

FOODS

and raw materials

Volume 12
Issue 1
2024

ISSN 2308-4057 (print)
ISSN 2310-9599 (online)



food production technology

food production
processes
and equipment

nutrition

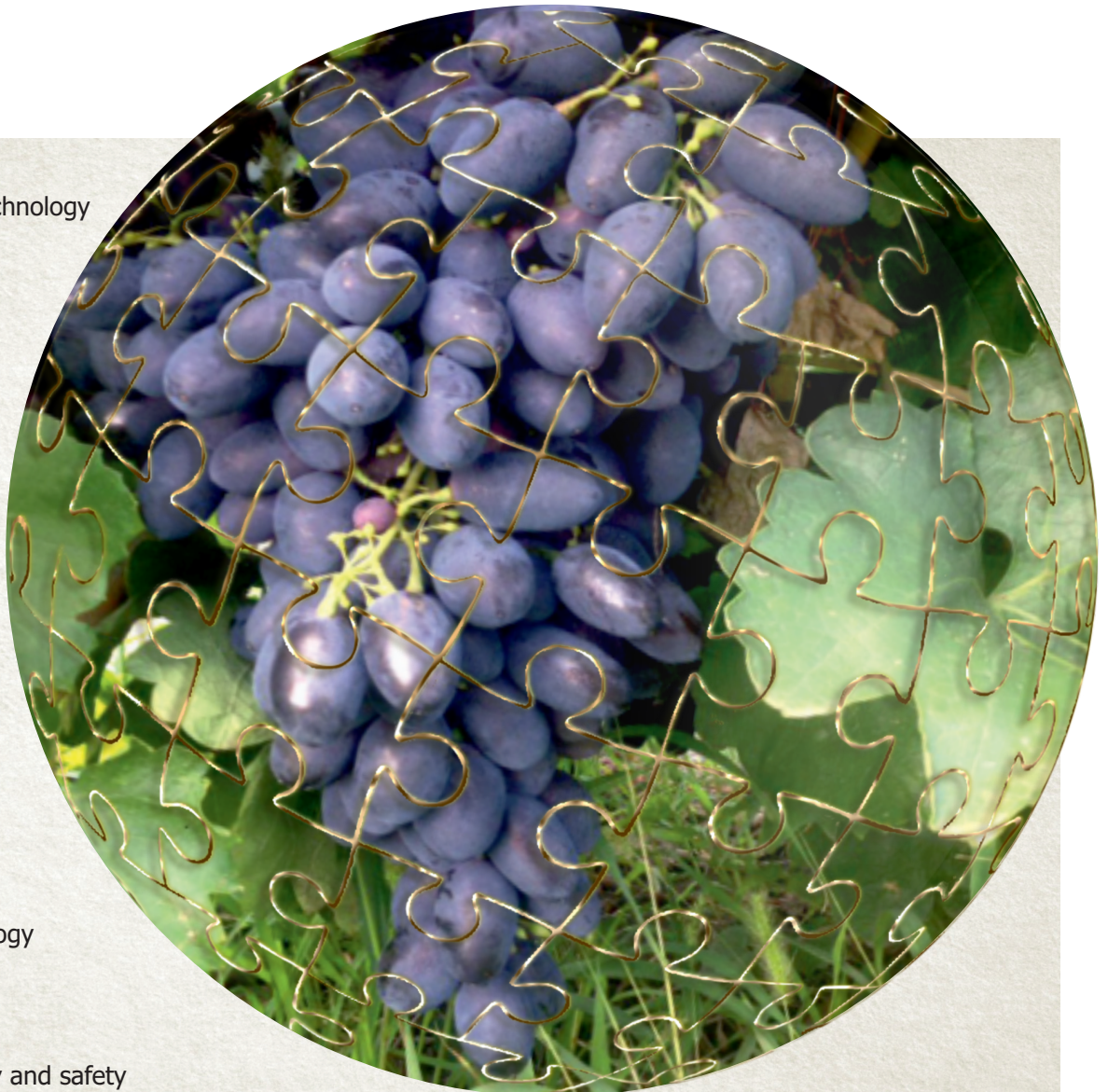
veterinary

biotechnology

biological sciences

chemistry and ecology

standardization,
certification, quality and safety



Foods and Raw Materials reports pioneering research in the food industry and agricultural science. We publish the results of fundamental and applied research as scientific papers, peer reviews, brief scientific reports, etc. The Journal is a single platform for scientific communication that bridges the gaps between regional, national, and international publications.

Foods and Raw Materials has been published in the English language since 2013. Two volumes a year come out in print and online.

All submitted manuscripts are checked for plagiarisms via *ithenticate.com* and *antiplagiat.ru* and undergo a double-blind peer review. Authors are responsible for the content of their article. As the Journal is fully supported by the Kemerovo State University, we do not charge for submission, translation, peer-review, or publication.

Foods and Raw Materials is an open access journal (CC BY 4.0). Our open access policy follows the Budapest Open Access Initiative (BOAI), which means that all our articles are available online immediately upon publication. Full-text electronic versions of all published materials appear in open access on *jfrm.ru/en* and *elibrary.ru*

Foods and Raw Materials is included in the following international data-bases: Emerging Sources Citation Index (Web of Science Core Collection), Scopus, DOAJ, CAS, FSTA, EBSCOhost, ResearchBib, WJCI, Dimensions, LENS.ORG, Scilit, CNKI, ProQuest, CABI, Agricola, Ulrich's, Google Scholar, OCLC WorldCat, and BASE.

For submission and subscription instructions, please visit us online at *jfrm.ru/en*

Editor-in-Chief

Alexander Yu. Prosekov, Dr. Sci. (Eng.), Dr. Sci. (Biol.), Professor, Corresponding Member of RAS, Kemerovo State University, Kemerovo, Russia.

Deputy Editor-in-Chief

Olga O. Babich, Dr. Sci. (Eng.), Associate Professor, Immanuel Kant Baltic Federal University, Kaliningrad, Russia.

Editorial Board

Levent Bat, Ph.D., Professor Dr., University of Sinop, Sinop, Turkey;

Irina M. Donnik, Dr. Sci. (Biol.), Professor, Academician of RAS, Kurchatov Institute, Moscow, Russia;

Sergey A. Eremin, Dr. Sci. (Chem.), Professor, Lomonosov Moscow State University, Moscow, Russia;

Palanivel Ganesan, Ph.D., Associate Professor, College of Biomedical and Health Science, Konkuk University, Chungju, South Korea;

Diako Khodaei, Ph.D., School of Science and Computing, Galway-Mayo institute of Technology, Galway, Ireland;

Nishant Kumar, Ph.D., National Institute of Food Technology Entrepreneurship and Management, Sonapat, India;

Fatumetuzzehra Küçükbay, Ph.D., Professor Dr., İnönü University, Malatya, Turkey;

Andrey B. Lisitsyn, Dr. Sci. (Eng.), Professor, Academician of RAS, V. M. Gorbатов Federal Research Center for Food Systems of Russian Academy of Sciences, Moscow, Russia;

Abdalbasit Adam Mariod, Ph.D., Professor, University of Jeddah, Alkamil, Saudi Arabia;

Philippe Michaud, Ph.D., Professor, Universite Clermont Auvergne, Polytech Clermont Ferrand, Aubiere, France;

Mehran Moradi, Doctor of Veterinary Medicine, Ph.D., Urmia University, Urmia, Iran;

Lev A. Oganesyants, Dr. Sci. (Eng.), Professor, Academician of RAS, All-Russian Research Institute of Brewing, Non-Alcoholic and Wine Industry, Moscow, Russia;

Gláucia Maria Pastore, Ph.D., Professor, Campinas University, Campinas, Brazil;

Andrey N. Petrov, Dr. Sci. (Eng.), Academician of RAS, All-Russia Dairy Research Institute, Moscow, Russia;

Shirish Hari Sonawane, Ph.D., Professor, National Institute of Technology Warangal, Telangana, India;

Rudolf Valenta, M.D., Professor for Allergology, Medical University of Vienna, Vienna, Austria.

Executive Editor

Anna I. Loseva, Ph.D. (Eng.), Kemerovo State University, Kemerovo, Russia.

Founder and Publisher: Kemerovo State University, 6, Krasnaya St., Kemerovo, Kemerovo region – Kuzbass, 650000, Russia

Editorial Office: Kemerovo State University, 6, Krasnaya St., Kemerovo, Kemerovo Region – Kuzbass, 650000, Russia; phone: +7(3842)58-81-19; e-mail: fjournal@mail.ru

Printing Office: Kemerovo State University, 73, Sovetskiy Ave., Kemerovo, Kemerovo Region – Kuzbass, 650000, Russia

Translators: Oxana Yu. Pavlova, Nadezda V. Rabkina

Publishing editors: Ekaterina V. Dmitrieva, Alena A. Kiryakova

Literary editor: Anastasia Yu. Kurnikova

Computer layout and design: Elena V. Volkova

Cover image: Ekaterina V. Dmitrieva. Photos credits: contributors

Date of publishing

February 05, 2024

Circulation 500 ex. Open price.

Subscription index in the Kniga-Servis online catalog – 40539.

The Federal Service for Supervision of Communications, Information Technology and Mass Media (Media Registration Certificate PI no. FS77-72606 dated April 04, 2018).

© 2024, Kemerovo State University. All rights reserved.



Editor's column

The wine industry is considered one of the oldest in Russian food science. It includes viticulture and winemaking, which shape budget revenues and socio-economic development of entire regions.

Russian viticulture dates back to Peter the Great. In the XIX century, Prince Golitsyn and Count Vorontsov turned the Crimea and the Krasnodar Region into the biggest wine-producers in Russia. They also provided the emerging Russian viticulture with its earliest scientific foundation. In Soviet times, the science of viticulture and winemaking kept developing and became one of the most advanced branches of agricultural science. Vineyards grew larger, new cultivars were introduced, and grapes became resistant to the harsh Russian climate. The anti-alcohol campaign of 1985-1987 hit the Russian wine industry hard, as did the roaring 1990s. Vineyards shrank, and some wine production technologies were lost. The industry still suffers from the after-shock of those events.

In 2019, the government adopted Federal Law No. 468-FZ On viticulture and winemaking in the Russian Federation, which established Russia's status as a wine-producing country. The new law boosted the development of the wine industry, based on a scientific approach to viticultural lands, their expansion, and novel production technologies. The law also protects Russian wine producers, especially those who grow their own grapes. The newly-adopted concept of Russian wine assigned it the status of an agricultural product. Thanks to the measures taken at the state level, the demand for Russian grapes has increased, and investors have acquired distribution guarantees.

Today, Russian viticulture is experiencing a renaissance. The wine-making regions expand their vineyards and increase their planting density. They renovate vineyards that are older than 10–15 years, as well as launch new wineries and tourism clusters. New wine-making areas are emerging in the Astrakhan Region, the Saratov Region, and in the Far East. These days, the total area of vineyards in Russia is 100,000 hectares, which is number 18 in the world. By 2030, it will have increased by 35%. Commercial grape production is concentrated in the south of Russia, i.e., in the regions of Krasnodar, Stavropol, the Crimea, Chechnya, Dagestan, Ingushetia, Kabardino-Balkaria, North Ossetia, Astrakhan, Volgo-

grad, Saratov, and Rostov. However, almost three quarters of all Russian vineyards are located in the Republic of Crimea and the Krasnodar Region. They grow international, Caucasian, autochthonous, and Soviet cultivars.

The Russian wine market is also developing at a pace to be envied. The production is expanding as it tries to keep up with the growing demand. The quality of domestic ripe wine meets world standards. According to forecasts, Russia's share in the global wine production will continue to grow and will have exceeded 3% by 2030. Today, 55% of Russian wine market is domestic wine. Domestic wine producers enjoy state support that help them create a competitive environment and stimulate public demand for Russian wines.

In Russia, wine tourism is a promising area of domestic tourism. In 2023, the government adopted a bill on advertising wine in grape-growing areas to support wine tourism and popularize the industry.


The state also supports scientific and technical development of the industry, e.g., various programs for technological renewal of viticulture and winemaking. Only advanced R&D can make the domestic wine industry efficient and successful.

Professor Anatoly M. Avidzba, Doctor of Agricultural Sciences and Member of the Russian Academy of Sciences, is a world-level specialist in viticulture and agricultural economics.

Professor Avidzba develops new methods aimed at improving viticultural technologies and wine production, as well as accelerating the selection process of new grape varieties. Professor Avidzba has invented new approaches to high-quality winemaking microzoning. He also studies polyphenols in various grape cultivars and wines. Functional grape product fortified with polyphenols can be part of dietary nutrition and medical treatment.

Professor Avidzba's contribution to the domestic viticulture and winemaking can hardly be overestimated. His scientific and practical achievements have been awarded at various levels. Professor Avidzba's articles, books, and patents have gained global recognition.

On February 10, we are happy to congratulate Anatoly Avidzba on his birthday. We wish Professor, his loved ones, colleagues, and students good health and optimism, inspiration for new ideas and scientific achievements, happiness and tranquility!

Editor-in-Chief,
Corresponding Member of the Russian Academy of Sciences,
Professor A. Yu. Prosekov 



Ionizing radiation effects on microorganisms and its applications in the food industry

Emmanuel Kormla Danyo*, Maria N. Ivantsova, Irina S. Selezneva

Ural Federal University named after the first President of Russia B.N. Yeltsin, Yekaterinburg, Russia

* e-mail: e.kdanyo@gmail.com

Received 04.10.2022; Revised 27.11.2022; Accepted 06.12.2022; Published online 30.05.2023

Abstract:

There are two main types of radiation: ionizing and non-ionizing. Radiations are widely distributed in the earth's crust with small amounts found in water, soil, and rocks. Humans can also produce them through military, scientific, and industrial activities. Ionizing and nonionizing radiations have a wide application in the food industry and medicine. γ -rays, X-rays, and electron beams are the main sources of radiation used in the food industry for food processing. This review discusses advantages and disadvantages of ionizing radiation on microorganisms and its potential applications in the food industry. Studies have revealed that ionizing radiation is used in the food industry to inactivate microorganisms in food products to improve hygiene, safety, and extend shelf life. Microorganisms such as bacteria and fungi are susceptible to high doses of irradiation. However, some bacterial and fungal species have developed an exceptional ability to withstand the deleterious effect of radiation. These organisms have developed effective mechanisms to repair DNA damage resulting from radiation exposure. Currently, radiation has become a promising technology for the food industry, since fruits, tubers, and bulbs can be irradiated to delay ripening or prevent sprouting to extend their shelf life.

Keywords: Ionizing radiation, activation, inactivation, food products, application, shelf life, microorganisms

Funding: The research was performed on the Ministry of Science and Higher Education of the Russian Federation (Minobrnauki) (Ural Federal University Program of Development within the Priority-2030 Program) is gratefully acknowledged.

Please cite this article in press as: Danyo EK, Ivantsova MN, Selezneva IS. Ionizing radiation effects on microorganisms and its applications in the food industry. *Foods and Raw Materials*. 2024;12(1):1–12. <https://doi.org/10.21603/2308-4057-2024-1-583>

INTRODUCTION

Ionizing radiation is a form of electromagnetic waves or particles which possess a significant amount of energy capable of ionizing an atom or a molecule. Too much exposure to ionizing radiation is harmful to living organisms. Some microorganisms have developed the capacity to survive in radioactive environments [1]. Living organisms are constantly faced with the challenge of surviving under extreme environmental conditions. Diverse groups of microorganisms such as bacteria, archaea, and eukaryotes can survive in harsh environments such as intense ultraviolet (UV) radiation, extreme temperatures, and desiccation. These conditions provide a lot of selection pressure for extremophiles [2].

Ionizing particles such as neutrons or α -particles can disrupt the DNA structure through a direct inter-

action with DNA, which can damage the sugar backbone and base pairs [3]. Radiation can induce genomic instability in living organisms by introducing either DNA single-strand breaks or double-strand breaks. When unrepaired, these errors may lead to cell death [4–6]. Reactive oxygen species produced by ionizing radiation in microorganisms can damage cellular macromolecules such as nucleic acids, proteins, lipids, and carbohydrates [7]. Post-translational addition of carbonyl groups to amino acid side chains increases after exposure to ionizing radiation. This results in a loss of protein function due to changes in protein folding [8, 9]. In order to overcome the deleterious effect of ionizing radiation, living organisms activate enzymatic and non-enzymatic antioxidant defense systems, DNA repair mechanisms, induction of protein folding, and degradation processes [10].

Irradiation food processing is a non-thermal method of administering specific doses of radiation to destroy microorganisms in food, thus enhancing its hygiene and safety and prolonging its shelf life [11]. The use of irradiation in food processing is highly recognized and well regulated. It can be applied to foods ranging from dried products like seasonings and spices to moisture-containing food such as meat. The presence of pathogens in fresh foods can cause foodborne illnesses. Irradiation technologies can decontaminate vegetables and fresh fruits without subjecting them to heat treatments [11]. Thermal methods such as sterilization and pasteurization have been effectively used to reduce fungi and mycotoxins in food products. However, processing at high temperatures can have a detrimental effect on the nutritional and sensory properties of food products. Therefore, we need to explore other technologies such as radiation [12]. In this review, we aimed to explore the effects of radiation on microorganisms and its applications in the food industry.

Radiation sources. Electromagnetic radiation is energy that travels at a constant speed through a sinusoidal path in different magnetic and electric fields. Its electromagnetic spectrum has different energies stretching from long-wavelength radio waves to short-wavelength γ -rays. In between these two limits, there are other forms of radiation such as microwave, infrared, visible light, ultraviolet, and X-ray [13]. There are two kinds of radiation, namely ionizing and non-ionizing. Non-ionizing radiation is a type of energy which can be generated by an instrument or machine in the form of electromagnetic waves with a specific wavelength [11]. Ionizing radiation, on the other hand, is a type of energy with a very short wavelength but high intensity capable of removing electrons from atoms. Its forms include X-rays, electron beams, and γ -rays [11, 13].

Radiations can emerge from both natural and artificial sources. Those from natural sources are due to the presence of several radiating elements found in the earth's crust, while those from artificial sources emerge from human scientific, military, and industrial activities [14]. The earliest radionuclides comprise uranium 238, thorium 232, potassium 40, radium 226, etc. They are mostly found in soils, rocks, and in many building materials. A good amount of environmental contamination with radioactive substances owes its source to nuclear power plant accidents, nuclear waste disposal, nuclear power testing, and mismanagement of radioactive materials [15].

Food processing can only use γ -radiation, X-rays, and accelerated electrons since other particles can induce radioactivity. Electron beam radiation is produced by an electron gun from which high-energy electron beams are emitted. A low penetration capacity (limited to approximately 2.5 cm) is a major drawback of applying electron beams to food. Therefore, this type of radiation cannot be used for a wide variety of foods. X-rays are high-energy photons that are also generated from

machine sources [16]. γ -radiations have a higher photon energy with a shorter wavelength. They are primarily produced from the decay of Cobalt-60 (^{60}Co) or Cesium 137 (^{137}Cs). ^{60}Co is obtained from loading small pellets of cobalt into sealed stainless steel or zirconium alloy tubes. ^{60}Co radionuclide is produced by the irradiation of ^{59}Co in a nuclear reactor by fast neutrons [17].

The effect of radiation on bacteria. Radiation, such as UV, causes indirect damage to proteins, lipids, and DNA, resulting in the formation of reactive oxygen species in bacteria. Radiation damages the bacterial DNA by stimulating single-strand breaks and causing pyrimidine dimers to form. Bacteria have many repair mechanisms in response to the damage caused by radiation. Some of them are post-replication recombination, nucleotide excision, and error-prone repairs [18, 19].

Bacteria belonging to the *Deinococcaceae* family are able to survive the deleterious effect of ionizing radiation. Among these radiation-resistant organisms is *Deinococcus radiodurans* [2, 20]. After exposing *D. radiodurans* to approximately 7 kGy of ionizing radiation, its genome was broken into fragments, but it did not have any effect on its survival [20].

There are no studies to justify a higher content of proteins involved in the double-strand breaks repair (such as RecA and PolA) in *D. radiodurans* than in other bacteria species such as *Escherichia coli* [21, 22]. Research shows that the ability of *D. radiodurans* to withstand radiation and desiccation is inherent in its Mn-dependent mechanisms which protect proteins from oxidative modifications that introduce carbonyl groups. The effect of γ -radiation on bacteria leads to a rise in protein carbonylation, which inhibits the catalytic activity of proteins and promotes cell death [10]. *D. radiodurans* bacteria possess about 300 times more Mn (II) ions than ionizing-radiation-sensitive bacteria such as *Thermus thermophiles* and *E. coli*. Due to high levels of intracellular Mn (II) ions, which protect proteins, *D. radiodurans* can resist the deleterious effect of 10 kGy ionizing radiation [23].

At the molecular and biological level, radiation targets the bacterial DNA, proteins, and cell membranes. The degree of damage depends on the genetic composition of bacteria. Each bacteria strain has several parameters which affect the yield of lesions per unit dose of radiation and the ability to cause cell death. Differences in sensitivity to radiation in different types of bacteria depend on the effectiveness of their cellular DNA repair mechanisms [24].

The effect of radiation on yeast. Yeasts are eukaryotic microorganisms which belong to the fungi kingdom. *Saccharomyces cerevisiae* is a type of yeast mostly used in the food industry for baking and brewing. Other species include *Candida*, *Saccharomyces*, *Debaryomyces*, *Hanseniaspora*, *Dekkera*, *Kluyveromyces*, *Rhodotorula*, *Meyerozyma*, *Pichia*, *Zygosaccharomyces*, and *Torulaspora* [25].

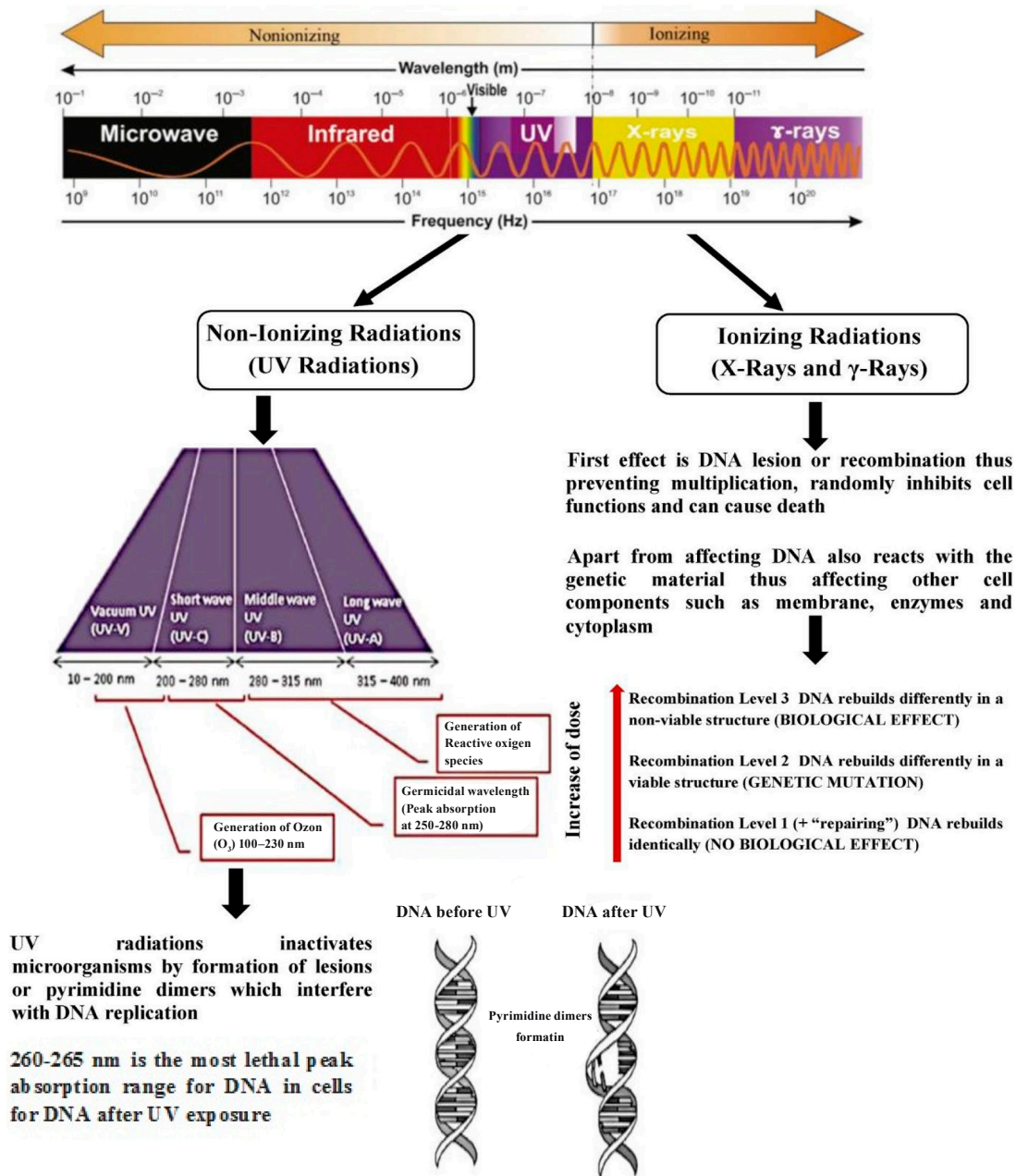


Figure 1 Effects of non-ionizing and ionizing radiation on microorganisms. Adapted from Bisht *et al.* [11]

A study conducted by Takeshita *et al.* exposed yeast cells to pulsed light and UV irradiation and showed differences in the proteins eluted from the yeast cells [19]. The elution of proteins is a possible indication of cell damage induced by irradiation. Pulse light irradiation is known to cause structural changes in yeast cells, enlarging vacuoles and distorting cell shape and cell membrane, as observed under transmission electron microscopy. These structural changes suggest that irradiation can cause damage to yeast cell membranes [19]. Ionizing radiation causes cellular damage to DNA, such as base damage, single-strand breaks, strand crosslinks, and double-strand breaks [26].

Budding yeasts exhibit resistance to ionizing radiation in the synthesis (S) and mitosis (M) phases

than nonbudding yeasts in the Gap 1 phase. Growing yeast cells in the synthesis/Gap 2 exhibit greater X-ray-induced instability than the stationary phase Gap 1/Gap 0 (G_1/G_0) yeast cells. It has been shown that yeast cells in the Gap 1 (G_1) phase are more sensitive to mutations caused by radiation, less sensitive in the early synthesis, and least sensitive in the late synthesis/Gap 2 (S/G_2) [27]. Yeast cells exhibit varied sensitivity to radiation at different growth stages. They are more resistant to radiation in the stationary phase (this resistance is different from what is observed in the cell cycle). However, cells are more sensitive to radiation in the exponential growth phase when the majority of cells are in the synthesis/Gap 2 phase. Studies have shown that budding yeasts are more resistant to the killing ef-

fect of radiation than nonbudding yeasts [28–30]. Also, yeasts show much greater resistance to environmental stressors than prokaryotes because of their ecological versatility [31]. Yeast cell membrane and DNA are susceptible to radiation damage and inactivation. There is a lack of information to support the effect of radiation on yeasts. Therefore, more studies are needed to show what damage is caused by their exposure to radiation.

The effect and response of fungi to radiation.

D. radiodurans bacterium is known to withstand higher levels of ionizing radiation. However, studies have also identified some fungal species with a greater potential to withstand the effects of radiation compared to this bacterium. After the explosion at the Chernobyl nuclear power plant in 1986, and several years down the line, over 2000 fungal species were isolated in that area [31]. Some of the species were remarkably radioresistant, including melanized fungal species (*Cladosporium* spp.), *Cryomyces antarcticus*, *Aureobasidium*, and yeast [31]. Melanized fungi were predominant compared to the other fungal species [32, 33].

A study by Dadachova *et al.* showed that melanized fungal species, such as *Cryptococcus neoformans* and *Wangiella dermatitidis*, experienced a higher cell growth compared to their non-melanized counterparts [34]. The authors found that ionizing radiation interfered with the electron transfer properties in melanin by analyzing the NADH-ferricyanide redox reaction. This suggests that melanized fungi can use radiation (γ -radiation) as an energy source to convert electromagnetic energy into chemical energy that the fungi can utilize [10]. Melanin protects fungal cells from various environmental stresses, including oxidative damage, heavy metals, and UV irradiation [35]. It plays an important role in radiation resistance by dispersing electrons and photons and serving as a radioprotective barrier against radiation and scavenging radiation-induced reactive oxygen species [36].

Transcriptome analysis was conducted by Jung *et al.* to explain the mechanism of radiation resistance in *C. neoformans* [37]. They found a significant variation in the *C. neoformans* genes. Out of 6962 identified genes, 37% showed different expression patterns after γ -radiation exposure. The genes involved in post-translational modification, DNA replication and repair, as well as protein turnover and chaperone function, were extremely upregulated during the early recovery time. However, the genes that participated in translation, transport, and amino acid metabolism were downregulated in the late recovery time. The transcriptome analysis of *C. neoformans* was similar to that of radiation-sensitive fungi such as *Schizosaccharomyces pombe* and *S. cerevisiae* [38, 39].

Fungi have developed several effective mechanisms to withstand the deleterious effect of radiation compared to other organisms. The genes involved in DNA damage repair and oxidative stress responses are upregulated during radiation exposure. Fungi produce protective molecules such as melanin, carotenoids, trehalose

1,3-glucan, and others. These molecules contribute to the fungi's exceptional ability to protect themselves against radiation and other harmful environmental stresses, such as dryness and salinity [31]. There is limited information in literature on the effects of radiation on fungi. Therefore, more research is needed to elucidate what kind of mechanisms are employed by fungi to overcome the deleterious effects of ionizing radiation.

Mechanisms of microbial inactivation. Ionizing and non-ionizing radiations have different effects on microorganisms because of the different energies they possess. Ionizing radiation produces free radicals in microorganisms and causes damage to genetic materials and other cellular components, contributing to cell death. However, microbial inactivation or destruction by non-ionizing radiation is facilitated by the thermal decomposition of proteins, lipids, and DNA, leading to cell rupture or disintegration. Spores produced by bacteria and fungi are resistant to irradiation because they contain a small amount of DNA and are very stable. Microorganisms respond differently to radiation due to differences in their physical and chemical structures and in their spore-producing capacity [13].

Ionizing radiation can destroy microbes and mycotoxins employing two major mechanisms, namely the direct interaction with the organism and the indirect action by water radiolysis. The direct interaction of radiation causes damage to genetic materials. In fungi, for instance, this can lead to the death of living cells, preventing the formation and release of mycotoxins. In the indirect method, radiation reacts with water molecules (radiolysis) to produce positively-charged water radicals (H_2O^+) and negative free solvated electrons (e^-). These interactions result in the formation of several reactive species such as H^+ , OH^+ , H_3O^+ , H_2O_2 , and OH . Subsequently, these free radicals attack cytoplasmic components and destroy organic molecules. The hydroxyl free radical removes hydrogen atoms from the bases within the DNA strands, causing death to organisms which cannot recover from this DNA damage [13]. Many studies have identified damage of deoxyribonucleic or ribonucleic acids coupled with the disintegration of cytoplasmic membranes as major mechanisms for microbial inactivation by ionizing radiation. The induction of single-strand breaks is not very destructive, but double- or multiple-strand breaks can render the microbe inactive [40]. Figure 2 shows how radiation can damage the DNA in microorganisms.

Justification of ionizing radiation in food processing. Food irradiation is a non-thermal method of exposing food to specific doses of non-ionizing or ionizing radiations to destroy microorganisms (bacteria, fungi, viruses, etc.) in food or agricultural products to improve their hygiene and safety, as well as prolong their shelf life [42, 43]. The use of radiation technology in food processing has proven to be effective and it is widely used for various kinds of foodstuffs from dried to moisturized food products [44]. The rise in different

kinds of food-borne diseases caused by consuming fresh foods contaminated with pathogens has made food irradiation an alternative approach to decontaminating fresh vegetables and fruits without heat treatments using sterilization or pasteurization [45].

Mycotoxin contamination of food products is raising several global concerns because it affects human health, causes economic loss to farmers, and leads to food wastage [46, 47]. Mycotoxins are produced in food contaminated with fungi. This can result in mycotoxin poisoning and various health consequences, such as gynecomastia, esophageal cancer, human nephropathies, hepatocellular carcinoma, liver cancers, hepatitis B, reduced levels of immunoglobulins, as well as increased morbidity and mortality [48–50].

Thermal food preservation methods used to eliminate enzymes, mycotoxins, and pathogenic microorganisms consume a lot of energy, thereby increasing the cost of preservation. Thermal treatment methods also cause loss of certain nutrients (vitamins, proteins, etc.) and sensory properties, affecting the overall quality of the food product [51–53]. To overcome this negative impact, the food industry is exploring alternative processing techniques, such as cold plasma, high pressure processing, and irradiation technologies [11].

Using electromagnetic radiation as an energy source is a better option to ensure microbial safety, improve sensory properties, and retain nutrients [54]. It does not leave residues and toxins in the product. Nor does it affect the odor, pH, flavor, or taste [55]. Parasites, such as *Toxoplasma gondii*, *Cysticercus* spp., *Taenia solium*, *Trichinella spiralis*, parasitic protozoa, and helminths in meat and fish, can be inactivated through 0.3 to 1 kGy irradiation to guarantee the product's safety for consumers [56].

Applications of ionizing radiation in the food industry. Food irradiation is a method used in food processing and preservation. This involves administering certain amounts of ionizing radiation to food in a radiation-protected chamber [57]. Radiation can be applied to food products to either pasteurize or sterilize them to reduce or eliminate pathogens and other microorganisms, except certain viruses, based on the radiation dose [16]. Microorganisms, such as *E. coli*, *Campylobacter*, *Salmonella*, and others, can be removed from food by irradiation to improve the product's shelf-life and guarantee safety. Sterile foods are very important for consumers, especially patients with a compromised or suppressed immune system who need to consume bacteria-free foods [16]. Practical doses of radiation given to food are classified into three main categories, as shown in Fig. 3 [56].

The focus of using this technology in the food industry is to maintain stability in stored products, eliminate insects or parasites, inhibit the activity of enzymes,

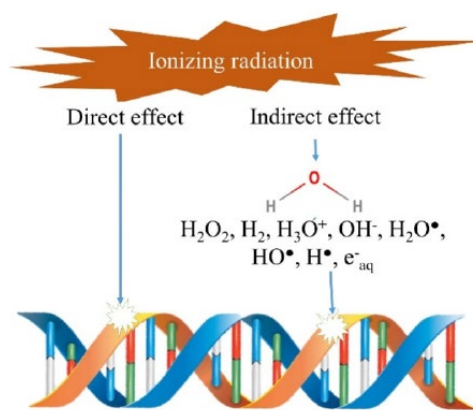


Figure 2 Effects of radiation on the genetic material (DNA) in microorganisms. Radiation can directly damage the DNA of microorganisms to kill/render them inactive or cause water molecules to undergo radiolysis to produce free radicals. These free radicals then attack the DNA and other organic molecules in the microbe causing them to die if they cannot recover from the radiation-induced damage. Adapted from [41]

and reduce food-borne contaminants such as bacteria, viruses, fungi, and mycotoxins [13]. The allowable dose of radiation delivered to food should not exceed 10 kGy, since this dose does not compromise the product's safety or affect its structure and functional properties [40]. Some applications of radiation technology in the food industry:

- irradiation of spices and condiments;
- control of sprouting in tubers and bulbs;
- insect disinfection in cereals;
- fruits and vegetables;
- fish and meat products; and
- application of irradiation in dairy products.

Irradiation of spices and condiments. Spices and condiments are naturally contaminated with numerous microorganisms or due to poor harvest and storage conditions [58]. Spices can be contaminated with pathogenic microorganisms such as *Clostridium perfringens*, *Bacillus cereus*, *Salmonella*, *E. coli*, and toxigenic molds. Several studies have confirmed that up to 10 kGy of irradiation can reduce the microbial load without any adverse chemical or organoleptic changes in spices [56, 59].

The use of spices to season processed foods without sterilization may increase food spoilage and even cause food-borne diseases. In the past, fumigants (methyl bromide and ethylene oxide) were used for insect, bacteria, and mold elimination because moist heat treatment was not suitable for dried products. However, these chemicals are highly toxic and raise safety and environmental concerns. Spice irradiation has been approved by many countries in recent times and the food industry is moving in this direction. Doses of 5–10 kGy are enough to eliminate mold spores, bacteria, and insects without any effects on the sensory or chemical properties of spices [60].

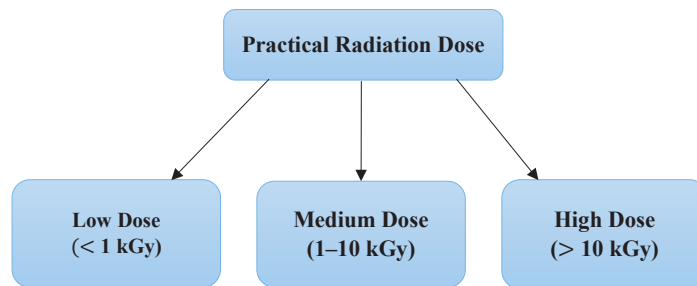


Figure 3 Radiation doses applied in the food industry for food processing

Control of sprouting in tubers and bulbs. Sprouting affects the shelf life of potatoes, garlic, onions, ginger shallots, and yam. These agricultural products have to be stored for several months to ensure adequate supplies to consumers, but due to sprouting, large losses are observed after harvesting [56]. Irradiation has proven to be effective for shelf-life extension [45, 61]. Low radiation doses of 0.02–0.2 and 0.25–1.0 kGy are used to prevent the sprouting of bulbs and tubers, respectively [56].

Sprouting and rotting of tubers and bulbs occur when they are stored under low temperatures (4–20°C) and high humidity (> 85%) [62]. Sprouting of tuber crops can be reduced by applying lower radiation doses (0.15 kGy) during the dormancy period. Although the dose needed for sprout prevention does not affect the physicochemical properties of the produce, in certain cases brownish discoloration can occur in the inner buds [17]. In a study by Tripathi *et al.*, several onion varieties (red dark, light red, yellow, and white) irradiated with 60 Gy of γ -radiation were stored for 6 months without sprouting, whereas 34.3% of the unirradiated onions developed sprouts [63].

Insect disinfection in cereals. Radiation is used for destroying insects in cereals, flours, and products made from them, since insects may damage some of these products. Insects can also serve as vectors for delivering pathogenic bacteria and parasites into food [58]. Radiation in the range of 100–1000 Gy is effective for inactivating insects in cereals [56, 64, 65]. Molds can be eliminated from cereals and grains by low dose irradiation. Doses > 1 kGy affect the quality of cereal grains and decrease flour viscosity. Also, they destroy starch and gluten, thus reducing the firmness, stickiness, and bulkiness of the dough [66].

Fruits and vegetables. Irradiation technology gives consumers access to the original taste, nutrients, appearance, and texture of fresh fruits and vegetables for extended periods of time. Radiation doses < 1 kGy are recommended for insect disinfection of fruits and vegetables, as well as to delay their ripening and senescence and inhibit sprouting [17]. The radiation doses needed to extend shelf life and enhance the quality of fruits and vegetables depend on their maturity, cultivar, and pre- and post-harvest handling [67]. Lower doses (0.2–0.4 kGy) can increase the shelf life of fruits,

while higher doses can lead to fruit decay [68]. The maximum irradiation dose for fresh fruit and vegetable disinfection and preservation must be < 1 kGy to receive approval from the United States Food and Drug Administration (FDA). Within the selected irradiation range, the sensitivity of the crop should be determined to enhance its quality without causing changes to its chemical and sensory properties [69].

The optimum dose for extending the shelf life of banana and plantain is within 150–300 Gy. At 500 Gy of irradiation, banana and plantain can develop a brown skin or gray scald due to increased polyphenol oxidase activity in the peels. Tissue damage can also be observed. Matured banana at harvest can tolerate quarantine radiation compared with less matured banana which develops peel injury after irradiation at 800 Gy [69]. Irradiation of fully matured green mangoes at 250–750 Gy can delay ripening. Tommy Atkins mangoes can be stored for 21 days at 12°C when exposed to radiation at ≤ 1000 Gy, while higher doses of ≥ 1500 Gy can result in fruit softening, peel scald, and flesh pitting [70–72].

Fish and meat products. The use of radiation in preserving fish can stabilize its market value and reduce wastage to ensure effective distribution of sea foods to the consumers [73]. Defrosted fish is contaminated with a lot of microorganisms, some of which move from the fish's gastrointestinal tract into the muscle tissue causing spoilage. The shelf life of fish is relatively short due to the action of spoilage microorganisms and enzymes. This contributes to fermentation and breakdown of fish proteins into free amino acids, destroying the sensory properties of the fish. Ionizing radiation is a promising technology that can be employed to increase the shelf life of defrosted fish by inactivating or killing pathogens and spoilage microorganisms [74]. The treatment of fish fillets with radiation (1–4 kGy) is more effective than traditional preservation methods because radiation destroys microorganisms without changing the physicochemical properties of the fish [75]. However, doses > 4.5 kGy can cause oxidative damage and destroy vitamins, for example, thiamine (B_1) [74]. Canned fish can be treated with low doses of irradiation after autoclaving to achieve good sterilization of the product. Exposure of cured fish to bacteria, fungi, and insects leads to its spoilage, so irradiation can be employed to reduce or eliminate these organisms in the product [73].

Meat is a perishable food product and the consumption of contaminated meat or meat products causes food-borne diseases. The most common pathogens that cause food-related outbreaks are *C. perfringens*, *Salmonella*, *Shiga-toxigenic*, *Listeria monocytogenes*, *Clostridium botulinum*, *E. coli*, *Staphylococcus aureus*, and *B. cereus* [76, 77]. Ultraviolet radiation (non-ionizing radiation) between 100–400 nm can be used to kill pathogenic microorganisms. Irradiation of fresh meat and meat products is considered a healthy and effective way to extend shelf life. Irradiation doses of 50 kGy or above can affect the meat color because of chemical changes caused to iron in myoglobin, while low doses (1–10 kGy) produce fewer changes in color, odor, and flavor [78]. Several studies confirmed the use of radiation to process meat products like ham, bacon, sausages, and beef burgers. Irradiation doses of 1–4 kGy can inactivate 90% of spoilage microorganisms in these products [79].

Dairy products. Milk and milk products form an important component in the food chain. Liquid, powdered, and concentrated milk is used in the food industry as a raw material for making different products. Consumers use milk for cooking and making beverages. Milk is susceptible to microbial contamination from cow's udder, as well as at various stages of production, processing, and distribution [80]. Pathogenic microorganisms, such as *L. monocytogenes*, *S. aureus*, and *Salmonella species*, can contaminate milk and cause food-borne illnesses [81]. Heat pasteurization and sterilization are effectively used to decrease the microbial load. However, psychotropic bacterial species can continue to grow in milk at low temperatures and this is a major concern for the dairy industry [82]. Irradiation can be explored as an alternative technology to reduce or destroy microorganisms in raw milk before using it for the preparation of dairy products. The practical application of radiation to dairy products is relatively low because most pathogens are effectively eliminated by heat pasteurization. Also, some studies report off-flavors in irradiated dairy products [80, 83].

Several studies have evaluated the suitability of using irradiation to preserve dairy products such as cheese and ice cream. They recommended packaging the products before irradiation treatment in order to kill post-processing microbial contaminants [80]. Prior to cheese production, milk is pasteurized to reduce the microbial load, but this does not guarantee absolute microbial safety because the chances of post-pasteurization contamination are still high. Therefore, there is a need for exploring other non-thermal sterilization methods, such as irradiation technologies, to inactivate microorganisms present in the final product even after packaging [84]. *Pseudomonas* spp. and *Enterobacteriaceae* are the main organisms responsible for cheese spoilage [85]. A study by Lacivita *et al.* showed that X-rays at 2 and 3 kGy inactivated these species and extended the shelf life of Fiordilatte cheese for more than 40 days, while the unirradiated

cheese remained unacceptable for about 10 days [83]. Food irradiation is safe and it has been approved in many countries. It can be applied to cheese to extend shelf life and maintain its nutritional and sensory properties [84].

Advantages and disadvantages of food irradiation.

Advantages. Exposure of food to ionizing radiation aims to reduce microbial load by destroying microorganisms and inactivating enzymes present in food to prevent its spoilage. Radiation also prevents gametes of parasitic insects from reproducing, resulting in various food preservation outcomes [86]. Perishable fruits (bananas, pears, mangoes) can be irradiated to improve their shelf life. As a result, they can be delivered to consumers fresh and in a timely manner [87]. Pathogenic microorganisms, such as *E. coli*, *Campylobacter*, *Listeria*, *Salmonella*, *Shigella*, and *Staphylococcus*, can be present in many foods. These organisms are responsible for different kinds of food-borne diseases. Irradiation offers a positive way of eliminating these pathogenic organisms, especially in foods where thermal inactivation is inapplicable [87].

Disadvantages. Irradiation also affects the nutritional and sensory properties of foods, just like any other food processing method. While low and medium doses of irradiation do not affect the nutritional content, doses > 10 kGy can degrade nutrients, as seen in thermal food processing methods such as cooking and pasteurization. Vitamins are the most affected components during food irradiation treatment [13]. Ionizing radiation causes chemical changes in food through radiolysis. Certain parameters, such as absorbed dose, presence or absence of oxygen, dose rate and temperature, affect the chemical reactions or transformations induced in food products. Ionizing radiation at 10 kGy does not usually have any effect on micronutrients (water and fat-soluble vitamins) or macronutrients (carbohydrates, proteins, and lipids) in food. However, at doses > 10 kGy, macromolecules, such as carbohydrates, are decomposed and lipids become rancid [88, 89].

Direct energy absorption by irradiated foods can cause chemical changes through radiolysis effects. Irradiation causes water molecules to lose an electron giving rise to OH^+ , which then reacts with other water molecules to produce hydrogen peroxide (H_2O_2), hydroxyl radicals ($\text{OH}\cdot$), molecular hydrogen, and oxygen. Since these molecules are free radicals, they cause oxidation and reduction reactions in food products [90, 91]. The effect of radiation on proteins depends on the protein structure, physical status, and amino acid content. The changes which can be induced in proteins include aggregation, dissociation, cross-linking, and oxidation [92]. For instance, γ -irradiation of hazelnuts at 10 kGy caused denaturation and protein aggregation [93]. The use of high radiation doses for processing muscle foods, such as meat and meat products, leads to the formation of free radicals, as well

as lipid and protein oxidation. This causes biochemical and physicochemical changes that affect the sensory and nutritional properties of the product [79].

CONCLUSION

Food spoilage and food-borne illnesses are caused by microorganisms which contaminate food during harvesting, manufacturing, and distribution. These microorganisms also reduce the shelf life of many processed and non-processed food products. The adoption of irradiation technologies to inactivate food spoilage microorganisms is gaining popularity among many food industries across the world. Food irradiation does not have much effect on the nutritional and chemical compositions of food. Thus, it is considered a good alternative to thermal processing methods. Ra-

diation can be used to extend the shelf life of different kinds of foods, such as fruits, meat, fish, spices, tubers, bulbs, and many others.

CONTRIBUTION

The authors were equally involved in writing the manuscript and are equally responsible for plagiarism.

CONFLICT OF INTEREST

The author declares that there is no conflict of interests regarding the publication of this article.

ACKNOWLEDGEMENTS

The research funding from the Ministry of Science and Higher Education of the Russian Federation (Ural Federal University Program of Development within the Priority-2030 Program) is gratefully acknowledged.

REFERENCES

1. Zhu J, Sun X, Zhang Z-D, Tang Q-Y, Gu M-Y, Zhang L-J, et al. Effect of ionizing radiation on the bacterial and fungal endophytes of the halophytic plant *Kalidium schrenkianum*. *Microorganisms*. 2021;9(5). <https://doi.org/10.3390/microorganisms9051050>
2. Confalonieri F, Sommer S. Bacterial and archaeal resistance to ionizing radiation. *Journal of Physics: Conference Series*. 2011;261. <https://doi.org/10.1088/1742-6596/261/1/012005>
3. Close DM, Nelson WH, Bernhard WA. DNA damage by the direct effect of ionizing radiation: Products produced by two sequential one-electron oxidations. *Journal of Physical Chemistry A*. 2013;117(47):12608–12615. <https://doi.org/10.1021/jp4084844>
4. Rich T, Allen RL, Wyllie AH. Defying death after DNA damage. *Nature*. 2000;407:777–783. <https://doi.org/10.1038/35037717>
5. Hoeijmakers JHJ. Genome maintenance mechanisms for preventing cancer. *Nature*. 2001;411:366–374. <https://doi.org/10.1038/35077232>
6. Azzam EI, Jay-Gerin J-P, Pain D. Ionizing radiation-induced metabolic oxidative stress and prolonged cell injury. *Cancer Letters*. 2012;327:1–2:48–60. <https://doi.org/10.1016/j.canlet.2011.12.012>
7. Madian AG, Regnier FE. Proteomic identification of carbonylated proteins and their oxidation sites. *Journal of Proteome Research*. 2010;9(8):3766–3780. <https://doi.org/10.1021/pr1002609>
8. Maisonneuve E, Ducret A, Khoueiry P, Lignon S, Longhi S, Talla E, et al. Rules governing selective protein carbonylation. *PLoS One*. 2009;4(10). <https://doi.org/10.1371/journal.pone.0007269>
9. Sukharev SA, Pleshakova OV, Moshnikova AB, Sadovnikov VB, Gaziev AI. Age- and radiation-dependent changes in carbonyl content, susceptibility to proteolysis, and antigenicity of soluble rat liver proteins. *Comparative Biochemistry and Physiology Part B: Biochemistry and Molecular Biology*. 1997;116(3):333–338. [https://doi.org/10.1016/S0305-0491\(96\)00232-5](https://doi.org/10.1016/S0305-0491(96)00232-5)
10. Jung K-W, Lim S, Bahn Y-S. Microbial radiation-resistance mechanisms. *Journal of Microbiology*. 2017;55:499–507. <https://doi.org/10.1007/s12275-017-7242-5>
11. Bisht B, Bhatnagar P, Gururani P, Kumar V, Tomar MS, Sinhmar R, et al. Food irradiation: Effect of ionizing and non-ionizing radiations on preservation of fruits and vegetables – a review. *Trends in Food Science and Technology*. 2021;114:327–385. <https://doi.org/10.1016/j.tifs.2021.06.002>
12. Wang C-Y, Huang H-W, Hsu C-P, Yang BB. Recent advances in food processing using high hydrostatic pressure technology. *Critical Reviews in Food Science and Nutrition*. 2016;56(4):527–540. <https://doi.org/10.1080/10408398.2012.745479>
13. Akhila PP, Sunooj KV, Aaliya B, Navaf M, Sudheesh C, Sabu S, et al. Application of electromagnetic radiations for decontamination of fungi and mycotoxins in food products: A comprehensive review. *Trends in Food Science and Technology*. 2021;114:399–409. <https://doi.org/10.1016/j.tifs.2021.06.013>
14. Alqadi MK, Alzoubi FY, Jaber MA. Assessment of radon gas using passive dosimeter in Amman and Al-Rusaifa cities, Jordan. *International Journal of Radiation Research*. 2016;14(4):367–371. <https://doi.org/10.18869/acadpub.ijrr.14.4.367>

15. Rafique M. Cesium-137 activity concentrations in soil and brick samples of Mirpur, Azad Kashmir; Pakistan. *International Journal of Radiation Research*. 2014;12(1):39–46.
16. Agbaka JI, Ibrahim AN. Irradiation: Utilization, advances, safety, acceptance, future trends, and a means to enhance food security. *Advances in Applied Science Research*. 2020;11(3).
17. Sharma P, Sharma SR, Mittal TC. Effects and application of ionizing radiation on fruits and vegetables: A review. *Journal of Agricultural Engineering*. 2020;57(2):97–126.
18. Fernández Zenoff V, Siñeriz F, Farías ME. Diverse responses to UV-B radiation and repair mechanisms of bacteria isolated from high-altitude aquatic environments. *Applied and Environmental Microbiology*. 2006;72(12). <https://doi.org/10.1128/AEM.01333-06>
19. Takeshita K, Shibato J, Sameshima T, Fukunaga S, Isobe S, Arihara K, et al. Damage of yeast cells induced by pulsed light irradiation. *International Journal of Food Microbiology*. 2003;85(1–2):151–158. [https://doi.org/10.1016/S0168-1605\(02\)00509-3](https://doi.org/10.1016/S0168-1605(02)00509-3)
20. Krisko A, Radman M. Protein damage and death by radiation in *Escherichia coli* and *Deinococcus radiodurans*. *Proceedings of the National Academy of Sciences*. 2010;107(32):14373–14377. <https://doi.org/10.1073/pnas.1009312107>
21. Blasius M, Hübscher U, Sommer S. *Deinococcus radiodurans*: What belongs to the survival kit? *Critical Reviews in Biochemistry and Molecular Biology*. 2008;43(3):221–238. <https://doi.org/10.1080/10409230802122274>
22. Daly MJ. A new perspective on radiation resistance based on *Deinococcus radiodurans*. *Nature Reviews Microbiology*. 2009;7:237–245. <https://doi.org/10.1038/nrmicro2073>
23. Sghaier H, Ghedira K, Benkahla A, Barkallah I. Basal DNA repair machinery is subject to positive selection in ionizing-radiation-resistant bacteria. *BMC Genomics*. 2008;9. <https://doi.org/10.1186/1471-2164-9-297>
24. Ginoza W. The effects of ionizing radiation on nucleic acids of bacteriophages and bacterial cells. *Annual Review of Microbiology*. 1967;21:325–368. <https://doi.org/10.1146/annurev.mi.21.100167.001545>
25. Riffo B, Henríquez C, Chávez R, Peña R, Sangorrín M, Gil-Duran C, et al. Nonionizing electromagnetic field: A promising alternative for growing control yeast. *Journal of Fungi*. 2021;7(4). <https://doi.org/10.3390/jof7040281>
26. Ward JF. DNA damage produced by ionizing radiation in mammalian cells: Identities, mechanisms of formation, and reparability. 1988;35:95–125. [https://doi.org/10.1016/S0079-6603\(08\)60611-X](https://doi.org/10.1016/S0079-6603(08)60611-X)
27. Hafer K, Rivina L, Schiestl RH. Cell cycle dependence of ionizing radiation-Induced DNA deletions and antioxidant radioprotection in *Saccharomyces cerevisiae*. *Radiation Research*. 2009;173(6):802–808. <https://doi.org/10.1667/RR1661.1>
28. Raju MR, Gnanapurani M, Stackler B, Madhvanath U, Howard J, Lyman JT, et al. Influence of linear energy transfer on the radioresistance of budding haploid yeast cells. *Radiation Research*. 1972;51(2):310–317. <https://doi.org/10.2307/3573612>
29. de Langguth EN, Beam CA. Repair mechanisms and cell cycle dependent variations in X-ray sensitivity of diploid yeast. *Radiation Research*. 1973;53(2):226–234. <https://doi.org/10.2307/3573527>
30. Beam CA, Mortimer RK, Wolfe RG, Tobias CA. The relation of radioresistance to budding in *Saccharomyces cerevisiae*. *Archives of Biochemistry and Biophysics*. 1954;49(1):110–122. [https://doi.org/10.1016/0003-9861\(54\)90172-1](https://doi.org/10.1016/0003-9861(54)90172-1)
31. Coleine C, Stajich JE, Selbmann L. Fungi are key players in extreme ecosystems. *Trends in Ecology and Evolution*. 2022;37(6):517–528. <https://doi.org/10.1016/j.tree.2022.02.002>
32. Zhdanova NN, Tugay T, Dighton J, Zheltonozhsky V, Mcdermott P. Ionizing radiation attracts soil fungi. *Mycological Research*. 2004;108(9):1089–1096. <https://doi.org/10.1017/S0953756204000966>
33. Vember VV, Zhdanova NN. Peculiarities of linear growth of the melanin-containing fungi *Cladosporium sphaerospermum* Penz. and *Alternaria alternata* (Fr.) Keissler. *Mikrobiologichnyĭ Zhurnal*. 2001;63(3):3–12.
34. Dadachova E, Bryan RA, Huang X, Moadel T, Schweitzer AD, Aisen P, et al. Ionizing radiation changes the electronic properties of melanin and enhances the growth of melanized fungi. *PLoS One*. 2007;2(5). <https://doi.org/10.1371/journal.pone.0000457>
35. Nosanchuk JD, Casadevall A. The contribution of melanin to microbial pathogenesis. *Cellular Microbiology*. 2003;5(4):203–223. <https://doi.org/10.1046/j.1462-5814.2003.00268.x>
36. Dadachova E, Bryan RA, Howell RC, Schweitzer AD, Aisen P, Nosanchuk JD, et al. The radioprotective properties of fungal melanin are a function of its chemical composition, stable radical presence and spatial arrangement. *Pigment Cell and Melanoma Research*. 2008;21(2):192–199. <https://doi.org/10.1111/j.1755-148X.2007.00430.x>
37. Jung K-W, Yang D-H, Kim M-K, Seo HS, Lim S, Bahn Y-S. Unraveling fungal radiation resistance regulatory networks through the genome-wide transcriptome and genetic analyses of *Cryptococcus neoformans*. *mBio*. 2016;7(6). <https://doi.org/10.1128/mBio.01483-16>


38. Watson A, Mata J, Bähler J, Carr A, Humphrey T. Global gene expression responses of fission yeast to ionizing Radiation. *Molecular Biology of the Cell*. 2004;15(2):851–860. <https://doi.org/10.1091/mbc.e03-08-0569>
39. Gasch AP, Huang M, Metzner S, Botstein D, Elledge SJ, Brown PO. Genomic expression responses to DNA-damaging agents and the regulatory role of the yeast ATR homolog Mec1p. *Molecular Biology of the Cell*. 2001;12(10):2987–3003. <https://doi.org/10.1091/mbc.12.10.2987>
40. Isemberlinova AA, Egorov IS, Nuzhnyh SA, Poloskov AV, Pokrovskaya EA, Vertinskiy AV, et al. The pulsed X-ray treatment of wheat against pathogenic fungi. *Nuclear Instruments and Methods in Physics Research Section B: Beam Interactions with Materials and Atoms*. 2021;503:75–78. <https://doi.org/10.1016/j.nimb.2021.07.011>
41. Munir MT, Federighi M. Control of foodborne biological hazards by ionizing radiations. *Foods*. 2020;9(7). <https://doi.org/10.3390/foods9070878>
42. Nair PM, Sharma A. Food irradiation. In: Knoerzer K, Muthukumarappan K, editors. *Innovative food processing technologies. A comprehensive review*. Elsevier; 2016. pp. 19–29. <https://doi.org/10.1016/B978-0-12-815781-7.02950-4>
43. Pathak B, Omre PK, Bisht B, Saini D. Effect of thermal and non-thermal processing methods on food allergens. *Progressive Research – An International Journal*. 2018;13(4):314–319.
44. Prakash A, Ornelas-Paz JJ. Irradiation of fruits and vegetables. In: Yahia EM, editor. *Postharvest technology of perishable horticultural commodities*. Duxford: Woodhead Publishing; 2019. pp. 563–589. <https://doi.org/10.1016/B978-0-12-813276-0.00017-1>
45. Barkai-Golan R, Follett PA. Sprout inhibition of tubers, bulbs, and roots by ionizing radiation. In: Barkai-Golan R, Follett PA, editors. *Irradiation for quality improvement, microbial safety and phytosanitation of fresh produce*. Cambridge: Academic Press; 2017. pp. 47–53. <https://doi.org/10.1016/B978-0-12-811025-6.00005-7>
46. Bytesnikova Z, Adam V, Richtera L. Graphene oxide as a novel tool for mycotoxin removal. *Food Control*. 2021;121. <https://doi.org/10.1016/j.foodcont.2020.107611>
47. Alshannaq A, Yu J-H. Occurrence, toxicity, and analysis of major mycotoxins in food. *International Journal of Environmental Research and Public Health*. 2017;14(6). <https://doi.org/10.3390/ijerph14060632>
48. Roohi R, Hashemi SMB, Mousavi Khaneghah A. Kinetics and thermodynamic modelling of the aflatoxins decontamination: A review. *International Journal of Food Science and Technology*. 2020;55(12):3525–3532. <https://doi.org/10.1111/ijfs.14689>
49. Mokhtarian M, Tavakolipour H, Bagheri F, Fernandes Oliveira CA, Corassin CH, Khaneghah AM. Aflatoxin B1 in the Iranian pistachio nut and decontamination methods: A systematic review. *Quality Assurance and Safety of Crops and Foods*. 2020;12(4):15–25. <https://doi.org/10.15586/qas.v12i4.784>
50. de Souza C, Mousavi Khaneghah A, Fernandes Oliveira CA. The occurrence of aflatoxin M₁ in industrial and traditional fermented milk: A systematic review study. *Italian Journal of Food Science*. 2021;33(SP1):12–23. <https://doi.org/10.15586/ijfs.v33iSP1.1982>
51. Barba FJ, Koubaa M, do Prado-Silva L, Orlie V, de Souza Sant’Ana A. Mild processing applied to the inactivation of the main foodborne bacterial pathogens: A review. *Trends in Food Science and Technology*. 2017;66:20–35. <https://doi.org/10.1016/j.tifs.2017.05.011>
52. Koca N, Urgu M, Saatli TE. Ultraviolet light applications in dairy processing. In: Koca N, editor. *Technological approaches for novel applications in dairy processing*. IntechOpen; 2018. <https://doi.org/10.5772/intechopen.74291>
53. Moreno-Vilet L, Hernández-Hernández HM, Villanueva-Rodríguez SJ. Current status of emerging food processing technologies in Latin America: Novel thermal processing. *Innovative Food Science and Emerging Technologies*. 2018;50:196–206. <https://doi.org/10.1016/j.ifset.2018.06.013>
54. Dogan Halkman HB, Yücel PK, Halkman AK. Non-thermal processing. Microwave. In: Batt CA, Tortorello ML, editors. *Encyclopedia of food microbiology. Reference work*. Academic Press; 2014. pp. 962–965. <https://doi.org/10.1016/B978-0-12-384730-0.00400-6>
55. McKeen L. Introduction to food irradiation and medical sterilization. In: McKeen L, editor. *The effect of sterilization on plastics and elastomers*. Elsevier; 2018. pp. 1–40. <https://doi.org/10.1016/B978-0-12-814511-1.00001-9>
56. Singh R, Singh A. Applications of food irradiation technology. *Defence Life Science Journal*. 2020;5(1):54–62. <https://doi.org/10.14429/dlsj.5.14398>
57. Singh R, Singh A. Food irradiation: An established food processing technology for food safety and security. *Defence Life Science Journal*. 2019;4(4):206–213. <https://doi.org/10.14429/dlsj.4.14397>
58. Mostafavi HA, Mirmajlessi SM, Fathollahi H. The potential of food irradiation: benefits and limitations. In: Eissa A, editor. *Trends in vital food and control engineering*. IntechOpen; 2012. pp. 43–68. <https://doi.org/10.5772/34520>

59. Thanushree MP, Sailendri D, Yoha KS, Moses JA, Anandharamakrishnan C. Mycotoxin contamination in food: An exposition on spices. *Trends in Food Science and Technology*. 2019;93:69–80. <https://doi.org/10.1016/j.tifs.2019.08.010>
60. Koopmans M, Duizer E. Foodborne viruses: an emerging problem. *International Journal of Food Microbiology*. 2004;90(1):23–41. [https://doi.org/10.1016/S0168-1605\(03\)00169-7](https://doi.org/10.1016/S0168-1605(03)00169-7)
61. Singh A, Rao SR, Singh R, Chacharkar MP. Identification and dose estimation of irradiated onions by chromosomal studies. *Journal of Food Science and Technology*. 1998;35(1):47–50.
62. Benkeblia N, Varoquaux P, Gouble B, Selselet-Attou G. Respiratory parameters of onion bulbs (*Allium cepa*) during storage. Effects of ionising radiation and temperature. *Journal of the Science of Food and Agriculture*. 2000;80(12):1772–1778. [https://doi.org/10.1002/1097-0010\(20000915\)80:12<1772::AID-JSFA700>3.0.CO;2-5](https://doi.org/10.1002/1097-0010(20000915)80:12<1772::AID-JSFA700>3.0.CO;2-5)
63. Tripathi PC, Sankar V, Mahajan VM, Lawande KE. Response of gamma irradiation on post harvest losses in some onion varieties. *Indian Journal of Horticulture*. 2011;68(4):556–560.
64. Boshra SA, Mikhael AA. Effect of gamma irradiation on pupal stage of *Ephestia calidella* (Guenée). *Journal of Stored Products Research*. 2006;42(4):457–467. <https://doi.org/10.1016/j.jspr.2005.09.002>
65. Azelmat K, Sayah F, Mouhib M, Ghailani N, ElGarrouj D. Effects of gamma irradiation on fourth-instar *Plodia interpunctella* (Hübner) (Lepidoptera: Pyralidae). *Journal of Stored Products Research*. 2005;41(4):423–431. <https://doi.org/10.1016/j.jspr.2004.05.003>
66. Erkmén O, Bozoglu TF. Food preservation by irradiation. In: Erkmén O, Bozoglu TF, editors. *Food microbiology: Principles into practice*. Wiley; 2016. pp. 106–126. <https://doi.org/10.1002/9781119237860.ch32>
67. Prakash A. Particular applications of food irradiation on fresh produce. *Radiation Physics and Chemistry*. 2016;129:50–52. <https://doi.org/10.1016/j.radphyschem.2016.07.017>
68. Zhang K, Deng Y, Fu H, Weng Q. Effects of Co-60 gamma-irradiation and refrigerated storage on the quality of Shatang mandarin. *Food Science and Human Wellness*. 2014;3(1):9–15. <https://doi.org/10.1016/j.fshw.2014.01.002>
69. Wall MM. Phytosanitary irradiation and fresh fruit quality: Cultivar and maturity effects. *Stewart Postharvest Review*. 2015;11(3):1–6. <https://doi.org/10.2212/spr.2015.3.6>
70. Thomas P. Irradiation of fruits and vegetables. In: Molins RA, editor. *Food irradiation: Principles and applications*. New York: John Wiley & Sons; 2001. pp. 213–240.
71. Reyes LF, Cisneros-Zevallos L. Electron-beam ionizing radiation stress effects on mango fruit (*Mangifera indica* L.) antioxidant constituents before and during postharvest storage. *Journal of Agricultural and Food Chemistry*. 2007;55(15):6132–6139. <https://doi.org/10.1021/jf0635661>
72. Moreno M, Castell-Perez ME, Gomes C, Da Silva PF, Moreira RG. Effects of electron beam irradiation on physical, textural, and microstructural properties of “Tommy Atkins” mangoes (*Mangifera indica* L.). *Journal of Food Science*. 2006;71(2):E80–E86. <https://doi.org/10.1111/j.1365-2621.2006.tb08900.x>
73. Vala RB, Vadher KH, Pampaniya NA, Parmar AM, Joshi A, Pushp A. Seafood irradiation – technology and application. *International Journal of Advanced Research*. 2016;4(6):132–136. <https://doi.org/10.21474/IJAR01/625>
74. Timakova RT, Tikhonov SL, Tikhonova NV, Shikhalev SV. Determining the dose of radiation and radurisation effects on the antioxidant activity of fish and the thermophysical characteristics of fish muscle tissue. *Foods*. 2019;8(4). <https://doi.org/10.3390/foods8040130>
75. Mohamed WS, El-Mossalami EI, Nosier SM. Evaluation of sanitary status of imported frozen fish fillets and its improvement by γ radiation. *Journal of Radiation Research and Applied Sciences*. 2009;2:921–931.
76. Omer MK, Álvarez-Ordoñez A, Prieto M, Skjerve E, Asehun T, Alvseike OA. A systematic review of bacterial foodborne outbreaks related to red meat and meat products. *Foodborne Pathogens and Disease*. 2018;15(10):598–611. <https://doi.org/10.1089/fpd.2017.2393>
77. Surveillance for foodborne disease outbreaks United States, 2017: Annual report. Atlanta: U.S. Department of Health and Human Services; 2019.
78. Rebezov M, Chughtai MFJ, Mehmood T, Khaliq A, Tanweer S, Semenova A, et al. Novel techniques for microbiological safety in meat and fish industries. *Applied Sciences*. 2022;12(1). <https://doi.org/10.3390/app12010319>
79. Jayathilakan K, Sultana K, Pandey MC. Radiation processing: An emerging preservation technique for meat and meat products. *Defence Life Science Journal*. 2017;2(2):133–141. <https://doi.org/10.14429/dlsj.2.11368>
80. Odueke OB, Farag KW, Baines RN, Chadd SA. Irradiation applications in dairy products: A review. *Food and Bioprocess Technology*. 2016;9:751–767. <https://doi.org/10.1007/s11947-016-1709-y>
81. Yagoub SO, Awadalla NE, El Zubeir IEM. Incidence of some potential pathogens in raw milk in Khartoum North Sudan and their susceptibility to antimicrobial agents. *Journal of Animal and Veterinary Advances*. 2005;4(3):341–344.

82. de Oliveira GB, Favarin L, Luchese RH, McIntosh D. Psychrotrophic bacteria in milk: How much do we really know? *Brazilian Journal of Microbiology*. 2015;46(2):313–321. <https://doi.org/10.1590/S1517-838246220130963>
83. Lacivita V, Mentana A, Centonze D, Chiaravalle E, Zambrini VA, Conte A, et al. Study of X-Ray irradiation applied to fresh dairy cheese. *LWT*. 2019;103:186–191. <https://doi.org/10.1016/j.lwt.2018.12.073>
84. Nyamakwere F, Esposito G, Dzama K, Gouws P, Rapisarda T, Belvedere G, et al. Application of gamma irradiation treatment on the physicochemical and microbiological quality of an artisanal hard cheese. *Applied Sciences*. 2022;12(6). <https://doi.org/10.3390/app12063142>
85. Mastromatteo M, Conte A, Lucera A, Saccotelli MA, Buonocore GG, Zambrini AV, et al. Packaging solutions to prolong the shelf life of Fiordilatte cheese: Bio-based nanocomposite coating and modified atmosphere packaging. *LWT – Food Science and Technology*. 2015;60(1):230–237. <https://doi.org/10.1016/j.lwt.2014.08.013>
86. Farkas J. Irradiation for better foods. *Trends in Food Science and Technology*. 2006;17(4):148–152. <https://doi.org/10.1016/j.tifs.2005.12.003>
87. Pricaz M, Uta A-C. Gamma radiation for improvements in food industry, environmental quality and healthcare. *Romanian Journal of Biophysics*. 2015;25(2):143–162.
88. Brewer MS. Irradiation effects on meat flavor: A review. *Meat Science*. 2009;81(1):1–14. <https://doi.org/10.1016/j.meatsci.2008.07.011>
89. Miller RB. *Electronic irradiation of foods: An introduction to the technology*. New York: Springer; 2005. 296 p. <https://doi.org/10.1007/0-387-28386-2>
90. Calucci L, Pinzino C, Zandomenoghi M, Capocchi A, Ghiringhelli S, Saviozzi F, et al. Effects of γ -irradiation on the free radical and antioxidant contents in nine aromatic herbs and spices. *Journal of Agricultural and Food Chemistry*. 2003;51(4):927–934. <https://doi.org/10.1021/jf020739n>
91. Black JL, Jaczynski J. Effect of water activity on the inactivation kinetics of *Escherichia coli* O157:H7 by electron beam in ground beef, chicken breast meat, and trout fillets. *International Journal of Food Science and Technology*. 2008;43(4):579–586. <https://doi.org/10.1111/j.1365-2621.2006.01480.x>
92. Mostafavi HA, Fathollahi H, Motamedi F, Mirmajlessi SM. Food irradiation: Applications, public acceptance and global trade. *African Journal of Biotechnology*. 2010;9(20):2826–2833.
93. Dogan A, Siyakus G, Severcan F. FTIR spectroscopic characterization of irradiated hazelnut (*Corylus avellana* L.). *Food Chemistry*. 2007;100(3):1106–1114. <https://doi.org/10.1016/j.foodchem.2005.11.017>

ORCID IDs

Emmanuel Kormla Danyo  <https://orcid.org/0000-0003-2183-308X>

Maria N. Ivantsova  <https://orcid.org/0000-0002-2389-0523>

Irina S. Selezneva  <https://orcid.org/0000-0002-7039-1874>



Chitosan complexes with amino acids and whey peptides: Sensory and antioxidant properties

Tatsiana M. Halavach^{1,*}, Vladimir P. Kurchenko¹, Ekaterina I. Tarun²,
Roman V. Romanovich³, Natalia V. Mushkevich¹, Alexander D. Kazimirov¹,
Aleksii D. Lodygin⁴, Ivan A. Evdokimov⁴

¹ Belarusian State University^{ROR}, Minsk, Republic of Belarus

² Sakharov International Environmental Institute of Belarusian State University^{ROR}, Minsk, Republic of Belarus

³ Center for Hygiene and Epidemiology of the Moskovsky District of Minsk, Minsk, Republic of Belarus

⁴ North-Caucasus Federal University^{ROR}, Stavropol, Russia

* e-mail: halavachtn@gmail.com

Received 27.12.2022; Revised 28.02.2023; Accepted 07.03.2023; Published online 30.05.2023

Abstract:

Chitosan reacts with amino acids and hydrolyzed whey proteins to produce biologically active complexes that can be used in functional foods. The research objective was to obtain chitosan biocomposites with peptides and amino acids with improved antioxidant and sensory properties.

The research featured biocomposites of chitosan and succinylated chitosan with whey peptides and amino acids. The methods of pH metry and spectrophotometry were employed to study the interaction parameters between polysaccharides and peptides, while colorimetry and spectrophotometry served to describe the amino acids content. The antiradical effect was determined by the method of fluorescence recovery. Pure compounds and their complexes underwent a sensory evaluation for bitterness.

Chitosan and succinylated chitosan formed complexes with whey peptides and such proteinogenic amino acids as arginine, valine, leucine, methionine, and tryptophan. The equimolar binding of tryptophan, leucine, and valine occurred in an aqueous chitosan solution (in terms of glucosamine). Methionine appeared to be the least effective in chitosan interaction, while arginine failed to complex both with chitosan and succinylated chitosan. Chitosan and succinylated chitosan biocomposites with peptides and leucine, methionine, and valine proved to be less bitter than the original substances. The samples with arginine maintained the same sensory properties. Chitosan complexes with tryptophan and peptides increased their antioxidant activity by 1.7 and 2.0 times, respectively, while their succinylated chitosan complexes demonstrated a 1.5-fold increase.

Chitosan and succinylated chitosan biocomplexes with tryptophan and whey protein peptides had excellent antioxidant and sensory properties. However, chitosan proved more effective than succinylated chitosan, probably, because it was richer in protonated amino groups, which interacted with negatively charged amino acids groups.

Keywords: Chitosan, succinylated chitosan, whey peptides, proteinogenic amino acids, chitosan biocomposites

Funding: This research was supported by the Ministry of Education of the Republic of Belarus^{ROR} as part of the research in Mechanisms of Amino Acids and Peptides Interaction with Chitosan and Its Derivatives, grant no. 20211584.

Please cite this article in press as: Halavach TM, Kurchenko VP, Tarun EI, Romanovich RV, Mushkevich NV, Kazimirov AD, *et al.* Chitosan complexes with amino acids and whey peptides: Sensory and antioxidant properties. *Foods and Raw Materials.* 2024;12(1):13–21. <https://doi.org/10.21603/2308-4057-2024-1-584>

INTRODUCTION

Milk proteins are a source of biologically active peptides that appear as a result of enzymic processes in the gastrointestinal tract. Milk proteins undergo enzymatic hydrolysis as part of the commercial hypoallergenic foods [1, 2]. Proteolysis forms bioactive functional

peptides [3]. Milk proteins lose their allergenicity because the antigenic determinants split in the structure of allergen proteins [4].

Hydrolyzed cow's milk proteins are short chain peptides and amino acids. Histidine, proline, phenylalanine, tyrosine, and tryptophan give them a characteristic bitter taste, which limits the use of hypoallergenic

hydrolysates in the food industry [5]. Hydrophobic chromatography improves the bitter taste of hydrolysates; other options include specific sorbents, isoelectric focus, and limited proteolysis [6]. Instrumental hydrolysate processing increases production costs and changes the amino acid composition because it removes essential amino acids. Moreover, instrumental processing requires specific enzymes and complex detoxication. Flavoring additives are an alternative solution that can camouflage the bitterness [7]. Still, food science is looking for new ways to reduce the bitterness of protein hydrolysates and amino acid mixes.

Cyclic oligosaccharides, or cyclodextrins, have a cone-like spatial structure with a hydrophobic inner cavity. As a result, they can form inclusion complexes with guest molecules, which are also called clathrates [8]. If bitter peptides and amino acids are encapsulated in cyclodextrins, their taste improves because the cone shields them from taste receptors [9, 10]. In addition, the method improves the biologically active potential of the encapsulated compounds [11, 12].

Aminopolysaccharide chitosan also can improve the sensory properties of bitter amino acids and peptides. Chitosan is a low-toxic substance, popular in the food industry as a filler, thickener, and stabilizer [13]. Food scientists obtain composites with more advantageous properties by complexing natural biopolymers and bioactive substances with chitosan and its derivatives.

Chitosan, a potential complexing agent, is able to interact with organic compounds due to its hydrophobic effect, as well as due to ionic and hydrogen bonds [14]. Although chitosan has good biocompatibility and adsorption, its solubility is rather limited [15]. As a result, chitosan is unpopular in the food industry and pharmacy. At $\text{pH} < 6.5$, its free amino groups are protonated, thus rendering it polycationic properties [16]. Soluble chitosan can be obtained by depolymerization and chemical modification [17]. For instance, Lee *et al.* introduced anionic succinate groups to produce succinylated chitosan [18]. This chitosan derivative was soluble at $\text{pH} > 7.0$ and < 4.5 .

Molecular modeling demonstrated that the complexation occurs as a result of the electrostatic interaction between the amino acid carboxyl group and the chitosan amino group [19]. Chitosan and its derivatives interact with amino acids in three different ways [20–28]:

1. Chitosan produces a gel-like base. This hydrogel acts as films or spheres and immobilizes amino acids inside the base or adsorbs it on its surface. As part of the film, amino acids can also be chemically crosslinked with chitosan molecules [20–23];

2. Molecules of chitosan and amino acid are chemically crosslinked. The resulting biocomposites serve as transport for various molecules [24–26]; and

3. Chitosan and amino acids interact in a solution as compounds bind with NH_2 -groups of chitosan. Different chitosan modifications interact with target molecules, which are normally used in gene therapy, packaging, drug delivery, wastewater treatment, etc. [27, 28].

This research focused on the third type of interaction because of its technical simplicity and low cost. The main goal was to use the biocomposites of chitosan and amino acids as a food component. According to the hypothesis, these high-molecular-weight biocomposites interact with bitter-taste receptors to improve the sensory properties of whey protein hydrolysates. The biocomposite releases its peptides and amino acids in the gastrointestinal tract because of weak electrostatic forces.

Biocomposites of chitosan and its derivatives with peptides and amino acids are promising functional ingredients. Chitosan complexing affects the antioxidant and sensory properties of amino acids and peptides.

The research objective was to obtain biocomposites of chitosan with peptides and amino acids with high antioxidant activity and improved sensory properties.

STUDY OBJECTS AND METHODS

The study involved chitosan with a molecular weight of 100 kDa and a degree of deacetylation of 90%. The succinylated chitosan had a molecular weight of 200 kDa and a degree of substitution of 75.1% (Bioprogress, Russia). The peptide mix had a molecular weight of ≤ 10 kDa. It was part of the Peptigen IF 3080 WPH whey protein hydrolysate with protein mass fraction 80% (Arla Foods Ingredients Group, Denmark). The experiment also featured such amino acids as L-arginine, L-valine, L-leucine, L-methionine, and L-tryptophan (Sigma, USA).

Complexing chitosan with whey protein hydrolysate. We prepared 0.1% aqueous solutions of chitosan and succinylated chitosan and 15% aqueous solution of hydrolysate, which was a mix of whey protein peptides. After that, we added 250 μL of the 15% hydrolysate solution to 50 mL of 0.1% chitosan solution and stirred. The solution was tested for active acidity and optical density at a wavelength of 640 nm. Then, the 0.1% chitosan solution was titrated with the 15% hydrolysate solution in the protein concentration range of 0.08–1.34%. The optical density and active acidity of the samples were evaluated after each hydrolysate cycle. The experiment with the succinylated chitosan followed the same procedure. The active acidity was determined using a HANNA HI 83141 pH-meter (Hanna Instruments, Germany). The optical density was monitored using a Metertech UV/VIS SP 8001 device (Meter-tech, Taiwan).

Obtaining chitosan biocomposites with amino acids. Variant 1 included 0.1% aqueous solutions of chitosan/succinylated chitosan with 0.5% aqueous solutions of arginine, valine, leucine, methionine, and tryptophan. The chitosan solution (0.1%, 20 mL) was titrated with a 0.5% amino acid solution. The amino acids were added by 80 μL until their concentration in the mix reached 0.002–0.05%. After each titration stage, we monitored the optical density and active acidity. The solution of succinylated chitosan (0.1%) was titrated under similar conditions.

Variant 2 involved aqueous solutions of 0.5% chitosan/succinylated chitosan and 0.5% proteinogenic amino acid, namely arginine, valine, leucine, or methionine. The tryptophan experiment included aqueous solutions of 0.1% chitosan/succinylated chitosan and 0.05% the amino acid. The resulting solutions were stirred at 25°C for 1 h. After that, we tested the samples for optical density and active acidity.

The chitosan and succinylated chitosan complexes with tryptophan were subjected to dialysis using a tubular cellulose membrane with a 14-kDa shut-off (Sigma, USA). The removal of unbound tryptophan took 4 h. After that, we measured amino acids in the dialysate and the optical density at a wavelength of 280 nm by using spectrophotometry. We also designed a calibration dependency curve for the optical density and tryptophan (0.0001–0.0016%). The curve made it possible to calculate the amount of tryptophan in the initial biocomposite solutions and dialysate samples.

The colorimetry test involved the Folin-Chocalteu reagent (Sigma, USA). We measured the optical density of the tryptophan complexes with chitosan/succinylated chitosan (variant 2) and the tryptophan calibration samples at a wavelength of 620 nm. We introduced 1000 µL of 0.5 M sodium hydroxide solution into 200 µL of the test sample, stirred, and added 240 µL of the Folin Ciocalteu reagent. The resulting mix was kept in a dark place for 20 min. Subsequently, the dyed samples were tested for optical density. The effect of the tryptophan content (0.0001–0.010%) on the optical density of the calibration samples was expressed as a dependency curve, which made it possible to calculate the amino acid concentration in the biocomposite solutions and the corresponding dialysates.

We introduced 500 µL of the test complexes (variant 2) into test tubes with centrifuge filters with a cut-off at 10 kDa (Merck Millipore, USA) to determine the concentration of free and bound arginine, valine, leucine, or methionine. The filtrates were obtained by centrifugation at 14 000 rpm for 15 min. We used the Kjeldahl method (State Standard 23327-98) to determine the total amount of nitrogen in the filtrate samples.

The statistical processing involved the arithmetic mean value \pm confidence interval ($n = 3$, $\alpha = 0.05$).

Determining the bitterness of pure compounds and chitosan complexes. The sensory evaluation followed a 10-point scale of bitterness: 0 – no bitterness detected; 1–2 – very weak; 3–4 – weak; 5–6 – mild; 7–8 – strong; 9–10 – very strong.

The severity of bitterness was determined using standard solutions of chitosan, amino acids, and peptides (Table 1). The mean value of bitterness was calculated after three repetitions.

Evaluating the antioxidant activity of chitosan biocomposites with tryptophan and hydrolysate. We used the Oxygen Radical Absorbance Capacity Assay (ORAC) to determine the antioxidant activity [29] following the procedure developed by Tarun *et al.*, who measured the antioxidant activity based on the results

of their interaction with hydroxyl radicals [30]. The radicals were generated using the Fenton system.

We determined the fluorescence fluorescein recovery (A, %) as the ratio of the signal intensity of the sample and the control fluorescein (100%). As a result, we obtained dependency curves for fluorescein fluorescence (A, %) and the solids. The curve made it possible to define the concentration of the sample necessary for a 50% suppression of fluorescein fluorescence (IC_{50}). The experiments were conducted in triplicates to obtain the arithmetic mean \pm confidence interval. We used the confidence interval method to calculate the significance of the differences between the samples.

RESULTS AND DISCUSSION

Interaction of chitosan and succinylated chitosan with whey protein hydrolysate. Chitosan and its succinylated derivative interacted with an extensive enzymatic hydrolysate of whey, which gave the resulting mix a bitter taste. The specific sensory properties of the hydrolysate resulted from the intensive breakdown of whey proteins, which released the bitter peptide and amino acid fraction.

Table 1 shows the bitterness of amino acids depending on their concentration in aqueous solutions.

We added a 0.1% solution of chitosan with whey protein hydrolysate in the concentration range of 0.08–1.34%, which increased the active acidity of the medium by 1.9 pH units (Fig. 1a).

Table 1 Bitterness of standard amino acids, hydrolysate, and chitosan

Solution	Bitterness, points	Sensory properties
1% arginine	9	Very strong
0.5% arginine	7	Strong
1% valine	6	Mild
0.5% valine	5	Mild
1% leucine	10	Very strong
0.5% leucine	8	Strong
1% methionine	9	Very strong
0.5% methionine	8	Strong
1% tryptophan	7	Strong
0.5% tryptophan	6	Mild
0.05% tryptophan	2	Very weak
0.01% tryptophan	2	Very weak
5% hydrolysate	8	Strong
1.3% hydrolysate	6	Mild
0.25% hydrolysate	0	Tasteless
1% chitosan	4	Weak*
0.5% chitosan	3	Weak*
0.1% chitosan	2	Very weak*
1% succinylated chitosan	4	Weak*
0.5% succinylated chitosan	2	Very weak*
0.1% succinylated chitosan	0	Tasteless

* – The sample possessed a specific astringent taste of chitosan

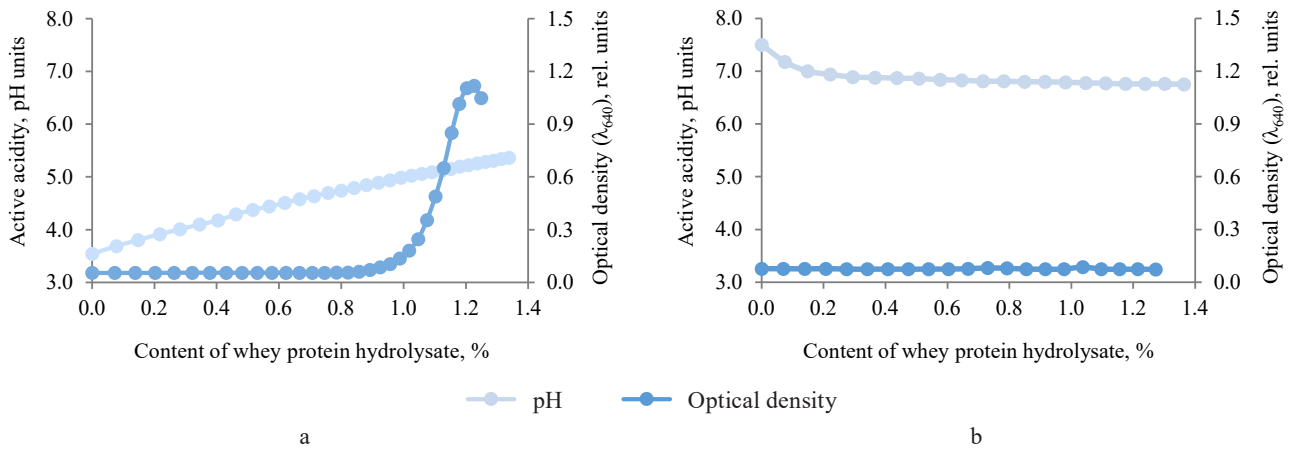


Figure 1 Effect of whey protein hydrolysate on optical density and active acidity of 0.1% solutions of chitosan (a) and succinylated chitosan (b)

When chitosan mixed with whey protein hydrolysate, the resulting protonation raised the active acidity of the medium. The optical density of the system increased by 1.1 relative units while the content of the hydrolysate changed from 1.0 to 1.3%. These consequences occurred because macromolecules of chitosan with those of peptides formed aggregates, which had a neutral total charge. The spectrophotometry test registered an equivalence point at a peptide concentration of 1.3% as the chitosan – hydrolysate protein system titrated.

Figure 1b summarizes the binding of succinylated chitosan and whey protein hydrolysate. When we added 0.08–1.34% hydrolysate to the 0.1% succinylated chitosan solution, the pH of the medium dropped by 0.75 units but the optical density of the system remained the same. According to the pH analysis, 0.25% hydrolysate resulted in an equivalent binding of succinylated chitosan to the peptide fraction.

Therefore, when the succinylated chitosan and whey protein hydrolysate had a lower pH, protons entered the medium. No changes occurred in the optical properties of the succinylated chitosan solution and the peptide fraction. Apparently, the same surface charges prevented a large-scale aggregation of macromolecular composites of succinylated chitosan with peptides.

In general, 1.0 g of chitosan interacted with 13.0 g of hydrolysate, while 1.0 g of succinylated chitosan bound with 2.5 g of hydrolysate. Good ability of chitosan to bind peptides results from its polycationic properties. In succinylated chitosan, anionic succinate groups replace 75.1% of amino groups, which decreases the number of potential interaction sites.

The next stage featured the sensory properties of protein hydrolysate, chitosan, its derivative, and their complexes (Fig. 2). We founded that it was hydrolysate that was responsible for the bitter taste. Chitosan and succinylated chitosan demonstrated a low bitterness and a specific astringency. The bitterness depended on the

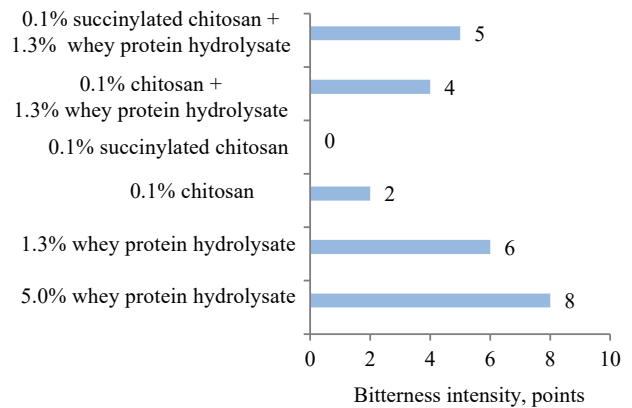


Figure 2 Bitterness of standard pure whey protein hydrolysate, chitosan, succinylated chitosan, and their biocomposites

concentration of the ingredients. The bitterness of hydrolysates in biocomposites dropped by 1–2 points, compared with its pure form.

Complexing chitosan and succinylated chitosan with amino acids. This stage involved the physicochemical parameters of prototypes obtained by mixing 0.1% solutions of chitosan/succinylated chitosan with 0.002–0.05% arginine/valine/leucine/methionine/tryptophan. The experiment revealed no significant changes in the optical density and active acidity of the solutions.

Other studies reported that amino acids could bind with polycationic chitosan as a result of electrostatic interaction [19, 31]. Unlike such macromolecular structures as proteins and peptide fractions, amino acids with their low molecular weight neither formed coagulating complexes with chitosan/succinylated chitosan solutions nor affected the pH of the medium.

To determine the optimal conditions for the interaction of tryptophan with chitosan and succinylated chitosan, we obtained solutions of 0.05% amino acids and 0.1% polysaccharide. The molar ratio of NH_2 -groups and tryptophan was 2:1 based on the content of amino

Table 2 Bound vs. free tryptophan in biocomposites with chitosan/succinylated chitosan

Parameter	Tryptophan concentration, %	
	Spectrophotometry, 280 nm	Colorimetry, 620 nm
Initial tryptophan content in biocomposites *	0.050	0.050
Tryptophan content in chitosan biocomposite (0.1% chitosan – 0.05% tryptophan)	0.0371 ± 0.0034	0.0400 ± 0.0037
Free tryptophan in the mix with chitosan (dialysis results)	0.0040 ± 0.0001	0.0030 ± 0.0003
Bound tryptophan in the mix with chitosan (dialysis results)**	0.0460 ± 0.0001	0.0471 ± 0.0004
Tryptophan content in succinylated chitosan biocomposite (0.1% succinylated chitosan – 0.05% tryptophan)	0.0441 ± 0.0054	0.0452 ± 0.0036
Free tryptophan in the mix with succinylated chitosan (dialysis results)	0.0222 ± 0.0004	0.0272 ± 0.0030
Bound tryptophan in the mix with succinylated chitosan (dialysis results)**	0.0278 ± 0.0004	0.0228 ± 0.0026

* – The amount of tryptophan introduced was as described in the process of obtaining its biocomposites with chitosan/succinylated chitosan

** – The estimated content of tryptophan was determined by subtracting the amount of unbound amino acid from the initial amount of tryptophan introduced into the mix according to the method described

groups in the composition of glucosamine (chitosan monomer). When we used succinylated chitosan, the molar ratio of tryptophan:glucosamine equaled 1:0.25, and that of tryptophan:succinylglucosamine was 1:1.3.

We subjected the experimental samples of chitosan/succinylated chitosan with tryptophan to dialysis to separate the unbound amino acid. Spectrophotometry and colorimetry made it possible to determine the proportion of tryptophan in the biocomposites. We determined the proportion of bound and free tryptophan in the complexes based on the amount of initial and dialyzed tryptophan.

The content of unbound amino acid in the solution did not change after dialysis. To determine the proportion of tryptophan in the complex, we subtracted the amount of dialyzed amino acid from its initial content (0.05%) (Table 2).

Both spectrophotometric and colorimetric methods yielded similar results. The mixes of chitosan/succinylated chitosan with amino acids had a low signal level in the ultraviolet and visible spectra, compared to the control 0.05% tryptophan solution. The resulting effect depended on the binding of the amino acid to the complexing agent and the change in the access to the amino acid radical.

Spectrophotometry and colorimetry also showed that the 0.1% chitosan solution bound 0.046 and 0.047% tryptophan, respectively, which means that 94% of the introduced amino acid entered the complex. The 0.1% succinylated chitosan solution bound 0.0278 and 0.0228% amino acid, respectively, which indicated a complex formation of 56% tryptophan. Thus, tryptophan bound with chitosan 1.7 times as effectively as with succinylated chitosan.

When the molar ratio of tryptophan:glucosamine was 1:0.25, a complete complexation of the amino acid occurred at 0.05% tryptophan and 0.2% succinylated chitosan. The optimal mass ratio of tryptophan:succinylated chitosan was 1:4 (Table 2).

As for the mix of amino acids and chitosan, the initial molar ratio of tryptophan:glucosamine was 1:2. When the solution contained 0.1% chitosan and 0.05%

tryptophan (mass ratio of 2:1), almost all the amino acid entered the complex, probably, as a result of the twofold excess of protonated amino groups. We expected an equimolar binding at a mass ratio of 1:1. The formation of biocomposites of chitosan/succinylated chitosan with tryptophan was confirmed by spectrophotometry and colorimetry.

The optimal mass ratio of tryptophan and chitosan/succinylated chitosan was 1:1 and 1:4, respectively. The binding of succinylated chitosan with tryptophan was quite weak because succinylation blocked amino groups. According to Deka & Bhattacharyya, it is the NH_2 -groups of the polysaccharide that have the most vigorous interaction with amino acids [19].

The experimental biocomposites of chitosan/succinylated chitosan with arginine/valine/leucine/methionine were filtered with a 10-kDa cut-off. The concentration of total nitrogen in the initial biocomposites and the proportion of amino acids in the biocomposites and filtrates were determined by calculation. Tables 3 and 4 illustrate the experimental data on the content of chitosan-bound amino acids.

Based on the preparation procedure and calculations, the biocomposites with arginine, valine, leucine, or methionine included 0.5% chitosan or succinylated chitosan, i.e., 5×10^{-5} mol/L of chitosan and 2.5×10^{-5} mol/L of succinylated derivative (0.0272 and 0.0032 mol/L of glucosamine monomer relative to chitosan and succinylated chitosan). Valine and leucine demonstrated the most effective interaction with chitosan, as evidenced by the equimolar saturation of glucosamine residues (NH_2 -groups) with amino acids (Tables 3 and 4). In case of tryptophan, almost all the introduced amino acid bound with chitosan (Tables 2–4). The complexing properties of succinylated chitosan with amino acids decreased as follows: methionine – tryptophan – leucine – valine.

The amount of the amino acids in the complexes with succinylated chitosan was low because succinylation blocked amino groups (75.1%). Arginine did not bind to polysaccharides (Tables 3 and 4).

In general, the properties of amino acid radicals are responsible for polysaccharide complexing. Thus,

Table 3 Amino acids in chitosan complexes: sensory evaluation

Composition	Amino acid		Amino acid bound with 1.0 g (0.0001 mol) of chitosan		Bitterness of free amino acid as part of complex, points
	%	mol/L	g	mol	
0.5% chitosan + 0.5% arginine	n.d.	n.d.	–	–	Strong (7)/strong (7)
0.5% chitosan + 0.5% valine	0.3276 ± 0.0034	0.0280 ± 0.0004	0.655 ± 0.009	0.0559 ± 0.0008	Mild (5)/weak (4)
0.5% chitosan + 0.5% leucine	0.3846 ± 0.0033	0.0293 ± 0.0004	0.769 ± 0.009	0.0586 ± 0.0008	Strong (8)/mild (5)
0.5% chitosan + 0.5% methionine	0.2437 ± 0.0125	0.0163 ± 0.0011	0.487 ± 0.030	0.0327 ± 0.0022	Strong (8)/mild (5)
0.1% chitosan + 0.05% tryptophan	0.0460 ± 0.0001	0.0023 ± 0.0001	0.460 ± 0.010	0.0225 ± 0.0005	Mild (6)/mild (5)*

* – bitterness of biocomposie 0.5% chitosan + 0.5% tryptophan

n.d. – not detected

Table 4 Amino acids in succinylated chitosan complexes: sensory evaluation

Composition	Amino acid		Amino acid bound with 1.0 g (0.0001 mol) of chitosan		Bitterness of free amino acid as part of complex, points
	%	mol/L	g	mol	
0.5% chitosan + 0.5% arginine	n.d.	n.d.	–	–	Strong (7)/strong (7)
0.5% chitosan + 0.5% valine	0.0192 ± 0.0034	0.0016 ± 0.0003	0.039 ± 0.007	0.0066 ± 0.0012	Mild (5)/weak (3)
0.5% chitosan + 0.5% leucine	0.0512 ± 0.0033	0.0039 ± 0.0003	0.102 ± 0.008	0.0156 ± 0.0013	Strong (8)/weak (4)
0.5% chitosan + 0.5% methionine	0.2687 ± 0.0125	0.0180 ± 0.0011	0.538 ± 0.030	0.0721 ± 0.0044	Strong (8)/mild (6)
0.1% chitosan + 0.05% tryptophan	0.0278 ± 0.0004	0.0014 ± 0.0001	0.278 ± 0.004	0.0272 ± 0.0004	Mild (6)/weak (3)*

* – bitterness for biocomposie 0.5% succinylated chitosan + 0.5% tryptophan

n.d. – not detected

polycationic chitosan binds with protonated amino groups if amino acids are in their anionic form (valine, leucine, methionine, and tryptophan). Arginine, on the contrary, remains in its protonated state in the solution, which prevents it from interacting with chitosan and its derivatives.

The sensory assessment of chitosan with tryptophan for bitterness was based on standard tryptophan samples (Table 1). A 0.5% chitosan solution is usually slightly bitter and astringent, which is also typical of succinylated chitosan (Table 1). Chitosan and succinylated chitosan improve the sensory properties of tryptophan: its bitterness decreases by 1–3 points compared to the pure amino acid sample (Tables 3 and 4). Bitterness was entirely absent when the concentration of polysaccharides and tryptophan was as low as 0.01–0.10%.

The bitterness of complexes of chitosan/succinylated chitosan with valine, leucine, and methionine lost 2–4 points, compared with the pure amino acid samples (Tables 3 and 4). Arginine biocomposites demonstrated no significant change in the level of bitterness. The resulting sensory profiles corresponded with the efficiency of complexation for valine, leucine, methionine, and tryptophan and the inability of arginine to bind with chitosan/succinylated chitosan.

Effect of complexation with chitosan and succinylated chitosan on the antioxidant properties of hydrolysate and tryptophan. This research also featured the antioxidant properties of tryptophan and whey protein hydrolysate in their complexes with chitosan and succinylated chitosan. We studied the an-

tioxidant potential of tryptophan, hydrolysate, chitosan, succinylated chitosan, and their biocomposites by restoring the fluorescein fluorescence at different antioxidant concentrations (0.0005–0.5 mg dry solids/mL). All the compounds were able to restore the fluorescein fluorescence (81–97%). The capacity to inhibit 50% hydroxyl radicals (IC_{50}) served as the main indicator of antioxidant activity.

The antioxidant effect of peptides is known to depend on the reducing effect of amino acid radicals, mainly methionine, cysteine, tyrosine, and tryptophan [32–34]. Natural polysaccharides, including chitin and chitosan, are potential antioxidants [35, 36]. The antioxidant activity index (IC_{50}) took into account the concentration of dry solids and the content of tryptophan (or protein) in the complexes (Table 5).

The restored fluorophore fluorescence reached 95 and 90% when chitosan and succinylated chitosan were introduced into the experimental system, respectively. Thus, the antioxidant activity index IC_{50} for chitosan reached 0.0352 mg of dry solids/mL and 0.0892 mg of dry solids/mL for succinylated chitosan. The chitosan samples had a better antioxidant profile probably because their amino groups were blocked by succinylation.

The peptide fraction had a relatively high antioxidant effect: its IC_{50} was as high as 0.0260 mg dry solids/mL and 0.0208 mg protein/mL.

Tryptophan had a much higher antioxidant effect than peptides: it increased by 2.2 and 1.8 times, respectively, in terms of nitrogen and solids.

Table 5 Antioxidant properties of tryptophan, whey protein hydrolysate, chitosan, succinylated chitosan, and biocomposites

Sample	IC ₅₀ , mg dry solids/mL	IC ₅₀ , mg hydrolysate (or tryptophan)/mL
Peptide fraction (whey protein hydrolysate)	0.0260 ± 0.0001	0.0208 ± 0.0001
Tryptophan	0.0119 ± 0.0001	0.0117 ± 0.0001
Chitosan	0.0352 ± 0.0003	0
Succinylated chitosan	0.0892 ± 0.0003	0
0.1% chitosan + 1.3% whey protein hydrolysate	0.0140 ± 0.0001	0.0104 ± 0.0001
0.1% succinylated chitosan + 0.25% whey protein hydrolysate	0.0244 ± 0.0010	0.0139 ± 0.0006
0.5% chitosan + 0.5% tryptophan	0.0139 ± 0.0001	0.0068 ± 0.0001
0.5% succinylated chitosan + 0.5% tryptophan	0.0157 ± 0.0001	0.0077 ± 0.0001

The antioxidant effect of the peptide fraction increased by 2.0 and 1.5 times as a result of interaction with chitosan and succinylated chitosan, respectively. The antioxidant activity of tryptophan increased by 1.7 times after binding with chitosan and by 1.5 times after binding with succinylated chitosan. The chitosan biocomposites of hydrolysate and tryptophan demonstrated a better antioxidant effect. The interaction of peptides and amino acids with succinylated chitosan proved less efficient. Probably, peptides and tryptophan had a better solubility during their biocomposing with chitosan and its derivative, which explains the antioxidant effect.

CONCLUSION

These experiments featured biocomposites of chitosan and succinylated chitosan with whey protein hydrolysate. The spectrophotometry and pH-metric analysis revealed that 1.0 g of chitosan interacted with 13.0 g of hydrolysate and 2.5 g of succinylated chitosan. The complexation of chitosan with whey peptides proved effective. The complexes had better sensory profiles than the original substances. Their bitterness score lost 1–2 points relative to the pure hydrolysate samples.

We also described the complexes of chitosan and succinylated chitosan with such amino acids as arginine, valine, leucine, methionine, and tryptophan. Valine, leucine, and tryptophan interacted with glucosamine residues in chitosan in an equimolar ratio. Succinylated chitosan had a low complexing potential because it contained few free amino groups, which were affected by succinic acid residues introduced into the structure. Arginine demonstrated no complexing with the polysaccharides. Valine, leucine, methionine, and tryptophan were anionic, which allowed them to bind with polycationic chitosan, whereas arginine was cationic. The sensory evaluation

revealed that the complexes of chitosan/succinylated chitosan with valine, leucine, methionine, and tryptophan had a lower bitterness (minus 1–4 points). The biocomplexes of chitosan/succinylated chitosan with arginine demonstrated no changes in bitterness.

Tryptophan and peptides of whey proteins demonstrated a good antioxidant potential. The antioxidant activity index IC₅₀ was 0.0117 mg tryptophan/mL for the amino acid and 0.0208 mg protein/mL for peptides. The experiments confirmed the antioxidant effect of chitosan (0.0352 mg chitosan/mL) and succinylated chitosan (0.0892 mg chitosan/mL). The antioxidant effect of tryptophan and peptides increased by 1.7 and 2.0 times, respectively, in the chitosan biocomposites and by 1.5 times in the succinylated chitosan biocomposites. Peptides and tryptophan were more effective in their binding with chitosan because they interacted with the amino groups of the polysaccharide, which improved their antioxidant properties.

The biocomposites of chitosan with whey peptides and amino acids had a high antioxidant activity and an improved sensory profile. As a result, they can be used in hypoallergenic functional foods.

CONTRIBUTION

T.N. Halavach supervised the project, designed the research, collected and interpreted the data, and wrote the manuscript. V.P. Kurchenko, A.D. Lodygin, and I.A. Evdokimov created the research concept and proofread the manuscript. E.I. Tarun, R.V. Romanovich, N.V. Mushkevich, and A.D. Kazimirov were responsible for the experimental part of the study and the methodology.

CONFLICT OF INTEREST

The authors declared no conflict of interest regarding the publication of this article.

REFERENCES

- Shivanna SK, Nataraj BH. Revisiting therapeutic and toxicological fingerprints of milk-derived bioactive peptides: An overview. *Food Bioscience*. 2020;38. <https://doi.org/10.1016/j.fbio.2020.100771>
- Zhao C, Ashaolu TJ. Bioactivity and safety of whey peptides. *LWT*. 2020;134. <https://doi.org/10.1016/j.lwt.2020.109935>
- Ye H, Tao X, Zhang W, Chen Y, Yu Q, Xie J. Food-derived bioactive peptides: production, biological activities, opportunities and challenges. *Journal of Future Foods*. 2022;2(4):294–306. <https://doi.org/10.1016/j.jfutfo.2022.08.002>

4. Nutten S, Schuh S, Dutter T, Heine RG, Kuslys M. Design, quality, safety and efficacy of extensively hydrolyzed formula for management of cow's milk protein allergy: What are the challenges? *Advances in Food and Nutrition Research*. 2020;93:147–204. <https://doi.org/10.1016/bs.afnr.2020.04.004>
5. Liceaga AM, Hall F. Nutritional, functional and bioactive protein hydrolysates. In: Melton L, Shahidi F, Varelis P, editors. *Encyclopedia of food chemistry*. Reference work. Vol. 3. Elsevier; 2019. pp. 456–464. <https://doi.org/10.1016/B978-0-08-100596-5.21776-9>
6. Iwaniak A, Minkiewicz P, Darewicz M, Hryniewicz M. Food protein-originating peptides as tastants – Physiological, technological, sensory, and bioinformatic approaches. *Food Research International*. 2016;89:27–38. <https://doi.org/10.1016/j.foodres.2016.08.010>
7. Murray NM, Jacquie JC, O'Sullivan M, Hallihan A, Murphy E, Feeney EL, et al. Using rejection thresholds to determine acceptability of novel bioactive compounds added to milk-based beverages. *Food Quality and Preference*. 2019;73:276–283. <https://doi.org/10.1016/j.foodqual.2018.10.014>
8. Gonzalez Pereira A, Carpena M, Garcia Oliveira P, Mejuto JC, Prieto MA, Simal Gandara J. Main applications of cyclodextrins in the food industry as the compounds of choice to form host–guest complexes. *International Journal of Molecular Sciences*. 2021;22(3). <https://doi.org/10.3390/ijms22031339>
9. Rudolph S, Riedel E, Henle T. Studies on the interaction of the aromatic amino acids tryptophan, tyrosine and phenylalanine as well as tryptophan-containing dipeptides with cyclodextrins. *European Food Research and Technology*. 2018;244(9):1511–1519. <https://doi.org/10.1007/s00217-018-3065-9>
10. Li J, Geng S, Liu B, Wang H, Liang G. Self-assembled mechanism of hydrophobic amino acids and β -cyclodextrin based on experimental and computational methods. *Food Research International*. 2018;112:136–142. <https://doi.org/10.1016/j.foodres.2018.06.017>
11. Halavach TM, Savchuk ES, Bobovich AS, Dudchik NV, Tsygankow VG, Tarun EI, et al. Antimutagenic and antibacterial activity of β -cyclodextrin clathrates with extensive hydrolysates of colostrum and whey. *Biointerface Research in Applied Chemistry*. 2021;11(2):8626–8638. <https://doi.org/10.33263/BRIAC112.86268638>
12. Halavach TM, Kurchenko VP, Tsygankow VG, Bondaruk AM, Tarun EI, Asafov VA. β -Cyclodextrin nanocomplexes with biologically active peptides from hydrolysed bovine whey and colostrum. *Biointerface Research in Applied Chemistry*. 2022;12(6):8502–8514. <https://doi.org/10.33263/BRIAC126.85028514>
13. Irastorza A, Zarandona I, Andonegi M, Guerrero P, de la Caba K. The versatility of collagen and chitosan: From food to biomedical applications. *Food Hydrocolloids*. 2021;116. <https://doi.org/10.1016/j.foodhyd.2021.106633>
14. Silva AO, Cunha RS, Hotza D, Francisco Machado RA. Chitosan as a matrix of nanocomposites: A review on nanostructures, processes, properties, and applications. *Carbohydrate Polymers*. 2021;272. <https://doi.org/10.1016/j.carbpol.2021.118472>
15. Ahmad SI, Ahmad R, Khan MS, Kant R, Shahid S, Gautam L, et al. Chitin and its derivatives: Structural properties and biomedical applications. *International Journal of Biological Macromolecules*. 2020;164:526–539. <https://doi.org/10.1016/j.ijbiomac.2020.07.098>
16. Wani TU, Pandith AH, Sheikh FA. Polyelectrolytic nature of chitosan: Influence on physicochemical properties and synthesis of nanoparticles. *Journal of Drug Delivery Science and Technology*. 2021;65. <https://doi.org/10.1016/j.jddst.2021.102730>
17. Benchamas G, Huang G, Huang S, Huang H. Preparation and biological activities of chitosan oligosaccharides. *Trends in Food Science and Technology*. 2021;107:38–44. <https://doi.org/10.1016/j.tifs.2020.11.027>
18. Lee JS, Nah H, Moon H-J, Lee SJ, Heo DN, Kwon IK. Controllable delivery system: A temperature and pH-responsive injectable hydrogel from succinylated chitosan. *Applied Surface Science*. 2020;528. <https://doi.org/10.1016/j.apsusc.2020.146812>
19. Deka BC, Bhattacharyya PK. DFT study on host-guest interaction in chitosan–amino acid complexes. *Computational and Theoretical Chemistry*. 2017;1110:40–49. <https://doi.org/10.1016/j.comptc.2017.03.036>
20. Medeiros Borsagli FGL, Carvalho IC, Mansur HS. Amino acid-grafted and *N*-acylated chitosan thiomers: Construction of 3D bio-scaffolds for potential cartilage repair applications. *International Journal of Biological Macromolecules*. 2018;114:270–282. <https://doi.org/10.1016/j.ijbiomac.2018.03.133>
21. Wang S, Shi L, Zhang S, Wang H, Cheng B, Zhuang X, et al. Proton-conducting amino acid-modified chitosan nanofibers for nanocomposite proton exchange membranes. *European Polymer Journal*. 2019;119:327–334. <https://doi.org/10.1016/j.eurpolymj.2019.07.041>
22. Rafiee F, Rezaie Karder F. Bio-crosslinking of chitosan with oxidized starch, its functionalization with amino acid and magnetization: As a green magnetic support for silver immobilization and its catalytic activity investigation. *International Journal of Biological Macromolecules*. 2020;146:1124–1132. <https://doi.org/10.1016/j.ijbiomac.2019.09.238>

23. Taketa TB, Mahl CRA, Calais GB, Beppu MM. Amino acid-functionalized chitosan beads for *in vitro* copper ions uptake in the presence of histidine. *International Journal of Biological Macromolecules*. 2021;188:421–431. <https://doi.org/10.1016/j.ijbiomac.2021.08.017>
24. Fernandes J, Ghate MV, Basu Mallik S, Lewis SA. Amino acid conjugated chitosan nanoparticles for the brain targeting of a model dipeptidyl peptidase-4 inhibitor. *International Journal of Pharmaceutics*. 2018;547(1–2):563–571. <https://doi.org/10.1016/j.ijpharm.2018.06.031>
25. Hefni HHH, Nagy M, Azab MM, Hussein MHM. O-Acylation of chitosan by L-arginine to remove the heavy metals and total organic carbon (TOC) from. *Egyptian Journal of Petroleum*. 2020;29(1):31–38. <https://doi.org/10.1016/j.ejpe.2019.10.001>
26. Wang Y, Han Q, Wang Y, Qin D, Luo Q, Zhang H. Self-assembly, rheological properties and antioxidant activities of chitosan grafted with tryptophan and phenylalanine. *Colloids and Surfaces A: Physicochemical and Engineering Aspects*. 2020;597. <https://doi.org/10.1016/j.colsurfa.2020.124763>
27. Pereira MBB, França DB, Araújo RC, Silva-Filho EC, Rigaud B, Fonseca MG, et al. Amino hydroxyapatite/chitosan hybrids reticulated with glutaraldehyde at different pH values and their use for diclofenac removal. *Carbohydrate Polymers*. 2020;236. <https://doi.org/10.1016/j.carbpol.2020.116036>
28. Torkaman S, Rahmani H, Ashori A, Najafi SHM. Modification of chitosan using amino acids for wound healing purposes: A review. *Carbohydrate Polymers*. 2021;258. <https://doi.org/10.1016/j.carbpol.2021.117675>
29. Zhong Y, Shahidi F. Methods for the assessment of antioxidant activity in foods. In: Shahidi F, editor. *Handbook of antioxidants for food preservation. A volume in Woodhead Publishing Series in Food Science, Technology and Nutrition*. Woodhead Publishing; 2015. pp. 287–333. <https://doi.org/10.1016/b978-1-78242-089-7.00012-9>
30. Tarun EI, Zaitseva MV, Kravtsova OI, Kurchenko VP, Golovach TN. Effect of whey protein peptides on recovery of fluorescence level in system with activated form of oxygen. *Proceedings of the Belarusian State University. Series of Physiological, Biochemical and Molecular Biology Sciences*. 2016;11(1):231–236. (In Russ.). <https://www.elibrary.ru/YMGPFB>
31. Hu Z, Qin YQ, Guang J, Cai Y. Preparation and characterization of chitosan amino acid salts. *IOP Conference Series: Materials Science and Engineering*. 2019;504. <https://doi.org/10.1088/1757-899X/504/1/012023>
32. Daroit DJ, Brandelli A. *In vivo* bioactivities of food protein-derived peptides – a current review. *Current Opinion in Food Science*. 2021;39:120–129. <https://doi.org/10.1016/j.cofs.2021.01.002>
33. Bielecka M, Cichosz G, Czczot H. Antioxidant, antimicrobial and anticarcinogenic activities of bovine milk proteins and their hydrolysates – A review. *International Dairy Journal*. 2022;127. <https://doi.org/10.1016/j.idairyj.2021.105208>
34. Galland F, de Espindola JS, Lopes DS, Taccola MF, Pacheco MTB. Food-derived bioactive peptides: Mechanisms of action underlying inflammation and oxidative stress in the central nervous system. *Food Chemistry Advances*. 2022;1. <https://doi.org/10.1016/j.focha.2022.100087>
35. Anraku M, Gebicki JM, Iohara D, Tomida H, Uekama K, Maruyama T, et al. Antioxidant activities of chitosans and its derivatives in *in vitro* and *in vivo* studies. *Carbohydrate Polymers*. 2018;199:141–149. <https://doi.org/10.1016/j.carbpol.2018.07.016>
36. Abd El-Hack ME, El-Saadony MT, Shafi ME, Zaberemawi NM, Arif M, Batiha GE, et al. Antimicrobial and antioxidant properties of chitosan and its derivatives and their applications: A review. *International Journal of Biological Macromolecules*. 2020;164:2726–2744. <https://doi.org/10.1016/j.ijbiomac.2020.08.153>

ORCID IDs

Tatsiana M. Halavach <https://orcid.org/0000-0002-2096-8030>
Vladimir P. Kurchenko <https://orcid.org/0000-0002-4859-2389>
Ekaterina I. Tarun <https://orcid.org/0000-0001-5711-6037>
Roman V. Romanovich <https://orcid.org/0000-0002-0465-8999>
Natalia V. Mushkevich <https://orcid.org/0000-0001-9020-2113>
Alexander D. Kazimirov <https://orcid.org/0000-0002-0987-3006>
Aleksei D. Lodygin <https://orcid.org/0000-0001-8460-2954>
Ivan A. Evdokimov <https://orcid.org/0000-0002-5396-1548>



Nanoemulsion-based active packaging for food products

Jaishankar Prasad¹, Aishwarya Dixit², Sujata P. Sharma^{1,*}, Anjelina W. Mwakosya³,
Anka T. Petkoska⁴, Ashutosh Upadhyay², Nishant Kumar^{2,**}

¹ Sharda University^{ROR}, Greater Noida, India

² National Institute of Food Technology Entrepreneurship and Management^{ROR}, Sonapat, India

³ University of Dar es Salaam^{ROR}, Dar es Salaam, Tanzania

⁴ St. Clement of Ohrid University of Bitola^{ROR}, Bitola, North Macedonia

* e-mail: sujata.sharma@sharda.ac.in

** e-mail: nishantniftem@gmail.com

Received 17.01.2023; Revised 08.02.2023; Accepted 07.03.2023; Published online 30.05.2023

Abstract:

Recently, there has been an increasing trend in the food and pharmaceutical industries towards using nanotechnological approaches to drug delivery and active packaging (edible coatings and films). In the food sector, nanoemulsions are the most promising technology for delivering active components and improving the barrier, mechanical, and biological properties of packaging to ensure the safety and quality of food products, as well as extend their shelf life.

For this review, we used several databases (Google Scholar, Science Direct, PubMed, Web of Science, Scopus, Research Gate, etc.) to collect information about nanoemulsions and their role in edible packaging.

We searched for articles published between 2015 and 2022 and described different scientific approaches to developing active packaging systems based on nanoemulsions, as well as their high-energy and low-energy synthesis methods. We also reviewed the uses of different types of essential oil-based nanoemulsions in the packaging of food products to prolong their shelf life and ensure safety. Non-migratory active packaging and active-release packaging systems were also discussed, as well as their advantages and disadvantages.

Keywords: Nanoemulsions, active packaging, essential oils, synthesis methods, shelf life, edible films

Please cite this article in press as: Prasad J, Dixit A, Sharma SP, Mwakosya AW, Petkoska AT, Upadhyay A, *et al.* Nanoemulsion-based active packaging for food products. *Foods and Raw Materials*. 2024;12(1):22–36. <https://doi.org/10.21603/2308-4057-2024-1-585>

INTRODUCTION

In recent years, there has been an increased interest in nanotechnological approaches and their applications in different areas, such as pharmaceuticals, medicine, cosmetics, rheology, polymer synthesis, drug delivery, and food industry. This interest is down to unique physical, chemical, and biological properties of nano-sized particles (with at least one dimension of 1–100 nm) and a large surface-to-volume ratio [1–11]. In the food sector, nanotechnology applications are divided into three key categories: 1) nano-structured foods, which contain nano-encapsulated or tailored nano-sized food additives or components; 2) smart food packaging, which uses nano-composite materials; and 3) materials and devices based on nanotechnologies, such as those used in nano-

filtration techniques for water treatment and nanosensors for the detection of food contaminants and food safety [12, 13].

The use of nanotechnology in food applications has received significant interest, and nanoemulsions are one of the most promising techniques for encapsulating and transporting functional components [8, 12, 14]. More particularly, nanoemulsions have diverse uses in the food and pharmaceutical industries in delivering active ingredients such as drugs, micronutrients, bioactive compounds, anti-microbial agents, antioxidants, preservatives, coloring and flavoring compounds, etc. [6, 15–17].

According to the Compound Annual Growth Rate's report (2022), the nanotechnology market is predicted to grow to USD 33.63 billion from 2021 to 2030, with applications in electronics, energy, chemicals, healthy food, and other sectors around the world [18]. In addi-

tion, the food industry demands novel technologies to improve shelf life of food and quality to gain higher consumer acceptability. Ameta *et al.* reported that the application of nanotechnology would mark a significant transformation in the food sectors, including production, processing, packaging, transportation, and consumption [19]. For example, according to previous studies, more than 40 000 scientists and 400 industries are using nanotechnology for developing food packaging [20, 21].

In the food sector, nanoemulsions have a variety of applications. In particular, they can mask unpleasant tastes or smells of bioactive compounds and protect bioactive compounds from evaporation, undesirable chemical interactions with other ingredients, or migration in food products. Nanoemulsions are also used to control drug delivery, extend the stability of bioactive compounds during processing and storage, and enhance the bioavailability of specific food components [22–26]. Most bioactive compounds, such as specific vitamins, antioxidants, and antimicrobial agents, are susceptible to chemical degradation, e.g., through oxidative reactions during food processing. Others are volatile and sensitive to food processing conditions, while certain bioactive compounds have low bioavailability. Due to their poor water solubility and high degradability under external conditions (pH, temperature, or light), these sensitive compounds are difficult to incorporate into food matrices. Therefore, nanoemulsions are used to effectively encapsulate, protect, and release bioactive compounds [27]. In addition, they lower concentrations of each ingredient added to the food systems, thus reducing changes in the food matrix's sensory qualities [22, 28].

Several types of nanomaterials and nano-scaled components are used to develop food packaging and improve the shelf life of fruits, vegetables, and other food products. They enhance the product's sensory characteristics and retard microbial growth and oxidation at all stages of production, from processing to packaging, transportation, storage, safety, and quality control [25, 29].

Numerous nanostructured materials, including nanoparticles, nanocomposites, and nanoemulsions, are used in food packaging to extend shelf life [8]. These materials deliver antioxidant, anti-browning, and antimicrobial agents into food packaging systems to protect food products [30–33]. For example, Suvorov *et al.* described packaging materials coated in a nanofilm with bactericidal and fungicidal characteristics based on silver nanoparticles [34].

In this study, we aimed to collect information about the roles of nanoemulsions in food packaging for food preservation and shelf life extension. We reviewed their properties, types, synthesis methods (high energy, low energy, thermal, isothermal), and their advantages in food packaging. We also described the process of nanoemulsion preparation and different types of nanoemulsion-based food packaging, such as non-migratory active packaging and active release packaging.

STUDY OBJECTS AND METHODS

For this review, we used reputable search engines such as Google Scholar, Science Direct, PubMed, Web of Science, Scopus, and Research Gate. The search was performed using keywords “nanoemulsion”, “active packaging”, “shelf life”, “essential oil”, “nanomaterials”, “synthesis”, “food packaging”, and others. The time frame was 1997 to 2023, with a focus on recent literature (2015–2022). Types of publications included review articles, research papers, book chapters, and official reports collected from reputed journals, books, conference proceedings, and official websites.

RESULTS AND DISCUSSION

Nanoemulsions. Nanoemulsions are nano-sized emulsions synthesized to enhance the delivery of active ingredients to food, also known as ultrafine emulsions, submicron emulsions, and mini-emulsions [35]. These are colloidal dispersions made up of oils, surfactants, and aqueous phases. They are isotropic, thermodynamically stable systems in which an emulsifying agent, such as a surfactant or a co-surfactant, combines two incompatible liquids into a single phase. Compared to thermodynamically stable microemulsions, nanoemulsions are unaffected by changes in pH or other physical or chemical factors [25, 36]. Nanoemulsions are more stable to droplet aggregation and gravitational separation than conventional emulsions, which can increase the shelf life of foods and beverages and mask the unpleasant smell of the ingredients [37]. Nanoemulsions typically have droplet sizes between 20 and 600 nm, and their transparency is due to their small size. In general, the size and shape of the particles dispersed in the continuous phase is the key difference between emulsions and nanoemulsions [25, 38–40]. As a result, nanoemulsions enhance drug delivery, improve the solubilization of poorly soluble drugs, and boost the therapeutic moiety's bioavailability. In order to synthesize a microemulsion, a variety of non-ionic surfactants and fatty acids are frequently utilized, and they have been approved as GRAS (generally recognized as safe) [41].

Nanoemulsions are classified into three categories, namely: 1) water-in-oil (W/O), where water is dispersed in the continuous oil phase; 2) oil-in-water (O/W), where oil is dispersed in the continuous aqueous phase; and 3) bi-continuous, where micro domains of water and oil are inter-dispersed within the system [42]. Based on the amount of energy required, there are high-energy and low-energy emulsification methods to obtain nanoemulsions. Ultrasonication and high-pressure homogenization utilizing either microfluidizers or high-pressure homogenizers are examples of high-energy emulsification techniques. Low-energy emulsification techniques include the phase inversion temperature method, the solvent displacement method, and the phase inversion composition method [43–45]. These techniques have gained more interest since they are delicate and non-destructive, and they do not affect encapsulated molecules.

Figure 1 graphically summarizes the process of nanoemulsion synthesis. In the food sector, nanoemulsions are used to deliver nutraceuticals, antimicrobials, drugs, proteins, vitamins, as well as coloring and flavoring ingredients into food products. In addition, nanoemulsion formulations of active components are used for developing biodegradable coatings and packaging films to improve the quality, functional properties, nutritional value, and shelf life of foods [17, 36, 46]. Biodegradable edible films are being developed as an alternative to traditional packaging [47]. They can decompose into substances that are neutral to the environment under the right conditions [48]. Biodegradable packaging materials seem promising due to their safety and capacity to increase the product’s shelf life [49].

Properties and advantages of nanoemulsions. Food-grade nanoemulsions can be used in the food packaging systems to improve their morphological, structural, and biological properties by encapsulating active agents, i.e., essential oils, plant extracts, phenolic compounds, antimicrobials, antioxidants, anti-browning agents, preservatives, flavors, coloring agents, nutraceuticals, etc. [27, 50, 51]. Furthermore, nanoemulsions incorporated into packaging may retard microbial growth, reduce color browning, and minimize lipid peroxidation, respiration rate, and water loss. This results in prolonged shelf life of food products such as fruits and vegetables [39, 52–54]. Active agents contained in nanoemulsions are incorporated in films and coatings for food packaging applications. These films and coatings comprised of biopolymer matrixes constitute the continuous phase because they are responsible for the

monodispersity and stability of nanoemulsion droplets. The droplet coalescence is inversely proportional to the viscosity of the continuous phase, as the former decreases when the latter increases [22]. In comparison to other materials, biopolymer materials offer a more beneficial feature as a thermal packaging medium [55]. For example, nanoemulsions containing thyme, lemongrass, and sage essential oils were incorporated in a film comprised of sodium alginate [56]. A nanoemulsion containing antimicrobial self-microemulsifying thyme essential oil was used to develop a biopolymer film based on calcium alginate [57]. A chitosan-based film developed by incorporating a nanoemulsion with thyme oil was used as a food packaging material. This film improved packaging properties, retarded the growth of food-borne pathogens, and increased the shelf life of food [58]. Cinnamon and clove essential oils were used to increase the antioxidant and antifungal activities, as well as oxidative stability of nanocapsules containing *Citrus reticulata* essential oil [59]. An active nanocomposite packaging film was developed by nano-encapsulating the *Cinnamodendron dinisii* Schwanke essential oil, utilizing zein as a wall material and a chitosan matrix [60]. A gelatin-chitosanbased film was developed by incorporating nanoemulsions loaded with active agents: 1) canola oil; 2) α -tocopherol/cinnamaldehyde; 3) α -tocopherol/garlic oil; or 4) α -tocopherol/cinnamaldehyde and garlic oil [61].

Synthesis of nanoemulsions. Since nanoemulsions are thermodynamically unstable systems, energy is required to develop them. Depending on the amount of energy required, nanoemulsions can be developed by

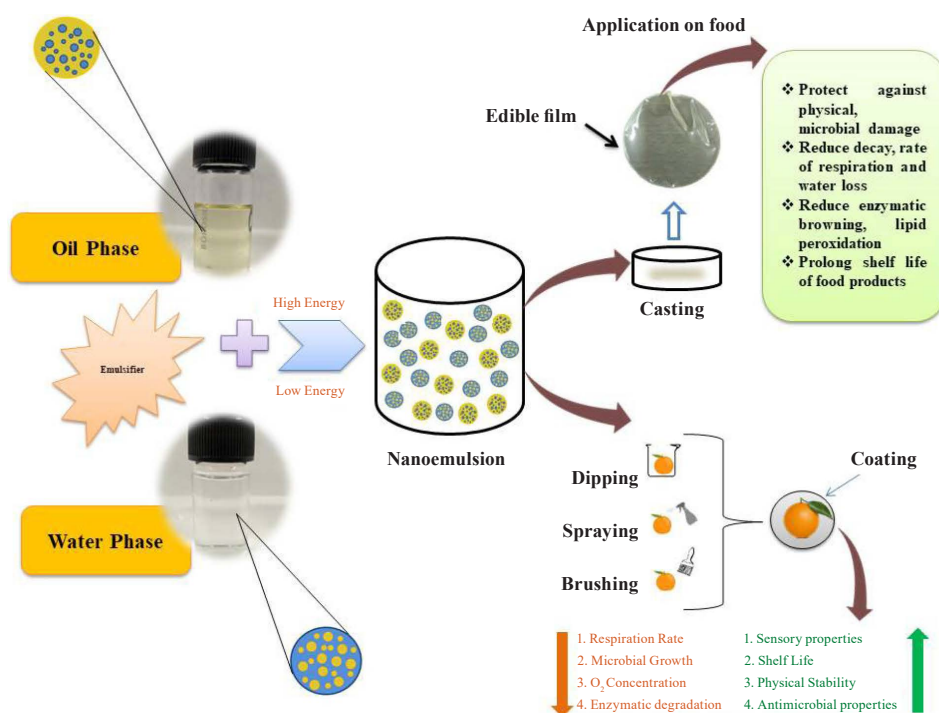


Figure 1 Preparation of nanoemulsions for food packaging applications

high-energy or low-energy emulsification methods, as well as by some of the current techniques such as the bubble-bursting method [43, 62–64]. High-energy emulsification methods include ultrasonication and high-pressure homogenization, while low-energy emulsification methods include phase inversion temperature, solvent displacement, and phase inversion composition [35, 44, 65–66].

High-energy emulsification methods. High mechanical energy is used to generate strong disruptive forces that split up large droplets into nano-sized droplets and create nanoemulsions with high kinetic energy. High-

energy methods rely on mechanical equipment to produce disruptive forces that generate high energies resulting in small oil droplets. They include high-shear stirring, ultrasonic emulsification, high-pressure homogenization, and, in particular, microfluidics and membrane emulsification [66–68]. The interior phase droplet size frequently exceeds the nanometer range when nanoemulsions are made using these methods. This is because dispersion requires a lot of energy, and there is an insufficient surfactant to completely adsorb all the droplets created during dispersion on the interface. Coalescence, which increases the average

Table 1 Applications and functions of nanoemulsion-based packaging

Type of packaging (carrier)	Essential oil (EO)	Composition	Emulsifier	Method of film formation	Key findings	Application	References
Film	Cinnamon and rutin	Chitosan/Gelatin polymer matrix	Tween 80	Solution casting method	Excellent antimicrobial and antioxidant activity and improved thermal and UV-blocking properties	Active food packaging	[99]
Coating	Oregano EO and Resveratrol EO	Pectin Biopolymer	Tween 80	Homogenization	Prolonged shelf-life and retarded physiochemical changes. Improved preservative function and stability of coating	Pork loin	[100]
Film	Thymus Daenensis EO	Hydroxypropylmethyl cellulose	Tween 80 and Lecithin	Sonication	Enhanced antimicrobial activity	–	[101]
Coating	Cardamom	Carboxymethyl cellulose	Tween 80	Ultrasonication	Enhanced antibacterial and antibiofilm activity against <i>Escherichia coli</i> and <i>Listeria monocytogens</i> . Increased the quality and shelf-life	Tomato	[102]
Film	Thyme oil	Calcium alginate and propylene glycol	Tween 80	Sonication	Excellent antimicrobial activity. Increased water-vapor permeability, opacity, and thickness	Ground beef	[57]
Film	Tea-Tree oil + TiO ₂ nanoparticles	Sodium alginate	–	–	Enhanced the retention property. Improved the barrier and UV blocking properties of the film. Improved the quality and reduced Anthracnose in stored banana	Banana	[84]

Type of packaging (carrier)	Essential oil (EO)	Composition	Emulsifier	Method of film formation	Key findings	Application	References
Coating	Ginger EO	Sodium casinate	Tween 80	Ultrasonication	Increased the shelf-life of chicken breast. Strong anti-microbial activity	Chicken breast	[86]
Film	Ginger EO + Montmorillonite (MMT)	Gelatin	Tween 20, Span 80 and Canola oil	Microfluidization	Improved antioxidant activity. Improved mechanical properties.	–	[103]
Film	Curcumin	Banana starch and glycerol	Tween 80	Emulsion phase inversion	Reduced the film's water vapor permeability and increased elongation at break	Aqueous and non-aqueous food stimulates	[104]
Film	Copaiba oil	Pectin	Tween 80	Ultrasonication	Reduced tensile strength, increased elongation at break and anti-microbial activity against <i>Staphylococcus aureus</i> and <i>E. coli</i>	–	[96]
Packaging (O ₂ absorber)	Cumin EO + Sunflower oil nanoemulsion	Oxygen absorber	–	Homogenization	Delayed the growth of <i>Mesophilic</i> and <i>Psychrotrophic</i> bacteria and enhanced shelf-life.	Lamb loin	[90]

droplet size, takes place in this case [35]. Particle size, stability, rheology, and color of the emulsion can be controlled more precisely using these methods with a variety of formulation components. High-energy nanoemulsion formulation techniques for food ingredients have the benefit of lowering the risk of spoilage and inactivation of food components without affecting food safety, nutritional value, or sensory attributes [67]. High-energy methods can be used to create nanoemulsions from any type of oil. However, they are most commonly used for oils with a high molecular weight and high viscosity. This allows for easier surfactant selection and generally requires a smaller amount of the surfactant. However, these methods seem to be inconvenient for drug delivery systems due to heat-sensitive ingredients [69].

High-speed stirring. High-speed stirring was found to be a very efficient technique for producing nanoemulsions. The method is rapid, economical, and suitable for mass production. Scholz & Keck created nanoemulsions with droplet sizes of 135 nm and narrow size distributions using this method [70]. The emulsions were physically stable for at least three months. This method produces an emulsion with slightly larger droplet sizes than high-pressure homogenization. Macroemulsions are usually created by high-speed stirring with rotor-stator homogenizers. According to earlier

research, rotor-stator systems might create emulsions with mean droplet sizes in the lower micrometer range [71, 72].

Ultrasonication. Nanoemulsions preparation by ultrasonic emulsification is a useful technique for small test samples since it reduces the mean droplet diameter size. Ultrasonication converts electrical waves into pressure waves with a reduced droplet size and increased sonication time, power, and emulsifier concentration [69]. Since this method produces more heat, it is inappropriate for heat-sensitive food components. The primary method of treatment with ultrasound is cavitation, and in liquid foods ultrasonic waves speed up chemical reactions, diffusion, and dissolving processes. Free ions produced by ultrasonic cavitation cause the ultrasonic acceleration of chemical reactions [73]. This method produces high droplet distributions with a particle size range of 150–700 nm, depending on the pre-emulsion preparation method [74]. Two mechanisms are thought to be involved in ultrasonic emulsification. First, when an acoustic field is applied, interfacial waves are created, and these waves eventually become unstable, causing the oil phase to erupt into the aqueous medium as droplets. Second, the use of low-frequency ultrasound induces acoustic cavitation, leading to the production and subsequent dissolution of micro bubbles caused by changes in sound wave pressure. Extreme levels

of intensely localized turbulence are produced by each bubble collapse. The primary oil droplets of the dispersed oil are effectively broken up into droplets of a sub-micron size by turbulent micro-implosions [75, 76].

High-pressure homogenization. High-pressure homogenization is one of the high-energy mechanical processing techniques for the formation of oil-in-water nanoemulsions. It is especially well suited for the continuous synthesis of finely dispersed emulsions [77]. When compared to the nanoemulsions synthesized by spontaneous emulsification, the nanoemulsions formed by high-pressure homogenization demonstrated a reduced droplet size and enhanced *in vitro* release [78, 79].

This method has the advantages of rapid emulsification, a small particle size, homogeneous distribution, a stable system, and a low surfactant amount [72].

Low-energy emulsification methods. Low-energy emulsification methods use the intrinsic chemical energy (or chemical potential of its constituents) of a system for the synthesis of nanoemulsions. These methods use slow stirring (1600 rpm), which leads to lower energy consumption. Low-energy emulsification methods are categorized into two types: isothermal and thermal. For bioactive substances, which are thermally sensitive, isothermal techniques are more appropriate [64, 69]. They include phase inversion temperature, solvent displacement, phase inversion composition, spontaneous emulsification, micro-emulsion dilution, and more recently developed techniques such as D-phase emulsification [43, 44, 69].

Isothermal methods. Low-energy isothermal processes do not require temperature change or a specific homogenizer to develop small droplets. Isothermal methods have numerous benefits. They are used to prepare nanoemulsions over a wide temperature range, without the need for temperature quenching after preparation, which may result in significant energy savings. Also, they allow for the encapsulation of heat-sensitive compounds [80].

Spontaneous emulsification. Numerous physicochemical processes can lead to this method: real spontaneous emulsification occurs when two immiscible liquids come into contact and emulsify on their own without the use of heat or mechanical forces. When surfactants are present or absent, solvents might be used to speed up the process [80].

Emulsion phase inversion. In emulsion phase inversion, an aqueous phase is added to a stirring organic phase. Since this method also involves mixing water with oil, it is sometimes referred to as “catastrophic phase inversion”. The emulsion phase inversion method is quite similar to the later steps of spontaneous emulsification, which include breaking down a microemulsion into tiny oil droplets. This process is also known as “phase inversion composition” [80].

Thermal methods. Phase inversion. Phase inversion makes use of the chemical energy liberated by phase changes that occur during emulsification. Transitions from structures with a surfactant film with an average

zero curvature play a key role in the formation of nanoemulsions, even though these phase transitions frequently require the inversion of the surfactant film curvature from positive to negative or vice versa. There are two methods for inducing phase transitions: phase inversion temperature and phase inversion composition. The former induces phase transition by changes in temperature, while the latter induces phase transition by changes in composition [38].

Nanoemulsion-based food packaging materials.

The four primary functions of packaging are restraint, convenience, communication, and protection. Among all, protection is the key function since packaging protects food from compressive pressures, vibration, shock, dust, microbial contamination, undesirable odors, gases, water vapor, and moisture [54]. The growth of foodborne pathogens is among the most common causes of a limited shelf life. Motivated by increased consumer interest in longer shelf life and easy food handling, researchers are developing improved food packaging such as active or intelligent packaging. The term “active packaging” refers to a system in which the packaging has been modified to preserve, protect, or enhance the food’s sensory attributes, safety, and quality [81, 82]. Active packaging has become a popular way to extend the shelf life of food products, reduce product losses, and guarantee customer safety.

Active packaging can be divided into two types: non-migratory active packaging and active-release packaging. Non-migratory packaging mainly refers to scavengers or absorbers such as oxygen scavengers, moisture scavengers, and ethylene absorbers. In contrast, active-release packaging systems include carbon dioxide emitters, antimicrobial packaging, and antioxidant packaging. The use of nanoemulsions is a recent technique for providing food packaging materials with antimicrobial, antioxidant, anticancer, antiinflammatory, and antiviral activities, as well as UV blocking, water vapor, and oxygen barrier properties [83–87].

Nanoemulsions can be integrated or incorporated into films and coatings in order to potentially be used in food packaging. Nanoemulsions containing bioactive compounds can be used to develop biodegradable films and coatings to enhance the quality, functionality, shelf life, and nutritional content. Biopolymer matrix-based films and coatings comprise the continuous phase because they provide mono dispersity and stability to nanoemulsions droplets [36].

Nanoemulsions in non-migratory active packaging.

Non-migratory active packaging refers primarily to absorbers and scavengers that are meant to eliminate or absorb undesirable gaseous elements from atmosphere inside the food package without intentional migration. Also, they provide a regulated influx of desired compounds into the packing environment, which favorably affects the food product by extending its shelf life. Active ingredients are incorporated into gas-absorbent packaging materials that can react with or absorb inside gases. Of all gas scavenging technologies,

the oxygen-scavenging packaging system has been the subject of most research and application [81]. This system extends the shelf life of foods while preserving their nutritional value and preventing discoloration, rancidity, oxidative browning, microbiological spoilage, and organoleptic deterioration, thus ensuring food safety [88].

Curcumin nanoemulsions were developed by high-pressure homogenization with varied surfactant (Tween 20) concentrations, and they were subsequently incorporated into the commercial milk system. Curcumin nanoemulsions exhibited efficient oxygen scavenging activity. Milk fortified with curcumin nanoemulsions showed considerably less lipid oxidation in comparison to unfortified milk, so these nanoemulsions are suitable for the beverage industry [89].

Hasani-Javanmardi *et al.* developed an oxygen absorber packaging incorporated with a nanoemulsion containing cumin and safflower essential oils and studied its effect on the quality of lamb loins throughout a 20-day chilled storage period [90]. The treatments were performed in three stages: single, binary, and ternary. They delayed the growth of mesophilic and psychrotrophic bacteria, *Enterobacteriaceae*, and lactic acid bacteria. Also, they retarded the physicochemical and sensory changes, but increased the rate of metmyoglobin production, total volatile nitrogen, lipid and protein oxidation, as well as sensory and color degradation. In another study, a food-grade vitamin E acetate nanoemulsion was developed using edible mustard oil and Tween 80. The nanoemulsion exhibited high bioactivity, as well as antioxidant and antibacterial effect, indicating that it may be used to extend the shelf life of fruit juice. The presence of vitamin E acetate was thought to account for antioxidant activity. As a result, it could scavenge reactive oxygen species produced in the body when lipids were oxidized, which could harm cells [91].

Palladium nanoparticles were developed with multi-layered poly (3-hydroxybutyrate) and polycaprolactone polymers, very effective oxygen scavengers, by using the electrospinning method. The resulting nanocomposites offered high oxygen-scavenging activity [92]. Ethylene scavengers are also needed in order to prolong the shelf life of fruits and vegetables. Ethylene is a well-known plant growth hormone that stimulates fruit ripening but can also cause over-ripening and even deterioration, giving fruits a restricted shelf life. Therefore, to reduce fruit waste, an ethylene scavenger can be created that is highly effective, safe, and sustainable and does not alter the physicochemical or physiological properties of the fruit.

Bio-based ethylene scavenger films were produced using paper towel microfibers coated with Zein – *Artemisia sphaerocephala* Krasch. Gum (ASKG) nanoparticles with core-shell structures were developed via electrospinning, and bananas coated with these films showed reduced browning, increased firmness, and extended shelf life [93]. Novel nanocomposites based

on polyolefin elastomer were developed, including nano-silica and nano clay impregnated with KMnO_4 . In comparison to neat polyolefin films, the resulting nanocomposites showed improved mechanical characteristics, a higher ethylene absorption, and a reduced water vapor permeability. Furthermore, the enhanced nanocomposite coatings could improve the shelf life of bananas by up to 15 days under ambient conditions [94]. The application of nanoemulsion coatings on apricot fruit had a significant impact on its quality characteristics. The nanoemulsion suppressed ascorbic acid and carotenoid contents, as well as decay rate, weight loss, and antioxidant activity. Similarly, it helped reduce the overall number of psychrophilic bacteria, yeast, and mold [95].

Nanoemulsions in active-release packaging. Active-release packaging systems release the required gases into the package environment to preserve product quality and freshness and lengthen shelf life. They are highly demanded to ensure food quality and safety. Active ingredients, such as antioxidants and antimicrobials, are incorporated into the packaging systems rather than added to the food itself so that the migration of these compounds can enrich the product.

There has been a great deal of interest in the systems' antimicrobial and antioxidant activities, as well as their water vapor and oxygen barrier properties. For example, a neem oil nanoemulsion in a pectin matrix exhibited enhanced mechanical attributes, diminished stiffness and water vapor permeability, increased extensibility, and showed excellent antifungal activity against *Aspergillus flavus* and *Penicillium citrinum* [97].

A clove essential oil nanoemulsion was incorporated into a chitosan coating to preserve fresh *Tremella fuciformis*. The coating exhibited high antibacterial activity against *Burkholderia gladioli* and increased the shelf-life of *T. fuciformis* to 9 days [97]. A bilayer film was developed based on a sodium alginate/tea tree essential oil nanoemulsion and containing TiO_2 nanoparticles to improve the postharvest losses of banana fruit and reduce the fungal disease (anthracnose). The addition of a specific amount of TiO_2 to sodium alginate significantly improved the film's UV blocking, water vapor, and oxygen barrier properties [84]. A bionanocomposite was developed in which different concentrations of a pracaxi oil nanoemulsion were incorporated into a xylitol pectin matrix. This bionanocomposite efficiently improved the shelf life and stability of butter against the oxidation process [85]. Clove- and cinnamon-based nanoemulsions were created via ultrasonication with varying concentrations of soy lecithin as a surfactant. The resulting nanoemulsions exhibited antioxidant activity, and the coated muffins maintained their texture and had lower weight loss, density, and moisture content. Additionally, the nanoemulsion-based coating helped extend the shelf life of the ingredients by up to 6 days without any quality loss, which made them more useful as functional components [98]. In another study, films were developed

with gelatin-chitosan (4:1) that included nanoemulsions loaded with various active substances, such as canola oil, tocopherol/cinnamaldehyde, tocopherol/garlic oil, tocopherol/cinnamaldehyde, and garlic oil. The nanoemulsions were synthesized in a microfluidizer using the casting method with biopolymers and glycerol as a plasticizer. The films loaded with nanoencapsulated active compounds showed strong antioxidant activity and were particularly effective against *Pseudomonas aeruginosa*. These active films could be used as packaging materials to extend the shelf life of foods [61].

Advantages and disadvantages of nanoemulsions in packaging. Researchers in the fields of food science, food technology, and food microbiology are all concerned about food safety due to the amount of food that is wasted after its shelf life has expired [105]. Food scientists have been fascinated by the development of more efficient nanotechnology-based methods in food packaging, along with significant progress in biotechnology in a broad range of industries, including cosmetic, agricultural, and pharmaceutical fields [54]. Many approaches can improve food packaging systems and reduce waste. For example, the use of essential oils can remove the limitations of conventional food packaging while lowering environmental risks [106, 107]. With the substantial growth of nanotechnology, there is an increasing interest in the use of nanoemulsion-based packaging systems for the real-time monitoring of food products [108]. They provide opportunities to streamline targeted compound distribution to large surface areas to improve stability, biodegradability, anti-oxidation, and antimicrobial qualities. There is a variety of methods for producing nanoemulsions.

In recent years, nanoemulsions have helped in food preservation, as well as in the development of stable, conventional food packaging systems. In addition, some edible coatings based on nanoemulsions containing essential oils have been created for food preservation. For example, a coating for strawberries was incorporated with a nanoemulsion based on pullulan and cinnamon essential. This coating retarded senescence and inhibited the decay of strawberry fruits during storage more efficiently than the control and pure pullulan coatings [105]. Strawberry cartilage and grey mold rot were controlled using a nanoemulsion made of cinnamon essential oil, which had antifungal properties. This nanoemulsion can replace chemical fungicides to minimize strawberry fruit post-harvest lesions [109].

Edible coatings provide food products with a glossy finished surface but one of their major advantages is that they are environmentally safe and, therefore, can replace plastic packaging to reduce waste and protect the environment. Natural coatings provide similar protection against oxygen, light, bacteria, and moisture as modified-environment packaging does by extending the shelf life of food products [110]. Recently developed active edible coatings are used to encapsulate active compounds in the form of nanoemulsions that play an

important role in increasing the functionality of edible packaging [111]. Nanoemulsions mixed with ground meat or fish products help uniformly distribute bioactive compounds throughout the product, while dipping or coating with nanoemulsions helps in preventing spoilage [105, 112].

Nanoemulsions that contain active components, such as antimicrobial agents and antioxidants, are incorporated into packaging films and coatings. The major application of these packaging systems is to protect the food against microbes, oxidation, denaturation, and changes in pH. However, they can also help control the release of active ingredients into the food. Active agents are incorporated into the packaging systems instead of being added directly to food. However, when added in a non-encapsulated form, these bioactive substances have an adverse effect on the optical and transparency properties of the films. Several disadvantages can also be seen throughout the film's development such as weak miscibility, phase separation, and the chemical or thermal degradation of bioactive compounds [113]. Moreover, the synthesis of nanoemulsions requires high-tech, expensive equipment, which may raise the total cost of the packaging system. High concentrations of emulsifiers used to develop nanoemulsions can prove to be highly toxic, inflicting serious harm to the human body, if consumed, and to the environment, if discarded.

Unless the most stable emulsifying conditions are used to develop nanoemulsions, instability in the form of flocculation or coalescence often occurs during storage. Nanoemulsions that are stored for a long time may become unstable, and their stability may also be affected by changes in pH and temperature [114]. Some processes reduce the interfacial area that occurs in them over time. The following processes lead to emulsion breakdown: 1) flocculation, which is the sticking together of dispersed phase droplets; 2) coalescence, which is the fusion of droplets; 3) sedimentation (creaming), which is the directed motion of particles (downward or upward); and 4) Ostwald ripening, also known as isothermal distillation, which is the transfer of material from smaller to larger droplets due to the difference in drop curvature radii [115, 116].

CONCLUSION

Nanoemulsions as a nanotechnological approach are gaining more attention due to their applications in the pharmaceutical, cosmetic, and food sectors to improve the stability of carrier agents. Their application in packaging systems is promising in terms of improving the packaging's physical, mechanical, barrier, and other functional properties, as well as extending the shelf life of fruits, vegetables, and other food categories. Furthermore, high-energy emulsification methods for preparing nanoemulsions, such as high-pressure homogenizers, ultrasonication, and others, are preferred to low-energy emulsification methods. The high-pressure homogenizer method has the best potential for impro-

ving the stability of nanoemulsions by reducing the particle size. In addition, different types of essential oils used as active components in nanoemulsion-based coatings and films improve their antimicrobial and antioxidant properties. They also help reduce post-harvest losses of fruits and vegetables by retarding their water and gas transpiration throughout the storage period. However, further research is needed to investigate the effects that essential oils may have on the stability of nanoemulsions and the retention of their volatile compounds on the surface of fruits and vegetables.

CONTRIBUTION

Jaishankar Prasad: Conceptualization, methodology, investigation, resources, and writing (original draft, review, and editing). Aishwarya Dixit: Writing (origi-

nal draft, review, and editing). Sujata Pandit Sharma: Supervision and writing (review and editing). Anjelina William Mwakosya: Writing (review and editing). Anka Trajkovska Petkoska: Writing (review and editing). Ashutosh Upadhyay: Writing (review and editing). Nishant Kumar: Conceptualization, methodology, formal analysis, visualization, and writing (original draft, review, and editing).

CONFLICT OF INTEREST

The authors declare no conflict of interest.

ACKNOWLEDGMENTS

The authors are grateful to their institutions for providing facility and infrastructural support.

REFERENCES

1. Wang L, Dong J, Chen J, Eastoe J, Li X. Design and optimization of a new self-nanoemulsifying drug delivery system. *Journal of Colloid and Interface Science*. 2009;330(2):443–448. <https://doi.org/10.1016/j.jcis.2008.10.077>
2. Wu X, Guy RH. Applications of nanoparticles in topical drug delivery and in cosmetics. *Journal of Drug Delivery Science and Technology*. 2009;19(6):371–384. [https://doi.org/10.1016/s1773-2247\(09\)50080-9](https://doi.org/10.1016/s1773-2247(09)50080-9)
3. Shah P, Bhalodia D, Shelat P. Nanoemulsion: A pharmaceutical review. *Systematic Reviews in Pharmacy*. 2010;1(1):24–32. <https://doi.org/10.4103/0975-8453.59509>
4. Cheng CJ, Tietjen GT, Saucier-Sawyer JK, Saltzman WM. A holistic approach to targeting disease with polymeric nanoparticles. *Nature Reviews Drug Discovery*. 2015;14(4):239–247. <https://doi.org/10.1038/nrd4503>
5. Singh Y, Meher JG, Raval K, Khan FA, Chaurasia M, Jain NK, *et al.* Nanoemulsion: Concepts, development and applications in drug delivery. *Journal of Controlled Release*. 2017;252:28–49. <https://doi.org/10.1016/j.jconrel.2017.03.008>
6. Salem MA, Ezzat SM. Nanoemulsions in food industry. In: Milani J, editor. *Some new aspects of colloidal systems in foods*. IntechOpen; 2019. <https://doi.org/10.5772/intechopen.79447>
7. Fytianos G, Rahdar A, Kyzas GZ. Nanomaterials in cosmetics: Recent updates. *Nanomaterials*. 2020;10(5). <https://doi.org/10.3390/nano10050979>
8. Nile SH, Baskar V, Selvaraj D, Nile A, Xiao J, Kai G. Nanotechnologies in food science: Applications, recent trends, and future perspectives. *Nano-Micro Letters*. 2020;12(1). <https://doi.org/10.1007/s40820-020-0383-9>
9. Rolland M, Truong NP, Parkatzidis K, Pilkington EH, Torzynski AL, Style RW, *et al.* Shape-controlled nanoparticles from a low-energy nanoemulsion. *JACS Au*. 2021;1(11):1975–1986. <https://doi.org/10.1021/jacsau.1c00321>
10. Mohammadi Z, Jafari SM. Detection of food spoilage and adulteration by novel nanomaterial-based sensors. *Advances in Colloid and Interface Science*. 2020;286. <https://doi.org/10.1016/j.cis.2020.102297>
11. Zhang Z, Qiu C, Li X, McClements DJ, Jiao A, Wang J, *et al.* Advances in research on interactions between polyphenols and biology-based nano-delivery systems and their applications in improving the bioavailability of polyphenols. *Trends in Food Science and Technology*. 2021;116:492–500. <https://doi.org/10.1016/j.tifs.2021.08.009>
12. Yalçınöz Ş, Erçelesi E. Potential applications of nano-emulsions in the food systems: An update. *Materials Research Express*. 2018;5(6). <https://doi.org/10.1088/2053-1591/aac7ee>
13. Huang J-Y, Li X, Zhou W. Safety assessment of nanocomposite for food packaging application. *Trends in Food Science and Technology*. 2015;45(2):187–199. <https://doi.org/10.1016/j.tifs.2015.07.002>
14. Liu K, Chen Y-Y, Pan L-H, Li Q-M, Luo J-P, Zha X-Q. Co-encapsulation systems for delivery of bioactive ingredients. *Food Research International*. 2022;155. <https://doi.org/10.1016/j.foodres.2022.111073>
15. Goindi S, Kaur A, Kaur R, Kalra A, Chauhan P. Nanoemulsions: an emerging technology in the food industry. In: Grumezescu AM, editor. *Emulsions. Nanotechnology in the agri-food industry, volume 3. A volume in nanotechnology in the agri-food industry*. Academic Press; 2016. pp. 651–688. <https://doi.org/10.1016/b978-0-12-804306-6.00019-2>

16. Abbasian Chaleshtari Z, Zhou M, Foudazi R. Nanoemulsion polymerization and templating: Potentials and perspectives. *Journal of Applied Physics*. 2022;131(15). <https://doi.org/10.1063/5.0081303>
17. Tan C, Zhu Y, Ahari H, Jafari SM, Sun B, Wang J. Sonochemistry: An emerging approach to fabricate biopolymer cross-linked emulsions for the delivery of bioactive compounds. *Advances in Colloid and Interface Science*. 2022;311. <https://doi.org/10.1016/j.cis.2022.102825>
18. Nanotechnology for Food Packaging Market: Segmented By Application; By Technology and Region – Global Analysis of Market Size, Share & Trends for 2019–2020 and Forecasts to 2030 CAGR 2022 [Internet]. [cited 2022 Dec 20]. Available from: https://reports.valuates.com/request/sample/ALLI-Manu-S71/Nanotechnology_Market
19. Ameta SK, Rai AK, Hiran D, Ameta R, Ameta SC. Use of nanomaterials in food science. In: Ghorbanpour M, Bhargava P, Varma A, Choudhary DK, editors. *Biogenic nano-particles and their use in agro-ecosystems*. Singapore: Springer Nature; 2020. pp. 457–488. https://doi.org/10.1007/978-981-15-2985-6_24
20. Neethirajan S, Jayas DS. Nanotechnology for the food and bioprocessing industries. *Food and Bioprocess Technology*. 2011;4(1):39–47. <https://doi.org/10.1007/s11947-010-0328-2>
21. Cerqueira MÂPR, McClements DJ, Pastrana-Castro LM. Nutrition, health and well-being in the world: The role of food structure design. In: Cerqueira MÂPR, Pastrana-Castro LM, editors. *Food structure engineering and design for improved nutrition, health and well-being*. Academic Press; 2023. pp. 3–15. <https://doi.org/10.1016/B978-0-323-85513-6.00015-3>
22. Artiga-Artigas M, Acevedo-Fani A, Martín-Belloso O. Effect of sodium alginate incorporation procedure on the physicochemical properties of nanoemulsions. *Food Hydrocolloids*. 2017;70:191–200. <https://doi.org/10.1016/j.foodhyd.2017.04.006>
23. Azmi NAN, Elgharbawy AAM, Motlagh SR, Samsudin N, Salleh HM. Nanoemulsions: Factory for food, pharmaceutical and cosmetics. *Processes*. 2019;7(9). <https://doi.org/10.3390/pr7090617>
24. Nedovic V, Kalusevic A, Manojlovic V, Levic S, Bugarski B. An overview of encapsulation technologies for food applications. *Procedia Food Science*. 2011;1:1806–1815. <https://doi.org/10.1016/j.profoo.2011.09.265>
25. McClements DJ. Advances in edible nanoemulsions: Digestion, bioavailability, and potential toxicity. *Progress in Lipid Research*. 2021;81. <https://doi.org/10.1016/j.plipres.2020.101081>
26. Reis DR, Ambrosi A, Luccio MD. Encapsulated essential oils: A perspective in food preservation. *Future Foods*. 2022;5. <https://doi.org/10.1016/j.fufo.2022.100126>
27. McClements DJ, Decker EA, Weiss J. Emulsion-based delivery systems for lipophilic bioactive components. *Journal of Food Science*. 2007;72(8):R109–R124. <https://doi.org/10.1111/j.1750-3841.2007.00507.x>
28. McClements DJ. Edible nanoemulsions: fabrication, properties, and functional performance. *Soft Matter*. 2011;7(6):2297–2316. <https://doi.org/10.1039/c0sm00549e>
29. Nanotechnology in the food industry: a short review [Internet]. [cited 2022 Dec 20]. Available from: <https://www.food-safety.com/articles/5193-nanotechnology-in-the-food-industry-a-short-review>
30. Cha DS, Chinnan MS. Biopolymer-based antimicrobial packaging: A review. *Critical Reviews in Food Science and Nutrition*. 2004;44(4):223–237. <https://doi.org/10.1080/10408690490464276>
31. Weiss J, Takhistov P, McClements DJ. Functional materials in food nanotechnology. *Journal of Food Science*. 2006;71(9):R107–R116. <https://doi.org/10.1111/j.1750-3841.2006.00195.x>
32. Sharma N, Kaur G, Khatkar SK. Optimization of emulsification conditions for designing ultrasound assisted curcumin loaded nanoemulsion: Characterization, antioxidant assay and release kinetics. *LWT*. 2021;141. <https://doi.org/10.1016/j.lwt.2021.110962>
33. Jiang T, Charcosset C. Encapsulation of curcumin within oil-in-water emulsions prepared by premix membrane emulsification: Impact of droplet size and carrier oil on the chemical stability of curcumin. *Food Research International*. 2022;157. <https://doi.org/10.1016/j.foodres.2022.111475>
34. Suvorov OA, Volozhaninova SYu, Balandin GV, Frolova YuV, Kozlovskaya AE, Fokina EN, et al. Antibacterial effect of colloidal solutions of silver nanoparticles on microorganisms of cereal crops. *Foods and Raw Materials*. 2017;5(1):100–107. <https://doi.org/10.21179/2308-4057-2017-1-100-107>
35. Koroleva MYu, Yurtov EV. Nanoemulsions: the properties, methods of preparation and promising applications. *Russian Chemical Reviews*. 2012;81(1):21–43. <https://doi.org/10.1070/rc2012v081n01abeh004219>
36. Aswathanarayan JB, Vittal RR. Nanoemulsions and their potential applications in food industry. *Frontiers in Sustainable Food Systems*. 2019;3. <https://doi.org/10.3389/fsufs.2019.00095>

37. Choi SJ, McClements DJ. Nanoemulsions as delivery systems for lipophilic nutraceuticals: Strategies for improving their formulation, stability, functionality and bioavailability. *Food Science and Biotechnology*. 2020;29(2):149–168. <https://doi.org/10.1007/s10068-019-00731-4>
38. Solans C, Izquierdo P, Nolla J, Azemar N, Garcia-Celma MJ. Nano-emulsions. *Current Opinion in Colloid and Interface Science*. 2005;10(3–4):102–110. <https://doi.org/10.1016/j.cocis.2005.06.004>
39. Jaiswal M, Dudhe R, Sharma PK. Nanoemulsion: an advanced mode of drug delivery system. *3 Biotech*. 2014;5(2):123–127. <https://doi.org/10.1007/s13205-014-0214-0>
40. Patel RB, Patel MR, Thakore SD, Patel BG. Nanoemulsion as a valuable nanostructure platform for pharmaceutical drug delivery. In: Grumezescu AM, editor. *Nano- and microscale drug delivery systems. Design and fabrication*. Elsevier; 2017. pp. 321–341. <https://doi.org/10.1016/b978-0-323-52727-9.00017-0>
41. Patravale V, Dandekar P, Jain R. Nanoparticulate systems as drug carriers: the need. In: Patravale V, Dandekar P, Jain R, editors. *Nanoparticulate drug delivery. Perspectives on the transition from laboratory to market. A volume in woodhead publishing series in biomedicine*. Woodhead Publishing; 2012. pp. 1–28. <https://doi.org/10.1533/9781908818195.1>
42. Gurpret K, Singh SK. Review of nanoemulsion formulation and characterization techniques. *Indian Journal of Pharmaceutical Sciences*. 2018;80(5):781–789. <https://doi.org/10.4172/pharmaceutical-sciences.1000422>
43. Gupta PK, Bhandari N, Shah HN, Khanchandani V, Keerthana R, Nagarajan V, et al. An update on nanoemulsions using nanosized liquid in liquid colloidal systems. In: Koh KS, Wong VL, editors. *Nanoemulsions – properties, fabrications and applications*. IntechOpen; 2019. <https://doi.org/10.5772/intechopen.84442>
44. Simonazzi A, Cid AG, Villegas M, Romero AI, Palma SD, Bermúdez JM. Nanotechnology applications in drug controlled release. In: Grumezescu AM, editor. *Drug targeting and stimuli sensitive drug delivery systems*. William Andrew; 2018. pp. 81–116. <https://doi.org/10.1016/b978-0-12-813689-8.00003-3>
45. Hashemnejad SM, Badruddoza AZM, Zarket B, Ricardo Castaneda C, Doyle PS. Thermoresponsive nanoemulsion-based gel synthesized through a low-energy process. *Nature Communications*. 2019;10(1). <https://doi.org/10.1038/s41467-019-10749-1>
46. Rehman A, Tong Q, Jafari SM, Korma SA, Khan IM, Mohsin A, et al. Spray dried nanoemulsions loaded with curcumin, resveratrol, and borage seed oil: The role of two different modified starches as encapsulating materials. *International Journal of Biological Macromolecules*. 2021;186:820–828. <https://doi.org/10.1016/j.ijbiomac.2021.07.076>
47. Bykov DE, Eremeeva NV, Makarova NV, Bakharev VV, Demidova AV, Bykova TO. Influence of plasticizer content on organoleptic, physico-chemical and strength characteristics of apple sauce-based edible film. *Foods and Raw Materials*. 2017;5(2):5–14. <https://doi.org/10.21603/2308-4057-2017-2-5-14>
48. Asyakina LK, Dolganyuk VF, Belova DD, Peral MM, Dyshlyuk LS. The study of rheological behavior and safety metrics of natural biopolymers. *Foods and Raw Materials*. 2016;4(1):70–78. <https://doi.org/10.21179/2308-4057-2016-1-70-78>
49. Giro TM, Beloglazova KE, Rysmukhambetova GE, Simakova IV, Karpunina LV, Rogojin AA, et al. Xanthan-based biodegradable packaging for fish and meat products. *Foods and Raw Materials*. 2020;8(1):67–75. <https://doi.org/10.21603/2308-4057-2020-1-67-75>
50. Chime SA, Kenechukwu FC, Attama AA. Nanoemulsions – Advances in formulation, characterization and applications in drug delivery. In: Sezer AD, editor. *Application of nanotechnology in drug delivery*. IntechOpen; 2014. <https://doi.org/10.5772/58673>
51. Nirmala MJ, Durai L, Gopakumar V, Nagarajan R. Preparation of celery essential oil-based nanoemulsion by ultrasonication and evaluation of its potential anticancer and antibacterial activity. *International Journal of Nanomedicine*. 2020;15:7651–7666. <https://doi.org/10.2147/IJN.S252640>
52. Donsi F. Applications of nanoemulsions in foods. In: Jafari SM, McClements DJ, editors. *Nanoemulsions. Formulation, applications, and characterization*. Cambridge: Academic Press; 2018. pp. 349–377. <https://doi.org/10.1016/B978-0-12-811838-2.00011-4>
53. Che Marzuki NH, Wahab RA, Abdul Hamid M. An overview of nanoemulsion: Concepts of development and cosmeceutical applications. *Biotechnology and Biotechnological Equipment*. 2019;33(1):779–797. <https://doi.org/10.1080/13102818.2019.1620124>
54. Ahari H, Naeimabadi M. Employing nanoemulsions in food packaging: Shelf life enhancement. *Food Engineering Reviews*. 2021;13:858–883. <https://doi.org/10.1007/s12393-021-09282-z>
55. Shershneva EG. Biodegradable food packaging: Benefits and adverse effects. *IOP Conference Series: Earth and Environmental Science*. 2022;988(2). <https://doi.org/10.1088/1755-1315/988/2/022006>



56. Acevedo-Fani A, Salvia-Trujillo L, Rojas-Graü MA, Martín-Belloso O. Edible films from essential-oil-loaded nanoemulsions: Physicochemical characterization and antimicrobial properties. *Food Hydrocolloids*. 2015;47:168–177. <https://doi.org/10.1016/j.foodhyd.2015.01.032>
57. Almasi L, Radi M, Amiri S, McClements DJ. Fabrication and characterization of antimicrobial biopolymer films containing essential oil-loaded microemulsions or nanoemulsions. *Food Hydrocolloids*. 2021;117. <https://doi.org/10.1016/j.foodhyd.2021.106733>
58. Elshamy S, Khadizatul K, Uemura K, Nakajima M, Neves MA. Chitosan-based film incorporated with essential oil nanoemulsion foreseeing enhanced antimicrobial effect. *Journal of Food Science and Technology*. 2021;58(9):3314–3327. <https://doi.org/10.1007/s13197-020-04888-3>
59. Mahdi AA, Al-Maqtari QA, Mohammed JK, Al-Ansi W, Cui H, Lin L. Enhancement of antioxidant activity, antifungal activity, and oxidation stability of *Citrus reticulata* essential oil nanocapsules by clove and cinnamon essential oils. *Food Bioscience*. 2021;43. <https://doi.org/10.1016/j.fbio.2021.101226>
60. Xavier LO, Sganzerla WG, Rosa GB, da Rosa CG, Agostinetto L, Veeck APDL, et al. Chitosan packaging functionalized with *Cinnamodendron dinisii* essential oil loaded zein: A proposal for meat conservation. *International Journal of Biological Macromolecules*. 2021;169:183–193. <https://doi.org/10.1016/j.ijbiomac.2020.12.093>
61. Pérez-Córdoba LJ, Norton IT, Batchelor HK, Gkatzionis K, Spyropoulos F, Sobral PJA. Physico-chemical, antimicrobial and antioxidant properties of gelatin-chitosan based films loaded with nanoemulsions encapsulating active compounds. *Food Hydrocolloids*. 2018;79:544–559. <https://doi.org/10.1016/j.foodhyd.2017.12.012>
62. Gupta A, Eral HB, Hatton TA, Doyle PS. Nanoemulsions: formation, properties and applications. *Soft Matter*. 2016;12(11):2826–2841. <https://doi.org/10.1039/c5sm02958a>
63. Nejatian M, Abbasi S. Application of bio-based emulsifiers in the formulation of food-grade nanoemulsions. In: Abd-El salam KA, Murugan K, editors. *Bio-based nanoemulsions for agri-food applications. A volume in nanobiotechnology for plant protection*. Elsevier; 2022. pp. 311–327. <https://doi.org/10.1016/B978-0-323-89846-1.00021-8>
64. Nain A, Tripathy DB, Gupta A, Dubey R, Kuldeep, Singh A. Nanoemulsions: Nanotechnological approach in food quality monitoring. In: Sharma A, Vijayakumar PS, Prabhakar EPK, Kumar R, editors. *Academic Press*; 2023. pp. 223–238. <https://doi.org/10.1016/B978-0-323-85791-8.00020-3>
65. Jasmina H, Džana O, Alisa E, Edina V, Ognjenka R. Preparation of nanoemulsions by high-energy and lowenergy emulsification methods. *CMBEBIH 2017. Proceedings of the International Conference on Medical and Biological Engineering*. 2017;62:317–322. https://doi.org/10.1007/978-981-10-4166-2_48
66. Chircov C, Grumezescu AM. Nanoemulsion preparation, characterization, and application in the field of biomedicine. In: Grumezescu AM, editor. *Nanoarchitectonics in biomedicine*. William Andrew; 2019. pp. 169–188. <https://doi.org/10.1016/b978-0-12-816200-2.00019-0>
67. Kumar M, Bishnoi RS, Shukla AK, Jain CP. Techniques for formulation of nanoemulsion drug delivery system: A review. *Preventive Nutrition and Food Science*. 2019;24(3):225–234. <https://doi.org/10.3746/pnf.2019.24.3.225>
68. Islam F, Saeed F, Afzaal M, Hussain M, Ikram A, Khalid MA. Food grade nanoemulsions: promising delivery systems for functional ingredients. *Journal of Food Science and Technology*. 2023;60(5):1461–1471. <https://doi.org/10.1007/s13197-022-05387-3>
69. Safaya M, Rotliwala YC. Nanoemulsions: A review on low energy formulation methods, characterization, applications and optimization technique. *Materials Today: Proceedings*. 2020;27:454–459. <https://doi.org/10.1016/j.matpr.2019.11.267>
70. Scholz P, Keck CM. Nanoemulsions produced by rotor–stator high speed stirring. *International Journal of Pharmaceutics*. 2015;482(1–2):110–117. <https://doi.org/10.1016/j.ijpharm.2014.12.040>
71. Zhang A, Wang L, Song T, Yu H, Wang X, Zhao X. Effects of high pressure homogenization on the structural and emulsifying properties of a vegetable protein: *Cyperus esculentus* L. *LWT*. 2022;153. <https://doi.org/10.1016/j.lwt.2021.112542>
72. Shi Y, Zhang M, Chen K, Wang M. Nano-emulsion prepared by high pressure homogenization method as a good carrier for Sichuan pepper essential oil: Preparation, stability, and bioactivity. *LWT*. 2022;154. <https://doi.org/10.1016/j.lwt.2021.112779>
73. Bredihin SA, Andreev VN, Martekha AN, Schenzle MG, Korotkiy IA. Erosion potential of ultrasonic food processing. *Foods and Raw Materials*. 2021;9(2):335–344. <https://doi.org/10.21603/2308-4057-2021-2-335-344>
74. Modarres-Gheisari SMM, Gavagsaz-Ghoachani R, Malaki M, Safarpour P, Zandi M. Ultrasonic nano-emulsification – A review. *Ultrasonics Sonochemistry*. 2019;52:88–105. <https://doi.org/10.1016/j.ultsonch.2018.11.005>

75. Kentish S, Wooster TJ, Ashokkumar M, Balachandran S, Mawson R, Simons L. The use of ultrasonics for nanoemulsion preparation. *Innovative Food Science and Emerging Technologies*. 2008;9(2):170–175. <https://doi.org/10.1016/j.ifset.2007.07.005>
76. Abbas S, Hayat K, Karangwa E, Bashiri M, Zhnag X. An overview of ultrasound-assisted food-grade nanoemulsions. *Food Engineering Reviews*. 2013;5:139–157. <https://doi.org/10.1007/s12393-013-9066-3>
77. Ruiz-Montañez G, Ragazzo-Sanchez JA, Picart-Palmade L, Calderón-Santoyo M, Chevalier-Lucia D. Optimization of nanoemulsions processed by high-pressure homogenization to protect a bioactive extract of jackfruit (*Artocarpus heterophyllus* Lam). *Innovative Food Science and Emerging Technologies*. 2017;40:35–41. <https://doi.org/10.1016/j.ifset.2016.10.020>
78. Sharma S, Sahni JK, Ali J, Baboota S. Effect of high-pressure homogenization on formulation of TPGS loaded nanoemulsion of rutin – pharmacodynamic and antioxidant studies. *Drug Delivery*. 2014;22(4):541–551. <https://doi.org/10.3109/10717544.2014.893382>
79. Hidajat MJ, Jo W, Kim H, Noh J. Effective droplet size reduction and excellent stability of limonene nanoemulsion formed by high-pressure homogenizer. *Colloids and Interfaces*. 2020;4(1). <https://doi.org/10.3390/colloids4010005>
80. Komaiko JS, McClements DJ. Formation of food-grade nanoemulsions using low-energy preparation methods: A review of available methods. *Comprehensive Reviews in Food Science and Food Safety*. 2016;15(2):331–352. <https://doi.org/10.1111/1541-4337.12189>
81. Ahmed MW, Haque MA, Mohibullah M, Khan MSI, Islam MA, Mondal MHT, et al. A review on active packaging for quality and safety of foods: Current trends, applications, prospects and challenges. *Food Packaging and Shelf Life*. 2022;33. <https://doi.org/10.1016/j.fpsl.2022.100913>
82. Yildirim S, Röcker B, Pettersen MK, Nilsen-Nygaard J, Ayhan Z, Rutkaite R, et al. Active packaging applications for food. *Comprehensive Reviews in Food Science and Food Safety*. 2017;17(1):165–199. <https://doi.org/10.1111/1541-4337.12322>
83. Lopes AT, Figueiredo BL, Michelon M, Chura SSD, de Souza AL, Teixeira LMC, et al. Use of essential oil-loaded nanoemulsions in active food packaging. In: Abd-Elsalam KA, Murugan K, editors. *Bio-based nanoemulsions for agri-food applications. A volume in nanobiotechnology for plant protection*. Elsevier; 2022. pp. 363–386. <https://doi.org/10.1016/b978-0-323-89846-1.00024-3>
84. Yang Z, Li M, Zhai X, Zhao L, Tahir HE, Shi J, et al. Development and characterization of sodium alginate/tea tree essential oil nanoemulsion active film containing TiO₂ nanoparticles for banana packaging. *International Journal of Biological Macromolecules*. 2022;213:145–154. <https://doi.org/10.1016/j.ijbiomac.2022.05.164>
85. Candido GS, Natarelli CVL, Carvalho EEN, Oliveira JE. Bionanocomposites of pectin and pracaxi oil nanoemulsion as active packaging for butter. *Food Packaging and Shelf Life*. 2022;32. <https://doi.org/10.1016/j.fpsl.2022.100862>
86. Noori S, Zeynali F, Almasi H. Antimicrobial and antioxidant efficiency of nanoemulsion-based edible coating containing ginger (*Zingiber officinale*) essential oil and its effect on safety and quality attributes of chicken breast fillets. *Food Control*. 2018;84:312–320. <https://doi.org/10.1016/j.foodcont.2017.08.015>
87. Espitia PJP, Fuenmayor CA, Otoni CG. Nanoemulsions: Synthesis, characterization, and application in bio-based active food packaging. *Comprehensive Reviews in Food Science and Food Safety*. 2018;18(1):264–285. <https://doi.org/10.1111/1541-4337.12405>
88. Maria Roberta A. Oxygen scavenging films and coating of biopolymers for food application. In: de Moraes MA, da Silva CF, Vieira RS, editors. *Biopolymer membranes and films. Health, food, environment, and energy applications*. Elsevier; 2020. pp. 535–551. <https://doi.org/10.1016/b978-0-12-818134-8.00022-5>
89. Joung HJ, Choi M-J, Kim JT, Park SH, Park HJ, Shin GH. Development of food-grade curcumin nanoemulsion and its potential application to food beverage system: Antioxidant property and *in vitro* digestion. *Journal of Food Science*. 2016;81(3):N745–N753. <https://doi.org/10.1111/1750-3841.13224>
90. Hasani-Javanmardi M, Fallah AA, Abbasvali M. Effect of safflower oil nanoemulsion and cumin essential oil combined with oxygen absorber packaging on the quality and shelf-life of refrigerated lamb loins. *LWT*. 2021;147. <https://doi.org/10.1016/j.lwt.2021.111557>
91. Dasgupta N, Ranjan S, Mundra S, Ramalingam C, Kumar A. Fabrication of food grade vitamin E nanoemulsion by low energy approach, characterization and its application. *International Journal of Food Properties*. 2015;19(3):700–708. <https://doi.org/10.1080/10942912.2015.1042587>
92. Cherpinski A, Szweczyk PK, Gruszczynski A, Stachewicz U, Lagaron JM. Oxygen-scavenging multilayered biopapers containing palladium nanoparticles obtained by the electrospinning coating technique. *Nanomaterials*. 2019;9(2). <https://doi.org/10.3390/nano9020262>

93. Fan X, Rong L, Li Y, Cao Y, Kong L, Zhu Z, et al. Fabrication of bio-based hierarchically structured ethylene scavenger films via electrospraying for fruit preservation. *Food Hydrocolloids*. 2022;133. <https://doi.org/10.1016/j.foodhyd.2022.107837>
94. Ebrahimi A, Zabihzadeh Khajavi M, Mortazavian AM, Asilian-Mahabadi H, Rafiee S, Farhoodi M, et al. Preparation of novel nano-based films impregnated by potassium permanganate as ethylene scavengers: An optimization study. *Polymer Testing*. 2021;93. <https://doi.org/10.1016/j.polymertesting.2020.106934>
95. Gull A, Bhat N, Wani SM, Masoodi FA, Amin T, Ganai SA. Shelf life extension of apricot fruit by application of nanochitosan emulsion coatings containing pomegranate peel extract. *Food Chemistry*. 2021;349. <https://doi.org/10.1016/j.foodchem.2021.129149>
96. Norcino LB, Mendes JF, Natarelli CVL, Manrich A, Oliveira JE, Mattoso LHC. Pectin films loaded with copaiba oil nanoemulsions for potential use as bio-based active packaging. *Food Hydrocolloids*. 2020;106. <https://doi.org/10.1016/j.foodhyd.2020.105862>
97. Wang H, Ma Y, Liu L, Liu Y, Niu X. Incorporation of clove essential oil nanoemulsion in chitosan coating to control *Burkholderia gladioli* and improve postharvest quality of fresh *Tremella fuciformis*. *LWT*. 2022;170. <https://doi.org/10.1016/j.lwt.2022.114059>
98. Prastuty, Kaur P, Singh A. Shelf life extension of muffins coated with cinnamon and clove oil nanoemulsions. *Journal of Food Science and Technology*. 2022;59(5):1878–1888. <https://doi.org/10.1007/s13197-021-05202-5>
99. Roy S, Rhim J-W. Fabrication of bioactive binary composite film based on gelatin/chitosan incorporated with cinnamon essential oil and rutin. *Colloids and Surfaces B: Biointerfaces*. 2021;204. <https://doi.org/10.1016/j.colsurfb.2021.111830>
100. Xiong Y, Li S, Warner RD, Fang Z. Effect of oregano essential oil and resveratrol nanoemulsion loaded pectin edible coating on the preservation of pork loin in modified atmosphere packaging. *Food Control*. 2020;114. <https://doi.org/10.1016/j.foodcont.2020.107226>
101. Moghimi R, Aliahmadi A, Rafati H. Antibacterial hydroxypropyl methyl cellulose edible films containing nanoemulsions of *Thymus daenensis* essential oil for food packaging. *Carbohydrate Polymers*. 2017;175:241–248. <https://doi.org/10.1016/j.carbpol.2017.07.086>
102. Das SK, Vishakha K, Das S, Chakraborty D, Ganguli A. Carboxymethyl cellulose and cardamom oil in a nanoemulsion edible coating inhibit the growth of foodborne pathogens and extend the shelf life of tomatoes. *Biocatalysis and Agricultural Biotechnology*. 2022;42. <https://doi.org/10.1016/j.bcab.2022.102369>
103. Alexandre EMC, Lourenço RV, Bittante AMQB, Moraes ICF, Sobral PJA. Gelatin-based films reinforced with montmorillonite and activated with nanoemulsion of ginger essential oil for food packaging applications. *Food Packaging and Shelf Life*. 2016;10:87–96. <https://doi.org/10.1016/j.fpsl.2016.10.004>
104. Sanchez LT, Pinzon MI, Villa CC. Development of active edible films made from banana starch and curcumin-loaded nanoemulsions. *Food Chemistry*. 2022;371. <https://doi.org/10.1016/j.foodchem.2021.131121>
105. Tripathi AD, Sharma R, Agarwal A, Haleem DR. Nanoemulsions based edible coatings with potential food applications. *International Journal of Biobased Plastics*. 2021;3(1):112–125. <https://doi.org/10.1080/24759651.2021.1875615>
106. Kamrul Hasan SM, Ferrentino G, Scampicchio M. Nanoemulsion as advanced edible coatings to preserve the quality of fresh-cut fruits and vegetables: A review. *International Journal of Food Science and Technology*. 2019;55(1):1–10. <https://doi.org/10.1111/ijfs.14273>
107. Zubair M, Shahzad S, Hussain A, Pradhan RA, Arshad M, Ullah A. Current trends in the utilization of essential oils for polysaccharide- and protein-derived food packaging materials. *Polymers*. 2022;14(6). <https://doi.org/10.3390/polym14061146>
108. Korotkaya EV. Biosensors: Design, classification, and applications in the food industry. *Foods and Raw Materials*. 2014;2(2):161–171. <https://doi.org/10.12737/5476>
109. Koroleva MYu, Yurtov EV. Ostwald ripening in macro- and nanoemulsions. *Russian Chemical Reviews*. 2021;90(3):293–323. <https://doi.org/10.1070/rcr4962>
110. Valencia-Chamorro SA, Palou L, del Río MA, Pérez-Gago MB. Antimicrobial edible films and coatings for fresh and minimally processed fruits and vegetables: A review. *Critical Reviews in Food Science and Nutrition*. 2011;51(9):872–900. <https://doi.org/10.1080/10408398.2010.485705>
111. Krishnamoorthy C, Chatterjee P, Paul U, Banerjee S, Kumar L, Chidambaram R. Nanoencapsulation of antimicrobial agents and antimicrobial effect of silver nanoparticles. In: Sharma A, Vijayakumar PS, Prabhakar EPK, Kumar R, editors. *Nanotechnology applications for food safety and quality monitoring*. Academic Press; 2023. pp. 435–456. <https://doi.org/10.1016/B978-0-323-85791-8.00023-9>

112. Gennadios A, Hanna MA, Kurth LB. Application of edible coatings on meats, poultry and seafoods: A review. *LWT – Food Science and Technology*. 1997;30(4):337–350. <https://doi.org/10.1006/fstl.1996.0202>
113. Yousefi M, Ehsani A, Jafari SM. Lipid-based nano delivery of antimicrobials to control food-borne bacteria. *Advances in Colloid and Interface Science*. 2019;270:263–277. <https://doi.org/10.1016/j.cis.2019.07.005>
114. Dasgupta N, Ranjan S. Food nanoemulsions: Stability, benefits and applications. In: Dasgupta N, Ranjan S, editors. *An introduction to food grade nanoemulsions*. Singapore: Springer; 2018. pp. 19–48. https://doi.org/10.1007/978-981-10-6986-4_2
115. Naserzadeh Y, Mahmoudi N, Pakina E. Antipathogenic effects of emulsion and nanoemulsion of cinnamon essential oil against *Rhizopus* rot and grey mold on strawberry fruits. *Foods and Raw Materials*. 2019;7(1):210–216. <https://doi.org/10.21603/2308-4057-2019-1-210-216>
116. Yüzer MO, Gençcelep H. Sesame seed protein: Amino acid, functional, and physicochemical profiles. *Foods and Raw Materials*. 2023;11(1):72–83. <https://doi.org/10.21603/2308-4057-2023-1-555>

ORCID IDs

Aishwarya Dixit  <https://orcid.org/0009-0004-7639-703X>
Anjelina William Mwakosya  <https://orcid.org/0000-0003-0617-3693>
Anka Trajkovska Petkoska  <https://orcid.org/0000-0002-9258-7966>
Ashutosh Upadhyay  <https://orcid.org/0000-0003-0886-0745>
Nishant Kumar  <https://orcid.org/0000-0003-0187-7544>



Composite exopolysaccharide-based hydrogels extracted from *Nostoc commune* V. as scavengers of soluble methylene blue

Nora Gabriela Herrera^{1,*} , Nelson Adrián Villacrés² ,
Lizbeth Aymara¹ , Viviana Román¹ , Mayra Ramírez¹ 

¹ Federico Villarreal National University , Lima, Peru

² National University of Engineering , Lima, Peru

* e-mail: nherrera@unfv.edu.pe

Received 26.12.2022; Revised 24.01.2023; Accepted 07.02.2023; Published online 11.07.2023

Abstract:


The industrial water contamination with synthetic dyes is currently a cause for concern. This paper introduces composite hydrogels as alternative scavengers of soluble dyes.

This research used kinetic models and adsorption isotherms to test composite exopolysaccharide hydrogels extracted from *Nostoc commune* V., pectin, and starch for their ability to remove methylene blue from water.

The exopolysaccharides demonstrated a rather low extraction yield and a crystallinity percentage of 38.21%. However, the crystallinity increased in the composite hydrogels (48.95%) with heterogeneous surface. The pseudo-second-order kinetic model served to explain the adsorption mechanism at pH 8 and pH 11, while the Elovich model explained the adsorption mechanism at pH 5. When in acid fluid, the hydrogels had a heterogeneous surface, whereas alkaline fluid resulted in a homogeneous surface. The Temkin adsorption model showed a good fit in the treatments.

At a basic pH value, composite exopolysaccharide-based hydrogels showed good results as scavengers of low-concentration methylene blue.

Keywords: Hydrogel, removal, methylene blue, adsorption, exopolysaccharide, *Nostoc commune* V.

Funding: This research was supported by the Vice-Rectorate for Research of the Federico Villarreal National University (UNFV)  as part of The Basic and Applied Research Projects Competition CANON 2019, project No. 5784-2019-CU-UNFV.

Please cite this article in press as: Herrera NG, Villacrés NA, Aymara L, Román V, Ramírez M. Composite exopolysaccharide-based hydrogels extracted from *Nostoc commune* V. as scavengers of soluble methylene blue. *Foods and Raw Materials*. 2024;12(1):37–46. <https://doi.org/10.21603/2308-4057-2024-1-587>

INTRODUCTION

The term *microalgae* refers to both eukaryotic (microalgae) and prokaryotic (cyanobacteria) microorganisms that perform oxygenic photosynthesis. These organisms live in aquatic and terrestrial habitats. They produce various compounds, e.g., polyunsaturated fatty acids, pigments, proteins, some enzymes, and exopolysaccharides. These compounds can be applied in various biotechnology sectors, i.e., food, energy, health, and biomaterials [1, 2].

Cyanobacterial exopolysaccharides possess unique biochemical properties due to their high molecular weight, anionic properties, and acidic profile [3]. Exopolysaccharides extracted from *Nostoc commune* V. can be applied in biomedicine and food industry to produce

hydrogels and films. However, the chemical structure of these exopolysaccharides is not yet known [3, 4].

Hydrogels consist of three-dimensional networks of intertwined polymer chains that are able to absorb and retain water molecules and solutes, including such ionic dyes as methylene blue [5].

Methylene blue is a cationic thiazine dye used in textile industries. However, it affects human health by causing asthma, cancer, and mutations [6]. Moreover, it affects the growth of aquatic organisms and generates mutagenic effects in fish [7, 8].

Industrial development facilitates economic prosperity but causes water pollution [9, 10]. This type of pollution occurs because various industries that deal with textile, dyes, and pharmaceuticals discharge

effluents that usually contain dyes and/or heavy metals [11]. For example, more than 700 000 tons of dyes are produced annually, of which approximately 1–2% are drained during production and around 10–15% are eliminated as effluents during application [12].

The list of modern wastewater treatment methods includes chemical precipitation, filtration, reverse osmosis, and photo-degradation [13–16]. However, not only are all these methods expensive and complex, but they also generate secondary products [17].

As a result, scientists are on the look for new absorbents, such as hydrogels, that could remove contaminants, e.g., dyes, from wastewater [18, 19].

This research extracted exopolysaccharides from the *N. commune* to prepare a new composite hydrogel that would remove soluble methylene blue.

STUDY OBJECTS AND METHODS

Materials. Pectin, starch, and calcium chloride dihydrate were purchased from Sigma-Aldrich. Petroleum ether, chloroform, propanol, ethanol, and methylene blue were obtained from Merck. The exopolysaccharides were extracted from cyanobacteria *Nostoc commune* V. collected in Conococha Lake, Province of Bolognesi, Ancash-Peru. These cyanobacteria were dried, crushed, and stored in an amber jar at room temperature.

Extracting the exopolysaccharide. We defatted 2 g of dry powder by maceration with 100 mL of petroleum ether, followed by filtering and oven-drying. This process was repeated with chloroform and then with ethanol. The extraction of the exopolysaccharide followed the procedure described by Rodríguez *et al.* [20]. The extractant was precipitated with propanol for subsequent drying, grinding, and storage in an amber bottle. The exopolysaccharide yield (Y_e , %) was calculated as follows:

$$Y_e = \frac{W_1}{W_2} \times 100 \quad (1)$$

where W_1 is the weight of exopolysaccharide, g; and W_2 is the weight of *N. commune* dried powder, g.

Preparation of hydrogels. We diluted 0.05 g of exopolysaccharide in distilled water to mix it with a pectin-starch solution in a ratio of 2:0.5, according to the methodology described by Dafe *et al.* [21]. After that, we poured the resulting mix drop by drop into a 0.2 M solution of $\text{CaCl}_2 \cdot 2\text{H}_2\text{O}$ under constant stirring at room temperature. The hydrogels were filtered and washed with distilled water. Before each application, the hydrogels were dried at 30°C for 36 h until a constant weight was obtained.

Characterization. The FTIR-ATR spectra (600 to 4000 cm^{-1}) were obtained using a Nicolet iS10 Thermo Scientific spectrophotometer. The thermogravimetric curves were gathered in an STA 6000 PerkinElmer device using 5.0 ± 0.1 mg of the sample in an N_2 atmosphere. The flow rate was 20 mL/min, and the temperature was between 20 and 600°C with a heating rate of 10°C/min. The XRD diffractograms were obtained

using a D2 Phaser (Brüker) equipment in a range of 10° to 60°. The crystallinity (%) index was determined using the ratio between the crystalline area and the total area (Eq. (2)). The specific surface area was determined using a Gemini VII 2390t micrometer with the nitrogen adsorption and desorption technique. The SEM images were obtained with an FEI Inspect S50 microscope. The samples were gold-plated in an 11430E-AX (SPI Supplies) high vacuum metallizer:

$$\text{Crystallinity} = \frac{\text{Crystalline area}}{\text{Total area}} \times 100 \quad (2)$$

Removing methylene blue. We added 0.1 g of hydrogel to 50 mL of methylene blue solution. For isothermal studies, the methylene blue concentration was $1.0\text{--}1.5 \times 10^{-6}$ mol/L at 25°C. The experiment involved five-time intervals (15, 30, 60, 90, and 120 min) and three pH levels (5, 8, and 11). The pH values were adjusted with NaOH (0.1 mol/L) and HCl (0.1 mol/L). The absorbance values ($\lambda_{\text{max}} = 668$ nm) were obtained using a Thermo Scientific/Spectronic GENESYS 20 Visible spectrophotometer by quantifying the adsorption capacity (q_e , mg/g) and removal percentage (%):

$$q_e = \frac{V \times (C_0 - C_e)}{W} \quad (3)$$

$$\text{Removal} = \frac{C_0 - C_e}{C_0} \times 100 \quad (4)$$

where C_0 and C_e are the initial and V equilibrium concentrations of methylene blue, mg/L, respectively; W is the volume of the solution, L; W is the mass of the hydrogel, g.

Isotherm and kinetic models. The adsorption isotherm illustrates the mobility or retention of a substance using a solid phase at a constant pH and temperature. The Langmuir isotherm (Eq. (5)) is an empirical model that describes the adsorption process on a homogeneous surface, forming a single layer without lateral interaction between the absorbed molecules. On the contrary, the Freundlich isotherm (Eq. (6)) assumes that the adsorption is carried out on a heterogeneous surface via a multilayer process, while the Temkin isotherm (Eq. (7)) considers the interaction between the adsorbent and the adsorbate:

$$\frac{C_e}{q_e} = \frac{1}{K_L \times q_{\text{max}}} + \frac{C_e}{q_{\text{max}}} \quad (5)$$

$$\ln q_e = \ln b + \frac{1}{n} \ln C_e \quad (6)$$

$$q_e = \frac{RT}{b_T} \ln C_e + \frac{RT}{b} \ln k_m \quad (7)$$

where C_e is the adsorbate equilibrium concentration, mg/L; q_e is the adsorbed amount at equilibrium, mg/g; q_{max} is the maximal amount of adsorbed surfactant, mg/g; K_L is the Langmuir constant, L/mg; b is the adsorption

capacity, L/mg; $1/n$ is the adsorption intensity or surface heterogeneity; R is the universal gas constant, J/mol/K; T is the temperature, K; b_T is the Temkin constant related to sorption heat, J/mol; k_m is the Temkin isotherm constant, L/g.

Finally, the separation factor or equilibrium parameter (Eq. (8)), denoted as R_L , checks if the adsorption is favorable ($R_L < 1$) or unfavorable ($R_L > 1$):

$$R_L = \frac{1}{1 + K_L \times C_0} \quad (8)$$

The pseudo-first-order (Eq. (9)) and pseudo-second-order (Eq. (10)) kinetic models differentiated the kinetic equations according to the adsorption capacity affected by the initial concentration of the dye. The Elovich model (Eq. (11)) assumes that the adsorbent surfaces are heterogeneous, and adsorption is performed in a multilayer process:

$$\ln \left[1 - \frac{q_t}{q_e} \right] = -k_1 \times t \quad (9)$$

$$\frac{1}{q_e - q_t} - \frac{1}{q_e} = k_2 \times t \quad (10)$$

$$q_t = \left(\frac{1}{\beta} \right) \times \ln \left(\frac{\alpha}{\beta} \right) + \left(\frac{1}{\beta} \right) \times \ln t \quad (11)$$

where q_e is the amount of the adsorbate at equilibrium, mg/g; q_t is the maximal uptake of adsorbate, mg/g; k_1 is the pseudo-first-order rate constant; k_2 is the pseudo-second-order rate constant; t is the contact time with

adsorbent, min; α is initial sorption rate, mg/g/min; β is the extent of surface coverage and activation energy for chemisorption, g/mg [22, 23].

RESULTS AND DISCUSSION

Exopolysaccharide profile. The exopolysaccharide obtained from the *Nostoc commune* V. had a brown-amber color (Fig. 1a); the extraction yield was 25% dw. However, Wang *et al.* managed to obtain a much greater yield of 96.7% [24].

X-ray analysis. The X-ray diffractogram (Fig. 1b) showed a broad peak at 20° and a bun-shaped curve, which suggested the non-crystallinity of the exopolysaccharides extracted from cyanobacteria [20]. This result was found consistent because the exopolysaccharide had crystallinity of 38.21% (Fig. 2b).

Thermogravimetry of exopolysaccharides. Figure 1c presents the TG thermogravimetric curve of the exopolysaccharide with mass losses assigned to the following thermal events: dehydration, depolymerization, degradation, and carbonization [20]. Table 1 shows the percentage of mass loss in each thermal event, with their respective temperature intervals.

FTIR of exopolysaccharides. Figure 1d illustrates the FTIR spectrum of the exopolysaccharide sample. The spectrum showed signals at 3325 cm^{-1} (hydroxyl groups), 2923 cm^{-1} (C-H vibrational stretch), 1586 cm^{-1} (asymmetric stretching of $-\text{COO}^-$), 1416 cm^{-1} (symmetric stretching of $-\text{COO}^-$), 1019 cm^{-1} (C-O-C vibrational stretch in cyclic glucose units), 889 cm^{-1} (β -glycosidic bond), and 795 cm^{-1} (glucopyranose units) [3, 25].

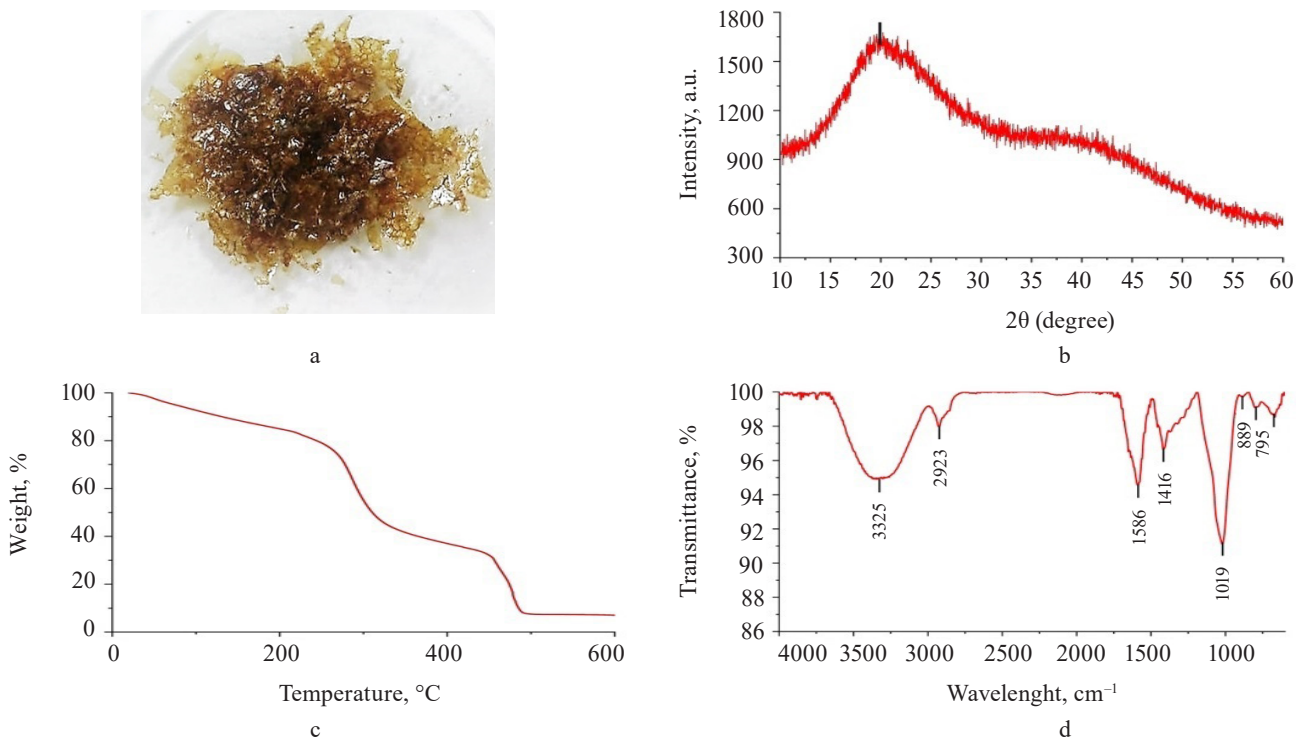


Figure 1 Extracted sample (a); XRD diffractogram (b); TG curve (c); and FTIR spectrum (d) of exopolysaccharide from *Nostoc commune*

Table 1 Mass loss values: thermogravimetric analysis of exopolysaccharide obtained from *Nostoc commune*

Weight, mg	Thermal event	ΔT , °C	Mass loss, %
4.965	Dehydration	20.0–186.0	14.1
	Depolymerization	186.0–413.0	49.9
	Degradation	413.0–558.0	28.8
	Carbonization	558.0–600.0	2.8

Table 2 Mass loss values: thermogravimetric analysis of exopolysaccharide-based composite hydrogels

Weight, mg	Thermal event	ΔT , °C	Mass loss, %
5.297	Dehydration	30.0–150.0	1.5
	Degradation	150.0–440.5	88.9
	Carbonization	440.5–600.0	3.3

Exopolysaccharide-based composite hydrogel profile. Exopolysaccharide-based composite hydrogels had crystallinity of 48.95% (Fig. 2a). The XRD diffractogram (Fig. 2b) showed peaks close to 15 and 22°, which corresponded to the gelatinized starch chains [26]. On the other hand, a peak around 34° corresponded to the crystalline structure of pectin [27]. However, the broad peak at 20°, which corresponded to the exopolysaccharides, disappeared, probably because the exopolysaccharide structure was destroyed.

Figure 2c presents the TG thermogravimetric curve of compound hydrogels with mass losses assigned to the stages of dehydration, degradation, and carbonization. According to Dash *et al.*, the second stage consists of

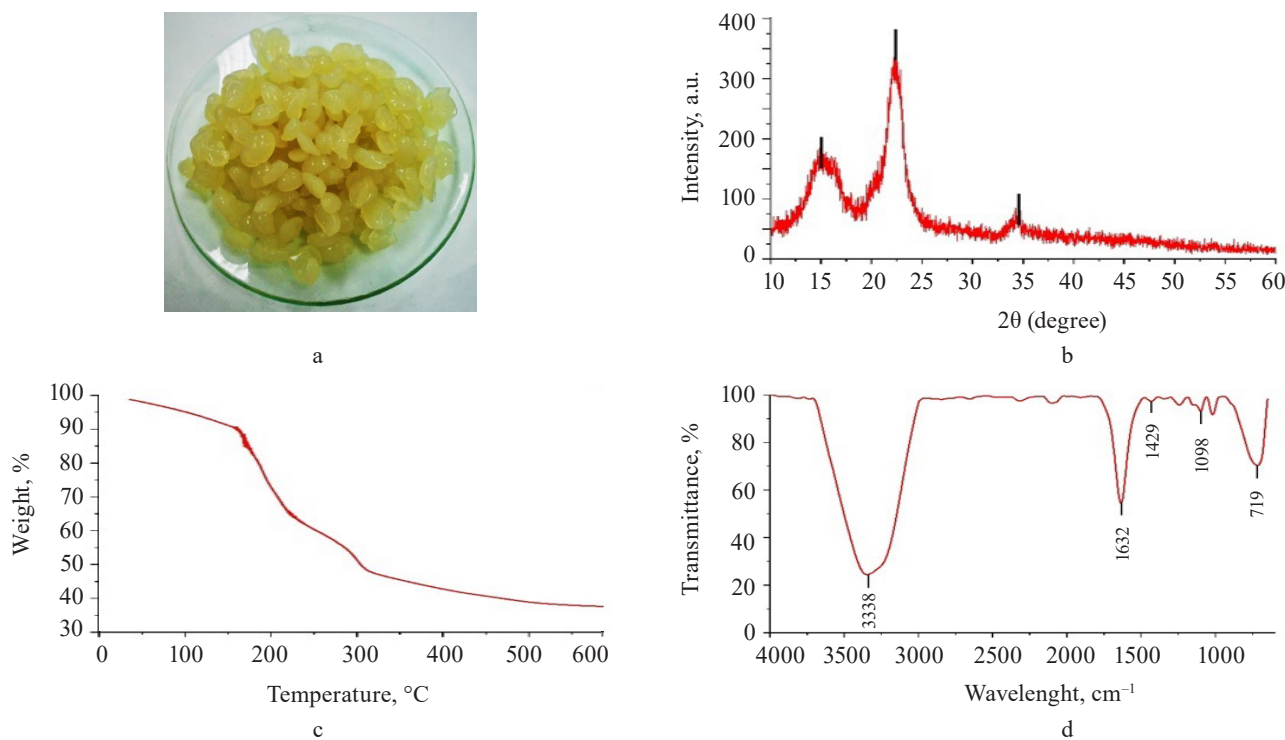
two continuous processes that follow pectin (200–280°C) and starch (290–425°C) degradation [28]. Table 2 shows the percentage of mass loss in each thermal event with their respective temperature intervals.

The FTIR spectrum of the hydrogels (Fig. 2d) shows additional signals to the spectrum of the exopolysaccharide (Fig. 1d). These signals corresponded to the C=O carbonyl group (1632 cm^{-1}) for pectin, while the peaks at 1429 and 1098 cm^{-1} could be attributed to C-O-O stretching and C-O-H bending modes in starch, respectively, and the signal at 719 cm^{-1} could be correlated with vibrations belonging of the polysaccharide ring [29–31].

The specific surface area of the composite hydrogel, as obtained from the BET isotherm model, was 0.5616 m^2/g . Figure 3 shows the N_2 adsorption-desorption process of the hydrogel before methylene blue scavenging. This process was a type VI isotherm, which is typical of solids with a uniform non-porous surface and represents a multilayer adsorption [31].

After the removal process, the composite hydrogels turned blue (Fig. 4a). Figure 4b shows a decrease in the band at 1632 cm^{-1} . However, the increase in pH to basic levels intensified the bands: at pH 11, the removal process probably occurred by electrostatic attraction [32, 33].

The SEM images of the hydrogels revealed the superficial changes in these materials during the methylene blue scavenging at different pH values. At pH 5 (Fig. 5b), the surface of the hydrogel became smoother and more homogeneous, compared to the hydrogel

**Figure 2** Samples (a); XRD diffractogram (b); TG curve (c); and FTIR spectrum (d) of exopolysaccharide-based composite hydrogel

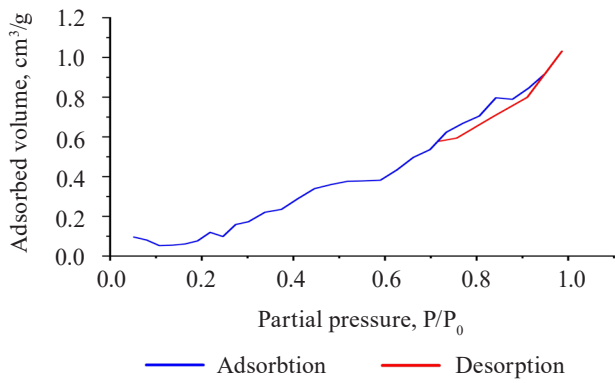


Figure 3 BET sorption-desorption isotherms for the exopolysaccharide-based composite hydrogel

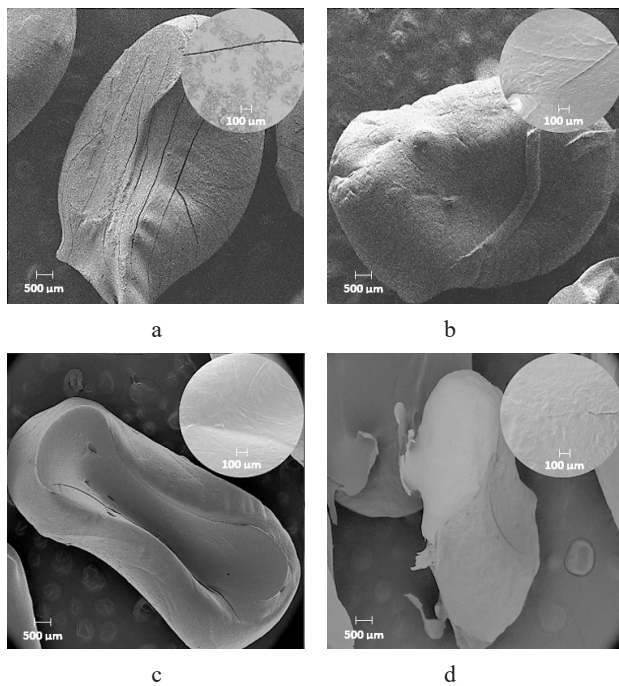


Figure 5 SEM images of hydrogels before (a) and after methylene blue removal at pH 5 (b), pH 8 (c), and pH 11 (d)

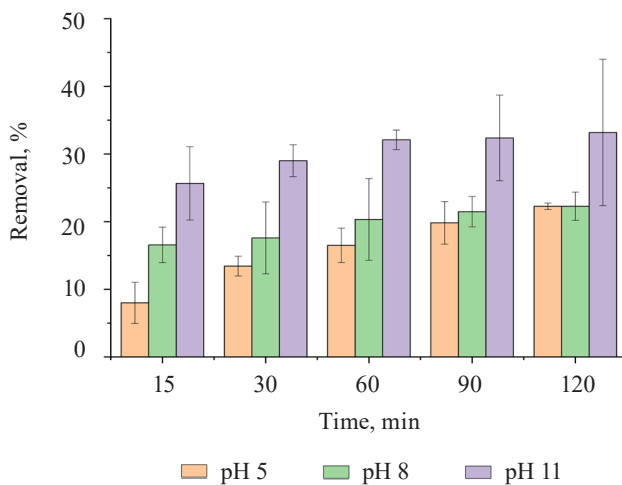


Figure 6 Methylene blue removal percentages at different pH and time values

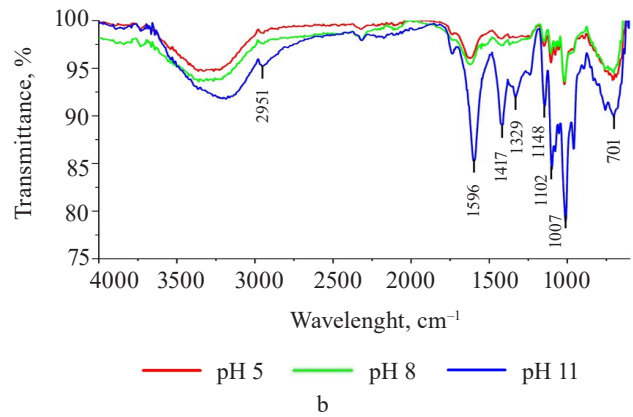
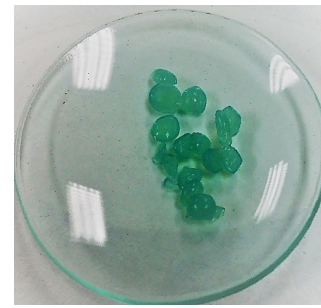


Figure 4 Samples (a) and FTIR spectrum (b) of exopolysaccharide-based composite hydrogel after methylene blue removal

before scavenging (Fig. 5a). At pH 8 (Fig. 5c), the hydrogel improved its surface homogeneity but changed shape. The same pattern occurred at pH 11 (Fig. 5d).

Methylene blue percentage removal. Figure 6 shows an increase in methylene blue scavenging at a basic pH value (pH 11) for 120 min. The increase could be explained by the more negative charge on the adsorbent surface, which generated a greater electrostatic attraction with the positively charged adsorbate [34]. Table 3 summarizes the methylene blue removal percentages at different pH levels and processing times.

Kinetic adsorption models. The pseudo-first-order, pseudo-second-order, and Elovich kinetic models were used to verify the experimental data (Fig. 7). Table 4 shows the values of the constants for the different kinetic models.

The pseudo-second-order model showed a higher R^2 value in the scavenging processes at pH 8 and pH 11. On the other hand, the Elovich model demonstrated a higher value at pH 5. Apparently, the mechanism of methylene blue sorption at pH 8 and pH 11 was caused by chemisorption. At pH 5, the surface of the hydrogel was heterogeneous, which was in line with Fig. 5b [35].

Adsorption isotherm models. We employed the Langmuir, Freundlich, and Temkin isotherms to verify the experimental data (Fig. 8). Table 5 shows the values that correspond to the adsorption isotherm models.

Negative R_L values were obtained from methylene blue removal at different pH values. At the three

Table 3 Methylene blue percentage removal and adsorption capacity

Time, min	pH	Initial methylene blue concentration, mg/L	Adsorption capacity, mg/g	Methylene blue removal, %
15	5	1.045×10^{-6}	4.669×10^{-7}	8.00
	8	1.014×10^{-6}	4.070×10^{-7}	16.57
	11	1.019×10^{-6}	3.623×10^{-7}	25.66
30	5	1.151×10^{-6}	4.817×10^{-7}	13.44
	8	1.117×10^{-6}	4.520×10^{-7}	17.59
	11	1.146×10^{-6}	4.067×10^{-7}	29.02
60	5	1.275×10^{-6}	5.054×10^{-7}	16.50
	8	1.209×10^{-6}	4.698×10^{-7}	20.34
	11	1.226×10^{-6}	4.231×10^{-7}	32.11
90	5	1.394×10^{-6}	5.587×10^{-7}	19.83
	8	1.286×10^{-6}	5.131×10^{-7}	21.48
	11	1.358×10^{-6}	4.936×10^{-7}	32.38
120	5	1.459×10^{-6}	6.054×10^{-7}	22.28
	8	1.429×10^{-6}	5.917×10^{-7}	22.28
	11	1.469×10^{-6}	5.503×10^{-7}	33.18

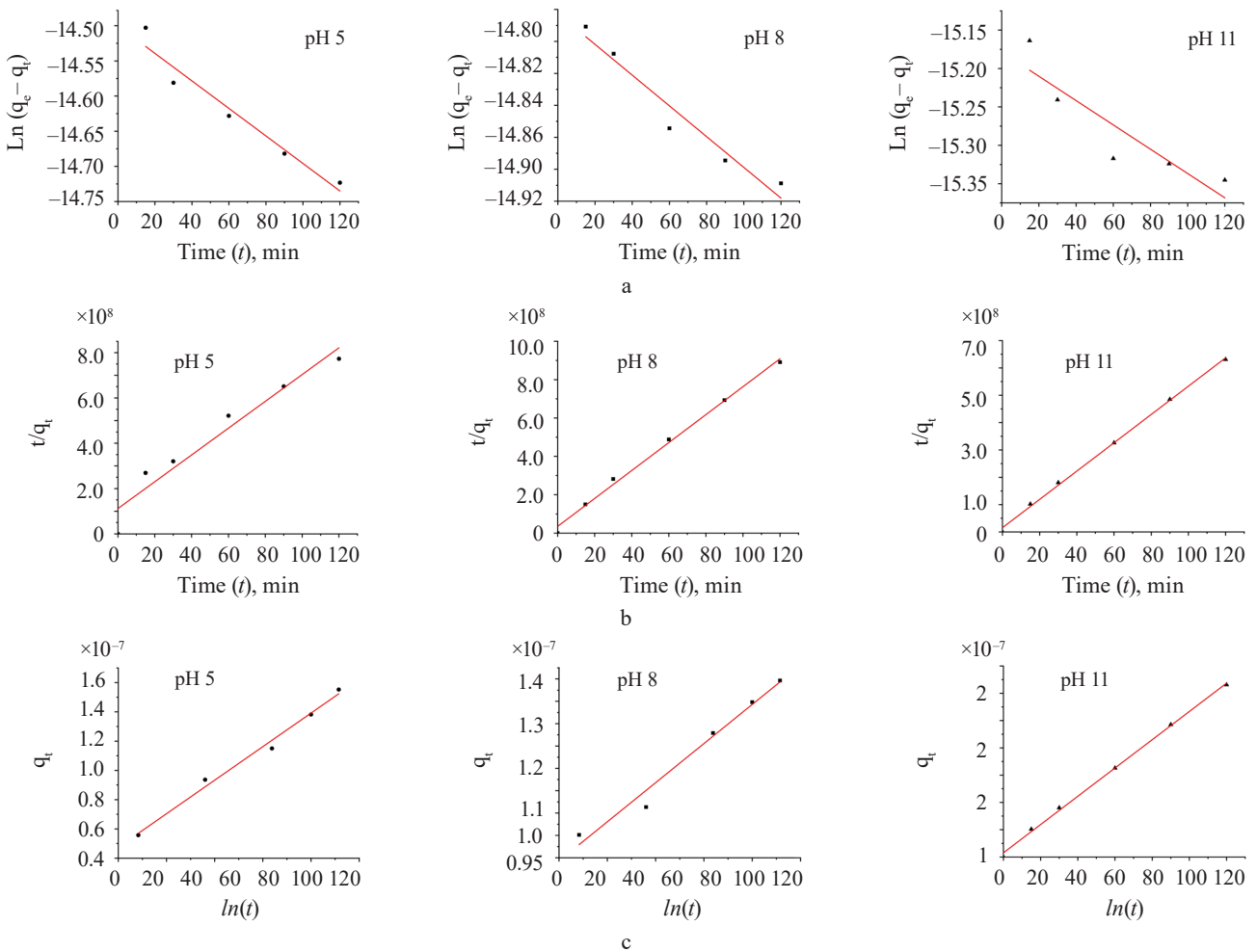


Figure 7 Linear plots for methylene blue adsorption: pseudo-first-order model (a); pseudo-second-order model (b); and Elovich kinetic model (c)

pH levels, the methylene blue removal did not fit the Langmuir isotherm [36, 37]. However, the adsorption intensity ($1/n$) in all the treatments was below one, which suggested that the active centers had less and less free enthalpy [38]. The b_T values were negative, so

the adsorption process in all the treatments were endothermic [39]. The results indicated a good fit (R^2) with the Temkin model; therefore, this model explained the adsorption process between the adsorbate and the adsorbent.

Table 4 Parameter values of methylene blue removal: kinetic studies

pH value	Kinetic model	R ²	K ₁	K ₂	α, mg/g/min	β, g/mg
pH 5	Pseudo-first-order	0.9331	-1.633×10 ⁻⁵	/	/	/
	Pseudo-second-order	0.9257	/	3.120×10 ⁵	/	/
	Elovich	0.9857	/	/	2.180×10 ⁷	1.059×10 ⁻⁸
pH 8	Pseudo-first-order	0.9324	-8.017×10 ⁻⁶	/	/	/
	Pseudo-second-order	0.9942	/	1.516×10 ⁶	/	/
	Elovich	0.9708	/	/	5.715×10 ⁷	3.147×10 ⁻⁷
pH 11	Pseudo-first-order	0.7549	-1.317×10 ⁻⁵	/	/	/
	Pseudo-second-order	0.9980	/	1.724×10 ⁶	/	/
	Elovich	0.9464	/	/	4.824×10 ⁷	1.911×10 ⁻⁶

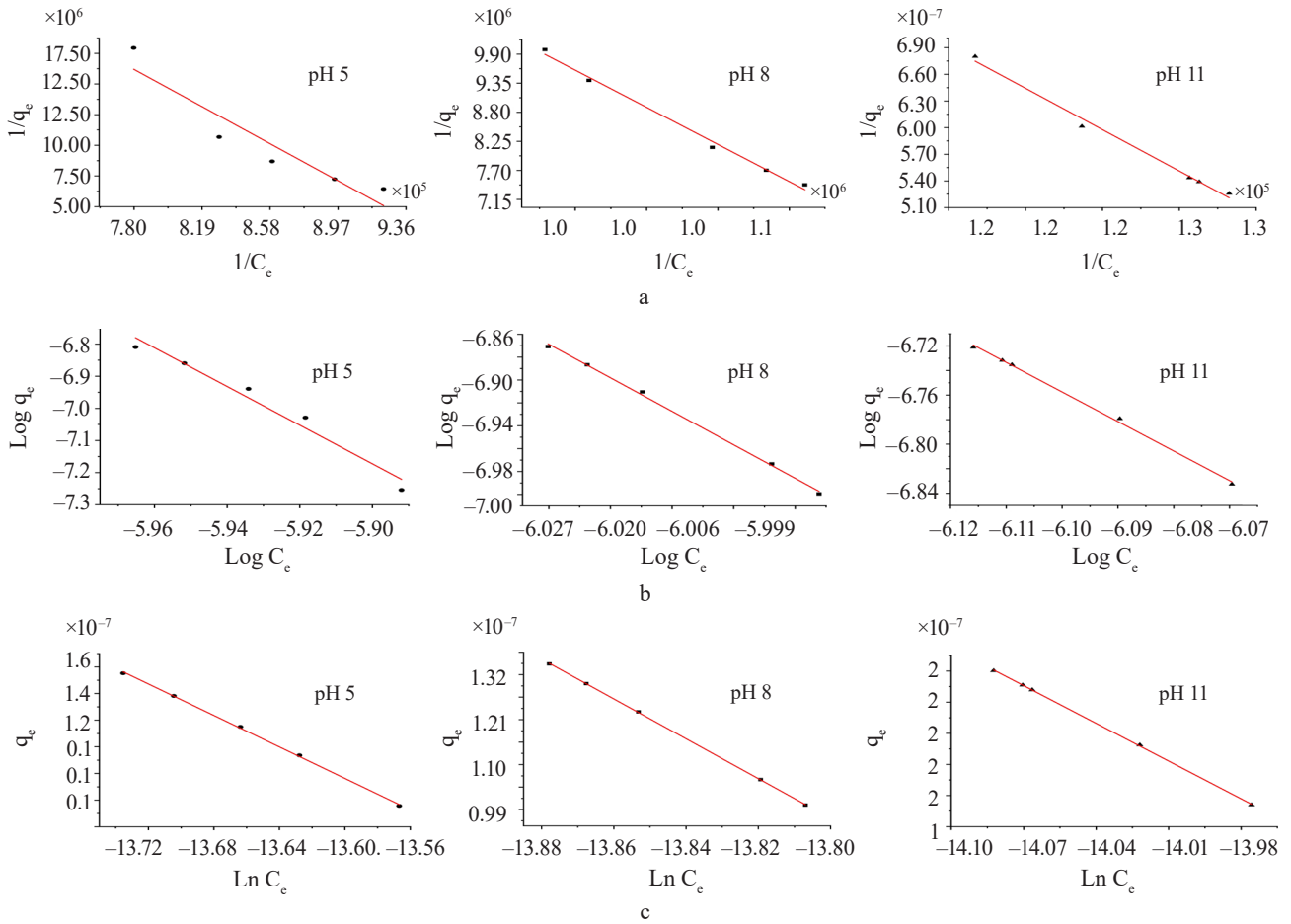


Figure 8 Linear plots for methylene blue adsorption: Langmuir model (a); Freundlich model (b); and Temkin model (c)

Table 5 Parameter values of methylene blue removal: adsorption studies

Type of isotherm	Parameters	Methylene blue removal		
		pH 5	pH 8	pH 11
Langmuir	K _L , L/mg	-9.89×10 ⁵	-1.273×10 ⁶	-1.753×10 ⁶
	q _{max} , mg/g	1.30×10 ⁻⁸	2.234×10 ⁻⁸	4.898×10 ⁻⁸
	R _L	-2.65	-1.86	-0.99
	R ²	0.8495	0.9912	0.9893
Freundlich	K _F , mg/g	2.09×10 ⁻⁴³	8.30×10 ⁻³³	3.51×10 ⁻²²
	1/n	-6.02	-4.18	-2.41
	R ²	0.9587	0.9978	0.9973
Temkin	K _m , L/g	7.08×10 ⁵	8.07×10 ⁵	8.15×10 ⁵
	b _T , J/mol	-5.901×10 ⁻⁷	-4.871×10 ⁻⁷	-4.04×10 ⁻⁷
	R ²	0.9991	0.9999	0.9997

CONCLUSION

Exopolysaccharides from *Nostoc commune* V. yielded composite hydrogels that could act as methylene blue scavengers. These materials had a non-porous and heterogeneous surface, which underwent changes at basic pH values during the removal process. The methylene blue adsorption mechanism depended on chemisorption and endothermic processes. The maximal removal was 33.18%, which proved that these composite hydrogels were not efficient as methylene blue scavengers. The result open pros-

pects for further research of exopolysaccharides with other adsorption materials.

CONTRIBUTION

The authors were equally involved in writing the manuscript and are equally responsible for any potential plagiarism.

CONFLICT OF INTEREST

The authors declare no conflict of interests regarding the publication of this article.

REFERENCES


1. Laroche C. Exopolysaccharides from microalgae and cyanobacteria: Diversity of strains, production strategies, and applications. *Marine Drugs*. 2022;20(5). <https://doi.org/10.3390/md20050336>
2. Miguel SP, Ribeiro MP, Otero A, Coutinho P. Application of microalgae and microalgal bioactive compounds in skin regeneration. *Algal Research*. 2021;58. <https://doi.org/10.1016/j.algal.2021.102395>
3. Montero X, Alves A, Ribeiro MP, Lazari M, Coutinho P, Otero A. Biochemical characterization of *Nostoc* sp. exopolysaccharides and evaluation of potential use in wound healing. *Carbohydrate Polymers*. 2021;254. <https://doi.org/10.1016/j.carbpol.2020.117303>
4. Gonzales KN, Troncoso OP, Torres FG, López D. Molecular α -relaxation process of exopolysaccharides extracted from *Nostoc commune* cyanobacteria. *International Journal of Biological Macromolecules*. 2020;161:1516–1525. <https://doi.org/10.1016/j.ijbiomac.2020.07.268>
5. Paulino AT, Guilherme MR, Reis AV, Campese GM, Muniz EC, Nozaki J. Removal of methylene blue dye from an aqueous media using superabsorbent hydrogel supported on modified polysaccharide. *Journal of Colloid and Interface Science*. 2006;301(1):55–62. <https://doi.org/10.1016/j.jcis.2006.04.036>
6. Shah SS, Ramos B, Teixeira ACSC. Adsorptive removal of methylene blue dye using biodegradable superabsorbent hydrogel polymer composite incorporated with activated charcoal. *Water*. 2022;14(20). <https://doi.org/10.3390/w14203313>
7. Varghese SA, Rangappa SM, Siengchin S, Parameswaranpillai J. Natural polymers and the hydrogels prepared from them. In: Chen Y, editor. *Hydrogels based on natural polymers*. Elsevier; 2020. pp. 17–47. <https://doi.org/10.1016/b978-0-12-816421-1.00002-1>
8. Shooto ND, Nkutha CS, Guilande NR, Naidoo EB. Pristine and modified mucuna beans adsorptive studies of toxic lead ions and methylene blue dye from aqueous solution. *South African Journal of Chemical Engineering*. 2020;31:33–43. <https://doi.org/10.1016/j.sajce.2019.12.001>
9. Hong G-B, Yu T-J, Lee H-C, Ma C-M. Using rice bran hydrogel beads to remove dye from aqueous solutions. *Sustainability*. 2021;13(10). <https://doi.org/10.3390/su13105640>
10. Drozdova MYu, Pozdnyakova AV, Osintseva MA, Burova NV, Minina VI. The microorganism-plant system for remediation of soil exposed to coal mining. *Foods and Raw Materials*. 2021;9(2):406–418. <https://doi.org/10.21603/2308-4057-2021-2-406-418>
11. Ren J, Wang X, Zhao L, Li M, Yang W. Effective removal of dyes from aqueous solutions by a gelatin hydrogel. *Journal of Polymers and the Environment*. 2021;29:3497–3508. <https://doi.org/10.1007/s10924-021-02136-z>
12. Hussain S, Khan N, Gul S, Khan S, Khan H. Contamination of water resources by food dyes and its removal technologies. In: Eyvaz M, Yüksel E, editors. *Water chemistry*. IntechOpen; 2019. <https://doi.org/10.5772/intechopen.90331>
13. Sane PK, Tambat S, Sontakke S, Nemade P. Visible light removal of reactive dyes using CeO₂ synthesized by precipitation. *Journal of Environmental Chemical Engineering*. 2018;6(4):4476–4489. <https://doi.org/10.1016/j.jece.2018.06.046>
14. Mansor ES, Ali H, Abdel-Karim A. Efficient and reusable polyethylene oxide/polyaniline composite membrane for dye adsorption and filtration. *Colloid and Interface Science Communications*. 2020;39. <https://doi.org/10.1016/j.colcom.2020.100314>
15. Wang J, Zhang T, Mei Y, Pan B. Treatment of reverse-osmosis concentrate of printing and dyeing wastewater by electro-oxidation process with controlled oxidation-reduction potential (ORP). *Chemosphere*. 2018;201:621–626. <https://doi.org/10.1016/j.chemosphere.2018.03.051>

16. Nayak S, Prasad SR, Mandal D, Das P. Carbon dot cross-linked polyvinylpyrrolidone hybrid hydrogel for simultaneous dye adsorption, photodegradation and bacterial elimination from waste water. *Journal of Hazardous Materials*. 2020;392. <https://doi.org/10.1016/j.jhazmat.2020.122287>
17. Ammari Y, El Atmani K, Bay L, Bakas I, Qourzal S, Ait Ichou I. Elimination of a mixture of two dyes by photocatalytic degradation based on TiO₂ P-25 Degussa. *Materials Today: Proceedings*. 2020;22:126–129. <https://doi.org/10.1016/j.matpr.2019.08.142>
18. ALSamman MT, Sánchez J. Recent advances on hydrogels based on chitosan and alginate for the adsorption of dyes and metal ions from water. *Arabian Journal of Chemistry*. 2021;14(12). <https://doi.org/10.1016/j.arabjc.2021.103455>
19. Elhady MA, Mousaa IM, Attia RM. Preparation of a novel superabsorbent hydrogel based on polyacrylic acid/shellac using gamma irradiation for adsorption removal of malachite green dye. *Polymers and Polymer Composites*. 2022;30. <https://doi.org/10.1177/09673911221074435>
20. Rodriguez S, Torres FG, López D. Preparation and characterization of polysaccharide films from the cyanobacteria *Nostoc commune*. *Polymers from Renewable Resources*. 2017;8(4):133–150. <https://doi.org/10.1177/204124791700800401>
21. Dafe A, Etemadi H, Dilmaghani A, Mahdavinia GR. Investigation of pectin/starch hydrogel as a carrier for oral delivery of probiotic bacteria. *International Journal of Biological Macromolecules*. 2017;97:536–543. <https://doi.org/10.1016/j.ijbiomac.2017.01.060>
22. Hii HT. Adsorption isotherm and kinetic models for removal of methyl orange and Remazol brilliant blue R by coconut shell activated carbon. *Tropical Aquatic and Soil Pollution*. 2021;1(1):1–10. <https://doi.org/10.53623/tasp.v1i1.4>
23. Kalam S, Abu-Khamsin SA, Kamal MS, Patil S. Surfactant adsorption isotherms: A review. *ACS Omega*. 2021;6(48):32342–32348. <https://doi.org/10.1021/acsomega.1c04661>
24. Wang H-B, Wu S-J, Liu D. Preparation of polysaccharides from cyanobacteria *Nostoc commune* and their antioxidant activities. *Carbohydrate Polymers*. 2014;99:553–555. <https://doi.org/10.1016/j.carbpol.2013.08.066>
25. Dubessay P, Andhare P, Kavitate D, Shetty PH, Ursu AV, Delattre C, et al. Microbial glucuronans and succinoglycans. In: Oliveira JM, Radhouani H, Reis RL, editors. *Polysaccharides of microbial origin*. Cham: Springer; 2021. pp. 1–23. https://doi.org/10.1007/978-3-030-35734-4_8-1
26. Abd El-Ghany NA, Mahmoud ZM. Synthesis, characterization and swelling behavior of high-performance antimicrobial amphoteric hydrogels from corn starch. *Polymer Bulletin*. 2020;78(1):6161–6182. <https://doi.org/10.1007/s00289-020-03417-8>
27. Sani IK, Geshlaghi SP, Pirsas S, Asdagh A. Composite film based on potato starch/apple peel pectin/ZrO₂ nanoparticles/microencapsulated *Zataria multiflora* essential oil; investigation of physicochemical properties and use in quail meat packaging. *Food Hydrocolloids*. 2021;117. <https://doi.org/10.1016/j.foodhyd.2021.106719>
28. Dash KK, Ali NA, Das D, Mohanta D. Thorough evaluation of sweet potato starch and lemon-waste pectin based-edible films with nano-titania inclusions for food packaging applications. *International Journal of Biological Macromolecules*. 2019;139:449–458. <https://doi.org/10.1016/j.ijbiomac.2019.07.193>
29. Nsom MV, Etape EP, Tendo JF, Namond BV, Chongwain PT, Yufanyi MD, et al. A green and facile approach for synthesis of starch-pectin magnetite nanoparticles and application by removal of methylene blue from textile effluent. *Journal of Nanomaterials*. 2019;2019. <https://doi.org/10.1155/2019/4576135>
30. Guo X, Duan H, Wang C, Huang X. Characteristics of two calcium pectinates prepared from citrus pectin using either calcium chloride or calcium hydroxide. *Journal of Agricultural and Food Chemistry*. 2014;62(27):6354–6361. <https://doi.org/10.1021/jf5004545>
31. Sing KSW, Everett DH, Haul RAW, Moscou L, Pierotti RA, Rouquérol J, et al. Reporting physisorption data for gas/solid systems with special reference to the determination of surface area and porosity (Recommendations 1984). *Pure and Applied Chemistry*. 1985;57(4):603–619. <https://doi.org/10.1351/pac198557040603>
32. Veisi Z, Gallant ND, Alcantar NA, Toomey RG. Responsive coatings from naturally occurring pectin polysaccharides. *Colloids and Surfaces B: Biointerfaces*. 2019;176:387–393. <https://doi.org/10.1016/j.colsurfb.2018.12.060>
33. Arayaphan J, Maijan P, Boonsuk P, Chantarak S. Synthesis of photodegradable cassava starch-based double network hydrogel with high mechanical stability for effective removal of methylene blue. *International Journal of Biological Macromolecules*. 2021;168:875–886. <https://doi.org/10.1016/j.ijbiomac.2020.11.166>
34. Pathania D, Sharma S, Singh P. Removal of methylene blue by adsorption onto activated carbon developed from *Ficus carica* bast. *Arabian Journal of Chemistry*. 2017;10:S1445–S1451. <https://doi.org/10.1016/j.arabjc.2013.04.021>
35. Sahoo TR, Prelot B. Adsorption processes for the removal of contaminants from wastewater. In: Bonelli B, Freyria FS, Rossetti I, Sethi R, editors. *Nanomaterials for the detection and removal of wastewater pollutants. A volume in micro and nano technologies*. Elsevier; 2020. pp. 161–222. <https://doi.org/10.1016/B978-0-12-818489-9.00007-4>


36. Linde MP, Marquez K. Alkali lignin from rice (*Oryza sativa* L.) husk as adsorbent for aqueous methyl orange and bromothymol blue: Analysis of the adsorption kinetics and mechanism. *Kimika*. 2021;32(1):19–33. <https://doi.org/10.26534/kimika.v32i1.19-33>
37. Asaolu SS, Adefemi SO, Ibigbami OA, Adekeye DK, Olagboye SA. Kinetics, isotherm and thermodynamic properties of the basement complex of clay deposit in Ire-Ekiti southwestern Nigeria for heavy metals removal. *Nature Environment and Pollution Technology an International Quarterly Scientific Journal*. 2020;19(3):897–907. <https://doi.org/10.46488/NEPT.2020.v19i03.001>
38. Ronka S, Bodylska W. Sorption properties of specific polymeric microspheres towards desethyl-terbuthylazine and 2-hydroxy-terbuthylazine: Batch and column studies. *Materials*. 2021;14(11). <https://doi.org/10.3390/ma14112734>
39. Fathy NA, El-Shafey OI, Khalil LB. Effectiveness of alkali-acid treatment in enhancement the adsorption capacity for rice straw: The removal of methylene blue dye. *ISRN Physical Chemistry*. 2013;2013. <https://doi.org/10.1155/2013/208087>


ORCID IDs

Nora Gabriela Herrera  <https://orcid.org/0000-0003-0595-8747>

Nelson Adrián Villacrés  <https://orcid.org/0000-0001-9499-3792>

Lizbeth Aymara  <https://orcid.org/0000-0001-9358-7688>

Viviana Román  <https://orcid.org/0000-0002-6614-3632>

Mayra Ramírez  <https://orcid.org/0000-0002-9143-4060>



Soybean testa spectral study

Olga N. Bugaets^{2,*}, Ivan A. Bugaets¹, Elena A. Kaigorodova², Sergey V. Zelentsov³,
Natalia A. Bugaets¹, Evgeny O. Gerasimenko¹, Elena A. Butina¹

¹ Kuban State Technological University^{ROR}, Krasnodar, Russia

² I.T. Trubilin Kuban State Agrarian University^{ROR}, Krasnodar, Russia

³ V.S. Pustovoit All-Russian Research Institute of Oilseeds^{ROR}, Krasnodar, Russia

* e-mail: obugaec@yandex.ru

Received 12.06.2022; Revised 28.12.2022; Accepted 10.01.2023; Published online 11.07.2023

Abstract:

The increasing production volumes of soy foods require new express methods for testing soybeans during processing and pre-sowing. This study assessed the efficiency of spectral pre-sowing assessment methods using Vilana soybeans.

The research featured soybeans of the Vilana cultivar. The control sample consisted of untreated whole soybeans while the test samples included soybeans pretreated with various modifiers. The methods involved spectrofluorimetry and IR-Fourier spectrometry.

A wide emission band at 400–550 nm corresponded to the fluorescence of the soybean testa. The band at 560–610 nm indicated the presence of such modifiers as Imidor insecticide and Deposit fungicide. The luminescence spectrum of the untreated soybean testa was maximal at 441 nm. The luminescence spectrum of the treated soybean samples was maximal at 446.5 and 585 nm when the excitation wavelength was 362 nm. The fluorescence was studied both spectrally and kinetically to establish the maximal luminescence time and the typical vibration frequencies.

The spectral studies of Vilana soybeans before and after treatment revealed which modifiers were adsorbed on the palisade epidermis and defined the type of interaction between the modifier and the soybean. The spectrofluorimetry and IR spectroscopy proved able to provide a reliable qualitative and quantitative analysis of Vilana soybean surface.

Keywords: Soybeans, Vilana variety, fluorescence, spectroscopy, kinetics, adsorption, chromophore groups, phytochromes, cryptochromes, photoreceptors

Funding: The authors used the equipment of the Research Center for Food and Chemical Technologies. This Collective Use Center at Kuban State Technological University (KUBSTU)^{ROR} (CKP_3111) is supported by the Ministry of Science and Higher Education of the Russian Federation (Minobrnauki)^{ROR} (Agreement N 075-15-2021-679). The research was part of the state task of the Minobrnauki, project no. FZEZ-2020-004.

Please cite this article in press as: Bugaets ON, Bugaets IA, Kaigorodova EA, Zelentsov SV, Bugaets NA, Gerasimenko EO, *et al.* Soybean testa spectral study. *Foods and Raw Materials*. 2024;12(1):47–59. <https://doi.org/10.21603/2308-4057-2024-1-589>

INTRODUCTION

Soy is a unique agricultural crop because its beans are extremely rich in native proteins and saturated fats. In fact, soybeans are superior to cereals, oilseeds, and legumes in terms of protein content and essential amino acids [1–4]. The food industry highly appreciates their plasticity, high enzymatic activity, therapeutic effect, and prophylactic properties.

According to the Oil World, 2021/22 saw an increase in the global soybean production. The Food and Agriculture Organization of the United Nations even developed the Soybean Information and Research Act

(<http://www.fao.org/3/bs958e/bs958e.pdf>). This document provides quality indicators for national soybean production. It also introduces a research program that aims at increasing production volumes, expanding domestic and foreign soybean markets, and popularizing soy products in the human diet.

New high-tech soybean production processes require new research methods. Pre-sowing treatment needs special control since it affects the yield. Other important methods include risk assessment and pre-calculation of maximal amounts of pesticide residue in soybean products [5].

Seeds maintain the viability of the embryo and preserve nutrients. However, the embryo protection is not the only function of the seed coat: it also affects seed germination. In soybeans, the testa and hilum are covered with two layers of palisade epidermis and wax. Agricultural soybean varieties have a thick palisade layer. Apparently, the chemical composition, location, and size of palisade cells delay swelling. The soybean testa contains 6.0% of protein, 2.7% fat, 34.3% fiber, 32.3% nitrogen-free extractives, and 10.6% ash. Soybeans include 13.0–21.7% of oils and 36.0–45.0% of protein. The activity of their trypsin inhibitors is 22.4 mg/g while the moisture content is 6.9–8.0% [6].

Soybean testa consists of metamorphosed integuments which form a narrow canal called micropyle. The part of the ovule opposite the micropyle is called the chalase. The chalazal part is responsible for tissue cells, or hypostasis, and their membranes are highly reflective. Flavones and flavonols absorb light in a shorter wavelength spectrum (280–320 nm) than anthocyanins. As a result, flavones and flavonols protect plant tissues, especially epidermis, from ultraviolet radiation. Phytochromes, cryptochromes, and phototropins are the most important photoreceptors of all the photomorphogenesis pigments because they absorb red and blue light. Cryptochromes and phototropins are blue light receptors. Cryptochromes consist of apoprotein and two chromophores, namely, pterin and flavin. Apoprotein has a high degree of homology with photolyase enzymes involved in the light-dependent DNA repair. The absorption spectrum of cryptochromes is ultraviolet (320–390 nm) and blue (390–500 nm), partially including green. The absorption region depends on the pterin chromophore functional group [7, 8].

Optical methods provide the most effective ways to control seeds and predict the optimal harvest time [9–11]. Luminescence and IR spectroscopy are environmentally friendly, non-destructive, remote, and fast. They are known for their high-precision and a wide variety of sampling options.

Photoluminescent devices that provide express diagnostics of ripeness, humidity, and germination are accurate and employ photodiodes or LEDs, depending on the test objective [12, 13]. Zelentsov *et al.* developed calibration models for MATRIX IR analyzers to monitor protein, oil, moisture, and trypsin inhibitor activity in laboratory soybeans [6]. The models gave satisfactory results and saved valuable selection material. To expand the spectrofluorimetric and IR-Fourier spectroscopic methods of seed control, scientists need new calibration models for different soybean varieties, as well as tailored equipment.

Agriculturists determine the pre-sowing seed quality and plan their chemical treatment by comparing the spectral profile of the seed testa of untreated and treated soybeans.

The research objective was to use spectral analysis, i.e., luminescence and IR spectroscopy, to assess the quality of Vilana soybean pre-sowing treatment.

The research involved the following tasks:

- determining the quality of pre-sowing treatment of Vilana soybeans with various modifiers;
- identifying the functional groups of modifiers on the palisade epidermis;
- studying the spectral profiles of untreated and experimental soybeans; and
- developing recommendations for spectral calibration models to assess soybean quality indicators and increase the yield.

STUDY OBJECTS AND METHODS

The soybeans of the Vilana cultivar were provided by the soybean department of the V.S. Pustovoit All-Russian Research Institute of Oilseeds (Krasnodar, Russia). This mid-season variety is highly productive and stress-resistant; it contains 40.8% of protein. Its yield is 2.5–3.0 tons/ha, which can reach 4.9–5.7 tons/ha if the moisture level is optimal. The plant has some gray floccose, the corolla of the flower is purple, and the bean folds are brown. The testa is yellow and dull, with no pigmentation. The hilum is medium, oval-elongated, and light brown [11].

For protection purposes, soybeans are treated with various chemical compounds before planting [14, 15]. We treated the Vilana soybeans with a mix of chemical and biological substances. It included insecticide Imidor, fungicide Deposit, fertilizer Rhizoform, and sticking agent Static. The procedure followed the one described in [16, 17]. Imidor is imidacloprid [4,5-dihydro-N-nitro-1-[(6-chloro-3-pyridyl)-methyl]-imidazolidin-2-yl-ene-amine] with neonicotinoid as the chemical active substance [18]. Deposit is a microemulsion that consists of 40 g/dm³ of fludioxonil [4-(2,2-difluoro-1,3-benzodioxol-4-yl)-pyrrole-3-carboxylic acid], 40 g/dm³ of [(±)-1-(β-allyloxy-2,4-dichlorophenylethyl)imidazole], and 30 g/dm³ of metalaxyl [methyl N-(methoxyacetyl)-N-(2,6-xylyl)-DL-alaninate]. Rhizoform is a liquid inoculant of *Bradyrhizobium japonicum* (2–3×10⁹ CFU/cm³). Rhizoform (<https://betaren.ru/catalog/spetsialnye-udobreniya/mikrobiologicheskie-preparaty/rizoform-soya>) always goes with Static, a stabilizer and sticking agent, which ensures the safety of viable bacteria on the surface of beans for up to 21 days. Static is a preservative that contains 0.5% of carbohydrates, 0.1% salts, and 100 cm³ water at pH 6.5–7.4.

To identify the spectral changes, we studied the luminescence parameters of the soybean testa in the untreated (control) samples and the experimental samples treated with separate modifiers and their mixes. Spectrofluorimetry involved the PanoramaPro software at 380–690 nm and copied the method described by Belyakov in [19], which was developed for a Fluorat-02-panorama spectrofluorimeter (Lumex-Marketing, Russia).

We interpreted the spectral bands of separate chemicals and their mixes to identify the vibration bands of each group on the surface of the biological object treated with a chemical mix. To reveal the

vibration bands of water, protein, starch, and fat, we studied the spectra of ground soybeans and the surface of untreated soybeans. Grinding and the IR spectroscopy were in line with State Standard R 53600-2009. The spectral studies followed the recommendations developed by the Agilent Food Testing & Agriculture LinkedIn in the spectral range between 350 and 7000 cm^{-1} using an Agilent Cary 630 FTIR spectrometer (Agilent Technologies, USA) [10].

RESULTS AND DISCUSSION

Spectrofluorimetry of soybeans. To register luminescence, we studied the spectral characteristics of luminescence excitation for a wide spectral range (Table 1, Figs. 1 and 2). Table 1 describes the excitation spectrum.

When the excitation length λ_c was 362 nm, the luminescence spectra of the untreated (control) soybean

testa demonstrated a typical wide luminescence band at 400–550 nm, which corresponded to the fluorescence of the soybean testa.

Table 2 shows the spectrum of the untreated soybeans.

In addition to the main maximum of the luminescence band at $\lambda_{f \max}$ 441 nm and intensity $I_f(\lambda)_{\max}$ 2.97 RU, the research revealed a minor shoulder at ~ 510 nm (Fig. 3).

The luminescence spectra of the whole soybean testa treated with a mix of modifiers (Fig. 4) also showed a typical wide luminescence band at 400–550 nm, which corresponded to the fluorescence of the soybean testa with a maximum $\lambda_{f1 \max}$ 446.5 nm and intensity $I_f(\lambda)_{1 \max}$ 2.48 RU. A second luminescence band of lower intensity appeared at 557–610 nm with a maximum at $\lambda_{f2 \max}$ 585 nm and $I_f(\lambda)_{2 \max}$ 1.19 RU, which matched the fluorescence of one adsorbed modifier.

The treated (experimental) seeds showed the following spectral changes: a 5-nm Stokes shift, a 5-nm bathochromic shift of the main peak, and a lower intensity of the main fluorescence peak. In addition, the shoulder at the main maximum disappeared at 510 nm, and a luminescence band of lower intensity appeared in the long-wavelength part of the spectrum (Table 3).

To reveal the luminescence of the modifiers, we treated the soybeans with each component of the mix separately, in line with the procedure described in [17] (Tables 4 and 5).

Table 1 Luminescence excitation spectra

Excitation spectrum, nm	Excitation wave intensity $I_c(\lambda)_{\max}$, RU	Excitation wavelength $\lambda_{c \max}$, nm	Registration wavelength, λ_{reg} , nm
240–430	2.54	362	445
	2.94	375	
	2.93	380	
308–430	1.18	362	585
	1.19	365	
	0.95	380	

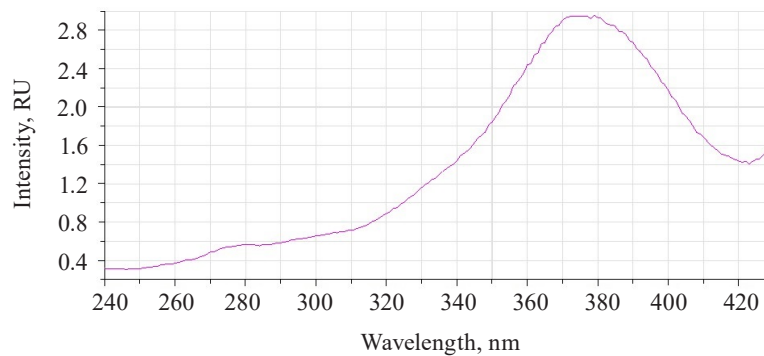


Figure 1 Excitation spectra at a registration wavelength of 445 nm

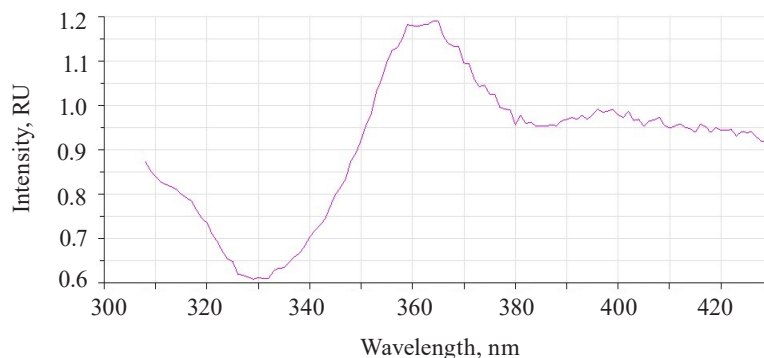


Figure 2 Excitation spectra at a registration wavelength of 585 nm

Table 2 Control Vilana soybean spectra

Excitation wavelength $\lambda_{e\max}$, nm	Stokes shift $\Delta\lambda$, nm	Luminescence wavelength $\lambda_{f\max}$, nm	Luminescence intensity $I_f(\lambda)_{\max}$, RU	Luminescence spectrum, nm
362	79	441	2.97	400–550

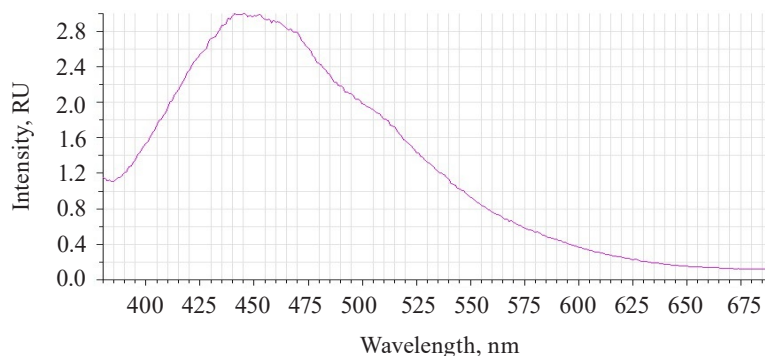


Figure 3 Luminescence spectra of untreated (control) whole soybean testa

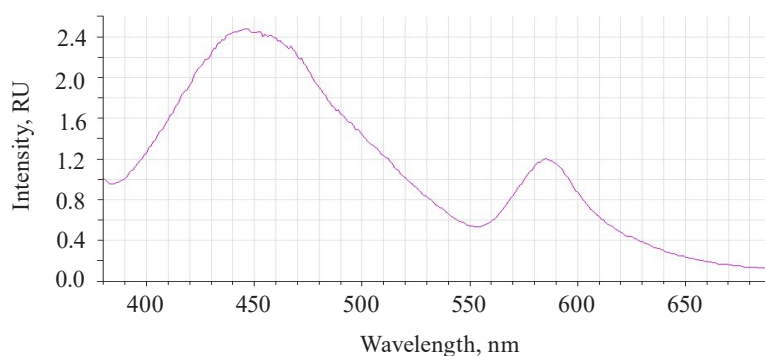


Figure 4 Luminescence spectra of soybean testa treated with various modifiers

Table 3 Experimental Vilana soybean spectra

Excitation wavelength $\lambda_{e\max}$, nm	Stokes shift $\Delta\lambda$, nm	Luminescence wavelength $\lambda_{f\max}$, nm	Luminescence intensity $I_f(\lambda)_{\max}$, RU	Luminescence wavelength	Luminescence intensity	Luminescence spectrum	
				$\lambda_{f\max}$, nm	$I_f(\lambda)_{\max}$, RU	λ_{f1} , nm	λ_{f2} , nm
362	84	446.5	2.48	585	1.19	390–550	560–615

Figures 5–8 show the luminescence spectra of the treated soybean samples.

The luminescence spectrum of the soybeans treated with Imidor showed two bands of different intensity (Fig. 5).

The first main band at 390–530 nm had a maximum at $\lambda_{f1\max}$ 445 nm, which corresponded to the luminescence of the testa. Relative to the mix-treated sample, the intensity of the main band decreased by 0.512 RU, the hypsochromic shift was 1.5 nm, and the Stokes shift reduced by 4 nm (Table 4).

The second band at 560–620 nm had a maximum at $\lambda_{f2\max}$ 585 nm, which corresponded to the Imidor luminescence. The maximum value of the second spectral band of the soybeans treated with a mix of modifiers coincided with that of the sample treated with Imidor.

The luminescence spectrum of the sample treated with Deposit showed a band of low intensity at 520–640 nm with a maximum of $\lambda_{f\max}$ 598 nm, which corresponded to the luminescence of Deposit (Fig. 6).

The Deposit treatment suppressed the luminescence of the testa at 390–550 nm. This result depended on the preparative form of the soybeans, which were ground to particles of 0.1–5 μm , and the composition of Deposit (https://betaren.ru/upload/medialibrary/d83/Depozit_ME_compressed.pdf). Deposit has a complex structure, and the substituent groups of the benzene ring bend the plane of the molecules, thus reducing their luminescent ability.

The absence of testa luminescence means that this microemulsion indeed protected the soybeans from ultraviolet radiation.

The luminescence spectrum of soybeans treated with Rhizoform had a band at 400–550 nm with a maximum at 449 nm, which corresponded to the luminescence of Rhizoform (Fig. 7). Relative to the mix-treated sample, the changes were as follows. The intensity of the main band reduced by 0.61 RU; the bathochromic peak shift was $\lambda_{f\text{ max}}$ 2.5 nm; and the Stokes shift $\Delta\lambda$ did not change.

The spectrum of soybeans treated with Static had a band at 392–560 nm with a maximum at $\lambda_{f\text{ max}}$ 447 nm, which corresponded to the luminescence of the sticking agent. Relative to the mix-treated sample, the intensity of the main band increased by 1.05 RU; the bathochromic shift of the maximum increased by 0.5 nm; and the long-wavelength shoulder of the main band became more obvious.

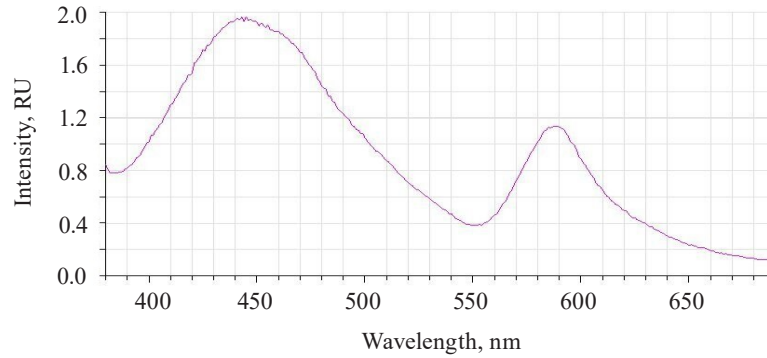


Figure 5 Luminescence spectra of soybeans treated with Imidor

Table 4 Luminescence spectra of soybean testa treated with Imidor

Excitation wavelength $\lambda_{e\text{ max}}$, nm	Stokes shift $\Delta\lambda$, nm	Luminescence wavelength	Luminescence intensity	Luminescence wavelength	Luminescence intensity	Luminescence spectrum	
		$\lambda_{f\text{ max}}$, nm	$I_f(\lambda)_{\text{ max}}$, RU	$\lambda_{f\text{ max}}$, nm	$I_f(\lambda)_{\text{ max}}$, RU	λ_{f1} , nm	λ_{f2} , nm
365	80	445	1.968	585	1.129	390–530	560–620

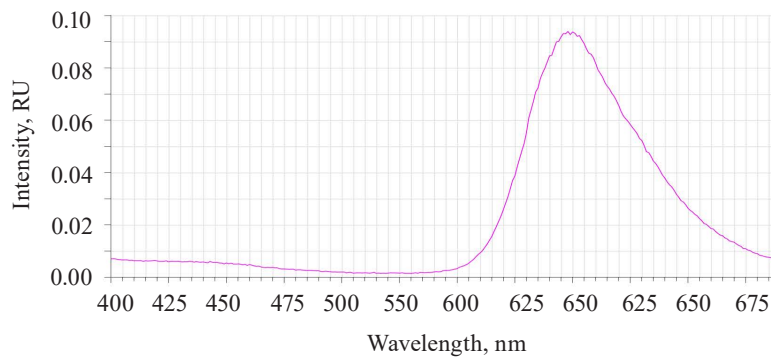


Figure 6 Luminescence spectra of soybeans treated with Deposit

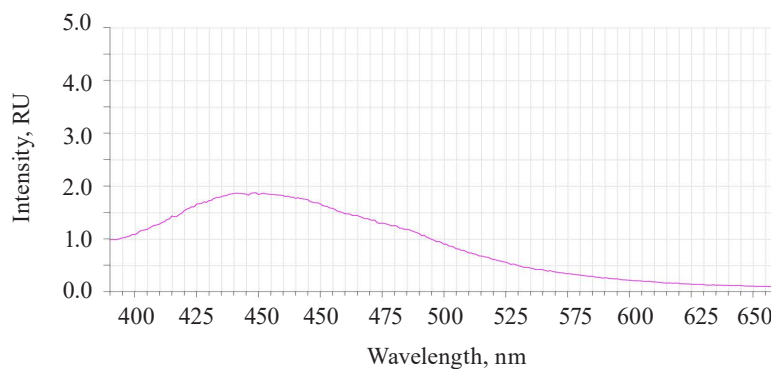


Figure 7 Luminescence spectra of soybeans treated with Rhizoform

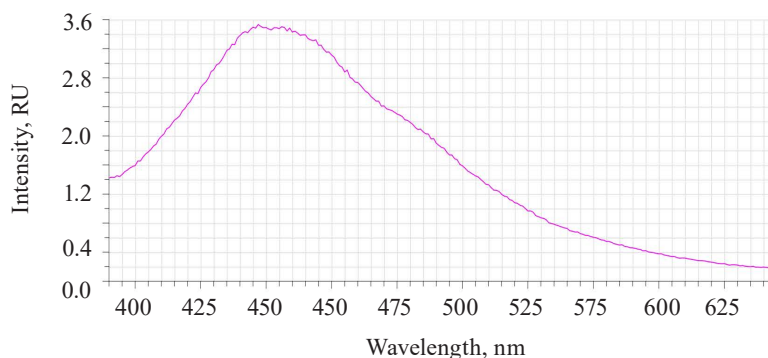


Figure 8 Luminescence spectra of soybeans treated with Static

Table 5 Luminescence spectrum of soybeans testa treated with Deposit, Rhizoform, and Static

Modifier	Excitation wavelength $\lambda_{c,max}$, nm	Stokes shift $\Delta\lambda$, nm	Luminescence wavelength $\lambda_{f,max}$, nm	Luminescence intensity $I_f(\lambda)_{max}$, RU	Luminescence spectrum, nm
Deposit	365	233	598	0.09	560–680
Rhizoform	365	84++	449	1.87	397–540
Static	365	82	447	3.53	392–560

Table 6 Luminescence kinetics of soybean testa

Soybean samples	Luminescence time τ_0 , μ s	Luminescence intensity $I_f(\lambda)_{t_0}$, RU	Luminescence time t_1 , μ s	$\lambda_f t_1$, RU	Luminescence time τ , μ s	$\lambda_f \tau$, RU
Untreated (control) λ_c 375 nm λ_{reg} 445 nm	2.05	1.11	1.2	0.408	17.05	0.0095
Mix-treated λ_c 375nm λ_{reg} 445 nm	1.95	0.369	1.3	0.698	17.25	0.0091
Mix-treated λ_c 365 nm λ_{reg} 585 nm	1.95	1.228	1.29	0.45	11.05	0.0086

Luminescence at 392–560 nm depended on Rhizoform and Static, while luminescence at 560–690 nm depended on Deposit and Imidor (Table 5). The luminescence spectrum of the treated soybeans coincided with the spectrum of Rhizoform and Static (Figs. 7 and 8).

The luminescence of Imidor at 560–620 nm overlapped the low-intensity luminescence of Deposit at 570–640 nm (Figs. 5 and 6). The pyridine ring of the neonicotinoids in Imidor used the methylene bridge to bind to the terminal electron-donating group of imine or ethene during the treatment.

The soybeans treated with a mix of modifiers had the second band at 560–615 nm that matched the luminescence of Imidor.

The untreated sample peaked at $\lambda_{f,max}$ 441 nm and $I_f(\lambda)_{max}$ 2.97 RU, $\Delta\lambda$ 79 nm. The treated samples had two peaks: $\lambda_{f1,max}$ 446.50 nm at $I_f(\lambda)_{1,max}$ 2.48 RU, $\Delta\lambda$ 84 nm, and $\lambda_{f2,max}$ 585 nm at $I_f(\lambda)_{2,max}$ 1.19 RU. Since cryptochromes had ultraviolet absorption spectrum (320–390 nm), the chromophore molecules at their basis were the luminescence centers of the soybean testa [12, 13].

Figure 9 illustrates the luminescence kinetics in the PanoramaPro software. The luminescence decay kinetics was analyzed at λ_c 365 and 375 nm and $\lambda_{registration}$ at 445 and 585 nm. The discreteness of the kinetic change was 0.05 μ s; the measure gate was 0.10 μ s; the gate delay was 0.05–30 μ s; and the gate delay step was 0.10 μ s (Table 6).

The luminescence decay parameters were expressed as the dependence of the luminescence intensity on time:

$$I(t) = Ae^{-t/\tau} \tag{1}$$

where A was the constant that depends on the nature of the substance; τ was the luminescence time, μ s.

Therefore, luminescence time t_1 could be calculated as follows:

$$t_1 = (\ln A - \ln I(t_0) + 1)\tau \tag{2}$$

where $I(t_0)$ was the maximal luminescence intensity at t_0 , %.

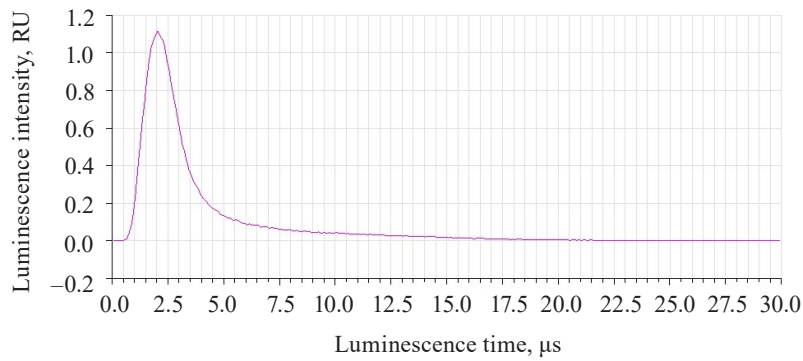


Figure 9 Luminescence kinetics of untreated soybeans

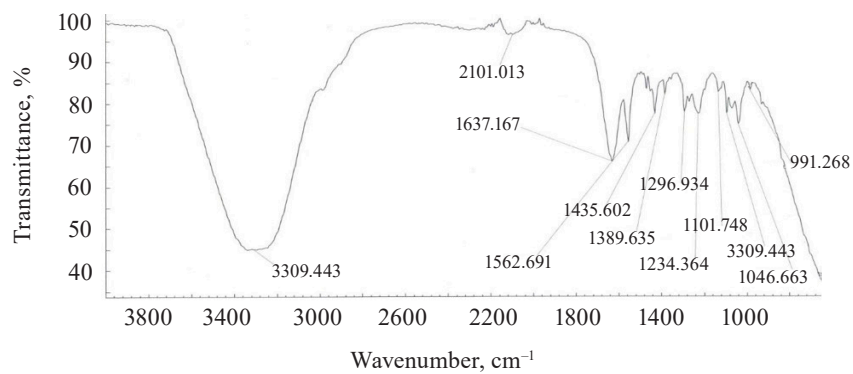


Figure 10 Imidor IR spectra

Table 7 Imidor IR spectroscopy

Wavenumber $\bar{\nu}$, cm^{-1}	Incident wavelength λ , μm	Transmittance, %	Vibration mode of the functional group
3309.45	3.02	53	ν_{OH}
2980.02	3.35	1	$\nu_{\text{C-H}}$
2101.01 (2240–1960)	4.76 (4.46–5.10)	5	Overtone and component bands
1637.16	6.11	15	σ_{HOH}
1561.70	6.40	12	$\nu_{\text{NO}_2}^{\text{as}}$
1435.60	6.97	10	$\nu_{\text{C-C}}$ in benzene ring
1389.64	7.20	4	$\nu_{\text{C-C}}$ in benzene ring
1296.94	7.72	5	$\nu_{\text{NO}_2}^{\text{s}}$
1234.36	8.12	6	$\nu_{\text{C-O-C}}^{\text{as}}$
1139.30	8.78	3	$\sigma_{\text{C-H}}$ (monosubstituted)
1101.75	9.08	4	$\sigma_{\text{C-H}}$ (1,3-substituted)
1046.66	9.56	5	$\nu_{\text{C-O-C}}^{\text{s}}$
991.27	10.09	2	$\gamma_{\text{C-H}}^{\text{w}}$ (position 1,2,4)

ν^{s} and ν^{as} are symmetric and asymmetric stretching vibrations

σ is the planar bending band

γ^{w} stands for bending wagging vibrations

In treated soybeans, the luminescence intensity $I_f(\lambda)$ reached its maximum by 0.1 μs sooner than in the untreated sample. Their luminescence time was longer by 0.09–0.1 μs . The shortest time of almost complete luminescence was λ_e 365 nm, and λ_{reg} 585 nm. The kinetic analysis proved that this luminescence could be classified as fluorescence.

IR spectroscopic analysis. We performed a separate IR spectroscopic analysis for each modifier, i.e., Imidor (Fig. 10), Deposit (Fig. 11), and Static (Fig. 12). Each of these substances, except for Rhizoform, is a complex aromatic compound. Fig. 13 illustrates the IR spectrum of Rhizoform. The grouping followed the typical vibration frequencies (Tables 7–9).

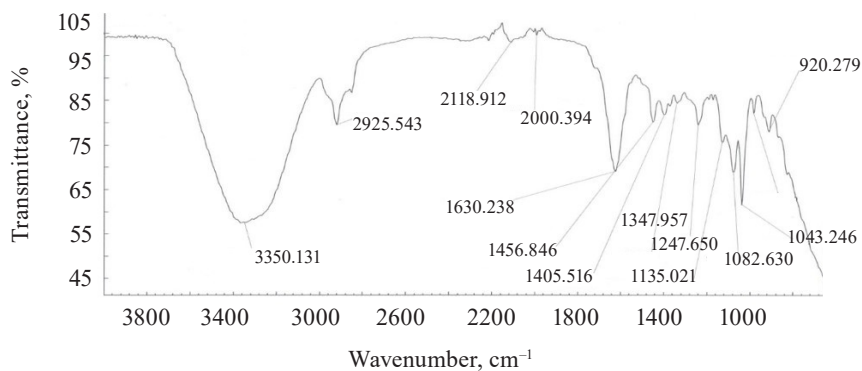


Figure 11 Deposit IR spectra

Table 8 Deposit IR spectroscopy

Wavenumber $\bar{\nu}$, cm^{-1}	Incident wavelength λ , μm	Transmittance, %	Vibration mode of the functional group
3350.13	2.98	32	ν_{OH}
2925.54	3.42	11	$\nu_{\text{C-H}}$
2118.92	4.72	4	Overtone and component bands
2000.39	5.01		
(2200–1940)	(4.54–5.15)		
1630.24	6.13	21	σ_{HOH}
1456.85	6.86	5	$\nu_{\text{C-C}}$ benzene ring
1405.52	7.11	2.5	$\nu_{\text{C-C}}$ benzene ring
1347.96	7.40	2	$\nu_{\text{C-C}}$ benzene ring
1247.65	8.02	6.5	$\nu_{\text{C-O-C}}^{\text{as}}$
1135.02	8.81	1.5	$\sigma_{\text{C-H}}$ (monosubstituted)
1082.63	9.24	8	$\sigma_{\text{C-H}}$ (position 1, 2, 3)
1043.25	9.58	14	$\nu_{\text{C-O-C}}^{\text{s}}$
990.60	10.10	3	$\gamma_{\text{C-H}}^{\text{w}}$ (orientation 1, 2, 4)
920.28	10.86	3	$\gamma_{\text{C-H}}^{\text{w}}$ (orientation 1, 2, 4)

ν^{s} and ν^{as} are symmetric and asymmetric stretching vibrations

σ is the planar bending band

γ^{w} stands for bending wagging vibrations

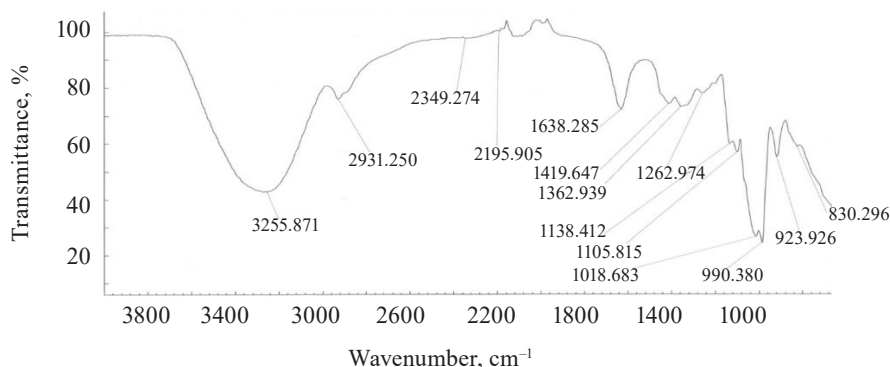


Figure 12 Static IR spectra

The spectra of Imidor (3309.45 cm^{-1}), Deposit (3350.13 cm^{-1}), and Static (3255.87 cm^{-1}) demonstrated an intense wide band of stretching vibrations of the hydroxyl group involved in the intermolecular hydrogen bond.

The spectra showed bands of stretching vibrations of C-H methyl groups: low-intensity at 2980.02 cm^{-1} for Imidor; average intensity at 2925.54 cm^{-1} for Deposit, and average intensity at 2931.25 cm^{-1} for Static [5].

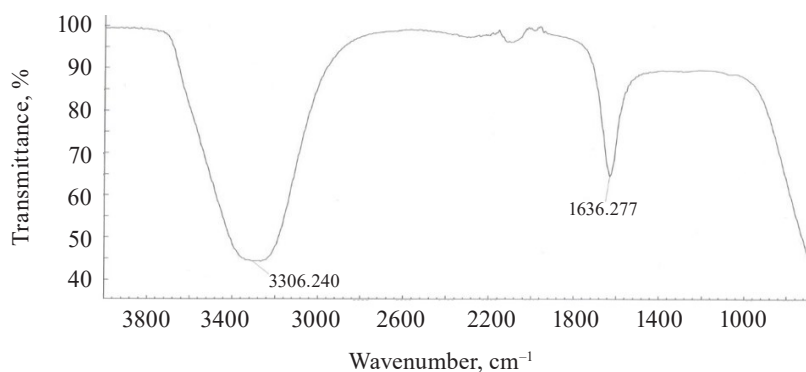
Table 9 Static IR spectroscopy

Wavenumber $\bar{\nu}$, cm^{-1}	Incident wavelength λ , μm	Transmittance, %	Vibration mode of the functional group
3255.87	3.07	39	ν_{OH}
2931.25	3.41	4.5	$\nu_{\text{C-H}}$
2118.60 (2200–1960)	4.72 (4.54–5.10)	6	Overtone bands
1638.28	6.01	18	σ_{HOH}
1419.65	7.05	4	$\nu_{\text{C-C}}$ benzene ring
1362.94	7.34	5	$\nu_{\text{C-C}}$ benzene ring
1262.97	7.91	2.5	$\nu_{\text{C-O-C}}^{\text{as}}$
1138.81	8.78	1.5	$\sigma_{\text{C-H}}$ (monosubstituted)
1105.68	9.05	5	$\sigma_{\text{C-H}}$ (position 1, 3)
1018.68	9.82	32	$\nu_{\text{C-O-C}}^{\text{s}}$
990.39	10.10	39	$\gamma_{\text{C-H}}^{\text{w}}$ (orientation 1, 2, 4)
923.93	10.82	12	$\gamma_{\text{C-H}}^{\text{w}}$ (1, 2, 4 orientation)
830.30	12.05	1	$\sigma_{\text{C-Cl}}$

ν^{s} and ν^{as} are symmetric and asymmetric stretching vibrations

σ is the planar bending band

γ^{w} stands for bending wagging vibrations

**Figure 13** Rhizoform IR spectra

The stretching vibrations of the C-C bonds in the benzene ring resulted in two bands of average intensity at 1435.6 and 1389.64 cm^{-1} for Imidor, 1456.85, 1405.52, and 1347.96 cm^{-1} for Deposit, and 1419.65 and 1362.94 cm^{-1} for Static [20].

The Imidor IR spectrum revealed stretching vibrations of the nitro group. As a result of the coupling, the ν of NO_2 bands shifted to the low-frequency region. The $\nu^{\text{as}}_{\text{NO}_2}$ band at 1561.7 cm^{-1} was more intense than the $\nu^{\text{s}}_{\text{NO}_2}$ band at 1296.94 cm^{-1} [21].

The location and intensity of the stretching vibrations of the C-O bond depend on the structural features of the molecule, mainly on the double bond and aromatic nucleus. The analyzed samples revealed two $\nu_{\text{C-O-C}}$ bands. The Imidor IR spectrum had $\nu^{\text{s}}_{\text{C-O-C}}$ at 1046.66 cm^{-1} and $\nu^{\text{as}}_{\text{C-O-C}}$ at 1234.36 cm^{-1} . The Deposit IR spectrum had $\nu^{\text{s}}_{\text{C-O-C}}$ at 1043.25 cm^{-1} and $\nu^{\text{as}}_{\text{C-O-C}}$ at 1247.65 cm^{-1} . The Static IR spectrum showed $\nu^{\text{s}}_{\text{C-O-C}}$ at 1018.68 cm^{-1} and $\nu^{\text{as}}_{\text{C-O-C}}$ at 1262.97 cm^{-1} .

The weak overtone bands at 2240–1940 cm^{-1} helped locate the substituents of the benzene ring. The bands

in this region had different contours depending on the nature of the substituent [7].

The IR spectra of the samples had plane bending vibrations of C-H at 1135–1082 cm^{-1} . In the Imidor spectrum, $\sigma_{\text{C-H}}$ at 1101.75 cm^{-1} matched positions 1, 3 of the substituents while $\sigma_{\text{C-H}}$ at 1139.3 cm^{-1} matched the monosubstitution. The out-of-plane molecular vibrations, e.g., the wagging vibrations of atoms in a molecule, had a low-intensity $\gamma_{\text{C-H}}$ band at 991.27 cm^{-1} and corresponded to positions 1, 2, 4 of the substituents. In the Deposit spectrum, $\sigma_{\text{C-H}}$ at 1082.63 cm^{-1} described positions 1, 2, 3 of the substituents while $\sigma_{\text{C-H}}$ at 1135.02 cm^{-1} matched the monosubstitution. The bending wagging vibrations of atoms in a molecule appeared as bands at γ_{max} 920.28 and 990.60 cm^{-1} , which was typical of orientations 1, 2, 4 of the substituents. The hypsochromic shift of the band γ_{max} at 920 cm^{-1} indicated the conjugation of the benzene ring substituent. In the Static spectrum, the absorption frequency $\sigma_{\text{C-H}}$ at 1105.68 cm^{-1} also corresponded to the meta position of the substituents while $\sigma_{\text{C-H}}$ at 1138.81 cm^{-1} matched the monosubstitution. The $\gamma_{\text{C-H}}$ bands at 990.39 and

923.93 cm^{-1} indicated positions 1, 2, 4 of the substituents. The spectrum contained a low-intensity bending band of C-Cl at 830.3 cm^{-1} .

In the IR spectra, the overtone bands at 2240–1960 cm^{-1} signified the main vibrations, namely $\nu_{\text{C-O-C}}$ and plane $\sigma_{\text{C-H}}$ with positions 1, 2, 3 and 1, 3 of substituents [22].

The Rhizoform IR spectrum showed ν_{OH} at 3306.24 cm^{-1} , bending vibrations of water molecules $\sigma_{\text{H}_2\text{O}}$ at 2080 cm^{-1} , and bending vibrations of the HOH stretch angle at 1636.28 cm^{-1} (Fig. 13).

The spectra of Imidor, Deposit, and Static also demonstrated bending vibrations of the HOH stretch angle at 1637.16, 1630.24, and 1638.28 cm^{-1} , respectively. They

allegedly indicated that the constancy of bending vibrations was caused by the intermolecular interaction: the bond angle of the water molecule changed as a result of the molecular interaction with each other, as well as with cations and anions [21].

To interpret the spectra of the biological sample treated with chemicals, we performed IR spectroscopy of the ground and whole samples (Fig. 13 and Table 10). The vibration frequencies indicated moisture, protein, fat, ash, carbohydrates, and hardness [23, 24].

The IR spectrum of ground soybeans (Fig. 14) had stretching vibrations of OH groups at 3277.25 cm^{-1} and bending vibrations of the HOH stretch angle at 1635.41 cm^{-1} .

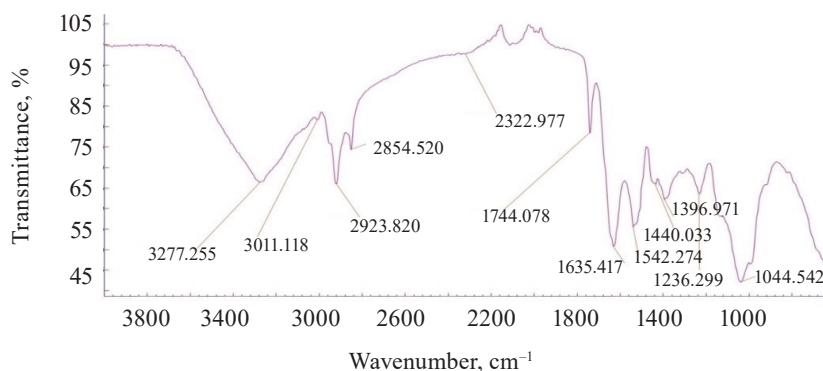


Figure 14 IR spectra of ground soybeans

Table 10 IR spectra of ground soybeans

Wavenumber $\bar{\nu}$, cm^{-1}	Incident wavelength λ , μm	Transmittance, %	Vibration mode of the functional group
3277.25 (3650–3000)	3.05	18	ν_{OH}
2854.52 (2800–3000)	3.50	4	Starch vibration in the C-H range
2923.82 (2800–3000)	3.41	18	
2080 (2080–1920)	4.80	4	Main band overtone C-O
1635.41	6.11	15	σ_{HOH}
1744.24	5.73	12	Vibration of amide I protein
1542.27	6.485	11	Vibration of amide II protein
1236.29	8.09	4	Stretching of C-C and C-O and bending of C-O-H and C-O-C
1044.54	9.57	18	

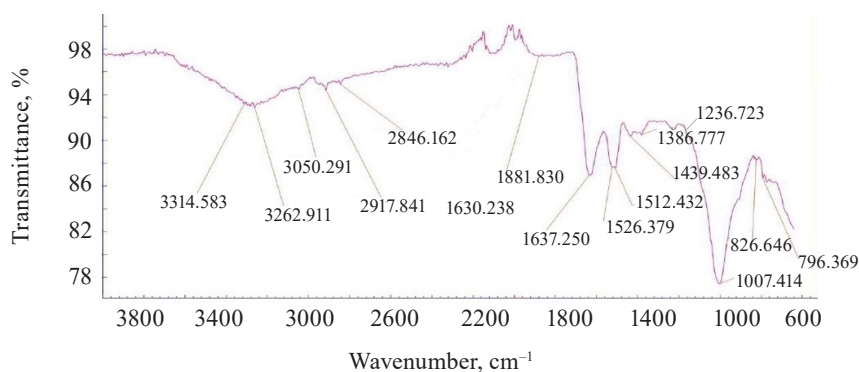


Figure 15 IR spectra of untreated whole soybeans

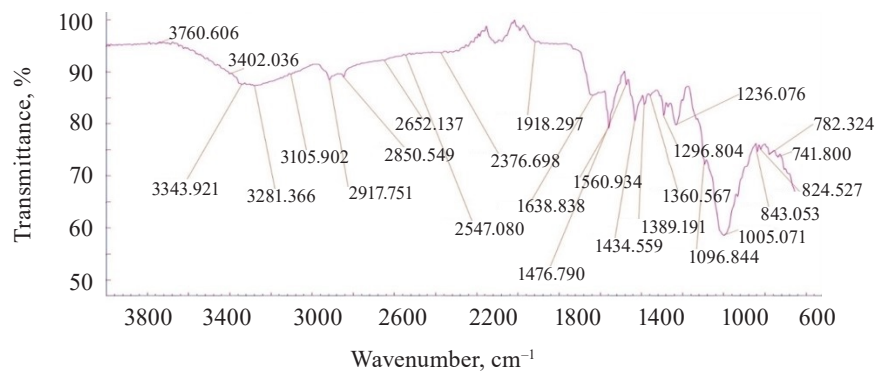


Figure 16 IR spectra of treated whole soybeans

Table 11 IR spectra of untreated (control) and treated (experimental) soybeans

Wavenumber, $\bar{\nu}$, cm^{-1}		Incident wavelength λ , μm		Transmittance, %		Vibration mode of the functional group
Treated	Untreated	Treated	Untreated	Treated	Untreated	
3281.36 (3640–3000 range)	3262.91 (range 3680–3100)	3.04	3.06	4.0	1.2	Stretching vibrations of OH groups
2917.75 (3000–2800)	3050.29 2917.84 (3400–2800)	3.428	3.27 3.42	3.3	1.3	Starch vibrations (C-H), $\nu_{\text{C-H}}$
2080 (2280–1880)	2080 (2250–1880)	4.80	4.80	4.50	2.0	Main band overtone (1003–1009 cm^{-1})
1638.83	1637.25	6.10	6.10	1.8	4	Bending vibrations of HOH stretch angle
1560.93		6.40		6.5		Stretching vibrations of the nitro group
	1526.37		6.55		4.0	Vibration of amide II protein
	1512.43		6.61			
1434.55		6.97		4.5		Stretching vibrations of C-C bond of benzene nucleus
1389.19		7.19		0.4		
1360.56		6.02				
1296.80		7.71		1.0		Stretching vibrations of nitro group
1236.07		8.09		4.5		Vibrations of C-O-C bond
1005.30	1007.41	9.95	9.93	17.5	12.0	Vibrations of C-O-C bond
843.05		11.86				Vibrations of the carbon-halogen bond

The vibration frequencies typical of amides I and II appeared at 1542.27 and 1744.24 cm^{-1} . The data differed from those reported by Migues *et al.*: our experiment revealed a bathochromic shift of 40 cm^{-1} and a hypsochromic shift of 8 cm^{-1} , respectively [7].

Vibrations typical of fats based on the C-H bond were observed at 1600–1750 and 1550–1570 cm^{-1} . The maxima of typical starch bands (2854.52 and 2923.82 cm^{-1}) were observed at 2800–3000 cm^{-1} in the C-H vibration region (Table 10). The strong absorption at 1200–900 cm^{-1} depended on the C-C and C-O stretching and the C-O-H and C-O-C bending [10].

The IR spectra of whole untreated (Fig. 15) and treated soybeans (Fig. 16) demonstrated stretching bands of OH groups at 3262.91 and 3281.36 cm^{-1} and bending bands of the HOH stretch angle at 1637.25 and 1638.83 cm^{-1} [7, 10].

Typical protein vibrations were registered at 1600–1700 and 1550–1570 cm^{-1} based on the associated amides I and II, respectively. Typical fat vibrations appeared in the same ranges, but they were based on the

C-H bond. Starch vibrations were observed at 2800–3000 cm^{-1} of the C-H stretch range at 2917.84 and 2917.75 cm^{-1} . The overtones had bands at 2080 cm^{-1} .

The vibrations typical of testa protein were observed in the spectrum of untreated soybeans at 1526.37 cm^{-1} . An intense band appeared at 1007.41 and 1005.30 cm^{-1} in the range of C-O-C vibrations at 1120–840 cm^{-1} (Table 11).

The bands at 1550–1200 cm^{-1} were strong and typical. This range made it possible to identify Imidor, Deposit, and Static on the hard soybean testa. The width and shape of the bands and the magnitude of the absorption band that occurred during the aggregate changes of the adsorbents revealed the magnitude and nature of intermolecular compounds and the treatment quality [21].

We registered five overlapping band maxima when comparing the spectra of the treated soybeans with the Imidor spectra. The bands at 1560.93 and 1561.7 cm^{-1} , as well as those at 1296.80 and 1296.94 cm^{-1} , corresponded to the stretching vibrations of the Imidor nitro group.

The bands at 1434.55 and 1435.6 cm^{-1} , as well as those at 1389.19 and 1389.64 cm^{-1} , matched the stretching vibrations of the C-C bond of the Imidor aromatic system. The typical C-O-C vibrations were visible at 1236.07 and 1234.36 cm^{-1} . The fact that the maxima of the absorption bands overlapped means that the interaction between Imidor and soybeans was, in fact, physical adsorption.

The spectra of the treated soybeans and the spectra of Static overlapped at 1360.56 and 1362.94 cm^{-1} , as well as in the range of 830–890 cm^{-1} . The comparison with the Deposit spectra revealed no overlaps, which indicated chemisorption on the soybean testa surface.

We tested the method of IR spectroscopy on complex organic adsorbed modifiers and detected certain structural elements with varying indicator values. The analysis revealed the presence of an aromatic system, the nature of functional groups, and the position of substituents.

CONCLUSION

The research featured the spectral-luminescent profile of untreated (control) and treated (experimental) soybeans and their infrared spectra. Both spectral profiles changed after the samples were treated with various modifiers. The comparative analysis of the infrared spectra gave the following results:

- the luminescence spectrum of the untreated Vilana soybean testa was 400–550 nm, with a maximum of $\lambda_{f \max}$ 441 nm and the Stokes shift of 79 nm;
- the luminescence spectrum of the treated soybeans had two bands: at 390–550 nm with a maximum of $\lambda_{f1 \max}$ 446.5 nm and at 560–615 nm with $\lambda_{f2 \max}$ 585 nm; the Stokes shift was 84 nm;
- the first band of the treated soybeans overlapped with the Rhizoform and Static spectra. The hypsochromic shift of the first band maximum was $\lambda_{f1 \max}$. The difference with the maxima of Rhizoform and Static was 2.5 and 0.5 nm, respectively;
- in the treated soybean sample, the second band at 560–615 nm with a maximum $\lambda_{f2 \max}$ 585 nm and intensity $I_f(\lambda)_{2 \max}$ 1.129 RU overlapped with the luminescence of Imidor;

- the luminescence of the treated and untreated soybean testa samples, as well as that of the modifiers, belonged to fluorescence;
- the modifiers on the surface of the treated soybeans could be identified at 1550–1200 cm^{-1} . We found five band maxima that overlapped with the Imidor spectra, two overlaps with the Static spectra, and no overlaps with the Deposit spectra;
- we detected the types of interaction between soybeans and modifiers. In case of Imidor, it was physical adsorption, while in case of Deposit, it was chemisorption.

Luminescence and IR spectroscopy provided a preliminary quality assessment of soybeans without germination. The spectral profile was able to define the heterogeneity of the crop seeds and helped select the best planting material.

The fluorescence level characterized the penetration of modifiers into plant tissues. This analysis made it possible to observe the pre-sowing treatment quality changes that may occur as a result of environmental changes, thus helping select the optimal processing conditions and the best modifier or their mix.

The methods of luminescence and IR spectroscopy were found prospective for new methods of qualitative and quantitative analysis of soybean surface before and after treatment.

CONTRIBUTION

Olga N. Bugaets performed the research, analyzed the obtained data, and wrote the article. Ivan A. Bugaets prosed the experimental data. Elena A. Kaigorodova designed the research and provided scientific counselling. Sergey V. Zelentsov prepared the research material and provided scientific counselling. Natalia A. Bugaets reviewed scientific publications. Evgeny O. Gerasimenko was responsible for the spectrofluorimetry. Elena A. Butina performed the IR-Fourier spectrometry.

CONFLICT OF INTEREST





The authors declare that there is no conflict of interests regarding the publication of this article.

REFERENCES

1. Messina M. Perspective: Soybeans can help address the caloric and protein needs of a growing global population. *Frontiers in Nutrition*. 2022;9. <https://doi.org/10.3389/fnut.2022.909464>
2. Abdelghany AM, Zhang S, Azam M, Shaibu AS, Feng Y, Qi J, et al. Natural variation in fatty acid composition of diverse world soybean germplasms grown in China. *Agronomy*. 2020;10(1). <https://doi.org/10.3390/agronomy10010024>
3. Sokolov DV, Bolkhonov BA, Zhamsaranova SD, Lebedeva SN, Bazhenova BA. Enzymatic hydrolysis of soy protein. *Food Processing: Techniques and Technology*. 2023;53(1):86–96. (In Russ.). <https://doi.org/10.21603/2074-9414-2023-1-2418>
4. Serba EM, Tadzhibova PYu, Rimareva LV, Overchenko MB, Ignatova NI, Volkova GS. Bioconversion of soy under the influence of *Aspergillus oryzae* strains producing hydrolytic enzymes. *Foods and Raw Materials*. 2021;9(1):52–58. <https://doi.org/10.21603/2308-4057-2021-1-52-58>
5. Zhang J, Li M, Kong Z, Bai T, Quan R, Gao T, et al. Model prediction of herbicide residues in soybean oil: Relationship between physicochemical properties and processing factors. *Food Chemistry*. 2022;370. <https://doi.org/10.1016/j.foodchem.2021.131363>

6. Zelentsov SV, Kohegura AV, Podkina DV, Trembak EN. Vilana Soybeans. Russia patent 03379607722. 1996.
7. Miguez VH, David JM, Gomes AF, David JP. Determination of soybean isoflavone by HPLC/DAD and simple UV spectroscopic analysis: A comparative study. *Food Analytical Methods*. 2022;15:367–376. <https://doi.org/10.1007/s12161-021-02120-2>
8. Desta KT, Hur O, Lee S, Yoon H, Shin M, Yi J, et al. Origin and seed coat color differently affect the concentrations of metabolites and antioxidant activities in soybean (*Glycine max* (L.) Merrill) seeds. *Food Chemistry*. 2022;381. <https://doi.org/10.1016/j.foodchem.2022.132249>.
9. Saito Y, Itakura K, Kuramoto M, Kaho T, Ohtake N, Hasegawa H, et al. Prediction of protein and oil contents in soybeans using fluorescence excitation emission matrix. *Food Chemistry*. 2021;365. <https://doi.org/10.1016/j.foodchem.2021.130403>
10. Yu D, Lord N, Polk J, Dhakal K, Li S, Yin Y, et al. Physical and chemical properties of edamame during bean development and application of spectroscopy-based machine learning methods to predict optimal harvest time. *Food Chemistry*. 2022;368. <https://doi.org/10.1016/j.foodchem.2021.130799>
11. Belyakov MV. Determination of seed germination of plants by the luminescence method. *The Bulletin of Izhevsk State Agricultural Academy*. 2017;52(3):35–40. (In Russ.). <https://elibrary.ru/ZRCNHZ>
12. Belyakov MV, Bereznikova LA. Innovative photoluminescent device control parameters of the plant seeds. *Bulletin NGIEI*. 2017;78(11):46–58. (In Russ.). <https://elibrary.ru/ZWPRFF>
13. Efimenko EG, Kucherenko LA, Efimenko SK, Nagalevskaya YaA. Evaluation of the general qualitative traits of soybean seeds using IR-spectrometry. *Oilseeds. Scientific and Technical Bulletin of the All-Russian Scientific Research Institute of Oilseed*. 2016;167(3):33–38. (In Russ.). <https://elibrary.ru/WWTJJD>
14. Valand R, Tanna S, Lawson G, Bengtström L. A review of Fourier Transform Infrared (FTIR) spectroscopy used in food adulteration and authenticity investigations. *Food Additives and Contaminants: Part A*. 2020;37(1):19–38. <https://doi.org/10.1080/19440049.2019.1675909>
15. Romero EL, Fairfax M, Colombo R, Gallup C, Biro A. Fungicide compounds and mixtures for control of fungal diseases of grain crops. Russia patent RU 2749224C2. 2021.
16. Tanaka A, Shimomura M, Nokura Y, Murakami S. Heterocyclic compound and agent containing it for the control of harmful arthropods. Russia patent RU 2748695C2. 2021.
17. Denisov A. Rhiziform for soybean seed processing. *International Agricultural Journal*. 2015;(2):65–67. (In Russ.). <https://elibrary.ru/TOASQH>
18. Anhalt JC, Moorman TB, Koskinen WC. Biodegradation of imidacloprid by an isolated soil microorganism. *Journal of Environmental Science and Health, Part B: Pesticides, Food Contaminants, and Agricultural Wastes*. 2007;42(5):509–514. <https://doi.org/10.1080/03601230701391401> PMID: 17562458.
19. Belyakov MV. Technique of studying the luminescent properties of plant seeds in “Flyuorat-02-Panorama” spectrofluorometer. *Scientific Life*. 2016;(3):18–26. (In Russ.). <https://elibrary.ru/VXMTLN>
20. Liu Q, Zhang W, Zhang B, Du C, Wei N, Liang D, et al. Determination of total protein and wet gluten in wheat flour by Fourier transform infrared photoacoustic spectroscopy with multivariate analysis. *Journal of Food Composition and Analysis*. 2022;106. <https://doi.org/10.1016/j.jfca.2021.104349>
21. Kazachenko AIS, Kazachenko AS, Chaplygina IA, Stupko TV. Using IR-spectroscopy in the analysis of grain (review). *Bulletin of KSAU*. 2019;150(9):134–142. (In Russ.). <https://elibrary.ru/COSTFD>
22. Keerati-U-Rai M, Miriani M, Iametti S, Bonomi F, Corredig M. Structural changes of soy proteins at the oil–water interface studied by fluorescence spectroscopy. *Colloids and Surfaces B: Biointerfaces*. 2012;93:41–48. <https://doi.org/10.1016/j.colsurfb.2011.12.002>
23. Marshall WE, Wartelle LH, Boler DE, Johns MM, Toles CA. Enhanced metal adsorption by soybean hulls modified with citric acid. *Bioresource Technology*. 1999;69(3):263–268. [https://doi.org/10.1016/S0960-8524\(98\)00185-0](https://doi.org/10.1016/S0960-8524(98)00185-0)
24. Li W, Zhao H, He Z, Zeng M, Qin F, Chen J. Modification of soy protein hydrolysates by Maillard reaction: Effects of carbohydrate chain length on structural and Interfacial properties. *Colloids and Surfaces B: Biointerfaces*. 2016;138:70–77. <https://doi.org/10.1016/j.colsurfb.2015.11.038>

ORCID IDs

Olga N. Bugaets  <https://orcid.org/0000-0002-8748-4137>
Ivan A. Bugaets  <https://orcid.org/0000-0002-9869-296X>
Elena A. Kaigorodova  <https://orcid.org/0000-0002-8286-515X>
Sergey V. Zelentsov  <https://orcid.org/0000-0003-0431-6021>
Natalia A. Bugaets  <https://orcid.org/0000-0003-4012-8837>
Evgeny O. Gerasimenko  <https://orcid.org/0000-0002-4267-9571>
Elena A. Butina  <https://orcid.org/0000-0003-0675-9643>



Nanoparticles of metals and their compounds in films and coatings: A review

Natalia B. Eremeeva

ITMO University , St. Petersburg, Russia

e-mail: eremeeva.itmo@gmail.com

Received 02.11.2022; Revised 28.12.2022; Accepted 10.01.2023; Published online 11.07.2023

Abstract:

Nanotechnology is important in food packaging because it increases shelf life, enhances food safety, and improves sensory characteristics and nutrient availability. We aimed to review scientific publications on the synthesis of nanoparticles, as well as their properties and applications in the food industry.

Research and review articles published from 2020 to 2022 were obtained from the database using the keywords “nanoparticles”, “film”, and “food”. They were on the synthesis of metal and metal oxide nanoparticles and their uses in food films and coatings.

We reviewed methods for synthesizing inorganic nanoparticles from metals and their compounds (silver, zinc, iron, etc.), as well as described their antimicrobial action against foodborne pathogens. By incorporating nanoparticles into films, we can create new materials with strong antimicrobial properties *in vitro*. Nanoparticles can be used to develop both polymer and biopolymer films, as well as their mixtures. Composite coatings can work synergistically with metal nanoparticles to create multifunctional food packaging systems that can act as compatibilizers. Particular attention was paid to metal nanoparticles in food coatings. We found that nanoparticles reduce the rate of microbial spoilage and inhibit lipid oxidation, thereby increasing the shelf life of raw materials and ready-to-eat foods. The safety of using nanoparticles in food coatings is an important concern. Therefore, we also considered the migration of nanoparticles from the coating into the food product.

Incorporating nanoparticles into polymer and biopolymer films can create new materials with antimicrobial properties against foodborne pathogens. Such composite films can effectively extend the shelf life of food products. However, the undesirable migration of metal ions into the food product may limit the use of such films.

Keywords: Nanoparticles, antibacterial effect, film, coating, packaging, food products

Funding: This study was financially supported by the Russian Science Foundation (RSF) (project No. 23-26-00056).

Please cite this article in press as: Eremeeva NB. Nanoparticles of metals and their compounds in films and coatings: A review. *Foods and Raw Materials*. 2024;12(1):60–79. <https://doi.org/10.21603/2308-4057-2024-1-588>

INTRODUCTION

The exploitation of oil resources and the production of various oil-based plastics are taking a heavy toll on the environment. Therefore, biopolymers are increasingly being used as an alternative material due to their biodegradability, safety, biocompatibility, and renewability [1]. Polysaccharides, proteins, and lipids are the main components of such composites.

Films based on biodegradable materials are often supplemented with bioactive substances, such as plant extracts or particles of inorganic metals, to meet the changing needs of modern consumers [2, 3].

Biosynthesized metal-based nanomaterials are used both for medical purposes (e.g., antimicrobial coatings,

drug delivery) and for catalytic water purification and environmental sensors [4–6]. Nanoparticles of inorganic metals (silver, gold, zinc oxide, titanium oxide, etc.) can act as antimicrobial agents in packaging films [7–9].

Nanoparticles of various metals, including titanium, copper, magnesium, and especially silver and gold, are known to have antimicrobial, antiviral, and antifungal properties [10, 11]. These nanoparticles are being actively studied as disinfectants, ingredients in the food industry, and as additives in clothing and medical devices [12].

He *et al.* described the antibacterial activity of gold nanoparticles against *Escherichia coli* [13]. In particular, they disrupt the membrane potential by inhibiting adenosine triphosphatase (ATPase) activity and decrease

cellular ATP levels. Another effect of gold nanoparticles is the inhibited binding of transfer RNA to the ribosome subunit.

Current studies of plant tissues and extracts as reducing agents are of great interest in the field of biosynthesized antibacterial nanoparticles. Biosynthesized nanoparticles may need to be purified from pathogenic or poisonous compounds, especially when used *in vivo* [14]. However, toxicity problems can be eliminated by using only well-studied and qualitative plant extracts for biosynthesis [15]. For example, green tea extract from camellia leaves is a widely used reducing agent for nanoparticle biosynthesis. Vaseeharan *et al.* used green tea extract to obtain silver nanoparticles in the study of antibacterial activity against *Vibrio harveyi* [16].

Several studies have described the antifungal activity of biosynthesized nanoparticles against *Aspergillus niger*. Gajbhiye *et al.* reported the antifungal properties of biosynthesized nanomaterials against *Phoma glomerata*, *Phoma herbarum*, *Fusarium semitectum*, *Trichoderma* sp., and *Candida albicans* in combination with fluconazole, a triazole antifungal drug [17].

Biosynthesized nanomaterials have been applied in almost all the areas where traditional nanomaterials have been in use. One of the challenges, however, has been in separating biogenic nanoparticles from biological material, since contamination with biological cells can cause allergens and pathogens to be unintentionally introduced into the product.

There is a growing interest in the production of packaging materials with nanocomponents used as antimicrobial agents, including biocoatings for food products [18–20].

The recent growth of publications on the synthesis of nanomaterials indicates much broader possibilities of their application to be discovered. Meanwhile, researchers are fine-tuning the synthesis methods used to create new biosynthetic forms of nanomaterials. Our interest was in metal nanoparticles with antibacterial action and their application in films and coatings, including those used for food products. We aimed to review the existing literature on the synthesis of nanoparticles, as well as their properties and applications in the food industry.

STUDY OBJECTS AND METHODS

We reviewed the latest Russian and foreign publications on the synthesis of metal nanoparticles and their compounds, as well as on their uses in films and coatings for food products. The data were correlated and classified.

A film was defined as a thin material based on synthetic and/or natural raw materials in various proportions that can be used as a packaging or a separating layer.

A coating was defined as a thin material applied directly to a food product.

A packaging material was defined as a material intended for the manufacture of packaging, containers, or auxiliary means of packaging.

Publications (articles and reviews) were searched in the Scopus-indexed journals (as of April 2022) using the keywords “nanoparticles”, “film”, and “food”. The search period was limited to 2020–2022. These search criteria ensured that the publications were from credible academic sources.

RESULTS AND DISCUSSION

Synthesis of nanoparticles. Nanotechnologies are important in food packaging since they increase shelf life and improve the food’s quality, safety, sensory characteristics, and nutrient availability. In the food industry, nanoparticles are used as part of active or smart packaging in the form of nanotubes, nanoemulsions, nanocomposites, nanocapsules, nanofibers, etc., which can be of both organic and inorganic origin [21]. This review covers inorganic particles obtained from transition metals (silver, iron) and metal oxides (zinc oxide, titanium dioxide). Such nanoparticles are the most promising due to their antibacterial properties and a high surface to volume ratio [22].

Nanoparticles can be synthesized in two ways: “bottom-up” and “top-down”. Methods for their synthesis can be divided into physical, chemical, and biological (Fig. 1).

In the bottom-up method, atoms, molecules, or small particles join together to form a nanostructured building block of nanoparticles. Its examples include physical and chemical vapor deposition, liquid state synthesis, chemical reduction, gas phase, and solvothermal methods [23]. In contrast, the top-down method involves reducing the size of the bulk material through various physical and chemical treatments. Some of the physical methods include lithography, laser ablation, sputtering, electrochemical pulse etching, and vapor deposition [24].

Zinc oxide nanoparticles obtained chemically were proposed as a superhydrophobic coating [25]. Such coatings can be used in the medical and food industries due to their high antimicrobial and hydrophobic properties, which help minimize surface contamination.

Biocompatible hybrid Ag-TiO₂ nanorods were obtained by successive synthesis of TiO₂ nanoparticles from titanium (IV) butoxide on a Teflon tube at 180°C for 18 h [26]. Next, they were mixed with a solution of silver nitrate at 120°C in nitrogen atmosphere and the resulting nanoparticles were stabilized in cyclohexane. Due to their ultra-small size and hybrid nature, the nanocomposites efficiently accumulated in breast cancer cells and generated large amounts of reactive oxygen species to ablate tumor cells. In addition, Ag-TiO₂ nanorods showed significant antibacterial activity against *Escherichia coli* and *Staphylococcus aureus* compared to TiO₂ nanoparticles, which was due to the synergistic properties of Ag and TiO₂ nanoparticles.

Biological (“green”) methods for synthesizing metal nanoparticles use plant material, bacteria, fungi, algae, and even viruses [27]. These economical methods produce environmentally friendly nanoparticles from

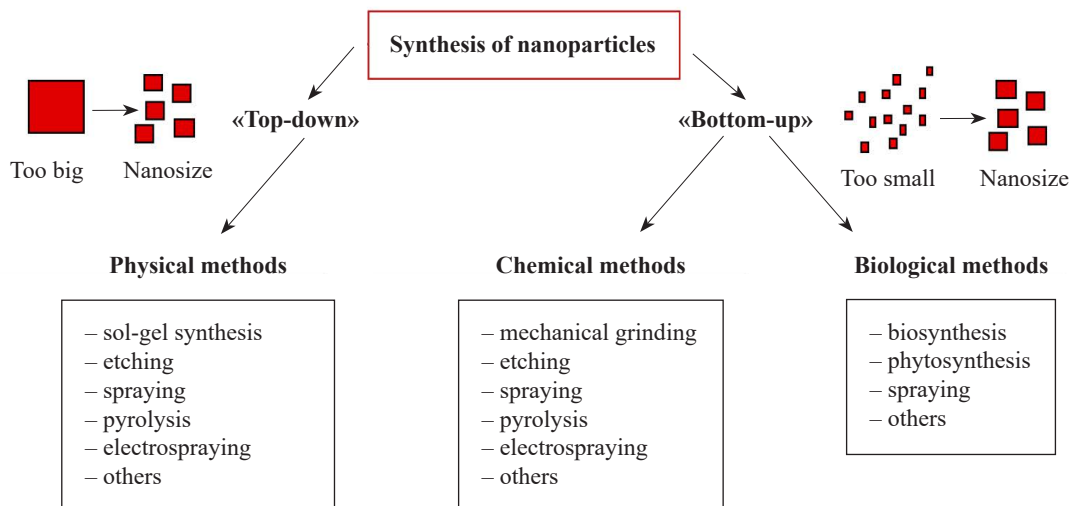


Figure 1 Methods for nanoparticles synthesis

biocompatible materials, since biological molecules are used as stabilizers and protective agents.

Biosynthetic ZnO nanoparticles obtained from *Aspergillus fumigata* leaf extract showed high antimicrobial activity against *E. coli* (Gram-negative bacteria) and *S. aureus* (Gram-positive bacteria), as well as strong antifungal activity [28]. *A. fumigata* leaf extract became more active in the presence of ZnO nanoparticles. Thus, the resulting nanoparticles can act as effective antimicrobial and antioxidant agents for commercial use in biomedicine and can be used as a substrate in drug therapy.

The biosynthesis of silver nanoparticles using an extract of *Ganoderma lucidum* can produce crystals with an average size of 11.38 ± 5.51 nm [29]. In biological tests, colloidal nanoparticles demonstrated antimicrobial activity against *S. aureus*, *E. coli*, *Pseudomonas aeruginosa*, *Salmonella enterica*, and *Candida albicans* with IC_{50} values of 17.97, 17.06, 1.32, 54.69, and $27.78 \mu\text{g}/\text{cm}^3$, respectively. The antioxidant capacity of silver nanoparticles was evaluated using 2,2-diphenyl-1-picrylhydrazyl (DPPH) free radical reagent ($IC_{50} = 447.120 \pm 0.084 \mu\text{g}/\text{cm}^3$). In addition, colloidal silver nanoparticles had better antitumor activity against human epidermal carcinoma cells with IC_{50} values of $190.06 \pm 3.62 \mu\text{g}/\text{cm}^3$, compared to a pure extract of *G. lucidum*.

Antibacterial action of metal nanoparticles. Nanoparticles are increasingly being used in the treatment of infectious diseases. In addition, they are used in the production of films and packaging that exhibit antibacterial activity against foodborne pathogens, thereby extending the product's shelf life.

Structurally, nanoparticles are three-dimensional particles ranging from 1 to 100 nm [30]. Their physicochemical properties, which underlie their antimicrobial activity, include size, charge, surface morphology, crystal structure, and zeta potential [31]. The small size is the main advantage of nanoparticles that ensures high

antimicrobial activity against intracellular bacteria since nanoparticles can easily penetrate through bacterial cell walls [32]. When nanoparticles electrostatically bind to bacterial cell walls, they damage the membrane, which ultimately leads to changes in its potential and depolarization [33]. As a result, bacterial cells lose their integrity and experience respiratory failure. Moreover, this causes imbalance within the bacteria, interrupts energy transduction, and ultimately leads to cell lysis.

The key processes that underlie the antimicrobial action of nanoparticles include the destruction of cell walls and membranes, which leads to oxidative stress, impaired energy transduction, enzyme inhibition, photocatalysis, and interference in DNA and RNA [34] (Fig. 2).

Destruction of cell walls and membranes. Cell walls and membranes are the first line of defense for bacteria. Both act as important protective barriers, helping bacteria maintain their shape and protecting them from the external environment [35]. Nanoparticles start their antimicrobial action by causing damage to cell walls and membranes, which leads to cell lysis. The pathway of nanoparticle adsorption is determined by the components of the bacterial cell membrane [36]. Nanoparticles have a stronger antimicrobial effect against Gram-positive bacteria than against Gram-negative ones. The cell wall of Gram-negative bacteria consists of lipoproteins, lipopolysaccharides, and phospholipids which allow only macromolecules to penetrate it, forming a barrier between the cell membrane and its environment. Conversely, the cell wall of Gram-positive bacteria contains a thick layer of peptidoglycan and teichoic acid with numerous pores that allow foreign molecules to easily penetrate the membrane. This leads to membrane disruption, loss of cytoplasmic constituents, and, ultimately, to apoptosis.

The degree of destruction of cell walls and membranes depends on the size and charge of nanoparticles. In particular, smaller-sized Ag nanoparticles showed

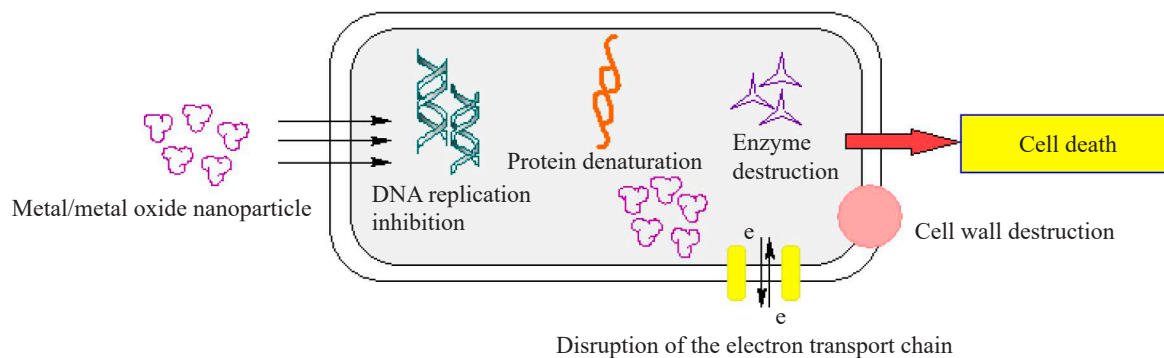


Figure 2 Bacterial cell death

lower values of minimum inhibitory and minimum bactericidal concentrations, exhibiting great antimicrobial activity [37].

Disruption of the mitochondrial electron transport chain. Another antimicrobial mechanism of nanoparticles is that they disrupt the mitochondrial electron transport chain. Flores-López *et al.* reported that the strong binding of Ag and Ag⁺ nanoparticles to thiol groups in cysteine residues impaired mitochondrial membrane proteins, membrane permeability, and mitochondrial functions [38]. Nanoparticles can accumulate in mitochondria, causing the mitochondrial membrane to depolarize and blocking the mitochondrial electron transport chain. This is due to the activation of an enzyme associated with nicotinamide adenine dinucleotide phosphate [39]. Blocking the mitochondrial electron transport chain further increases cellular levels of reactive oxygen species through electron transport.

Overproduction of reactive oxygen species. Mitochondria play a major role in the regulation of intracellular levels of reactive oxygen species. Therefore, the disruption of the mitochondrial electron transport chain leads to their excessive production [40]. The control over reactive oxygen species production regulates certain processes such as the initiation of defense against pathogens, programmed cell lysis, and energy generation through mitochondria.

Inhibition of proteins and enzymes. As a result of interacting with nanoparticles, vital proteins lose their important functions and enzymes become inhibited. In particular, nanoparticles cause structural changes in the proteins adsorbed on them. For example, new secondary bonds are formed and the initial bonds are destroyed during protein adsorption on Au nanoparticles, and such changes are irreversible [41]. Structural changes in proteins, which are caused by interactions between proteins and peptides binding to nanoparticles, can lead to chemical denaturation and the formation of fibrils due to thermodynamic instability. This subsequently leads to the loss of protein functions. The possibility of interaction between nanoparticles and proteins is quite high, since proteins make up to 35% of biological fluids by volume.

Oxidative damage to DNA and RNA. DNA is the fundamental molecule of a living organism. DNA strand breakage is a standard biomarker of DNA damage, natural or caused by other factors [42]. It is believed that nanoparticles can induce DNA damage by inhibiting DNA replication. Nanoparticles can change the ability of cells to repair induced DNA damage due to the overproduction of reactive oxygen species [43]. DNA is particularly susceptible to oxidative damage since the production of HO• from Fenton reactions can attack nucleic bases or sugar phosphate and lead to the fragmentation of saccharides and strand breakage. Nanoparticles can also initiate a double-strand break by modulating replication forks, which further leads to apoptosis.

Properties of nanoparticle-based films. By using nanoparticles in the production of films, scientists can create new materials with strong antimicrobial properties *in vitro*. Nanoparticles of metals, oxides, or their combinations have been used to develop polymer and biopolymer films, as well as their mixtures. There is a trend towards using nanomaterials based on particles of silver or zinc. The effects of metal nanoparticles on the physicochemical and antibacterial properties of films are described below.

Silver. Polyethylene nanocomposite films containing synthesized silver and titanium dioxide nanoparticles showed antibacterial efficacy against *E. coli* and *S. aureus* in the cultural research method [44]. Polyethylene films obtained by extrusion and containing Ag/TiO₂/montmorillonite clay had bactericidal properties and therefore potential applications in medicine and food packaging to prevent bacterial contamination. In addition, irradiation of the composites obtained by reducing ions to nanosilver on the surface of TiO₂/montmorillonite clay caused complete death to the pathogens tested. Those composites which had a smaller size due to the irradiation of surface films showed a more stable bactericidal activity.

The scientists developed a two-layer food packaging film with unique properties. Particularly, the film prevented bacterial growth, inhibited oxidative processes, increased the safety of food products, blocked UV penetration, and was oil-resistant and transparent. It had

an Ag-organometallic basis with p-coumaric acid, chitosan nanoparticles, and a mixture of polyvinyl alcohol and starch. As described in [45], a two-layer film is composed of separate previously obtained components to be subsequently used as a packaging material.

An environmentally friendly method was applied for the biosynthesis of hybrid Ag/AgCl nanoparticles using Levan from *Bacillus mojavensis*. Such nanoparticles can be used as highly efficient antimicrobial agents against a wide range of foodborne bacteria [46]. The morphological and physicochemical characteristics of Levan Ag/AgCl nanoparticles were studied by transmission electron microscopy, X-ray diffraction, UV visual spectroscopy, dynamic light scattering, and thermogravimetric analysis. Levan-Ag/AgCl was analyzed for antibacterial activity against foodborne pathogenic bacteria (*E. coli*, *Klebsiella pneumoniae*, *S. enterica*, *P. aeruginosa*, *S. aureus*, *Micrococcus luteus*, *Listeria monocytogenes*, *Enterococcus faecalis*, *Bacillus subtilis*, and *Bacillus thuringiensis*) by diffusion on agar. The study demonstrated high antimicrobial activity of Levan-Ag/AgCl nanoparticles as a potent inhibitor against all the tested strains, with higher efficacy against Gram-negative than against Gram-positive bacteria. Due to these properties, Levan-Ag/AgCl nanoparticles can be used as a component in packaging films to increase the shelf life of beef. Their antimicrobial activity may be due to a slow release of silver ions and their interaction with negatively charged biomolecules. These biomolecules damage the cell wall, cause structural changes in the protein and its biofunction, and ultimately lead to cell death.

The size of metal and oxide nanoparticles significantly affects the transmission of light through a film [47]. A number of studies have shown that metal nanoparticles increase the hydrophobicity of film materials. For examples, silver nanoparticles caused a 77% increase in the hydrophobicity of a film based on polyvinyl alcohol and guar gum, compared to the control group.

A biocomposite consisting of sodium alginate, oxidized nanocellulose, and silver nanoparticles was introduced into a paper matrix for food packaging. It inhibited the growth of Gram-positive (*S. aureus*, *B. subtilis*) and Gram-negative (*E. coli*, *Pseudomonas aeruginosa*) bacteria [48].

A sandwich-like chitosan nanocomposite film was produced from corn stalk as a green reducing agent, silver nanoparticles, and graphene oxide nanoparticles used for stabilization and controlled release of nano-silver in the inner layer and chitosan in the outer one [49]. The results showed that the sandwich-like film released silver nanoparticles during 14 days, with a total amount of only 1.9%. The nanocomposite film had a high antibacterial activity against *E. coli* and *S. aureus* and did not exhibit toxicity to cells.

Silver nanoparticles synthesized using *Saraca asoca* leaf extract were used to produce nanocomposite films based on rice starch [50]. They had a spherical shape with a diameter of 27 to 45 nm. Silver nanoparticles im-

proved the tensile at break of rice starch films and reduced their elongation at break. In addition, the films showed lower water solubility, water-holding capacity, and vapor permeability. Silver nanoparticles in the form of colloids or discrete films exhibited high antibacterial activity against common foodborne pathogens (*E. coli*, *S. aureus* and *B. subtilis*).

Silver nanoparticles can be synthesized *in situ* in a pectin matrix using γ -irradiation at 2.5 and 5 kGy. They provide nanocomposite films with antibacterial activity against *E. coli* and *Salmonella typhimurium*, as shown by the total colony count [51].

Dash *et al.* studied the physicochemical, mechanical, barrier, and thermal properties of flax protein-alginate films produced with various concentrations of silver nanoparticles [52]. The study showed that all the films with silver nanoparticles had a strong antibacterial effect, compared to the control film. According to the inhibition zones, the antibacterial activity against Gram-negative bacteria (*E. coli*) was higher than that against Gram-positive bacteria (*S. aureus*).

The amount of active ions released also affects the film's antimicrobial properties. In a study by Wang *et al.*, silver nanoparticles in polymer films based on chitosan or polyvinyl alcohol (PVA) affected the growth of *Pseudomonas fluorescens* differently [53]. The study was carried out both on agar and on a model food hydrogel. In particular, the film based on PVA exhibited a stronger antimicrobial effect than the one based on chitosan. This correlated with a larger amount of silver ions released from the PVA film into hydrogel. The study showed that the strength of interaction between silver nanoparticles and the film polymer is a key factor that determines the release of antimicrobials and, therefore, the antimicrobial activity of the packaging film.

Sallak *et al.* created a film from corn starch containing *Satureja khuzestanica* essential oil and Ag-TiO₂ nanocomposites (sized 30–60 nm) and assessed its antimicrobial, morphological, physical, and mechanical characteristics [54]. The film showed a reduction in *S. aureus* and *E. coli* of 3–4 and 6–7 log (CFU/mL), respectively, compared to the control.

Silver nanoparticles based on *Ricinus communis* leaf extract exhibited high antioxidant activity by absorbing DPPH (2,2-diphenyl-1-picrylhydrazyl) radicals [55]. They also showed antibacterial activity against Gram-positive (*S. aureus*) and Gram-negative (*E. coli*, *P. aeruginosa*) bacteria, as determined by agar plate diffusion.

Zinc. A nanocomposite based on a copolymer of lactic and glycolic acids and nanozinc oxide promoted the formation of long-lived reactive protein species [56]. It also caused 8-oxoguanine, a key biomarker of oxidative stress, to appear in DNA. The nanocomposite exhibited significant bacteriostatic properties, which depended on the concentration of nanoparticles. Its surface was non-toxic to eukaryotic cells and did not prevent their adhesion, growth, or division. Due to its low cytotoxicity and bacteriostatic properties, this nanocomposite

can be used as a coating material in the food industry, an additive for textiles, and in biomedicine.

A nanocomposite film consisting of polylactic acid (PLA), zinc oxide (ZnO) nanoparticles, and graphene oxide (GO) is a biodegradable polymer that can be used as food packaging [57]. ZnO and GO increased the strength of the resulting packaging material and gave it antibacterial properties against *E. coli* and *B. subtilis* cells, as determined by counting viable colonies. The PLA/ZnO/GO composite was synthesized by a successive mixing of graphene oxide and zinc oxide nanoparticles in acetone under ultrasound at 40°C and a subsequent addition of a PLA solution with vigorous stirring for 3 h. The resulting composite was dried at room temperature on an acrylic plate.

A functional film based on carrageenan/agar was obtained by combining tea tree oil emulsion and zinc sulfide nanoparticles, which were uniformly dispersed in a binary polymer matrix [58]. Zinc sulfide nanoparticles improved the film's mechanical strength, while the tea tree oil emulsion slightly reduced it. However, due to their combined use, the film retained its mechanical strength and became slightly more flexible. These components slightly increased the vapor barrier, water resistance, and thermal stability of the film. In addition, the composite membrane showed pronounced antioxidant and antibacterial activity.

Tymczewska *et al.* described a “green” method for obtaining active films based on gelatin/polyvinyl alcohol, black cumin cake extract, and zinc oxide nanoparticles [59]. The nanoparticles were preliminarily synthesized from zinc nitrate hexahydrate and an aqueous extract of black cumin cake in an alkaline medium at 60°C. The film had strong antibacterial properties against Gram-positive bacteria (*M. luteus*, *L. monocytogenes*, and *S. aureus*). Black cumin cake extract and zinc oxide nanoparticles also increased the films' antioxidant activity, as determined by the DPPH and ABTS methods (2,2-azino-di-[3-ethylbenzthiazoline sulfonate). In addition, these components affected the physicochemical characteristics of the films. In particular, they reduced their tensile at break and vapor permeability and increased their opacity and elongation at break. These nanocomposite materials can be recommended to reduce microbial spoilage and inhibit oxidative rancidity of packaged foods.

Zinc oxide nanoparticles are also used in nanofibrous membranes for wound dressings [60]. Titanium oxide nanoparticles in silk fibers and collagen, which are synthetic membranes for skin tissue regeneration, exhibit antibacterial activity against *S. aureus* and *E. coli* [61].

In another study, a functional biodegradable food packaging film was produced from soy protein isolate, a natural antimicrobial agent (mangosteen peel extract, 10 wt.%), and functional modifiers (zinc oxide nanoparticles) at various concentrations by solution casting [62]. The triple combined composite films exhibited significantly improved mechanical properties, water vapor permeability, water solubility, UV barrier, antioxi-

dant properties, and thermal stability. Due to the antibacterial properties of the plant extract and ZnO nanoparticles, the composite films showed excellent antibacterial action against *E. coli* and *S. aureus*.

Zinc nanoparticles were used to prepare a functional composite film based on pectin/agar [63]. Their integration significantly improved the film's physical properties, such as mechanical and UV protective properties, without affecting its transparency too much. In addition, zinc nanoparticles had no effect on the film's hydrophobicity, vapor barrier, and thermal properties. Finally, the composite film showed strong antibacterial activity against pathogenic foodborne bacteria *E. coli* and *L. monocytogenes*.

Lee *et al.* analyzed the antibacterial activity of composite films based on chicken skin gelatin/tapioca starch and zinc oxide nanoparticles (0–5%) obtained by casting [64]. They found that the inhibition zones for both Gram-positive *S. aureus* (16–20 mm) and Gram-negative *E. coli* (15–20 mm) were greater in the film with 5% zinc oxide. Overall, the films based on chicken skin gelatin and tapioca starch with 3% zinc oxide nanoparticles were found to be optimally formulated and have good physical, mechanical, and antibacterial properties.

Well-dispersed zinc oxide (ZnO) nanoparticles were placed *in situ* on a non-toxic natural palygorskite (PAL) nanorod to form an antibacterial composite PAL@ZnO nanorod. This nanorod was embedded in a chitosan/gelatin-based film to obtain composite films with markedly improved mechanical properties and antibacterial activity against *S. aureus* and *E. coli* bacteria (inhibition zones of 21.82 ± 0.95 and 16.36 ± 1.64 mm, respectively) [65]. In addition, PAL@ZnO nanorods significantly improved the film's water and heat resistance.

In another study, bionanocomposite films based on bovine gelatin supplemented with chitosan and zinc oxide nanoparticles showed better thermal stability and tensile at break, as well as lower elongation at break and solubility [66]. In addition, gelatin-based biocomposite films exhibited antibacterial properties against *S. aureus* and *E. coli*.

The physicochemical properties of nanomaterials depend on their size and shape, the key factors for biomedical applications. Hasanzadeh *et al.* used the hydrothermal method to obtain ZnO nanostructures of various shapes, including nanospheres, nanoplates, and nanopyramids [67]. They studied the antibacterial activity (colony count) of nanostructures against *E. coli* and found that ZnO nanopyramids obtained at 70°C had a stronger inhibitory effect than nanospheres and nanoplates.

Iron. Appu *et al.* biosynthesized chitosan-coated Fe₃O₄ nanocomposites by mixing solutions of iron chloride and broccoli extract while heating to be subsequently leached [68]. Next, the resulting Fe₃O₄ nanoparticles were mixed with a solution of chitosan in acetic acid at 60°C. The nanocomposite material was analyzed by Fourier-transform infrared spectroscopy, X-ray photoelectron spectroscopy, electron microscopy,

an X-ray diffractometer, and a vibrating sample magnetometer. In addition, the nanoparticles exhibited significant antibacterial efficacy against foodborne bacterial pathogens, such as *S. aureus* and *E. coli*, with inhibition zones of 11.5 and 13.5 mm, respectively.

Yaseen *et al.* compared the antibacterial, antioxidant, and larvicidal activity of *Alstonia scholaris* and *Polyalthia longifolia* extracts and that of Fe₂MgO₄ nanoparticles based on them [69]. The study objects were active against Gram-positive (*B. subtilis*, *S. aureus*) and Gram-negative (*P. aeruginosa*, *S. typhimurium*, and *E. coli*) bacteria in the following order: *A. scholaris*-based Fe₂MgO₄ > *P. longifolia*-based Fe₂MgO₄ > *A. scholaris* extract > *P. longifolia* extract. A similar correlation was observed for larvicidal activity against *Aedes albopictus* larvae. In particular, Fe₂MgO₄ nanoparticles exhibited excellent larvicidal activity with an LD₅₀ of 5–10 µg/cm³, a much lower dose than for the plant extracts. The antioxidant potential of Fe₂MgO₄ nanoparticles was determined by DPPH and phosphomolybdenum assays. It showed that Fe₂MgO₄ nanoparticles performed better than pure plant extract (controls).

Nickel. Ramji and Vishnuvarthanan created nanocomposite films based on polylactic acid with silica and nickel oxide nanoparticles in various concentrations (0.25, 0.5, 0.75, and 1 wt.%) and studied the nanoparticles' effect on the film's extensibility, barrier, surface color, opacity, and antibacterial properties [70]. The authors found that the films had good antibacterial activity against Gram-positive (*L. monocytogenes*) and Gram-negative (*Salmonella*) bacteria.

In another study, active nanocomposite films were obtained by incorporating nickel oxide nanoparticles (3, 6, and 9 wt.%) into chitosan-based films [71]. They were synthesized by burning the solution, and the films were obtained by casting in solvents. Fourier-transform infrared spectroscopy and X-ray diffraction analysis confirmed the formation of new interactions and an increase in crystallinity. In addition, the nanocomposite films showed good antibacterial activity against Gram-positive (*S. aureus*) and Gram-negative (*S. typhimurium*) bacteria.

Titanium. According to antibacterial tests, none of the bacterial species was sensitive to TiO₂ nanoparticles at any concentration under dark conditions, indicating that their antibacterial effects were due to photocatalytic reactions. Without light excitation, TiO₂ nanoparticles were not toxic to bacteria, as shown by CFU values. The nanoparticles only adsorbed on the bacterial cell wall. To ensure the adsorption–desorption equilibrium of TiO₂ nanoparticles doped with phosphorus and fluorine (PF-TiO₂), they were thoroughly mixed with bacterial suspensions under dark conditions and incubated for 15 min [72]. Light can induce charge separation in nanoparticles, and redox reactions can subsequently occur on their surface. The photocatalytic reactions confirmed the presence of hydroxyl (OH•) and superoxide (O₂^{•-}) radicals, as well as singlet oxygen.

Ezati *et al.* synthesized nanoparticles of titanium dioxide (TiO₂) and Cu-active-TiO₂ (Cu-TiO₂) by the sol-gel method, using carboxymethylcellulose (CMC) as a nanofiller to obtain functional packaging films [73]. The nanoparticles increased the films' mechanical and thermal stability, as well as their vapor barrier properties. Unlike the CMC/TiO₂ film, the CMC/Cu-TiO₂ film exhibited significant antibacterial activity against foodborne pathogenic bacteria (*L. monocytogenes* and *E. coli*) under visible light. The CMC/Cu-TiO₂ film also significantly delayed the browning of bananas when stored at 25°C for 14 days under visible light. The researchers assumed that the nanoparticles exhibited photocatalytic activity in visible light. Therefore, they can be used in functional packaging films to extend the shelf life of fruits after harvest, as well as in active packaging.

Films with antibacterial properties are mainly obtained from solutions and suspensions of film components that are molded by casting and dried under various conditions. Table 1 presents various films with metal and metal oxide nanoparticles used as antibacterial agents.

Nanoparticles incorporated in food coatings. The food industry involves a range of processes, including the preparation of raw materials, production, packaging, storage, etc. Packaging ensures food quality and safety, affecting the product's shelf life and marketing. Traditionally, packaging performs the following functions: storage; transportation; protection from physical damage, as well as chemical or biological deterioration; and branding [84–86].

Growing consumer concern and interest in health, nutritional value, food safety, and environmental issues has driven the development of biodegradable packaging. Since synthetic packaging materials are not biodegradable, they contribute to environmental pollution, climate change, and the depletion of natural resources. Despite excellent properties, high mechanical strength, low production cost, and process optimization, these non-renewable materials have a significant environmental impact in terms of greenhouse gas emissions, as well as land and water footprints [87]. Therefore, alternative ways of obtaining biopolymers are gaining more attention, since they address environmental issues, including the end-of-life treatment of plastic film waste.

Biodegradable films are commonly made from renewable sources mainly composed of proteins, carbohydrates, and lipids. Biopolymers have been extensively studied due to their abundance, good film-forming ability, transparency, and excellent barrier properties against O₂, CO₂, and lipids [88].

Currently, biopolymer food packaging is produced from a variety of materials, including natural agents, plant extracts, and nanomaterials. Such technologies can work synergistically along with nanotechnologies, creating multifunctional food packaging systems of high quality that can act as compatibilizers [89].

Table 1 Synthesis and antibacterial properties of films with metal and metal oxide nanoparticles

Composition	Synthesis	Bacteria strains	Method	Antimicrobial activity of films	References
CMC-PVA/ ZnO	1. $Zn(CH_3COO)_2 \cdot 2H_2O$ + NaOH solution, 3 h 60°C, sediment separation by centrifugation, drying at 600°C 2. Casting a mixture of CMC, PVA, and ZnO	<i>Escherichia coli</i> and <i>Staphylococcus aureus</i>	Agar disc diffusion	Synergistic effect of antimicrobial activity against <i>E. coli</i> and <i>S. aureus</i> in inhibition zones of 2.15 ± 0.42 and 3.25 ± 0.47 mm, respectively	[74]
Chitosan/ ZnO/bamboo leaves	1. 1:0.25 dispersion of powders in 1% acetic acid at 25°C, addition of glycerin 2. Incorporating bamboo leaf antioxidants, film casting	<i>E. coli</i> and <i>S. aureus</i>	Agar disc diffusion	ZnO NPs increased the antimicrobial activity of the chitosan film due to the interaction between Zn^{2+} ions and intracellular contents. Bamboo leaf antioxidants also increase antimicrobial properties through a synergistic effect	[75]
PLA/ Acelized cellulose nanocrystals/ ZnO	1. Dispersion of acelated cellulose nanocrystals in chloroform under ultrasound, addition of ZnO NPs under ultrasound. 2. Incorporating PMC 3. Solution casting. Drying at room temperature	<i>E. coli</i> and <i>S. aureus</i>	Shaking of the flask	The antibacterial activity of triple composite films increased with higher contents of ZnO NPs. The growth inhibition rate of 99.9% for both bacteria in the film with 5% ZnO nanoparticles demonstrated a great antibacterial effect. The antibacterial activity against <i>E. coli</i> was higher than against <i>S. aureus</i> . This was because the peptidoglycan layer of the cell wall was thicker in the Gram-positive <i>S. aureus</i> than in the Gram-negative <i>E. coli</i> , protecting it from destruction	[76]
Gelatin/ tragacanth/ ZnO	1. ZnO + water ($25 \pm 1^\circ C$, 400 rpm, 1 h), ultra sound (30°C, 40 kHz, 30 min) 2. Adding gelatin (40°C, 600 rpm, 30 min) 3. Mixing with a tragacanth solution at 700 rpm and then 1000 rpm. Adding a glycerin solution 4. Casting onto a 15 cm polyethylene plate. Drying (25°C, 48 h)	<i>E. coli</i> and <i>S. aureus</i>	Agar disc diffusion	The control film had no antimicrobial activity against either Gram-negative (<i>E. coli</i>) or Gram-positive (<i>S. aureus</i>) bacteria. All the nanocomposites showed antimicrobial activity dependent on the ZnO content against both bacteria. The small size of ZnO NPs caused higher interactions with bacterial cells	[77]
Gelatin/CuS	1. A suspension of CuS in water stirred under ultra sound 2. Adding a solution of glycerin and gelatin at 80°C 3. Casting on Teflon-coated glass. Drying	<i>E. coli</i> and <i>Listeria monocytogenes</i>	Counting viable colonies	The nanocomposite film with CuS nanoparticles integrated into gelatin sharply reduced the viability of <i>E. coli</i> cells, but had no significant effect on the growth of <i>L. monocytogenes</i> . The antimicrobial effect of CuS varied depending on its concentration. The low concentration (0.5 wt.%) of CuS was insufficient to inhibit microbial growth. However, its high concentration (2.0 wt.%) caused sufficiently strong antibacterial activity to completely inhibit the growth of <i>E. coli</i> after 9 h of exposure. The gelatin/CuS-based film showed stronger antibacterial activity against Gram-negative than Gram-positive bacteria	[78]

Composition	Synthesis	Bacteria strains	Method	Antimicrobial activity of films	References
CMC/glycerin/ <i>Dioscorea</i> <i>opposita</i> extract/ ZnO NPs	1. Mixing components in various concentrations at 50°C, centrifugation at 5000 rpm 2. Casting and drying at 50°C for 36 h	<i>E. coli</i> and <i>S. aureus</i>	Counting viable colonies	The films with ZnO NPs exhibited significant antibacterial activity against both target bacteria and <i>S. aureus</i> , which was stronger against <i>E. coli</i> . Inhibition rates of about 95% were achieved at each concentration for both Gram-positive and Gram-negative bacteria. Higher concentrations of the <i>D. opposita</i> extract reduced the antibacterial affect against <i>E. coli</i> at various concentrations of film-forming solutions	[79]
ZnO/corn starch/ chitosan/glycerin	1. Successive mixing of a chitosan solution (in a solution of malic acid), corn starch, glycerol, and ZnO NPs, followed by degassing by ultrasonication 2. Solution casting	<i>E. coli</i> and <i>S. aureus</i>	Agar disc diffusion	Longer times of delayed release of the composite films decreased the diameters of inhibition zones. Compared to the control, the composite films with ZnO NPs showed positive antibacterial activity against both <i>S. aureus</i> and <i>E. coli</i> . The inhibition zones against <i>S. aureus</i> had diameters of 29.36 ± 2.40 , 24.90 ± 0.40 , and 22.00 ± 0.34 mm, respectively, after 0, 7, and 14 days of prolonged release. They were larger than the inhibition zones of the composite films without ZnO	[80]
PVA/orange peel powder/Ag NPs	1. Successive incorporation of PVA, orange peel powder and AgNO ₃ into distilled water and constant stirring until complete dissolution 2. Solution casting	<i>E. coli</i> , <i>Pseudomonas aeruginosa</i> , <i>Streptococcus oralis</i> , and <i>S. aureus</i>	Agar disc diffusion	The clear inhibition zones formed by the composite films were larger than those formed by pure PVA or a mixture of PVA and orange peel powder. The hybrid biocomposite film with 5 mM silver NPs formed the clearest zones against both Gram-negative and Gram-positive bacteria	[81]
Gelatin/cellulose nanofibers/ZnO and/or Se NPs – nanoparticles, PVA – polyvinyl alcohol, US – ultrasound, PLA – polylactic acid	1. Successive incorporation of gelatin powder, a suspension of cellulose nanofiber, glycerin, and a solution of ZnO and Se, or their mixture, into distilled water with constant stirring 2. Solution casting	<i>E. coli</i> , <i>L. monocytogenes</i> , <i>S. aureus</i> , and <i>Pseudomonas fluorescens</i>	Agar disc diffusion	All the films containing NPs had an antibacterial effect against the studied strains. The largest inhibition zone was formed for <i>L. monocytogenes</i> , while the smallest zone was observed for <i>P. fluorescens</i>	[82]
Gelatin/ β -glucan/ ZnO	1. Successive incorporation of gelatin powder, glycerin, and a ZnO NP solution into distilled water with constant stirring. Adding a β -glucan solution. 2. Solution casting. Drying at 40°C for 24 h	<i>P. aeruginosa</i> , <i>Salmonella typhimurium</i> , <i>S. aureus</i> , and <i>E. coli</i>	Agar disc diffusion	The incorporation of ZnO NPs into the films ensured inhibitory activity against all the studied bacteria. Higher concentrations of ZnO NPs significantly enhanced the antibacterial activity of the films. The combination of ZnO NPs with β -glucan in a gelatin-based film significantly reduced the antibacterial activity against all the bacteria. However, increased concentrations of β -glucan did not cause a significant difference in the antibacterial activity of films with ZnO NPs. The highest inhibitory activity was shown against <i>S. aureus</i> , indicating that it was higher against Gram-positive than against Gram-negative bacteria	[83]

NPs – nanoparticles, PVA – polyvinyl alcohol, US – ultrasound, PLA – polylactic acid

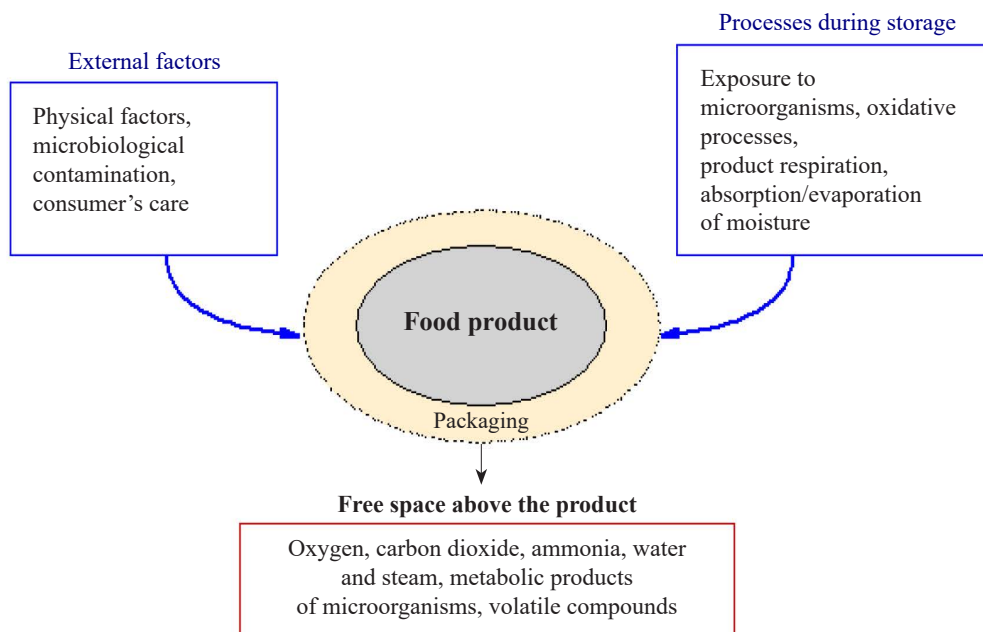


Figure 3 Changes in the product-packaging system over time

In recent years, bioactive films and smart technologies have been in wide use for packaging in the food sector [90, 91]. Plastic films have served as a barrier to protect food from heat, moisture, micro-organisms, dust, and dirt. Recent advances, such as smart packaging, active packaging, and intellectual packaging, have provided barrier films with extra functions [92–96]. These packaging systems are an effective way to extend the shelf life of foods produced through simplified processes or with a minimal use of preservatives [97, 98]. Yet, there cannot be a single package to suit all food products, since they vary greatly in chemical and microbiological components. In addition, food products are complex systems that change over time. Therefore, it is extremely important to develop optimal packaging for different types of products that meets their specific requirements. Figure 3 shows changes in the product-packaging system over time.

Cheese. Cheeses are mainly produced from pasteurized milk and usually have a low risk of microbiological contamination. However, foodborne pathogens can appear in cheese due to its improper handling during processing or due to re-opening of the packaging during storage [99]. Soft cheeses are an excellent environment for pathogenic microflora due to their high water activity, high protein content, and a moderate amount of fat [100].

Han *et al.* described the preparation of a nanosilver/graphene/PLA coating and its use as a package for curd cheese [101]. Three days of storage showed no difference in sensory parameters, regardless of the type of packaging. The cheese packaged in a nanosilver/graphene/PLA coating had minimal changes in appearance and color. It was uniform, slightly matte, white, and slightly pungent. The scientists also evaluated a possibility of re-using the active packaging.

The soft cheese samples were packaged in alginate composite coatings (ZnO nanoparticles and lemongrass essential oil) and stored at $4 \pm 1^\circ\text{C}$ and 75% relative humidity for 14 days [102]. The control sample packaged in a pure alginate coating became quite hard and translucent with visible signs of spoilage, while the test samples were whiter and softer, and retained the original creamy texture. The weight loss of the cheeses increased linearly with storage time due to the continuous movement of water vapor from the cheese into the environment. The pH values were monitored daily and found to be in the range of 4.45–4.57, indicating little change. However, the pH of the control sample dropped to 4.33, probably due to increased fermentation stimulated by microorganisms.

In another study, a coating with TiO_2 nanoparticles or a combination of TiO_2 and Ag in the PLA matrix increased the shelf life of chilled Yunnan curd from 5–7 days to 25 days at $5 \pm 1^\circ\text{C}$ [103]. Yet, no changes were observed in pH, as well as physicochemical and sensory indicators. The incorporation of nanoparticles effectively inhibited the growth of microorganisms, including yeasts and molds. The authors also tested the migration of nanoparticles from the composite coating in line with the standards of the European Food Safety Authority. Although the levels of metal ion migration reached $20.04 \pm 1.38 \mu\text{g}/\text{kg}$ at the end of the shelf life, those values were below the acceptable migration limit of $104 \mu\text{g}/\text{kg}$ for food contact materials.

Meat and poultry. Meat and poultry, as well as their products, are very sensitive to storage conditions. When refrigerated, they have a shelf life of only a few days due to microbial growth and lipid oxidation [104]. Large amounts of moisture and nutrients make them perishable products. Bacterial growth causes unpleasant smell

and taste, as well as mucus. Moreover, lipid oxidation changes the sensory characteristics of meat and poultry, which also limits their shelf life [105].

A simple method was proposed to obtain translucent antimicrobial nanocomposite films using regenerated cellulose and zinc oxide nanoparticles. The resulting nanocomposite coatings were transparent enough for food packaging, including meat products. They showed good mechanical strength, UV barrier properties, water vapor permeability, and antimicrobial activity against six pathogenic foodborne bacteria [106]. According to the tests, adding 3 wt.% zinc oxide nanoparticles effectively inhibited the growth of pathogenic Gram-positive (*Bacillus cereus*, *S. aureus*, and *L. monocytogenes*) and Gram-negative (*E. coli*, *S. typhimurium*, and *Vibrio parahaemolyticus*) bacteria. The UV transmission and oxygen permeability of the coatings reduced by 32 and 37%, respectively.

Despite high antibacterial activity, silver nanoparticles pose potential danger to human health. Therefore, they need to be incorporated into safer compounds. Zhao *et al.* used iturin A to synthesize silver nanoparticles to obtain a composite that can prevent chicken from bacterial contamination [107]. The composite material showed a broader antimicrobial spectrum, a lower concentration of silver, and higher antibacterial and antifungal activity, compared to the control. When applied to paper packaging for chicken, the iturin-Ag nanoparticle complex showed no silver residue, which demonstrated its high potential for food preservation.

Minced meat was placed in composite coatings (gelatin, chickpea protein, copper sulfide nanoparticles, and microencapsulated *Nigella sativa* essential oil) and stored for 14 days at 4°C [108]. The microbiological tests (*L. monocytogenes*, *S. aureus*, *Enterobacteriaceae*, and *Pseudomonas* spp.) showed that the simultaneous use of microencapsulated essential oil and CuS nanoparticles had a positive synergistic effect in increasing the shelf life of minced meat, compared to other samples.

Alginate-based nanocomposite coatings containing TiO₂ nanoparticles and caraway essential oil showed a high potential for extending the shelf life of beef [109]. The researchers studied their effect on chemical processes (changes in pH, total volatile basic nitrogen, peroxide value, and thiobarbituric acid-reactive substances) and microbial spoilage (changes in viable enterobacteria, lactic acid bacteria, *L. monocytogenes*, and *Pseudomonas* spp.) during 24 days of storage (4°C). The active coatings significantly reduced lipid oxidation, microbial growth, and total volatile basic nitrogen. They also improved the beef's sensory properties, retained its color for longer, and increased its shelf life from 4 to 16 days.

Hybrid chitosan-ZnO nanoparticles in combination with clove essential oil were found to have a good potential in active packaging materials [110]. The scanning electron microscope images showed a uniform distribution of the components with their minimal aggregation in the nanocomposite coatings. These components improved the film's tensile at break (~ 39.82%), film

hydrophobicity (~ 35.36%), ability to block ultraviolet light, water vapor barrier (~ 84.64%), and oxygen barrier (~ 57.66%), compared to the control film. In addition, they increased antioxidant activity and antibacterial activity against *P. aeruginosa*, *S. aureus*, and *E. coli*. The nanocomposite coatings extended the shelf life of chicken meat up to 5 days when stored at 8 ± 2°C. The researchers also determined the total migration limit in distilled water, 3% acetic acid, and 50% ethanol. According to the results, the coatings had a total migration rate below the allowable limit of 1000 µg/dL for model systems. The overall migration limit increased in the following order depending on the solvent: distilled water < 50% ethanol < 3% acetic acid.

Fish and seafood. Like meat and its products, fish and seafood have a short shelf life that is limited to a greater extent by microbiological spoilage.

Paidari and Ahari studied the effect of nanosilver and nanoclay incorporated into packaging materials on the growth of pathogens (*V. parahaemolyticus*, *S. aureus*, and *E. coli*) in shrimp stored for 6 days at 4°C [111]. They found that nanopackaging reduced the number of colonies by more than one logarithmic cycle, which is a significant reduction ($p < 0.05$). A synergistic effect was also observed for packaging with both nanosilver and nanoclay particles. Plasma-mass spectroscopy showed no migration of coating components (Ag, Al, and Si) in the shrimp samples on day 6 of the experiments.

Incorporating anthocyanins into packaging materials helps control the process of food spoilage. For example, pH-sensitive and antibacterial coatings based on chitosan/polyvinyl alcohol/ZnO nanoparticles and containing extracts of purple potato or rosella helped monitor the degree of freshness in shrimp by changing the color from purple to light green [112]. The coatings absorbed total volatile nitrogen released from the spoiled shrimp, which caused hydroxide ions to form and induce discoloration of the anthocyanins in the coating matrix. Therefore, such coatings have promising potential as active and intelligent packaging materials for food.

Efatian *et al.* studied a possibility of using a composite coating for packaging Nile tilapia fish stored at 4 and -20°C for 5 and 10 days [113]. The coating consisted of low-density polyethylene, silver nanoparticles, or a mixture of silver, copper, and titanium oxide nanoparticles. Antibacterial tests showed that the PNP/Ag + Cu/TiO₂ nanocomposite coating exhibited strong antibacterial activity against *E. coli* and *L. monocytogenes*. The researchers also evaluated the chemical characteristics (pH, protein and fat concentrations, free fatty acid profile) of the coated fish samples, as well as the migration of nanoparticles. According to the results, the samples packaged in Ag + Cu coatings had the least changes in pH and a free fatty acid profile, compared to fresh samples ($p < 0.05$). The migration of Ag and Cu nanoparticles from the coating into the tilapia samples was negligible, with Ag and Cu releases of < 2.0 and < 10 µg/kg, respectively.

Fresh fruits. Fresh fruits contain minerals, vitamins, phenolic compounds, and other nutrients. However, if not properly preserved, they quickly deteriorate and have a shelf life of only 5–7 days after harvest [114]. Currently, various types of processing (drying, jamming, etc.) are used to maintain post-harvest quality, but such processing leads to a loss of nutrients. However, coatings incorporated with nanoparticles can improve the preservation of these perishable products and extend their shelf life.

Strawberry fruits were packaged in multifunctional thin films (polylactic acid, antibacterial agents, and silver nanoparticles obtained from mango peel extract) and stored for 7 days at room temperature [115]. The films showed strong antimicrobial properties against *E. coli* and *S. aureus*. As we know, consumers are concerned about the migration of nanomaterials from food containers into food products posing potential risk to health. In this study, however, the total amount of silver migration was within the standard range throughout the storage period. The membrane also exhibited lower cytotoxicity, and the cells exposed to the composite film had an 80% survival.

The blotting paper layer of the packaging material incorporated with a mixture of plant extracts and silver nanoparticles as an antibacterial, anti-mold, anti-yeast, and anti-viral functional additive increased the shelf life of perishable products [116]. The coated paper showed good antibacterial activity against *E. coli* and *Motlagh S. aureus*. Freshly harvested tomatoes and coriander leaves packaged in the coated paper retained their quality characteristics for 15 and 30 days. However, when stored in plastic bags or outdoors, they showed partial spoilage and wilting.

Silver nanoparticles were obtained from an acidic polysaccharide isolated from the fruits of *Rosa roxburghii* [117]. This polysaccharide promoted the reduction of AgNO_3 into composites of Ag nanoparticles by a one-stage, environmentally friendly process. The resulting composites exhibited excellent antimicrobial activity against *S. aureus* and *E. coli*. The coating based on silver nanoparticles with chitosan showed a preservative effect on cherry tomatoes.

Paper packaging incorporated with silver nanoparticles bound with iturin A was used to prevent bacterial spoilage of chicken and protect oranges from fungal contamination [107].

Ready-to-eat products. Ready-to-eat foods, including ready-made salads, are the most vulnerable to microbiological spoilage. Their shelf life under standard conditions of $4 \pm 2^\circ\text{C}$ is no more than 24 h.

Motlagh *et al.* studied the effect of polyethylene packages containing silver nanoparticles in various concentrations (0.02 and 0.04%) on the shelf life, appearance, as well as microbiological and sensory properties of Olivier salad on days 2, 12, and 22 of storage [118]. According to the tests, the total count of microorganisms and molds increased with longer storage time and decreased with higher concentrations of nanoparticles.

In addition, *E. coli* decreased over time in all three packages, while the concentration of nanoparticles had no effect on the coliforms. Sensory characteristics were better in the samples stored in the packages with silver nanoparticles. The most optimal shelf life was 14 days in a package with 404.93 ppm of silver nanoparticles. The migration of silver ions from the package into the salad was measured by atomic absorption and was found to be within acceptable limits.

Table 2 summarizes the key characteristics of coatings based on nanoparticles that have not been covered above.

Although increasing the shelf life of food products, metals and their oxides can affect human health due to toxic effects [128, 129]. Therefore, their migration into products is undesirable and must be carefully controlled. As noted above, most studies have been devoted to antibacterial nanoparticles of silver and zinc in films and coatings. Therefore, the migration of coating components into food systems has also been described using these nanoparticles.

After ingestion, food products can release nanoparticles into the gastrointestinal environment [130]. According to *in vitro* studies, silver nanoparticles can disrupt the function of intestinal apical epithelial cells [131]. Moreover, they can induce inflammatory changes and oxidative stress in intestinal cells [132].

Other studies determined the toxicity of nanoparticles of metals and their oxides depending on the dose of exposure. They found that low concentrations of nanoparticles had no detrimental effect *in vitro* or *in vivo*. Particularly, the values of the starting point of transcriptomics for silver nanoparticles were significantly lower than the concentrations associated with changes in the calcium channel, oxidative stress, and membrane potential [128]. According to [133], ZnO nanoparticles are able to pass through the intestinal barrier and move from the intestinal lumen to hemolymph. However, no general toxicity was observed, and no oxidative stress was found in hemolymph cells (hemocytes).

Thus, there is still a lack of studies on the effect of films with nanoparticles of metals and their compounds on ready-to-eat products, so this area is worth pursuing in further research. The existing data are contradictory and therefore they cannot clearly indicate whether films and coatings with metal nanoparticles are safe or not, including those that are in contact with food.

CONCLUSION

Nanotechnology is a rapidly developing field of science. Researchers have been searching for ways to create nanoparticles with specified parameters using environmentally friendly methods, including biosynthesis based on plant extracts, plant parts, bacteria, and viruses. Such nanoparticles are widely used in films for various purposes. Nanoparticles of metals and metal oxides can act as antibacterial agents that are active even at low concentrations.

Table 2 Antibacterial effect of metal and compound nanoparticles incorporated into coatings for some food products

Nanoparticles	Coating components	Pathogens	Method	Product	References
ZnO	Acetylated cassava starch, polybutylene adipate-terephthalate, glycerin	<i>Staphylococcus aureus</i> , <i>Escherichia coli</i> , <i>Enterobacteriaceae</i> , <i>Pseudomonas</i> spp.	Counting viable cell colonies	Meat	[119]
Ag/AgCl-levan	Polyvinyl acetate	<i>E. coli</i> , <i>Klebsiella pneumoniae</i> , <i>Salmonella enterica</i> , <i>Pseudomonas aeruginosa</i> , <i>S. aureus</i> , <i>Micrococcus luteus</i> , <i>Listeria monocytogenes</i> , and <i>Enterococcus faecalis</i>	Agar disc diffusion	Minced meat	[46]
SiO ₂ -ZnO	γ -carrageenan/cassava starch	<i>E. coli</i> and <i>S. aureus</i>	Agar disc diffusion	Minced chicken	[120]
Ag	Agar, glycerin	<i>L. monocytogenes</i> and <i>E. coli</i>	Counting viable cell colonies	Beef loin	[121]
ZrO ₂	Apple peel pectin, potato starch, glycerin, <i>Zataria multiflora</i> microencapsulated essential oil	<i>E. coli</i> and <i>S. aureus</i>	Agar disc diffusion	Quail meat	[122]
TiO ₂	Gelatin, κ -carrageenan, saffron or barberry extract	<i>E. coli</i> and <i>S. aureus</i>	Agar disc diffusion	Trout	[123]
Fe ₂ TiO ₅	Sodium alginate, calcium chloride, glycerin	<i>Bacillus subtilis</i> , <i>E. coli</i> , <i>Bacillus cytotoxicus</i> , <i>S. enteritidis</i>	Agar disc diffusion	Strawberry	[124]
Ag	Soy protein isolate, chitin, glycerin	<i>S. aureus</i> , <i>E. coli</i> , <i>P. aeruginosa</i> , <i>Bacillus</i>	Agar disc diffusion	Bread	[125]
ZnO	Sodium alginate, aloe vera gel, glycerin	<i>S. aureus</i> , <i>E. coli</i> , <i>Syncephalastrum racemosum</i>	Agar disc diffusion	Tomatoes	[126]
ZnO	Soy protein isolate, red grape	Total microbial count	Agar disc diffusion	Pork	[127]

Nanoparticles have unique properties associated with their small size. They can attach and electrostatically bind to bacterial cell walls, causing membrane damage and, eventually, cell lysis. This explains their superior antimicrobial activity.

We studied the potential of incorporating nanoparticles into polymer and biopolymer films to obtain new materials with strong antimicrobial properties *in vitro*. We saw a trend towards a widespread use of silver or zinc nanoparticles, compared to other types of metal nanoparticles. The films under study exhibited antibacterial properties against major food pathogens, such as *Escherichia coli*, *Staphylococcus aureus*, *Listeria monocytogenes*, *Pseudomonas aeruginosa*, *Streptococcus oralis*, *Salmonella typhimurium*, etc. Many of them also showed improved physicochemical properties, such as water vapor permeability, water solubility, UV barrier, antioxidant properties, and others.

Bioactive coatings with nanoparticles of metals or their compounds are increasingly being studied as potential packaging for food raw materials and ready-to-eat products. Such composite films can extend the product's shelf life by reducing the rate of microbial spoilage and lipid oxidation. In addition, they have no, or only a slight, effect on the sensory characteristics of food products.

However, the migration of metal ions into a food product is highly undesirable, which may prevent composite films with metal nanoparticles from wide use. Further research into the migration of nanoparticles from the film into the food matrix might show if such films can be safely used for products with different chemical compositions.

CONFLICT OF INTEREST

The author declare no conflict of interest.

REFERENCES

- Chesnokova NYu, Prikhodko YuV, Kuznetsova AA, Kushnarenko LV, Gerasimova VA. Anthocyanin films in freshness assessment of minced fish. *Food Processing: Techniques and Technology*. 2021;51(2):349–362. (In Russ.). <https://doi.org/10.21603/2074-9414-2021-2-349-362>
- Bhargava N, Sharanagat VS, Mor RS, Kumar K. Active and intelligent biodegradable packaging films using food and food waste-derived bioactive compounds: A review. *Trends in Food Science and Technology*. 2020;105:385–401. <https://doi.org/10.1016/j.tifs.2020.09.015>

3. Koosha M, Hamed S. Intelligent Chitosan/PVA nanocomposite films containing black carrot anthocyanin and bentonite nanoclays with improved mechanical, thermal and antibacterial properties. *Progress in Organic Coatings*. 2019;127:338–347. <https://doi.org/10.1016/j.porgcoat.2018.11.028>
4. Gubitosa J, Rizzi V, Lopodota A, Fini P, Laurenzana A, Fibbi G, *et al.* One pot environmental friendly synthesis of gold nanoparticles using *Punica Granatum* Juice: A novel antioxidant agent for future dermatological and cosmetic applications. *Journal of Colloid and Interface Science*. 2018;521:50–61. <https://doi.org/10.1016/j.jcis.2018.02.069>
5. Rolima WR, Pelegrino MT, de Araújo Lima B, Ferraza LS, Costa FN, Bernardes JS, *et al.* Green tea extract mediated biogenic synthesis of silver nanoparticles: Characterization, cytotoxicity evaluation and antibacterial activity. *Applied Surface Science*. 2019;463:66–74. <https://doi.org/10.1016/j.apsusc.2018.08.203>
6. Piñón-Segundo E, Mendoza-Muñoz N, Quintanar-Guerrero D. Nanoparticles as dental drug-delivery systems. In: Subramani K, Ahmed W, editors. *Nanobiomaterials in clinical dentistry. A volume in micro and nano technologies*. Elsevier; 2019. pp. 567–593. <https://doi.org/10.1016/B978-0-12-815886-9.00023-1>
7. Qin Y, Liu Y, Yuan L, Yong H, Liu J. Preparation and characterization of antioxidant, antimicrobial and pH-sensitive films based on chitosan, silver nanoparticles and purple corn extract. *Food Hydrocolloids*. 2019;96:102–111. <https://doi.org/10.1016/j.foodhyd.2019.05.017>
8. Sun J, Jiangm H, Wu H, Tong C, Pang J, Wu C. Multifunctional bionanocomposite films based on konjac glucomannan/chitosan with nano-ZnO and mulberry anthocyanin extract for active food packaging. *Food Hydrocolloids*. 2020;107. <https://doi.org/10.1016/j.foodhyd.2020.105942>
9. Gmshinski IV, Ananyan MA, Shipelin VA, Riger NA, Trushina EN, Mustafina OK, *et al.* Effect of dihydroquercetin on the toxic properties of nickel nanoparticles. *Foods and Raw Materials*. 2023;11(2):232–242. <https://doi.org/10.21603/2308-4057-2023-2-572>
10. Khan SA, Noreen F, Kanwal S, Iqbal A, Hussain G. Green synthesis of ZnO and Cu-doped ZnO nanoparticles from leaf extracts of *Abutilon indicum*, *Clerodendrum infortunatum*, *Clerodendrum inerme* and investigation of their biological and photocatalytic activities. *Materials Science and Engineering: C*. 2018;82:46–59. <https://doi.org/10.1016/j.msec.2017.08.071>
11. Rai M, Yadav A, Gad A. Silver nanoparticles as a new generation of antimicrobials. *Biotechnology Advances*. 2009;27(1):76–83. <https://doi.org/10.1016/j.biotechadv.2008.09.002>
12. Marambio-Jones C, Hoek EMV. A review of the antibacterial effects of silver nanomaterials and potential implications for human health and the environment. *Journal of Nanoparticle Research*. 2010;12:1531–1551. <https://doi.org/10.1007/s11051-010-9900-y>
13. Cui Y, Zhao Y, Tian Y, Zhang W, Lü X, Jiang X. The molecular mechanism of action of bactericidal gold nanoparticles on *Escherichia coli*. *Biomaterials*. 2012;33(7):2327–2333. <https://doi.org/10.1016/j.biomaterials.2011.11.057>
14. Dhayalan M, Denison MIJ, Ayyar M, Gandhi NN, Krishnan K, Abdulhadi B. Biogenic synthesis, characterization of gold and silver nanoparticles from *Coleus forskohlii* and their clinical importance. *Journal of Photochemistry and Photobiology B: Biology*. 2018;183:251–257. <https://doi.org/10.1016/j.jphotobiol.2018.04.042>
15. Kumar KP, Paul W, Sharma CP. Green synthesis of gold nanoparticles with *Zingiber officinale* extract: Characterization and blood compatibility. *Process Biochemistry*. 2011;46(10):2007–2013. <https://doi.org/10.1016/j.procbio.2011.07.011>
16. Vaseeharan B, Ramasamy P, Chen JC. Antibacterial activity of silver nanoparticles (AgNps) synthesized by tea leaf extracts against pathogenic *Vibrio harveyi* and its protective efficacy on juvenile *Fenneropenaeus indicus*. *Letters in Applied Microbiology*. 2010;50(4):352–356. <https://doi.org/10.1111/j.1472-765X.2010.02799.x>
17. Gajbhiye M, Kesharwani J, Ingle A, Gade A, Rai M. Fungus-mediated synthesis of silver nanoparticles and their activity against pathogenic fungi in combination with fluconazole. *Nanomedicine: Nanotechnology, Biology, and Medicine*. 2009;5(4):382–386. <https://doi.org/10.1016/j.nano.2009.06.005>
18. Tankhiwale R, Bajpai SK. Preparation, characterization and antibacterial applications of ZnO-nanoparticles coated polyethylene films for food packaging. *Colloids and Surfaces B: Biointerfaces*. 2012;90:16–20. <https://doi.org/10.1016/j.colsurfb.2011.09.031>
19. Bang Y-J, Shankar S, Rhim J-W. *In situ* synthesis of multi-functional gelatin/resorcinol/silver nanoparticles composite films. *Food Packaging and Shelf Life*. 2019;22. <https://doi.org/10.1016/j.fpsl.2019.100399>
20. Liu J, Ma Z, Liu Y, Zheng X, Pei Y, Tang K. Soluble soybean polysaccharide films containing in-situ generated silver nanoparticles for antibacterial food packaging applications. *Food Packaging and Shelf Life*. 2022;31. <https://doi.org/10.1016/j.fpsl.2021.100800>
21. Perera KY, Jaiswal S, Jaiswal AK. A review on nanomaterials and nanohybrids based bio-nanocomposites for food packaging. *Food Chemistry*. 2022;376. <https://doi.org/10.1016/j.foodchem.2021.131912>
22. Khodashenas B, Ghorbani HR. Synthesis of silver nanoparticles with different shapes. *Arabian Journal of Chemistry*. 2019;12(8):1823–1838. <https://doi.org/10.1016/j.arabjc.2014.12.014>

23. Dzulkharnien NSF, Rohani R. A review on current designation of metallic nanocomposite hydrogel in biomedical applications. *Nanomaterials*. 2022;12(10). <https://doi.org/10.3390/nano12101629>
24. Rosli NA, Teow YH, Mahmoudi E. Current approaches for the exploration of antimicrobial activities of nanoparticles. *Science and Technology of Advanced Materials*. 2021;22(1):885–907. <https://doi.org/10.1080/14686996.2021.1978801>
25. Shaikh S, Nazam N, Rizvi SMD, Ahmad K, Baig MH, Lee EJ, *et al.* Mechanistic insights into the antimicrobial actions of metallic nanoparticles and their implications for multidrug resistance. *International Journal of Molecular Sciences*. 2019;20(10). <https://doi.org/10.3390/ijms20102468>
26. Beyth N, Hourri-Haddad Y, Domb A, Khan W, Hazan R. Alternative antimicrobial approach: Nano-antimicrobial materials. *Evidence-Based Complementary and Alternative Medicine*. 2015;2015. <https://doi.org/10.1155/2015/246012>
27. Jamkhande PG, Ghule NW, Bamer AH, Kalaskar MG. Metal nanoparticles synthesis: An overview on methods of preparation, advantages and disadvantages, and applications. *Journal of Drug Delivery Science and Technology*. 2019;53. <https://doi.org/10.1016/j.jddst.2019.101174>
28. Balasooriya ER, Jayasinghe CD, Jayawardena UA, Ruwanthika RWD, de Silva RM, Udagama PV. Honey mediated green synthesis of nanoparticles: New era of safe nanotechnology. *Journal of Nanomaterials*. 2017;2017. <https://doi.org/10.1155/2017/5919836>
29. Lyu J, Xing S, Meng Y, Wu N, Yin C. Flexible superhydrophobic ZnO coating harvesting antibacterial and washable properties. *Materials Letters*. 2022;314. <https://doi.org/10.1016/j.matlet.2022.131730>
30. Hou Y, Mushtaq A, Tang Z, Dempsey E, Wu Y, Lu Y, *et al.* ROS-responsive Ag-TiO₂ hybrid nanorods for enhanced photodynamic therapy of breast cancer and antimicrobial applications. *Journal of Science: Advanced Materials and Devices*. 2022;7(2). <https://doi.org/10.1016/j.jsamd.2022.100417>
31. Maťátková O, Michailidu Ja, Miškovská A, Kolouchová I, Masák J, Čejková A. Antimicrobial properties and applications of metal nanoparticles biosynthesized by green methods. *Biotechnology Advances*. 2022;58. <https://doi.org/10.1016/j.biotechadv.2022.107905>
32. Chinnapaiyan M, Selvam Y, Bassyouni F, Ramu M, Sakkaraveeranan C, Samickannian A, *et al.* Nanotechnology, green synthesis and biological activity application of zinc oxide nanoparticles incorporated argemone mexicana leaf extract. *Molecules*. 2022;27(5). <https://doi.org/10.3390/molecules27051545>
33. Dat TD, Viet ND, Dat NM, My PLT, Thinh DB, Thy LTM, *et al.* Characterization and bioactivities of silver nanoparticles green synthesized from Vietnamese *Ganoderma lucidum*. *Surfaces and Interfaces*. 2021;27. <https://doi.org/10.1016/j.surfin.2021.101453>
34. Singh P, Garg A, Pandit S, Mokkalapati VRSS, Mijakovic I. Antimicrobial effects of biogenic nanoparticles. *Nanomaterials*. 2018;8(12). <https://doi.org/10.3390/nano8121009>
35. Liu Z, Persson S, Sánchez-Rodríguez C. At the border: the plasma membrane–cell wall continuum. *Journal of Experimental Botany*. 2015;66(6):1553–1563. <https://doi.org/10.1093/jxb/erv019>
36. Swaminathan M, Sharma NK. Antimicrobial activity of the engineered nanoparticles used as coating agents. In: Martínez LMT, Kharissova OV, Kharisov BI, editors. *Handbook of ecomaterials*. Cham: Springer; 2017. pp. 1–15. https://doi.org/10.1007/978-3-319-48281-1_1-1
37. Dong Y, Zhu H, Shen Y, Zhang W, Zhang L. Antibacterial activity of silver nanoparticles of different particle size against *Vibrio natriegens*. *PLoS ONE*. 2019;14(9). <https://doi.org/10.1371/journal.pone.0222322>
38. Flores-López LZ, Espinoza-Gómez H, Somanathan R. Silver nanoparticles: Electron transfer, reactive oxygen species, oxidative stress, beneficial and toxicological effects. Mini review. *Journal of Applied Toxicology*. 2018;39(1):16–26. <https://doi.org/10.1002/jat.3654>
39. Dai Y, Wang Z, Zhao J, Xu L, Xu L, Yu X, *et al.* Interaction of CuO nanoparticles with plant cells: internalization, oxidative stress, electron transport chain disruption, and toxicogenomic responses. *Environmental Science: Nano*. 2018;5(10):2269–2281. <https://doi.org/10.1039/C8EN00222C>
40. Muntean DM, Sturza A, Dănilă MD, Borza C, Duicu OM, Mornoș C. The role of mitochondrial reactive oxygen species in cardiovascular injury and protective strategies. *Oxidative Medicine and Cellular Longevity*. 2016;2016. <http://doi.org/10.1155/2016/8254942>
41. Liu J, Peng Q. Protein-gold nanoparticle interactions and their possible impact on biomedical applications. *Acta Biomaterialia*. 2017;55:13–27. <https://doi.org/10.1016/j.actbio.2017.03.055>
42. Wang LL, Hu C, Shao LQ. The antimicrobial activity of nanoparticles: present situation and prospects for the future. *International Journal of Nanomedicine*. 2017;12:1227–1249. <https://doi.org/10.2147/IJN.S121956>
43. Kaur P, Nene AG, Sharma D, Somani PR, Tuli HS. Synergistic effect of copper nanoparticles and antibiotics to enhance antibacterial potential. *Bio-Materials and Technology*. 2019;1(1):33–47.

44. Oliani WL, Pusceddu FH, Parra DF. Silver-titanium polymeric nanocomposite non ecotoxic with bactericide activity. *Polymer Bulletin*. 2022;79:10949–10968. <https://doi.org/10.1007/s00289-021-04036-7>
45. Zhang M, Zheng Y, Jin Y, Wang D, Wang G, Zhang X, *et al.* Ag@MOF-loaded p-coumaric acid modified chitosan/chitosan nanoparticle and polyvinyl alcohol/starch bilayer films for food packing applications. *International Journal of Biological Macromolecules*. 2022;202:80–90. <https://doi.org/10.1016/j.ijbiomac.2022.01.074>
46. Haddar A, Ayed EB, Sila A, Putaux J-L, Bougatef A, Boufic S. Hybrid levan–Ag/AgCl nanoparticles produced by UV-irradiation: Properties, antibacterial efficiency and application in bioactive poly(vinyl alcohol) films. *RSC Advance*. 2021;11:38990–39003. <https://doi.org/10.1039/D1RA07852F>
47. Gasti T, Hiremani VD, Kesti ShS, Vanjeri VN, Goudar N, Masti SP, *et al.* Physicochemical and antibacterial evaluation of poly (vinyl alcohol)/guar gum/silver nanocomposite films for food packaging applications. *Journal of Polymers and the Environment*. 2021;29:3347–3363. <https://doi.org/10.1007/s10924-021-02123-4>
48. Adel AM, Al-Shemy MT, Diab MA, El-Sakhawy M, Toro RG, Montanari R, *et al.* Fabrication of packaging paper sheets decorated with alginate/oxidized nanocellulose-silver nanoparticles bio-nanocomposite. *International Journal of Biological Macromolecules*. 2021;181:612–620. <https://doi.org/10.1016/j.ijbiomac.2021.03.182>
49. Gu B, Jiang Q, Luo B, Liu C, Ren J, Wang X, *et al.* A sandwich-like chitosan-based antibacterial nanocomposite film with reduced graphene oxide immobilized silver nanoparticles. *Carbohydrate Polymers*. 2021;260. <https://doi.org/10.1016/j.carbpol.2021.117835>
50. Khurshid S, Arif S, Ali TM, Iqbal HM, Shaikh M, Khurshid H, *et al.* Effect of silver nanoparticles prepared from *Saraca asoca* leaf extract on morphological, functional, mechanical, and antibacterial properties of rice starch films. *Starch – Stärke*. 2022;74(5–6). <https://doi.org/10.1002/star.202100228>
51. Ardjoum N, Shankar S, Chibani N, Salmieri S, Lacroix M. *In situ* synthesis of silver nanoparticles in pectin matrix using gamma irradiation for the preparation of antibacterial pectin/silver nanoparticles composite films. *Food Hydrocolloids*. 2021;121. <https://doi.org/10.1016/j.foodhyd.2021.107000>
52. Dash KK, Kumar A, Kumari S, Malik MA. Silver nanoparticle incorporated flaxseed protein-alginate composite films: Effect on physicochemical, mechanical, and thermal properties. *Journal of Polymers and the Environment*. 2021; 29:3649–3659. <https://doi.org/10.1007/s10924-021-02137-y>
53. Wang L, Periyasami G, Aldalbahi A, Fogliano V. The antimicrobial activity of silver nanoparticles biocomposite films depends on the silver ions release behaviour. *Food Chemistry*. 2021;359. <https://doi.org/10.1016/j.foodchem.2021.129859>
54. Sallak N, Moghanjoughi AM, Ataee M, Anvar A, Golestan L. Antimicrobial biodegradable film based on corn starch/*Satureja khuzestanica* essential oil/Ag–TiO₂ nanocomposites. *Nanotechnology*. 2021;32(40). <https://doi.org/10.1088/1361-6528/ac0a15>
55. Mintiwab A, Jeyaramraja PR. Evaluation of phytochemical components, antioxidant and antibacterial activities of silver nanoparticles synthesized using *Ricinus communis* leaf extracts. *Vegetos*. 2021;34:606–618. <https://doi.org/10.1007/s42535-021-00244-8>
56. Burmistrov DE, Simakin AV, Smirnova VV, Uvarov OV, Ivashkin PI, Kucherov RN, *et al.* Bacteriostatic and cytotoxic properties of composite material based on ZnO nanoparticles in PLGA obtained by low temperature method. *Polymers*. 2022;14(1). <https://doi.org/10.3390/polym14010049>
57. Ching LW, Keesan FWM, Muhamad II. Optimization of ZnO/GO nanocomposite-loaded polylactic acid active films using response surface methodology. *Journal of King Saud University – Science*. 2022;34(3). <https://doi.org/10.1016/j.jksus.2022.101835>
58. Saedi S, Shokri M, Priyadarshi R, Rhim J-Wh. Carrageenan-based antimicrobial films integrated with sulfur-coated iron oxide nanoparticles (Fe₃O₄@SNP). *ACS Applied Polymer Materials*. 2021;3(10):4913–4923. <https://doi.org/10.1021/acsapm.1c00690>
59. Tymczewska A, Furtado BU, Nowaczyk J, Hryniewicz K, Szydłowska-Czerniak A. Functional properties of gelatin/polyvinyl alcohol films containing black cumin cake extract and zinc oxide nanoparticles produced via casting technique. *International Journal of Molecular Sciences*. 2022;23(5). <https://doi.org/10.3390/ijms23052734>
60. Abolhassani S, Alipour H, Alizadeh A, Nemati MM, Najafi H, Alavi O. Antibacterial effect of electrospun polyurethane-gelatin loaded with honey and ZnO nanoparticles as potential wound dressing. *Journal of Industrial Textiles*. 2022;5(1S):954S–968S. <https://doi.org/10.1177/15280837211069871>
61. Khalid H, Iqbal H, Zeeshan R, Nasir M, Sharif F, Akram M, *et al.* Silk fibroin/collagen 3D scaffolds loaded with TiO₂ nanoparticles for skin tissue regeneration. *Polymer Bulletin*. 2021;78:7199–7218. <https://doi.org/10.1007/s00289-020-03475-y>
62. Huang X, Zhou X, Dai Q, Qin Z. Antibacterial, antioxidation, uv-blocking, and biodegradable soy protein isolate food packaging film with mangosteen peel extract and ZnO nanoparticles. *Nanomaterials*. 2021;11(12). <https://doi.org/10.3390/nano11123337>

63. Roy S, Rhim J-W. Preparation of pectin/agar-based functional films integrated with zinc sulfide nano petals for active packaging applications. *Colloids and Surfaces B: Biointerfaces*. 2021;207. <https://doi.org/10.1016/j.colsurfb.2021.111999>
64. Lee SW, Said NS, Sarbon NM. The effects of zinc oxide nanoparticles on the physical, mechanical and antimicrobial properties of chicken skin gelatin/tapioca starch composite films in food packaging. *Journal of Food Science and Technology*. 2021;58(11):4294–4302. <https://doi.org/10.1007/s13197-020-04904-6>
65. Ding J, Hui A, Wang W, Yang F, Kang Y, Wang A. Multifunctional palygorskite@ZnO nanorods enhance simultaneously mechanical strength and antibacterial properties of chitosan-based film. *International Journal of Biological Macromolecules*. 2021;189:668–677. <https://doi.org/10.1016/j.ijbiomac.2021.08.107>
66. Ahmad AA, Sarbon NM. A comparative study: Physical, mechanical and antibacterial properties of bio-composite gelatin films as influenced by chitosan and zinc oxide nanoparticles incorporation. *Food Bioscience*. 2021;43. <https://doi.org/10.1016/j.fbio.2021.101250>
67. Hasanzadeh Y, Hamidinezhad H, Ashkarran AA. Shape dependent antibacterial activity of various forms of ZnO nanostructures. *BioNanoScience*. 2021;11:893–900. <https://doi.org/10.1007/s12668-021-00870-1>
68. Appu M, Lian Z, Zhao D, Huang J. Biosynthesis of chitosan-coated iron oxide (Fe₃O₄) hybrid nanocomposites from leaf extracts of *Brassica oleracea* L. and study on their antibacterial potentials. *3 Biotech*. 2021;11. <https://doi.org/10.1007/s13205-021-02820-w>
69. Yaseen MW, Sufyan M, Nazir R, Naseem A, Shah R, Sheikh AA, *et al*. Simple and cost-effective approach to synthesis of iron magnesium oxide nanoparticles using *Alstonia scholaris* and *Polyalthia longifolia* leaves extracts and their antimicrobial, antioxidant and larvicidal activities. *Applied Nanoscience*. 2021;11:2479–2488. <https://doi.org/10.1007/s13204-021-02051-8>
70. Ramji V, Vishnuvarthanan M. Influence of NiO supported silica nanoparticles on mechanical, barrier, optical and antibacterial properties of polylactic acid (PLA) bio nanocomposite films for food packaging applications. *Silicon*. 2022;14:531–538. <https://doi.org/10.1007/s12633-020-00839-x>
71. Marand SA, Almasi H, Marand NA. Chitosan-based nanocomposite films incorporated with NiO nanoparticles: Physicochemical, photocatalytic and antimicrobial properties. *International Journal of Biological Macromolecules*. 2021;190:667–678. <https://doi.org/10.1016/j.ijbiomac.2021.09.024>
72. Al-Tayyar NA, Youssef AM, Al-hindi R. Antimicrobial food packaging based on sustainable Bio-based materials for reducing foodborne Pathogens: A review. *Food Chemistry*. 2020;310. <https://doi.org/10.1016/j.foodchem.2019.125915>
73. Ezati P, Riahi Z, Rhim J-W. CMC-based functional film incorporated with copper-doped TiO₂ to prevent banana browning. *Food Hydrocolloids*. 2022;122. <https://doi.org/10.1016/j.foodhyd.2021.107104>
74. Helmiyati H, Hidayat ZSZ, Sitanggang IFR, Liftyawati D. Antimicrobial packaging of ZnO–Nps infused into CMC–PVA nanocomposite films effectively enhances the physicochemical properties. *Polymer Testing*. 2021;104. <https://doi.org/10.1016/j.polymertesting.2021.107412>
75. Liu J, Huang J, Hu Z, Li G, Hu L, Chen X, *et al*. Chitosan-based films with antioxidant of bamboo leaves and ZnO nanoparticles for application in active food packaging. *International Journal of Biological Macromolecules*. 2021;189:363–369. <https://doi.org/10.1016/j.ijbiomac.2021.08.136>
76. Yu F, Fei X, He Y, Li H. Poly(lactic acid)-based composite film reinforced with acetylated cellulose nanocrystals and ZnO nanoparticles for active food packaging. *International Journal of Biological Macromolecules*. 2021;186:770–779. <https://doi.org/10.1016/j.ijbiomac.2021.07.097>
77. Shahvalizadeh R, Ahmadi R, Davandeh I, Pezeshki A, Seyed Moslemi SA, Karimi S, *et al*. Antimicrobial bio-nanocomposite films based on gelatin, tragacanth, and zinc oxide nanoparticles – Microstructural, mechanical, thermo-physical, and barrier properties. *Food Chemistry*. 2021;354. <https://doi.org/10.1016/j.foodchem.2021.129492>
78. Roy S, Rhim J-W. Gelatin-based film integrated with copper sulfide nanoparticles for active packaging applications. *Applied Science*. 2021;11(14). <https://doi.org/10.3390/app11146307>
79. Li X, Ren Z, Wang R, Liu L, Zhang J, Ma F, *et al*. Characterization and antibacterial activity of edible films based on carboxymethyl cellulose, *Dioscorea opposita* mucilage, glycerol and ZnO nanoparticles. *Food Chemistry*. 2021;349. <https://doi.org/10.1016/j.foodchem.2021.129208>
80. Lian R, Cao J, Jiang X, Rogachev AV. Physicochemical, antibacterial properties and cytocompatibility of starch/chitosan films incorporated with zinc oxide nanoparticles. *Materials Today Communications*. 2021;27. <https://doi.org/10.1016/j.mtcomm.2021.102265>
81. Rathinavel S, Saravanakumar SS. Development and analysis of silver nano particle influenced PVA/natural particulate hybrid composites with thermo-mechanical properties. *Journal of Polymers and the Environment*. 2021;29:1894–1907. <https://doi.org/10.1007/s10924-020-01999-y>

82. Tymczewska A, Furtado BU, Nowaczyk J, Hryniewicz K, Szydłowska-Czerniak A. Functional properties of gelatin/polyvinyl alcohol films containing black cumin cake extract and zinc oxide nanoparticles produced via casting technique. *International Journal of Molecular Sciences*. 2022;23(5). <https://doi.org/10.3390/ijms23052734>
83. Azari SSh, Alizadeh A, Roufegarinejad L, Asefi N, Hamishhekar H. Preparation and characterization of gelatin/ β -glucan nanocomposite film incorporated with ZnO nanoparticles as an active food packaging system. *Journal of Polymers and the Environment*. 2021;29:1143–1152. <https://doi.org/10.1007/s10924-020-01950-1>
84. Drago E, Campardelli R, Pettinato M, Perego P. Innovations in smart packaging concepts for food: An extensive review. *Foods*. 2020;9(11). <https://doi.org/10.3390/foods9111628>
85. Risch SJ. Food packaging history and innovations. *Journal of Agricultural Food Chemistry*. 2009;57(18):8089–8092. <https://doi.org/10.1021/jf900040r>
86. Shaikh S, Yaqoob M, Aggarwal P. An overview of biodegradable packaging in food industry. *Current Research in Food Science*. 2021;4:503–520. <https://doi.org/10.1016/j.crf.2021.07.005>
87. Brizga J, Hubacek K, Feng K. The unintended side effects of bioplastics: Carbon, land, and water footprints. *One Earth*. 2020;3(4):515–516. <https://doi.org/10.1016/j.oneear.2020.09.004>
88. Etxabide A, Uranga J, Guerrero P, de la Caba K. Development of active gelatin films by means of valorisation of food processing waste: A review. *Food Hydrocolloids*. 2017;68:192–198. <https://doi.org/10.1016/j.foodhyd.2016.08.021>
89. Said NS, Howell NK, Sarbon NM. A review on potential use of gelatin-based film as active and smart biodegradable films for food packaging application. *Food Reviews International*. 2021;39(2):1063–1085. <https://doi.org/10.1080/87559129.2021.1929298>
90. Sohail M, Sun D-W, Zhu Z. Recent developments in intelligent packaging for enhancing food quality and safety. *Critical Reviews in Food Science and Nutrition*. 2018;58(15):2650–2662. <https://doi.org/10.1080/10408398.2018.1449731>
91. Nogueira GF, Soares CT, Cavasini R, Fakhouri FM, de Oliveira RA. Bioactive films of arrowroot starch and blackberry pulp: Physical, mechanical and barrier properties and stability to pH and sterilization. *Food Chemistry*. 2019;275:417–425. <https://doi.org/10.1016/j.foodchem.2018.09.054>
92. Vanderroost M, Ragaert P, Devlieghere F, de Meulenaer B. Intelligent food packaging: The next generation. *Trends in Food Science and Technology*. 2014;39(1):47–62. <https://doi.org/10.1016/j.tifs.2014.06.009>
93. Kerry JP, O’Grady MN, Hogan SA. Past, current and potential utilisation of active and intelligent packaging systems for meat and muscle-based products: A review. *Meat Science*. 2006;74(1):113–130. <https://doi.org/10.1016/j.meatsci.2006.04.024>
94. Han J-W, Ruiz-Garcia L, Qian J-P, Yang X-T. Food packaging: A comprehensive review and future trends. *Comprehensive Reviews in Food Science and Food Safety*. 2018;17(4):860–877. <https://doi.org/10.1111/1541-4337.12343>
95. Schaefer D, Cheung WM. Smart packaging: Opportunities and challenges. *Procedia CIRP*. 2018;72:1022–1027. <https://doi.org/10.1016/j.procir.2018.03.240>
96. Müller P, Schmid M. Intelligent packaging in the food sector: A brief overview. *Foods*. 2019;8(1). <https://doi.org/10.3390/foods8010016>
97. Janjarasskul T, Suppakul P. Active and intelligent packaging: The indication of quality and safety. *Critical Reviews in Food Science and Nutrition*. 2018;58(5):808–831. <https://doi.org/10.1080/10408398.2016.1225278>
98. Wicochea-Rodríguez JD, Chalier P, Ruiz T, Gastaldi E. Active food packaging based on biopolymers and aroma compounds: How to design and control the release. *Frontiers in Chemistry*. 2019;7. <https://doi.org/10.3389/fchem.2019.00398>
99. Youssef AM, EL-Sayed SM, EL-Sayed HS, Salama HH, Dufresne A. Enhancement of Egyptian soft white cheese shelf life using a novel chitosan/carboxymethyl cellulose/zinc oxide bionanocomposite film. *Carbohydrate Polymers*. 2016;151:9–19. <https://doi.org/10.1016/j.carbpol.2016.05.023>
100. Al-Nabulsi A, Osaili T, Sawalha A, Olaimat AN, Albiss BA, Mehyar G, *et al*. Antimicrobial activity of chitosan coating containing ZnO nanoparticles against *E. coli* O157:H7 on the surface of white brined cheese. *International Journal of Food Microbiology*. 2020;334. <https://doi.org/10.1016/j.ijfoodmicro.2020.108838>
101. Peter A, Cozmuta LM, Nicula C, Cozmuta AM, Talasman CM, Drazic G, *et al*. Chemical and organoleptic changes of curd cheese stored in new and reused active packaging systems made of Ag-graphene-TiO₂-PLA. *Food Chemistry*. 2021;363. <https://doi.org/10.1016/j.foodchem.2021.130341>
102. Motelica L, Fikai D, Oprea O, Fikai A, Trusca R-D, Andronescu E, *et al*. Biodegradable alginate films with zno nanoparticles and citronella essential oil – A novel antimicrobial structure. *Pharmaceutics*. 2021;13(7). <https://doi.org/10.3390/pharmaceutics13071020>

103. Li W, Li L, Zhang H, Yuan M, Qin Y. Evaluation of PLA nanocomposite films on physicochemical and microbiological properties of refrigerated cottage cheese. *Journal of Food Processing and Preservation*. 2018;42(1). <https://doi.org/10.1111/jfpp.13362>
104. Hosseinzadeh S, Partovi R, Talebi F, Babaei A. Chitosan/TiO₂ nanoparticle/*Cymbopogon citratus* essential oil film as food packaging material: Physico-mechanical properties and its effects on microbial, chemical, and organoleptic quality of minced meat during refrigeration. *Journal of Food Processing and Preservation*. 2020;44(7). <https://doi.org/10.1111/jfpp.14536>
105. Marcous A, Rasouli S, Ardestani F. Low-density polyethylene films loaded by titanium dioxide and zinc oxide nanoparticles as a new active packaging system against *Escherichia coli* O157:H7 in fresh calf minced meat. *Packaging Technology and Science*. 2017;30(11):693–701. <https://doi.org/10.1002/pts.2312>
106. Saedi S, Shokri M, Kim JT, Shin GH. Semi-transparent regenerated cellulose/ZnONP nanocomposite film as a potential antimicrobial food packaging material. *Journal of Food Engineering*. 2021;307. <https://doi.org/10.1016/j.jfoodeng.2021.11066>
107. Zhao X, Wang K, Ai C, Yan L, Jiang C, Shi J. Improvement of antifungal and antibacterial activities of food packages using silver nanoparticles synthesized by iturin A. *Food Packaging and Shelf Life*. 2021;28. <https://doi.org/10.1016/j.fpsl.2021.100669>
108. Rasul NH, Asdagh A, Pirsas S, Ghazanfarirad N, Sani IK. Development of antimicrobial/antioxidant nanocomposite film based on fish skin gelatin and chickpea protein isolated containing Microencapsulated *Nigella sativa* essential oil and copper sulfide nanoparticles for extending minced meat shelf life. *Materials Research Express*. 2022;9. <https://doi.org/10.1088/2053-1591/ac50d6>
109. Sayadi M, Langroodi AM, Amiri S, Radi M. Effect of nanocomposite alginate-based film incorporated with cumin essential oil and TiO₂ nanoparticles on chemical, microbial, and sensory properties of fresh meat/beef. *Food Science and Nutrition*. 2022;10(5):1401–1413. <https://doi.org/10.1002/fsn3.2724>
110. Gasti T, Dixit S, Hiremani VD, Chougale RB, Masti SP, Vootla SK, *et al.* Chitosan/pullulan based films incorporated with clove essential oil loaded chitosan-ZnO hybrid nanoparticles for active food packaging. *Carbohydrate Polymers*. 2022;277. <https://doi.org/10.1016/j.carbpol.2021.118866>
111. Paidari S, Ahari H. The effects of nanosilver and nanoclay nanocomposites on shrimp (*Penaeus semisulcatus*) samples inoculated to food pathogens. *Journal of Food Measurement and Characterization* volume. 2021;15:3195–3206. <https://doi.org/10.1007/s11694-021-00905-x>
112. Liu J, Huang J, Ying Y, Hu L, Hu Y. pH-sensitive and antibacterial films developed by incorporating anthocyanins extracted from purple potato or roselle into chitosan/polyvinyl alcohol/nano-ZnO matrix: Comparative study. *International Journal of Biological Macromolecules*. 2021;178:104–112. <https://doi.org/10.1016/j.ijbiomac.2021.02.115>
113. Efatian H, Ahari H, Shahbazzadeh D, Nowruzzi B, Yousefi S. Fabrication and characterization of LDPE/silver-copper/titanium dioxide nanocomposite films for application in Nile Tilapia (*Oreochromis niloticus*) packaging. *Journal of Food Measurement and Characterization*. 2021;15:2430–2439. <https://doi.org/10.1007/s11694-021-00836-7>
114. Yinzhe R, Shaoying Z. Effect of carboxymethyl cellulose and alginate coating combined with brewer yeast on postharvest grape preservation. *International Scholarly Research Notices*. 2013;2013. <https://doi.org/10.1155/2013/871396>
115. Cheng J, Lin X, Wu X, Liu Q, Wan S, Zhang Y. Preparation of a multifunctional silver nanoparticles polylactic acid food packaging film using mango peel extract. *International Journal of Biological Macromolecules*. 2021;188:678–688. <https://doi.org/10.1016/j.ijbiomac.2021.07.161>
116. Chaitanya Kumari S, Naga Padma P, Anuradha K. Green silver nanoparticles embedded in cellulosic network for fresh food packaging. *Journal of Pure and Applied Microbiology*. 2021;15(3):1236–1244. <https://doi.org/10.22207/JPAM.15.3.13>
117. Wang L, Tian Y, Zhang P, Li C, Chen J. Polysaccharide isolated from *Rosa roxburghii* Tratt fruit as a stabilizing and reducing agent for the synthesis of silver nanoparticles: antibacterial and preservative properties. *Journal of Food Measurement and Characterization*. 2022;16:1241–1251. <https://doi.org/10.1007/s11694-021-01248-3>
118. Motlagh NV, Aghazamani J, Gholami R. Investigating the effect of nano-silver contained packaging on the olivier salad shelf-life. *BioNanoScience*. 2021;11:838–847. <https://doi.org/10.1007/s12668-021-00876-9>
119. Phothisarattana D, Wongphan P, Promhuad K, Promsorn J, Harnkarnsujarit N. Blown film extrusion of PBAT/TPS/ZnO nanocomposites for shelf-life extension of meat packaging. *Colloids and Surfaces B: Biointerfaces*. 2022;214. <https://doi.org/10.1016/j.colsurfb.2022.112472>
120. Praseptianga D, Widyaastuti D, Panatarani C, Joni IM. Development and characterization of semi-refined iota carrageenan/ SiO₂-ZnO bionanocomposite film with the addition of cassava starch for application on minced chicken meat packaging. *Foods*. 2021;10(11). <https://doi.org/10.3390/foods10112776>

121. Hong S-I, Cho Y, Rhim J-W. Effect of Agar/AgNP composite film packaging on refrigerated beef loin quality. *Membranes*. 2021;11(10). <https://doi.org/10.3390/membranes11100750>
122. Sani IK, Geshlaghi SP, Pirsas S, Asdagh A. Composite film based on potato starch/apple peel pectin/ZrO₂ nanoparticles/microencapsulated *Zataria multiflora* essential oil; investigation of physicochemical properties and use in quail meat packaging. *Food Hydrocolloids*. 2021;117. <https://doi.org/10.1016/j.foodhyd.2021.106719>
123. Sani MA, Tavassoli M, Salim SA, Azizi-lalabadi M, McClements DJ. Development of green halochromic smart and active packaging materials: TiO₂ nanoparticle- and anthocyanin-loaded gelatin/κ-carrageenan films. *Food Hydrocolloids*. 2022;124. <https://doi.org/10.1016/j.foodhyd.2021.107324>
124. Rizzotto F, Vasiljevic ZZ, Stanojevic G, Dojcinovic MP, Jankovic-Castvan I, Vujancevic JD, *et al.* Antioxidant and cell-friendly Fe₂TiO₅ nanoparticles for food packaging application. *Food Chemistry*. 2022;390. <https://doi.org/10.1016/j.foodchem.2022.133198>
125. Koshy RR, Reghunadhan A, Mary SK, Sadanandan S, Jose S, Thomas S, *et al.* AgNP anchored carbon dots and chitin nanowhisker embedded soy protein isolate films with freshness preservation for active packaging. *Food Packaging and Shelf Life*. 2022;33. <https://doi.org/10.1016/j.fpsl.2022.100876>
126. Abdel Aziz MS, Salama HE. Development of alginate-based edible coatings of optimized UV-barrier properties by response surface methodology for food packaging applications. *International Journal of Biological Macromolecules*. 2022;212:294–302. <https://doi.org/10.1016/j.ijbiomac.2022.05.107>
127. Ran R, Chen S, Su Y, Wang L, He S, He B, *et al.* Preparation of pH-colorimetric films based on soy protein isolate/ZnO nanoparticles and grape-skin red for monitoring pork freshness. *Food Control*. 2022;137. <https://doi.org/10.1016/j.foodcont.2022.108958>
128. Xu K, Mittal K, Ewald J, Rulli S, Jakubowski JL, George S, *et al.* Transcriptomic points of departure calculated from human intestinal cells exposed to dietary nanoparticles. *Food and Chemical Toxicology*. 2022;170. <https://doi.org/10.1016/j.fct.2022.113501>
129. Wang S, Kang X, Alenius H, Wong SH, Karisola P, El-Nezami H. Oral exposure to Ag or TiO₂ nanoparticles perturbed gut transcriptome and microbiota in a mouse model of ulcerative colitis. *Food and Chemical Toxicology*. 2022;169. <https://doi.org/10.1016/j.fct.2022.113368>
130. Liu Y, Huang Y, Mou Z, Li R, Hossen A, Dai J, *et al.* Characterization and preliminary safety evaluation of nano-SiO₂ isolated from instant coffee. *Ecotoxicology and Environmental Safety*. 2021;224. <https://doi.org/10.1016/j.ecoenv.2021.112694>
131. Cornu R, Chrétien C, Pellequer Y, Martin H, Béduneau A. Small silica nanoparticles transiently modulate the intestinal permeability by actin cytoskeleton disruption in both Caco-2 and Caco-2/HT29-MTX models. *Archives of Toxicology*. 2020;94:1191–1202. <https://doi.org/10.1007/s00204-020-02694-6>
132. Xu K, Basu N, George S. Dietary nanoparticles compromise epithelial integrity and enhance translocation and antigenicity of milk proteins: An *in vitro* investigation. *NanoImpact*. 2021;24. <https://doi.org/10.1016/j.impact.2021.100369>
133. Alaraby M, Annangi B, Hernández A, Creus A, Marcos R. A comprehensive study of the harmful effects of ZnO nanoparticles using *Drosophila melanogaster* as an *in vivo* model. *Journal of Hazardous Materials*. 2015;296:166–174. <https://doi.org/10.1016/j.jhazmat.2015.04.053>

ORCID IDs

Natalia B. Eremeeva  <https://orcid.org/0000-0002-9632-6296>



Hematological parameters of free-ranging moose *Alces alces* (Linnaeus 1758) (*Ruminantia*, *Cervidae*)

Maria A. Perevozchikova* , Igor A. Domsy , Alexey A. Sergeyev

Professor Zhitkov Russian Research Institute of Game Management and Fur Farming, Kirov, Russia

* e-mail: mperevozchikova@mail.ru

Received 28.03.2023; Revised 18.04.2023; Accepted 02.05.2023; Published online 30.08.2023

Abstract:

Comparative studies that feature the physiology of wild and domestic animals replenish the fundamental knowledge in the field of biology and adaptive potential, thus increasing the efficiency of domestication. Semi-free conditions and artificial environment create prerequisites for epidemics and stress. However, early detection can prevent critical situations. This research provides new data on moose biology and physiology by establishing age and sex hematological parameters.

The study featured moose blood samples ($n = 55$) obtained in the Kirov Region in the northeast of European Russia. Hematological tests relied on a veterinary version of a MicroCC-20 Plus automatic analyzer (High Technology).

This research was the first of its kind to introduce a comparative hematological analysis of local European moose according to age and sex. Adults and calves demonstrated significant differences ($p < 0.05$) in red blood cells, hemoglobin, hematocrit, mean corpuscular volume, mean concentration hemoglobin, mean corpuscular hemoglobin concentration, platelet distribution width, red blood cell distribution width, platelet crit, platelets, leukocytes, and eosinophils. Females and males also had significant differences ($p < 0.05$) in red blood cells, hemoglobin, mean corpuscular volume, red blood cell distribution width, platelet distribution width, platelets, and eosinophil content. The single- and multivariate analysis made it possible to establish the effect of physiological factors on the blood parameters in moose.

The hematological values were in line with the most indicators reported in other publications on wild artiodactyls. The existing differences in blood parameters depended on the species, habitat, food supply, age, and sex.

Keywords: *Alces alces*, moose females, moose males, adult animals, calves, hematology, erythrocytes, leukocytes, platelets

Funding. This research was partially supported by the Russian Academy of Sciences (RAS) FSZZ-2019-0001 (AAAA-A19-119020190132-5). It was performed on the premises of the Professor Zhitkov Russian Research Institute of Game Management and Fur Farming (VNIIOZ profi Zhitkov).

Please cite this article in press as: Perevozchikova MA, Domsy IA, Sergeyev AA. Hematological parameters of free-ranging moose *Alces alces* (Linnaeus 1758) (*Ruminantia*, *Cervidae*). Foods and Raw Materials. 2024;12(1):80–90. <https://doi.org/10.21603/2308-4057-2024-1-592>

INTRODUCTION

The European moose (*Alces alces*, Linnaeus, 1758) is one of the largest representatives of the taiga fauna. The species has a significant ecological variability and acclimatizes quite easily to new habitats. The moose is a traditional game species in many countries [1–3]. Nowadays, moose are bred in semi-free conditions and artificial habitats. Their complete commercial development is possible only on farms. Moose are a source of meat and milk, which has a chemical composition of a high-quality food product. Moose skin can be processed into top-grade suede. In addition, moose can be used for transport purposes.

Moose possess numerous valuable qualities, including rapid growth and maturation. Under normal conditions, the fecundity approximates 1.5 calves per mature female. This indicator depends on the habitat, climate, and individual characteristics. Both females and males become breedable at 18 months [4].

An important advantage is that moose experience no forage competition from farm animals. In their year-round free-ranging, they rely on trees and shrubs of a certain composition and age. Moose diet varies from habitat to habitat and from season to season [4].

The bottle-neck of moose breeding is the veterinary and sanitary measures against non-communicable and

contagious diseases. Thus, moose farming requires not only hunting and biotechnical procedures, but also a number of veterinary measures.

Peripheral blood is highly sensitive to environmental conditions. As a result, it can be used to assess the health, adaptive capabilities, and stability of moose organism. Hematology currently occupies a leading place in veterinary science as it links physiology with clinical evidence. By establishing the effect of age, sex, and season on blood parameters, veterinarians can detect the slightest changes in animal physiology [5]. In addition, hematological studies are important because blood performs numerous and complex functions. Diagnostic hematology relies on the morphology, quantity, and ratio of blood cells. These studies include the diagnostics of hematopoietic and other organs and tissues because their malfunction affects blood morphology and biochemistry [5]. Hematology allows veterinarians to detect deviations from the norm. These methods can also be used to assess the state of wild animal populations [6].

Therefore, hematological methods are important tools in studying the health of individual animals and whole populations. They provide such valuable input data as challenging breeding conditions, semi-free or artificial habitat, acclimatization, population decline, epizootics, etc.

The first moose blood studies belonged to Ponder, who reported them as mammals with the largest red blood cells. Knorre & Knorre studied the concentration of red blood cells and hemoglobin in moose blood at the Pechoro-Ilychsky Reserve in the Komi Republic, Russia [7, 8]. Indeed, all publications report the large size of moose red blood cells, as well as their low concentration, which indicates a relatively low oxygen transportation [9].

Very few modern studies in moose hematology are now available. As a rule, they rely on insufficient sampling, provide no sex or age differences, or involve only animals kept in captivity [6, 10–11]. However unrepresentative, these studies are of considerable scientific value.

The purpose of this research was to obtain new data in the field of biology and physiology of moose and to establish hematological parameters for various age and sex groups.

STUDY OBJECTS AND METHODS

Moose blood samples ($n = 55$) were collected from 13 young females, 11 adult females, 10 young males, and 21 adult males.

The animals were caught in 2011–2020 during hunting seasons between October and December. All the animals were clinically healthy and demonstrated no signs of disease at the time of sampling.

The body weight varied as follows: 127.0–185.0 kg in young females, 363.0–432.0 kg in adult females, 178.0–201.5 in young males, and 280.0–420.5 in adult males.

The sampling covered the experimental game farm at the Professor Zhitkov Russian Research Institute of

Game Management and Fur Farming. It is located in the southern taiga of the north-east of European Russia, namely, in Slobodsky, Zuevsky, and Belokholunsky districts of the Kirov Region with the geographical center in the village of Rogovoe (58°33'04"N, 50°43'42"E). The total area of the experimental farm is 66 250 ha. The climate is continental, with moderately cold winters and warm summers. All the animals were wild and roamed freely within the farm, feeding on local vegetation.

Blood samples were obtained by cutting the jugular vein (*Venae jugularis* L.) immediately after shooting: 4 cm³ of blood was collected into UNIVAC vacuum tubes with dipotassium ethylenediaminetetraacetic acid (K₂EDTA) anticoagulant. The tubes were kept refrigerated until sent to the laboratory.

The hematological studies took place on days 1–3 using a veterinary modification of a MicroCC-20 Plus automatic analyzer (High Technology, USA). The leukocyte formula was calculated by the microscopy of blood smears stained with dye-fixative eosin methylene blue according to May-Grunwald and azure-eosin dye according to Romanovsky (MiniMed-M-G, Russia).

Each blood sample was studied for red blood cells, hemoglobin, hematocrit, mean corpuscular volume, mean concentration hemoglobin, mean corpuscular hemoglobin concentration, red blood cell distribution width, platelet distribution width, platelet crit, platelet count, white blood cells, and eosinophils.

The statistical analysis involved MS Excel (Office 2019), Statgraphics (19-X64) software, and standard methods [12]. The mean (M), standard deviation (SD), median (Me), and the 25th and 75th percentiles served to describe the samples. The Mann-Whitney U test and the Kruskal-Wallis H test were applied to compare the groups. Single- and multivariate analysis of variance made it possible to assess the effect of age, sex, and body weight on the hematological parameters. The effect was considered significant at $p < 0.05$.

RESULTS AND DISCUSSION

Blood analysis assesses the state of health or the course of a pathological process in the animal body. In the recent past, veterinary practice did not rely on hematology because blood testing methods were underdeveloped, the equipment was lacking, and no data on blood composition in wild species were available. Moreover, veterinary science possessed very poor evidence about the relationship between the qualitative composition of blood and the course of pathological processes. Blood testing opened up good prospects for understanding various pathologies and their control. Blood changes can facilitate diagnosis and prognosis.

Thus, the baseline values for various hemogram parameters can indicate the state of specimen and populations of game animals that are exposed to the environment conditions, pathogenic microorganisms, parasites, toxins, etc.

The research delivered reliable data on red blood cells, while blood cells, and platelets of wild moose

Table 1 Red blood cell parameters for free-ranging moose given for calves and adult animals (n = 55)

Parameters, min – max M ± SD Me 25–75%	Calves ≤ 1 y.o., ♀	Adults, ♀	Calves ≤ 1 y.o., ♂	Adults, ♂
Red blood cells, ×10 ¹² /L	3.60–5.98 4.72 ± 0.66 4.72 ^{A,B} 4.30–5.18	4.36–7.24 5.88 ± 0.94 5.87 ^{A,B} 5.12–6.52	4.54–5.90 5.29 ± 0.42 5.35 ^{A,B} 5.00–5.58	4.77–9.10 6.95 ± 1.11 7.35 ^{A,B} 6.20–7.71
Hemoglobin, g/L	93–140 117.07 ± 14.13 115 ^{A,B} 109–124	105–173 143.54 ± 21.34 143 ^A 127.0–166.0	100–139 121.50 ± 11.91 122 ^{A,B} 114–129	121–199 158.04 ± 23.47 159 ^A 144–173
Hematocrit, %	23.7–34.4 28.84 ± 3.03 29.4 ^A 27.2–30.7	31.8–58.7 45.56 ± 8.82 44.1 ^A 38–52.1	30.5–42.3 35.52 ± 3.18 36.25 ^A 33.5–36.4	33.1–60.4 45.98 ± 7.73 47.6 ^A 41.2–51
Mean corpuscular volume, fl	57.2–65.3 61.33 ± 2.26 61.6 ^{A,B} 60.1–62.7	60.1–79.0 68.79 ± 5.64 68.5 ^A 62.6–72.8	58.9–79.8 70.24 ± 7.10 70.95 ^B 64.1–75.6	63.4–86.0 72.12 ± 6.15 71.8 67.9–75.1
Mean concentration hemoglobin, pg	19.3–24.5 21.80 ± 1.60 21.6 ^A 21.1–22.5	22.2–25.3 24.05 ± 0.83 24 ^A 23.6–24.8	19.5–26.1 22.85 ± 2.25 22.45 21.9–25.1	21.9–26.0 23.90 ± 1.18 23.9 23.1–24.7
Mean corpuscular hemoglobin concentration, g/L	324–373 346.69 ± 13.73 346 ^A 343–351	339–386 361.00 ± 13.73 362 ^A 350–371	247–374 329.70 ± 44.58 341.5 ^A 327–361	337–400 365.28 ± 17.47 363 ^A 352–379
Red blood cell distribution width (standard deviation), %	13–15.3 14.37 ± 0.70 14.4 ^{A,B} 13.9–14.8	13.8–16.8 15.10 ± 0.87 15.2 ^{A,B} 14.3–15.7	13.8–18.1 15.90 ± 1.32 15.9 ^B 15.0–16.4	14.5–18.3 16.36 ± 0.98 16.4 ^B 15.7–17.0

^A – differences between calves and adult animals are significant ($p < 0.05$); ^B – differences between females and males are significant ($p < 0.05$)

depending on sex and age. Table 1 structures the red blood cell count for adult wild moose and calves (n = 55).

Table 2 features platelet parameters in adult wild moose and calves (n = 55).

Table 3 describes while blood cells and leukocytic formula for adult wild moose and calves.

Our single- and multivariate analysis revealed the effect of age, sex, and weight on blood parameters. Sex and age proved to have a significant effect on red blood cells ($p = 0.00$, $p = 0$, respectively), mean corpuscular volume ($p = 0.00$, $p = 0.00$), red blood cell distribution width ($p = 0.00$, $p = 0.03$), platelet distribution width ($p = 0.00$, $p = 0.00$), and eosinophils ($p = 0.00$, $p = 0$). Age had a significant effect on hemoglobin ($p = 0.00$), hematocrits ($p = 0.00$), mean concentration hemoglobin ($p = 0.00$), mean corpuscular hemoglobin concentration ($p = 0.00$), platelets ($p = 0.00$), white blood cells ($p = 0.00$), and monocytes ($p = 0.02$).

The moose of different sex and age differed significantly in body weight, which affected the following hematological parameters: red blood cells ($p = 0.00$), hemoglobin ($p = 0.00$), hematocrits ($p = 0.00$), mean corpuscular volume ($p = 0.00$), mean concentration he-

moglobin ($p = 0.00$), red blood cell distribution width ($p = 0.00$), platelet distribution width ($p = 0.00$), platelets ($p = 0.00$), white blood cells ($p = 0.00$), and eosinophils ($p = 0.00$).

Respiratory phylo- and ontogenesis of blood in vertebrates has one common trend: erythrocytes lose their nucleus, lifespan increases, and size and shape change [13]. In precocial species, blood becomes denuclearized as early as in embryogenesis. Non-nucleated erythrocytes break down glucose to lactic acid, and this metabolic process is responsible for the gas transport function in mammals [14].

The respiratory function of blood also depends on the development of the skeleton and the musculoskeletal system [15]. In newborn mammals, the entire red bone marrow is engaged in hematopoiesis. In mature animals, a certain part of red bone marrow is replaced by yellow adipose marrow [16]. In newborn reindeer, the weight of the bone marrow is 13% body weight and 58.3% skeleton weight; 60% of bone marrow is in the peripheral skeleton [14].

Between birth and puberty, blood volume, red blood cells, and hemoglobin increase together with live weight gain. In wild animals, the mean blood volume

Table 2 Platelet parameters for free-ranging moose given for calves and adult animals (n = 55)

Parameters, min – max M ± SD Me 25–75 %	Calves ≤ 1 y.o., ♀	Adults, ♀	Calves ≤ 1 y.o., ♂	Adults, ♂
Mean platelet volume, fl	7–9.5 8.43 ± 0.71 8.5 8.0–8.9	7.4–10.5 9.03 ± 0.95 9 8.3–9.6	5.6–9.8 8.18 ± 1.43 8.35 7.1–9.5	6.6–10.8 8.48 ± 1.07 8.5 7.8–9.1
Platelet distribution width, %	9.5–13.8 11.66 ± 1.15 12 ^{A, B} 10.8–12.2	11.1–18.3 15.22 ± 2.23 15.5 ^A 13.2–16.9	10.1–18.8 14.72 ± 2.97 14.9 ^B 12.1–17.5	12.0–21.9 16.57 ± 2.82 16.3 14.3–18.8
Platelet crit, %	0.127–0.178 0.15 ± 0.01 0.149 ^A 0.145–0.163	0.047–0.183 0.11 ± 0.04 0.121 ^A 0.085–0.161	0.110–0.206 0.14 ± 0.03 0.152 0.112–0.175	0.074–0.247 0.14 ± 0.05 0.14 0.095–0.197
Platelets, 10 ⁹ /L	144–241 194.76 ± 27.01 200 ^B 182–212	134–296 211.36 ± 49.89 214 185–252	135–254 172.50 ± 36.27 172.5 ^{A, B} 142–188	137–372 234.85 ± 61.70 236 ^A 213–264

^A – differences between calves and adult animals are significant ($p < 0.05$); ^B – differences between females and males are significant ($p < 0.05$)

Table 3 White blood cell and leukocytic formulas for free-ranging moose given for calves and adult animals, % (n = 55)

Parameters, min – max M ± SD Me 25–75 %	Calves ≤ 1 y.o., ♀	Adults, ♀	Calves ≤ 1 y.o., ♂	Adults, ♂
White blood cells, ×10 ⁹ /L	1.9–3.6 2.73 ± 0.44 2.6 ^A 2.5–3.0	2.0–5.1 3.28 ± 0.79 3.2 ^A 2.8–3.7	1.8–4.2 3.00 ± 0.77 3 ^A 2.4–3.8	2.1–5.3 3.77 ± 0.98 3.6 ^A 3.1–4.4
Leukocytic formulas, %				
Rod-shaped neutrophils	0–4 2.076 ± 1.320 2 1–3	0–4 1.36 ± 1.50 1 0–3	0–5 2.00 ± 1.88 1.5 0–4	1–4 2.38 ± 1.02 2 2–3
Segmental neutrophils	24–44 30.69 ± 6.25 27 27–31	4–49 26.27 ± 16.79 27 7–40	14–45 28.60 ± 9.77 27.5 20–37	18–47 32.52 ± 10.26 28 24–42
Monocytes	0–2 1.23 ± 0.72 1 1–2	0–3 0.81 ± 1.07 0 0–2	0–3 1.30 ± 1.15 1 0–2	0–2 0.57 ± 0.67 0 0–1
Lymphocytes	53–70 61.92 ± 6.42 65 55–68	45–87 65.27 ± 15.98 68 46–80	50–76 62.30 ± 8.26 59.5 58–69	43–69 59.28 ± 9.07 63 49–67
Eosinophils	0–7 2.69 ± 1.93 2 ^A 1–4	2–9 6.27 ± 2.14 7 ^A 5–8	0–6 4.20 ± 2.04 4.5 ^{A, B} 3–6	5–10 7.80 ± 1.50 8 ^{A, B} 7–9

^A – differences between calves and adult animals are significant ($p < 0.05$); ^B – differences between females and males are significant ($p < 0.05$)

per unit of body weight hardly changes during postnatal ontogenesis. In domestic ungulates, body weight in ontogenesis increases faster than the mean blood volume and hemoglobin.

A large volume of circulating blood and its high hemoglobin content allow wild ungulates to endure the intense muscle load and the high energy exchange associated with physical activity [14]. Korzhuev

formulated this phenomenon as a greater “provision” of wild animals with blood [15].

The blood of wild ungulates undergoes significant changes in the first six months of life because calves need to prepare for winter [16]. Like other wild ungulates, moose grow very fast after birth: in fact, their body weight increases by ≥ 10 times over the summer [9]. Newborn calves have a significant blood content, which may reach 10.6–16.2% body weight [9]. During the first post-natal week, the concentration of red blood cells and hemoglobin decreases because the plasma volume increases in a matter of days, while the count of red blood cells remains the same or decreases slightly. The blood becomes less saturated with cells, while its total volume goes up [9]. Moose calves are reported to eat clay and drink rusty marsh water to consume ferrous iron. This need to replenish the iron supply during intensive hematopoiesis is an important ecological feature [9]. Newborn moose, like reindeer, demonstrated a high blood percentage but no anemia [9, 17].

After this temporary inhibition, the hematopoietic activity increases by the time calves are 30 days old. The count of red blood cells increases by an average of 48.9%, and erythrocytes and hemoglobin soon regain their initial count. Since the weight of moose calves rapidly increases during this period, the mean volume of blood and hemoglobin drops by 15 and 25%, respectively [9]. The rapid growth was reported by Knorre & Knorre and Petrov [8, 18]. In addition, the fast growth rate increases together with the activity of hematopoietic organs: one-year-old calves and adult moose have the same blood-to-body weight ratio.

In wild moose, blood volume keeps pace with body weight much better than in domestic animals. According to Petrov, it takes the same time for calf’s skeleton to increase by 10 times as it takes its heart to grow by 30 times [19]. A larger heart means a larger blood volume. Thus, adult moose have much larger mean blood content than cows, sheep, and horses: it is 9–12% in moose and only 6–9% in farm animals [20]. In this respect, the moose is similar to the reindeer and the argali. However, these wild ungulates have much higher hemoglobin (1 g per 1 kg body weight). Moose make poor long-distance runners, and their low hemoglobin can be explained by their lower mobility.

To sum it up, all processes inside animal organisms affect the morphological, biochemical, and immunological parameters of blood. External factors also have a significant effect. However, the changes that take place in blood composition as a result of external and internal factors cannot be assessed without a reliable reference range. Still, this range should be considered as a rough guide, not an iconic reference because free-ranging wild animals seldom make a large sample.

Veterinary laboratories of the early XXI century saw a rapid automatization. Unlike traditional methods, automatic hematology analyzers are highly accurate and efficient. They illustrate cell distribution as histograms and require very little biological material. Mo-

dern analyzers cover 20 parameters, some of which cannot be established by microscopy, e.g., red blood cell distribution width, platelet distribution width, mean corpuscular hemoglobin concentration, mean platelet volume, etc. These parameters have significant clinical and diagnostic value [21]. In addition, automatic hematology analyzers are more objective compared to the manual method. Thus, automated blood testing offers new diagnostic possibilities for wildlife studies.

Erythrocyte indicators. Red blood cells are one of the most important erythrocyte indicators. Automated blood tests provide coefficient of variation for this parameter below 1% [21]. Polycythemia, or erythrocytosis, is a high red blood cell count caused by various processes. The list of physiological causes usually includes prolonged physical stress and high altitudes while pathological causes involve chronic lung diseases, kidney diseases associated with erythropoietin, chronic heart failure, tumors, etc. Relative polycythemia develops if the volume of circulating plasma increases, e.g., as a result of long diarrhea and vomiting. It can also be caused by redistribution and deposition of blood or its superfluous release from the blood pool, as well as by acute hypoxia and stress, accompanied by an increase in blood norepinephrine, adrenaline, and glucocorticoids.

Erythropenia is a low red blood count caused by various anemias, kidney diseases associated with low erythropoietin, infectious and autoimmune diseases, hyper- and hypofunction of the thyroid gland, hemoglobinuria, hemoglobinopathies, radiation sickness, etc.

Hematocrit represents the volume percentage of red blood cells. Hematocrit levels that are too high can indicate symptomatic erythrocytosis or erythremia, trauma, shock, or dehydration caused by severe diarrhea, vomiting, or burn disease. Low hematocrit levels indicate severe blood loss, various anemias, or an increase in circulating blood volume.

Hemoglobin reflects the concentration of hemoglobin in the blood. Automatic hematological analyzers provide the variation coefficient below 2% [21]. Hemoglobin levels that are too high may reflect physiological changes and diseases associated with high red blood cell count. Low hemoglobin is typical of anemia and may be caused by blood loss, impaired hematopoiesis, or hemolysis. Though anemia can be an independent disease, it is usually a symptom of another chronic disease.

Mean cell volume, or mean corpuscular volume, is calculated by dividing the total red blood cells by their number. In an automated blood test, it indicates the volume of the entire cell population. The mean cell volume can have a normal value even in case of a pronounced macro- and microcytosis. Then, the real sizes of erythrocytes can be determined by analyzing histograms of cell distribution in the population. Microcytic, normocytic, and macrocytic anemias depend on the mean cell volume [21].

Mean concentration of hemoglobin, or mean cell hemoglobin, in an erythrocyte is calculated by dividing the hemoglobin concentration by the number of red

blood cells per unit volume. The clinical significance of this parameter is similar to the blood color index. Anemias are divided into normochromic, hypochromic, and hyperchromic ones, depending on mean cell hemoglobin.

Mean cell hemoglobin concentration, or mean corpuscular hemoglobin concentration, reflects the degree of saturation of erythrocytes with hemoglobin. It is the ratio of hemoglobin values to hematocrit, multiplied by 100. The mean corpuscular hemoglobin concentration is a concentration index that does not depend on the cell volume, which makes it a sensitive indicator of a hemoglobin formation problem.

An increase in the mean corpuscular hemoglobin concentration may be associated with a microspherocytic hemolytic anemia unless it is a technical error. Low mean corpuscular hemoglobin concentrations accompany impaired hemoglobin synthesis in cases such as hemoglobinopathies and iron deficiency anemia.

Red blood cell distribution width is an indicator of erythrocyte volume heterogeneity and anisocytosis. It determines the degree of anisocytosis, i.e., fluctuations in the size of red blood cells [21].

In laboratory practice, the abovementioned red blood cell parameter usually serves to diagnose anemia of various etiologies. However, red blood cell distribution width appeared to be a reliable laboratory indicator that can be used to diagnose diseases that are not associated with anemia. Thus, automatic hematological analyzers provide erythrocyte indices and histograms that can serve as a useful diagnostic tool for a wide range of pathologies.

The hematological parameters obtained in this research somewhat differed from the results reported by foreign and domestic scientists, but the trend between adult animals and calves was similar in most indicators.

We established significant differences ($p < 0.05$) for all red blood cell parameters between calves and mature animals. Females and males in both age groups also demonstrated significant differences.

The Pechoro-Ilychsky Reserve (Komi Republic) conducted a comprehensive study of hematological parameters in moose. According to Kochanov, moose hardly differed in red blood cells: calves – 5.52×10^6 per 1 mm^3 , one-year-olds – 5.63×10^6 per 1 mm^3 , adult females – 5.41×10^6 per 1 mm^3 [22]. The hemoglobin percentage slightly increased with age and reached 8.99, 9.25, and 9.7 g%, respectively. Knorre & Knorre reported data similar to our findings on red blood cells in one-year-olds and adult moose [8]. Adult moose had a gradual decrease in hemoglobin, which dropped from 11.5 to 8.16 g%, unlike three-month-old calves. Irzhak reported bigger numbers for one-month-olds in spring: their red blood cell count was by 2 million/ mm^3 higher than in adults (6.2 and 4.2 million, respectively), and the hemoglobin was by 0.7 g% higher (8 and 7.3 g%, respectively) [23].

Norwegian moose had higher indicators than those obtained in this research. Calves had by 25% more

red blood cells and by 20.47% more hemoglobin while adult moose had hemoglobin by 6.22% more than in our work [6]. Adult female American moose (*Alces americanus shirasi*, Nelson 1914) in northwestern Wyoming, USA, exceeded our results in the red blood cell count by 26.72% and hemoglobin by 13.96% [10]. Adult female California wapiti (*Cervus elaphus nannodes*, Merriam 1905) that live in California, USA, had more hemoglobin by 17.35% and more hematocrit by 13.7% [24]. The difference could probably be explained by their habitat. Most of the territory of Norway is more than 490 m above sea level; the highest point of Wyoming is 4207 m while the state of California is 4421 m above sea level. In the Kirov Region, the difference in absolute heights ranges from 56 to 337 m. In all the abovementioned studies, the mean corpuscular volume, mean concentration hemoglobin, and mean corpuscular hemoglobin concentration were almost identical with our results.

The black-and-white cattle (*Bos taurus*, Linnaeus, 1758) from Tajikistan mountains also showed a higher red blood cell count in adult males: it was by 7.55% higher than our data for the moose from the Kirov Region [25]. Yaks (*Bos mutus*, Przewalski, 1883) also had a higher total red blood cell count [25]. For young yak females and males, the figures were higher by 28.6 and 18.2%, respectively, while the hemoglobin count was higher by 16.67% for young females and by 7.58% for young males. The hypsometric levels of Tajikistan mountains range from 300 to 7495 m above sea level.

The West Caucasian tur (*Capra caucasica severtzovi*, Menzbier 1887) from the Karachay-Cherkessia had the total red blood cell count 50% as high as that of the moose from the Kirov Region [26]. Their mean corpuscular hemoglobin concentration also was by 13.5% higher. The pastures of the Karachay-Cherkessia Republic are 1650 m above sea level.

Domesticated Nenets reindeer (*Rangifer tarandus*, Linnaeus 1758) in the Yamalo-Nenets Autonomous Region had the total red blood cell count in the peripheral blood by 18.2% higher than in this research [27]. The Transuralian area is 200–500 m above sea level.

Adult free-range wild reindeer in southwestern Norway showed higher red blood cell counts by 38.23% and hemoglobin by 12.72% [28]. However, they had lower figures for the mean erythrocyte volume, mean concentration hemoglobin, and red blood cell distribution width by 37.28, 32.09, and 8.875, respectively. The hematocrit and mean corpuscular hemoglobin concentration coincided with our results.

The moose from the Pechoro-Ilychsky Reserve of the Komi Republic had very similar blood parameters to those reported in this study [11]. The Reserve is 150–175 m above sea level.

Animals use different anatomical, physiological and biochemical means to adapt to different heights, i.e., to the amount of oxygen available [29]. High altitudes trigger certain transformations in the oxygen transport

system. The partial pressure of oxygen is not enough to saturate the blood, so the total oxygen-transportation capacity increases. The low capacity of hemoglobin to carry oxygen requires more circulating respiratory pigment. The regulatory effect of 2,3-diphosphoglycerate increases to facilitate the release of oxygen by hemoglobin in the tissues. Behavioral and physiological adaptations include low muscle activity and low oxygen demand, as well as increased heart rate and breathing, which increases the amount of oxygen delivered to tissues. However, adaptive shifts that occur at the molecular level eliminate this phenomenon. First, a greater red blood cell count increases the oxygen-carrying capacity. Second, hemoglobin gives more oxygen to tissues, because the concentration of 2,3-DPG in erythrocytes increases [29].

Climate is as important as altitude. The review above included animals that inhabited different climatic zones, from the Mediterranean, California, and subtropical Tajikistan to the Yamalo-Nenets area in the Far North with its sharply continental climate.

Most animals are excellent survivors under harsh winter conditions. The reindeer would simply not be able to live in a warm habitat because it lacks sweat glands. However, these animals maintain a high level of hemoglobin during the winter period: it reaches 1.5 per 100 kg of live weight, which is 0.6–1.2 kg in other animals, and its blood volume reaches 11% live weight [30, 31].

Moose demonstrate significant age-related differences in blood counts. Some studies [11, 32] report physiological anemia as normal for young animals that are low in red blood cells, hemoglobin, hematocrit, and leukocytes. Males have a higher red blood cell count than females because red blood cells increase testosterone under the action of erythropoietin. As a result, male moose increase their blood volume before the rut season, which presupposes fights and wounds. By the beginning of the rut season, they develop mature antlers [33, 34]. The percentage of red blood cell weight and hemoglobin increases. Fluctuations in hematocrit can also be caused by different water intake, intestinal disorders, etc. [34].

Our sampling was performed by hunting. The chase-related stress and hyperventilation can cause spleen contraction and an increase in hematocrit by 10% or more, as well as in red blood cells and hemoglobin [35].

Platelet indicators. Automated hematological blood tests also provide valuable information on platelets, their mean volume, distribution width, and crit.

Total platelet count, or platelets, is an important indicator that can detect thrombocytosis, an increase in platelets typical of chronic myeloproliferative diseases, acute and chronic inflammatory processes, amyloidosis, blood loss, malignant neoplasms, and hemolytic anemia. Thrombocytopenia is a decrease in platelets caused by their destruction and inhibited formation [5].

Mean platelet volume describes the size of platelets based on their volumetric distribution. Mean platelet vo-

lume is inversely proportional to platelet count, which maintains hemostasis and constant mass. Consequently, the more numerous they are, the smaller they get. A pathology might violate this proportion. Intensive thrombocytopoiesis, increased aging, and various activators can change the proportions between the mean volume and count.

Platelet crit represents the ratio of mean platelet volume and total blood volume. It depends on the number of platelets and their size. In clinical practice, this indicator assesses the risk of bleeding and thrombosis. Platelet distribution width reflects the size heterogeneity in terms of size, i.e., the anisocytosis degree. Platelet aggregates, microerythrocytes, and platelet fragments may increase this indicator. Myeloproliferative diseases also affect platelet distribution width [21].

This research established significant ($p < 0.05$) age differences in terms of mean platelet distribution width and platelet crit between young and adult females. Another correlation included platelet count in young and adult males. We also revealed significant sex differences in mean platelet distribution width between young females and males, as well as in platelet count in adults.

The moose from the Kirov Region differed in platelet parameters from Norwegian moose in that adult Russian moose had a larger platelet count by 27.28% [6]. The platelets in young Norwegian moose exceeded our figures by 19.31%. The same dynamics was typical of the mean platelet volume: our data were higher by 22.34% in calves and 32.31% in adults. Norwegian adult female moose also had fewer platelets by 26.75% [10].

Leukocyte indicators. Leukocyte count and composition are the most important leukocyte indicators. Leukogramic changes often precede the clinical signs of certain diseases and indicate pathological processes. Leukocytosis is an increase in the number of leukocytes. It may be the result of leukemia, acute inflammatory and infectious processes, myocardial infarction, malignant tumors, burns, thrombosis of peripheral arteries accompanied by gangrene, uremia, significant blood loss, toxic poisoning, and ionizing radiation. Leukopenia is a decrease in the leukocyte count. It accompanies viral diseases, aplastic anemia, agranulocytosis, some acute leukemias, radiation sickness, systemic diseases, endocrine pathology, chronic gastritis, colitis, and cholecystitis [5, 21]. All leukocytes perform the protective function, but each type does this in a special way.

We established significant ($p < 0.05$) age differences in leukocytes and eosinophils in females and males, as well as a certain gender-related difference in eosinophils.

We also studied the lymphocytic profile of moose blood. In moose, lymphocytes are mostly medium in size, with fewer small and large varieties. Some young females had 90% of lymphocytes. Segmented neutrophils had polysegmented nuclei and poorly visible granularity. Kizhina *et al.* obtained similar data on lymphocytes and cell morphology for moose from Karelia [36].

They reported that moose had a lymphocytic blood profile with 85% lymphocytes, which averaged $54.50 \pm 17.03\%$.

We detected significant differences in the leukoformula content of eosinophils, which had a large number of small granules in their composition, between young and adult females, as well as between young and adult males. Adult moose had a much greater eosinophil count than domestic or young animals. Apparently, these cells were parasitic infection frontliners. Some moose had as many as 23–27% of eosinophils, but we did not exclude them from the statistics.

According to Kochanova, moose experience a rather sharp increase in leukocytes when they approach their first birthday, but this indicator stabilizes as they grow older: it is 7460 per 1 mm^3 in young animals, 10 600 per 1 mm^3 in one-year-olds, and 10 840 in adult female moose [22].

Knorre & Knorre detected a sharp decrease in leukocytes in adult moose, which dropped from 8625 to 4000, compared with three-month-old calves [8].

However, Rostal *et al.* reported no differences in leukocytes between adult and young moose below one year old ($3.2 \times 10^9/\text{L}$) [6]. In their research, adult moose had approximately the same ratio of lymphocytes and neutrophils: calves moved from a predominantly lymphocytic (51%) and lower neutrophilic (33%) leukocyte profile to a more even distribution of 45% neutrophils and 42% lymphocytes in adult moose. These age-related changes in the ratio of neutrophils and lymphocytes were recorded in other ruminant species and, probably, reflected the maturation of the immune system [32, 37–38].

According to Shideler, Californian wapiti had 60% (44–74%) of lymphocytes in adult females and 29% (5–45%) in adult males [24].

Two-year-old black-and-white male yaks from Tajikistan highlands had $7.32 \pm 0.49 \times 10^9/\text{L}$ of leukocytes [25]. Eight-month-old female yaks had $6.11 \pm 0.72 \times 10^9/\text{L}$ of leukocytes, while for males it was $6.24 \pm 0.33 \times 10^9/\text{L}$. Two-year-old female yaks had $6.84 \pm 0.44 \times 10^9/\text{L}$ while for males it was $6.51 \pm 0.311 \times 10^9/\text{L}$.

Bagirov *et al.* reported $13.3 \times 10^9/\text{L}$ leukocytes for the West Caucasian tur and $12.4 \times 10^9/\text{L}$ for domestic goats of the Karachay breed [26]. Novak *et al.* reported $6.09 \pm 0.21 \times 10^9/\text{L}$ leukocytes for adult domesticated reindeer [27]. Domesticated reindeer that inhabited the Yakutian tundra had $4.20 \pm 0.95 \times 10^9/\text{L}$ leukocytes in winter and $45.2 \pm 1.8\%$ lymphocytes [39].

The differences between the abovementioned data and those obtained in this research probably depend on the species, individual characteristics, and environmental conditions. Protein digestion depends on the proteolytic enzymes of neutrophils, while the lipolytic enzymes of lymphocytes affect fat digestion. Myogenic leukocytosis is more typical of animals that live in the Caucasus or the highlands of Tajikistan because intensive muscular activity requires redistribution of blood cells caused by the changes in vasomotors and metabolism.

Reshetnikov linked the drop in lymphocytes in autumn with the poor winter diet [40]. The sharp changes under the weather conditions triggered a stress response to the challenges of winter foraging, which released lymphocytes into the peripheral blood.

No information is currently available on the effect of different methods of moose blood sampling on the hematological parameters. However, a series of studies of white-tailed deer (*Odocoileus virginianus*, Zimmermann 1780) showed that if blood was sampled immediately after immobilization, the hemogram variations did not depend on the trapping method [41–44]. Therefore, we made no difference for blood sampling methods.

Our baseline hematology data for this moose population had some limitations that should be considered in comparative studies. They included the differences in hematological analyzers, laboratory diagnostics, and animal habitats [45]. In addition, a delay of $\geq 72 \text{ h}$ between the blood sampling and laboratory analysis could affect the blood composition [46]. Probably, this time gap caused the decrease in platelets, leukocytes, lymphocytes, monocytes, and basophils, as well as the associated increase in hematocrit. Thus, our results should be interpreted with these factors in mind.

The moose blood profile had seasonal differences. Thus, the red blood cell parameters were higher in autumn than in spring because animals prepare for winter forage [34].

Thus, the hematological values we obtained in this study follow the patterns reported by other studies of wild artiodactyls. The differences depended on the species, sex, age, climate, environment, and food supply.

CONCLUSION

1. The research revealed the hematological parameters for the European moose (*Alces alces*, Linnaeus 1758) of different sex and age from the Kirov Region, Russia. Adults and calves demonstrated significant differences ($p < 0.05$) in red blood cells, hemoglobin, hematocrit, mean corpuscular volume, mean concentration hemoglobin, mean corpuscular hemoglobin concentration, platelet distribution width, red blood cell distribution width, platelet crit, platelets, leukocytes, and eosinophils. Females and males had significant differences ($p < 0.05$) in red blood cells, hemoglobin, mean corpuscular volume, platelet distribution width, red blood cell distribution width, platelets, and eosinophils.

2. The single- and multivariate analysis established the effect of such physiological factors as age, sex, and weight on blood parameters. Sex and age had a significant effect on red blood cells, mean corpuscular volume, platelet distribution width, red blood cell distribution width, and eosinophils. Age had a significant effect on hemoglobin, hematocrit, mean concentration hemoglobin, mean corpuscular hemoglobin concentration, platelets, leukocytes, and monocytes. Weight affected ery-

throcytes, hemoglobin, hematocrit, mean corpuscular volume, mean concentration hemoglobin, platelet distribution width, red blood cell distribution width, platelets, leukocytes, and eosinophils.

3. By comparing the physiology of wild and domestic animals, scientists replenished the fundamental and practical knowledge in the field of biology and the adaptive potential of species, thus increasing the efficiency of their domestication. Animals kept in semi-free conditions and artificial habitats may fall victim to epidemics and stress. As a result, any disease must be detected at the earliest stage possible. Modern automated devices make it possible to monitor the physiological state of animals and register the very first signs of various health issues.

CONTRIBUTION

All the authors contributed equally to the study and bear equal responsibility for information published in this article.

CONFLICT OF INTEREST

The authors declare that there is no conflict of interests regarding the publication of this article.

ACKNOWLEDGMENTS

We are grateful to hunters of Russian Research Institute of Game Management and Fur Farming for their help in collecting biological material. We also thank Dr. Boris Zarubin for his help and assistance with data collection.

REFERENCES

1. Litvinov VF, Podoshvelev DA, Kovalev NA. Breeding and resettlement of game animals in Belarus. Relevant Issues of Nature Management, Hunting, and Fur Farming: Proceedings of the International scientific and practical conference dedicated to the 95th anniversary of B.M. Zhitkov All-Russian Research Institute of Hunting and Fur Breeding; 2017; Kirov. Kirov: B.M. Zhitkov All-Russian Research Institute of Hunting and Fur Breeding; 2017. p. 387–390. (In Russ.).
2. Likhatskiy Yu, Likhatskiy E, Atamanov P. Semi-free breeding of ungulates in the Deer nature reserve. Relevant Issues of Nature Management, Hunting, and Fur Farming: Proceedings of the International scientific and practical conference dedicated to the 95th anniversary of B.M. Zhitkov All-Russian Research Institute of Hunting and Fur Breeding; 2017; Kirov. Kirov: B.M. Zhitkov All-Russian Research Institute of Hunting and Fur Breeding; 2017. p. 391–394. (In Russ.).
3. Urosevic IM, Deutz A, Petrovic J, Ristic AZ, Mirceta J. Deer farming in European Union and Serbia: Veterinary legislation perspective. International Symposium on Animal Science 2016; 2016; Belgrade. Belgrade – Zemun: University of Belgrade; 2016. p. 391–398.
4. Veber AEh, Simakov AF, Chuv'yurova NI, Chalyshev AV, Badlo LP, Kochan TI, et al. Physiology of nutrition and metabolism in moose. Syktyvkar: Komi Scientific Center of the Ural Branch of the Russian Academy of Sciences; 1992. 126 p. (In Russ.).
5. Azaubaeva GS. Blood pattern in animals and birds. Kurgan: Zaural'e; 2004. 167 p. (In Russ.).
6. Rostal MK, Evans AL, Solberg EJ, Arnemo JM. Hematology and serum chemistry reference ranges of free-ranging moose (*Alces alces*) in Norway. *Journal of Wildlife Diseases*. 2012;48(3):548–559. <https://doi.org/10.7589/0090-3558-48.3.548>
7. Ponder E. The mammalian red cell and the properties of haemolytic systems. *Protoplasma*. 1935;22:492–494.
8. Knorre EP, Knorre EK. Physiological characteristics of the moose. Proceedings of the Pechoro-Ilych State Reserve. 1959;7:133–167. (In Russ.).
9. Irzhak LI. Moose blood physiology. Proceedings of the Pechoro-Ilych State Reserve. 1964;11:61–66. (In Russ.).
10. Becker SA, Kauffman MJ, Anderson SH. Nutritional condition of adult female Shiras moose in northwest Wyoming. *Alces*. 2010;46:151–166.
11. Moysenko NA. Components of red blood in young moose. *Alces*. 2002;2:93–97.
12. Ivanter EhV, Korosov AV. Elementary biometrics. Petrozavodsk: PetrGU; 2005. 104 p. (In Russ.).
13. Mogalev NP. Nuclear-cytoplasmic ratio and shape of erythroid cells in reindeer embryos. *Archives of Anatomy, Histology, and Embryology*. 1987;92(5):45–48. (In Russ.).
14. Chermnykh NA. Ecological physiology of the reindeer. Ekaterinburg: UrO RAN; 2008. 196 p. (In Russ.).
15. Korzhuev PA. Hemoglobin. *Comparative Physiology and Biochemistry*. Moscow: Nauka; 1964. 287 p. (In Russ.).
16. Korzhuev PA. The respiratory function of blood and the vertebrate skeleton. *Uspekhi Sovremennoi Biologii*. 1955;39(2):163–195. (In Russ.).
17. Gorodetsky VK. Ecological and physiological parameters of reindeer blood. Abstract cand. bio. sci. diss. Moscow: Moscow Order of Lenin and the Order of the Red Banner of Labor State University. M.V. Lomonosov; 1962. 18 p. (In Russ.).

18. Petrov AK. Moose vs. cattle: growth and development. Abstract dr. bio. sci. diss. Moscow: Moscow Veterinary Academy; 1958. 28 p. (In Russ.).
19. Petrov AK. Patterns of heart development in moose. *Zoologicheskiy Zhurnal*. 1961;40(3):447–453. (In Russ.).
20. Irzhak LI. Morphology of mammalian erythrocytes and the age-related changes in red blood cells. *Biophysics, Biochemistry, and Pathology of Erythrocytes: Conference proceedings*. Krasnoyarsk; 1960. p. 64–68. (In Russ.).
21. Egorova EN, Pustovalova RA, Gorshkova MA. Clinical and diagnostic significance of red blood cell indices, defined automatic hematological analyzers. *Volga Medical Journal*. 2014;12(3):34–41. (In Russ.).
22. Kochanova NE. Moose metabolism in summer. *Proceedings of the Pechoro-Ilych State Reserve*. 1964;11:31–54. (In Russ.).
23. Irzhak LI. Physiology of the moose in the Pechoro-Ilychsky Reserve. *News of the Komi Branch of the All-Union Geographical Society*. 1963;(8):88–89. (In Russ.).
24. Shideler SE, Stoops MA, Gee NA, Tell LA. Hematologic values for Tule elk (*Cervus elaphus nannodes*). *Journal of Wildlife Diseases*. 2002;38(3):589–597. <https://doi.org/10.7589/0090-3558-38.3.589>
25. Kosilov VI, Irgashev TA, Shabunova BK, Akhmedov D. Clinical and hematological parameters of black-spotted cattle of different genotypes and yaks under the mountainous conditions of Tadzhikistan. *Izvestia Orenburg State Agrarian University*. 2015;51(1):112–115. (In Russ.).
26. Bagirov VA, Aybazov MM, Mamontova TV. Morphometric and biological indicators of the west C. Caucasia. *Proceedings of the Stavropol Research Institute of Animal Husbandry and Forage Production*. 2014;3(7):33–40. (In Russ.).
27. Novak G, Bodrova L. Hematologic parameters of blood in reindeers with different types of feeding. *Bulletin of the BSSA named after V.R. Filippov*. 2014;36(3):22–27. (In Russ.).
28. Miller AL, Evans AL, Os Ø, Arnemo JM. Biochemical and hematologic reference values for free-ranging, chemically immobilized wild Norwegian Reindeer (*Rangifer tarandus tarandus*) during early winter. *Journal of Wildlife Diseases*. 2013;49(2):221–228. <https://doi.org/10.7589/2012-04-115>
29. Hochachka P, Somero J. *Biochemical adaptation strategy*. Moscow: Mir; 1977. 398 p. (In Russ.).
30. Lyakh SP. *Adaptation of microorganisms to low temperatures*. Moscow: Nauka; 1976. 160 p. (In Russ.).
31. Sroslova GA, Postnova MV, Zimina YuA. Features of adaptation of living organisms. *Science of VolSU. Natural Sciences*. 2017;7(4):32–38. (In Russ.). <https://doi.org/10.15688/jvolsu11.2017.4.5>
32. Taylor JA, Feldman BF, Zinki JG, Jain NC. Leukocyte responses in ruminants. In: Feldman BF, Zinkl JG, Jain NC, editors. *Schalm's veterinary hematology*. Wiley; 2000. pp. 391–393.
33. Irzhak LI. *Respiratory function of blood in mammals*. Moscow; Leningrad: Nauka; 1964. 183 p. (In Russ.).
34. Marma BB. Veterinary and physiological observations of moose in a zoo. *Proceedings of the Pechoro-Ilych State Reserve*. 1967;12:74–86. (In Russ.).
35. Brenner KV, Gurtler H. Further investigations on metabolic and hematological reactions of pigs restraint by means of a rope round the upper jaw. *Journal of Experimental Veterinary Medicine*. 1981;35:401–407.
36. Kizhina AG, Uzenbaeva LB, Panchenko DV, Ilyukha VA. Morphofunctional organization of blood cells in Nordic *Cervidae*. *Dynamics of the game animals populations in Northern Europe: Book of abstracts. The 7th International symposium*; 2018; Petrozavodsk. Petrozavodsk: KRC RAS; 2018. p. 52–54. (In Russ.).
37. Thorn NE, Feldman BF, Zinki JG, Jain NC. Hematology of the deer. In: Feldman BF, Zinkl JG, Jain NC, editors. *Schalm's veterinary hematology*. Wiley; 2000. pp. 1179–1183.
38. Vegad JL, Feldman BF, Zinki JG, Jain NC. Normal blood values of the water buffalo (*Bubalus bubalis*). In: Feldman BF, Zinkl JG, Jain NC, editors. *Schalm's veterinary hematology*. Wiley; 2000. pp. 1085–1088.
39. Koryakina LP, Maksimov VI, Machakhtyrov GN. Morphophysiological parameters and enzyme blood profile in domestic reindeer by seasons in the taiga and mountain taiga zones of Yakutia. *Agrarian Bulletin of the Urals*. 2008;43(1):48–50. (In Russ.).
40. Reshetnikov IS. Effect of natural conditions and seasons on the reindeer *thymus lymphocytes*. *Adaptations to Natural Conditions: Proceedings of the VI All-Union Conference on Ecological Physiology*; 1982; Syktyvkar. Syktyvkar: Komi filiala AN SSSR; 1982. p. 46. (In Russ.).
41. Kocan AA, Glenn BL, Thedford TR, Doyle R, Waldrup K, Kubat G, et al. Effects of chemical immobilization on hematologic and serum chemical values in captive white-tailed deer. *Journal of the American Veterinary Medical Association*. 1981;179(11):1153–1156.

42. Wolfe G, Kocan AA, Thedford TR, Barron SJ. Hematologic and serum chemical values of adult female Rocky Mountain elk from New Mexico and Oklahoma. *Journal of Wildlife Diseases*. 1982;18(2):223–227. <https://doi.org/10.7589/0090-3558-18.2.223>
43. Mautz WW, Seal US, Boardman CB. Blood serum analysis of chemically restrained white-tailed deer. *Journal of Wildlife Management*. 1980;44:343–351.
44. Wesson JA, Sanlon PF, Kirkpatrick RL, Mosby HS. Influence of chemical immobilization and physical restraint on packed cell volume, total protein, glucose, and blood urea nitrogen in blood in white-tailed deer. *Canadian Journal of Zoology*. 1979;57(4):756–767. <https://doi.org/10.1139/z79-093>
45. Kazakova MS, Lugovskaya SA, Dolgov VV. The reference values of indicators of total blood analysis of adult working population. *Clinical Laboratory Diagnostics*. 2012;(6):43–49. (In Russ.).
46. Bleul U, Sorbiraj A, Bostedt H. Effects of duration and storage temperature on cell counts of bovine blood samples as determined by an automated haematology analyser. *Comparative Clinical Pathology*. 2002;11:211–216. <https://doi.org/10.1007/s005800200021>

ORCID IDs

Maria A. Perevozchikova  <https://orcid.org/0000-0003-3638-3712>

Igor A. Domskey  <https://orcid.org/0000-0003-1633-1341>

Alexey A. Sergeev  <https://orcid.org/0000-0002-9461-5131>



Effect of a new probiotic on *Artemia* cysts determined by a convolutional neural network

Ivan Yu. Evdokimov^{1,*}, Angelina V. Malkova¹, Alena N. Irkitova¹,
Maxim V. Shirmanov¹, Dmitrii V. Dementev²

¹ Altai State University^{ROR}, Barnaul, Russia

² Aرسال LLC, Yarovoye, Russia

* e-mail: ivan.evdokimov.92@mail.ru

Received 09.01.2023; Revised 23.02.2023; Accepted 07.03.2023; Published online 30.08.2023

Abstract:

One of the problems in sea farming is infections that cause mass mortality of crustaceans. To fight infections and improve sanitary conditions, farmers are actively using probiotic preparations. We aimed to study the effect of a new probiotic based on *Bacillus toyonensis* B-13249 and *Bacillus pumilus* B-13250 strains on the incubation of *Artemia franciscana* cysts. Another purpose was to test a possibility of using a convolutional neural network for fast automatic counting of cysts, nauplii, and embryos.

A pilot batch of the probiotic was prepared at the Prombiotech Engineering Center, Altai State University, from two strains of spore bacteria from the Center's collection: *B. toyonensis* B-13249 and *B. pumilus* B-13250.

The recommended amount of the probiotic was experimentally determined as 0.1 per 2 g of cysts. This concentration increased the number of hatched cysts by 1.4 and 10% in the batches from Lake Bolshoye Yarovoye (Z29.04) and from Lake Kuchuk (C9). It also increased the biomass yield to 7.40 ± 0.69 and 6.80 ± 0.43 g in these two batches, respectively, compared to the control samples where the yields were 5.30 ± 0.60 and 4.60 ± 0.50 g, respectively. The robot counter reduced the sample processing time 15 times and saved the data for further use.

The probiotic based on *B. toyonensis* B-13249 and *B. pumilus* B-13250 had a positive effect on the hatching rate and biomass yield of *A. franciscana*. The new method for rapid counting of *Artemia*, which was based on the convolutional neural network and developed as an application of the Artemeter-1 robot, reduced the processing time and lowered labor costs.

Keywords: *Bacillus pumilus*, *Bacillus toyonensis*, *Artemia franciscana*, aquaculture, probiotics, convolutional neural network, bacteria counting

Please cite this article in press as: Evdokimov IYu, Malkova AV, Irkitova AN, Shirmanov MV, Dementev DV. Effect of a new probiotic on *Artemia* cysts determined by a convolutional neural network. Foods and Raw Materials. 2024;12(1):91–100. <https://doi.org/10.21603/2308-4057-2024-1-590>

INTRODUCTION

Aquaculture, one of the most promising branches of agriculture, is becoming an important source of nutrition for many people. Aquatic animals are widely bred and grown in coastal countries, such as India, Thailand, Mexico, and others [1–3]. Shrimp production exceeds millions of tons per year but fish farming is still the most common kind of aquaculture [4, 5].

Aquatic animals are grown in artificial ecosystems which have their peculiarities. For example, the larvae of many commercially cultivated species of marine fish, mollusks, and shrimps need live food at the early stages of their development (from a few days to 3–5 weeks).

Grouper, bream, and other popular species show excellent growth when feeding on live plankton as a starter feed. Yet, this is only critical to shrimps, since there are no alternative artificial feeds. Shrimps actively feed (and, therefore, grow) on independently-moving aquatic organisms, ignoring motionless or free-floating food particles. This is true not only of predatory species, such as the tiger shrimp (*Penaeus monodon* Fabricius, 1798), but also of popular omnivorous species, such as the white-legged shrimp (*Penaeus vannamei* Boone, 1931) or the Rosenberg shrimp (*Macrobrachium rosenbergii* De Man, 1879) [6].

Considering the nutrition needs of the crustaceans, manufacturers began to use planktonic halophilic crustaceans of the genus *Artemia* as an optimal starter feed. These planktonic crustaceans are native to the saline lakes of Western Siberia (Russia and Kazakhstan), China, Tibet, and Iran. They can also be found in the Mediterranean region, New Zealand, Canada, and the USA [7, 8]. Brine shrimps are convenient to use since they can propagate under adverse conditions with cysts covered with a thick chitin membrane. Simple technical manipulations can preserve their cysts for a long time (up to 14 years) to be stored or transported. Biochemical processes can be easily activated in the cysts (salt water, light, aeration, etc.) to obtain, within 24 h, microscopic (0.4–0.45 mm) nauplii, an ideal food for the cultivated shrimp larvae.

Niu *et al.* explored alternatives to using brine shrimp as a starter feed for the *Litopenaeus vannamei* shrimp most commonly farmed in China and in the West [9]. During cultivation, its larvae get infected with diseases, including those carried by live organisms they feed on (rotifers and brine shrimp). In other words, these live organisms are a source of both food and disease (parasites) in the aquaculture. Therefore, the lack of efficient commercial methods is still the main obstacle to a sustainable, healthy farming of this species of shrimp. To overcome it, the scientists created an alternative fortified artificial food without live organisms. They found that the shrimp had a survival rate of 81–87% under constant cholesterol level monitoring. According to Malkova *et al.*, a probiotic preparation for *Artemia* crustaceans could facilitate the commercial production of the shrimp [10]. As a result, they could still be used as a live starter feed.

Large-scaled sea farming (invertebrates and fish) is accompanied by various infections that may cause mass mortality. Among the most common pathogenic microorganisms in the aquatic environment are those of the genera *Vibrio*, *Salmonella*, *Escherichia*, and others [11]. Antibiotics have been used for many years to prevent large losses, which has made a lot of microflora resistant to them [12]. Thus, we need to seek safer ways to fight microbes so that bacterial resistance to antibiotics does not lead to an ecological catastrophe [13–15].

The above-mentioned problems in aquaculture can be overcome with modern probiotic preparations [16–18]. Ahmadifard *et al.* fortified brine shrimp with a probiotic based on *Bacillus subtilis*. They found that it had a positive effect on the growth, reproduction, and microflora of ornamental fish *Poecilia latipinna*, as well as its resistance to *Aeromonas hydrophila*. At the same time, there were no significant differences in the ontogeny of the fortified and non-fortified *Artemia* groups [19].

A research team from Korea found that strains *B. subtilis* KA1 and *B. subtilis* KA3 improved food absorption by the shrimp *Palaemon paucidens* and contributed to their survival from a white spot syndrome virus [20]. A group of Chinese scientists proved that the probiotic bacteria [21]. *Bacillus coagulans* ATCC 7050 improved

the growth, intestinal morphology, immune response, and resistance to *Vibrio parahaemolyticus* in the shrimp *L. vannamei*. Fernandes *et al.* found that the bacteria *B. subtilis*, *Bacillus amyloliquefaciens*, *Bacillus licheniformis*, and *Pseudomonas* sp. were safe as biological inoculants. In addition, they increased enzymatic activity in the intestines of *L. vannamei* shrimp, contributing to higher weight gain [23]. According to Thai researchers, the *Bacillus aryabhatai* TBRC8450 was not only antagonistically active against *Vibrio harveyi* and *V. parahaemolyticus*, but also improved antioxidant activity in animal plasma [4].

Wang *et al.* from Taiwan experimentally confirmed that a multicomponent probiotic based on *Lactobacillus pentosus* BD6, *Lactobacillus fermentum* LW2, *B. subtilis* E20, and *Saccharomyces cerevisiae* P13 improved shrimp health and performance more effectively than monocomponent preparations with the same strains [23]. A team of Spanish scientists fortified *Artemia* metanauplii with a *Lactobacillus rhamnosus*-based probiotic and found its positive effect against potentially pathogenic microorganisms of the *Vibrionaceae* family [11].

A group of Indian scientists fortified brine shrimp, to be fed as live food to freshwater shrimp *M. rosenbergii*, with a probiotic supplement based on *Lactobacillus sporogenes* at different concentrations. The experiments showed that the fortification resulted in *M. rosenbergii*'s better survival, rapid growth, and higher contents of protein, amino acids, carbohydrates, and lipids. The *L. sporogenes* concentration of 6×10^8 CFU/g was found to be optimal for feed fortification [24].

In a similar study by scientists from India, brine shrimp nauplii fortified with a probiotic based on *Saccharomyces boulardii* showed an improved resistance to *Vibrio* bacteria they had been artificially infected with [25].

Another group of Indian scientists fortified *Artemia parthenogenetica* nauplii with *L. rhamnosus* and *B. coagulans* [26]. They studied the probiotic supplement's load on the intestines of brine shrimp nauplii and its retention time in their intestines. According to the results, the nauplii fortified with *L. rhamnosus* and *B. coagulans* had a full intestine after 39 and 39.5 min, respectively. The load on the intestines and the retention time varied in the experimental groups.

As can be seen in the above studies, probiotic preparations are mainly made from well-studied microorganisms of the *Lactobacillus* and *Bacillus* genera. For the sustainable development of aquaculture, however, we need to expand the pool of probiotic microorganisms and make more preparations based on microbial consortia, rather than monocultures.

Until now, brine shrimp farmers have done the counting visually, using a binocular and/or a microscope, as well as with the naked eye. Time-consuming and tiring, these methods do not always produce accurate results. Moreover, additional devices have to be used to save the data.

To reduce statistical errors, experiments need to be conducted in at least eight repetitions. In order to shorten the counting time, improve accuracy, and save data, we used a brine shrimp counter robot, for the first time in Russia, based on a convolutional neural network that used the YOLO (You Only Look Once) algorithm [27].

The main difference between the YOLO algorithm and other neural network algorithms lies in its instantaneous detection of objects in real time. In the YOLO algorithm, a full-size image completely passes through the convolutional neural network only once, while other algorithms involve many repetitions.

When we started our study, YOLOv4 (2020) was one of the most productive neural networks for object detection. We tested several neural networks from the MS COCO (2017) set of 127 287 images and found YOLOv4 to be the most efficient. Its algorithm works twice as fast as EfficientDet, one of the most accurate models. Compared to the earlier version (YOLOv3), the Average Precision metric and performance (FPS) of YOLOv4 have been improved by 10 and 12%, respectively [28]. Therefore, YOLOv4 was used as a platform for creating an Artemeter-1 robot for counting organisms.

We aimed to study the effectiveness of a new probiotic preparation based on a consortium of rhizosphere strains *Bacillus toyonensis* B-13249 and *Bacillus pumilus* B-13250 for the incubation of *Artemia franciscana* cysts. We also explored a possibility of using a counter robot based on a convolutional neural network for fast automatic counting of cysts, nauplii, and embryos after decapsulation.

STUDY OBJECTS AND METHODS

Microorganisms in probiotics. A probiotic was based on two strains of spore bacteria from the collection of the Prombiotech Engineering Center. Both strains are patented and deposited in the Russian National Collection of Industrial Microorganisms. They were isolated in 2017 (Novye Zori village, Altai Krai, Russia). The *Bacillus toyonensis* B-13249 strain was isolated from the rhizosphere of the genus *Helianthus*, while the *Bacillus pumilus* B-13250 strain was isolated from the rhizosphere of the *Cichorium* genus.

These strains form oval spores located terminally or subterminally and withstand heating at 80°C for 30 min. The morphology of their colonies is shown in Fig. 1.

Culture media for probiotic production. A pilot batch of probiotics was prepared using the following culture media:

1. Solid L(Luria)-medium for counting bacteria;
2. Liquid L-medium for cultivating the inoculum in flasks;
3. Endo medium for checking the samples for coliform bacteria;
4. A protective (cryoprotective) medium for protecting cells and spores during the freezing period; and
5. A fermentation (molasses-corn) medium used as the main nutrient medium in the fermentation apparatus.



Figure 1 Colony morphology of the strains on L-medium (10×): a – *Bacillus toyonensis* B-13249; b – *Bacillus pumilus* B-13250



Figure 2 Incubation cones with *Artemia* cysts

A pilot batch of probiotics. A pilot batch of probiotics to be tested on *Artemia* crustaceans was produced at the Prombiotech Engineering Center (Barnaul, Russia), using the technology developed by this institution earlier [29].

The inoculum (seed) was cultivated in shake flasks in an Innova 44 shaker-incubator (New Brunswick). The cultivation methods were scaled on the laboratory batch fermentation units with a capacity of 15 and 250 L. After 24 h of cultivation, the accumulated biomass was concentrated in a GTGQ-1251 tubular centrifuge at 15 600 rpm. Then, the bacterial concentrate was mechanically removed from the centrifuge rotor, mixed with a cryoprotective medium (1:1), frozen, and subsequently freeze-dried in an SP Scientific 25L Genesis SQ Super ES-55 semi-industrial freeze-dryer. The resulting concentrate was mixed with a filler (maltodextrin) until the final titer of the probiotic preparation (at least 1×10^{10} CFU/g) [29].

Incubation and analysis of *Artemia* cysts. We used cysts of the branchial crustacean *Artemia franciscana* from two different lakes: batch Z29.04 from Lake Bolshoye Yarovoye and batch C9 from Lake Kuchuk. The cysts were incubated in cones (Fig. 2) for 48 h with constant air bubbling under standard conditions: incubation solution – 1 L, salinity – 30‰, temperature – 25–30°C, pH – 8.0–8.5, redox potential – 148–220 mV, illumina-

tion – 1500–2000 lux, cysts – 2.0 g, and activator – 0.2 cm³ of 3% H₂O₂ solution.

We produced one control and three test samples for each batch of cysts in 24 repetitions. At the start of nauplii incubation, probiotics were introduced directly into the cones at the following amounts: 0 (control) and 0.05, 0.1, and 0.2 g. After 48 h of incubation, we counted the number of crustaceans or nauplii (*N*), unhatched cysts (*C*), and half-hatched embryos or umbrellas (*U*) in each cone. According to the standard method, the crustaceans were counted in two stages [30].

At the first stage, a few drops (about 0.1 cm³) of concentrated Lugol's solution was added to a liquid sample from the incubator (0.05–0.1 cm³) in order to immobilize the crustaceans and make formed elements more contrasting in color. Some 20–30 min later, nauplii (*N*) and embryos (*U*) were counted, then proceeding to the second stage of cyst count.

At the second stage, a sodium hypochlorite (NaOCl) solution was added to the stained samples to dissolve empty shells from hatched cysts, leaving only the interior of unhatched cysts (*C*). The amount of hypochlorite (and the exposure time) depended on the number of cysts in the sample, averaging 0.2–0.3 cm³ of 8% sodium hypochlorite for each sample.

As a result, we obtained the counts of nauplii (*N*), embryos (*E*), and cysts (*C*) in 0.05–0.1 cm³ of incubation suspension. Analyzing the data, we calculated the relative quality indicators of cysts (*HR*[−] and *HR*⁺).

The hatching rate (*HR*) is of great importance when using brine shrimp in farming. This indicator shows the percentage of nauplii hatched from the total number of cysts incubated. Thus, the higher the hatching rate, the greater the amount of live feed in the water. There are two *HR*s for each sample: *HR*[−] indicates the percentage of fully-hatched nauplii (*N*) and *HR*⁺ shows the percentage of fully-hatched (*N*) and half-hatched (*U*) nauplii. The *HR*s were calculated using the following formulas:

$$HR^{-} = \frac{\Sigma N}{\Sigma N + \Sigma C + \Sigma U} \times 100 \quad (1)$$

$$HR^{+} = \frac{\Sigma N + \Sigma U}{\Sigma N + \Sigma C + \Sigma U} \times 100 \quad (2)$$

$$HR = \frac{HR^{-} + HR^{+}}{2} \quad (3)$$

where *HR*[−] is the hatching rate without embryos, %; *HR*⁺ is the hatching rate with embryos, %; *HR* is the average between *HR*[−] and ; ΣN is the sum of nauplii; ΣC is the sum of cysts; ΣU is the sum of embryos (umbrellas), half-hatched nauplii.

To determine the biomass yield, we turned off aeration at the end of incubation, while leaving the lighting on. After 10 min, the biomass (live nauplii) was separated from waste (shells and unhatched cysts on the bottom and walls of the cone) by sedimentation and simultaneous concentration of mobile nauplii in the illuminated middle part of the cone. Then, the liquid

with nauplii was drained through a cone-shaped sieve (100 μm pores) with a 4–6 mm silicone tube from the middle part of the cone, leaving the waste on its walls and bottom. The sieved biomass was washed in fresh water and squeezed out at least five times. Then, it was left to drain excess moisture for 2 min and weighed on a laboratory balance with an accuracy of 0.01 g.

Biomass yield. Biomass yield is an indicator of incubation effectiveness that shows the amount of *Artemia* biomass incubated. This indicator is used in farming because of its simplicity: dry cysts are weighed at the beginning of incubation and compared with the weight of nauplii at the end of incubation. Although its accuracy is much lower than that of the classical method, we used it to double-check the results, trying to minimize possible errors [30]. The main problem in measuring biomass is that water runs down differently from the samples. Before weighing, the samples are kept in a sieve (100–150 μm) for some time to minimize the effect of water mass on the *Artemia* biomass.

In our study, we used the same kind of 50 cm³ gas net, which was twisted 720 degrees twice (to squeeze out most of the water), and then left for 5 min to drain excess residual liquid. Only after this double manipulation (the same for all samples), the resulting *Artemia* biomass was weighed on a laboratory balance. Then, we calculated the biomass coefficient corresponding to a multi-fold difference between the final wet weight and the weight of dry cysts introduced at the beginning of incubation.

Neural network operation. Nowadays, many farmers of *Artemia* crustaceans do the counting by using binoculars, microscopes, or magnifiers. To save data, they have to use additional devices, such as cameras or smartphones, and manually enter the data into logbooks or spreadsheets. All these manipulations take a lot of time and effort.

The Artemeter-1 robot counter based on a convolutional neural network that uses the YOLO algorithm is designed to significantly reduce the counting time, as well as improve the quality and accuracy of measurements. It ensures a one-time graphic fixation of *Artemia* and storage of all data, as well as saves researchers having to use other instruments. Therefore, we employed this robot counter in our study and we know of no other studies in Russia that have used it before.

The neural network was trained using a dataset of 1200 manually labeled microphotographs of *Artemia* samples (Fig. 3). Each sample amounted to 0.1 cm³ of incubator water with a random number of unhatched cysts, embryos, and hatched nauplii.

All the objects that were to be counted by the neural network were marked on each sample. The total number of labeled images (dataset) was divided into two unequal parts: 1) a training sample (about 800 images) that the network learns from, and 2) a test sample (400 images) that the network uses to check itself [31]. Figure 4 shows some examples of the images in the corresponding resolution.

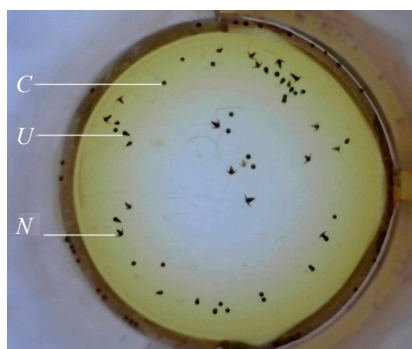


Figure 3 The sample under the binocular (9×): *C* – cysts; *U* – embryos; *N* – nauplii



Nauplii (*N*) Umbrellas (*U*) Cysts (*C*)

Figure 4 Objects for detection in the sample

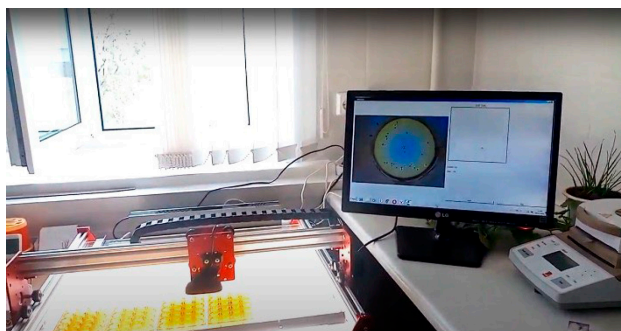


Figure 5 Artemeter-1 robot for *Artemia* counting

The images were enlarged in size. The number of pixels per unit area was sufficient for the neural network to operate, since the real size of the objects in the detector's visibility was commensurate with that of the samples used to train it.

The neural network was trained in the GoogleColab cloud service connected to Nvidia K80s, T4s, P4s, and P100s GPUs. As a result, so-called “neural network weights” were obtained, i.e. parameter settings that the neural network used for most accurate detection of objects in the image. Further, the weights were downloaded from the cloud service to be used offline.

The mechanical part of the Artemeter-1 robot for nauplii counting was also designed and manufactured in Russia (Fig. 5).

The network detects three types of objects (nauplii, cysts, and umbrellas), whose ratio indicates the quality of the product. It also marks these objects

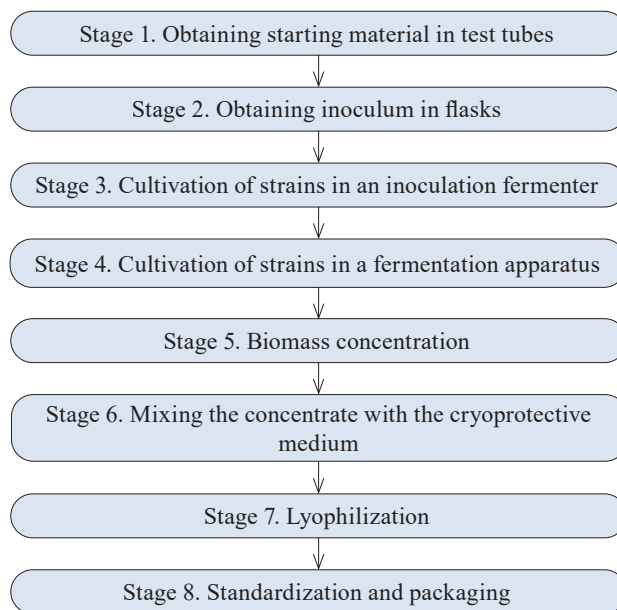


Figure 6 Process chart for probiotic production

in the original JPEG file and saves the data in both EXCEL tables and processed images. The robot is designed for both producers and large consumers of *Artemia* cysts [27].

Statistical processing. One-way analysis of variance (Student's t-test, Statistica 13, MS Excel 2016) was used to determine significant variations between *Artemia* groups counted by different methods. The data were presented as means (AV) with standard deviation (SD). All the data showed significance at $p < 0.05$. The coefficient of variation (CV) was also determined for the hatching rate (HR).

RESULTS AND DISCUSSION

Probiotic production. We developed a technology for producing a new probiotic for aquaculture (Fig. 6).

Each stage of the process produced an intermediate result, namely:

Stage 1. Starting mother culture for further scaling in stepwise increasing inoculation containers.

Stage 2. Primary inoculum for sowing a small (1 L) fermentation apparatus, which was about 10% of the loaded medium (inoculation apparatus – 15 L, estimated nutrient medium – 10 L).

Stage 3. Inoculum for deep cultivation in commercial media on a semi-industrial bioreactor, with a volume of about 5% of the main fermenter (bioreactor – 250 L, estimated fermentation medium – about 120 L).

Stage 4. Each strain fermented in 120 L of nutrient medium separately, under the same cultivation conditions.

Stage 5. About 3 kg of concentrated biomass from two fermentations (one per each strain) with a residual moisture of 15–20% after flow centrifugation.

Table 1 Incubation of *Artemia* cysts, batch Z29.04 (Lake Bolshoye Yarovoye), 48 h

Samples (probiotic weight, g)	Hatching rate (AV \pm SD, %)	Coefficient of variation, % (as to HR)	Biomass yield
Control (0)	95.19 \pm 2.98	3.1	2.65
Test (0.05)	94.61 \pm 4.89	5.2	3.40
Test (0.10)	96.53 \pm 2.91	3.0	3.70
Test (0.20)	93.01 \pm 5.09	5.5	3.55

HR – hatching rate, AV – average value, SD – standard deviation. Mean differences between the control and each of the test cones are significant at $p < 0.05$

Table 2 Incubation of *Artemia* cysts, batch C9 (Lake Kuchuk), 48 h

Samples (probiotic weight, g)	Hatching rate (AV \pm SD, %)	Coefficient of variation, % (as to HR)	Biomass yield
Control (0)	79.23 \pm 9.37	11.8	2.30
Test (0.05)	79.85 \pm 12.74	16.0	3.20
Test (0.10)	88.76 \pm 5.66	6.4	3.40
Test (0.20)	83.69 \pm 8.23	9.8	2.55

HR – hatching rate, AV – average value, SD – standard deviation. Mean differences between the control and each of the test cones are significant at $p < 0.05$.

Stage 6. The concentrated biomass mixed with 3 L of cryoprotective medium (1:1), poured into trays, and frozen.

Stage 7. The freeze-dried concentrate of bacteria with a total weight of about 2.5 kg and at least 1×10^{11} CFU/g for each strain, additionally ground in a blender to homogeneous powder.

Stage 8. The concentrate standardized to a titer of 1×10^{10} CFU/g, packaged in plastic bags, sealed, and placed in three-layer kraft bags, which were sewn up to prevent the probiotic from getting wet.

As a result, we obtained a pilot batch of the probiotic with a titer of at least 1×10^{10} CFU/g to be used in full-scale tests.

The probiotic's effect on the incubation of *Artemia franciscana* cysts. Shrimp need live feed in the early stages of development. Therefore, shrimp prelarvae are fed on live, freshly hatched *Artemia* nauplii. However, the incubation solution for *A. franciscana* is a favorable environment for any microorganisms, including pathogenic microflora, which affects the quality of shrimp. The number of pathogenic microorganisms in *Artemia* increases exponentially while the nauplii are hatching and becoming enriched with nutrients. For this reason, producers add probiotic and prebiotic preparations to reduce the development of pathogens in shrimp prelarvae [32].

Artemia nauplii begin to hatch from cysts in large numbers after 20 h of incubation and start feeding actively 6–8 h after birth. Thus, during 48 h of incubation, *Artemia* cysts not only inseminate the surface of nauplii, but also populate their gastrointestinal tract with probiotic bacilli. Our study showed a positive effect of the probiotic we had developed on both batches of *Artemia* cysts, which manifested in increased biomass yield compared to the control. In addition, the consortium of *Bacillus toyonensis* B-13249 and *Bacillus pumilus* B-13250 appeared to favorably change

the habitat conditions for *Artemia*, stimulating the hatching process. This could also be associated with the antagonistic properties of these bacilli against pathogens. The test results for cyst batches Z29.04 and batch C9 are shown in Tables 1 and 2, respectively. For both batches, the highest biomass yield was provided by 0.1 g of the probiotic per 2 g of dry cysts.

The probiotic added to batch Z29.04 increased the hatching rate by 1.4%, compared to the control (Table 1). The coefficient of variation from 3 to 5% indicated a slight spread of values and the validity of the results.

The probiotic added to batch C9 increased the hatching rate by about 10%, compared to the control (Table 2). The coefficient of variation for this batch was significantly higher (6.4–11.8%) than the one for batch Z29.04, but it was within an allowable range and therefore indicative of reliable results. The smallest variation was noted in the test group with 0.1 g of the probiotic.

The biomass yield shows the mass of *A. franciscana* incubated. Figure 7 presents the correlation between the amount of the probiotic and the biomass yield from two independent batches taken from two different lakes.

As can be seen in Fig. 7, the maximum biomass yield was obtained with a probiotic weight of 0.1/2 g of cysts in both experimental batches, which corresponded to the data in Tables 1 and 2.

A. franciscana cysts from batches C9 and Z29.04 had different hatching rates and biomass yield in the control cones. However, these indicators decreased in both batches with the addition of 0.2 g of the probiotic, compared to the best result in the cone with 0.1 g of the probiotic. The effect of the probiotic was more pronounced in batch C9 with the initially low hatching rate and biomass yield. Test batch Z29.04 (Lake Bolshoye Yarovoye) showed a significantly higher hatching rate, which was normal for this batch and was not associated with the probiotic. Batch C9 (Lake Kuchuk) had minimum

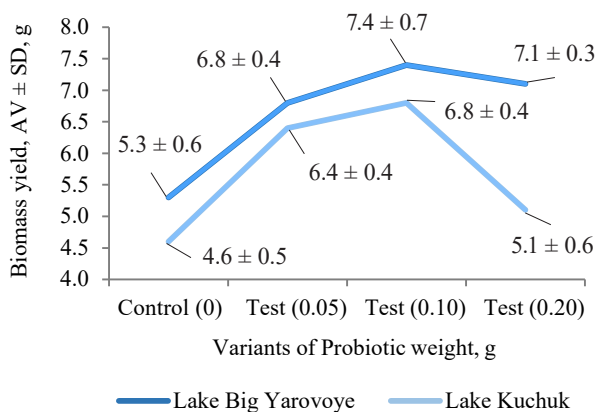


Figure 7 Correlation between the probiotic concentration and the biomass yield

differences in the indicators when we added 0.1 g of the probiotic. This might indirectly indicate the stabilizing effect of the probiotic on hatching. The differences in the hatching rates between the two batches of *Artemia* cysts were due to the fact that they were obtained from different salt lakes, i.e., different ecosystems where they evolved.

The biomass yield indicates the number of times that the mass of *Artemia* increased after incubation. Tables 1 and 2 present the correlation between the amount of the probiotic and the biomass yield in the studied batches.

Thus, the new probiotic preparation based on *B. toyo-nensis* B-13249 and *B. pumilus* B-13250 had a positive effect on the hatching rate and biomass yield of *A. franciscana*. According to our results, the optimal concentration of the probiotic was 0.1 per 2 g of cysts. This concentration increased the hatching rates by 1.4 and 10% in batches Z29.04 and C9, respectively. The biomass yields in the control cones were 5.30 ± 0.60 and 4.60 ± 0.50 g in batches Z29.04 and C9, respectively. The addition of 0.1 g of the probiotic increased the biomass yield to 7.40 ± 0.69 and 6.80 ± 0.43 g, respectively.

Counting reliability. To ensure the reliability of automatic counting results, we used the classical (mechanical) method for the entire batch of 192 images (Table 3).

We found no significant differences between the automatic and mechanical methods of counting. However, the automatic counting proved to be faster and more accurate. Slight differences were observed in the control and the sample with 0.05 g of the probiotic in the batch from Lake Bolshoye Yarovoye. In cone 1 (control), the mechanical and automatic methods revealed 833 and 848 nauplii, 34 and 26 cysts, and 41 and 38 embryos, respectively. The sample with the lowest concentration of the probiotic (0.05 g), also showed slightly different counts. These differences could be explained by a large number of objects to be observed in each sample, as well as the impossibility of marking the observed objects during mechanical counting. The different counts of morphologically different objects (nauplii, cysts, and embryos) could also be explained by higher accuracy of the

Table 3 Classical (mechanical) vs. automatic counting of *Artemia* nauplii

Sample (probiotic weight, g)	Total number of nauplii	Total number of cysts	Total number of embryos
Classical (mechanical) counting (45 sec/sample)			
Lake Bolshoye Yarovoye			
Control (0)	833	34	41
Test (0.05)	757	44	28
Test (0.10)	782	16	26
Test (0.20)	739	42	41
Lake Kuchuk			
Control (0)	394	96	20
Test (0.05)	390	95	15
Test (0.10)	488	56	16
Test (0.20)	469	86	26
Automatic counting (3 sec/sample)			
Lake Bolshoye Yarovoye			
Control (0)	848	26	38
Test (0.05)	758	33	28
Test (0.10)	782	16	26
Test (0.20)	739	42	41
Lake Kuchuk			
Control (0)	394	96	20
Test (0.05)	390	95	15
Test (0.10)	488	56	16
Test (0.20)	469	86	26

robot counter, which compared the objects under observation with those it was trained on. The robot can instantly count all the objects and mark them on each sample, and if it fails to identify the objects correctly, it can be retrained. However, the differences between the counts were too insignificant to affect the final results. Both methods showed similar counts in the other samples. The entire set of images was saved for further research.

Figure 8 shows an example of saved images from the test set. The robot can determine and count both individual morphological forms (for more specific identification) and their different types (nauplii, cysts, and embryos).

The advantages of the *Artemia* robot counter based on the convolutional neural network outweigh its limitations. These advantages include a simultaneous use of multiple devices, a reduced data processing time, a possibility of saving data for later use, and less operator presence.

The absence of significant differences between the mechanical and automatic counting methods confirms high accuracy of the robot counter. Its large-scale use will optimize the counting of *Artemia* nauplii, cysts, and embryos in further research.

Thus, our study was the first in Russia that successfully tested the new robotic system for counting nauplii based on machine learning. It significantly reduced the processing time (15 times per 1 sample) and labor costs, as well as saved the data for further use.

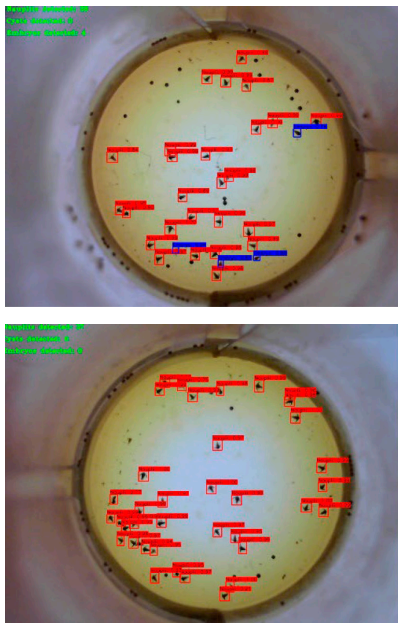


Figure 8 Test images

CONCLUSION

We found that the new probiotic preparation based on *Bacillus toyonensis* B-13249 and *Bacillus pumilus* B-13250 had a positive effect on the biomass yield

of *Artemia franciscana*. In particular, it increased the hatching rate in batches Z29.04 and C9 by 1.4 and 10%, respectively. While the biomass yields in the control cones were 5.30 ± 0.60 and 4.60 ± 0.50 g for batches Z29.04 and C9, respectively, the probiotic increased this indicator to 7.40 ± 0.69 and 6.80 ± 0.43 g, respectively.

As a result of our tests, we recommend 0.1 g of the probiotic per 2 g of cysts.

Just as important was the development and testing of the Artemeter-1 robot based on the convolutional neural network for rapid and accurate counting of *Artemia* during decapsulation. Our study was the first in Russia that utilized this new robotic system based on machine learning. It reduced the sample processing time 15 times, lowered labor costs, and saved the data in electronic form for further use.

Our results may be useful to farmers working in aquaculture, as well as researchers interested in this field.

CONTRIBUTION

The authors were equally involved in writing the manuscript and are equally responsible for any potential plagiarism.

CONFLICT OF INTEREST

The authors declare no conflict of interest.





REFERENCES

- Salunke M, Kalyankar A, Khedkar CD, Shingare M, Khedkar GD. A review on shrimp aquaculture in India: Historical perspective, constraints, status and future implications for impacts on aquatic ecosystem and biodiversity. *Reviews in Fisheries Science and Aquaculture*. 2020;28(3):283–302. <https://doi.org/10.1080/23308249.2020.1723058>
- Sampantamit T, Ho L, Lachat C, Sutumawong N, Sorgeloos P, Goethals P. aquaculture production and its environmental sustainability in Thailand: Challenges and potential solutions. *Sustainability*. 2020;12(5). <https://doi.org/10.3390/su12052010>
- Cortes A, Casillas-Hernandez R, Cambeses-Franco C, Borquez-Lopez R, Magallon-Barajas F, Quadros-Seiffert W, et al. Eco-efficiency assessment of shrimp aquaculture production in Mexico. *Aquaculture*. 2021;544. <https://doi.org/10.1016/j.aquaculture.2021.737145>
- Tepaamorndech S, Chantarasakha K, Kingcha Y, Chaiyapechara S, Phromson M, Sriariyanun M, et al. Effects of *Bacillus aryabhatai* TBRC8450 on vibriosis resistance and immune enhancement in Pacific white shrimp, *Litopenaeus vannamei*. *Fish and Shellfish Immunology*. 2019;86:4–13. <https://doi.org/10.1016/j.fsi.2018.11.010>
- Naylor RL, Hardy RW, Buschmann AH, Bush SR, Cao L, Klinger DH, et al. A 20-year retrospective review of global aquaculture. *Nature*. 2021;591:551–563. <https://doi.org/10.1038/s41586-021-03308-6>
- Joshua WJ, Kamarudin MS, Ikhsan N, Yusoff FM, Zulperi Z. Development of enriched *Artemia* and *Moina* in larviculture of fish and crustaceans: A review. *Latin American Journal of Aquatic Research*. 2022;50(2):144–157.
- Kovacheva NP, Litvinenko LI, Saenko EM, Zhigin AV, Kryahova NV, Semik AM. Current state and prospects of aquaculture artemia in Russia. *Trudy VNIRO*. 2019;178:150–171. (In Russ.). <https://doi.org/10.36038/2307-3497-2019-178-150-171>
- Sellami I, Naceur HB, Kacem A. Study of cysts biometry and hatching percentage of the brine shrimp *Artemia salina* (Linnaeus, 1758) from the Sebkhfa of Sidi El Hani (Tunisia) according to successive generations. *Aquaculture Studies*. 2020;21(1):41–46. https://doi.org/10.4194/2618-6381-v21_1_05
- Niu J, Chen P-F, Tian L-X, Liu Y-J, Lin H-Z, Yang H-J, et al. Excess dietary cholesterol may have an adverse effect on growth performance of early post-larval *Litopenaeus vannamei*. *Journal of Animal Science and Biotechnology*. 2012;3(1). <https://doi.org/10.1186/2049-1891-3-19>

10. Malkova A, Evdokimov I, Shirmanov M, Irkitova A, Demytyev D. New bacilli-based probiotic for aquaculture: Efficacy study on *Macrobrachium rosenbergii*. *BIO Web of Conferences*. 2022;42. <https://doi.org/10.1051/bioconf/20224201011>
11. Ofelio C, Planas M, Pintado J. Administration of the probiotic *Lactobacillus rhamnosus* IMC 501 as a strategy for the control of *Vibrio* bacteria in the brine shrimp *Artemia*. *Letters in Applied Microbiology*. 2021;73(3):336–342. <https://doi.org/10.1111/lam.13518>
12. Schar D, Zhao C, Wang Yu, Larsson DGJ, Gilbert M, Boeckel van TP. Twenty-year trends in antimicrobial resistance from aquaculture and fisheries in Asia. *Nature Communications*. 2021;12(1). <https://doi.org/10.1038/s41467-021-25655-8>
13. Wall S. Prevention of antibiotic resistance – an epidemiological scoping review to identify research categories and knowledge gaps. *Global Health Action*. 2019;12. <https://doi.org/10.1080/16549716.2020.1756191>
14. Uddin TM, Chakraborty AJ, Khusro A, Zidan BMRM, Mitra S, Emran TB, et al. Antibiotic resistance in microbes: History, mechanisms, therapeutic strategies and future prospects. *Journal of Infection and Public Health*. 2021;14(12):1750–1766. <https://doi.org/10.1016/j.jiph.2021.10.020>
15. Larsson DGJ, Flach C-F. Antibiotic resistance in the environment. *Nature Reviews Microbiology*. 2022;20:257–269. <https://doi.org/10.1038/s41579-021-00649-x>
16. Goh JXH, Tan LT-H, Law JW-F, Khaw K-Y, Zengin G, Chan K-G, et al. Probiotics: Comprehensive exploration of the growth promotion mechanisms in shrimps. *Progress in Microbes and Molecular Biology*. 2023;6(1). <https://doi.org/a10.36877/pmmb.0000324>
17. da Costa Sousa N, do Couto MVS, Paixão PEG, dos Santos Medeiros E, de Souza JCN, Barros FAL, et al. Enriched *Artemia nauplii* with commercial probiotic in the larviculture of angelfish *Pterophyllum scalare* Lichtenstein (1823). *Journal of Fisheries Science*. 2020;2(1):17–21. <https://doi.org/10.30564/jfsr.v2i1.1569>
18. Volkova GS, Serba EM. New Multistrain Bacterial consortium for Feed Probiotics. *Food Processing: Techniques and Technology*. 2021;51(2):260–269. (In Russ.). <https://doi.org/10.21603/2074-9414-2021-2-260-269>.
19. Ahmadifard N, Aminlooi VR, Tukmechi A, Agh N. Evaluation of the impacts of long-term enriched *Artemia* with *Bacillus subtilis* on growth performance, reproduction, intestinal microflora, and resistance to *Aeromonas hydrophila* of ornamental fish *Poecilia latipinna*. *Probiotics Antimicrobial Proteins*. 2019;11:957–965. <https://doi.org/10.1007/s12602-018-9453-4>
20. Sekar A, Kima M, Jeonb H, Kima K. Screening and selection of bacteria inhibiting white spot syndrome virus infection to *Litopenaeus vannamei*. *Biochemistry and Biophysics Reports*. 2019;19. <https://doi.org/10.1016/j.bbrep.2019.100663>
21. Amoah K, Huang Q-C, Tan B-P, Zhang S, Chi S-Y, Yang Q-H, et al. Dietary supplementation of probiotic *Bacillus coagulans* ATCC 7050, improves the growth performance, intestinal morphology, microflora, immune response, and disease confrontation of Pacific white shrimp, *Litopenaeus vannamei*. *Fish and Shellfish Immunology*. 2019;87:796–808. <https://doi.org/10.1016/j.fsi.2019.02.029>
22. Fernandes V, Sabu EA, Shivaramu MS, Gonsalves MJBD, Sreepada RA. Dynamics and succession of plankton communities with changing nutrient levels in tropical culture ponds of whiteleg shrimp. *Aquaculture Environment Interactions*. 2019;11:639–655. <https://doi.org/10.3354/aei00341>
23. Wang Y-C, Hu S-Y, Chiu C-S, Liu C-H. Multiple-strain probiotics appear to be more effective in improving the growth performance and health status of white shrimp, *Litopenaeus vannamei*, than single probiotic strains. *Fish and Shellfish Immunology*. 2019;84:1050–1058. <https://doi.org/10.1016/j.fsi.2018.11.017>
24. Seenivasan C, Bhavan PS, Radhakrishnan S, Shanthi R. Enrichment of *Artemia nauplii* with *Lactobacillus sporogenes* for enhancing the survival, growth and levels of biochemical constituents in the post-larvae of the freshwater prawn *Macrobrachium rosenbergii*. *Turkish Journal of Fisheries and Aquatic Sciences*. 2012;12:23–31.
25. Patra SK, Mohamed KS. Enrichment of *Artemia nauplii* with the probiotic yeast *Saccharomyces boulardii* and its resistance against a pathogenic *Vibrio*. *Aquaculture International*. 2003;11:505–514. <https://doi.org/10.1023/b:aqui.0000004193.40039.54>
26. Isamma A, Divya, KR, Ramasubramanian V, Arunjith TS, Sureshkumar S. Standardization of the bioencapsulation of probiotics and oil emulsion in *Artemia parthenogenetica*. *International Journal of Research in Fisheries and Aquaculture*. 2014;4(3):122–125.
27. Dement'ev DV, Komyshev GB, Semyonov PA. The convolutional neural network for determining the quality of *Artemia*. Patent RU 2021663036. 2021. <https://www.elibrary.ru/ERHLL>

28. Bochkovskiy A, Wang C-Y, Liao H-YM. YOLOv4: Optimal speed and accuracy of object detection. <https://doi.org/10.48550/arXiv.2004.10934>
29. Malkova AV, Evdokimov IYu, Shirmanov MV, Irkitova AN, Dudnik DE. Development of a probiotic for animals and aquaculture based on *Bacillus toyonensis* B-13249 and *Bacillus pumilus* B-13250 strains. *Proceedings of Universities. Applied Chemistry and Biotechnology*. 2021;11(3):393–402. (In Russ.). <https://doi.org/10.21285/2227-2925-2021-11-3-393-402>
30. Baert P, Bosteels T, Sorgeloos P. Pond production. In: Lavens P, Sorgeloos P, editors. *Manual on the production and use of live food for aquaculture*. Rome: FAO; 1996. pp. 196–251.
31. Jabir B, Rabhi L, Falih N. RNN- and CNN-based weed detection for crop improvement: An overview. *Foods and Raw Materials*. 2021;9(2):387–396. <https://doi.org/10.21603/2308-4057-2021-2-387-396>
32. Hamsah, Widanarni, Alimuddin, Yuhana M, Zairin M. The nutritional value of *Artemia* sp. enriched with the probiotic *Pseudoalteromonas piscicida* and the prebiotic mannan-oligosaccharide. *AAFL Bioflux*. 2017;10(1):8–17.

ORCID IDs

Ivan Yu. Evdokimov  <https://orcid.org/0000-0002-6218-3151>
Angelina V. Malkova  <https://orcid.org/0000-0002-4053-036X>
Alena N. Irkitova  <https://orcid.org/0000-0002-2664-1995>
Maxim V. Shirmanov  <https://orcid.org/0000-0002-1628-2546>
Dmitrii V. Dementev  <https://orcid.org/0000-0002-6954-8563>



A thermophilic L-lactic acid producer of high optical purity: Isolation and identification

Mariia V. Romanova^{ID}, Anastasiia N. Dolbunova^{ID}, Yulia M. Epishkina^{ID},
Svetlana A. Evdokimova^{ID}, Mikhail R. Kozlovskiy^{ID}, Alexander Ye. Kuznetsov^{ID},
Natalya Yu. Khromova^{ID}, Andrey V. Beloded*^{ID}

Dmitry Mendeleev University of Chemical Technology of Russia^{OR}, Moscow, Russia

* e-mail: beloded.a.v@muctr.ru

Received 22.03.2023; Revised 26.04.2023; Accepted 02.05.2023; Published online 30.08.2023

Abstract:

Biodegradable polymers, specifically polylactide, are an important part of food packaging and medical devices. Microbiological synthesis uses cheap renewable raw materials and industrial waste to produce a high yield of lactic acid, the monomer of polylactide. This method needs new effective lactic acid producing strains, e.g., thermophilic bacteria.

The research involved thermophilic bacterial strains isolated from soil and compost samples. Their ability to produce organic acids and extracellular enzymes was tested using the method of high-performance liquid chromatography (HPLC) and microbiological tests respectively. The real-time polymerase chain reaction method (PCR) detected L-lactate dehydrogenase structural genes of L-lactate dehydrogenase of *Bacillaceae*. Strain T7.1 was fermented using glucose and yeast extract as carbon and nitrogen sources, respectively. The optical purity of lactic acid was evaluated using quantitative gas chromatography on a chiral column to separate lactate isomers. The molecular genetic analysis of the 16S rRNA gene sequence was applied to identify strain T7.1.

The chromatographic analysis proved that 10 out of 13 isolated thermophilic strains were effective lactic acid producers. They demonstrated proteolytic, amylolytic, or cellulase activities. During the fermentation, strain T7.1 produced 81 g/L of lactic acid with a peak productivity at 1.58 g/(L·h). The optical purity of the product exceeded 99.9% L-lactate. The genetic analysis identified strain T7.1 as *Weizmannia coagulans* (*Bacillus coagulans*).

The research revealed a promising thermophilic producer of optically pure L-lactic acid. Further research is needed to optimize the cultivation conditions, design an effective and cheap nutrient medium, and develop engineering and technological solutions to increase the yield.

Keywords: Thermophilic bacteria, *Bacillus*, *Weizmannia coagulans*, lactic acid, L-lactate, polylactide

Funding: The research was supported by the foundation of Dmitry Mendeleev University of Chemical Technology of Russia (Mendeleev University)^{OR} as part of strategic academic leadership Program Priority 2030 (project no. 2022-040).

Please cite this article in press as: Romanova MV, Dolbunova AN, Epishkina YuM, Evdokimova SA, Kozlovskiy MR, Kuznetsov AY, *et al.* A thermophilic L-lactic acid producer of high optical purity: Isolation and identification. *Foods and Raw Materials*. 2024;12(1):101–109. <https://doi.org/10.21603/2308-4057-2024-1-591>

INTRODUCTION

Lactic acid is widely used in food production, pharmacy, and cosmetics. The global production of lactic acid amounted to 1.39 million tons in 2021 and will have reached 2.65 million tons by 2029 [1]. The demand for local acid keeps increasing, following the increase in production of foods, beverages, and biodegradable polymers [2]. Lactic acid serves as a preservative and acidity regulator in pickled and fermented foods, chee-

ses, yoghurts, fermented dairy products, bakery, confectionery, etc. [3]. In addition, environmentally-aware consumers, manufacturers, and scientists encourage the development of sustainable products and processes. This trend affects packaging methods, since environmental pollution by synthetic polymers is approaching a critical level [4, 5].

Lactic acid is a precursor for the synthesis of green solvents, lactide and polylactide. It should be noted that lactic acid can at least partially solve the tremendous

problem of plastic pollution because it is a source of polylactide, which is a biodegradable polymer of high transparency and excellent mechanical strength. Polylactide has good barrier properties to food smell, as well as chemical resistance to fats and oils [6, 7]. It is a prospective material for biodegradable films and plasticware [2].

Lactic acid has two stereoisomers. As a result, it can produce poly-L-lactide, poly-D-lactide, and poly-L,D-lactides with different isomer content. The mechanical properties of particular polymer depend on the ratio of L- and D-isomers. For instance, polylactide with 90% of poly-L-lactide has a semi-crystalline structure, while polylactide with a higher content of D-lactate is an amorphous material with poor mechanical properties [8].

Chemical and microbiological syntheses are two commercial methods of lactic acid production. However, chemical synthesis forms racemic L,D-lactic acid, which makes it difficult to produce polylactide with required properties. Biotechnological synthesis yields optically pure isomers of lactic acid from cheap and renewable raw materials, e.g., industrial waste [9]. A proper pretreatment, such as grinding, chemical or enzymatic hydrolysis, etc., can increase the yield. For example, Alexandri *et al.* used a hydrolysate of bread production waste as a substrate to obtain optically pure L-lactic acid and cultivate *Bacillus coagulans* [10]. They also substituted yeast extract with a more accessible alfalfa juice. The productivity for batch cultivation was 2.59 g/(L·h) with the final lactic acid titer of 62.2 g/L. The combination of these two substrates (50:50) in a continuous process with cell recycling raised the efficiency up to 11.28 g/(L·h).

Some lignocellulosic substrates are fit for simultaneous saccharification and fermentation. The pretreatment occurs, wholly or partly, in a fermenter, where the lactic acid producer is cultivated. Hu *et al.* used the method of simultaneous saccharification and fermentation, as well as corn straw as substrate, to cultivate *Lactobacillus pentosus* FL0421 (37°C, pH 6.0) [11]. They also added cellulases and yeast extract to the medium with the pretreated substrate. The final lactic acid titer and the product efficiency were 92.30 g/L and 1.92 g/(L·h), respectively.

The yield and optical purity of microbiologically-synthesized lactic acid depends on gene expression, enzymatic activity, stereospecificity of lactate dehydrogenases (LDH), lactate racemases, and some enzymes of amino acid metabolism. For instance, enzymes L-LDH and D-LDH catalyze the conversion of pyruvic acid to L-lactic acid and D-lactic acid, respectively. They can be present, together or separately, in different types of microorganisms [12].

Lactate racemases provide the mutual conversion of lactate isomers. They can be found in some lactic acid bacteria, but not necessarily in *Bacillaceae*, which also can produce lactic acid [13]. *Bacillaceae* strains are known as effective producers of optically pure lactic acid. Unlike the more popular *Lactobacillaceae*, *Bacillaceae* are thermotolerant and/or thermophilic.

Thermophilic lactic acid producers have some advantages over mesophilic microorganisms. They demonstrate accelerated metabolism and increase the solubility of substrates in the fermentation medium during thermal processing, thus boosting the yield. In addition, they reduce the risk of contamination during fermentation [14]. Thermophilic microorganisms have the same optimal growth temperatures as commercial enzyme preparations, which increases the efficiency of saccharification of complex raw materials in a bioreactor [15]. Thermotolerant *Bacillaceae*, e.g., *B. coagulans* (*Weizmannia coagulans*), are prospective lactic acid producers as they have a low need for growth factors and can utilize a wide range of substrates [16]. Some *Bacillaceae* are resistant to inhibitory substances contained in some hydrolysates, e.g., to furfural and its derivatives [17]. In addition, *Bacillaceae* have their own hydrolytic enzymes, i.e., proteases, amylases, and cellulases. As a result, saccharification requires less enzymes during simultaneous saccharification and fermentation [9].

Fed-batch culture, as well as semi-continuous and continuous fermentation, can increase the lactate yield during biosynthesis. Continuous cultivation methods, including those based on a membrane bioreactor, facilitate substrate conversion in the fermentation medium into the target product and reduce inhibitory effects [18]. The efficiency of bioreactors depends on how well they are able to maintain the culture in a certain physiological state at a given medium supply rate [19]. Long-term cultivation during continuous fermentation requires process stability, a low contamination risk, and a highly-active and stable producer. As a result, the food science keeps looking for new lactic acid producers with high optical purity and their assessment methods. The research objective was to isolate and identify thermophilic bacterial strains capable of homofermentative conversion of carbohydrates into lactic acid, as well as to evaluate the optical purity of the product.

STUDY OBJECTS AND METHODS

Microorganisms and culture conditions. The research featured strains of thermophilic bacteria isolated from various samples of natural origin on nutrient media with different glucose and lactate amounts as a carbon source and elective element. To obtain enrichment cultures, we added 1 g of the sample to nutrient media and cultivated at 50°C for 24 h. After that, we seeded the cultures into a liquid medium and its tenfold dilutions on agar nutrient medium. The medium composition, g/L, was as follows: glucose – 20, tryptone – 20, yeast extract – 5, K₂HPO₄·3H₂O – 2, MgSO₄·7H₂O – 0.2, MnSO₄·5H₂O – 0.05, and CaCO₃ – 10. For further research, we selected those colonies that demonstrated zones of calcium carbonate dissolution caused by organic acids. The profiling of low molecular weight metabolites was carried out using a similar but tryptone-free liquid medium after 24 h of cultivation in test tubes under anaerobic or microaerophilic conditions. The nature of colony growth on agar media revealed its

ability to synthesize extracellular proteases, amylases, and cellulases. The medium contained skimmed milk powder, starch, and carboxymethyl cellulose, respectively [20].

To produce lactic acid, the strains were cultivated in a five-liter Minifors fermenter (INFORS, Switzerland). The inoculum was grown at 50°C under microaerophilic conditions on a nutrient medium for 24 h. The medium included, g/L: glucose – 20, yeast extract – 5, $K_2HPO_4 \cdot 3H_2O$ – 2, $MgSO_4 \cdot 7H_2O$ – 0.2, and $MnSO_4 \cdot 5H_2O$ – 0.05. All the fermentation medium components were sterilized separately to avoid the formation of inhibiting compounds. The operating volume of the medium in the fermenter was 3 L, and the concentrations of the components, g/L, were as follows: glucose – 100, yeast extract – 5, $K_2HPO_4 \cdot 3H_2O$ – 2, $MgSO_4 \cdot 7H_2O$ – 0.2, and $MnSO_4 \cdot 5H_2O$ – 0.05. The inoculum was added as 10% of the medium volume. The fermentation occurred under anaerobic conditions while the medium was stirred at 250 rpm. During cultivation, temperature and pH were recorded and controlled using the Iris V5 software. The fermentation medium was automatically titrated to neutralize lactic acid with 25% ammonia solution until pH reached 7.0. The bacterial biomass was measured by the optical density of tenfold dilutions at $\lambda = 590$ nm.

Determining the content of organic acids and glucose. To analyze the metabolites in the culture broth of thermophilic strains and glucose consumption, we used the method of high-performance liquid chromatography (HPLC). The procedure involved an Agilent 1220 Infinity chromatograph (Agilent, USA) with an Agilent Hi-Plex H column (250×4.6 mm). The concentration was determined by the refractometric signal after standard calibration. As pretreatment, the culture broth was centrifuged at 12 000 rpm for 15 min and filtered through 0.45- μ m cellulose acetate membranes (MF-Millipore, USA). The analysis was performed at 50°C and a mobile phase flow rate (0.002 M H_2SO_4) of 0.3 mL/min.

Evaluating the optical purity of lactate. To determine the individual optical isomers of lactic acid in the fermentation products, the culture broth was purified from biomass by ultrafiltration on an AR-100 hollow fiber device with a cut-off limit of 100 kDa. Nonutilized components of the nutrient medium and interfering metabolic products were adsorbed: the cell-free broth was filtered through a layer of activated carbon. After that, the lactate was converted into salt, and from salt into acid. This process involved ion-exchange H-form resin Amberlyst 70. The entire lactic acid was converted into the trimethylsilyl derivative using N,O-Bis(trimethylsilyl)trifluoroacetamide (BSTFA) as a silylating agent. We took 0.03 g of the sample, thoroughly mixed it with 1 mL of ethyl acetate, and added extra BSTFA. The mix was incubated at 60°C for 30 min. We used the same conditions to convert all forms of lactic acid to derivatives of ditrimethylsilyl ethers (diTMS esters) suitable for gas chromatography.

The optical isomers of the obtained lactic acid derivatives were determined by quantitative gas chromatography using a column for the separation of chiral isomers Cyclosil-B, 30 m×0.25 mm×0.25 μ m (Agilent, USA). The procedure also involved a Kristall 5000.1 gas chromatograph (Khromatek, Russia) with a flame-ionization detector and Khromatek Analyst 2.6 software. Nitrogen served as the mobile phase at a pressure of 75 kPa. The initial temperature of the column (35°C) was maintained for 20 min, then the temperature was raised to 100°C at a rate of 1°C/min and then to 250°C at a rate of 10°C/min. The optical purity (OP) of L-lactic acid was calculated as follows:

$$OP = \frac{SL}{SL + SD} \times 100$$

where *SL* is the peak area of the diTMS-ester of L-lactic acid; and *SD* is the peak area of the diTMS-ester of D-lactic acid.

Screening L-LDH genes. The structural genes of L-lactate dehydrogenase were detected using the real-time polymerase chain reaction method (PCR). Degenerate primers for genetic screening were selected based on the sequences typical of *Bacillaceae*, in particular *Bacillus coagulans* and *Bacillus subtilis*: 5'-CGGSCTGCCGAAAGAAC-3' (forward primer) and 5'-GCCGTGYTCGCCGATAAT-3' (reverse primer). The genomic DNA isolation involved a 24-h culture and a genomic DNA isolation kit (Dia-M, Russia). The PCR analysis was performed in a CFX96 Touch Deep Well Real-Time PCR Detection System (Bio-Rad Laboratories, USA).

The reaction mix had a volume of 25 μ L and included 5 μ L of 5x qPCRmix-HS SYBR reagent (Evrogen, Russia). In total the reaction mix contained *Taq* DNA Polymerase, dNTPs, buffer, $MgCl_2$ and SYBR Green I, 1 μ L of each primer with final concentration of 200 nM, 1 μ L of the culture lysate, and bidistilled water.

The PCR had the following temperature conditions: preliminary denaturation at 95°C for 3 min followed by 35 cycles of denaturation at 95°C for 15 s, annealing at 55°C for 15 s, and elongation at 72°C for within 25 s.

The PCR data analysis involved melting curves constructed when the samples were heated at 65–95°C at 0.5°C intervals.

Strain identification. The bacteria were identified by their morphological and biochemical features, as well as by molecular genetic analyses of the 16S rRNA gene nucleotide sequence. The genomic DNA isolation involved a 24-h culture and a kit for isolating genomic DNA from bacterial cells.

The classical PCR was performed in a CFX96 Touch Deep Well Real-Time PCR Detection System with a Hot Start *Taq*-DNA polymerase PCR kit (Dia-M, Russia). The universal primers 8F (5'-AGAGTTTGATCCTGGCT-CAG-3') and 1492R (5'-TACGGYTACCTTGTTACGACT-T-3') were used at a final concentration of 240 nM to amplify the 16S rRNA gene region.

The process proceeded under the following conditions: pre-denaturation at 95°C for 5 min followed by 35 cycles of denaturation at 95°C for 30 s, annealing at 54°C for 30 s, elongation at 72°C for 90 s, and the final elongation at 72°C for 10 min.

The sequencing of the obtained PCR fragments of the 16S rRNA genes followed the Sanger method with preliminary purification (Evrogen, Russia). The sequencing involved the same universal primers as those used for amplification. The amplicons were sequenced in forward and reverse directions. The resulting nucleotide sequences were compared to the 16S rRNA gene sequences from the NCBI GenBank database using the BLAST search tool. The phylogenetic analysis relied on the neighbor-joining method in the MEGA software [19].

RESULTS AND DISCUSSION

Isolating the thermophilic strains and their metabolite profiling. We isolated and profiled 13 thermophilic bacterial strains using the enrichment culture method. The samples were obtained from soils of Moscow urban forests, summer gardens, and natural ecosystems of the Moscow Region. Seven strains deve-

loped calcium carbonate dissolution zones on agar media with glucose as a carbon source, which proved that they released organic acids. The isolated acid-forming strains were characterized by rod-shaped morphology. They were classified as aerotolerant anaerobes and facultative anaerobes. The chromatography of the thermophilic culture broth grown under microaerophilic conditions showed that the bacteria released lactic, acetic, and propionic acids (Table 1).

Figure 1 shows a typical chromatogram of T6.1 culture broth grown on a glucose medium under microaerophilic conditions. The bacteria proved able to perform homofermentative lactic acid fermentation.

Strains T1.1, T5.1, T6.1, and T7.1 converted glucose into lactic acid in large quantities with minimal by-product organic acids. The lactic acid yield and fermentation selectivity depended both on the strain and culture conditions.

Further research involved detection of extracellular enzymatic activities on agar media with respective substrates. Table 2 introduces the screening results for extracellular hydrolases in cultures.

Table 1 Glucose consumption and formation of organic acids by thermophilic bacterial strains

Strain	Dissolution of calcium carbonate	Glucose consumption, g/L	Lactic acid, g/L	Acetic acid, g/L	Propionic acid, g/L
T1.1	+	2.34	2.24	n.d.	n.d.
T1.2	+	1.05	2.13	n.d.	0.54
T1.3	+	4.40	2.36	n.d.	0.79
T2.1	+	2.62	2.17	n.d.	0.57
T2.2	n.d.	0.80	0.06	0.39	n.d.
T3.1	n.d.	6.00	2.18	n.d.	1.53
T3.2	n.d.	3.00	2.07	n.d.	0.61
T3.3	n.d.	3.01	1.85	n.d.	0.58
T4.1	n.d.	2.15	0.09	0.29	0.65
T4.2	n.d.	2.30	0.08	0.41	n.d.
T5.1	+	1.74	2.58	n.d.	0.37
T6.1	+	2.79	2.60	n.d.	0.37
T7.1	+	2.42	2.66	n.d.	n.d.

n.d. – not detected

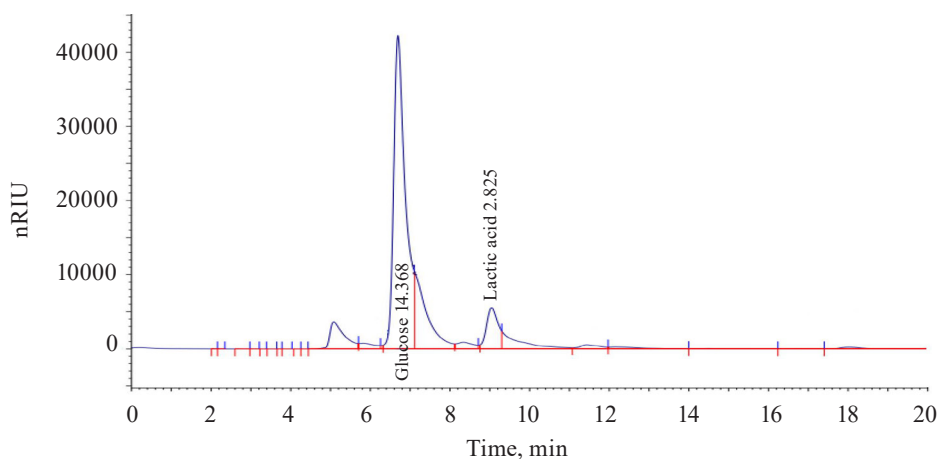
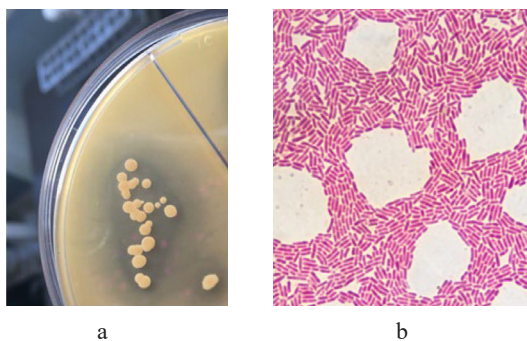


Figure 1 Thermophilic acid-forming strain T6.1 culture broth: chromatogram

Table 2. Extracellular hydrolases of thermophilic strains: enzymatic activity

Strain	Proteolytic activity	Amylase activity	Cellulase activity
T1.1	–	+	–
T1.2	–	–	+
T1.3	–	+	–
T2.1	–	–	–
T2.2	+++	+++	+++
T3.1	+	++	++
T3.2	+	++	++
T3.3	+	++	++
T4.1	++	++	++
T4.2	++	+++	+++
T5.1	–	–	–
T6.1	–	+	–
T7.1	–	+	–

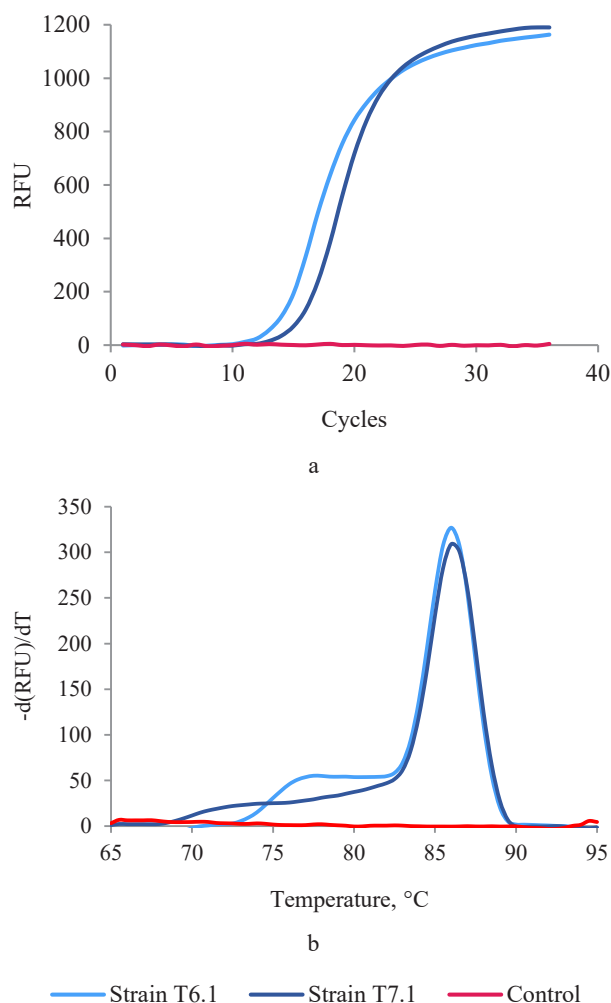
+++ – prominent enzymatic activity under the test conditions; ++ – positive enzymatic activity under the test conditions; + – enzymatic activity confirmed by the tests; and – – no enzymatic activity detected

**Figure 3** Colony growth on the medium with calcium carbonate (a) and cell morphology of strain T 7.1, 1000× (b)

The experiments demonstrated that six out of thirteen strains possessed proteolytic activity, ten strains showed amylase activity, and seven strains had cellulase activity. These results could be used to develop a new nutrient medium for synthesis of lactic acid, e.g., for acid-forming strains T3.1, T6.1, and T7.1. Starch-containing vegetable raw materials could serve as a potential source of carbon.

Genetic screening for LDH genes. Promising lactic acid producers T6.1 and T7.1 underwent genetic screening. According to their morphological and physiological characteristics, they were previously assigned to *Bacillaceae*. The PCR analysis detected the bacillary *L-ldh* gene in both strains. It is responsible for the synthesis of L-lactate (Fig. 2a). The melting curves showed that the fragments were homogeneous and contained no PCR by-products (Fig. 2b).

Thermophilic strains T6.1 and T7.1 were close to some representatives of the *Bacillus* genus and were found potentially capable of synthesizing the L-enantiomer of lactic acid. Genome of some *Bacillus* representatives, e.g., in particular *Bacillus coagulans*, contains

**Figure 2** Amplification curves of *L-ldh* gene fragments of thermophilic strains T6.1 and T7.1 (a) and melting curves of PCR products (b)

both structural genes. However, L-lactate-producing *B. coagulans* have a much more expressed *L-ldh* than *D-ldh* [20].

Profiling the promising thermophilic acid-forming strains. Strain T7.1 was as a spore-forming facultative anaerobe, resistant to slightly acidic pH. On agar, it developed white colonies with a diameter of 2–4 mm with a smooth surface. Strain T7.1 hydrolyzed starch but not casein. On the medium with calcium carbonate, it formed clean zones, which indicated the release of acids (Fig. 3a). The cell morphology was rod-shaped and typical for *Bacillaceae* (Fig. 3b).

For strain T7.1 identification, the 16S rRNA gene was amplified with standard bacterial primers, purified, and sequenced by the Sanger method.

The bioinformatic analysis of the nucleotide sequence included sequence alignment of reference bacterial 16S rRNA and a phylogenetic analysis.

The phylogenetic analysis relied on the 16S rRNA sequences deposited in the GenBank NCBI. The strains were selected with $\geq 92\%$ similarity of the gene. Strain T7.1 shared 99.86% with *Weizmannia coagulans*

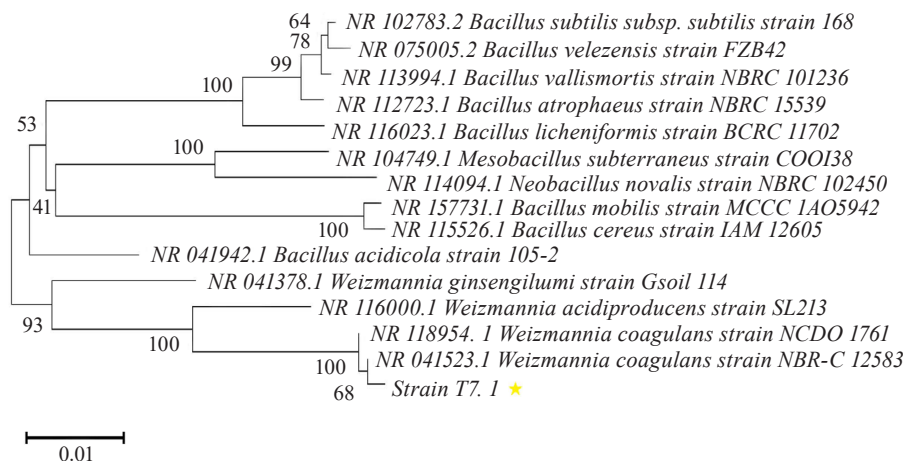


Figure 4 Phylogenetic tree constructed by the neighbor-joining method: nucleotide sequences of 16S rRNA for thermophilic strain T7.1 and reference *Bacillaceae*

NBRC 12583, which was the maximal similarity achieved for this gene (Fig. 4).

Thus, strain T7.1 was identified as *W. coagulans*. The result correlated with the morphological, physiological, and biochemical characteristics of the test culture.

Simple batch cultivation of strain T7.1 on the medium with high initial glucose content. Strain T7.1 was chosen for further studies of lactic acid synthesis by thermophilic bacteria. It underwent batch fermentation for 70 h. Figure 5 illustrates the main results of the fermentation: culture growth, consumption, and lactic acid synthesis.

Thermophilic strain T7.1 utilized 86 out of 95 g/L glucose to form 81 g/L of lactic acid with a peak productivity at 1.58 g/(L·h). The substrate conversion exceeded 90% while the yield of lactate was 94%. The chromatography showed no by-product organic acids at the end of cultivation (Fig. 6).

The fermentation data indicated that the sugars in the medium were metabolized by homofermentative lactic acid fermentation. Both in lactic acid and glucose conversion, the maximal productivity was observed at a residual glucose concentration of ≈ 50 g/L and lactate accumulation ≤ 45 g/L in the medium. The process occurred when the culture entered the stationary phase. The subsequent productivity decreased because the final product inhibited it. Further research is required to explain the effect of the medium composition and cultivation physicochemical parameters on the lactic acid synthesis.

Fed-batch cultivation and continuous fermentation, e.g., membrane bioreactors, could remove the inhibitory effect of metabolites and maintain cells in the required physiological state [23]. This engineering and technological approach is known to boost the efficiency of mesophilic cultures in lactic acid production. Logically, isolated thermophilic cultures should also demonstrate high process performance, especially because strain T7.1 produced exclusively lactic acid under the conditions of batch fermentation. In addition, T7.1 was thermophilic

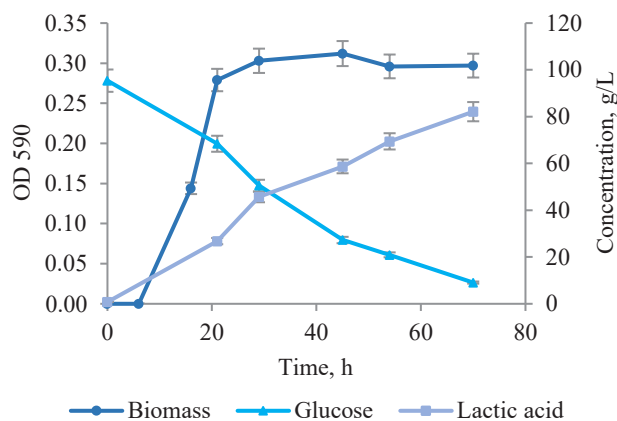


Figure 5 Growth curve, glucose consumption, and lactic acid synthesis by thermophilic strain T7.1 during cultivation in the Minifors bioreactor

and had much lower requirements for the growth factor content in the medium, compared to *Lactobacilli*.

Lactic acid optical purity analysis. Lactic acid intended for the food industry or polylactide synthesis requires excellent optical purity. As a result, the next step was to determine the content of L- and D-isomers formed during fermentation.

We used the method of gas chromatography of volatile acid derivatives using an optically active column to identify and analyze the optical isomers of lactic acid in the fermentation products. We tested the method on standard samples of L-lactic acid and a racemic mix of D,L-lactic acid obtained by mesolactide hydrolysis. Table 3 and Fig. 7 illustrate the separation of optical isomers of lactic acid. The chromatogram shows separate yields of D-lactic acid (peak 1 at 57.393 min) and L-lactic acid (peak 2 at 57.640 min).

Table 4 and Fig. 8 represent the chromatographic data for the sample of the culture broth obtained during the fermentation of the thermophilic strain T7.1. The D-lactate peak was hardly visible.

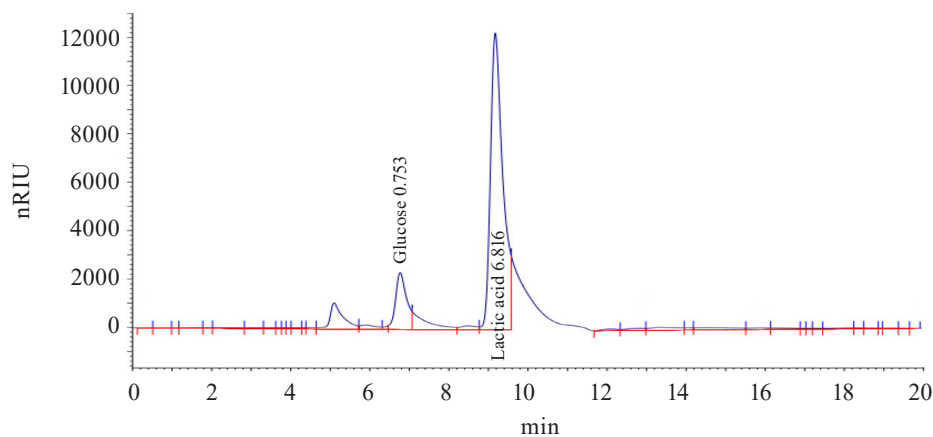


Figure 6 T.7.1 culture broth after 70 h of cultivation, diluted by 12.05 times: chromatogram

Table 3 Chromatographic separation of mesolactide hydrolysis products

Time, min	Component	Area	Area, %
57.393	D-lactic acid_diTMS	33.771	42.729
57.640	L-lactic acid_diTMS	45.264	57.271

Table 4 Optical purity of L-lactate produced by strain T.7.1

Time, min	Component	Area	Area, %
57.340	L-lactic acid_diTMS	0.039	0.028
57.659	D-lactic acid_diTMS	139.586	99.972

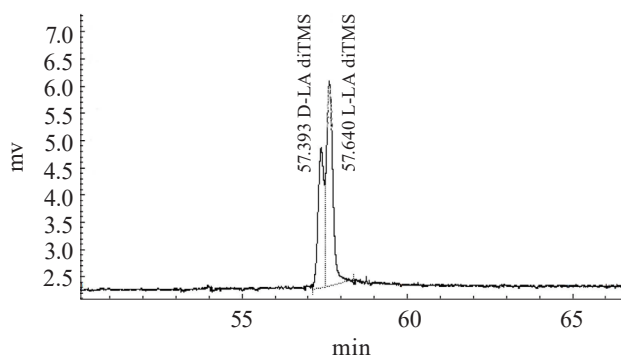


Figure 7 Separation of D- and L-isomers of lactic acid: chromatogram

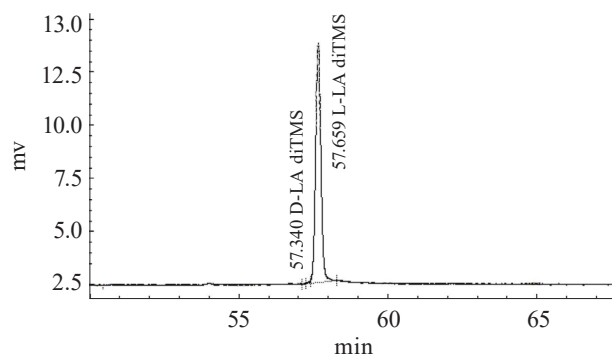


Figure 8 Separation of lactate isomers synthesized by thermophilic strain T.7.1: chromatogram

The optical purity of lactate produced by strain T.7.1 during fermentation at a high content of glucose in the medium correlated with other studies of *B. coagulans*. For example, Zhou *et al.* fermented *B. coagulans* WCP10-4 with glucose (source of carbon) and yeast extract (source of nitrogen) [24]. The optical purity of the obtained lactic acid was 99.8%, and the total concentration of by-product organic acids was below 1 g/L. Other publications [25, 26] explained the high optical purity of the obtained L-lactate by the absence of the lactate racemase gene in *B. coagulans* and related species. Further research on the development of a new technology for high optical purity lactic acid production will test various carbon sources, including plant hydrolysates, and analyze their effect on the optical purity.

CONCLUSION

The research resulted in a highly effective thermophilic acid-forming strain. Strain T.7.1, which possesses the bacillary L-lactate dehydrogenase gene, pro-

ved able to ferment homofermentative lactic acid. The molecular genetic analysis identified this strain as *Weizmannia coagulans* (*Bacillus coagulans*). The process of batch fermentation provided L-lactate of high optical purity ($\geq 99.9\%$) with a yield of 94% glucose. Therefore, strain T.7.1 is a promising thermophilic producer of lactic acid. It could be part of a highly efficient process for obtaining optically pure L-lactic acid in a membrane bioreactor. Lactic acid is intended for the food and chemical industries, namely for polylactide synthesis, biodegradable materials and green packaging producing, etc.

CONTRIBUTION

M.V. Romanova, N.Yu. Khromova, and A.V. Beloded developed the research concept. N.Yu. Khromova and A.V. Beloded were responsible for data curation, wrote the review and proofread the manuscript. N.Yu. Khromova, Yu.M. Epishkina, A.V. Beloded, and A.Ye. Kuznetsov performed the formal analy-

sis. M.V. Romanova, A.N. Dolbunova, A.Ye. Kuznetsov, M.R. Kozlovskiy and S.A. Evdokimova conducted the laboratory research. M.V. Romanova worked with the software, provided infographics, wrote the original draft. N.Yu. Khromova provided research funds, supervised the project, responsible for the validation of the results. A.V. Beloded developed the methodology. All the au-

thors discussed the results and contributed to the final manuscript. All the authors read and agreed to the published version of the manuscript.

CONFLICT OF INTEREST









The authors declare that there is no conflict of interests regarding the publication of this article.

REFERENCES

1. Lactic acid market key players, sales, demand, business strategy and forecast 2030 [Internet]. [cited 2023 Mar 6]. Available from: <https://www.digitaljournal.com/pr/lactic-acid-market-key-players-sales-demand-business-strategy-and-forecast-2030#ixzz7uLkASYIk>
2. Lactic acid market – Global industry analysis, size, share, growth, trends, regional outlook, and forecast 2022–2030 [Internet]. [cited 2023 Mar 6]. Available from: <https://www.precedenceresearch.com/lactic-acid-market>
3. Krasnova IS, Ganina VI, Semenov GV. Fruit and vegetable purees as cryoprotectants for vacuum freeze-dried fermented milk products. *Foods and Raw Materials*. 2023;11(2):300–308. <https://doi.org/10.21603/2308-4057-2023-2-578>
4. Panseri S, Martino PA, Cagnardi P, Celano G, Tedesco D, Castrica M, et al. Feasibility of biodegradable based packaging used for red meat storage during shelf-life: A pilot study. *Food Chemistry*. 2018;249:22–29. <https://doi.org/10.1016/j.foodchem.2017.12.067>
5. Kryuk RV, Kurbanova MG, Kolbina AYu, Plotnikov KB, Plotnikov IB, Petrov AN, et al. Color sensors in smart food packaging. *Food Processing: Techniques and Technology*. 2022;52(2):321–333. (In Russ.). <https://doi.org/10.21603/2074-9414-2022-2-2366>
6. Ncube LK, Ude AU, Ogunmuyiwa EN, Zulkifli R, Beas IN. Environmental impact of food packaging materials: A review of contemporary development from conventional plastics to polylactic acid based materials. *Materials*. 2020;13(21). <https://doi.org/10.3390/ma13214994>
7. Singha S, Hedenqvist MS. A review on barrier properties of poly(lactic acid)/clay nanocomposites. *Polymers*. 2020;12(5). <https://doi.org/10.3390/polym12051095>
8. Farah S, Anderson DG, Langer R. Physical and mechanical properties of PLA, and their functions in widespread applications – A comprehensive review. *Advanced Drug Delivery Reviews*. 2016;107:367–392. <https://doi.org/10.1016/j.addr.2016.06.012>
9. Aulitto M, Fusco S, Bartolucci S, Franzén CJ, Contursi P. *Bacillus coagulans* MA-13: a promising thermophilic and cellulolytic strain for the production of lactic acid from lignocellulosic hydrolysate. *Biotechnology for Biofuels and Bioproducts*. 2017;10. <https://doi.org/10.1186/s13068-017-0896-8>
10. Alexandri M, Blanco-Catalá J, Schneider R, Turon X, Venus J. High L(+)-lactic acid productivity in continuous fermentations using bakery waste and lucerne green juice as renewable substrates. *Bioresource Technology*. 2020;316. <https://doi.org/10.1016/j.biortech.2020.123949>
11. Hu J, Lin Y, Zhang Z, Xiang T, Mei Y, Zhao S, et al. High-titer lactic acid production by *Lactobacillus pentosus* FL0421 from corn stover using fed-batch simultaneous saccharification and fermentation. *Bioresource Technology*. 2016;214:74–80. <https://doi.org/10.1016/j.biortech.2016.04.034>
12. Kilcawley K, O’Sullivan M. Cheese flavour development and sensory characteristics. In: Papademas P, Bintsis T, editors. *Global cheesemaking technology: Cheese quality and characteristics*. Wiley; 2017. pp. 45–70. <https://doi.org/10.1002/9781119046165.ch0c>
13. Poudel P, Tashiro Y, Sakai K. New application of *Bacillus* strains for optically pure L-lactic acid production: general overview and future prospects. *Bioscience, Biotechnology, and Biochemistry*. 2016;80(4):642–654. <https://doi.org/10.1080/09168451.2015.1095069>
14. Urbietta MS, Donati ER, Chan K-G, Shahar S, Sin LL, Goh KM. Thermophiles in the genomic era: Biodiversity, science, and applications. *Biotechnology Advances*. 2015;33(6):633–647. <https://doi.org/10.1016/j.biotechadv.2015.04.007>
15. Blumer-Schuette SE, Brown SD, Sander KB, Bayer EA, Kataeva I, Zurawski JV, et al. Thermophilic lignocellulose deconstruction. *FEMS Microbiology Reviews*. 2014;38(3):393–448. <https://doi.org/10.1111/1574-6976.12044>
16. Wang Y, Cao W, Luo J, Wan Y. Exploring the potential of lactic acid production from lignocellulosic hydrolysates with various ratios of hexose versus pentose by *Bacillus coagulans* IPE22. *Bioresource Technology*. 2018;261:342–349. <https://doi.org/10.1016/j.biortech.2018.03.135>
17. Bischoff KM, Liu S, Hughes SR, Rich JO. Fermentation of corn fiber hydrolysate to lactic acid by the moderate thermophile *Bacillus coagulans*. *Biotechnology Letters*. 2010;32:823–828. <https://doi.org/10.1007/s10529-010-0222-z>

18. Fan R, Ebrahimi M, Czermak P. Anaerobic membrane bioreactor for continuous lactic acid fermentation. *Membranes*. 2017;7(2). <https://doi.org/10.3390/membranes7020026>
19. Ma K, Hu G, Pan L, Wang Z, Zhou Y, Wang Y, et al. Highly efficient production of optically pure l-lactic acid from corn stover hydrolysate by thermophilic *Bacillus coagulans*. *Bioresource Technology*. 2016;219:114–122. <https://doi.org/10.1016/j.biortech.2016.07.100>
20. Thebti W, Riahi Y, Gharsalli R, Belhadj O. Screening and characterization of thermo-active enzymes of biotechnological interest produced by thermophilic *Bacillus* isolated from hot springs in Tunisia. *Acta Biochimica Polonica*. 2016;63(3):581–587. https://doi.org/10.18388/abp.2016_1271
21. Tamura K, Stecher G, Kumar S. MEGA11: Molecular evolutionary genetics analysis version 11. *Molecular Biology and Evolution*. 2021;38(7):3022–3027. <https://doi.org/10.1093/molbev/msab120>
22. Sun L, Zhang C, Lyu P, Wang Y, Wang L, Yu B. Contributory roles of two l-lactate dehydrogenases for l-lactic acid production in thermotolerant *Bacillus coagulans*. *Scientific Report*. 2016;6. <https://doi.org/10.1038/srep37916>
23. Kuznetsov A, Beloded A, Derunets A, Grosheva V, Vakar L, Kozlovskiy R, et al. Biosynthesis of lactic acid in a membrane bioreactor for cleaner technology of polylactide production. *Clean Technologies and Environmental Policy*. 2017;19:869–882. <https://doi.org/10.1007/s10098-016-1275-z>
24. Zhou X, Ye L, Wu JC. Efficient production of L-lactic acid by newly isolated thermophilic *Bacillus coagulans* WCP10-4 with high glucose tolerance. *Applied Microbiology and Biotechnology*. 2013;97:4309–4314. <https://doi.org/10.1007/s00253-013-4710-7>
25. Wang L, Cai Y, Zhu L, Guo H, Yu B. Major role of NAD-dependent lactate dehydrogenases in the production of l-lactic acid with high optical purity by the thermophile *Bacillus coagulans*. *Applied and Environmental Microbiology*. 2014;80(23). <https://doi.org/10.1128/AEM.01864-14>
26. Bosma EF, van de Weijer AHP, van der Vlist L, de Vos WM, van der Oost J, van Kranenburg R. Establishment of markerless gene deletion tools in thermophilic *Bacillus smithii* and construction of multiple mutant strains. *Microbial Cell Factories*. 2015;14. <https://doi.org/10.1186/s12934-015-0286-5>

ORCID IDs

Mariia V. Romanova  <https://orcid.org/0000-0003-3109-8445>
Anastasiia N. Dolbunova  <https://orcid.org/0009-0003-7884-3198>
Yulia M. Epishkina  <https://orcid.org/0000-0002-7776-2922>
Svetlana A. Evdokimova  <https://orcid.org/0000-0002-4808-5002>
Mikhail R. Kozlovskiy  <https://orcid.org/0000-0003-0774-2886>
Alexander Ye. Kuznetsov  <https://orcid.org/0000-0003-2574-2118>
Natalya Yu. Khromova  <https://orcid.org/0000-0001-9852-9401>
Andrey V. Beloded  <https://orcid.org/0000-0002-4425-8068>



Nutritional significance of finger millet and its potential for using in functional products

Vaibhav Gaikwad¹, Jaspreet Kaur¹, Prasad Rasane^{1,*}, Sawinder Kaur¹,
Jyoti Singh¹, Ankit Kumar², Ashwani Kumar³, Nitya Sharma⁴,
Chandra Mohan Mehta¹, Avinash Singh Patel⁵

¹ Lovely Professional University^{ROR}, Phagwara, India

² Baba Farid Group of Institution, Bhatinda, India

³ Rani Lakshmi Bai Central Agricultural University, Jhansi, India

⁴ Indian Institute of Technology Delhi^{ROR}, New Delhi, India

⁵ North Carolina State University^{ROR}, Raleigh, United States

* e-mail: rasaneprasad@gmail.com

Received 11.01.2023; Revised 06.02.2023; Accepted 07.03.2023; Published online 30.08.2023

Abstract:

Finger millet (*Eleusine coracana* L.), ragi or mandua, is one of essential minor millets extensively grown in the Indian and African subcontinents. It is a staple food in India, particularly for people belonging to low-socioeconomic groups. Finger millet is highly valued for its content of macro- and micronutrients. It is rich in carbohydrates, protein, and fat. Its micronutrients include calcium (0.38%), dietary fiber (18%), and phenolic compounds (0.3–3%), such as catechin, epicatechin, as well as ferulic, salicylic, protocatechuic, cinnamic, and hydroxybenzoic acids, etc. Finger millet is also recognized as a source of vital amino acids, including isoleucine, leucine, methionine, and phenylalanine, which are otherwise deficient in starchy meals. In addition, finger millet is well appreciated for its pharmacological properties such as anti-diabetic, anti-tumorigenic, anti-atherosclerogenic, antioxidant, and antimicrobial effects. To improve its nutritional and sensory properties, this grain can be processed by various traditional and advanced methods (soaking, malting, cooking, fermentation, popping, and radiation). These processing techniques equally assist in the reduction of anti-nutritional factors (tannins, phytic acid, oxalic acid, protein inhibitors, glucans) and their inhibitory effects. In this review, we highlighted the nutritional composition, health attributes, and uses of finger millet for the development of functional food products.

Researchers and producers can further explore the opportunities and scope for utilizing finger millet and develop more products in the same line to solve the current issues of food and nutrition security.

Keywords: Finger millet, cultivation, nutritional composition, health benefits, processing, fortification

Please cite this article in press as: Gaikwad V, Kaur J, Rasane P, Kaur S, Singh J, Kumar A, *et al.* Nutritional significance of finger millet and its potential for using in functional products. *Foods and Raw Materials*. 2024;12(1):110–123. <https://doi.org/10.21603/2308-4057-2024-1-593>

INTRODUCTION

Millet is a minor cereal belonging to the *Poaceae* grass family that is well known in India as ragi or mandua [1]. Cultivated in arid and sub-arid regions, it is considered a poor people's food [2, 3]. Since time immemorial, millets have been a well-known food for humans but in recent years they have been replaced by wheat and rice [4]. Globally, annual millet production amounts to 30.73 million tons, including 11.42 million tones (37% of the global yield) in India alone. India and Africa are the leading producers of finger millet,

followed by Uganda, Nepal, and China [4]. India is one of the largest cultivators of millets, especially finger millet (*Eleusine coracana* L.), which accounts for about 85% of all minor millets [5]. Karnataka is the leading state that cultivates 58% of total finger millet production in India [6].

Finger millet is well recognized for its high nutritional profile, including protein (6–13%), calcium (0.34%), dietary fiber (18%), phenolic compounds (0.3–3%), and minerals (2.5–3.5%). In addition, it is a good source of a vitamin B complex (thiamine and riboflavin), as well

as essential amino acids (methionine, isoleucine, leucine, phenylalanine, etc.) [1, 7–10]. Finger millet contains 30 times as much calcium as rice, namely 344 mg/100 g, which plays a positive role in bone development and maintenance, as well as in the functioning of nerves and muscles [4, 11, 12]. According to studies, finger millet possesses various medicinal and nutritional properties. It is well known for its biological properties (anti-tumorigenic, anti-atherosclerogenic, anti-diabetic, antioxidant, and antimicrobial) mainly due to polyphenols and dietary fiber [13, 14]. Also, finger millet prevents oxidation of low-density lipoproteins, hypertension, hypercholesterolemia, and diabetes mellitus, as well as improves gastrointestinal tract functioning and vascular fragility [8, 15]. Being an aboriginal crop, minor millet is utilized in formulations of geriatric and weaning foods, as well as health foods both in natural and malted forms [16]. Malted finger millet flour can be used to prepare bread, papad, chips, chapatti, bakery products, porridge, chakli, idli, biscuits, cookies, and beer, as well as gruel for new-born babies [17, 18]. Our review highlights various aspects of finger millet, including its nutritional composition, various effects of processing, as well as its utilization for the development of functional products.

STUDY OBJECTS AND METHODS

For this review, we searched for publications in Google Scholar, ResearchGate, ScienceDirect, and PubMed. Synonyms and alternative words were identified and used to obtain current literature in English. Our major search terms and key words were “millets”, “millet phytochemicals”, “major bioactive compounds in finger millets”, “health benefits of millets bioactive compounds”, “finger millet processing”, and “finger millet products”. Most of the research articles mentioned in the manuscript are recent and published between 2012–2019.

RESULTS AND DISCUSSION

Cultivation of finger millet. In Nepal and India, finger millet is grown on 274 350 hectares of land, yielding 305 588 million tons with an average productivity of 1115 kg/ha, as a kharif and rain-fed crop on marginal lands and in hilly regions. Finger millet is primarily farmed in Africa, widely in Uganda, Kenya, and Tanzania, as well as in Ethiopia, Eritrea, Mozambique, Rwanda, Malawi, Sudan, Namibia, Senegal, Niger, Nigeria, Madagascar, Zambia, Zimbabwe (to a minimal degree), and India [19]. India, as a leading producer, cultivates 1.98 million tons of finger millet on 1.19 million hectares of land, with a productivity of 1661 kg/ha [20].

In Asia, the major cultivators are India, Nepal, Malaysia, China, Japan, Iran, Afghanistan, and Sri Lanka [21, 22]. In the eastern, central, and western parts of India (Uttar Pradesh, Bihar, Tamil Nadu, Karnataka, and Andhra Pradesh), this crop is cycled along with maize in a mixed cropping system. In the mid and far western regions, however, it is monocultured [23].

Finger millet is highly tolerant to biotic and abiotic stimuli and is highly adaptable to the local climate. It can adapt to harsh weather conditions, requiring minimum inputs, and has higher nutritional characteristics when grown in desert environments [24, 25]. Scientific emphasis has been placed on the crop's capacity to grow in warm altitudes, on soils with minimal moisture and low fertility [26]. Finger millet is a short plant that needs a minimum day duration of around 12 h and flourishes at higher elevations, where other major grains fail to survive. It can grow between 500 and 2400 m above sea level. On average, it demands 500 mm of yearly rainfall, but it can also withstand 300–4000 mm of precipitation. The crop performs best in the tropical regions of India and Africa, where the average maximum temperature approaches 27°C and the average minimum temperature does not drop below 18°C. Dry weather encourages the harvest of healthy grains at maturity, whereas rainy weather causes grain blackening. Finger millet prefers climates where the average temperature ranges from 11 to 28°C, although it can also tolerate higher temperatures [20]. The crop is grown from sea level to higher elevations in the Himalayas, up to 2400 m above sea level [27].

Finger millet is a desirable crop in an intensive cropping system since it requires less time to grow and can be farmed in all seasons. The seeds have a long lifespan (more than five years) and are resistant to storage pests, which makes them an excellent reserve for food security crisis periods [28]. Finger millet grows well in a wide range of soils, including red lateritic soil, mixed grey soil, and unaltered soils with coarse parent materials. In the tropics, it is typically grown in reddish-brown lateritic soils which require proper drainage [29]. However, the crop is more prevalent in sandy loam textured soils where it receives evenly distributed rainfall.

Finger millet is a drought-resistant and weather-tolerable crop due to its efficient C4 photosynthetic pathway [28, 30, 31]. It is cultivated in abundance in the Koraput district of Odisha, accounting for 16% of the total gross cropped area and 28% of the total area under cereal crop cultivation. In Koraput, it thrives in temperatures ranging from 14 to 40°C, with an annual average rainfall of 1320–1520 mm. In this district, tribal groups mostly farm local finger millet land races, such as telugu mandia, dasara mandia, san mandia, and bada mandia by adopting traditional agronomic ways. Finger millet can also resist slight moisture stress, though too much dampness or stagnant water would limit its growth and yield potential. It also declines the growth of weeds and resists numerous diseases [32]. In addition, finger millet appears to be more capable of using rock phosphate than other grains [33].

Nutritional composition of finger millet. Finger millet is well known for its high contents of calcium, dietary fiber, and phenolic compounds [8]. It is also a good source of carbohydrates, proteins, vitamins, and iron [34]. Chandra *et al.* compared the nutritional composition of finger millet, wheat, maize, sorghum, and

rice [1]. They found that finger millet was superior to the other cereals with respect to dietary fiber, calcium, and some micronutrients. The husk of finger millet is a rich source of phenolic compounds, minerals, and dietary fiber [35]. The nutritional profile of finger millet is presented in Table 1.

Carbohydrates. The total carbohydrate content of finger millet has been reported to be in the range of 72–79.5%, consisting of free sugars (1.04%), starch (65.5%), and non-starchy polysaccharides or dietary fiber (11.5%) [40]. The dietary fiber content is much higher in finger millet (11.5%) than in brown rice, polished rice, and all other millets, namely foxtail, little, kodo, and barnyard millet. The carbohydrate content of finger millet is comparable to that of wheat but lower than that of polished rice. However, the starch content of finger millet is lower in amylose (16%) than that of the other millets. Also, finger millet starch has the highest set back viscosity (560 BU) followed by cooling which further favors retrogradation [3].

Protein. According to Ambre *et al.*, the protein content of finger millet depends on its varieties and ranges

from 5 to 12% [16]. Swami *et al.* had malted finger millet for 8, 12, 16, 20, and 24 h and reported that longer germination times led to higher protein contents (14–17.5%) [41]. By induced hydrolytic activity, the germination of finger millet seeds increased the nutritional value [42]. Finger millet is a rich source of amino acids, including methionine (3.1 g), isoleucine (4.4 g), leucine (9.5 g), and phenylalanine (5.2 g) [43]. Of all amino acids present in finger millet, 44.7% are essential, such as methionine and tryptophan. Their content is higher than the required 33.9% of essential amino acids in the FAO's reference protein [16].

Finger millet is mainly valued for its content of methionine, which is lacking in the diets of millions of poor people who mainly depend on starchy staples along with cassava, plantain, polished rice, or maize meals [44]. Finger millet's protein composition looks comparatively well-balanced because it has more lysine, threonine, and valine than other millet grains.

Minerals. Among all cereals and millets, finger millet comprises the highest calcium and potassium amounts of 344 and 408 mg, respectively [3]. Singh and Raghuvanshi reported a huge variation in the mineral content of finger millet, depending mainly on genetic factors and environmental conditions [45]. Yet, the importance of minerals in human nutrition cannot be overestimated [11].

Lipids. Kumar *et al.* reported that the lipid content in millets is comparable to that of wheat and rice (2.0 and 2.7%, respectively) and ranges from 1.43 to 6.0 g/100 g [38]. Finger millet lipids carry 70–72% of neutral lipids (primarily triglycerides and traces of sterols), 10–12% of glycolipids, 5–6% of phospholipids, 46–62% of oleic acid, 8–27% of linoleic acid, 20–35% of palmitic acid, and traces of linolenic acid. Finger millet has the lowest lipid content among all varieties. This could be one of the major factors contributing to its long-life properties, compared to other varieties [3].

Vitamins. Micronutrients present in finger millet, including vitamins, are required for the typical development and self-maintenance of human body. Vitamins are divided into two major groups, fat-soluble and water-soluble [13]. Most of the probiotic food consists of fatty acids, vitamins, and other vital nutrients that enhance the body's resistance against pathogenic microorganisms [2]. Thapliyal and Singh stated that the fermentation of finger millet enhances the concentration of vitamins, including riboflavin (0.60 mg/100 g), pantothenic acid (1.6 mg/100 g), and niacin (4.2 mg/100 g) [8].

Anti-nutrients. Being a good source of vital nutrients, finger millet also comprises several antinutritional factors that significantly affect its nutritional value. They lead to poor digestion of proteins and a low bioavailability of carbohydrates and minerals such as calcium, iron and, copper. Major antinutritional factors present in finger millet include tannins, polyphenols, flavonoids, HCN, phytates, oxalic acid, digestive enzyme inhibitors (amylase inhibitor function, trypsin inhibitory activity), and goitrogens [40, 46].

Table 1 Nutritional components of finger millet

Constituents	Amount	References
Moisture, g/100 g	7.15–13.1	[36]
Carbohydrate, g/100 g	72.6–83.3	[8, 36]
Protein, g/100 g	6.0–8.2	[24, 37]
Lipid, g/100 g	1.8–3.5	[36, 38]
Dietary fiber, g/100 g	15.0–22.0	[24, 36]
Minerals, mg/100 g:		
Calcium	220–398	[7, 24, 36, 39]
Phosphorous	130–250	
Sodium	49	
Potassium	430–490	
Magnesium	78–201	
Iron	3.30–14.89	
Manganese	17.61–48.43	
Zinc	2.3	
Vitamins, mg/100 g:		
Retinol	6.0	[3, 24, 36]
Thiamine	0.20–0.48	
Riboflavin	0.12–0.19	
Niacin	1.00–1.30	
Ascorbic acid	1.0	
Amino acids, g/100 g:		
Isoleucine	4.4	[7, 24, 36, 37]
Leucine	6.6–9.5	
Methionine	2.5–3.1	
Phenylalanine	4.1–5.2	
Valine	4.9–6.6	
Threonine	3.4–4.2	
Lysine	2.2	
Tryptophan	1.1–1.5	
Fatty acids, %:		
Oleic acid	49	[14]
Linoleic acid	25	
Palmitic acid	25	

Phytates and tannins are two major anti-nutrients that reduce the bioavailability of vital nutrients, which can be eliminated by employing food processing methods such as fermentation and germination. Kumari *et al.* reported that non-processed brown finger millet had a higher radical quenching activity than the processed one and postulated that tannins and phytic acid were responsible for the activity [12, 47]. The seed coat of finger millet contains quite a few phytochemicals which might also have health benefits [3]. The brown variety of finger millet was found to exhibit the highest level of phenolic compounds, compared to other varieties [3].

Health benefits of finger millet. Finger millet is well known for its health-beneficial properties, such as hypoglycemic effects, as well as antioxidant and antimicrobial activities [48]. Kumari *et al.* reported that the non-processed brown finger millet had a higher radical quenching activity than the processed one due to tannins and phytic acid [12, 47]. Apart from that, finger millets exhibit several health-beneficial effects. In particular, they lower glucose and cholesterol levels and have neuro-protective, antioxidant, wound-healing, and anti-cataractogenesis properties [35]. Tatala *et al.* reported an improved status of hemoglobin in children who were given finger millet-based food [49]. As it is a gluten-free grain, it is highly beneficial for those who are suffering from celiac disease [43]. Lee *et al.* found that finger millet may prevent the risk of cardiovascular diseases by reducing the plasma triglycerides levels in hyperlipidemic rats [50].

Effects of processing on finger millet. Finger millet is pulverized in order to prepare food products, such as roti, kazhi, and kanji with health-promoting proper-

ties [3]. Table 2 illustrates the effects of different processing methods on the functional and nutritional qualities of finger millet. Figure 1 represents various processing methods for developing functional products from finger millets. A brief account of processing methods and quality characteristics is given below.

Soaking. Soaking is a process where finger millet grains are steeped in distilled water overnight at a room temperature of about 30–60°C, followed by the discarding of the water and cleaning of finger millet grains thoroughly by using clean water to remove unwanted particles. Afterwards, they are dried and then milled at 60°C for 90 min to reduce the moisture content [42, 59]. During the soaking, the water needs to be changed once or twice in order to prevent the excessive growth of microorganisms [51]. Rajasekhar *et al.* reported that after soaking, finger millet had an increase in true density, porosity, hardness and angle of repose, as well as a decrease in longitudinal and lateral diameter, sphericity, surface area, 1000 kernel weight, bulk density, color (L^* , a^* , b^*), and terminal velocity [60]. Ocheme and Chinma observed a slight increase in protein, ash, dry matter, water absorption capacity, hygroscopicity, and swelling ability of millet flour resulting from soaking and germination, as well as a decrease in fat, phytic acid, gelation capacity, and viscosity [61].

Milling or grinding. Generally, finger millet is pulverized to obtain flour for food products. Firstly, finger millet is cleaned to remove foreign particles, such as stalks, stones, chaffs, etc. Then, it is passed through abrasive or friction mills to remove the non-edible cellulose tissue. Sometimes, decortication or pearling are also used to dehusk the finger millet grain [14]. During the milling process, grains undergo different operations

Table 2 Effects of processing on finger millet

Processing	Effects	References
Soaking	Enhances the bioavailability of minerals, improves digestibility, nutritional value and sensory attributes	[51, 52]
Milling or grinding	Influences the yield by separating out glumes (non-edible cellulosic tissue) Leads to the loss of fiber and phytochemicals when grain is milled to obtain flour	[1] [46]
Popping or puffing	Improves the nutritional value by inactivating some of the anti-nutritional factors Enhances aroma (due to the Maillard reaction), color, taste, and appearance of processed raw materials	[13, 51]
Malting	Improves digestibility, lowers down anti-nutrients, and enhances nutritional value	[53]
Cooking	Enhances soluble phenolic acids and inactivates heat-labile anti-nutritional factors Makes food more palatable, safe, and suitable for consumption	[54, 55]
Fermentation	Reduces anti-nutritional factors, leads to biochemical changes, decreases pH, and increase total sugar Helps preserve food products	[2, 51]
Drying	Increases protein content, digestibility, bioavailable micronutrients, desired moisture content, and color retention	[18]
Roasting	Increases the bio-availability of minerals like calcium and iron Increases the shelf life of food	[8, 9]
Decortication/Dehulling	Reduces polyphenolic pigments and phytate content Decreases the total mineral content but increases the bio-accessibility of calcium, iron, and zinc	[17, 56]
Extrusion	Modifies texture and other physical properties, gelatinization of starch and denaturation of protein, starch fragmentation	[57]

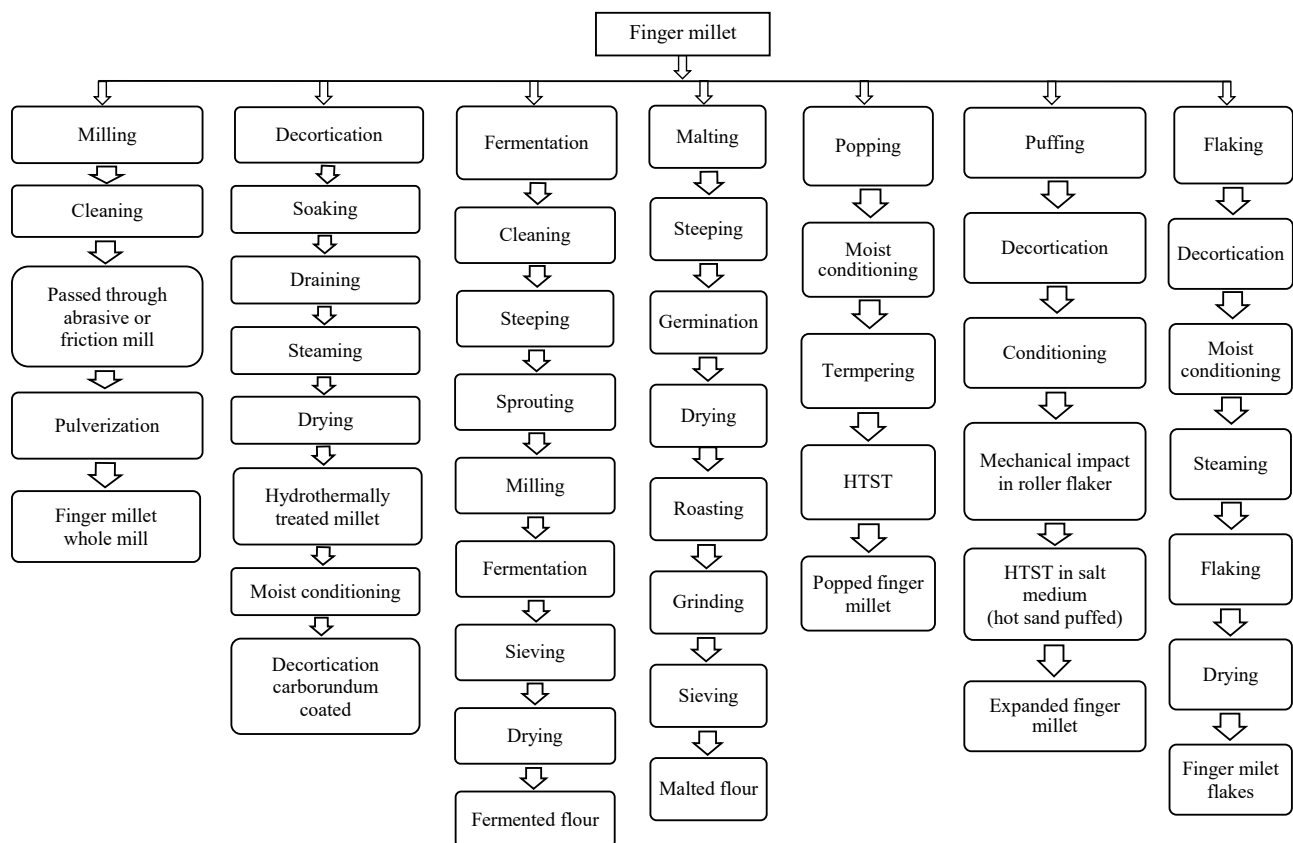


Figure 1 Processing techniques for finger millet products [3, 14, 58]

such as cleaning, sorting, hulling, branning, and kilning [62]. About 10% of water is added to help the removal of fibrous husk. Generally, milling is used to remove the fibrous bran or the seed coat of millet grains. During this process, some phytochemicals like tannins and phytates become lower, enhancing the bioavailability of iron [45]. Finger millet is usually milled by roller or hammer mills, while a centrifugal sheller can also be used to dehull/decorticate small millets. There is no uniformity in the size of particles when milling in a hammer mill, so it is not suitable for the preparation of stiff and thin porridge with rough texture. However, it can be used to prepare baked or smooth-textured foods [63].

Popping or puffing. Popping is a process where starch is gelatinized and expanded. For this, finger millet grains are kept at high temperature for a short time, which results in vapor production and expansion of endosperm [64]. This technique can also reduce anti-nutritional factors in finger millet. In addition, it is less expensive and easy to use [40]. Both popping and puffing are the oldest traditional methods of cooking grains. The popping of finger millet grains inactivates some antinutrients and enhances protein and carbohydrate digestibility (Table 2). Popped millets also have improved color, taste, appearance, and aroma. For puffing, extra water is added during the conditioning process to increase moisture up to the limit of 18–20%,

which is then kept for 4–6 h under normal temperature. After conditioning, the puffing process is carried out by agitation on a hot sand layer at about 230–250°C for a short time. A highly desired aroma develops in the millet due to the sugar present in the aleurone layer from the reaction with amino acids that causes the Maillard reaction. Modern air puffing machines can be the best solution for sand particles sticking to the product [51].

There are various types of popping and puffing methods, including sand and salt treatment, hot air popping, gun puffing, popping in hot oil, conventional method, and microwave heating [64]. A decrease in the calcium content and an increase in the iron content have been observed during the popping of finger millet, whereas the amount of anti-nutritional factors, such as trypsin inhibitor and oxalic acid, decreased gradually. Thus, popping of finger millet results in lowered anti-nutritional factors and increased nutritional content [65].

Malting. Shahidi and Chandrasekara reported changes in the composition of free and bound polyphenol contents in the malted finger millet [43]. Malting can gradually help lower anti-nutritional factors, as well as enhance the nutrient content [38, 53]. Sprouting of finger millets at 30°C for 48 h improves protein digestibility and reduces oxalate, phytic acid, and tannin contents by 45, 46, and 29%, respectively. Germination is a tradi-

tional process in which dehusked grains are steeped in distilled water for 2–24 h and then incubated at 30°C for 48 h [59].

In a study by Hithamani and Srinivasan, finger millet grains were soaked overnight in distilled water [66]. On the following day, the grains were removed from water and kept under normal temperature for 48 h, with water sprayed over them periodically. The germination process is stopped by drying the germinated grain in a hot-air oven. The drying time and temperature play an important role because they not only affect enzymatic activity but also help in developing the color and flavor of compounds [67]. Kumar *et al.* reported that malting enhanced the bio accessibility of iron and manganese in millet by 300 and 17%, respectively [38]. Malting increases the nutrient content by inducing hydrolytic activity. Banusha and Vasantharuba reported that malting gradually increased the reducing sugar and free amino acid contents [42].

Germination of finger millets, which has been used for hundreds of years, helps soften the kernel structure and enhance nutrient contents. It also increases the contents of vitamins, minerals, essential amino acids, and carbohydrates, thus enhancing the useful optical properties of the grains [68]. Malting of finger millet increases the vitamin C content, phosphorus availability, as well as synthesizes lysine and tryptophan [69].

Cooking. Cooking is a processing method which involves boiling of finger millet grains in water until their structure becomes soft. It is the most commonly used traditional method of food processing which aids in reducing anti-nutritional factors (e.g., tannin content by 30%) and also makes the food palatable [54]. Also, cooking decreases the microbial load and thus enhances the sensory properties of cooked grains [34]. Porridge can be prepared by mixing boiled water with flour [18]. Cooking was found to increase the resistant starch content in finger millet, as compared to other processes [3].

Fermentation. As reported by Ilango and Antony, the fermentation of finger millet led to the breakdown of long-chain fatty acids and starch molecules [70]. The pH value dropped by 2.1 units and the contents of lactic and acetic acids rapidly increased by 6.5 and 3.7%, respectively. Also, the total fat content reduced by 42.9%, which helped lower the phytic acid content by 72 and 54% in 96 and 72 h, respectively. Finger millet is a rich source of calcium as it is, but its contents of iron, manganese, and calcium can be further increased by fermentation [71].

Fermentation is more effective than malting in reducing phytic acid since it enhances the chemical and physiological accessibility of micronutrients in the body and reduces anti-nutritional factors such as phytates and tannins. The nutritional value of millet grains becomes higher due to an increase in the bioavailability of nutrients [71]. Fermentation is widely employed all over the world, as it significantly increases the shelf life of food products. Fermented products have more intense sensory characteristics such as aroma, taste, and

flavor [63]. It is the most effective and oldest method to increase the shelf life of products, i.e., food preservation [54].

Drying. In a study by Emmambux and Taylor, germinated finger millet was dried at temperature ranging between 40 and 70°C using a fluidized bed dryer [18]. This process increased the protein content, digestibility, and bioavailability of micronutrients. The flour made from dried sprouted finger millet can be utilized to prepare papad, noodles, bread, and several other Indian dishes, such as idli, chakli, and porridge. A decrease in the lightness of finger millet seeds was observed [15]. Finger millet can be dried by bed dryers, drum dryers, and in the sun. In sun drying, which is a traditional method, grains are generally spread and kept under sunlight for a specific period of time. After drying, the grains can be stored in bags for 5–10 years. These grains are highly effective in preventing disease, but they are very small and not easy to handle, which is a major obstacle [52, 72].

Roasting. Roasting of finger millet grains enhances the contents of carbohydrates and ash, increases the bio-availability of minerals (calcium and iron), and reduces moisture, fat, protein, phenols, and antioxidant activity [9]. Roopa and Premavalli reported an increase in resistant starch, which reduced in all the other processing methods [73]. Chandrasekara *et al.* revealed a decrease in the free radical quenching activity during the roasting process [74]. In another study, roasting caused higher total phenolics, protein, and amylose contents, as well as a lower moisture content [75]. The food products from roasted finger millet grains contained the highest amount of resistant starch (3.1%), compared to other products [3]. In India, sand roasting is quite a popular method, which is mainly performed by street vendors to prepare various types of food products [76].

Decortication or dehulling. Before consumption, finger millet grains undergo dehulling and debranning processes which remove large portions of husk and bran [36]. Centrifugal shellers can be used to dehull or decorticate small millets [63].

Extrusion. Extrusion involves the development of a food material using high pressure and mechanical shear [77]. A study by Kumar *et al.* reported a reduction in phytates and tannins during the extrusion cooking or HTST, as well as an increase in the bioavailability of minerals [38]. Another study revealed that the extruded products had high cold paste viscosity, but their cooked paste viscosity was significantly lower [78]. The extruded products exhibited a greater digestibility of protein, but there was no difference in the *in-vitro* carbohydrate digestibility [77].

Utilization of finger millet in functional products. Finger millet can be used in a variety of ways and it can be a great substitute for other starchy grains such as rice. Nowadays, finger millet is being popularized in India for its functional characteristics [79].

Bakery products. *Cookies.* Abioye *et al.* prepared cookies using blends of wheat flour, germinated finger

millet, and African yam bean [80]. The cookies were rich in nutrients and functional characteristics of the flour, but low in anti-nutritional factors. In another study, multigrain cookies were formulated with finger millet and sorghum in various proportions. The cookies containing 60% of fructo-oligosaccharides, 20% of finger millet, and 30% of sorghum showed good acceptability [81]. Sharma *et al.* evaluated the nutritional and sensory characteristics of finger millet-based cookies [82]. The samples with 30 and 50% of finger millet showed good acceptability and had a higher content of fiber and minerals, such as calcium, phosphorus, copper, and zinc. In another study, cookies were prepared from malted finger millet and wheat flour mixture (4:1) where jaggery melted in milk was introduced [83]. The cookies were baked at 170°C for 15 min.

Muffins. Two samples of muffins were prepared from: 1) plain finger millet (60%) and wheat flour (40%) and 2) malted finger millet (20%) and wheat flour (80%). The sensory acceptance of the former sample was 8.4 and the overall acceptability of the latter was 8.5. The shelf life of the muffins was estimated as 3 days at ambient temperature and 6 days at refrigerated temperature. The sensory properties of finger millet degraded during the storage period. Those muffins which were stored in aluminum foil at refrigerated temperature showed good quality, as compared to those stored in polypropylene bags at ambient temperature [84]. Muffins are very popular snacks mostly consumed by children. Finger millet flour can easily replace wheat flour, without any loss in taste or other characteristics. Furthermore, the addition of finger millet flour enhances the nutritional content of muffins [84]. Thus, the utilization of finger millets in bakery products is a healthy choice [51].

Bread. Bread is a very good source of nutrients that has a positive impact on human health. Its nutrient content can be enhanced by incorporating cereal grain flour [85]. Millet has been called a “nutri-cereal” for its nutrient content. Generally, wheat flour is used in breadmaking but finger millet could substitute for wheat flour because of its composition. Kaur *et al.* reported that the bread prepared from a blend of finger millet and wheat flour showed similar sensory scores [86]. Another study evaluated the sensory and textural properties of bread samples from composite flour [87]. Malted finger millet and red kidney bean were used to substitute 20 and 100 g of wheat flour, respectively. The results confirmed that the bread sample with malted finger millet had a better sensory score and textural attributes than the one with red kidney bean. However, the latter showed a better mineral and nutrient content than the former. Finger millet bread or hot porridge is commonly eaten with banana juice or sugar in the eastern and northern parts of Uganda [79].

Cake. In the bakery industry, cake is one of the most popular products among consumers. Malted finger millet and wheat flour were used in different ratios to formulate a cake [69]. The samples fortified with

malted ragi flour were richer in minerals (calcium, iron, phosphorus) and crude fiber than the control sample. The sensory score was found to be the same at a ratio of 50:50. The cake with 70% of malted finger millet showed the highest mineral and fiber content, but had lower sensory characteristics due to the loss of sponginess and increased intensity of brown color. In another study, finger millet (nagli rava) was mixed together with butter milk to prepare batter. Subsequently, jaggery syrup, white butter, and baker’s yeast were added, while the flavor was enhanced with cardamom. Fermentation was achieved after 1 and the cake was baked at 180°C for 20 min [83].

Biscuits. Biscuits were prepared from two compositions of finger millet and wheat flour, 60:40 and 70:30 w/w. The quality of dough and biscuits was evaluated and their hardness was measured by the textural profile analysis. According to the results, the samples with the 60:40 ratio of finger millet and wheat flour were harder than those with the 70:30 ratio, because wheat flour makes the dough more adhesive. Another study reported the advantages of the 60:40 ratio of finger millet and wheat flour [88]. During milling, malting, and decortication of finger millet grain, the outer layer of a seed coat forms a by-product. Krishnan *et al.* reported that the seed coat matter contained 9.5–12% of protein, 2.6–3.7% of fat, 40–48% of dietary fiber, 3–5% of polyphenols, and 700–860 mg/100 g of calcium [89]. Seed coat matter can be used in flour blends to prepare biscuits. According to the sensory evaluation, 20% of malted millet, hydrothermally processed millet, and 10% of seed coat matter could be used in composite biscuit flour.

Alcoholic beverages. Beer. Beer is known as doro, hwahwa, mhamba, or utshwala in various regions of Zimbabwe. Opaque beer is a popular alcoholic beverage in the southern part of Africa [90]. Millet beer ranges in alcohol content and taste between ethnic groups. For traditional brewing processes, mostly Bulrush (*Pennisetum typhoideum*) and finger millet malts are preferred [91]. Opaque beer is generally produced from millet with a high level of tannins. Malted finger millet and barley flour are blended together in various proportions (100:0, 50:50, and 0:100) for beer brewing. Gull *et al.* reported that the optimal conditions for beer production were a 68:32 ratio of finger millet and barley, a kilning temperature of 50°C, and a slurry ratio of 1:7 [14]. There are various cultivars of finger millet such as brown, light brown, and white [12, 36, 63]. In South Africa, mainly brown cultivar is used for brewing of traditional opaque beer [52].

Extruded products. Noodles. Blends of finger millet flour (30–50%) and refined wheat flour were used to develop noodles for diabetic patients. The sensory analysis showed that noodles prepared with 30% of finger millet flour had better acceptance than the other samples [92]. Two ratios of finger millet flour and rice flour (50:50 and 100:0) were used to prepare noodles. Water was added to increase moisture up to 35% and

to cause pellets to form. Pellets were steamed to make sheets and form noodles by extrusion. Afterwards, the noodles were sterilized at 100°C and dried. The samples with both ratios of finger millet and rice flours showed good acceptance, but the sample with 100% of finger millet flour had better acceptability in color than the one with 50% of finger millet flour. Noodles can be packed in PET/LDPE bags for more than 1.5 years without any deterioration [93].

Fermented products. *Dosa.* Dosa is an Indian breakfast food. Sinthiya prepared dosa from finger millet flour and horse gram [94]. It was inexpensive and had a high protein content. Fermentation was carried out for 24 h in different proportions. The results showed a decrease in pH by 2.4 in 16 h. Fermented dosa showed higher sensory acceptance. Also, the study showed that dosa might help in overcoming malnutrition. In another study, finger millet, rice, and urad dal flours (2:2:1) were mixed with jaggery syrup and dry yeast to make batter which was fermented for 10 h with the adding of salt [83].

Koozh. Koozh is a popular fermented beverage. Generally, it is produced in rural India by traditional methods. Rich in nutrients, it also carries some health-promoting properties. Koozh is considered a unique fermented food because it undergoes fermentation twice, before and after cooking. Also, it takes two days to process [70]. Koozh is generally prepared from finger millet and it is well known for its flavor and nutritious value. In south India, it is consumed every day for breakfast [95].

Weaning food. The sprouting of finger millet is an important process in the preparation of infant food. Hejazi and Orsat stated that sprouted finger millet and amaranth grains enhanced the availability and digestibility of protein, which is an essential nutrient for infants' growth [53]. Nowadays, micronutrient deficiency is a global issue. Finger millet grain is popular in eastern and northern Uganda as a highly nutritious food. Finger millet bread or hot porridge is eaten with banana juice or sugar [79]. Different processes during the preparation of weaning food, such as roasting, help enhance the bioavailability of iron [8, 45]. Finger millet has special properties which make it an excellent source of nutrients, compared to other grains. It is a rich food due to its malting characteristics. Malted finger millet has been traditionally used to develop infant food and beverages either with milk or lukewarm water with the addition of sugar [51, 69].

Chapatti (roti). Dough is prepared from finger millet flour, water, a pinch of salt, and oil. To make chapatti, the dough is kneaded into small balls, which are flattened and then put over a hot pan. Shobana *et al.* stated that the wheat chapatti had a better digestibility index than the finger millet chapatti [3]. The latter had a resistant starch content of about 4.5%. Sharma *et al.* prepared chapatti from a blend of finger millet and wheat flours (3:1) [82]. The blended flour showed higher levels of phenols and higher antioxidant activity than

wheat flour. The chapatti from blended flour had a high level of starch which was slow in digestion.

Panghal *et al.* found that the chapatti prepared from finger millet flour (40%) and wheat flour had poor dough sheeting and handling properties [96]. Moreover, it was low in the level of redness and phenolic content. A 7:3 ratio of finger millet and wheat flours was considered suitable for the preparation of chapatti, although the color of chapatti was still slightly dark. Finger millet flour incorporated into the dough improved the taste of chapatti. In addition, it efficiently controls the level of sugars in diabetic patients. Its fiber content can also help solve the problem of constipation [16].

Papad. According to a report by Verma and Patel, papad is prepared using 60% of finger millet flour in Karnataka [51]. First, the flour is cooked in distilled water until it gets gelatinized. Then, the dough is prepared by adding water. It is rolled, flattened, cut into shapes of a desirable size, and then dried until required moisture. In India, papad is a very popular snack and it is as thin as wafers. Generally, it has a round shape and is consumed roasted. The moisture content of papad is about 14–15%. Papad prepared from a blend of finger millet and soy flours can be stored for up to two months. In a study by Kazi and Auti, finger millet grains were soaked for 16 h and germinated for 48 h. They were then dried at room temperature to reduce moisture and ground into fine powder. To enhance the flavor of papad, malted flour and cumin seeds were added to boiling water. The mixture was stirred until it became thicker in consistency and sun-dried for 2 days [83].

Porridge. Porridge is a staple food mainly consumed in southern India, especially in rural areas. Porridge is prepared by mixing finger millet flour with water to attain a dough-like consistency [47]. Porridge made from different varieties of finger millets had a reduced content of phenolic compounds (by 41%) and tannins (by 35%), while its iron and zinc bio-accessibility was 6 and 13%, respectively [55]. Finger millets were roasted at various temperatures and during different times to prepare porridge. Ambre *et al.* reported that longer time and higher temperature decreased viscosity by 50–60% [16]. Mainly brown and white cultivars were used to prepare porridge [36, 52].

Non-food uses. Finger millet is an unconventional crop that can be used not only to formulate nutritious foods but also as an excellent source of biomass for bioethanol production. Finger millet seeds are mainly utilized in the production of ethanol, while African countries mostly use them for beer production [97]. Finger millet straw and agricultural waste can be converted into bioethanol. The current problems of global warming, turbulent oil prices, and environmental pollution have prompted most of consumers around the world to sharply increase their use of “green” fuels. Bioethanol is commonly derived from the conversion of carbon-based feeds. However, bioethanol from bio-sources is the main alternative to fossil fuels for road

transport vehicles [98]. Finger millet straw can be used for feeding Mandya sheep or any other animals [99].

Future prospects for research. Our literature review shows that finger millet is an excellent source of nutrients and health-benefitting properties, which are comparable to those of major cereals such as wheat, rice, and maize. Its edible content and nutritional value can be increased by various processing technologies such as soaking, fermentation, germination, popping, and puffing. The use of finger millet grain is lower in some rural areas compared to urban areas. This is due to the lack of innovative millet-processing technologies to provide easy-to-handle, ready-to-cook, or ready-to-eat products and meals on a commercial scale.

Finger millet is not only used as a coarse grain, but it is also considered a nutrient grain, or a nutrient crop, and a possible solution to food and nutrition security globally. Its high nutritional value and tolerance towards various biological and azotic stresses make it an excellent crop for the currently growing population in the conditions of climate change.

A super grain can be created in the future by genetically combining various agriculturally important traits of the finger millet genus. Advanced finger millet varieties can be cultivated through different types of breeding and genetic modification to enhance the crop's nutritional composition. The production of finger millet can be improved with modern agricultural practices and a timely management of the crop's condition.

CONCLUSION

Finger millet is a promising raw material for obtaining food products with a high nutritional value. In addition to meeting the food requirements of the population, it has a large number of nutritional (vitamins, minerals, fatty acids, calcium, antioxidants) and medicinal properties. Its nutritional and functional properties were found to be superior to those of other cereal grains. Processing and value-addition technologies have made it possible to process and prepare functional products for both rural and urban consumers. In rural areas, the utilization of finger millet as a food product is still limited, so it needs to be widely popularized. Specially formulated region-specific and group-specific foods can help promote millet consumption and thereby improve the nutritional intake of consumers.

CONTRIBUTION

Vaibhav Gaikwad, Jaspreet Kaur and Prasad Rasane designed and planned the research, and wrote the manuscript. Sawinder Kaur and Jyoti Singh created the tables and figures, as well as interpreted the data. Ankit Kumar, Ashwani Kumar, Nitya Sharma, Chandra Mohan Mehta and Avinash Singh Patel reviewed and modified the manuscript.

CONFLICT OF INTEREST

The authors declare no conflict of interest.

REFERENCES

1. Chandra D, Chandra S, Pallavi, Sharma AK. Review of finger millet (*Eleusine coracana* (L.) Gaertn): A power house of health benefiting nutrients. *Food Science and Human Wellness*. 2016;5(3):149–155. <https://doi.org/10.1016/j.fshw.2016.05.004>
2. Abd Salem MH, Hippen AR, Salem MM, Assem FM, El-Aassar M. Survival of probiotic *Lactobacillus casei* and *Enterococcus fecium* in Domiati cheese of high conjugated linoleic acid content. *Emirates Journal of Food and Agriculture*. 2012;2(24):98–104.
3. Shobana S, Krishnaswamy K, Sudha V, Malleshi NG, Anjana RM, Palaniappan L, et al. Finger millet (*Ragi*, *Eleusine coracana* L.): A review of its nutritional properties, processing, and plausible health benefits. *Advances in Food and Nutrition Research*. 2013;69:1–39. <https://doi.org/10.1016/B978-0-12-410540-9.00001-6>
4. Sakamma S, Umesh KB, Girish MR, Ravi SC, Satishkumar M, Bellundagi V. Finger millet (*Eleusine coracana* L. Gaertn.) production system: Status, potential, constraints and implications for improving small farmer's welfare. *Journal of Agricultural Science*. 2018;10(1):162–179. <https://doi.org/10.5539/jas.v10n1p162>
5. Divya GM, Krishnamurthy KN, Gowda DM. Growth and instability analysis of finger millet crop in Karnataka. *Mysore Journal of Agricultural Science*. 2013;47(1):35–39.
6. Mushtari Begum J, Begum S, Pandey A. Nutritional evaluation of finger millet malt. *International Journal of Science, Environment and Technology*. 2016;5(6):4086–4096.
7. Palanisamy BD, Rajendran V, Sathyaseelan S, Bhat R, Venkatesan BP. Enhancement of nutritional value of finger millet-based food (Indian *dosa*) by co-fermentation with horse gram flour. *International Journal of Food Sciences and Nutrition*. 2011;63(1):5–15. <https://doi.org/10.3109/09637486.2011.591367>
8. Thapliyal V, Singh K. Finger millet: Potential millet for food security and power house of nutrients. *International or Research in Agriculture and Forestry*. 2015;2(2):22–33.
9. Singh N, David J, Thompkinson DK, Seelam BS, Rajput H, Morya S. Effect of roasting on functional and phytochemical constituents of finger millet (*Eleusine coracana* L.). *The Pharma Innovation Journal*. 2018;7(4): 414–418.

10. Zyaynitdinov DR, Ewteew AV, Bannikova AV. Properties of polyphenols and xylooligosaccharides obtained biotechnologically from processed millets. *Food Processing: Techniques and Technology*. 2021;51(3):538–548. (In Russ.). <https://doi.org/10.21603/2074-9414-2021-3-538-548>
11. Soetan KO, Olaiya CO, Oyewole OE. The importance of mineral elements for humans, domestic animals and plants – A review. *African Journal of Food Science*. 2010;4(5):200–222.
12. Devi PB, Vijayabharathi R, Sathyabama S, Malleshi NG, Priyadarisini VB. Health benefits of finger millet (*Eleusine coracana* L.) polyphenols and dietary fiber: A review. *Journal of Food Science and Technology*. 2011;51(6):1021–1040. <https://doi.org/10.1007/s13197-011-0584-9>
13. Yang X, Wan Z, Perry L, Lu H, Wang Q, Zhao C, et al. Early millet use in northern China. *Proceedings of the National Academy of Sciences*. 2012;109(10):3726–3730. <https://doi.org/10.1073/pnas.1115430109>
14. Gull A, Gulzar Ahmad N, Prasad K, Kumar P. Technological, Processing and nutritional approach of finger millet (*Eleusine coracana*) – A mini review. *Journal of Food Processing and Technology*. 2016;7. <https://doi.org/10.4172/2157-7110.1000593>
15. Shingare SP, Thorat BN. Effect of drying temperature and pretreatment on protein content and color changes during fluidized bed drying of finger millets (Ragi, *Eleusine coracana*) sprouts. *Drying Technology*. 2013;31(5):507–518. <https://doi.org/10.1080/07373937.2012.744033>
16. Ambre PK, Sawant AA, Sawant PS. Processing and value addition: A finger millet review. *Journal of Pharmacognosy and Phytochemistry*. 2020;9(2):375–380.
17. Krishnan R, Dharmaraj U, Malleshi NG. Influence of decortication, popping and malting on bioaccessibility of calcium, iron and zinc in finger millet. *LWT – Food Science and Technology*. 2012;48(2):169–174. <https://doi.org/10.1016/j.lwt.2012.03.003>
18. Naushad Emmambux M, Taylor JRN. Morphology, physical, chemical, and functional properties of starches from cereals, legumes, and tubers cultivated in Africa: A review. *Starch – Stärke*. 2013;65(9–10):715–729. <https://doi.org/10.1002/star.201200263>
19. Dida MM, Devos KM. Finger millet. In: Kole C, editor. Heidelberg: Springer Berlin; 2006. pp. 333–343. https://doi.org/10.1007/978-3-540-34389-9_10
20. Sood S, Joshi DC, Chandra AK, Kumar A. Phenomics and genomics of finger millet: current status and future prospects. *Planta*. 2019;250:731–751. <https://doi.org/10.1007/s00425-019-03159-6>
21. Chandrashekar A. Finger millet: *Eleusine coracana*. *Advances in Food and Nutrition Research*. 2010;59:215–262. [https://doi.org/10.1016/S1043-4526\(10\)59006-5](https://doi.org/10.1016/S1043-4526(10)59006-5)
22. Dass A, Sudhishri S, Lenka NK. Integrated nutrient management to improve finger millet productivity and soil conditions in hilly region of Eastern India. *Journal of Crop Improvement*. 2013;27(5):528–546. <https://doi.org/10.1080/15427528.2013.800828>
23. Adhikari BN, Pokhrel BB, Shrestha J. Evaluation and development of finger millet (*Eleusine coracana* L.) genotypes for cultivation in high hills of Nepal. *Farming and Management*. 2018;3(1):37–46.
24. Gull A, Jan R, Nayik GA, Prasad K, Kumar P. Significance of finger millet in nutrition, health and functional products: A review. *Journal of Environmental Science, Computer Science and Engineering and Technology*. 2014;3(3):1601–1608.
25. Lata C. Advances in genomics for enhancing abiotic stress tolerance in millets. *Proceedings of the Indian National Science Academy*. 2015;81(2):397–417. <https://doi.org/10.16943/ptinsa/2015/v81i2/48095>
26. Shukla A, Lalit A, Sharma V, Vats S, Alam A. Pearl and finger millets: The hope of food security. *Applied Research Journal*. 2015;1(2):59–66.
27. Sood S, Gupta AK, Kant L, Pattanayak A. Assessment of parametric and non-parametric methods for selecting stable and adapted finger millet (*Eleusine coracana* (L.) Gaertn.) genotypes in sub-mountainous Himalayan region. *International Journal of Basic and Applied Agricultural Research*. 2015;13:283–288.
28. Rurinda J, Mapfumo P, van Wijk MT, Mtambanengwe F, Rufino MC, Chikowo R, et al. Comparative assessment of maize, finger millet and sorghum for household food security in the face of increasing climatic risk. *European Journal of Agronomy*. 2014;55:29–41. <https://doi.org/10.1016/j.eja.2013.12.009>
29. Goron TL, Bhosekar VK, Shearer CR, Watts S, Raizada MN. Whole plant acclimation responses by finger millet to low nitrogen stress. *Frontiers in Plant Science*. 2015;6. <https://doi.org/10.3389/fpls.2015.00652>
30. Upadhyaya HD, Gowda CLL, Pundir RPS, Gopal Reddy V, Singh S. Development of core subset of finger millet germplasm using geographical origin and data on 14 quantitative traits. *Genetic Resources and Crop Evolution*. 2006;53:679–685. <https://doi.org/10.1007/s10722-004-3228-3>










31. Parashuram DP, Gowda J, Satish RG, Mallikarjun NM. Heterosis and combining ability studies for yield and yield attributing characters in finger millet (*Eleusine coracana* (L.) Gaertn.). *Electronic Journal of Plant Breeding*. 2011;2:494–500.
32. Samarajeewa KBDP, Horiuchi T, Oba S. Finger millet (*Eleusine coracana* L. Gaertn.) as a cover crop on weed control, growth and yield of soybean under different tillage systems. *Soil and Tillage Research*. 2006;90(1–2):93–99. <https://doi.org/10.1016/j.still.2005.08.018>
33. Neshamba SM. Variability for drought tolerance in finger millet (*Eleusine coracana* (L.) Gaertn.) accessions from Zambia. Master of Science thesis. University of Zambia; 2010
34. Khamgaonkar SG, Singh A, Chand K, Shahi NC, Lohani UC. Processing technologies of Uttarakhand for lesser known crops: An overview. *Journal of Academic Industry Research*. 2013;1(8):447–452.
35. Shobana S. Investigations on the carbohydrate digestibility of finger millet (*Eleusine coracana*) with special reference to the influence of its seed coat constituents. Doctoral dissertation. University of Mysore; 2009. 283 p.
36. Ramashia SE, Anyasi TA, Gwata ET, Meddows-Taylor S, Jideani AIO. Processing, nutritional composition and health benefits of finger millet in sub-saharan Africa. *Food Science and Technology*. 2019;39(2):253–266. <https://doi.org/10.1590/fst.25017>
37. Amadou I, Gounga ME, Le G-W. Millets: Nutritional composition, some health benefits and processing – A review. *Emirates Journal of Food and Agriculture*. 2013;25(7):501–508. <https://doi.org/10.9755/ejfa.v25i7.12045>
38. Kumar A, Tomer V, Kaur A, Kumar V, Gupta K. Millets: a solution to agrarian and nutritional challenges. *Agriculture and Food Security*. 2018;7. <https://doi.org/10.1186/s40066-018-0183-3>
39. Ambati K, Sucharitha KV. Millets-review on nutritional profiles and health benefits. *International Journal of Recent Scientific Research*. 2019;10(7):33943–33948.
40. Singh E, Sarita. Potential functional implications of finger millet (*Eleusine coracana*) in nutritional benefits, processing, health and diseases: A review. *International Journal of Home Science*. 2016;2(21):151–155.
41. Swami SB, Thakor NJ, Gurav HS. Effect of soaking and malting on finger millet (*Eleusine coracana*) grain. *Agricultural Engineering International: CIGR Journal*. 2013;15(1):194–200.
42. Banusha S, Vasantharuba S. Effect of malting on nutritional contents of finger millet and mung bean. *American-Eurasian Journal of Agriculture and Environmental Science*. 2013;13(12):1642–1646.
43. Shahidi F, Chandrasekara A. Millet grain phenolics and their role in disease risk reduction and health promotion: A review. *Journal of Functional Foods*. 2013;5(2):570–581. <https://doi.org/10.1016/j.jff.2013.02.004>
44. Lande SB, Thorats S, Kulthe AA. Production of nutrient rich vermicelli with malted finger millet (Ragi) flour. *International Journal of Current Microbiology and Applied Sciences*. 2017;6(4):702–710. <https://doi.org/10.20546/ijemas.2017.604.086>
45. Singh P, Raghuvanshi RS. Finger millet for food and nutritional security. *African Journal of Food Science*. 2012;6(4):77–84. <https://doi.org/10.5897/ajfsx10.010>
46. Nakarani UM, Singh D, Suthar KP, Karmakar N, Faldu P, Patil HE. Nutritional and phytochemical profiling of nutraceutical finger millet (*Eleusine coracana* L.) genotypes. *Food Chemistry*. 2021;341. <https://doi.org/10.1016/j.foodchem.2020.128271>
47. Kumari D, Chandrasekara A, Shahidi F. Bioaccessibility and antioxidant activities of finger millet food phenolics. *Journal of Food Bioactives*. 2019;6:100–109. <https://doi.org/10.31665/jfb.2019.6187>
48. Chethan S, Malleshi NG. Finger millet polyphenols: Characterization and their nutraceutical potential. *American Journal of Food Technology*. 2007;2(7):582–592. <https://doi.org/10.3923/ajft.2007.582.592>
49. Tatala S, Ndossi G, Ash D, Mamiro P. Effect of germination of finger millet on nutritional value of foods and effect of food supplement on nutrition and anaemia status in Tanzania children. *Tanzania Journal of Health Research*. 2007;9(2):77–86. <https://doi.org/10.4314/thrb.v9i2.14308>
50. Lee SH, Chung I-M, Cha Y-S, Park Y. Millet consumption decreased serum concentration of triglyceride and C-reactive protein but not oxidative status in hyperlipidemic rats. *Nutrition Research*. 2010;30(4):290–296. <https://doi.org/10.1016/j.nutres.2010.04.007>
51. Verma V, Patel S. Value added products from nutri-cereals: Finger millet (*Eleusine coracana*). *Emirates Journal of Food and Agriculture*. 2013;25(3):169–176. <https://doi.org/https://doi.org/10.9755/ejfa.v25i3.10764>
52. Sood S, Kumar A, Babu BK, Gaur VS, Pandey D, Kant L, et al. Gene discovery and advances in finger millet [*Eleusine coracana* (L.) Gaertn.] genomics – An important nutri-cereal of future. *Frontiers in Plant Science*. 2016;7. <https://doi.org/10.3389/fpls.2016.01634>
53. Hejazi SN, Orsat V. Malting process optimization for protein digestibility enhancement in finger millet grain. *Journal of Food Science and Technology*. 2016;53(4):1929–1938. <https://doi.org/10.1007/s13197-016-2188-x>

54. Kakade SB, Hathan BS. Finger millet processing: Review. *International Journal of Agriculture Innovations and Research*. 2015;3(4):1003–1008.
55. Gabaza M, Shumoy H, Louwagie L, Muchuweti M, Vandamme P, du Laing G, et al. Traditional fermentation and cooking of finger millet: Implications on mineral binders and subsequent bioaccessibility. *Journal of Food Composition and Analysis*. 2018;68:87–94. <https://doi.org/10.1016/j.jfca.2017.05.011>
56. Jaybhaye RV, Pardeshi IL, Vengaiyah PC, Srivastav PP. Processing and technology for millet-based food products: A review. *Journal of Ready to Eat Food*. 2014;1(2):32–48.
57. Tumuluru JS, Sokhansanj S, Bandyopadhyay S, Bawa AS. Changes in moisture, protein, and fat content of fish and rice flour coextrudates during single-screw extrusion cooking. *Food and Bioprocess Technology*. 2012;6:403–415. <https://doi.org/10.1007/s11947-011-0764-7>
58. Ushakumari SR. Technological and physico-chemical characteristics of hydrothermally treated finger millet. Doctoral dissertation. University of Mysore; 2009. 282 p.
59. Shimray CA, Gupta S, Venkateswara Rao G. Effect of native and germinated finger millet flour on rheological and sensory characteristics of biscuits. *International Journal of Food Science and Technology*. 2012;47(11):2413–2420. <https://doi.org/10.1111/j.1365-2621.2012.03117.x>
60. Rajasekhar M, Edukondalu L, Smith DD, Veeraprasad G. Changes in engineering properties of finger millet (*PPR-2700, Vakula*) on hydrothermal treatment. *The Andhra Agricultural Journal*. 2018;65(2):420–429.
61. Ocheme OB, Chinma CE. Effects of soaking and germination on some physicochemical properties of millet flour for porridge production. *Journal of Food Technology*. 2008;6(5):185–188.
62. Rasane P, Jha A, Sabikhi L, Kumar A, Unnikrishnan VS. Nutritional advantages of oats and opportunities for its processing as value added foods – A review. *Journal of Food Science and Technology*. 2015;52(2):662–675. <https://doi.org/10.1007/s13197-013-1072-1>
63. Rathore S, Singh K, Kumar V. Millet grain processing, utilization and its role in health promotion: A review. *International Journal of Nutrition and Food Sciences*. 2016;5(5):318–329. <https://doi.org/10.11648/j.ijnfs.20160505.12>
64. Mishra G, Joshi DC, Panda BK. Popping and puffing of cereal grains: A review. *Journal of Grain Processing and Storage*. 2014;1(2):34–46.
65. Chauhan ES, Sarita. Effects of processing (germination and popping) on the nutritional and anti-nutritional properties of finger millet (*Eleusine coracana*). *Current Research in Nutrition and Food Science Journal*. 2018;6(2):566–572. <https://doi.org/10.12944/crnfsj.6.2.30>
66. Hithamani G, Srinivasan K. Effect of domestic processing on the polyphenol content and bioaccessibility in finger millet (*Eleusine coracana*) and pearl millet (*Pennisetum glaucum*). *Food Chemistry*. 2014;164:55–62. <https://doi.org/10.1016/j.foodchem.2014.04.107>
67. Hübner F, Arendt EK. Germination of cereal grains as a way to improve the nutritional value: A review. *Critical Reviews in Food Science and Nutrition*. 2013;53(8):853–861. <https://doi.org/10.1080/10408398.2011.562060>
68. Pushparaj FS, Urooj A. Influence of Processing on dietary fiber, tannin and *in vitro* protein digestibility of pearl millet. *Food and Nutrition Sciences*. 2011;2(8):895–900. <https://doi.org/10.4236/fns.2011.28122>
69. Desai AD, Kulkarni SS, Sahoo AK, Ranveer RC, Dandge PB. Effect of supplementation of malted ragi flour on the nutritional and sensorial quality characteristics of cake. *Advance Journal of Food Science and Technology*. 2010;2(1):67–71.
70. Ilango S, Antony U. Assessment of the microbiological quality of koozh, a fermented millet beverage. *African Journal of Microbiology Research*. 2014;8(3):308–312. <https://doi.org/10.5897/ajmr2013.6482>
71. Makokha AO, Oniang'o RK, Njoroge SM, Kamar OK. Effect of traditional fermentation and malting on phytic acid and mineral availability from sorghum (*Sorghum bicolor*) and finger millet (*Eleusine coracana*) Grain varieties grown in Kenya. *Food and Nutrition Bulletin*. 2002;23(3):241–245. <https://doi.org/10.1177/15648265020233s147>
72. Usai T, Nyamunda BC, Mutonhodza B. Malt quality parameters of finger millet for brewing commercial opaque beer. *International Journal of Science and Research*. 2013;2(9):146–149.
73. Roopa S, Premavalli K. Effect of processing on starch fractions in different varieties of finger millet. *Food Chemistry*. 2008;106(3):875–882. <https://doi.org/10.1016/j.foodchem.2006.08.035>
74. Chandrasekara A, Nacz M, Shahidi F. Effect of processing on the antioxidant activity of millet grains. *Food Chemistry*. 2012;133(1):1–9. <https://doi.org/10.1016/j.foodchem.2011.09.043>

75. Mahajan H, Gupta M. Nutritional, functional and rheological properties of processed sorghum and ragi grains. *Cogent Food and Agriculture*. 2015;1(1). <https://doi.org/10.1080/23311932.2015.1109495>
76. Kora AJ. Applications of sand roasting and baking in the preparation of traditional Indian snacks: nutritional and antioxidant status. *Bulletin of the National Research Centre*. 2019;43. <https://doi.org/10.1186/s42269-019-0199-2>
77. Brahma S, Martínez I, Walter J, Clarke J, Gonzalez T, Menon R, et al. Impact of dietary pattern of the fecal donor on *in vitro* fermentation properties of whole grains and brans. *Journal of Functional Foods*. 2017;29:281–289. <https://doi.org/10.1016/j.jff.2016.12.042>
78. Dharmaraj U, Malleshi NG. Changes in carbohydrates, proteins and lipids of finger millet after hydrothermal processing. *LWT – Food Science and Technology*. 2011;44(7):1636–1642. <https://doi.org/10.1016/j.lwt.2010.08.014>
79. Kannan S. Finger millet in nutrition transition: an infant weaning food ingredient with chronic disease preventive potential. *British Journal of Nutrition*. 2010;104(12):1733–1734. <https://doi.org/10.1017/s0007114510002989>
80. Abioye VF, Olatunde SJ, Elias G. Quality attributes of cookies produced from composite flours of wheat, germinated finger millet flour and African yam bean. *International Journal of Research – Granthaalayah*. 2018;6(11):172–183. <https://doi.org/10.5281/zenodo.1845427>
81. Handa C, Goomer S, Siddhu A. Effects of whole-multigrain and fructoligosaccharide incorporation on the quality and sensory attributes of cookies. *Food Science and Technology Research*. 2010;17(1):45–54. <https://doi.org/10.3136/Fstr.17.45>
82. Sharma B, Gujral HS, Solah V. Effect of incorporating finger millet in wheat flour on mixolab behavior, chapatti quality and starch digestibility. *Food Chemistry*. 2017;231:156–164. <https://doi.org/10.1016/j.foodchem.2017.03.118>
83. Kazi T, Auti SG. Calcium and iron rich recipes of finger millet. *IOSR Journal of Biotechnology and Biochemistry*. 2017;3(3):64–68.
84. Rajiv J, Soumya C, Indrani D, Venkateswara Rao G. Effect of replacement of wheat flour with finger millet flour (*Eleusine coracana*) on the batter microscopy, rheology and quality characteristics of muffins. *Journal of Texture Studies*. 2011;42(6):478–489. <https://doi.org/10.1111/j.1745-4603.2011.00309.x>
85. Onyango C, Noetzold H, Bley T, Henle T. Proximate composition and digestibility of fermented and extruded *uji* from maize–finger millet blend. *LWT – Food Science and Technology*. 2004;37(8):827–832. <https://doi.org/10.1016/j.lwt.2004.03.008>
86. Kaur KD, Jha A, Sabikhi L, Singh AK. Significance of coarse cereals in health and nutrition: A review. *Journal of Food Science and Technology*. 2012;51(8):1429–1441. <https://doi.org/10.1007/s13197-011-0612-9>
87. Bhol S, Bosco SJD. Influence of malted finger millet and red kidney bean flour on quality characteristics of developed bread. *LWT – Food Science and Technology*. 2014;55(1):294–300. <https://doi.org/10.1016/j.lwt.2013.08.012>
88. Saha S, Gupta A, Singh SRK, Bharti N, Singh KP, Mahajan V, et al. Compositional and varietal influence of finger millet flour on rheological properties of dough and quality of biscuit. *LWT – Food Science and Technology*. 2011;44(3):616–621. <https://doi.org/10.1016/j.lwt.2010.08.009>
89. Krishnan R, Dharmaraj U, Sai Manohar R, Malleshi NG. Quality characteristics of biscuits prepared from finger millet seed coat based composite flour. *Food Chemistry*. 2011;129(2):499–506. <https://doi.org/10.1016/j.foodchem.2011.04.107>
90. Mgonja MA, Lenné JM, Manyasa E, Sreenivasaprasad S. Finger millet blast management in East Africa. Creating opportunities for improving production and utilization of finger millet. Andhra Pradesh: International Crops Research Institute for the Semi-Arid Tropics; 2007. 196 pp.
91. Bvochora JM, Zvauya R. Biochemical changes occurring during the application of high gravity fermentation technology to the brewing of Zimbabwean traditional opaque beer. *Process Biochemistry*. 2001;37(4):365–370. [https://doi.org/10.1016/s0032-9592\(01\)00224-2](https://doi.org/10.1016/s0032-9592(01)00224-2)
92. Shukla K, Srivastava S. Evaluation of finger millet incorporated noodles for nutritive value and glycemic index. *Journal of Food Science and Technology*. 2011;51(3):527–534. <https://doi.org/10.1007/s13197-011-0530-x>
93. Dissanayake BDMPB, Jayawardena HS. Development of a method for manufacturing noodles from finger millet. *Procedia Food Science*. 2016;6:293–297. <https://doi.org/10.1016/j.profoo.2016.02.058>
94. Vaishnavi Devi N, Sinthiya R. Development of functional product from finger millet (*Eleusine coracana*). *International Journal of Research – Granthaalayah*. 2018;6(2):109–119. <https://doi.org/10.29121/granthaalayah.v6.i2.2018.1551>

95. Thirumangaimannan G, Gurumurthy K. A study on the fermentation pattern of common millets in *Koozh* preparation – A traditional South Indian food. *Indian Journal of Traditional Knowledge*. 2013;12(3):512–517.
96. Panghal A, Khatkar BS, Yadav DN, Chhikara N. Effect of finger millet on nutritional, rheological, and pasting profile of whole wheat flat bread (chapatti). *Cereal Chemistry*. 2019;96(1):86–94. <https://doi.org/10.1002/cche.10111>
97. Yemets AI, Blume RYa, Rakhmetov DB, Blume YaB. Finger millet as a sustainable feedstock for bioethanol production. *The Open Agriculture Journal*. 2020;14(1):257–272. <https://doi.org/10.2174/1874331502014010257>
98. Larson NI, Story M, Wall M, Neumark-Sztainer D. Calcium and dairy intakes of adolescents are associated with their home environment, taste preferences, personal health beliefs, and meal patterns. *Journal of the American Dietetic Association*. 2006;106(11):1816–1824. <https://doi.org/10.1016/j.jada.2006.08.018>
99. Arun PN, Chittaragi B, Prabhu TM, Siddalingamurthy HK, Suma N, Gouri MD, et al. Effect of replacing finger millet straw with jackfruit residue silage on growth performance and nutrient utilization in Mandya sheep. *Animal Nutrition and Feed Technology*. 2020;20(1):103–109. <https://doi.org/10.5958/0974-181x.2020.00010.4>

ORCID IDs

Jaspreet Kaur  <https://orcid.org/0000-0003-3718-5734>
Prasad Rasane  <https://orcid.org/0000-0002-5807-4091>
Sawinder Kaur  <https://orcid.org/0000-0002-4500-1053>
Jyoti Singh  <https://orcid.org/0000-0003-0838-6393>
Ankit Kumar  <https://orcid.org/0000-0001-9124-0269>
Ashwani Kumar  <https://orcid.org/0000-0001-6315-5710>
Nitya Sharma  <https://orcid.org/0000-0002-0203-6061>
Chandra Mohan Mehta  <https://orcid.org/0000-0001-7261-9732>
Avinash Singh Patel  <https://orcid.org/0000-0002-8520-7670>



Antihyperglycemic activity of colostrum peptides

Sergei L. Tikhonov^{1,2,*}, Natalia V. Tikhonova², Irina F. Gette³,
Ksenia V. Sokolova³, Irina G. Danilova³

¹ Russian State Agrarian University – Moscow Timiryazev Agricultural Academy^{ROR}, Moscow, Russia

² Ural State Agrarian University^{ROR}, Yekaterinburg, Russia

³ Institute of Immunology and Physiology of the Ural Branch of the Russian Academy of Sciences^{ROR}, Yekaterinburg, Russia

* e-mail: tikhonov75@bk.ru

Received 31.10.2022; Revised 28.11.2022; Accepted 06.12.2022; Published online 30.08.2023

Abstract:

Peptides of plant and animal origin have good anti-diabetic prospects. The research objective was to use bovine colostrum peptides to reduce hyperglycemia in diabetic rats.

Bovine colostrum peptides were obtained by trypsin hydrolysis of colostrum proteins with preliminary extraction of triglycerides. The study involved four groups of Wistar rats with seven animals per group. Group 1 served as control; group 2 received 300 mg/kg of trypsin hydrolysate of bovine colostrum as part of their daily diet for 30 days. Groups 3 and 4 had diabetes mellitus caused by intraperitoneal injections of 110 mg/kg of nicotinamide and 65 mg/kg of streptozotocin. Group 4 also received 300 mg/kg trypsin hydrolysate of bovine colostrum intragastrically five times a week for 30 days.

Three peptides were isolated from the trypsin hydrolysate of bovine colostrum and tested for the sequence of amino acids and molecular weight. Their identification involved the Protein NCBI database, followed by 2D and 3D modeling, which revealed their chemical profile, pharmacological properties, and antioxidant activity. The diabetic rats treated with colostrum peptides had lower glucose, glycated hemoglobin, malondialdehyde, and catalase activity but a higher content of glutathione in the blood. Their leukocytes and erythrocytes also demonstrated less deviation from the standard. The antioxidant effect of colostrum protein hydrolysate depended on a peptide with the amino acid sequence of SQKKKNCPNGTRIRVPGPGP and a mass of 8.4 kDa. Colostrum peptides reduced hyperglycemia and oxidative stress in diabetic rats. The research revealed good prospects for isolating individual colostrum peptides to be tested for antidiabetic properties.

Keywords: Peptides, bovine colostrum, diabetes mellitus, glucose, glycated hemoglobin, antioxidant activity

Please cite this article in press as: Tikhonov SL, Tikhonova NV, Gette IF, Sokolova KV, Danilova IG. Antihyperglycemic activity of colostrum peptides. *Foods and Raw Materials*. 2024;12(1):124–132. <https://doi.org/10.21603/2308-4057-2024-1-586>

INTRODUCTION

Diabetes mellitus, or type II diabetes, is the most common type of diabetes [1–3]. It causes such chronic complications as cardiovascular disease and neurological disorders, which have become a real pandemic of the XXI century. Medical science is constantly looking for new methods to curb the pathogenic factors that determine this socially significant disease and its chronic complications.

The list of targeted antidiabetic compounds includes dipeptidyl peptidase 4 (DPP4), intestinal maltase glucomylase, hepatic receptor homologue 1 (NR5A2), pancreatic alpha-amylase, peroxisome proliferator-activated receptor alpha (PPARA), protein tyrosine phosphatase, and retinol-binding protein-4 (RBP4) [4–6].

Protein hydrolysates of plant and animal origin contain a number of biologically active regulatory peptides with antidiabetic properties [7–13]. Antidiabetic peptides inhibit DPP4 activity, which prolongs the insulin-secreting action of incretins. Antioxidant peptides inactivate reactive oxygen species, scavenge free radicals, chelate prooxidant transition metals, and increase the activity of intracellular antioxidant enzymes [10]. Angiotensin-converting enzyme inhibitors have a hypotensive effect and reduce the risk of atherosclerosis, which is one of the main chronic complications of diabetes mellitus. Peptides that inhibit DPP-IV and angiotensin-converting enzyme have been found in protein hydrolysates obtained from chlorella, spirulina, amaranth, tuna milk, and lactic acid products [7–9, 12, 14, 15].

The peptide obtained from *Chlorella pyrenoidosa* contained ten amino acids: Leu-Leu-Val-Val-Try-Pro-Trp-Thr-Gln-Arg. It was reported to inhibit the activity of pancreatic lipase and prevent the accumulation of fatty acids and triglycerides in cells [16]. Peptide hydrolysates synthesized from quinoa (*Chenopodium quinoa* L.) and chickpea (*Cicer arietinum* L.) proteins were able to inhibit the activity of α -amylase and α -glucosidase, thus reducing glucose uptake and hyperglycemia [17, 18].

Bovine colostrum is the first cow's milk which is obtained after calving. It is a promising source of peptides. Colostrum contains more protein, peptides, lipids, hormones, minerals, and vitamins than whole milk [19, 20].

Colostrum contains antioxidants (vitamins C, A, E, β -carotene, selenium), as well as vitamins B₁, B₂, PP, B₅, B₆, B₁₂, D, orotic acid, and enzymes with peroxidase activity [21]. The protein component of colostrum is represented mainly by such whey proteins as albumins and globulins. Casein appears only on lactation days 3–4, and its amount gradually increases but never prevails.

The whey fraction of colostrum contains factors that provide passive immunity: immunoglobulins, lactoferrin, interferon, lysozyme, and defensins are partially synthesized by udder cells and partially formed by milk lymphocytes. Numerous studies have confirmed the antiviral, antifungal, and antibacterial properties of colostrum [21].

Colostrum contains such growth factors and protein hormones as epidermal growth factor (EGF), IGF-1, IGF-2, TGF α , TGF β , fibroblast growth factor, gonadotropin-releasing hormone, somatotropin, and growth hormone releasing factor (GHRF) [21, 22]. Growth factors promote regeneration, regulate blood glucose levels, and stimulate lipolysis. Glucagon-like peptide 1 (GLP-1) regulates glucose homeostasis by stimulating insulin secretion. A long-term colostrum diet increased the level of GLP-1 in the blood plasma of calves [23]. Colostrum casein hydrolysate appears under the action of lactic acid bacterial proteinases. Hydrolysis yields peptides with hypotensive, antimicrobial, antifungal, and immunoprotective effects. Bovine colostrum whey hydrolysates were reported to contain angiotensin-converting enzyme inhibitors, as well as proteins with antioxidant, antimicrobial, immunomodulatory, and opioid effects [24].

Agarkova *et al.* hydrolyzed casein by digestive enzymes to obtain 23 peptides with DPP-IV inhibitory activity, which exhibited no side effects typical of DPP-IV inhibitors [25]. A greater degree of hydrolysis reduces the allergenic properties of proteins. Colostrum hydrolysate contains peptides with a lower molecular weight compared to milk hydrolysate. Golovach *et al.* detected antioxidant activity in colostrum peptides, which increased together with the degree of hydrolysis [26].

Colostrum is safe as it cannot be overdosed and has demonstrated no side effects of clinical significance so far. Colostrum and its protein hydrolysates have a potential therapeutic and preventive use due to their an-

tibacterial and immunoregulatory peptides, as well as growth factors. Colostrum-based functional products may accompany synthetic drugs in the prevention and treatment of diabetes mellitus. These encouraging results require further studies to confirm these effects, as well as to define the optimal amount and treatment time.

The present research objective was to reveal the possibility of reducing hyperglycemia in diabetic rats under the action of bovine colostrum peptides.

STUDY OBJECTS AND METHODS

Colostrum peptides were obtained on the first day after calving by enzymatic hydrolysis of colostrum with trypsin. We removed the fat fraction by centrifugation at 3900 rpm for 10 min in an SM-12-06 centrifuge (TAGLER, Russia). After that, we introduced the enzyme trypsin (Samson-Med, Russia) at 0.15% colostrum weight in a phosphate buffer solution at pH 7.4. The solution consisted of disodium hydrogen phosphate dodecahydrate (Rosspolymer, Russia). The hydrolysis lasted 12 h at a temperature of 36°C until it was raised to 75°C to inactivate the enzyme.

The molecular weight distribution of the peptides was carried out by mass spectrometry and identified by MALDI-TOF and MS/MS mass spectrometry using an Ultraflex MALDI time-of-flight mass spectrometer (Bruker, Germany). The mass spectra analysis involved the Mascot program, Peptide Fingerprint option (Matrix Science, USA), and the Protein NCBI database.

The score was calculated by the following formula:

$$\text{Score} = \frac{50000}{M_{\text{prot}} \times P_{\text{mmi}}} \quad (1)$$

where M_{prot} is the molecular weight for each matched protein; P_{mmi} is the product calculated from the Mowse matrix of weights M for each match with the experimental data and peptide masses calculated based on the Protein NCBI genomic database. The spatial structure of the isolated peptides was modeled using the Schrodinger Maestro molecular modeling program (USA).

The antioxidant activity of the peptides was determined by their ability to scavenge free radicals DPPH (2,2-diphenyl-1-picrylhydrazyl) and ABTS (2,2'-azino-bis(3-ethylbenzothiazoline-6-sulfonate), as well as by their reducing power when interacting with the Fe(III)-2,4,6-tripyridyl-s-triazine complex by the ferric-reducing antioxidant power method (FRAP). The experiment followed the procedure described in [27] with some modifications.

To determine the antioxidant activity by the DPPH method, we mixed 20 μ L of protein hydrolysate or standard solution with 300 μ L of a fresh 0.1 mM solution of 2,2-diphenyl-1-picrylhydrazyl. The mix was incubated in the dark at room temperature for 30 min. The optical density decreased at 515 nm, compared to the control.

To determine antioxidant activity by the ABTS method, we used a ABTS radical solution. The ABTS radical was generated by mixing aliquots of 7.0 mM

ABTS solution and 2.45 mM potassium persulfate solution. The solution was kept in the dark at room temperature for 16 h. Then, we added 20 μ L of the hydrolysate or standard to 300 μ L of the solution of the ABTS⁺ radical cation. The absorbance was measured at 734 nm after the mix was incubated for 15 min at 37°C in the dark.

To determine the restoring power of the peptides, we prepared a FRAP reagent by mixing 10 parts of 0.3 M acetate buffer (pH 3.6), one part of a 10 mM solution of 2,4,6-tripyridyl-s-triazine in 40 mM HCl, and one part aqueous 20 mM solution of iron chloride FeCl₃·6H₂O. The reaction was initiated by mixing 300 μ L of the FRAP reagent and 20 μ L of the test peptide sample or standard solution. The reaction lasted 10 min at 37°C in the dark. The increase in optical density occurred at 593 nm, compared to the control.

We used a trolox solution (6-hydroxy-2,5,7,8-tetramethylchroman-2-carboxylic acid) of known concentration as a standard solution in all the methods. The results of the analyzes were expressed in mmol Trolox equivalents/l.

All the spectrophotometric measurements were performed using a CLARIOstar microplate reader (BMG Labtech, Germany).

The experiment involved twelve-week-old male Wistar rats that weighed 345 \pm 11 g. The rats were purchased from the Institute of Immunology and Physiology of the Ural Branch of the Russian Academy of Sciences. They lived five animals per cage under standard laboratory conditions at 20 \pm 2°C and a 12-h light-dark cycle, with free access to water and food. They were fed on 2020X Teklad rodent food without soy protein (Envigo, Huntingdon, UK). All manipulations followed the EU Council Directive 2010/63/EU and were approved by the ethics committee of the Institute of Physics, Ural Branch of the Russian Academy of Sciences.

The rats were divided into four groups with seven animals in each. Group 1 included control animals. Group 2 received 300 mg/kg of trypsin hydrolysate of bovine colostrum every day for 30 days. Rats in groups 3 and 4 acquired diabetes mellitus. After 16 h of fasting, they were administered 65 mg/kg of streptozotocin in citrate buffer pH 4.5 intraperitoneally, following a preliminary administration of an aqueous solution of 110 mg/kg of nicotinamide [28]. Group 4 received 300 mg/kg of trypsin hydrolysate of bovine colostrum for 30 days. A DE006A 18G×50 mm probe (Great Britain) was used for intragastric administration of colostrum peptides. All the animals were weighed every week.

All the animals were withdrawn from the experiment by intramuscular administration of 40 mg/kg of sodium pentobarbital. Blood samples for biochemical studies were collected from the tail vein with anticoagulant heparin. The content of glycated hemoglobin (HbA1c) was determined in whole blood by affinity gel chromatography using a GLYCOHEMOTEST kit (ELTA, Russian Federation). Blood plasma was separated from the new elements by centrifugation at 1000 g for 10 min. The content of glucose in blood plasma was determined by the glucose oxidase method using a Glucose-Novo reagent

kit (Vector-Best, Russian Federation). The blood plasma was tested for free radical oxidation products that react with thiobarbituric acid, including malondialdehyde malondialdehyde (MDA) [29]. The amount of reduced glutathione (GSH) and other thiols in the blood plasma was defined using Ellman's reagent (5,5'-dithiobis(2-nitrobenzoic acid) [30].

Erythrocytes were mixed with distilled water in a ratio of 1:18, cooled at 4°C for 1 h, and centrifuged again at 1000 g for 10 min. After that, the hemoglobin content was determined to recalculate the indicators of the free radical oxidation – antioxidant protection system (FRO-AOD) per gram of hemoglobin. The procedure involved a Vital reagent kit (Vital Development Corporation, Russian Federation). In the erythrocyte hemolysate, the catalase activity (Enzyme Commission number EC 1.11.1.6) was determined by the decrease in the amount of hydrogen peroxide, which formed a dyed complex with ammonium molybdate [31].

The optical density was measured with a Beckman DU-800 spectrophotometer (USA).

The hematological parameters were obtained using an automated hematological analyzer Celly 70 (Biocode Hycel), designed to study experimental animal blood.

The statistical analysis relied on the OriginPro 9.0 software (OriginlabCorporation, USA). The data were presented as mean \pm standard error. The statistical significance of differences in the data obtained was assessed using the nonparametric Mann-Whitney test (U). The difference in the mean values within a group had a 5% significance level ($p < 0.05$).

RESULTS AND DISCUSSION

Table 1 describes three biologically active peptides isolated from hydrolyzed bovine colostrum proteins. Peptide 1 with a mass of 8.4 kDa contained 20 amino acids and demonstrated a significant antioxidant activity in comparison with other samples, as revealed by the FRAP method.

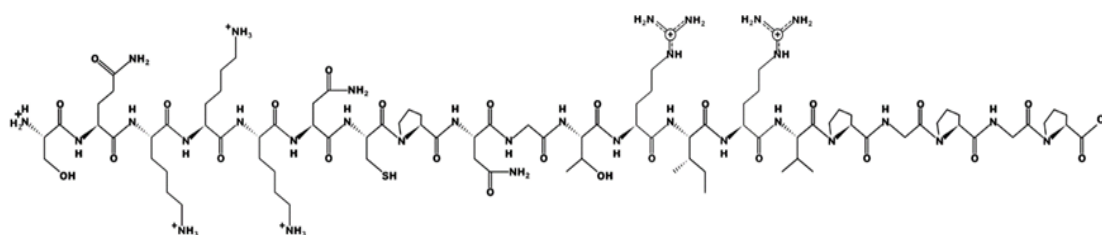
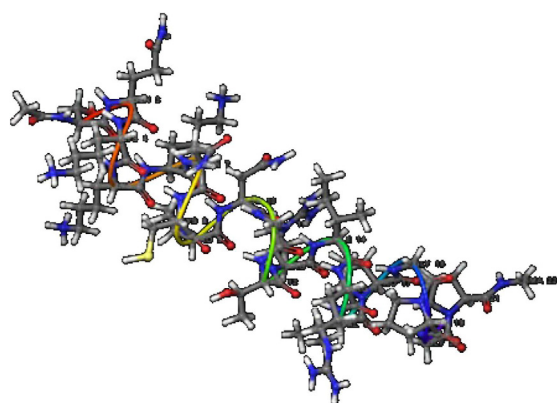
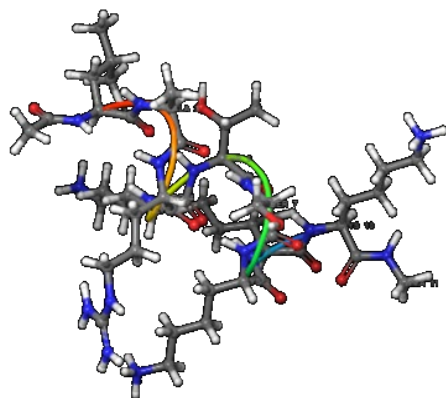
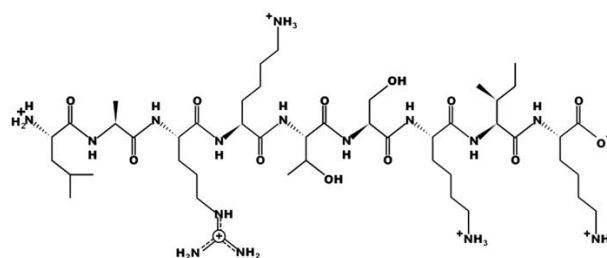
The antioxidant activity against DPPH and ABTS radicals demonstrated by peptide 1 indicated that the mix of peptides and amino acids was able to suppress DPPH and ABTS. Probably, the result was due to the pairing of one unpaired electron present in these radicals. We found ambiguous data regarding the FRAP-measured relationship between the average molecular weight of the peptide and its iron-reducing capacity. Sonklin *et al.* found that peptides with a low molecular weight (< 3 kDa) demonstrated a lower FRAP value while peptides with a molecular weight of 3–5 and 5–10 kDa had a higher FRAP level [32]. However, Meza-Espinoza *et al.* reported that soybean hydrolysate with an average molecular weight of peptides \leq 1 kDa had a greater FRAP-measured antioxidant activity than those with higher molecular weight fractions [33]. Thus, both our results and review proved that molecular weight may not be the most important factor affecting the ability of peptides to reduce ferric ions.

Scientific publications report peptides with hydrophobic amino acids to have a higher antioxidant activity:

Table 1 Peptides isolated from trypsin hydrolysate of bovine colostrum

Peptide sample	1	2	3
Amino acid sequence	SQKKKNC PNGTRIRV PGPGP	LARKT SKIK	MHNNETN SASNTVN HTVTPFK ISSHKHI RTRTKKN EGKAGTI LSTALTR
Number of amino acids	20	9	49
Molecular weight, kDa	8.4	13.0	18.0
Score	90	76	89
Peptide identification	POSSUM_01-POSSUM-C- EMBRYO-2KB, Trichosurus Vulpecula	A similar peptide was not found because the level of coverage with known peptides is low	CO950255 protein, sus scrofa
Functions	n.d.	n.d.	n.d.
Antioxidant activity DPPH	1.128 ± 0.008	n.d.	n.d.
FRAP antioxidant activity	1.183 ± 0.014	n.d.	n.d.
ABTS antioxidant activity	1.079 ± 0.009	n.d.	n.d.

n.d. – no data

**Figure 1** Peptide 1: 2D structure**Figure 2** Peptide 1: 3D structure**Figure 4** Peptide 2: 3D structure**Figure 3** Peptide 2: 2D structure

alanine (Ala), lysine (Lys), proline (Pro), leucine (Leu), histidine (His), tyrosine (Tyr), and methionine (Met) [33]. Methionine (Met), cysteine (Cys), tyrosine (Tyr), tryptophan (Trp), histidine (His), and lysine (Lys) increased the iron-reducing ability of peptides while the aromatic amino acids enhanced the antiradical activity of peptides [34–36].

A comparative analysis of ABTS, DPPH, and FRAP antioxidant tests revealed that the antioxidant activity of peptides depended on the amino acid composition of peptide sequences. The low molecular weight peptides exhibited higher antioxidant activity against the DPPH radical compared to those with a high molecular weight. The samples with a lower average molecular weight consisted of shorter and more active peptides that acted as electron donors. They reacted with free radicals and turned them into more stable substances, thus stopping free radical chain oxidation reactions.

Figures 1–6 show simulated 2D and 3D structures of the peptides.

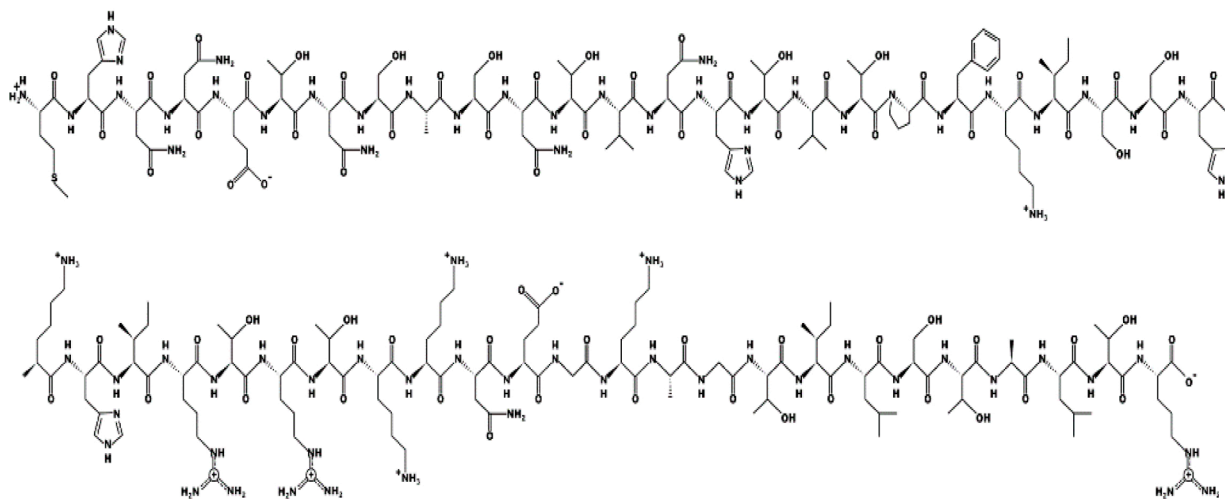


Figure 5 Peptide 3: 2D structure

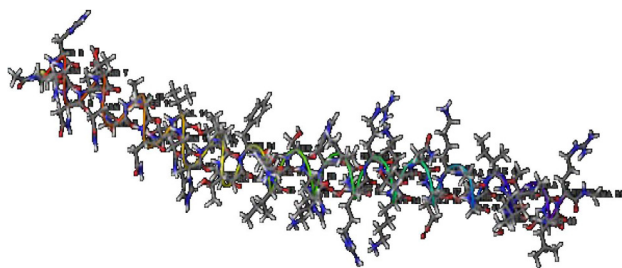


Figure 6 Peptide 3: 3D structure

The spatial models of peptides isolated from fermented bovine colostrum hydrolysate established that the amino acid sequences formed secondary structures. These structures were mostly represented by an alpha helix since they contained little aromatic amino acid residues. This fact explained the lack of antiradical activity in peptides 2 and 3. According to Wang *et al.*, aromatic amino acids enhance the antioxidant activity of peptides [36].

All the peptides in this study had the isoelectric point in a highly-alkaline medium. Peptide 1 had the isoelectric point at pH 11.62 while peptide 2 had it at pH 11.79. The points depended not on the number of amino acids but on the predominance of amine or carboxyl groups in the peptide.

The peptide structure modeling revealed the range of peptide hydrophilicity from +16.95 Kcal/mol in peptide 2 to +48.34 Kcal/mol in peptide 3. Peptide 1 had a hydrophilicity level of +25.51 Kcal/mol.

The 3D model showed that peptide 3 with its charge of +6 had a higher chemical activity than the rest: peptide 1 had a charge of +4, and peptide 2 had a charge of +5.

The intragastric administration of colostrum peptides caused no significant changes in body weight, glucose, and glycated hemoglobin in healthy rats, compared to the control (Table 2).

Unlike the healthy and control rats, the experimental diabetic rats demonstrated a lower body weight, higher glucose levels, and more glycated hemoglobin by day 30 (Table 2). The administration of colostrum peptides to diabetic rats did not prevent weight loss, but the hyperglycemia was less severe, unlike in group 3 (untreated diabetic rats), which included untreated diabetic rats (Table 2).

The administration of colostrum peptides to healthy animals did not increase the amount of malondialdehyde in the blood plasma (Table 3). However, group 2, which included healthy rats treated with colostrum peptides, had a higher content of reduced glutathione and catalase activity compared to the control. The intragastric administration procedures definitely caused stress, which inevitably disturbed homeostasis in the free radical oxidation-antioxidant protection system. The fact that the malondialdehyde did not increase in group 2 indicated a slight increase in the free radical oxidation and a compensation for this process.

Diabetic rats started accumulating malondialdehyde, and the level of reduced glutathione dropped by 5.2 times. They demonstrated a greater catalase activity than the healthy rats (Table 3). Despite the catalase activation, the diabetic rats lacked the non-enzymatic link of antioxidant protection but accumulated secondary products of free radical oxidation, which indicated the development of oxidative stress.

The diabetic rats treated with colostrum peptides (Group 4) had a lower content of malondialdehyde and catalase activity while their level of reduced glutathione stabilized, compared to the untreated diabetic rats (Table 3). While glutathione was the only indicator that stabilized in Group 4, this change can still be assessed as a decrease in the severity of oxidative stress under the action of colostrum. Glutathione contains γ -glutamic acid, cysteine, and glycine. In the diabetic rats treated with colostrum peptides, it could increase because its synthesis increased under the action of colostrum peptide amino acids.

Table 2 Indicators of diabetes mellitus

Parameter	Group 1 Healthy rats (Control)	Group 2 Healthy rats treated with colostrum peptides	Group 3 Untreated diabetic rats	Group 4 Diabetic rats treated with colostrum peptides
Body weight at the start of the experiment, g	332 ± 19	332 ± 19	352 ± 17	307 ± 26
Body weight at the end of the experiment, g	393 ± 8	361 ± 17	264 ± 18* ²	295 ± 17* ²
Glucose, mmol/L	6.0 ± 0.2	6.1 ± 0.3	18.6 ± 1.2* ²	11.2 ± 1.9* ^{2,3}
HbA1c, %	4.7 ± 0.3	4.5 ± 0.2	10.1 ± 0.3* ²	7.4 ± 0.5* ^{2,3}

* – the difference with the indicator in the control is significant at $p < 0.05$

^{2,3} – the difference with groups 2 and 3 is significant at $p < 0.05$

Table 3 Indicators of oxidative stress

Parameter	Group 1 Healthy rats (Control)	Group 2 Healthy rats treated with colostrum peptides	Group 3 Untreated diabetic rats	Group 4 Diabetic rats treated with colostrum peptides
Malondialdehyde, $\mu\text{mol/L}$	2.01 ± 0.06	2.23 ± 0.18	3.44 ± 0.22* ²	2.89 ± 0.06* ^{2,3}
Glutathione, $\mu\text{mol/L}$	24.38 ± 2.88	41.84 ± 3.61*	4.67 ± 0.71* ²	23.46 ± 6.50* ^{2,3}
Catalase, mmol/min·g Hb	57.86 ± 2.79	70.36 ± 3.94*	99.19 ± 1.68* ²	74.60 ± 3.77* ³

* – the difference with the indicator in the control is significant at $p < 0.05$

^{2,3} – the difference with groups 2 and 3 is significant at $p < 0.05$

Table 4 Hematological indicators

Parameter	Group 1 Healthy rats (Control)	Group 2 Healthy rats treated with colostrum peptides	Group 3 Untreated diabetic rats	Group 4 Diabetic rats treated with colostrum peptides
Leukocytes, thousand/ μL	10.18 ± 1.14	11.17 ± 0.74	7.43 ± 0.85 ²	8.78 ± 0.65 ²
Lymphocytes, thousand/ μL	7.63 ± 0.91	8.21 ± 0.73	4.53 ± 0.54* ²	5.77 ± 0.57 ²
Monocytes, thousand/ μL	0.27 ± 0.03	0.33 ± 0.03	0.25 ± 0.03	0.30 ± 0.03
Granulocytes, thousand/ μL	2.28 ± 0.25	2.63 ± 0.10	2.65 ± 0.31	2.72 ± 0.23
Lymphocytes, %	74.5 ± 1.4	72.6 ± 2.2	60.5 ± 1.5* ²	65.4 ± 3.2*
Monocytes, %	2.8 ± 0.1	3.2 ± 0.2	3.9 ± 0.2	3.5 ± 0.2
Granulocytes, %	22.8 ± 1.5	24.2 ± 2.1	35.6 ± 1.4*	31.2 ± 3.1
Erythrocytes, mln/ μL	8.50 ± 0.12	8.72 ± 0.09	10.00 ± 0.20*	9.93 ± 0.39
Hemoglobin, g/L	164.3 ± 3.1	166.4 ± 1.4	192.7 ± 4.3*	190.2 ± 5.7*
Hematocrit, %	45.6 ± 0.8	45.9 ± 0.6	53.4 ± 1.1*	52.7 ± 1.5*
MCV, fl	53.7 ± 0.8	52.7 ± 0.6	53.4 ± 0.6	53.2 ± 0.9
MCH, pg	19.3 ± 0.3	19.0 ± 0.2	19.2 ± 0.2	19.2 ± 0.3
MCHC, g/L	360.2 ± 1.4	362.4 ± 2.2	360.7 ± 2.1	360.7 ± 1.2
RDW, %	12.2 ± 0.3	12.2 ± 0.2	12.1 ± 0.4	12.4 ± 0.2
Platelets, thousand/mkl	1067 ± 129	1198 ± 91	1300 ± 184	1282 ± 129
MPV, fl	6.23 ± 0.11	6.39 ± 0.19	6.32 ± 0.21	6.37 ± 0.29
PDV, %	15.7 ± 0.1	15.7 ± 0.1	15.9 ± 0.1	15.8 ± 0.2
Pct, %	0.44 ± 0.14	0.66 ± 0.01	0.63 ± 0.06	0.62 ± 0.03

* – the difference with the indicator in the control is significant at $p < 0.05$

^{2,3} – the difference with groups 2 and 3 is significant at $p < 0.05$

The diabetic rats treated with colostrum hydrolysate demonstrated a less severe oxidative stress because the hydrolysate contained a peptide with antioxidant properties, namely peptide 1.

The hematological analysis revealed no abnormalities in leukocyte, erythrocyte, or platelet parameters in healthy rats treated with colostrum peptides (Table 4). The untreated diabetic rats demonstrated a lower absolute and relative number of leukocytes due to the fraction of lymphocytes with a greater proportion of granulocytes.

Leukopenia and lymphopenia in diabetic rats might have been caused by the destructive processes in the organs of the immune system [37]. The untreated diabetic rats also had a greater number of erythrocytes, and the hemoglobin content also increased by 1.2 times, affected by a larger number of erythrocytes. Therefore, the hematocrit increased by 1.2 times relative to the healthy rats. Other hematological parameters remained within the norm (Table 4). The high content of erythrocytes and hemoglobin in the diabetic rats may be a consequence

of hypoxia caused by diabetes mellitus. In the diabetic rats treated with colostrum peptides, the values of leukocytes and erythrocytes approached those in the healthy rats, but the relative number of granulocytes and the number of erythrocytes were the only parameters that stabilized (Table 4).

CONCLUSION

1. The intragastric administration of 300 mg/kg of bovine colostrum peptides to the healthy rats caused minor and compensated changes in the antioxidant system but did not affect the level of glycemia and hematological parameters.

2. The rats with diabetes mellitus developed hyperglycemia, oxidative stress, leukopenia, and a slight increase in the number of red blood cells and hemoglobin.

3. The diabetic rats treated with 300 mg/kg of colostrum peptides had a lower hyperglycemia and oxidative stress, as well as better hematological parameters.

4. The peptide with the amino acid sequence SQKKKNCPNGTRIRVPGPGP and a mass of 8.4 kDa added the antioxidant effect to colostrum hydrolysate.

Thus, the isolation of individual colostrum peptides is relevant for studying their antidiabetic properties in the future.

CONTRIBUTION

The authors were equally involved in the writing of the manuscript and bear equal responsibility.

CONFLICT OF INTEREST

The authors declared no conflict of interests regarding the publication of this article.

REFERENCES

1. International Diabetes Federation: Diabetes Atlas 8th edition. 2017.
2. Ademosun AO. Glycemic properties of soursop-based ice cream enriched with moringa leaf powder. *Foods and Raw Materials*. 2021;9(2):207–214. <https://doi.org/10.21603/2308-4057-2021-2-207-214>
3. Zaytseva LV, Ruban NV, Tsyganova TB, Mazukabzova EV. Fortified confectionery creams on vegetable oils with a modified carbohydrate profile. *Food Processing: Techniques and Technology*. 2022;52(3):500–510. (In Russ.). <https://doi.org/10.21603/2074-9414-2022-3-2377>
4. Artasensi A, Pedretti A, Vistoli G, Fumagalli L. Type 2 diabetes mellitus: A review of multi-target drugs. *Molecules*. 2020;25(8). <https://doi.org/10.3390/molecules25081987>
5. Holst JJ. From the incretin concept and the discovery of GLP-1 to today's diabetes therapy. *Frontiers in Endocrinology*. 2019;10. <https://doi.org/10.3389/fendo.2019.00260>
6. Pereira ASP, Banegas-Luna AJ, Peña-García J, Pérez-Sánchez H, Apostolides Z. Evaluation of the anti-diabetic activity of some common herbs and spices: Providing new insights with inverse virtual screening. *Molecules*. 2019;24(22). <https://doi.org/10.3390/molecules24224030>
7. Lin Y-H, Chen G-W, Yeh CH, Song H, Tsai J-S. Purification and identification of angiotensin I-converting enzyme inhibitory peptides and the antihypertensive effect of *Chlorella sorokiniana* protein hydrolysates. *Nutrients*. 2018;10(10). <https://doi.org/10.3390/nu10101397>
8. Andreeva A, Budenkova E, Babich O, Sukhikh S, Ulrikh E, Ivanova S, et al. Production, purification, and study of the amino acid composition of microalgae proteins. *Molecules*. 2021;26(9). <https://doi.org/10.3390/molecules26092767>
9. Li Y, Aiello G, Bollati C, Bartolomei M, Arnoldi A, Lammi C. Phycobiliproteins from *Arthrospira platensis* (spirulina): A new source of peptides with dipeptidyl peptidase-IV inhibitory activity. *Nutrients*. 2020;12(3). <https://doi.org/10.3390/nu12030794>
10. Novoselova MV, Prosekov AYu. Technological options for the production of lactoferrin. *Foods and Raw Materials*. 2016;4(1):90–101. <https://doi.org/10.21179/2308-4057-2016-1-90-101>
11. Manzanares P, Gandía M, Garrigues S, Marcos JF. Improving health-promoting effects of food-derived bioactive peptides through rational design and oral delivery strategies. *Nutrients*. 2019;11(10). <https://doi.org/10.3390/nu11102545>
12. Suo S-K, Zheng S-L, Chi C-F, Luo H-Y, Wang B. Novel angiotensin-converting enzyme inhibitory peptides from tuna byproducts-milts: Preparation, characterization, molecular docking study, and antioxidant function on H₂O₂-damaged human umbilical vein endothelial cells. *Frontiers in Nutrition*. 2022;9. <https://doi.org/10.3389/fnut.2022.957778>
13. Ryazantseva KA, Agarkova EYu, Fedotova OB. Continuous hydrolysis of milk proteins in membrane reactors of various configurations. *Foods and Raw Materials*. 2021;9(2):271–281. <https://doi.org/10.21603/2308-4057-2021-2-271-281>.
14. Ayala-Niño A, Rodríguez-Serrano GM, González-Olivares LG, Contreras-López E, Regal-López P, Cepeda-Saez A. Sequence identification of bioactive peptides from amaranth seed proteins (*Amaranthus hypochondriacus* spp.). *Molecules*. 2019;24(17). <https://doi.org/10.3390/molecules24173033>

15. Rubak YuT, Nuraida L, Iswantini D, Prangdimurti E. Angiotensin-I-converting enzyme inhibitory peptides in milk fermented by indigenous lactic acid bacteria. *Veterinary World*. 2020;13(2):345–353. <https://doi.org/10.14202/vetworld.2020.345-353>
16. Zhang R, Chen J, Mao X, Qi P, Zhang X. Separation and lipid inhibition effects of a novel decapeptide from *Chlorella pyrenoidose*. *Molecules*. 2019;24(19). <https://doi.org/10.3390/molecules24193527>
17. Valenzuela Zamudio F, Segura Campos MR. Amaranth, quinoa and chia bioactive peptides: a comprehensive review on three ancient grains and their potential role in management and prevention of Type 2 diabetes. *Critical Reviews in Food Science and Nutrition*. 2020;62(10):2707–2721. <https://doi.org/10.1080/10408398.2020.1857683>
18. Quintero-Soto MF, Chávez-Ontiveros J, Garzón-Tiznado JA, Salazar-Salas NY, Pineda-Hidalgo KV, Delgado-Vargas F, et al. Characterization of peptides with antioxidant activity and antidiabetic potential obtained from chickpea (*Cicer arietinum* L.) protein hydrolyzates. *Journal of Food Science*. 2021;86(7):2962–2977. <https://doi.org/10.1111/1750-3841.15778>
19. Uyama T, Kelton DF, Winder CB, Dunn J, Goetz HM, LeBlanc SJ, et al. Colostrum management practices that improve the transfer of passive immunity in neonatal dairy calves: A scoping review. *PLoS ONE*. 2022;17(6). <https://doi.org/10.1371/journal.pone.0269824>
20. Tikhonov SL, Tikhonova NV, Tursunov KhKh, Danilova IG, Lazarev VA. Peptides of trypsin hydrolyzate in bovine colostrum. *Food Processing: Techniques and Technology*. 2023;53(1):150–158. (In Russ.). <https://doi.org/10.21603/2074-9414-2023-1-2422>
21. Playford RJ, Weiser MJ. Bovine colostrum: Its constituents and uses. *Nutrients*. 2021;13(1). <https://doi.org/10.3390/nu13010265>
22. Brenmoehl J, Ohde D, Wirthgen E, Hoeflich A. Cytokines in milk and the role of TGF-beta. *Best Practice and Research Clinical Endocrinology and Metabolism*. 2018;32(1):47–56. <https://doi.org/10.1016/j.beem.2018.01.006>
23. Inabu Y, Pyo J, Pletts S, Guan LL, Steele MA, Sugino T. Effect of extended colostrum feeding on plasma glucagon-like peptide-1 concentration in newborn calves. *Journal of Dairy Science*. 2019;102(5):4619–4627. <https://doi.org/10.3168/jds.2018-15616>
24. Ashok NR, Aparna HS. Empirical and bioinformatic characterization of buffalo (*Bubalus bubalis*) colostrum whey peptides & their angiotensin I-converting enzyme inhibition. *Food Chemistry*. 2017;228:582–594. <https://doi.org/10.1016/j.foodchem.2017.02.032>
25. Agarkova EYu, Ryazantseva KA, Kruchinin AG. Anti-diabetic activity of whey proteins. *Food Processing: Techniques and Technology*. 2020;50(2):306–318. (In Russ.). <https://doi.org/10.21603/2074-9414-2020-2-306-318>
26. Golovach TN, Kurchenko VP, Tarun EI. Protein-peptide composition and radical reducing properties of fermented bovine colostrum. *Food Industry: Science and Technologies*. 2016;33(3):57–63. (In Russ.). <https://elibrary.ru/XAMKJF>
27. Feduraev P, Skrypnik L, Nebreeva S, Dzhobadze G, Vatagina A, Kalinina E, et al. Variability of phenolic compound accumulation and antioxidant activity in wild plants of some *Rumex* species (*Polygonaceae*). *Antioxidants*. 2022;11(2). <https://doi.org/10.3390/antiox11020311>
28. Spasov AA, Vorohkova MP, Snegur GL, Cheplyaeva NI, Chepurnova MV. Experimental model of a type 2 diabetes. *Journal Biomed*. 2011;(3):12–18. (In Russ.). <https://elibrary.ru/OJBTOH>
29. Stal'naya ID, Garishvili TG. Determining malondialdehyde with thiobarbituric acid. In: Orekhovicha VN, editor. *Modern methods in biochemistry*. Moscow: Meditsina; 1977. pp. 66–68. (In Russ.).
30. Verevkin IV, Tochilkin AI, Popova NA. Colorimetric determination of SH-groups and –SS-bonds in proteins with 5,5'-dithiobis(2-nitrobenzoic) acid. In: Orekhovicha VN, editor. *Modern methods in biochemistry*. Moscow: Meditsina; 1977. pp. 223–231. (In Russ.).
31. Korolyuk MA, Ivanova LN, Mayorova IG, Tokarev VE. Determining catalase activity. *Laboratory Sphere*. 1988;(4): 44–47. (In Russ.).
32. Sonklin C, Laohakunjit N, Kerdchoechuen O. Assessment of antioxidant properties of membrane ultrafiltration peptides from mungbean meal protein hydrolysates. *PeerJ*. 2018;6. <https://doi.org/10.7717/peerj.5337>
33. Meza-Espinoza L, Sáyo-Ayerdi SG, García-Magaña ML, Tovar-Pérez EG, Yahia EM, Vallejo-Cordoba B, et al. Antioxidant capacity of egg, milk and soy protein hydrolysates and biopeptides produced by *Bromelia pinguin* and *Bromelia karatas*-derived proteases. *Emirates Journal of Food and Agriculture*. 2018;30(2):122–130. <https://doi.org/10.9755/ejfa.2018.v30.i2.1604>

34. Samaranyaka AGP, Li-Chan ECY. Food-derived peptidic antioxidants: A review of their production, assessment, and potential applications. *Journal of Functional Foods*. 2011;3(4):229–254. <https://doi.org/10.1016/j.jff.2011.05.006>
35. Carrasco-Castilla J, Hernández-Álvarez AJ, Jiménez-Martínez C, Jacinto-Hernández C, Alaiz M, Girón-Calle J, et al. Antioxidant and metal chelating activities of *Phaseolus vulgaris* L. var. Jamapa protein isolates, phaseolin and lectin hydrolysates. *Food Chemistry*. 2012;131(4):1157–1164. <https://doi.org/10.1016/j.foodchem.2011.09.084>
36. Wang Y-Y, Wang C-Y, Wang S-T, Li Y-Q, Mo H-Z, He J-X. Physicochemical properties and antioxidant activities of tree peony (*Paeonia suffruticosa* Andr.) seed protein hydrolysates obtained with different proteases. *Food Chemistry*. 2021;345. <https://doi.org/10.1016/j.foodchem.2020.128765>
37. Queiroz LAD, Assis JB, Guimarães JPT, Sousa ESA, Milhomem AC, Sunahara KKS, et al. Endangered lymphocytes: The effects of alloxan and streptozotocin on immune cells in type 1 induced diabetes. *Mediators Inflammation*. 2021;2021. <https://doi.org/10.1155/2021/9940009>

ORCID IDs

Sergei L. Tikhonov  <https://orcid.org/0000-0003-4863-9834>
Natalia V. Tikhonova  <https://orcid.org/0000-0001-5841-1791>
Irina F. Gette  <https://orcid.org/0000-0003-3012-850X>
Ksenia V. Sokolova  <https://orcid.org/0000-0002-7024-4110>
Irina G. Danilova  <https://orcid.org/0000-0001-6841-1197>



Coffee pulp pretreatment methods: A comparative analysis of hydrolysis efficiency

Do Viet Phuong*, Luu Thao Nguyen

Industrial University of Ho Chi Minh City^{ROR}, Ho Chi Minh, Vietnam

* e-mail: dovietphuong@iuh.edu.vn

Received 05.01.2023; Revised 28.02.2023; Accepted 07.03.2023; Published online 30.08.2023

Abstract:

The Vietnamese food industry produces a lot of coffee pulp, which is a valuable and abundant source of agricultural by-products. It contains a lot of cellulose, which can be converted into bioethanol. However, coffee pulp needs an extensive pretreatment to reduce the amount of lignin and hemicellulose while retaining the initial cellulose composition. This study compared several pre-hydrolysis and pre-fermentation pretreatment methods which involved H_2SO_4 , NaOH, microwaves, and white rot fungus *Phanerochaete chrysosporium*.

The hemicellulose dropped by 43.8% after the acidic pretreatment, by 47.1% after the alkaline pretreatment, and by 12.8% after the microbial pretreatment. The lignin contents dropped by 4.2, 76.6, and 50.2% after acidic, alkaline, and microbial pretreatment, respectively. The removal of hemicellulose and lignin in the coffee pulp was much more efficient when two or three of the pretreatment methods were combined. The microwave-assisted acid and alkaline pretreatment was the most efficient method: it removed 71.3% of hemicellulose and 79.2% of lignin. The combined method also had the highest amount of reducing sugars and glucose in hydrolysate. Additionally, concentrations of such yeast inhibitors as 5-hydroxymethyl-2-furaldehyde (HMF) and furfural were 2.11 and 3.37 g/L, respectively.

The acid pretreatment was effective only in removing hemicellulose while the alkaline pretreatment was effective in lignin removal; the fungal pretreatment had low results for both hemicellulose and lignin removals. Therefore, the combined pretreatment method was found optimal for coffee pulp.

Keywords: Coffee pulp, hydrolysis, lignin, hemicellulose, reducing sugars, acidic pretreatment, alkaline pretreatment

Please cite this article in press as: Phuong DV, Nguyen LT. Coffee pulp pretreatment methods: A comparative analysis of hydrolysis efficiency. *Foods and Raw Materials*. 2024;12(1):133–141. <https://doi.org/10.21603/2308-4057-2024-1-594>

INTRODUCTION

No ethanol can be obtained from lignocellulose biomass without some kind of pre-fermentation pretreatment which converts carbohydrate polymers in lignocellulose into simpler sugar. This conversion usually involves hydrolytic enzymes. Lignocellulose biomass possesses heterogeneous and very complex properties, e.g., cellulose crystallization, degree of coincidence, humidity, surface area, bonding level of lignin and hemicellulose, etc. As a result, this biomass requires special processing to be able to regulate the hydrolytic activity of the enzyme. The pretreatment also decreases the amount of lignin and hemicellulose in the raw material while retaining cellulose components and reducing the crystallization of cellulose (Fig. 1).

Coffee pulp is one of the most abundant sources of lignocellulose biomass in Vietnam. Coffee pulp is the

first by-product obtained from wet processing during coffee production. The global coffee production is responsible for around 22 million tons of fresh pulp per year, 2.4 million tons of mucilage, and about 8.6 million tons of parchment. The Vietnamese coffee industry dumps about 0.5 million tons of dried pulp into the environment [2]. A combined effort of technology, economics, and environmentalism is needed to cope with this waste issue. The main chemical components of coffee pulp include cellulose (25.88%), hemicellulose (3.6%), lignin (20.07%), protein (9.52%), total sugars (9.18%), and ash (6.29%). Coffee pulp has a high nutritional value, which makes it a valuable source of animal feed. However, coffee pulp also contains some non-nutritional ingredients, such as tannins (8.69%) and caffeine (0.78%), which are bad for food metabolism [3].

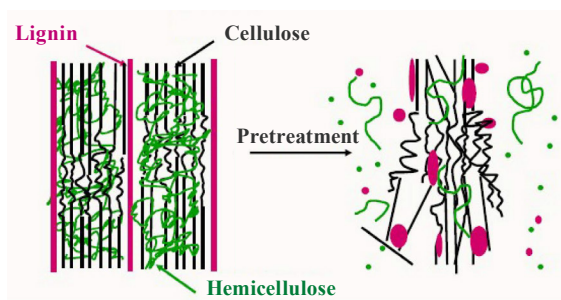


Figure 1 Material structure before and after pretreatment [1]

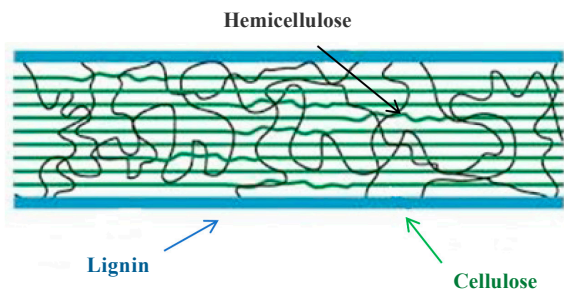


Figure 2 Lignocellulose structure [1]

Several recent studies reported that coffee pulp has a great potential for ethanol production [4–6]. Unfortunately, it also contains a lot of hemicellulose and lignin, which bind to cellulose (Fig. 2) to form a barrier that protects cellulose molecules from the attack of chemicals and enzymes. Therefore, ethanol production needs new pretreatment methods to remove lignin while retaining cellulose in the raw material prior to hydrolysis and fermentation.

The list of pretreatment methods that remove lignin and hemicellulose includes acid pretreatment, alkaline pretreatment, steam explosion pretreatment, microwave pretreatment, hydrothermal pretreatment, and microbial pretreatment [7–12]. Chemical and thermal pretreatment methods all share the same disadvantages, such as environmental pollution, equipment corrosion, high cost, and production of yeast inhibitors. Microbial pretreatment method overcomes these disadvantages but has a long processing time and low effectiveness of lignin and hemicellulose removal.

Lignin is one of the main components that make up plant and algal cells. It is the most abundant component found in tree trunks, and it is often called “wood matter”. In coffee pulp, lignin accounts for about 17.5–20.07%, while lignin contents in straw, corn cores, sugarcane, and grass are 4.65, 15, 20, and 12–18%, respectively [3, 13]. Coffee pulp has a higher lignin content than other sources of lignocellulose biomass, which is a major challenge for its pretreatment processing before hydrolysis and fermentation. Therefore, ethanol production needs more in-depth surveys of pretreatment methods and their combinations that would remove lignin and hemicellulose components while retaining cellulose.

STUDY OBJECTS AND METHODS

Biomass samples. Fresh coffee berries were collected in Pong Drang commune, Krong Buk district, Dak Lak province, Vietnam, in November and December. They went through a rubbing machine to remove the peel. After that, the pulp was left to dry at 60°C for 12 h until the humidity was 5–8% prior to being ground in a disc mill. The resulting powder was sifted through a multi-layer sifting system with sieve diameters of 0.25, 0.5, 1, and 2 mm. The powder that did not sift through the two-millimeter sieve grid underwent re-crushing. The study involved only the powder that went through the sieve grids of 1–2 mm (Fig. 3).

Chemicals, enzymes, and microorganism strains.

The research involved the following chemicals:

- DNS Reagents (Guangzhou, Guangdong, China);
- CTAB (sigma-Aldrich, Singapore);
- EDTA (Guangzhou, Guangdong, China);
- lignin (Sigma-Aldrich, USA);
- CMC (Sigma-Aldrich, USA);
- TBP (Sigma-Aldrich, USA);
- glucose (Sigma-Aldrich, USA);
- Viscozyme® Cassava C (Bagsvaerd, Denmark): > 450 EGU/g;
- glucosidase (Novozyme 188) (Novozyme, Denmark): > 750 CBU/g; and
- *Phanerochaete chrysosporium* (Southern Institute of Biotechnology and Microbiological Application, SIAMB, Ho Chi Minh, Vietnam).

Acid, alkaline, and microwave pretreatment methods. We put 50 g of dried coffee pulp into a one-liter round bottom flask and added 500 mL of 2% H₂SO₄ (w/w).

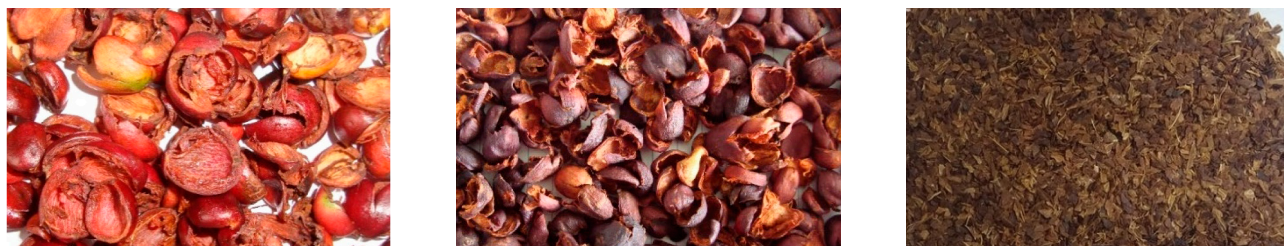


Figure 3 Fresh coffee pulp (a); dry coffee pulp (b); and grid coffee pulp (c)

The raw material was pretreated in a sterilized steamer at 140°C for 45 min and cooled to room temperature before being filtered to collect the solid residue [14, 15]. The residue was washed several times with water until neutral pH and dried at 60°C for 12 h. Then, we placed dried material into a 500-mL round bottom flask and added 2% (w/w) NaOH solution (2 g NaOH per 100 g of raw material). The alkaline pretreatment lasted 20 min at 120°C and was followed by the microwave pretreatment at 300 W for 20 min [8, 10, 16, 17]. The pretreated material was then filtered, washed in neutral pH water, and dried. The control was only pretreated with hot water under the same conditions. The effectiveness of the pretreatment process was tested using surface SEM scans for the remaining fiber content and the reducing sugar in the pretreatment solution.

The concentrations of cellulose, hemicellulose, and lignin remaining in the pretreated material were calculated according to the equation below [7]:

$$R_x = \frac{A_p}{A_i} \times 100 \quad (1)$$

where R_x is the percentage of cellulose (R_C), hemicellulose (R_H), or lignin (R_L) remaining in the pretreated pulp, %; A_i is the amount of the constituent in the initial dried coffee pulp, g; A_p is the amount of the constituent after pretreatment of the dried coffee pulp, g.

Fungi pretreatment method. White rot fungus *P. chrysosporium* was cultured in a semi-solid medium, which contained 2 g of rice bran, 8 g of coconut, 25 g of fishmeal, 25 g of oil cake, and 0.15 g of sugar rust (Fig. 4). The cultivation lasted 7 days. After that, the mass was filtered and centrifuged at 5000 rpm to obtain the fungal biomass. The pretreatment with *P. chrysosporium* took place at 35°C with the biomass to raw material ratio of 1.5%. A portion of the raw material was taken for cellulose, hemicellulose, and lignin quantification after 10, 20, 30, 40, and 50 days.

Hydrolysis method. We put 15 g of the pretreated raw material into a 250 mL Erlenmeyer flask and added 150 mL of citrate buffer (0.05 mol/L, pH 4.8), 25 FPU/g of Viscozyme Cassava, and 34 CBU/g of Novozyme 188. The hydrolysis occurred on a shaker at 150 rpm under 50°C and lasted 72 h. The hydrolysis mix was centrifuged at 2500 rpm for 10 min to collect the supernatant for the reducing sugar and glucose analysis [3]. The processing involved the control sample, in which raw material was omitted. The hydrolysis performance (YEH, %) was calculated according to the following formula [7]:

$$YEH = \frac{0.9(G_e - G_w)}{C_p} \times 100 \quad (2)$$

where G_e is the glucose concentration at the end of the enzymatic hydrolysis, g glucose/L; G_w is the glucose concentration without enzyme treatment, g glucose/L; and C_p is the cellulose concentration in the pretreated material, g cellulose/L.

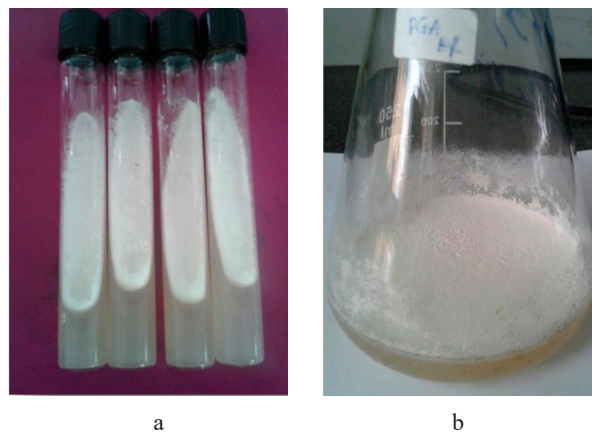


Figure 4 *Phanerochaete chrysosporium* strains (a); *Phanerochaete chrysosporium* on PGA (b)

Analytical methods. The reducing sugar content was determined using the dinitrosalicylic acid (Miller/DNS) method [19]. The glucose content was determined by optical measurement at a wavelength of 540 nm using an oxidase/peroxidase system [20]. The cellulose and hemicellulose content was determined using the ADF and NDF methods [21]. The lignin content was determined according to U.S. TAPPI standards (TAPPI T. 222 OM-02 Acid-insoluble lignin in wood and pulp).

The filter paper (FPU, U/mL) assay tested the saccharifying of cellulase: it was based on the hydrolysis of filter paper by cellulase solution [22]. The amount of glucose produced was determined using the dinitrosalicylic acid method [19].

$$FPU = \frac{0.37}{\text{enzyme concentration to release 2 mg glucose}} \quad (3)$$

The carboxymethyl cellulase (CMC, U/mL) assay for endo- β -1,4 glucanase measured the carboxymethyl cellulase hydrolysis by cellulase solution [22]. The amount of glucose produced was determined using the dinitrosalicylic acid method [19].

$$CMCase = \frac{0.185}{\text{enzyme concentration to release 0.5 mg glucose}} \quad (4)$$

The cellobiase assay (CBU, U/mL) involved cellobiose hydrolysis by cellulase solution [22]. The amount of glucose produced was determined using the dinitrosalicylic acid method [19].

$$CBU = \frac{0.0926}{\text{enzyme concentration to release 1 mg glucose}} \quad (5)$$

Statistical analysis. The experiments were randomly arranged and performed in triplicates with one or two variables. We employed the ANOVA software to conclude the discrepancy between the average of the tests. The Statgraphics Centurion 15.2 software was used to process the obtained statistics. The average and standard deviation was calculated using the Excel

software. The results of the previous experiment were selected as fixed parameters for the experiments to follow.

RESULTS AND DISCUSSION

Formation of reducing sugar in pretreatment solution. Pretreatment methods increase the area of biomass surface, improve the porosity of raw materials, reduce cellulose crystallization, and remove hemicellulose and lignin. Both hemicellulose and lignin are important factors in the formation of lignocellulose biomass, and they bond with cellulose. A single pretreatment method is only good for a certain aspect but provides no resolution of the aforementioned requirements.

Therefore, a combination of many pretreatment methods can perform several tasks at once: save cellulose, reduce its crystallization, increase the surface area of contact with hydrolyzed enzymes, remove more lignin, and recover more hemicellulose.

The combination of acid and alkaline pretreatments in different orders yielded unexpected results. Most samples pretreated with alkaline, acid, or fungus resulted in a much larger content of reducing sugar in the pretreatment solution compared to the water-pretreated control samples. In particular, the acid pretreatment produced a higher amount of reducing sugar when pretreated with alkaline (Fig. 5).

Previous studies of lignocellulose biomass pretreatment showed that the lignocellulose biomass pretreated with *Phanerochaete chrysosporium* gave a low removal efficiency of 20–40%. Meanwhile, acid or alkaline pretreatment proved to be more efficient because the processing time was shorter. However, the processing temperature was much higher, which required complex and expensive equipment. Moreover, the acid or alkaline pretreatment methods resulted in a greater cellulose loss than the microbial pretreatment and could produce some yeast inhibitors. Therefore, an optimal pretreatment method or their combination depend on the nature of the

raw material and the objective, and a proper combination of different pretreatment methods can provide a greater efficiency compared to a single method.

Changes in cellulose, hemicellulose, and lignin content. The reducing sugar content in the pretreatment fluid is not the only factor to be considered when comparing different pretreatment methods. A more comprehensive comparison involves the changes in fiber composition, especially the decline of lignin and hemicellulose. Other important factors include the formation of yeast inhibitors and the content of reducing sugars that appear during hydrolysis.

Figure 6 shows that the coffee pulp pretreated with H₂SO₄ 2% (w/w) demonstrated a decrease in hemicellulose content, which dropped from 3.67 to 2.06% (equivalent to 43.8% reduction of hemicellulose). It also triggered a minor change in lignin content: only 4.18% was decomposed. The coffee pulp pretreated with 2% H₂SO₄ (w/w) was further pretreated with 2% NaOH (w/w). And as a result, the hemicellulose content went on decreasing and dropped to 1.15%, which was equivalent to a 68.6% reduction after two pretreatment steps. The lignin content saw a dramatic decrease with 77.5% of lignin being decomposed, which was equivalent to a 78.5% reduction after two pretreatment steps.

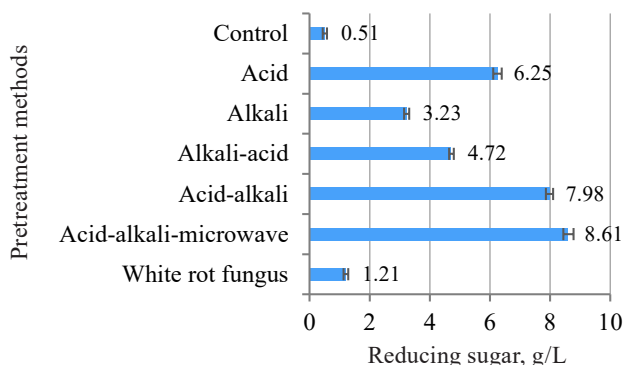


Figure 5 Effect of different pretreatment methods on the reducing sugar content in the pretreatment solution

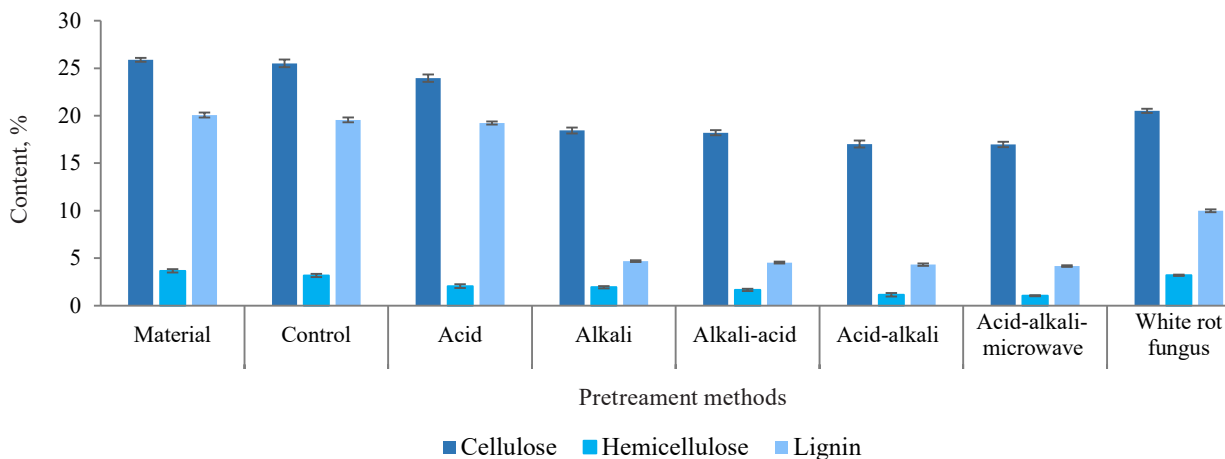


Figure 6 Changes in the composition of coffee pulp fiber

In reverse order, the hemicellulose content from coffee pulp pretreated with 2% NaOH decreased from 3.67 to 1.94%, which was equivalent to a 47.1% reduction, and the lignin decomposed by 76.6%. The coffee pulp was further pretreated with H₂SO₄, which resulted in a 54.7% reduction of hemicellulose and a 77.3% reduction of lignin after two pretreatment steps (Fig. 6).

Thus, different orders of chemical use yielded different results in coffee pulp pretreatment. Figures 5 and 6 show that the use of acid and alkaline order in pretreatment was more effective than the opposite order. The reducing sugar content in the pretreatment liquid and the reduction degree of the hemicellulose content in acid-alkaline pretreatment were both higher than those in the alkaline-acid pretreatment. Probably, the hemicellulose hydrolysis under the action of diluted acid was the same as cellulose hydrolysis. Hemicellulose was initially hydrolyzed into long oligomers, short oligomers, or monomers, depending on the temperature, acid concentration, and hydrolysis time [7].

In our experiment, hemicellulose was hydrolyzed mostly into oligomers under the action of diluted alkaline, and the number of monomers was very small. Therefore, the reducing sugar content and the reduction level of hemicellulose content in the acid-alkaline pretreatment was higher than those in the alkaline-acid pretreatment.

The pretreatment of lignocellulose biomass with diluted alkaline increased the contact surface area and reduced both coincidence and crystallization by separating the bonds between lignin and cellulose or between hemicellulose and cellulose or by disrupting the structure of lignin (Fig. 7c).

Figure 7 also illustrates the difference between the raw sample and the processed sample. The raw sample had a hard structure which was very compact and non-porous. The sample processed by diluted alkaline sho-

wed increased porosity and a larger surface area, which was due to the removal of lignin and hemicellulose.

Furfural and 5-hydroxymethyl-2-furaldehyde (HMF) formation in hydrolysis solution. The pretreatment with diluted acid or diluted alkaline at high temperatures (> 140°C) resulted in a partial hydrolyzation of cellulose and a complete hydrolyzation of hemicellulose into single sugars, e.g., glucose, xylose, arabinose, mannose, galactose, as well as acetic acid. It could also cause a partial breakdown of lignin into phenol derivatives, i.e., para-hydroxyphenyl, guaiacyl, and syringyl. In addition to that, this pretreatment method formed 5-hydroxymethyl-2-furaldehyde (HMF) and 2-furaldehyde (furfural). Organic acids, such as acetic acid or trifluoroacetic acid (TFA), appeared as a result of the decomposition of pentose and hexose [7].

Of all these intermediate products, furfural and HMF are toxic to ethanol fermentation yeast. Therefore, they had to be removed or minimized. These toxic substances often develop immediately after the pretreatment process and partially dissolve in the pretreatment solution while the rest remains in the raw material residue. Therefore, they need to be removed immediately after the pretreatment or eliminated in the hydrolysis solution prior to fermentation. Removing them immediately after the pretreatment could be difficult because they are almost evenly distributed and penetrate deep inside the raw material, which means a complex extraction. Removing them during hydrolysis seems more effective because hydrolysis is a process of extracting and diffusing toxic substances from the raw material. Therefore, removing furfural and HMF in the hydrolysis solution is more cost-effective than in the raw material.

Furfural appeared as a result of decomposing pentose sugar, which was mainly xylose. HMF resulted from the breakdown of hexose, mainly glucose and fructose. Figure 8 illustrates the furfural and HMF content in the

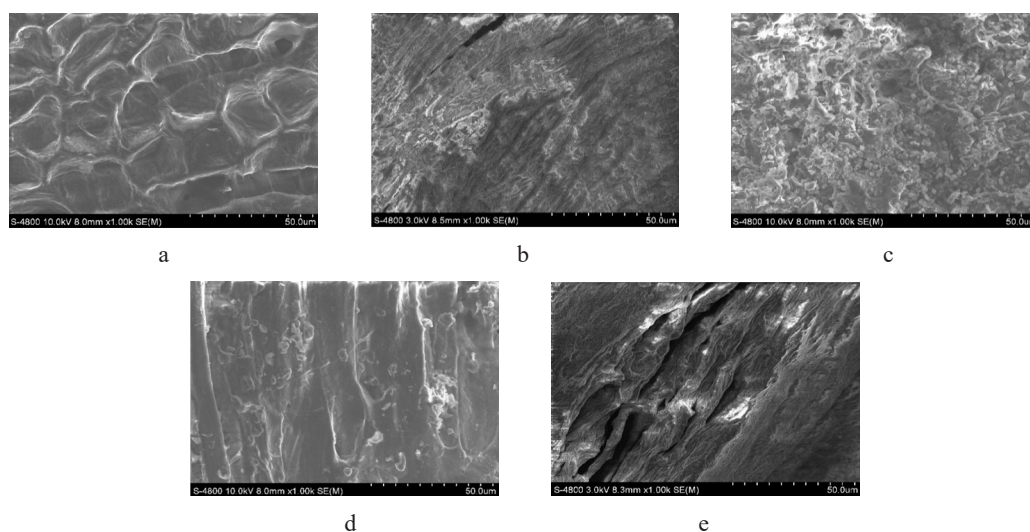


Figure 7 Scanning electron microphotographs of coffee pulp: (a) no pretreatment raw materials; (b) pretreatment with H₂SO₄ 2%; (c) pretreatment with NaOH 2%; (d) pretreatment with white rot fungus; and (e) pretreatment of acid-alkaline-microwave combination

hydrolyzed solution. The pretreatment with 2% H₂SO₄ at 140°C for 45 min provided the highest content of furfural (3.61 g/L) because diluted acid had a hydrolysis effect on hemicellulose to form xylose, which continued to decompose into furfural under high temperature. Meanwhile, two samples pretreated by acid-alkaline and acid alkaline-microwave pretreatment methods had a slightly lower furfural content because both treatments involved a neutral soaking process. As a result, water washed away and damaged a lot of furfural. The pretreatment with 2% NaOH at 120°C for 20 min also produced the highest HMF content of 2.43 g/L because alkaline had a partial hydrolysis effect on cellulose to form glucose, which was then broken down into HMF at high temperature.

The furfural and HMF contents in hydrolysis solution correlated with the cellulose and hemicellulose contents, which degraded after the pretreatment. The microbial pretreatment samples showed no signs of furfural or HMF in the hydrolysis solution because the temperature was as low as 35°C, and no acid or alkaline was involved. As the hydrolysis process by cellulase also presupposed low temperatures, no furfural or HMF were detected. The control sample was only pretreated in hot water at 140°C without acid, alkaline, or microwaves. In this case, only a small amount of hemicellulose and cellulose were hydrolyzed and decomposed into furfural and HMF (Fig. 8).

In most pretreatment methods, when the furfural and HMF content exceed 1 g/L, they have a strong inhibitory effect on microbial cell growth, especially yeast [23]. To limit their formation, pretreatment usually involves low temperatures, which affects the pretreatment efficiency. Therefore, if the pretreatment process is thermal, furfural and HMF should be removed from the hydrolysis solution prior to fermentation.

Formation of reducing sugars and glucose in hydrolysis solution. A comprehensive effectiveness test of coffee pulp pretreatment cannot be reduced to the targeted lignin or hemicellulose removal and the percentage of cellulose retained. It should involve such factors as the reduction of crystallized cellulose, the structural hollowing, the surface contact area, etc. These factors improve the hydrolysis process and control the formation of some yeast inhibitors. All of the aforementioned considerations are to be verified through the material hydrolysis process after the pretreatment process is carried out.

Therefore, we compared the effectiveness of the pretreatment processes using the content of glucose and reducing sugars released under the action of commercial cellulase enzymes, represented here by Viscozyme Cassava C and Novozyme 188 (Novo, Denmark). The hydrolysis process occurred under the following conditions. The hydrolyzed temperature was 50°C at pH 4.8. The shaking mode was 150 rpm, and the hydrolyzation time was 72 h. The concentration of Viscozyme Cassava was 25 FPU/g cellulose and that of Novozyme 188 was 34 CBU/g β-glucosidase, based on dry shell weight [24].

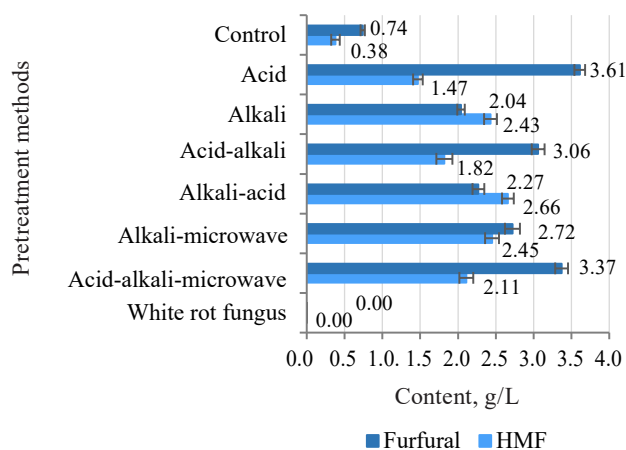


Figure 8 Effect of various pretreatment methods on 5-hydroxymethyl-2-furaldehyde (HMF) and 2-furaldehyde (furfural) in hydrolyzed solution

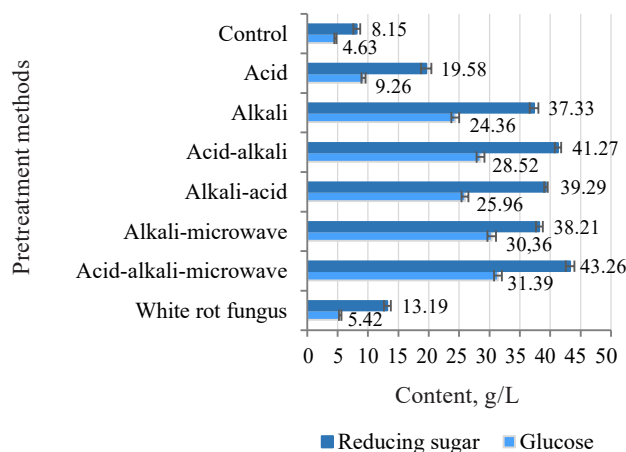


Figure 9 Effect of different pretreatment methods on the formation of glucose and reducing sugars after hydrolysis

The hydrolyzed liquid was centrifuged at 2500 rpm for 10 min. Figure 9 shows the results of the analysis of glucose and sugar content.

The purpose of the pretreatment process was to increase the sensitivity of cellulose to the hydrolyzed enzyme system. Therefore, the glucose and reducing sugar were the two components that characterized the action of the cellulase system on the cellulose component found in the coffee pulp after hydrolysis. According to Fig. 9, all the experimental samples demonstrated a better hydrolysis performance than the control sample, which involved water pretreatment under the same conditions. The glucose and reducing sugar reached the highest contents when the combined pretreatment followed the order of acid → alkaline → microwave. The glucose content was 31.39 g/L, and the reducing sugar content was 43.26 g/L.

The microbial pretreatment demonstrated the lowest results when the glucose content dropped to 5.42 g/L, and the reducing sugar content was as low as 13.19 g/L. *P. chrysosporium* secreted some extracellular enzymes,

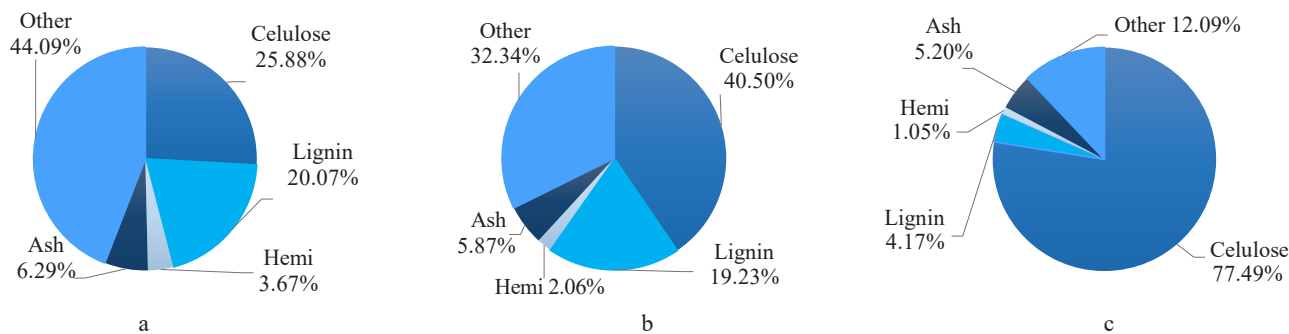


Figure 10 Coffee pulp components after different pretreatments: (a) no pretreatment; (b) acidic pretreatment; and (c) pretreatment of acid-alkaline-microwave combination

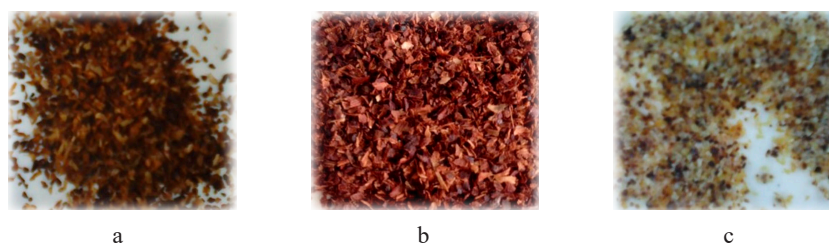


Figure 11 Color and shape of coffee pulp after different pretreatments: (a) no pretreatment; (b) acidic pretreatment; and (c) pretreatment of acid-alkaline-microwave combination

mainly active lignin hydrolysis, into the environment during the pretreatment process with only 50.2% of lignin being hydrolyzed. This rate was much lower than in the case of the acid-alkaline-microwave combination when up to 79.2% lignin was removed. *P. chrysosporium* also failed to break down hemicellulose, but was able to alter the content and the crystal structure of cellulose molecules (Fig. 7d). Therefore, the material structure was less porous, and the contact surface area and the sensitivity to hydrolysis enzymes were low. This led to a less efficient hydrolysis performance in comparison with the acid-alkaline-microwave pretreatment.

In addition, the hydrolysis performance of the enzyme was lower in the case of acid-alkaline pretreatment. The acid pretreatment resulted in 9.26 g/L of glucose and 19.58 g/L of reducing sugar. The alkaline pretreatment helped release much higher amounts of sugar than the acid pretreatment: the glucose content was 24.36 g/L, and the reducing sugar content was 37.33 g/L. The amount of reducing sugar in the alkaline pretreatment solution was lower than that in the acid pretreatment solution (Fig. 5). As the diluted acid pretreatment was the most efficient hemicellulose hydrolysis mode, the highest amount of reducing sugar appeared in the pretreatment solution. NaOH cut off the endomolecular ester bonds between hemicellulose and other molecules, including lignin. As a result, the material became porous, thus increasing the contact surface area and the amorphous region of cellulose [25].

Although the microwave pretreatment did not really degrade lignin and hemicellulose (Fig. 6), it somewhat changed the surface structure of material (Fig. 7e). Mic-

rowaves trigger two types of bipolar interactions and ion interactions which cause rotation/collision between the bipolar molecules and the ions present in the material. As a result, they generate heat and disrupt the supermolecule structure of lignocellulose biomass, both inside and outside [17, 26]. The results were truly surprising when the combination of acid-alkaline-microwave pretreatment methods followed by the hydrolysis yielded the glucose content of 31.39 g/L. The yield exceeded the result of the acid treatment by 64.9% and was by 22.8% higher than in the alkaline-pretreated samples. The reducing sugar content was 43.26 g/L, which was by 42.6% higher than after the acidic pretreatment and by 17.3% higher than after the alkaline pretreatment (Fig. 9).

Thus, the combined acid-alkaline-microwave pretreatment gave the best results based on the fiber composition, the content of reducing sugar, and the change in the surface structure. This method reduced hemicellulose by 71.4 to 1.05% (g/100 g db) and lignin by 79.2 to 4.17% (g/100 g db). The remaining material consisted of 77.49% cellulose (calculated according to the original cellulose content), ash, and some other substances (Fig. 10). After this pretreatment, the coffee pulp looked like yellow-brown soft foam and had good water permeability ($\leq 85\%$) (Fig. 11).

CONCLUSION

This study led to four important conclusions:

1. The combined acid-alkaline-microwave pretreatment method possessed the best lignin and hemicellulose removal efficiency.

2. The acid pretreatment method had the lowest loss of cellulose.

3. The combined acid-alkaline-microwave pretreatment had the highest concentrations of reducing sugars and glucose.

4. The pretreatment with white rot fungus *Phanerochaete chrysosporium* was safe, inexpensive, and green, although the hydrolysis efficiency was not as high as after other pretreatment methods. In addition, it produced no yeast inhibitory substances during ethanol fermentation.

CONTRIBUTION

D.V. Phuong developed the research concept, designed the study, collected the data, and drafted the

manuscript. L.T. Nguyen wrote the abstract and proof-read the manuscript; both the authors performed the experimental work and designed the research methodology.

CONFLICT OF INTEREST

The authors declared no conflict of interests regarding the publication of this article.

ACKNOWLEDGEMENTS

The authors would like to thank the Institute of Biotechnology and Food Technology, Industrial University of Ho Chi Minh City, Vietnam, and their co-workers for the technical and equipment support of this study.


REFERENCES

1. Sheng Y, Lam SS, Wu Y, Ge S, Wu J, Cai L, et al. Enzymatic conversion of pretreated lignocellulosic biomass: A review on influence of structural changes of lignin. *Bioresource Technology*. 2021;324. <https://doi.org/10.1016/j.biortech.2020.124631>
2. Coffee: World markets and trade. United States Department of Agriculture; 2020. 9 p.
3. Phuong DV, Quoc LPT, Tan PV, Duy LND. Production of bioethanol from Robusta coffee pulp (*Coffea robusta* L.) in Vietnam. *Foods and Raw Materials*. 2019;7(1):10–17. <https://doi.org/10.21603/2308-4057-2019-1-10-17>
4. Dadi D, Beyene A, Simoens K, Soares J, Demeke MM, Thevelein JM, et al. Valorization of coffee byproducts for bioethanol production using lignocellulosic yeast fermentation and pervaporation. *International Journal of Environmental Science and Technology*. 2018;15:821–832. <https://doi.org/10.1007/s13762-017-1440-x>
5. Shankar K, Kulkarni NS, Jayalakshmi SK, Sreeramulu K. Saccharification of the pretreated husks of corn, peanut and coffee cherry by the lignocellulolytic enzymes secreted by *Sphingobacterium* sp. ksn for the production of bioethanol. *Biomass and Bioenergy*. 2019;127. <https://doi.org/10.1016/j.biombioe.2019.105298>
6. Duarte A, Uribe JC, Sarache W, Calderón A. Economic, environmental, and social assessment of bioethanol production using multiple coffee crop residues. *Energy*. 2021;216. <https://doi.org/10.1016/j.energy.2020.119170>
7. Solarte-Toro JC, Romero-García JM, Martínez-Patiño JC, Ruiz-Ramos E, Castro-Galiano E, Cardona-Alzate CA. Acid pretreatment of lignocellulosic biomass for energy vectors production: A review focused on operational conditions and techno-economic assessment for bioethanol production. *Renewable and Sustainable Energy Reviews*. 2019;107:587–601. <https://doi.org/10.1016/j.rser.2019.02.024>
8. Woiciechowski AL, Dalmas Neto CJ, de Souza Vandenbergh LP, de Carvalho Neto DP, Sydney ACN, Letti LAJ, et al. Lignocellulosic biomass: Acid and alkaline pretreatments and their effects on biomass recalcitrance – Conventional processing and recent advances. *Bioresource Technology*. 2020;304. <https://doi.org/10.1016/j.biortech.2020.122848>
9. Ziegler-Devin I, Chruscziel L, Brosse N. Steam explosion pretreatment of lignocellulosic biomass: A mini-review of theoretical and experimental approaches. *Frontiers in Chemistry*. 2021;9. <https://doi.org/10.3389/fchem.2021.705358>
10. Hoang AT, Nizetić S, Ong HC, Mofijur M, Ahmed SF, Ashok B, et al. Insight into the recent advances of microwave pretreatment technologies for the conversion of lignocellulosic biomass into sustainable biofuel. *Chemosphere*. 2021; 281. <https://doi.org/10.1016/j.chemosphere.2021.130878>
11. Scapini T, dos Santos MSN, Bonatto C, Wancura JHC, Mulinari J, Camargo AF, et al. Hydrothermal pretreatment of lignocellulosic biomass for hemicellulose recovery. *Bioresource Technology*. 2021;342. <https://doi.org/10.1016/j.biortech.2021.126033>
12. Mishra S, Singh PK, Dash S, Pattnaik R. Microbial pretreatment of lignocellulosic biomass for enhanced biomethanation and waste management. *3 Biotech*. 2018;8. <https://doi.org/10.1007/s13205-018-1480-z>
13. Wang W, Lee D-J. Lignocellulosic biomass pretreatment by deep eutectic solvents on lignin extraction and saccharification enhancement: A review. *Bioresource Technology*. 2021;339. <https://doi.org/10.1016/j.biortech.2021.125587>
14. Sahoo D, Ummalyma SB, Okram AK, Pandey A, Sankar M, Sukumaran RK. Effect of dilute acid pretreatment of wild rice grass (*Zizania latifolia*) from Loktak Lake for enzymatic hydrolysis. *Bioresource Technology*. 2018;253:252–255. <https://doi.org/10.1016/j.biortech.2018.01.048>

15. Martínez-Patiño JC, Lu-Chau TA, Gullon B, Ruiz E, Romero I, Castro E, *et al.* Application of a combined fungal and diluted acid pretreatment on olive tree biomass. *Industrial Crops and Products*. 2018;121:10–17. <https://doi.org/10.1016/j.indcrop.2018.04.078>
16. Łukajtis R, Rybarczyk P, Kucharska K, Konopacka-Łyskawa D, Słupek E, Wychodnik K, *et al.* Optimization of saccharification conditions of lignocellulosic biomass under alkaline pre-treatment and enzymatic hydrolysis. *Energies*. 2018;11(4). <https://doi.org/10.3390/en11040886>
17. Hassan SS, Williams GA, Jaiswal AK. Emerging technologies for the pretreatment of lignocellulosic biomass. *Bioresource Technology*. 2018;262:310–318. <https://doi.org/10.1016/j.biortech.2018.04.099>
18. Sun Z, Mao Y, Liu S, Zhang H, Xu Y, Geng R, *et al.* Effect of pretreatment with *Phanerochaete chrysosporium* on physicochemical properties and pyrolysis behaviors of corn stover. *Bioresource Technology*. 2022;361. <https://doi.org/10.1016/j.biortech.2022.127687>
19. Miller GL. Use of dinitrosalicylic acid reagent for determination of reducing sugar. *Analytical Chemistry*. 1959;31(3):426–428. <https://doi.org/10.1021/ac60147a030>
20. Sadasivam S, Manickam A. *Biochemical Methods*. New Delhi: New Age International (P) Ltd. Publishers; 1996. 272 p.
21. van Soest PJ, Robertson JB, Lewis BA. Methods for dietary fiber, neutral detergent fiber, and nonstarch polysaccharides in relation to animal nutrition. *Journal of Dairy Science*. 1991;74(10):3583–3597. [https://doi.org/10.3168/jds.S0022-0302\(91\)78551-2](https://doi.org/10.3168/jds.S0022-0302(91)78551-2)
22. Ghose T. Measurement of cellulase activities. *Pure and Applied Chemistry*. 1987;59(2):257–268.
23. Sun C, Liao Q, Xia A, Fu Q, Huang Y, Zhu X, *et al.* Degradation and transformation of furfural derivatives from hydrothermal pre-treated algae and lignocellulosic biomass during hydrogen fermentation. *Renewable and Sustainable Energy Reviews*. 2020;131. <https://doi.org/10.1016/j.rser.2020.109983>
24. Agrawal R, Verma A, Singhania RR, Varjani S, Di Dong C, Patel AK. Current understanding of the inhibition factors and their mechanism of action for the lignocellulosic biomass hydrolysis. *Bioresource Technology*. 2021;332. <https://doi.org/10.1016/j.biortech.2021.125042>
25. Periyasamy S, Isabel JB, Kavitha S, Karthik V, Mohamed BA, Gizaw DG, *et al.* Recent advances in consolidated bioprocessing for conversion of lignocellulosic biomass into bioethanol – A review. *Chemical Engineering Journal*. 2022;453. <https://doi.org/10.1016/j.cej.2022.139783>
26. Chen Z, Wan C. Ultrafast fractionation of lignocellulosic biomass by microwave-assisted deep eutectic solvent pretreatment. *Bioresource Technology*. 2018;250:532–537. <https://doi.org/10.1016/j.biortech.2017.11.066>

ORCID IDs

Do Viet Phuong  <https://orcid.org/0000-0002-0081-0930>


Luu Thao Nguyen  <https://orcid.org/0000-0002-8146-1102>



The effect of post-packaging pasteurization on physicochemical and microbial properties of beef ham

Nasim Azizpour^{1,*} , Seyed Hadi Razavi² , Mehran Azizpour³ , Esmail Khazaei Poul¹ 

¹ Urmia University , Urmia, Iran

² University of Tehran , Tehran, Iran

³ University of Manitoba , Winnipeg, Canada

* e-mail: nasimazizpour95@gmail.com

Received 10.11.2022; Revised 31.03.2023; Accepted 04.04.2023; Published online 11.10.2023

Abstract:

In this study, we aimed to investigate the impact of three different post-packaging pasteurization temperatures (55, 65, and 75°C) on the physicochemical (pH, drip loss, texture profile, and color), microbial (lactic acid bacteria, mesophilic and psychrotrophic bacteria, as well as mold and yeast), and sensory (odor, taste, texture, color, slime, exudates, swelling, and overall acceptability) characteristics of vacuum-packed beef ham during 30 days of storage at two different temperatures (5 and 12°C).

Lactic acid bacteria and total mesophilic and psychrotrophic counts were reduced to zero by post-packaging pasteurization at 65 and 75°C. Higher post-packaging pasteurization temperatures resulted in a significant increase in drip loss in the treated samples at 65 and 75°C, as well as a small rise in pH in all the samples. Furthermore, higher post-packaging pasteurization temperatures decreased lightness, yellowness, and h° values while increasing redness and ΔE . During post-packaging pasteurization, Chroma remained constant. The textural profile analysis revealed that post-packaging pasteurization and storage had a significant impact on the texture of beef ham. The sensory analysis showed no changes after post-packaging pasteurization in the samples, and the sensory parameters remained stable during their storage at 65 and 75°C.

Finally, our investigation showed that 65°C is an optimal post-packaging pasteurization temperature for increasing the shelf-life of beef ham under refrigeration.

Keywords: Ready-to-eat foods, meat products, thermal pasteurization, post-packaging pasteurization, shelf-life, lactic acid bacteria

Please cite this article in press as: Azizpour N, Razavi SH, Azizpour M, Khazaei Poul E. The effect of post-packaging pasteurization on physicochemical and microbial properties of beef ham. *Foods and Raw Materials*. 2024;12(1):142–155. <https://doi.org/10.21603/2308-4057-2024-1-596>

INTRODUCTION

Ready-to-eat products are really popular in modern lifestyles because they are easy to prepare. Meat products like ham are preferred among ready-to-eat foods due to their excellent nutritional, protein, vitamin, and mineral contents. Processed meats are highly perishable and have a short shelf-life despite the preservation technologies employed in these products. Because of their low salt content of 2%, pH of 6, and water activity of 0.9, as well as high protein, water, and nutrient contents, these products are highly susceptible to contamination by spoilage microorganisms, particularly lactic acid bacteria species [1–3]. This can happen during manipulation processes before the final packaging, such as slicing [4].

Symptoms of lactic acid bacteria spoilage include in-package souring, swelling, slime, milky exudates, off-flavors, off-odors, and discoloration [3]. The food industry is constantly concerned about lactic acid bacteria spoilage because it causes economic problems for producers who have to recall their products and may also harm their reputation [2]. On the one hand, meat companies attempt to create a high-quality product with financial advantages. On the other hand, people are becoming more conscious of the hazards of artificial additives used in ready-to-eat products [5]. Therefore, post-package pasteurization may be used to improve microbial safety and extend the shelf-life of vacuum-packed meat products. This method is easier to use and it is less expensive than other techniques used by meat

companies. Post-package pasteurization is a thermal process known as a low-temperature decontamination method that can increase the shelf-life of ready-to-eat meat products [4, 6, 7].

Most previous studies used post-package pasteurization to control *Listeria monocytogenes*, *Escherichia coli*, *Salmonella* spp., and *coliforms* on a variety of products [6, 8–11]. To the best of our knowledge, there is a lack of research on the impact of different temperatures of post-package pasteurization on controlling spoilage bacteria, primarily lactic acid bacteria, in beef ham. Moreover, there are few studies on the quality changes during the post-package pasteurization process, primarily sensory attributes, which is limited to Vahabi Anaraki *et al.*, who applied post-package pasteurization to turkey breast at 80°C for 5.5 min [4]. The heating process can cause changes in the quality of meat, such as denaturation, fiber shrinkage, and collagen solubilization [12]. Therefore, choosing an appropriate heating temperature is a critical step in producing a high-quality product.

According to previous studies [8, 13–16], the temperatures selected for post-package pasteurization ranged between 50 and 95°C. Since higher thermal treatments cause more quality changes, we attempted to find an optimum temperature in lower thermal ranges that could efficiently eliminate bacteria while still ensuring product quality. For this, we examined the effect of post-package pasteurization at different temperatures on the microbial, physical, chemical, and sensory quality of fully cooked, vacuum-packed 90% beef ham. In addition, we evaluated post-package pasteurization's effect on the shelf-life of beef ham during 30 days of storage at temperatures of 5 and 12°C, which are the average house and market temperatures.

STUDY OBJECTS AND METHODS

In this study, we evaluated the impact of post-package pasteurization on the microbial activity (lactic acid bacteria, aerobic mesophilic and psychrotrophic bacteria, mold, and yeast) and on the physicochemical changes (pH, drip loss, color coordinates, texture profile) and sensory analysis in vacuum-packed 90% beef ham at three post-package pasteurization temperatures (55, 65, and 75°C) and during 30 days of storage at two storage temperatures (5 and 12°C).

Cooked ham model. Sliced cooked hams were prepared using traditional techniques in an industrial meat factory in Amol, Iran (Kalleh Company). According to the manufacturer's instructions, the hams were produced from boneless beef cuts (90%), salt (1.5%), sodium polyphosphate (0.3%), ascorbic acid (0.05%), sodium nitrite (0.01%), seasonings (1.14%), water (2%), and wheat starch (5%). After mixing the ingredients, the mixture was tumbled (2–4°C) and packed into an artificial casing and cooked until the core temperature reached 72°C, which was measured by inserting a thermometer (Model Testo 103, Germany) into the center of a sample pack. After cooking, the product was

immediately cooled in a refrigerator (4°C) for about 2 h until the core temperature reached 5°C. The hams were then sliced (~ 0.2×11×14 cm) by using a slicing machine and vacuum-packed in polyethylene-polyamide-polyethylene (100 μ diameter) bags weighing around 300 g (~ 300 g sliced ham per package).

Heat treatment. The vacuum-packed hams were divided into four groups: control (non-pasteurized samples) and experimental pasteurized samples that were transported to saturated steam chambers at three different temperatures of 60, 70, and 80°C until the core temperature reached 55, 65, and 75°C, respectively. The temperature was measured by inserting a thermometer (Model Testo 103, Germany) into the center of a sample pack. Each treatment group required 60 min to reach the core temperature. The packs were then cooled in a refrigerator (4°C) for about 2 h until the core temperature reached 5°C. Following that, both pasteurized and non-pasteurized samples were transferred to the laboratory and refrigerated for 30 days at two temperatures of 5 and 12°C. For each category (pasteurized and non-pasteurized) of treatments, 30 out of a total of 120 packed hams were used. All analyses were carried out at least three times on days 0, 15, and 30 at temperatures of 5 and 12°C.

pH measurement. The pH of the product was calculated according to the procedure described by Khorsandi [17]. After mixing 10 g of a chopped sample with 90 mL of distilled water of room temperature, we measured pH with a digital pH meter (Model C860, Consort, Belgium). On each measurement day, the pH meter was calibrated at room temperature using buffers with pH of 4.01 and 6.97. All pH measurements were replicated three times.

Drip loss measurement. Drip loss was recorded on each slice of the sample immediately after packaging or processing at both storage temperatures by removing the cover of the hams, drying the exudates with a paper towel, and reweighing the hams with the wrapping. The drip loss was calculated as follows [18]:

$$\text{Drip loss} = \frac{W_1 - W_2}{W_1} \times 100 \quad (1)$$

where W_1 is the meat weight at packaging, g; W_2 is the meat weight at sampling day, g.

The measurements were replicated at least three times.

Microbiological analysis. All microbiological analyses were performed according to Menéndez *et al.* [19]. Before each microbial analysis, sample packages were sterilized with 70% ethanol and opened aseptically using a sterile scalpel. Ham samples (25 g) were transferred aseptically to 0.1% sterile peptone water (225 mL) and homogenized in a stomacher (Lab Blender, Seward, London, UK) for 2 min. Further decimal dilutions were made using the same diluent, and they were then examined for aerobic mesophilic and psychrotrophic microorganisms, lactic acid bacteria, molds, and yeasts under the following conditions: lactic acid bacteria on

Man Rogosa Sharpe agar at 30°C for 3 days; mesophilic and psychrotrophic bacteria on plate count agar at 30°C for 48 h and 10°C for 7 days, respectively; yeasts and molds on Rose Bengal with chloramphenicol agar at 25°C for 5 days. The tests were run in duplicate on agar plates using three samples for each treatment, and the results were represented as logarithms of the number of colony-forming units (log CFU/g).

Color analysis. The color coordinates (CIELAB) were calculated using a Minolta CR-400 colorimeter (Minolta Camera Co., Osaka, Japan; an aperture of 8 mm), illuminant D65, and a 2° observation angle, as described in [20]. L^* denotes lightness and ranges from black (0) to white (100); a^* denotes redness and ranges from (+) red to (−) green; and b^* denotes yellowness and ranges from (+) yellow to (−) blue. A standard Minolta reflector plate was used to calibrate the colorimeter before each color measurement. Total color difference (ΔE), saturation index or Chroma (C^*), and hue angle (h°), which indicate the divergence from the color space's true red axis, were determined as follows [21]:

$$\Delta E = \sqrt{(L^* - L_0)^2 + (a^* - a_0)^2 + (b^* - b_0)^2} \quad (2)$$

$$C^* = \sqrt{(a^{*2} + b^{*2})} \quad (3)$$

$$h^\circ = \tan^{-1}(b^* / a^*) \quad (4)$$

Where L^* , a^* , and b^* are the measured values of treated and control hams on different days, and L_0 , a_0 , and b_0 are the standard color parameters. In L^* , a^* , and b^* color spaces, ΔE is the difference between two colors [22]. The Chroma or saturation scale runs from 0 for fully unsaturated (neutral gray, black, or white) to 100 for extremely high Chroma or “color purity”. The hue angle (h°) of the saturated color in the color space ranges from 0° (red), 90° (yellow), 180° (green), 270° (blue), and 360° (red) [21].

Texture profile analysis. The textural properties of hams were evaluated using a texture analyzer (M350-10CT, Testometric, UK) controlled by the comprehensive WinTest Analysis software. Samples were fixed on the central part of the texture profile analysis plate at room temperature and compressed twice to 50% of their original height through a 2-bite mechanism with a P/4 cylindrical probe (4.0 mm in diameter), a load cell of 50 kg, and a crosshead speed of 60 mm/min. The rest time between the two compressions was 10 s. The following parameters were determined: hardness, springiness, adhesiveness, cohesiveness, gumminess, and chewiness. The measurements were repeated at least three times at different points for each sample.

Sensory analysis. The sensory analysis was performed as described in [23], with eight trained panelists. The following sensory attributes were evaluated: odor, taste, texture, slime formation, pack swelling, color, exudates, and overall acceptability. The panelists rated the sensory attributes on a five-point hedonic scale:

1 for “extremely bad”, 2 for “bad”, 3 for “moderate”, 4 for “good”, and 5 for “extremely good”. The evaluations of every characteristic were repeated three times. The sensory evaluations were performed on days 0, 15, and 30 at both storage temperatures (5 and 12°C).

Statistical analysis. To evaluate the differences ($p < 0.05$), all the data were analyzed using one-way ANOVA. Duncan's multiple range tests ($p < 0.05$) were performed to evaluate whether there were changes in the means of the treatments. The SPSS software was used for the analysis (SPSS 23.0 for Windows, SPSS Inc., Chicago, IL, USA).

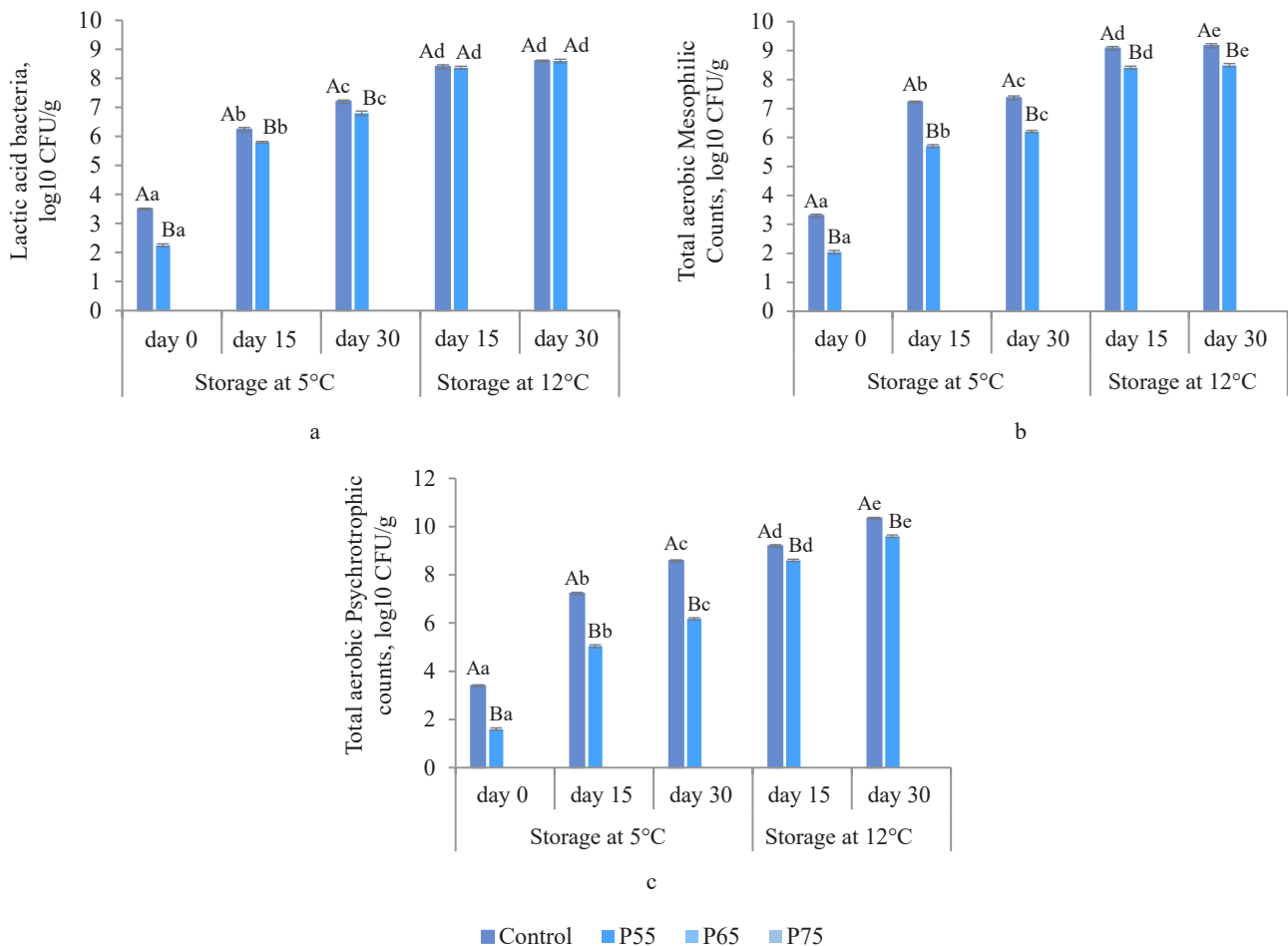
RESULTS AND DISCUSSION

Microbiological analysis. Figure 1 depicts total aerobic mesophilic counts, total psychrotrophic counts, and lactic acid bacteria counts after post-package pasteurization and under different storage conditions. As can be seen in Fig. 1a, post-package pasteurization considerably reduced the lactic acid bacteria counts of the treated samples. No colony of lactic acid bacteria was counted during 30 days of storage in the samples pasteurized at 65 (P65) and 75°C (P75). The initial count of lactic acid bacteria was 3.5 log₁₀ CFU/g in the control samples. Compared to the control group, this amount significantly reduced to 2.25 log₁₀ CFU/g in the P55 samples ($p < 0.05$) (Fig. 1a). These results of lactic acid bacteria are similar to those reported by [3] and [24], who obtained a one-log reduction in the value of *Lactobacillus sakei*, *Lactobacillus plantarum*, *Leuconostoc mesenteroides*, and *Leuconostoc curvatus* in vacuum-packed sausages in less than 60 s at 55 and 57°C.

We found that on the first day of storage, the value of log₁₀ CFU/g of mesophilic bacteria in non-pasteurized samples was 3.3 log₁₀ CFU/g. Compared to the non-pasteurized group, this amount significantly reduced ($p < 0.05$) to 2.04 log₁₀ CFU/g in the P55 ham and reached zero in the P65 and P75 samples (Fig. 1b). Similarly, Pinggen *et al.* observed 1.75 log₁₀ CFU/g reductions in total aerobic mesophilic counts at 53°C in pork loins, and Jeong *et al.* observed a 3.67 log₁₀ CFU/g reduction in total aerobic mesophilic counts after 45 min of post-package pasteurization treatment at 61°C in pork ham [9, 25].

In our study, the initial count of psychrotrophic bacteria in the control group was 3.4 log₁₀ CFU/g on the first day of storage. Compared to the control group, post-package pasteurization significantly reduced total psychrotrophic counts to 1.6 log₁₀ CFU/g in the P55 ham and zero in the P65 and P75 samples ($p < 0.05$) (Fig. 1c). Our total psychrotrophic counts results were consistent with those of [10], who reported a 4 log₁₀ CFU/g reduction in psychrotrophic counts in lamb loins after the post-package pasteurization process at 60°C for 6 h.

There were no mold or yeast counts after post-package pasteurization or during 30 days of storage at 5 or 12°C in either the non-pasteurized or pasteurized samples. The number of bacteria in our study increased significantly during storage in both control and the P55



P55, P65 and P75 are the samples pasteurized at 55, 65, and 75°C

Averages with different capital (A–C) and small (a–c) letters indicate statistically significant difference ($p < 0.05$) between treatments and in treatments, respectively, at both storage temperatures (5 and 12°C). Each point represents the mean \pm SD

Figure 1 Microbiological analysis of control and post-package pasteurization-treated hams during 30 days of storage at 5 and 12°C: lactic acid bacteria count (a); total aerobic Mesophilic Counts (b); and total aerobic Psychrotrophic counts (c)

samples ($p < 0.05$). The control samples had a significantly higher lactic acid bacteria count during 30 days of storage at 5°C, but at 12°C, this amount increased to 8.6 log₁₀ CFU/g at the end of storage for both the control and the P55 ham ($p < 0.05$) (Fig. 1a).

At both storage temperatures (5 and 12°C), the amount of increase in total aerobic mesophilic counts and total psychrotrophic counts was constantly higher in the control group than in the P55 ham (Fig. 1b and c). Post-package pasteurization at 65 and 75°C effectively eliminated the number of lactic acid bacteria, total aerobic mesophilic counts, and total psychrotrophic counts by 3.5, 3.3, and 3.4 log₁₀ CFU/g, respectively, whereas post-package pasteurization at 55°C significantly eliminated these bacteria by 1.25, 1.26, and 1.8 log₁₀ CFU/g, respectively. Furthermore, post-package pasteurization inhibited the growth of these microorganisms in both the P65 and P75 samples during cold storage (5 and 12°C), further increasing the product's safety.

pH values. Table 1 shows variations in pH values of the treatments as a result of post-package pasteurization

and cold storage. As can be seen, the pH of pasteurized hams increased with a higher post-package pasteurization temperature, but this trend was not statistically significant ($p > 0.05$). This could be related to a decrease in muscle acidic groups and the formation of free hydrogen sulfide as thermal temperatures rise [26]. This finding was consistent with the findings of [27] and [28], who discovered a slight increase in the pH of chicken and pork samples after heat treatment.

In our study, during storage at 5°C only the pH in the control samples decreased significantly ($p < 0.05$), and at 12°C, this trend was only seen in the control and P55 samples (Table 1). When the lactic acid bacteria counts reached 7 log₁₀ CFU/g, the pH dropped faster. Similarly, when the lactic acid bacteria population reached 7 log₁₀ CFU/g, Khadijeh *et al.* and Khorsandi *et al.* discovered a significant decrease in pH [3, 17]. According to our findings, there were no significant ($p > 0.05$) changes in the pH of the P65 and P75 samples during storage. While the pH drop has been related to lactic acid bacteria growth, these findings may

Table 1 Effect of post-package pasteurization on drip loss and pH of beef ham within 30 days of storage at 5 and 12°C. Values are expressed as mean ± SD

Attribute	Days	Control	P55	P65	P75
Storage temperature 5°C					
pH	0	6.32 ± 0.03 ^{Aa}	6.35 ± 0.02 ^{Aa}	6.37 ± 0.05 ^{Aa}	6.40 ± 0.05 ^{Aa}
	15	6.30 ± 0.05 ^{Aa}	6.34 ± 0.01 ^{Aa}	6.39 ± 0.02 ^{Aa}	6.37 ± 0.04 ^{Aa}
	30	5.36 ± 0.04 ^{Ab}	6.34 ± 0.02 ^{Ba}	6.37 ± 0.03 ^{Ba}	6.36 ± 0.03 ^{Ba}
Drip loss, %	0	2.60 ± 0.46 ^{Aa}	3.10 ± 0.25 ^{Aa}	4.35 ± 0.32 ^{Ba}	5.66 ± 0.53 ^{Ca}
	15	2.73 ± 0.29 ^{Aa}	3.34 ± 0.37 ^{Aa}	4.24 ± 0.54 ^{Ba}	5.88 ± 0.85 ^{Ca}
	30	3.65 ± 0.49 ^{Ab}	3.47 ± 0.57 ^{Aab}	4.60 ± 0.69 ^{Ba}	5.82 ± 0.84 ^{Ca}
Storage temperature 12°C					
pH	0	6.32 ± 0.03 ^{Aa}	6.35 ± 0.02 ^{Aa}	6.37 ± 0.05 ^{Aa}	6.40 ± 0.05 ^{Aa}
	15	5.09 ± 0.03 ^{Ac}	5.10 ± 0.02 ^{Ab}	6.34 ± 0.02 ^{Ba}	6.34 ± 0.02 ^{Ba}
	30	4.92 ± 0.05 ^{Ac}	4.93 ± 0.01 ^{Ab}	6.33 ± 0.05 ^{Ba}	6.36 ± 0.03 ^{Ba}
Drip loss, %	0	2.60 ± 0.46 ^{Aa}	3.10 ± 0.25 ^{Aa}	4.35 ± 0.32 ^{Ba}	5.66 ± 0.53 ^{Ca}
	15	3.53 ± 0.14 ^{Ab}	3.64 ± 0.12 ^{Aab}	4.60 ± 0.14 ^{Ba}	5.77 ± 0.16 ^{Ca}
	30	5.65 ± 0.29 ^{Ac}	4.18 ± 0.15 ^{Bb}	4.68 ± 0.16 ^{Ba}	5.79 ± 0.09 ^{Ca}

P55, P65 and P75 are the samples pasteurized at 55, 65, and 75°C

Averages with different capital (A–C) letters in the same row indicate statistically significant difference ($p < 0.05$) between treatments at the same storage time. Averages with different small (a–c) letters in the same column indicate statistically significant difference ($p < 0.05$) within treatments during different storage times

be due to a lack of lactic acid bacteria growth in these treatments [4]. On day 30, the pH of the P55 ham was significantly lower at 12°C than that at 5°C. Our findings demonstrated that post-package pasteurization at 65 and 75°C could inhibit lactic acid bacteria growth while maintaining the pH of the samples unchanged.

Drip loss analysis. Table 1 shows changes in drip loss in the samples caused by post-package pasteurization and during cold storage. Higher temperatures of post-package pasteurization increased the drip loss rate of the P65 and P75 samples, which was also significant between the experimental groups ($p < 0.05$). This increase in drip loss could be due to thermal treatment, which causes myofibrillar protein structures in muscle to become more rigid in the longitudinal axis due to protein denaturation. As a result, more muscle sarcoplasmic fluid is released due to this procedure [23]. Our findings agree with those of [8] in pork loin. Drip loss increased considerably in the control and P55 treatments during cold storage at both storage temperatures ($p < 0.05$) (Table 1). Because the water-holding capacity of muscle proteins is highly pH-dependent, this can be explained by a decrease in pH in these samples around the isoelectric point of proteins (particularly myosin with PI = 5.4) [4, 29].

Wang *et al.* and Ozaki *et al.* reported a rising trend in drip loss in their samples during storage, which is consistent with our findings [30, 31]. According to our data, post-package pasteurization significantly increased drip loss in the P65 and P75 samples, which is a downside to selecting high temperatures. This parameter rose during cold storage in both the control and the P55 ham sample, which was connected to lactic acid bacteria growth and a pH drop.

Color analysis. The L^* and b^* values. Table 2 shows changes in the color coordinates (CIELAB) (L^* , a^* ,

and b^*) of all the samples. The L^* and b^* values of the pasteurized samples followed the same trend, decreasing considerably as the temperature increased up to 65°C and then leveling out at 75°C ($p < 0.05$). One possible explanation for the L^* value's decrease is higher drip loss in these samples, which causes moisture loss and may result in a decrease in lightness [32]. Reduced b^* values may be attributed to metmyoglobin denaturation, which finally results in brown meat coloring because of ferrihemochrome production [33]. Several investigations have shown comparable findings for the L^* value and b^* value during post-package pasteurization [9, 16, 34]. In our study, only in the control samples (at both storage temperatures) and P55 samples (only at 12°C) did the L^* value decrease significantly during cold storage ($p < 0.05$) (Table 2). This phenomenon could be explained by a loss of the water-holding capacity in the meat emulsion or a decrease in the pH of the samples [35, 36].

The b^* value, on the other hand, increased significantly during cold storage in all the samples ($p < 0.05$) (Table 2). The increasing b^* values observed in the control and P55 samples can be explained by pigment and lipid oxidation as a result of pH reduction [18, 37]. However, in the P65 and P75 samples, this increase could be attributed to lipid oxidation caused by released non-heme iron groups as thermal temperatures rise [38]. The b^* values during the storage period in our study agreed with those obtained in [37] and [18]. Post-package pasteurization significantly increased the L^* and b^* values of the pasteurized samples, as well as induced darkness and blueness, according to our findings.

The a^* value. Unlike the L^* and b^* values, the a^* values of the pasteurized samples increased significantly as the post-package pasteurization temperature rose

Table 2 Effect of post-package pasteurization on color coordinates (L^* , a^* , and b^*), total color difference (ΔE), Chroma (C^*), and hue angle (h°) of 90% beef ham within 30 days of storage at 5 and 12°C. Values are expressed as mean \pm SD

Color attribute	Days	Control	P55	P65	P75
Storage temperature 5°C					
L^*	0	29.98 \pm 0.22 ^{Aa}	29.53 \pm 0.28 ^{Ba}	28.34 \pm 0.23 ^{Ca}	28.30 \pm 0.22 ^{Ca}
	15	29.97 \pm 0.29 ^{Aa}	29.52 \pm 0.25 ^{Ba}	28.32 \pm 0.31 ^{Ca}	28.28 \pm 0.20 ^{Ca}
	30	29.61 \pm 0.24 ^{Ab}	29.51 \pm 0.21 ^{Aa}	28.30 \pm 0.22 ^{Ca}	28.25 \pm 0.28 ^{Ca}
a^*	0	15.56 \pm 0.23 ^{Aa}	15.92 \pm 0.26 ^{Ba}	16.54 \pm 0.22 ^{Ca}	16.52 \pm 0.31 ^{Ca}
	15	15.41 \pm 0.25 ^{Aa}	15.74 \pm 0.29 ^{Ba}	16.35 \pm 0.20 ^{Cab}	16.27 \pm 0.29 ^{Cab}
	30	15.01 \pm 0.23 ^{Abc}	15.44 \pm 0.22 ^{Bb}	16.23 \pm 0.27 ^{Cab}	16.19 \pm 0.23 ^{Cb}
b^*	0	19.44 \pm 0.23 ^{Aa}	18.98 \pm 0.25 ^{Ba}	18.31 \pm 0.21 ^{Ca}	18.20 \pm 0.29 ^{Ca}
	15	19.62 \pm 0.28 ^{Aab}	19.15 \pm 0.20 ^{Bab}	18.46 \pm 0.21 ^{Cab}	18.45 \pm 0.22 ^{Cab}
	30	19.81 \pm 0.23 ^{Abc}	19.34 \pm 0.24 ^{Bbc}	18.69 \pm 0.36 ^{Cbc}	18.70 \pm 0.27 ^{Cbc}
ΔE	0	0 ^{Aa}	0.76 \pm 0.26 ^{Ba}	2.22 \pm 0.22 ^{Ca}	2.30 \pm 0.18 ^{Da}
	15	0.64 \pm 0.15 ^{Ab}	0.73 \pm 0.27 ^{Ba}	2.22 \pm 0.17 ^{Ca}	2.23 \pm 0.14 ^{Cb}
	30	0.76 \pm 0.13 ^{Ac}	0.66 \pm 0.12 ^{Bb}	2.11 \pm 0.08 ^{Cb}	2.11 \pm 0.26 ^{Cc}
C^*	0	24.90 \pm 0.23	24.77 \pm 0.25	24.67 \pm 0.31	24.58 \pm 0.30
	15	24.95 \pm 0.27	24.79 \pm 0.25	24.66 \pm 0.35	24.59 \pm 0.34
	30	24.85 \pm 0.33	24.75 \pm 0.33	24.75 \pm 0.35	24.73 \pm 0.25
h°	0	51.32 \pm 0.17 ^{Aa}	50.01 \pm 0.04 ^{Ba}	47.91 \pm 0.16 ^{Ca}	47.77 \pm 0.11 ^{Ca}
	15	51.85 \pm 0.20 ^{Ab}	50.58 \pm 0.05 ^{Bb}	48.47 \pm 0.06 ^{Cb}	48.59 \pm 0.10 ^{Cb}
	30	52.85 \pm 0.15 ^{Ac}	51.40 \pm 0.13 ^{Bc}	49.03 \pm 0.08 ^{Cc}	49.11 \pm 0.07 ^{Cc}
Storage temperature 12°C					
L^*	0	29.98 \pm 0.22 ^{Aa}	29.53 \pm 0.28 ^{Ba}	28.34 \pm 0.23 ^{Ca}	28.30 \pm 0.22 ^{Ca}
	15	29.50 \pm 0.21 ^{Ab}	29.19 \pm 0.20 ^{Bb}	28.26 \pm 0.45 ^{Ca}	28.23 \pm 0.28 ^{Ca}
	30	29.42 \pm 0.23 ^{Ab}	29.12 \pm 0.38 ^{Bb}	28.24 \pm 0.25 ^{Ca}	28.21 \pm 0.19 ^{Ca}
a^*	0	15.56 \pm 0.24 ^{Aa}	15.92 \pm 0.26 ^{Ba}	16.54 \pm 0.20 ^{Ca}	16.52 \pm 0.31 ^{Ca}
	15	14.93 \pm 0.24 ^{Abc}	15.07 \pm 0.21 ^{Ac}	16.20 \pm 0.42 ^{Bb}	16.16 \pm 0.20 ^{Bb}
	30	14.73 \pm 0.28 ^{Ac}	14.81 \pm 0.25 ^{Ac}	16.15 \pm 0.21 ^{Bb}	16.10 \pm 0.22 ^{Bb}
b^*	0	19.44 \pm 0.23 ^{Aa}	18.98 \pm 0.25 ^{Ba}	18.31 \pm 0.21 ^{Ca}	18.20 \pm 0.29 ^{Ca}
	15	19.91 \pm 0.28 ^{Abc}	19.35 \pm 0.33 ^{Bbc}	18.71 \pm 0.24 ^{Cbc}	18.72 \pm 0.39 ^{Cbc}
	30	20.02 \pm 0.35 ^{Ac}	19.55 \pm 0.35 ^{Bc}	18.75 \pm 0.22 ^{Cbc}	18.77 \pm 0.21 ^{Cbc}
ΔE	0	0 ^{Aa}	0.76 \pm 0.26 ^{Ba}	2.22 \pm 0.22 ^{Ca}	2.30 \pm 0.18 ^{Da}
	15	0.94 \pm 0.18 ^{Ad}	0.65 \pm 0.22 ^{Bb}	2.14 \pm 0.36 ^{Cb}	2.13 \pm 0.15 ^{Cc}
	30	1.16 \pm 0.10 ^{Ac}	0.56 \pm 0.18 ^{Bc}	2.24 \pm 0.22 ^{Ca}	2.21 \pm 0.20 ^{Cb}
C^*	0	24.90 \pm 0.33	24.77 \pm 0.35	24.67 \pm 0.31	24.58 \pm 0.27
	15	24.88 \pm 0.36	24.53 \pm 0.27	24.75 \pm 0.33	24.73 \pm 0.40
	30	24.85 \pm 0.32	24.53 \pm 0.30	24.75 \pm 0.31	24.73 \pm 0.31
h°	0	51.32 \pm 0.17 ^{Aa}	50.01 \pm 0.04 ^{Ba}	47.91 \pm 0.16 ^{Ca}	47.77 \pm 0.11 ^{Ca}
	15	53.13 \pm 0.05 ^{Ac}	52.10 \pm 0.07 ^{Bd}	49.11 \pm 0.04 ^{Cc}	49.20 \pm 0.10 ^{Cc}
	30	53.64 \pm 0.04 ^{Ad}	52.85 \pm 0.12 ^{Be}	49.26 \pm 0.16 ^{Cc}	49.38 \pm 0.13 ^{Cc}

P55, P65 and P75 are the samples pasteurized at 55, 65, and 75°C

Averages with different capital (A–C) letters in the same row indicate statistically significant difference ($p < 0.05$) between treatments at the same storage time. Averages with different small (a–c) letters in the same column indicate statistically significant difference ($p < 0.05$) within treatments at different storage times

up to 65°C before leveling off at 75°C ($p < 0.05$). The cured red color formation in meats (Fe^{2+} -nitrosylhemochrom pigment) as a result of the thermal process is related to the increasing redness during post-package pasteurization [25]. Our findings were consistent with those in [11] for fillet fish heated from 50 to 70°C. Conversely, during both storage temperatures, a significant reduction ($p < 0.05$) was observed for a^* values in all the samples (Table 2), which could be attributed to the nitrosylmyoglobin pigment oxidation and metmyoglobin formation [39, 40]. Furthermore, nonenzymatic browning as a result of oxidative reac-

tions upon heating can be responsible for a^* value changes in the P65 and P75 samples, which is consistent with previous studies in sausage and pork ham [35, 41, 42].

Higher post-package pasteurization temperatures (primarily up to 65°C) were found to induce the cure meat color in beef ham, which is a desirable quality for consumer preference. This indicates that 65°C is a suitable temperature for post-package pasteurization.

Total color difference (ΔE), Chroma (C^*), and hue angle (h°). As can be seen in Table 2, post-package pasteurization significantly increased ($p < 0.05$) the

total color differences of the pasteurized samples, ranging from 0.76 to 2.3, when compared to the non-pasteurized (control) samples. According to Fernández-López *et al.*, the actual visual difference of the product occurs when the total color difference of samples is greater than 3 [22]. Increasing the post-package pasteurization temperatures reduced the h^* value of all the pasteurized samples from 50.01 to 47.77 ($p < 0.05$) (Table 2). There were no significant differences in Chroma between the pasteurized treatments during post-package pasteurization ($p > 0.05$) (Table 2). This might be due to insufficient thermal temperatures, which could not affect the Chroma value.

The total color differences of the non-pasteurized samples increased significantly at both cold storage temperatures, whereas this parameter decreased significantly in all the pasteurized samples (except P65 at 12°C) ($p < 0.05$) (Table 2). However, according to Fernández-López *et al.*, this reduction was not detectable by the untrained eye [22].

The hue angle results for all the pasteurized and non-pasteurized samples showed a significant increase ($p < 0.05$) at the two cold storage temperatures (Table 2), with values ranging from 47.77 to 53.64, indicating an increase in yellowness during storage. However, we observed no change in the Chroma values in any of the treatments during storage at both temperatures ($p > 0.05$) (Table 2).

According to the hue angle data, higher thermal temperatures caused more redness in the samples. Furthermore, it can be assumed that temperatures in our study were not high enough to have a significant impact on the Chroma or ΔE that could be detected.

Textural profile analysis. Hardness, gumminess, and chewiness. Table 3 shows the effects of various heating and storage temperatures on the texture parameters of beef ham. Post-package pasteurization had a significant effect on the hardness, gumminess, and chewiness of the samples. Compared to the control groups, there was a significant decrease in hardness, gumminess, and chewiness in the pasteurized samples up to 65°C, followed by a significant increase in these parameters at 75°C ($p < 0.05$). Bertola *et al.* discovered the lowest hardness values at 60 and 64°C and relatively higher hardness values between 81 and 90°C [13]. In addition, Tornberg reported an increase in meat toughness during heating between 65 and 80°C caused by connective tissue shrinkage. The increase in meat tenderness during heating up to 65°C is caused by sarcoplasmic protein aggregation, gelation of fibers and fiber bundles, and decreased fracture stress [43].

Furthermore, this author connected a reduction in shear force to a weakening of collagenous connective tissue, and Shen *et al.* suggested that changes in the myofibrillar protein structure during heating are another factor that leads to meat hardness at temperatures above 70°C [11, 43].

The decrease in gumminess during post-package pasteurization is also caused by the heat denaturation of myosin, whereas the increase in gumminess can be related to the unfolding of actin and sarcoplasmic proteins [44]. Rabeler and Feyissa and Rigdon *et al.* observed a similar trend for gumminess when heating between 50 and 95°C [16, 45].

The decreased chewiness during post-package pasteurization could be attributed to the loss of the myosin structure, whereas the increased chewiness can be related to gel formation due to the denaturation of connective tissue and collagen that begins at temperatures above 70°C [14, 46, 47]. Roldán *et al.* found a similar trend for chewiness during post-package pasteurization in lamb loins [10].

Furthermore, these texture parameters declined during the two cold storage periods in all the samples. In general, the degradation of proteins and lipids by microorganisms or enzymatic activity, as well as the loosening of myofibrils, the degeneration of connective tissue, and the reduction of actin-myosin junctions, are associated with decreased hardness and increased softness of meat during storage [36, 48, 49]. In our study, this decreased trend was coincidental with the increase in the number of lactic acid bacteria, total aerobic mesophilic counts, and total psychrotrophic counts in the control and P55 samples (Fig. 1a, b, and c). Thus, decreased gumminess during storage could be due to ionic reaction loss [42]. Additionally, decreased gumminess and chewiness in the control and P55 samples might be due to the degradation of meat protein due to pH reduction, while decreased gumminess and chewiness in both P65 and P75 samples could be due to proteolysis caused by chemical and enzymatic activity and lipid oxidation during the thermal treatment [11, 50, 51].

Our results for hardness, gumminess, and chewiness during storage were consistent with those of [28, 36], [42, 48], and [28, 48], respectively. We found that the firmness of the treated samples decreased as a result of post-package pasteurization up to 65°C. However, the P65 samples had the highest firmness at the end of day 30 of refrigerated storage at both 5 and 12°C. According to these findings, 65°C could be considered the optimum post-package pasteurization temperature for maintaining the firmness quality of beef ham during cold storage.

Adhesiveness and cohesiveness. As shown in Table 3, none of the post-package pasteurization temperatures affected the adhesiveness and cohesiveness of the pasteurized samples, with the exception of the P55 ham sample, which had the lowest value when compared to the other treatments ($p < 0.05$). These results were consistent with those of D'sa *et al.* for adhesiveness and Rabeler and Feyissa for cohesiveness [15, 16].

The adhesiveness and cohesiveness of all the samples remained unchanged during cold storage ($p > 0.05$). Thus, meat products such as ham cannot have high adhesiveness because they must have a firm texture and not stick when touched [52]. Rahman *et al.* relates ionic interaction loss to the cohesiveness of the

Table 3 Effect of post-package pasteurization on texture profile analysis of beef ham within 30 days of storage at 5 and 12°C. Values are expressed as mean ± SD

Days	Attribute	Control	P55	P65	P75
Storage temperature 5°C					
0	Hardness, N	0.976 ± 0.060 ^{Aa}	0.947 ± 0.180 ^{Aa}	0.85 ± 0.02 ^{Ba}	1.19 ± 0.03 ^{Ca}
	Cohesiveness	0.243 ± 0.010	0.24 ± 0.01	0.23 ± 0.01	0.25 ± 0.01
	Springiness, mm	1.000 ± 0 ^A	0.98 ± 0.02 ^{AB}	0.93 ± 0.03 ^{Ba}	1.000 ± 0 ^A
	Gumminess, N	0.23 ± 0.02 ^{Aa}	0.227 ± 0.040 ^{ABCa}	0.198 ± 0.010 ^{Ba}	0.301 ± 0.010 ^{Ca}
	Chewiness, N/mm	0.235 ± 0.040 ^{Aa}	0.223 ± 0.040 ^{Aa}	0.184 ± 0.010 ^{Ba}	0.301 ± 0.010 ^{Ca}
	Adhesiveness, Kgf·s	0.12 ± 0.02 ^{Aa}	0.110 ± 0.016 ^A	0.10 ± 0.01 ^A	0.020 ± 0.001 ^B
15	Hardness, N	0.71 ± 0.10 ^{Ab}	0.837 ± 0.030 ^{Bb}	0.763 ± 0.050 ^{ABa}	0.80 ± 0.04 ^{ABb}
	Cohesiveness	0.236 ± 0.050	0.23 ± 0.01	0.23 ± 0.01	0.247 ± 0.010
	Springiness, mm	0.977 ± 0.030	1.000 ± 0	0.997 ± 0.010 ^{ab}	0.947 ± 0.080
	Gumminess, N	0.167 ± 0.020 ^{Ab}	0.192 ± 0.010 ^{Aa}	0.176 ± 0.010 ^{Aa}	0.198 ± 0.010 ^{Ab}
	Chewiness, N/mm	0.163 ± 0.020 ^{Ab}	0.192 ± 0.020 ^{Aa}	0.176 ± 0.010 ^{Aab}	0.187 ± 0.020 ^{Ab}
	Adhesiveness, Kgf·s	0.07 ± 0.01 ^{ab}	0.06 ± 0.01	0.060 ± 0.002	0.033 ± 0.002
30	Hardness, N	0.477 ± 0.020 ^{Ac}	0.477 ± 0.020 ^{Ac}	0.61 ± 0.04 ^{Bb}	0.56 ± 0.04 ^{ABc}
	Cohesiveness	0.23 ± 0.01	0.21 ± 0.02	0.23 ± 0.01	0.23 ± 0.02
	Springiness, mm	0.993 ± 0.010	0.987 ± 0.010	0.998 ± 0 ^{ab}	0.98 ± 0.03
	Gumminess, N	0.109 ± 0.010 ^{ABc}	0.101 ± 0.010 ^{Ab}	0.14 ± 0.01 ^{Bb}	0.129 ± 0.010 ^{ABc}
	Chewiness, N/mm	0.109 ± 0.010 ^{ABc}	0.10 ± 0.02 ^{Ab}	0.14 ± 0.02 ^{Bb}	0.124 ± 0.020 ^{ABc}
	Adhesiveness, Kgf·s	0.050 ± 0.003 ^{ab}	0.060 ± 0.008	0.05 ± 0.01	0.020 ± 0.001
Storage temperature 12°C					
0	Hardness, N	0.976 ± 0.060 ^{Aa}	0.947 ± 0.180 ^{Aa}	0.85 ± 0.02 ^{Ba}	1.19 ± 0.03 ^{Ca}
	Cohesiveness	0.243 ± 0.010	0.24 ± 0.01	0.23 ± 0.01	0.25 ± 0.01
	Springiness, mm	1.000 ± 0	0.98 ± 0.02	0.93 ± 0.03	1.000 ± 0
	Gumminess, N	0.23 ± 0.02 ^{Aa}	0.227 ± 0.040 ^{ABCa}	0.198 ± 0.010 ^{Ba}	0.301 ± 0.010 ^{Ca}
	Chewiness, N/mm	0.235 ± 0.040 ^{Aa}	0.223 ± 0.040 ^{Aa}	0.184 ± 0.010 ^{Ba}	0.301 ± 0.010 ^{Ca}
	Adhesiveness, Kgf·s	0.12 ± 0.02 ^{Aa}	0.110 ± 0.016 ^A	0.10 ± 0.01 ^A	0.020 ± 0.001 ^B
15	Hardness, N	0.463 ± 0.010 ^{Ac}	0.477 ± 0.010 ^{Ac}	0.66 ± 0.04 ^{Bb}	0.59 ± 0.04 ^{Bc}
	Cohesiveness	0.22 ± 0.01	0.210 ± 0.005	0.22 ± 0.01	0.23 ± 0.02
	Springiness, mm	1.000 ± 0	0.99 ± 0.01	1.03 ± 0.10 ^b	0.963 ± 0.010
	Gumminess, N	0.101 ± 0.010 ^{Ac}	0.100 ± 0.002 ^{Ab}	0.148 ± 0.010 ^{Bab}	0.136 ± 0.010 ^{ABc}
	Chewiness, N/mm	0.101 ± 0.010 ^{Ac}	0.100 ± 0.002 ^{Ab}	0.15 ± 0.01 ^{Bab}	0.13 ± 0.02 ^{ABc}
	Adhesiveness, Kgf·s	0.040 ± 0.005 ^b	0.050 ± 0.004	0.070 ± 0.001	0.040 ± 0.001
30	Hardness, N	0.463 ± 0.010 ^{Ac}	0.467 ± 0.010 ^{Ac}	0.61 ± 0.04 ^{Bb}	0.55 ± 0.04 ^{ABc}
	Cohesiveness	0.21 ± 0.01	0.200 ± 0.002	0.225 ± 0.010	0.229 ± 0.020
	Springiness, mm	1.000 ± 0	1.000 ± 0	0.987 ± 0.010 ^{ab}	0.993 ± 0.010
	Gumminess, N	0.097 ± 0.002 ^{ABc}	0.090 ± 0.003 ^{Ab}	0.134 ± 0.010 ^{Bb}	0.136 ± 0.010 ^{ABc}
	Chewiness, N/mm	0.097 ± 0.002 ^{ABc}	0.093 ± 0.010 ^{Ab}	0.132 ± 0.020 ^{Bb}	0.125 ± 0.020 ^{ABc}
	Adhesiveness, Kgf·s	0.060 ± 0.001 ^{ab}	0.040 ± 0.002	0.070 ± 0.001	0.040 ± 0.002

P55, P65 and P75 are the samples pasteurized at 55, 65, and 75°C

Averages with different capital (A–C) letters in the same row indicate statistically significant difference ($p < 0.05$) between treatments at the same storage time. Averages with different small (a–c) letters in the same column indicate statistically significant difference ($p < 0.05$) within treatments during different storage times

samples during storage [49]. Similar findings have been observed for adhesiveness in fish and sausage and for cohesiveness during cold storage in sausage [48, 52, 53].

It has been reported that adhesiveness and cohesiveness can play an important role in product slicing and that increasing adhesiveness and cohesiveness results in increased product stickiness, which is an undesirable attribute for consumer preference [54]. In our study, post-package pasteurization had no effect on the product's adhesiveness or cohesiveness, and these parameters remained unchanged during cold storage.

Springiness. Post-package pasteurization had no effect on the springiness of the samples ($p > 0.05$) (Table 3). However, when compared to the control and P55 samples, the P65 samples had the lowest springiness ($p < 0.05$), which can be attributed to collagen and sarcoplasmic transitions that occurred between 65 and 67°C [43]. A similar result was observed for springiness during the heating of chicken breast meat at 50–90°C [16]. Similarly, another study discovered that the springiness of the samples treated at 65°C was lower than that of the samples treated at 72°C [27].

The springiness of the samples did not change significantly at any of the storage temperatures ($p > 0.05$). Since an increase in springiness has been linked to a decrease in pH, while a decrease in springiness has been linked to an increase in drip loss, our results for springiness during storage may be related to the interaction of these factors [48, 55]. Feng *et al.* found no significant changes in the springiness of sausages after 58 days of refrigerated storage [48]. Our findings revealed that post-package pasteurization had no effect on the springiness of the samples. Additionally, this parameter remained constant across all storage temperatures (5 and 12°C), suggesting that post-package pasteurization can preserve the texture quality of beef ham.

Sensory analysis. Taste, odor, and texture. Figure 2 depicts the sensory analysis of the samples after post-package pasteurization and during cold storage. Post-package pasteurization had no effect on the taste, odor, or texture of the samples, according to the panelists ($p > 0.05$) (Figs. 2a–c), which was consistent with previous post-package pasteurization studies [27, 56] on sausage and pork. The sensory scores of taste and odor in the control and the P55 samples decreased significantly ($p < 0.05$) during cold storage at both 5 and 12°C, reaching 1 at the end of storage (Figs. 2a and b). The decreased taste and odor scores during storage could be attributed to an increase in microbial growth, free fatty acid formation, and oxidative rancidity [52]. Odors and off-tastes become noticeable when bacterial counts, particularly lactic acid bacteria, reach 7 logs, according to our findings and other studies [17, 52].

The sensory scores of texture decreased significantly at both storage temperatures in the control, P55, and P75 samples, according to the panelists ($p < 0.05$). However, these scores did not fall below 3 (Fig. 2c). Lower texture scores in the control and P55 samples can be related to a drop in pH, which changes muscle protein interaction and, as a result, changes textural structures [57]. The decrease in product firmness during storage has been attributed to enzymatic and microbiological activity [49]. It could also be due to the residual proteolysis activity of the protease after thermal heating during cold storage in the P75 hams [51]. Our findings were compatible with those reported by Feki *et al.* for sausage and Sani *et al.* for lamb meat [52, 58]. Our study revealed that post-package pasteurization had no effect on the taste, odor, or texture of the product. These findings also demonstrated that taste and odor in the P65 and P75 samples, as well as texture in P65, could be preserved during both cold storage periods.

Slime formation, color, and swelling. As depicted in Figs. 2d–f, post-package pasteurization had no noticeable impact on slime formation, color, or swelling in the samples ($p > 0.05$). These results were consistent with those of Vahabi Anaraki *et al.* [4].

Slime formation, color, and swelling scores in the control samples, as well as swelling scores in the P55

samples, decreased significantly ($p < 0.05$) at both storage temperatures, and those scores fell below 3. Slime formation and pack swelling during storage are linked to the growth of lactic acid bacteria, primarily *Leuconostoc mesenteroides* [59]. The decreased color score during storage can be related to pigment and lipid oxidation, which causes non-enzymatic browning of lipids and amino acids [52]. The results of color analysis in our study agree with those of Feki *et al.* and Sani *et al.* in beef sausage and lamb meat, respectively [52, 58]. Our study showed no statistically significant differences in these sensory qualities in the pasteurized samples. Furthermore, only the non-pasteurized samples had lower scores for slime formation and color after 30 days of cold storage (5 and 12°C), and pack swelling scores only decreased in the control and P55 samples.

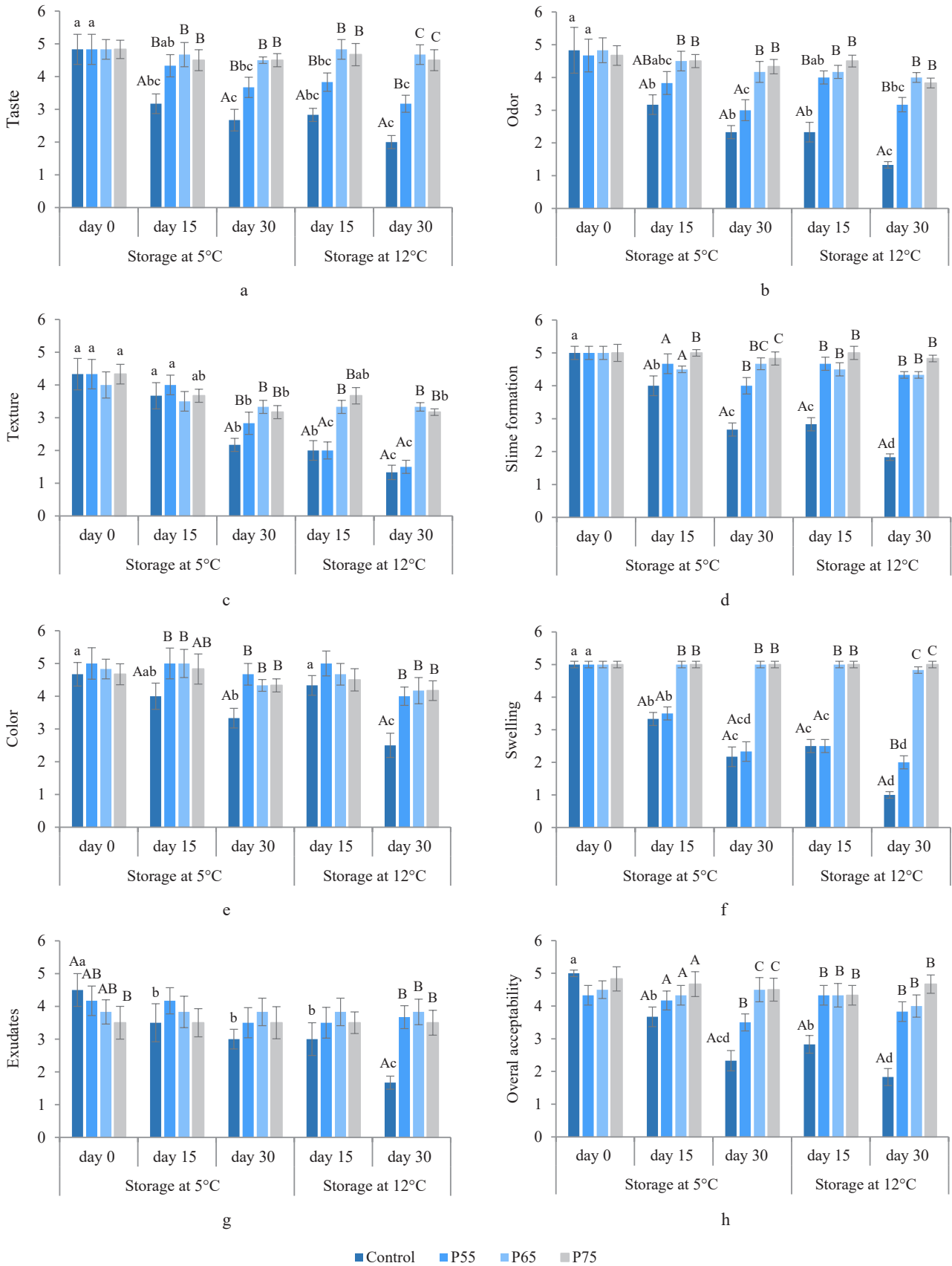
Exudates. As displayed in Fig. 2g, the exudate scores for the pasteurized samples showed a pattern of decreasing acceptability as the post-package pasteurization temperatures rose. Heat treatment-induced protein denaturation is related to an increase in exudates [60].

The exudates scores decreased significantly during cold storage in the control and P55 ham samples ($p < 0.05$). Although the decrease in P55 was lower than in the control group and remained above 3, while the scores in the control group reached 4 at 5°C and fell below 2 at 12°C, this decline could be attributed to a decrease in pH, which caused protein denaturation and aggregation disarray, resulting in moisture loss [50]. Our results for exudates agree with those reported by Vahabi Anaraki *et al.* in turkey breast [4]. According to our results, post-package pasteurization had a negative effect on the exudates score of the pasteurized samples. After 30 days of cold storage at both 5 and 12°C, the score for this parameter did not decrease in either the P65 or P75 samples, reflecting the absence of microbial growth in these samples.

Overall acceptability. As illustrated in Fig. 2h, the overall acceptability of the P55, P65, and P75 ham samples remained from “moderate” to “very good” and never fell below 3. In the control samples, however, the scores dropped significantly to “bad” and “very bad”, and on the 30th day of cold storage, the overall acceptability fell below 3 at 5°C and below 2 at 12°C ($p < 0.05$). The higher sensory quality of the P65 and P75 samples was due to the lack of spoilage microorganisms in these samples, and the higher overall acceptability scores for the P55 ham, compared to the control samples, might be due to the inhibitory effect of post-package pasteurization on microbial growth in these samples. According to our findings, we can conclude that post-package pasteurization can maintain the sensory characteristics of beef ham in pasteurized samples stored at 5 and 12°C.

CONCLUSION

Our study revealed that post-package pasteurization could significantly reduce number of lactic acid bacteria, total aerobic mesophilic counts, and total



P55, P65 and P75 are the samples pasteurized at 55, 65, and 75°C

The different capital (A–C) and small (a–c) letters indicate statistically significant difference ($p < 0.05$) between treatments and in treatments, respectively, during both storage temperatures (5 and 12°C). Each point represents the mean \pm SD

Figure 2 Sensory attributes of control and post-package pasteurization-treated hams during 30 days of storage at 5 and 12°C: taste (a); odor (b); texture (c); slime formation (d); color (e); swelling (f); exudates (g); and overall acceptability (h)

psychrotrophic counts. Furthermore, we found that post-package pasteurization significantly increased drip loss and exudates in the treated samples. Fortunately, post-package pasteurization had no negative effect on the texture, color analysis, or sensory properties of beef ham, such as taste, odor, slime, swelling, color, texture, or overall acceptability. Also, it could significantly maintain these qualities in the P65 and P75 samples until the end of day 30 during cold storage at both 5 and 12°C. According to our findings, 65°C was the optimum temperature for post-package pasteurization application in 90% beef ham.

Our study indicated that post-package pasteurization can be easily applied on an industrial scale, and the only downside to it is increased drip loss during the heating of the product. This issue could be resolved by using a

different starch or phosphate in the formulation of this product to increase the water-holding capacity during post-package pasteurization.

CONTRIBUTION

The authors were equally involved in writing the manuscript and are equally responsible for any potential plagiarism.

CONFLICT OF INTEREST

The authors declare no potential conflict of interest.

ACKNOWLEDGMENTS

The authors would like to express their thanks to the Kalleh Meat Products Company in Iran for providing financial support for this study.

REFERENCES

1. Corrêa JAF, dos Santos JVG, Evangelista AG, Pinto ACSM, de Macedo REF, Luciano FB. Combined application of phenolic acids and essential oil components against *Salmonella* Enteritidis and *Listeria monocytogenes* in vitro and in ready-to-eat cooked ham. *LWT*. 2021;149. <https://doi.org/10.1016/j.lwt.2021.111881>
2. Vinnikova L, Synytsia O, Shlapak H, Azarova N, Glushkov O. Decrease of repeated contamination of packed delicious meat products. *EUREKA: Life Sciences*. 2019;(5):58–63. <https://doi.org/10.21303/2504-5695.2019.00996>
3. Abhari K, Jafarpour D, Shekarforoush SS. Effects of in-package pasteurization on preventing spoilage in emulsion vacuum packaged sausages during refrigerated storage. *Foods and Raw Materials*. 2018;6(1):40–46. <https://doi.org/10.21603/2308-4057-2018-1-40-46>
4. Vahabi Anaraki N, Abbasvali M, Bonyadian M. Effects of post-packaging pasteurization process on microbial, chemical, and sensory qualities of ready-to-eat cured vacuum-packed Turkey breast. *Journal of Food Safety*. 2020;40. <https://doi.org/10.1111/jfs.12776>
5. Horita CN, Baptista RC, Caturla MYR, Lorenzo JM, Barba FJ, Sant'Ana AS. Combining reformulation, active packaging and non-thermal post-packaging decontamination technologies to increase the microbiological quality and safety of cooked ready-to-eat meat products. *Trends in Food Science and Technology*. 2018;72:45–61. <https://doi.org/10.1016/j.tifs.2017.12.003>
6. Wang Q, Zhang M, Adhikari B, Cao P, Yang C-H. Effects of various thermal processing methods on the shelf-life and product quality of vacuum-packaged braised beef. *Journal of Food Process Engineering*. 2019;42(4). <https://doi.org/10.1111/jfpe.13035>
7. Huang L, Hwang C-A, Fang T. Improved estimation of thermal resistance of *Escherichia coli* O157:H7, *Salmonella* spp., and *Listeria monocytogenes* in meat and poultry – The effect of temperature and fat and A global analysis. *Food Control*. 2019;96:29–38. <https://doi.org/10.1016/j.foodcont.2018.08.026>
8. Hwang S-I, Lee E-J, Hong G-P. Effects of temperature and time on the cookery properties of sous-vide processed pork loin. *Food Science of Animal Resources*. 2019;39(1):65–72. <https://doi.org/10.5851/kosfa.2019.e4>
9. Jeong K, Hyeonbin O, Shin SY, Kim Y-S. Effects of sous-vide method at different temperatures, times and vacuum degrees on the quality, structural, and microbiological properties of pork ham. *Meat Science*. 2018;143:1–7. <https://doi.org/10.1016/j.meatsci.2018.04.010>
10. Roldán M, Antequera T, Martín A, Mayoral AI, Ruiz J. Effect of different temperature–time combinations on physicochemical, microbiological, textural and structural features of sous-vide cooked lamb loins. *Meat Science*. 2013;93(3):572–578. <https://doi.org/10.1016/j.meatsci.2012.11.014>
11. Shen S, Chen Y, Dong X, Liu F, Cai W, Wei J, et al. Changes in food quality and microbial composition of Russian sturgeon (*Acipenser gueldenstaedti*) fillets treated with low temperature vacuum heating method during storage at 4°C. *Food Research International*. 2020;138. <https://doi.org/10.1016/j.foodres.2020.109665>
12. Haghghi H, Belmonte AM, Masino F, Minelli G, Lo Fiego DP, Pulvirenti A. Effect of time and temperature on physicochemical and microbiological properties of sous vide chicken breast fillets. *Applied Sciences*. 2021;11(7). <https://doi.org/10.3390/app11073189>

13. Bertola NC, Bevilacqua AE, Zaritzky NE. Heat treatment effect on texture changes and thermal denaturation of proteins in beef muscle. *Journal of Food Processing and Preservation*. 1994;18(1):31–46. <https://doi.org/10.1111/j.1745-4549.1994.tb00240.x>
14. Cai W, Wei J, Chen Y, Dong X, Zhang J, Bai F, et al. Effect of low-temperature vacuum heating on physicochemical properties of sturgeon (*Acipenser gueldenstaedti*) fillets. *Journal of the Science of Food and Agriculture*. 2020;100(12):4583–4591. <https://doi.org/10.1002/jsfa.10517>
15. D'sa EM, Harrison MA, Williams SE, Broccoli MH. Effectiveness of two cooking systems in destroying *Escherichia coli* O157:H7 and *Listeria monocytogenes* in ground beef patties. *Journal of Food Protection*. 2000;63(7):894–899. <https://doi.org/10.4315/0362-028X-63.7.894>
16. Rabeler F, Feyissa AH. Kinetic modeling of texture and color changes during thermal treatment of chicken breast meat. *Food and Bioprocess Technology*. 2018;11:1495–1504. <https://doi.org/10.1007/s11947-018-2123-4>
17. Khorsandi A, Eskandari MH, Aminlari M, Shekarforoush SS, Golmakani MT. Shelf-life extension of vacuum packed emulsion-type sausage using combination of natural antimicrobials. *Food Control*. 2019;104:139–146. <https://doi.org/10.1016/j.foodcont.2019.04.040>
18. Dang TT, Rode TM, Skipnes D. Independent and combined effects of high pressure, microwave, soluble gas stabilization, modified atmosphere and vacuum packaging on microbiological and physicochemical shelf life of precooked chicken breast slices. *Journal of Food Engineering*. 2021;292. <https://doi.org/10.1016/j.jfoodeng.2020.110352>
19. Menéndez RA, Rendueles E, Sanz JJ, Santos JA, García-Fernández MC. Physicochemical and microbiological characteristics of diverse Spanish cured meat products. *CyTA – Journal of Food*. 2018;16(1):199–204. <https://doi.org/10.1080/19476337.2017.1379560>
20. Contador R, Ortiz A, del Rosario Ramírez M, García-Torres S, López-Parra MM, Tejerina D. Physico-chemical and sensory qualities of Iberian sliced dry-cured loins from various commercial categories and the effects of the type of packaging and refrigeration time. *LWT*. 2021;141. <https://doi.org/10.1016/j.lwt.2021.110876>
21. Hamdi M, Nasri R, Dridi N, Moussa H, Ashour L, Nasri M. Improvement of the quality and the shelf life of reduced-nitrites turkey meat sausages incorporated with carotenoproteins from blue crabs shells. *Food Control*. 2018;91:148–159. <https://doi.org/10.1016/j.foodcont.2018.03.048>
22. Fernández-López J, Lucas-González R, Viuda-Martos M, Sayas-Barberá E, Navarro C, Haros CM, et al. Chia (*Salvia hispanica* L.) products as ingredients for reformulating frankfurters: Effects on quality properties and shelf-life. *Meat Science*. 2019;156:139–145. <https://doi.org/10.1016/j.meatsci.2019.05.028>
23. Herman RA, Adzitey F, Teye GA. The shelf life of coarse beef sausage using dawadawa (*Parkia biglobosa*) pulp powder as an extender. *Journal of Postharvest Technology*. 2019;7(2):62–68.
24. Franz CMAP, von Holy A. Thermotolerance of meat spoilage lactic acid bacteria and their inactivation in vacuum-packaged Vienna sausages. *International Journal of Food Microbiology*. 1996;29(1):59–73. [https://doi.org/10.1016/0168-1605\(95\)00022-4](https://doi.org/10.1016/0168-1605(95)00022-4)
25. Pinggen S, Sudhaus N, Becker A, Krischek C, Klein G. High pressure as an alternative processing step for ham production. *Meat Science*. 2016;118:22–27. <https://doi.org/10.1016/j.meatsci.2016.03.014>
26. Ku S-K, Kim J, Kim S-M, Yong HI, Kim B-K, Choi Y-S. Combined effects of pressure cooking and enzyme treatment to enhance the digestibility and physicochemical properties of spreadable liver sausage. *Food Science of Animal Resources*. 2022;42(3):441–454. <https://doi.org/10.5851/kosfa.2022.e14>
27. Ji D-S, Kim J-H, Yoon D-K, Kim J-H, Lee H-j, Cho W-Y, et al. Effect of different storage-temperature combinations on *Longissimus dorsi* quality upon sous-vide processing of frozen/thawed pork. *Food Science of Animal Resources*. 2019;39(2):240–254. <https://doi.org/10.5851/kosfa.2019.e19>
28. Wang Z, Shi Y, Zhou K, Zhou H, Li X, Li C, et al. Effects of different thermal temperatures on the shelf life and microbial diversity of Dezhou-braised chicken. *Food Research International*. 2020;136. <https://doi.org/10.1016/j.foodres.2020.109471>
29. Sorapukdee S, Jansa S, Tangwatcharin P. Partial replacement of pork backfat with konjac gel in Northeastern Thai fermented sausage (Sai Krok E-san) to produce the healthier product. *Asian-Australasian Journal of Animal Sciences*. 2019;32(11):1763–1775. <https://doi.org/10.5713/ajas.18.0811>
30. Wang Z-C, Yan Y, Fang Z, Nisar T, Sun L, Guo Y, et al. Application of nitric oxide in modified atmosphere packaging of tilapia (*Oreochromis niloticus*) fillets. *Food Control*. 2019;98:209–215. <https://doi.org/10.1016/j.foodcont.2018.11.043>
31. Ozaki MM, Munekata PES, Jacinto-Valderrama RA, Efraim P, Pateiro M, Lorenzo JM, et al. Beetroot and radish powders as natural nitrite source for fermented dry sausages. *Meat Science*. 2021;171. <https://doi.org/10.1016/j.meatsci.2020.108275>

32. Zhang L, Du H, Zhang P, Kong B, Liu Q. Heterocyclic aromatic amine concentrations and quality characteristics of traditional smoked and roasted poultry products on the northern Chinese market. *Food and Chemical Toxicology*. 2020;135. <https://doi.org/10.1016/j.fct.2019.110931>
33. Lee S, Choi Y-S, Jo K, Jeong HG, Yong HI, Kim T-K, et al. Processing characteristics of freeze-dried pork powder for meat emulsion gel. *Food Science of Animal Resources*. 2021;41(6):997–1011. <https://doi.org/10.5851/kosfa.2021.e51>
34. Aleson-Carbonell L, Fernández-López J, Pérez-Alvarez JA, Kuri V. Functional and sensory effects of fibre-rich ingredients on breakfast fresh sausages manufacture. *Food Science and Technology International*. 2005;11(2):89–97. <https://doi.org/10.1177/1082013205052003>
35. Alirezalu K, Hesari J, Nemati Z, Munekata PES, Barba FJ, Lorenzo JM. Combined effect of natural antioxidants and antimicrobial compounds during refrigerated storage of nitrite-free frankfurter-type sausage. *Food Research International*. 2019;120:839–850. <https://doi.org/10.1016/j.foodres.2018.11.048>
36. Cao J, Wang Q, Ma T, Bao K, Yu X, Duan Z, et al. Effect of EGCG-gelatin biofilm on the quality and microbial composition of tilapia fillets during chilled storage. *Food Chemistry*. 2020;305. <https://doi.org/10.1016/j.foodchem.2019.125454>
37. Santovito E, Elisseeva S, Cruz-Romero MC, Duffy G, Kerry JP, Papkovsky DB. A Simple sensor system for onsite monitoring of O₂ in vacuum-packed meats during the shelf life. *Sensors*. 2021;21(13). <https://doi.org/10.3390/s21134256>
38. Zhang Y, Tian X, Jiao Y, Wang Y, Dong J, Yang N, et al. Free iron rather than heme iron mainly induces oxidation of lipids and proteins in meat cooking. *Food Chemistry*. 2022;382. <https://doi.org/10.1016/j.foodchem.2022.132345>
39. Cava R, García-Parra J, Ladero L. Effect of high hydrostatic pressure processing and storage temperature on food safety, microbial counts, colour and oxidative changes of a traditional dry-cured sausage. *LWT*. 2020;128. <https://doi.org/10.1016/j.lwt.2020.109462>
40. Yu HH, Kim YJ, Park YJ, Shin D-M, Choi Y-S, Lee N-K, et al. Application of mixed natural preservatives to improve the quality of vacuum skin packaged beef during refrigerated storage. *Meat Science*. 2020;169. <https://doi.org/10.1016/j.meatsci.2020.108219>
41. Alirezalu K, Hesari J, Yaghoubi M, Khaneghah AM, Alirezalu A, Pateiro M, et al. Combined effects of ε-polylysine and ε-polylysine nanoparticles with plant extracts on the shelf life and quality characteristics of nitrite-free frankfurter-type sausages. *Meat Science*. 2021;172. <https://doi.org/10.1016/j.meatsci.2020.108318>
42. Ran M, He L, Li C, Zhu Q, Zeng X. Quality changes and shelf-life prediction of cooked cured ham stored at different temperatures. *Journal of Food Protection*. 2021;84(7):1252–1264. <https://doi.org/10.4315/JFP-20-374>
43. Tornberg E. Effects of heat on meat proteins – Implications on structure and quality of meat products. *Meat Science*. 2005;70(3):493–508. <https://doi.org/10.1016/j.meatsci.2004.11.021>
44. Truong BQ, Buckow R, Nguyen MH, Stathopoulos CE. High pressure processing of barramundi (*Lates calcarifer*) muscle before freezing: The effects on selected physicochemical properties during frozen storage. *Journal of Food Engineering*. 2016;169:72–78. <https://doi.org/10.1016/j.jfoodeng.2015.08.020>
45. Rigdon M, Thippareddi H, McKee RW, Thomas CL, Stelzleni AM. Texture of fermented summer sausage with differing pH, endpoint temperature, and high pressure processing times. *Meat and Muscle Biology*. 2020;4(1). <https://doi.org/10.22175/mmb.9476>
46. Villacís M, Rastogi NK, Balasubramaniam VM. Effect of high pressure on moisture and NaCl diffusion into turkey breast. *LWT – Food Science and Technology*. 2008;41(5):836–844. <https://doi.org/10.1016/j.lwt.2007.05.018>
47. Kumar M, Sharma BD. The storage stability and textural, physico-chemical and sensory quality of low-fat ground pork patties with Carrageenan as fat replacer. *International Journal of Food Science and Technology*. 2003;39(1): 31–42. <https://doi.org/10.1111/j.1365-2621.2004.00743.x>
48. Feng C-H, Wang W, Makino Y, García-Martín JF, Alvarez-Mateos P, Song X-Y. Evaluation of storage time and temperature on physicochemical properties of immersion vacuum cooled sausages stuffed in the innovative casings modified by surfactants and lactic acid. *Journal of Food Engineering*. 2019;257:34–43. <https://doi.org/10.1016/j.jfoodeng.2019.03.023>
49. Rahman MS, Seo J-K, Zahid MdA, Park J-Y, Choi S-G, Yang H-S. Physicochemical properties, sensory traits and storage stability of reduced-fat frankfurters formulated by replacing beef tallow with defatted bovine heart. *Meat Science*. 2019;151:89–97. <https://doi.org/10.1016/j.meatsci.2019.01.011>
50. Lau ATY, Arvaj L, Strange P, Goodwin M, Barbut S, Balamurugan S. Effect of cranberry pomace on the physicochemical properties and inactivation of *Salmonella* during the manufacture of dry fermented sausages. *Current Research in Food Science*. 2021;4:636–645. <https://doi.org/10.1016/j.crfs.2021.09.001>
51. Akoğlu I, Bıyıklı M, Akoğlu A, Kurhan Ş. Determination of the quality and shelf life of sous vide cooked turkey cutlet stored at 4 and 12°C. *Brazilian Journal of Poultry Science*. 2018;20(1):001–008. <https://doi.org/10.1590/1806-9061-2017-0571>

52. Feki A, Sellem I, Hamzaoui A, Amar WB, Mellouli L, Zariat A, et al. Effect of the incorporation of polysaccharide from *Falkenbergia rufolanosa* on beef sausages for quality and shelf life improvement. *LWT*. 2021;143. <https://doi.org/10.1016/j.lwt.2021.111139>
53. Sutikno LA, Bashir KMI, Kim H, Park Y, Won NE, An JH, et al. Improvement in physicochemical, microbial, and sensory properties of common squid (*Todarodes pacificus* Steenstrup) by superheated steam roasting in combination with smoking treatment. *Journal of Food Quality*. 2019;2019. <https://doi.org/10.1155/2019/8721725>
54. Safaei F, Abhari K, Khosroshahi NK, Hosseini H, Jafari M. Optimisation of functional sausage formulation with konjac and inulin: using D-Optimal mixture design. *Foods and Raw Materials*. 2019;7(1):177–184. <https://doi.org/10.21603/2308-4057-2019-1-177-184>.
55. Jung E-Y, Yun I-R, Go G, Kim G-D, Seo H-W, Joo S-T, et al. Effects of *radix puerariae* extracts on physicochemical and sensory quality of precooked pork sausage during cold storage. *LWT – Food Science and Technology*. 2012;46(2):556–562. <https://doi.org/10.1016/j.lwt.2011.11.007>
56. Inmanee P, Kamonpatana P, Pirak T. Ohmic heating effects on *Listeria monocytogenes* inactivation, and chemical, physical, and sensory characteristic alterations for vacuum packaged sausage during post pasteurization. *LWT*. 2019;108:183–189. <https://doi.org/10.1016/j.lwt.2019.03.027>
57. Shin D-J, Lee HJ, Lee D, Jo C, Choe J. Fat replacement in chicken sausages manufactured with broiler and old laying hens by different vegetable oils. *Poultry Science*. 2020;99(5):2811–2818. <https://doi.org/10.1016/j.psj.2020.01.008>
58. Sani MA, Ehsani A, Hashemi M. Whey protein isolate/cellulose nanofibre/TiO₂ nanoparticle/rosemary essential oil nanocomposite film: Its effect on microbial and sensory quality of lamb meat and growth of common foodborne pathogenic bacteria during refrigeration. *International Journal of Food Microbiology*. 2017;251:8–14. <https://doi.org/10.1016/j.ijfoodmicro.2017.03.018>
59. Samelis J, Kakouri A. Growth inhibitory and selective pressure effects of sodium diacetate on the spoilage microbiota of frankfurters stored at 4°C and 12°C in Vacuum. *Foods*. 2021;10(1). <https://doi.org/10.3390/foods10010074>
60. Hassoun A, Aït-Kaddour A, Sahar A, Cozzolino D. Monitoring thermal treatments applied to meat using traditional methods and spectroscopic techniques: A review of advances over the last decade. *Food and Bioprocess Technology*. 2021;14:195–208. <https://doi.org/10.1007/s11947-020-02510-0>

ORCID IDs

Nasim Azizpour  <https://orcid.org/0000-0002-4362-1611>

Seyed Hadi Razavi  <https://orcid.org/0000-0002-5815-4411>

Mehran Azizpour  <https://orcid.org/0000-0001-9124-4091>

Esmail Khazaei Poul  <https://orcid.org/0009-0001-9149-0994>



Chemical, rheological, and sensory properties of wheat biscuits fortified with local buckwheat

Ahmed M. S. Hussein¹, Hala A. Abd El-Aal²,
Nahla M. Morsy², Mohamed M. Hassona^{2,3,*}

¹ National Research Center, Cairo, Egypt

² University of Sadat City^{ROR}, Sadat, Egypt

³ Hamad bin Khalifa University^{ROR}, Doha, Qatar

* e-mail: mmamh83@gmail.com

Received 12.01.2023; Revised 13.02.2023; Accepted 07.03.2023; Published online 11.10.2023

Abstract:

The research featured two species of buckwheat: *Fagopyrum esculentum* Moench. and *Fagopyrum tataricum* (L.) Gaertn.

The authors used 10, 20, or 30% of buckwheat flour to substitute soft wheat flour in order to obtain biscuits with improved sensory and nutritional properties.

The biscuits were tested for chemical composition, rheology, color, baking quality, sensory properties, and texture. The sample made of soft wheat flour and *F. tataricum* contained less protein and fat than the sample with *F. esculentum*. The samples with *F. tataricum* demonstrated greater amounts of fiber and ash while the samples made of soft wheat flour were rich in carbohydrates. The additional increment enhanced the arrival time, dough development time, dough stability, the mixing tolerance index, and weakening. Compared to the control, the samples with *F. esculentum* demonstrated lower peak, trough, breakdown, final, and setback viscosities. *F. tataricum*, on the contrary, increased the viscosity readings. The biscuits fortified with *F. esculentum* and *F. tataricum* contained more protein, fat, ash, and crude fiber the control. The control biscuits also exceeded the total carbohydrates. The experimental biscuits with *F. esculentum* and *F. tataricum* were darker in color than the control: the lightness (L^*) and redness values (b^*) decreased as the proportion of *F. esculentum*/*F. tataricum* rose. However, the experimental biscuits had a higher level of yellowness (a^*). As the replacement levels rose, *F. esculentum* and *F. tataricum* reduced biscuit weight and volume.

According to the research results, 30% *F. esculentum* and 20% *F. tataricum* proved able to yield nutritious biscuits with outstanding physical properties. Greater proportions of *F. esculentum*/*F. tataricum* resulted in poor sensory ratings for color, taste, flavour, texture, appearance, and overall acceptability.

Keywords: *Fagopyrum tataricum*, *Fagopyrum esculentum*, semolina, biscuit, chemical composition, color, baking quality, sensory evaluation, texture

Please cite this article in press as: Hussein AMS, Abd El-Aal HA, Morsy NM, Hassona MM. Chemical, rheological, and sensory properties of wheat biscuits fortified with local buckwheat. *Foods and Raw Materials*. 2024;12(1):156–167. <https://doi.org/10.21603/2308-4057-2024-1-597>

INTRODUCTION

Cereals products constitute an essential part of human diet. They are responsible for carbohydrates, proteins, fats, dietary fiber, B-group vitamins, and minerals. Whole grains are an essential ingredient in many processed foods [1]. In Egypt, biscuits are a popular bakery item consumed by nearly all social groups. They are affordable, nutritious, shelf-stable, and diverse in shape and taste. Bakery products are often fortified with various nutritional ingredients [2–4]. A basic biscuit

formulation includes such essential primary ingredients as flour, fats, water, and sugar. Fats provide plasticity and incorporate air during dough formation. They enable the dough to withstand the baking temperatures without losing shape [5].

Buckwheat is a so-called pseudocereal that derives from the genus of *Fagopyrum*. The common buckwheat (*Fagopyrum esculentum* Moench.) is the most prevalent buckwheat species [6]. Buckwheat is highly adaptable and thrives in various conditions [7]. It contains such flavonoids as quercetin, vitexin, orientin, isovitexin, and

isoorientin. The flavonoid content depends on numerous factors, e.g., testa, seed size and shape, flower color, seeding time, soil placement, environment, climate, growth phases, region, etc. [8]. Buckwheat seeds are also abundant in dietary fibre, which has a beneficial physiological effect on the gastrointestinal system and facilitates the metabolism of other nutrients [9]. In addition, buckwheat seeds are gluten-free and suitable for people with celiac disease [10]. Buckwheat flour is a highly nutritional component often used in pasta, noodles, pancakes, bread, biscuits, etc. [11]. The research objective was to develop a new biscuit formulation from different combinations of the common buckwheat (*F. esculentum*) and the green, or Tatar, buckwheat (*Fagopyrum tataricum* (L.) Gaertn.), as well as to determine the effect of processing procedures on the chemistry, rheology, color, backing quality, sensory properties, and texture of the finished product.

STUDY OBJECTS AND METHODS

This research involved *Fagopyrum esculentum* Moench. (California) and *Fagopyrum tataricum* (L.) Gaertn. (Hong Kong) seeds. The samples possessed a state-certified identification label that provided the scientific, local, and English names of the species, as well as some data on germination and purity ratios. The seeds were sowed, planted, and harvested in the city of Belbies (Sharkia governorate, Egypt; coordinates: 30.4196° N, 31.5619° E) and the city of Sadat (Monofiya, Egypt; coordinates: 30.3594° N, 30.5327° E) in 2018–2019 and 2019–2020 to evaluate the growth and quality of the buckwheat at various growing times. This research involved only hand-picked grains. After initial drying in the field for 3–4 days, they were put in a clean, shaded place for further drying and kernel separation. The soft wheat flour was supplied by South Cairo Mill Company (Giza, Egypt) and accounted for 72% of the total weight. Sugar, eggs, salt (sodium chloride), shortening, baking powder, and vanilla were purchased at a local market (Giza, Egypt).

The list of analytical reagent-grade chemicals and solvents included trichloroacetic acid, thiobarbituric acid, and DPPH (2,2-Diphenyl-1-picryl-hydrazyl). They were obtained from El-Gomhouria Co. for Trading Drugs, Chemicals, and Medical Supplies (Cairo, Egypt).

Technological treatment. Preparing the flour mixes. *F. esculentum* and *F. tataricum* grains were cleaned, tempered (15% moisture), milled (Quadrumat Junior flour mill), filtered through a 40-mesh screen, and packaged in plastic bags. The blends of soft wheat flour (72% extraction) with *F. esculentum* and *F. tataricum* flour had the following ratios: 100:0, 90:10, 80:20, and 70:30 w/w.

Rheology of dough. The farinograph and rapid-visco-analyzer tests followed the guidelines developed by the American Association of Cereal Chemists to determine the rheological qualities of the samples [12].

Preparing the biscuits. We mixed 200 g of soft wheat flour with 10, 20 and 30% of *F. esculentum* or *F. tataricum*. The biscuits were cooked according to the formulation recommended by The Association of Official Analytical Chemists with some modifications (Table 1) [13]. The dry ingredients (flour, sugar, salt, and baking powder) were thoroughly mixed in a bowl by hand for 3 min. Then, egg was added and kneaded in. The dough was rolled and sliced with a five-millimeter biscuit cutter. The biscuits were baked on trays at 200°C for 25 min. After that, they were cooled, packaged in plastic bags, and stored at 28 ± 2°C before the analytical and sensory assessment.

Baking quality. The weight, volume, specific volume, diameter, thickness, and spread ratio were measured in triplicates.

Color attributes. The color of both mixes and biscuits were measured using a Spectro-Colorimeter (Tristimulus Color Machine) with a CIE lab color scale (Hunter, Lab Scan XE, Reston VA.) calibrated using a white Hunter Lab color standard tile (LXNO. 16379): X = 77.26, Y = 81.94, and Z = 88.14. The Hunter-Scotfield's equation was used to measure the color difference (*E*) using Hunter *a*, *b*, and *L* scales:

$$\Delta E = (\Delta a^2 + \Delta b^2 + \Delta L^2)^{1/2},$$

$$a = a - a_0, b = b - b_0, L = L - L_0$$

where 0 stood for the control color.

The hue angle and saturation index were calculated in line with the procedure described by Sapers & Douglas [14].

Table 1 Biscuit formulation

Samples	Control	<i>Fagopyrum esculentum</i>			<i>Fagopyrum tataricum</i>		
		10%	20%	30%	10%	20%	30%
Buckwheat biscuit formulation							
Soft wheat flour	100	90	80	70	90	80	70
Buckwheat flour	–	10	20	30	10	20	30
Salt	0.93	0.93	0.93	0.93	0.93	0.93	0.93
Sucrose	35	35	35	35	35	35	35
Shortening	28	28	28	28	28	28	28
Egg	30	30	30	30	30	30	30
Baking powder	1.5	1.5	1.5	1.5	1.5	1.5	1.5
Vanilla	1	1	1	1	1	1	1

Sensory evaluation. The sensory evaluation relied on the method developed by Hussein *et al.* [15]. Each formulation was analyzed by twenty panelists. Each panelist gave the product a score between 0 and 20 based on its color, smell, taste, texture, appearance, and general acceptability.

Texture analysis. The biscuit samples underwent a texture analysis using a texturometer (Brookfield, CT3-10 kg, USA) with a cylinder probe (TA. AACCC36). The hardness, stickiness, resilience, cohesion, springiness, gumminess, and chewiness were measured using the method of texture profile analysis, which was programmed for two cycles of measurements to generate a two-bit texture profile curve. The trigger load was 9.00 N g, and the test speed was 2.5 mm/s.

Analytical methods. Chemical composition. The ash, crude fiber, fat, and protein levels were calculated using the standards developed by The Association of Official Analytical Chemists [13]. The carbohydrate content was determined as follows:

$$\text{Carbohydrates} = 100 - (\% \text{ protein} + \% \text{ fat} + \% \text{ ash} + \% \text{ crude fiber})$$

Statistical analysis. The obtained results were evaluated statistically using the analysis of variance reported by McClave & Benson [16].

RESULTS AND DISCUSSION

Chemical composition of raw materials. The soft wheat flour, *Fagopyrum tataricum* (L.) Gaertn., and *Fagopyrum esculentum* Moench. were analyzed for mois-

ture, ash, crude protein, lipid, crude fiber, and carbohydrates. Table 2 displays the acquired values for the chemical composition of soft wheat flour, *F. tataricum*, and *F. esculentum*. The soft wheat flour had the most effective moisture content (11.65%), followed by *F. esculentum* (9.17%) and *F. tataricum* (8.78%). *F. esculentum* had higher protein and fat concentrations (14.90 and 2.18%) than soft wheat flour (11.81 and 1.57%) and *F. tataricum* (11.32 and 1.66%). *F. tataricum* contained more fiber and ash than *F. esculentum* (12.51 and 2.58%) and soft wheat flour (0.79 and 0.81%), respectively (22.08 and 2.85%). Soft wheat flour had a more significant proportion of total carbohydrates than *F. tataricum* and *F. esculentum*. The results obtained were consistent with those published elsewhere [17–21].

Rheological parameters. Farinograph parameters. Table 3 and Fig. 1 illustrate the effects of 10, 20, and 30% *F. esculentum*/*F. tataricum* on the farinograph test parameters. The findings demonstrated the effect of combining *F. esculentum*/*F. tataricum* at 10, 20, and 30% with soft wheat flour on such farinograph parameters as water absorption, arrival time, dough development time, dough stability, and dough deterioration. The water absorption value of the soft wheat flour sample was 61.2%. Its combinations with different proportions of *F. esculentum*/*F. tataricum* resulted both in a progressive decline and an increase. In tandem with the extra increase, the arrival time, dough development time, dough stability, mixing tolerance index, and weakening went down, compared to the control. The increased dough development time and stability may have been

Table 2 Proximate chemical composition of raw materials, %

Samples	Chemical composition					
	Moisture	Ash	Fiber	Protein	Lipids	Total carbohydrates
Soft wheat flour	11.65 ± 0.25	0.81 ± 0.10	0.79 ± 0.09	11.32 ± 0.11	1.66 ± 0.14	85.37 ± 0.31
<i>Fagopyrum esculentum</i>	9.17 ± 0.17	2.58 ± 0.07	12.51 ± 0.32	14.90 ± 0.27	2.18 ± 0.05	59.08 ± 0.56
<i>Fagopyrum tataricum</i>	8.78 ± 0.29	2.85 ± 0.01	22.08 ± 0.37	11.81 ± 0.25	1.57 ± 0.03	52.60 ± 0.85

Table 3 Effect of *Fagopyrum esculentum*/*Fagopyrum tataricum* on farinograph parameters

Samples	Water absorption, %	Arrival time, min	Dough development time, min	Dough stability, min	Mixing tolerance Index, Brabender unit	Weakening, Brabender unit
Control (100% soft wheat flour)	61.2	1.5	1.5	3.5	60	90
10% <i>Fagopyrum esculentum</i> + 90% soft wheat flour	60.8	1.0	1.5	6.0	40	80
20% <i>Fagopyrum esculentum</i> + 80% soft wheat flour	60.6	1.5	2.5	6.5	50	90
30% <i>Fagopyrum esculentum</i> + 70% soft wheat flour	60.4	2.0	5.0	8.5	70	70
10% <i>Fagopyrum tataricum</i> + 90% soft wheat flour	61.0	1.0	1.5	3.0	60	100
20% <i>Fagopyrum tataricum</i> + 80% soft wheat flour	61.2	1.5	3.0	5.5	80	110
30% <i>Fagopyrum tataricum</i> + 70% soft wheat flour	61.8	2.0	3.5	5.0	100	120

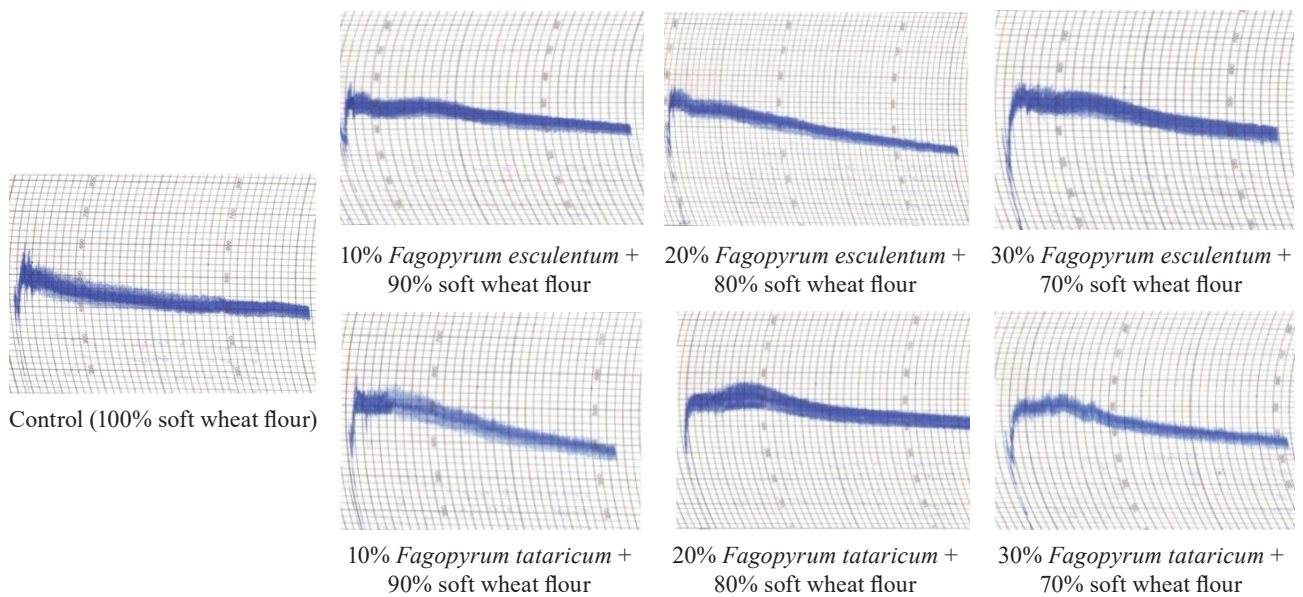


Figure 1 Farinograph parameters of dough samples with 10, 20, and 30% *Fagopyrum esculentum*/*Fagopyrum tataricum*

Table 4 Effect of *Fagopyrum esculentum*/*Fagopyrum tataricum* on pasting properties

Samples	Peak viscosity, cP	Trough viscosity, cP	Break down viscosity, cP	Final viscosity, cP	Setback viscosity, cP	Peak time, min	Pasting temperature, °C	Peak temperature, °C
Control (100% soft wheat flour)	2508	1659.92	977.8	2573	-64.92	12.1	42.4	94.5
10% <i>Fagopyrum esculentum</i> + 90% soft wheat flour	3008	1452.7	1555	2648	359.7	9.67	64.8	94.8
20% <i>Fagopyrum esculentum</i> + 80% soft wheat flour	1869	1070.58	798	1863	5.58	9.4	66.1	94.6
30% <i>Fagopyrum esculentum</i> + 70% soft wheat flour	2528	1521.52	1139	2595	66.52	9.23	63.5	94.6
10% <i>Fagopyrum tataricum</i> + 90% soft wheat flour	3671	1463.6	2208	2946	724.8	9.9	64.3	94.4
20% <i>Fagopyrum tataricum</i> + 80% soft wheat flour	3445	1421.7	2023	2910	535.2	9.9	64.3	94.6
30% <i>Fagopyrum tataricum</i> + 70% soft wheat flour	3022	1707.9	1613	2838	183.9	9.97	63.6	94.6

induced by a slower water hydration rate and gluten formation due to the increased fiber content. The higher mixing tolerance and extension value might have resulted from the interactions between gluten and fiber [3]. As gluten diluted in the flour samples, it could not interact with starch, thus resulting in a greater mixing tolerance index [22, 23].

Pasting profile. Table 4 and Fig. 2 demonstrate the pasting properties of the flour mixes. The control sample with soft wheat flour showed the following pasting viscosities: peak viscosity – 2508 cP, trough viscosity – 1659.92 cP, breakdown viscosity – 977.8 cP, final viscosity – 2573 cP, setback viscosity – 64.92 cP. The sample with *F. esculentum* reduced the peak, trough, breakdown, final, and setback viscosities of soft wheat flour from 2508 to 1869 cP, 1659.92 to 1070.58 cP, 977.8 to 798 cP, and 2573 to 1863 cP, respectively. In contrast,

the samples with *F. tataricum* enhanced all the viscosity parameters: peak viscosity – 3022 cP, trough viscosity – 1707.9 cP, breakdown viscosity – 1613 cP, final viscosity – 2838 cP, setback viscosity – 183.9 cP. The thermal data for both *F. esculentum* and *F. tataricum* samples were as follows: peak time – 9.23–9.97 min, pasting temperature – 66.1–63.5°C, peak temperature – 94.6–94.8°C. According to Hallen *et al.*, the degradation of the pasting profile might occur as a result of the fact that less starch is available for gelatinization [24]. Symons & Brennan reported similar findings [25]. They replaced wheat starch with 5% barley β-glucan fiber fractions, and the peak viscosity went down because less starch was available for gelatinization and less water was available for the first swelling of the starch granule. Adebowale *et al.* linked the pasting temperature with the water-binding capacity [26]. In other studies [24, 27],

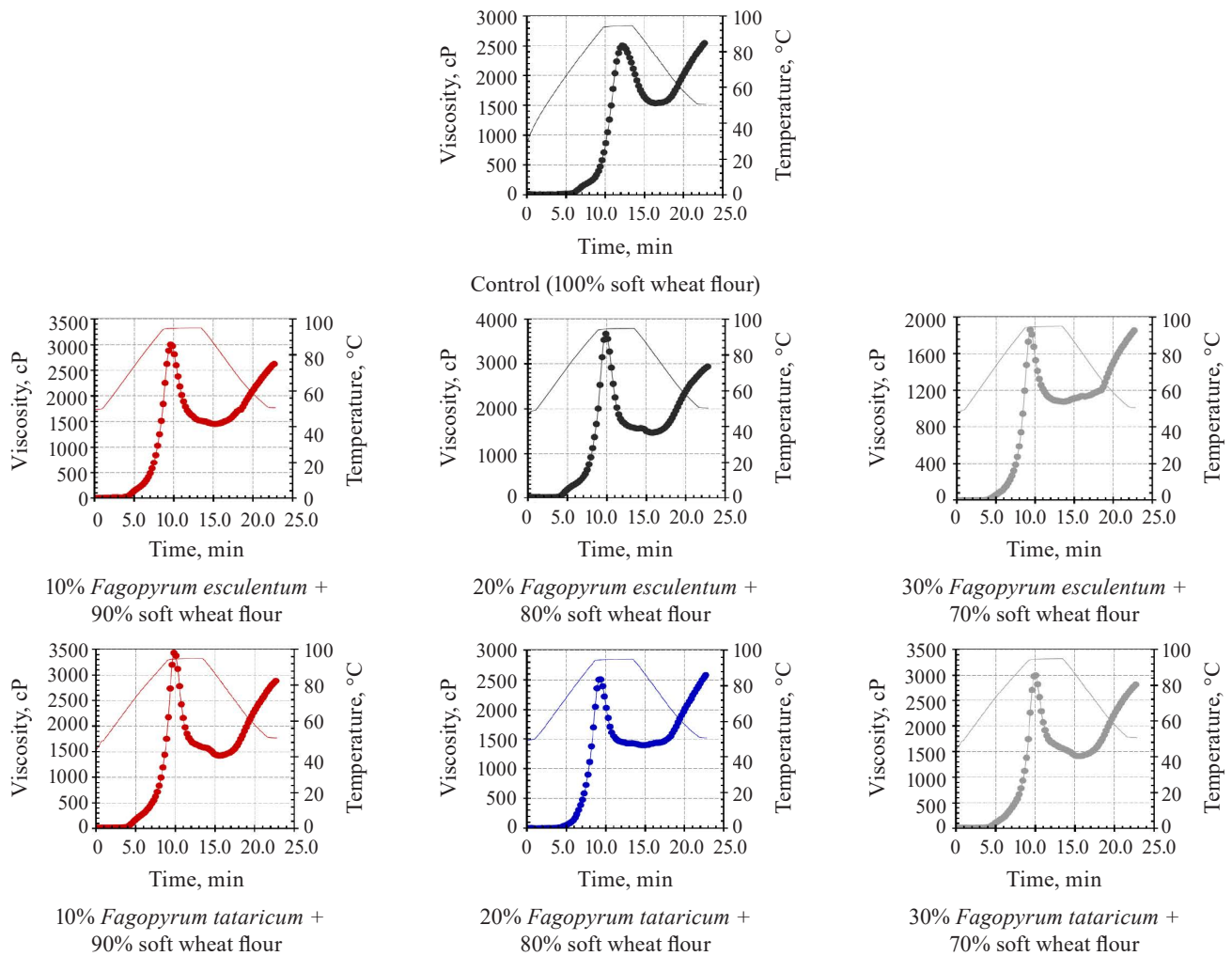


Figure 2 Rapid viscoanalyzer parameters of dough samples with 10, 20, and 30% *Fagopyrum esculentum*/*Fagopyrum tataricum*

the pasting profile of flour samples also revealed that flour blends had lower viscosities and pasting temperature. Gluten-free flour proved able to alter the amylose/amylopectin ratios of starches and the gluten content [28, 29].

Chemical composition of biscuit samples. This research stage featured the effect of adding 10, 20, and 30% *F. esculentum*/*F. tataricum* to soft wheat flour. The biscuits fortified with *F. esculentum*/*F. tataricum* contained more protein, fat, ash, and crude fiber than the control sample fortified with soft wheat flour (Table 5). The biscuits with 72% soft wheat flour had more carbohydrates than total carbohydrates. *F. esculentum* and *F. tataricum* were rich in iron, copper, and magnesium, which could be responsible for the increased ash concentration [30]. The rise in the moisture content may be attributed to the higher protein content. Mustafa *et al.* demonstrated that the moisture content of bread rose as the protein level increased [31]. The fat content of the biscuit samples with *F. esculentum* and *F. tataricum* was higher than that of the biscuits with soft wheat flour because buckwheat flour tends to retain oil during baking [32–34]. Higher oil retention improves the texture and flavor retention of biscuits. The protein content in

the biscuits increased together with the concentration of *F. esculentum*/*F. tataricum*, probably, because soft wheat flour was low-protein.

Color parameters. Color is a crucial sensory element that directly affects customer choice for any product, especially bakery items. We analyzed the color properties of the biscuits using a Hunter laboratory colorimeter (Table 6). The Hunter *L* scale spanned from 0 black to 100 white, whereas Hunter *b* scale ranged from negative blue to positive yellow. The biscuits with *F. esculentum*/*F. tataricum* were darker than the control. The lightness (*L*^{*}) and redness (*b*^{*}) values decreased as the percentage of *F. esculentum*/*F. tataricum* increased. The yellowness (*a*^{*}) increased together with the share of *F. esculentum*/*F. tataricum*. Both *F. esculentum* and *F. tataricum* flours were darker (lower *L*^{*}) than soft wheat flour. Naturally, the biscuits with *F. esculentum*/*F. tataricum* were darker in color. These results concurred with other publications [35–37]. The Maillard browning and sugar caramelization during baking are believed to cause brown pigments [38]. These browning events depend on several variables, including water activity, pH, temperature, sugars, and the type and proportion of amino compounds [39, 40]. Sugar caramelization

Table 5 Chemical composition of biscuits with *Fagopyrum esculentum*/*Fagopyrum tataricum*, %wd

Samples	Moisture	Protein	Oil	Ash	Fiber	Carbohydrate
Control (100% soft wheat flour)	4.50 ^c ± 0.08	10.65 ^f ± 0.15	28.37 ^f ± 0.22	0.35 ^c ± 0.01	0.72 ^f ± 0.10	59.91 ^a ± 0.65
10% <i>Fagopyrum esculentum</i> + 90% soft wheat flour	4.75 ^d ± 0.05	10.90 ^d ± 0.17	28.50 ^d ± 0.15	0.40 ^d ± 0.03	1.15 ^e ± 0.09	59.05 ^b ± 0.52
20% <i>Fagopyrum esculentum</i> + 80% soft wheat flour	5.00 ^{bc} ± 0.07	11.15 ^b ± 0.10	28.65 ^b ± 0.12	0.42 ^{cd} ± 0.05	1.50 ^d ± 0.07	58.28 ^c ± 0.48
30% <i>Fagopyrum esculentum</i> + 70% soft wheat flour	5.15 ^{ab} ± 0.10	11.35 ^a ± 0.19	28.70 ^a ± 0.17	0.45 ^{bc} ± 0.07	1.85 ^c ± 0.11	57.65 ^d ± 0.29
10% <i>Fagopyrum tataricum</i> + 90% soft wheat flour	4.80 ^{cd} ± 0.12	10.80 ^e ± 0.22	28.40 ^e ± 0.14	0.42 ^{cd} ± 0.09	1.50 ^d ± 0.08	58.88 ^c ± 0.42
20% <i>Fagopyrum tataricum</i> + 80% soft wheat flour	5.05 ^{ab} ± 0.9	11.00 ^e ± 0.13	28.50 ^d ± 0.10	0.48 ^b ± 0.06	2.00 ^b ± 0.15	58.02 ^f ± 0.35
30% <i>Fagopyrum tataricum</i> + 70% soft wheat flour	5.25 ^a ± 0.11	11.15 ^b ± 0.16	28.60 ^e ± 0.19	0.55 ^a ± 0.04	2.45 ^a ± 0.19	57.25 ^e ± 0.22
LSD at 0.05	0.235	0.033	0.021	0.035	0.136	0.0414

The results are presented as means for triplicate analyses ± standard deviation (SD)

The data marked with superior letters are significantly different ($p \leq 0.05$)

Table 6 Color attributes of biscuits with *Fagopyrum esculentum*/*Fagopyrum tataricum*

Samples	<i>L</i> *	<i>a</i> *	<i>b</i> *	<i>a/b</i>	Saturation	ΔE^*
Control (100% soft wheat flour)	65.10 ^a ± 0.45	6.80 ^f ± 0.16	32.50 ^a ± 0.35	0.21 ^e ± 0.01	33.20 ^a ± 0.22	73.08 ^a ± 1.15
10% <i>Fagopyrum esculentum</i> + 90% soft wheat flour	60.80 ^b ± 0.54	10.80 ^d ± 0.19	27.71 ^c ± 0.40	0.39 ^e ± 0.30	29.74 ^{bc} ± 0.35	67.68 ^b ± 1.22
20% <i>Fagopyrum esculentum</i> + 80% soft wheat flour	55.41 ^c ± 0.49	12.50 ^b ± 0.25	25.15 ^d ± 0.39	0.50 ^e ± 0.01	28.09 ^c ± 0.17	62.12 ^d ± 1.33
30% <i>Fagopyrum esculentum</i> + 70% soft wheat flour	49.68 ^d ± 0.64	13.26 ^a ± 0.13	22.56 ^e ± 0.50	0.59 ^b ± 0.04	26.19 ^{cd} ± 0.19	56.15 ^e ± 1.38
10% <i>Fagopyrum tataricum</i> + 90% soft wheat flour	58.20 ^{bc} ± 0.75	10.10 ^e ± 0.11	29.00 ^b ± 0.29	0.35 ^f ± 0.00	30.71 ^b ± 0.27	65.80 ^c ± 1.19
20% <i>Fagopyrum tataricum</i> + 80% soft wheat flour	49.33 ^d ± 0.62	11.00 ^e ± 0.25	25.50 ^d ± 0.32	0.43 ^d ± 0.02	27.77 ^{dc} ± 0.15	56.61 ^e ± 1.29
30% <i>Fagopyrum tataricum</i> + 70% soft wheat flour	38.40 ^e ± 0.55	13.20 ^a ± 0.16	21.19 ^f ± 0.25	0.62 ^a ± 0.03	24.96 ^f ± 0.26	45.80 ^f ± 1.11
LSD at 0.05	0.128	0.105	0.346	0.0175	1.751	1.365

The results are presented as means for triplicate analyses ± standard deviation (SD)

The data marked with superior letters are significantly different ($p \leq 0.05$)

and the Maillard processes also cause browning in high-sugar biscuit formulations [41].

Baking quality. Table 7 describes the following baking parameters of biscuits: weight (g), volume (cm³), specific volume (v/w), diameter (cm), thickness (cm), and spread ratio (%). The diameter of the *F. esculentum*/*F. tataricum* biscuits decreased slightly with increasing the substitution percentage compared to control biscuits. The samples with 10% *F. esculentum* had the biggest diameter (6.63 cm), while the samples with 20% *F. esculentum* had a small diameter (6.52 cm). However, the height of *F. esculentum*/*F. tataricum* biscuits decreased relative to the control sample, except for the sample with 10% *F. esculentum*. The spread ratio normally corresponds to the diameter-to-height ratio, which serves as a quality indicator. Therefore, premium biscuits should have a high spread ratio [42]. *F. esculentum*/*F. tataricum*

proved to enhance the spread ratio, although the sample with 20% *F. tataricum* had the lowest spread ratio value of 6.06 cm. The rise in spread ratio may be due to the dilution of gluten caused by the increased proportion of *F. esculentum*/*F. tataricum* in the formulation. The samples with *F. esculentum*/*F. tataricum* had a greater protein and dietary fiber content, which reduced the spread ratio because these ingredients have a greater water-binding capacity. As a result, they reduced the amount of water available to dissolve sugars and prevented the biscuits from spreading [43, 44]. As the gluten protein diluted and the fiber and gluten interacted, the extra fiber added to wheat flour together with *F. esculentum*/*F. tataricum* had a decisive impact on the development of gluten networks [43, 45]. *F. esculentum*/*F. tataricum* decreased the weight and volume of biscuits as the replacement levels rose. The formulation of biscuits

Table 7 Baking quality of biscuits with *Fagopyrum esculentum*/*Fagopyrum tataricum*

Samples	Weight, g	Volume, cm ³	Specific volume, cm ³ /g	Diameters	Height	Spread ratio
Control (100% soft wheat flour)	26.25 ^a ± 1.02	36.75 ^b ± 0.11	1.40 ^a ± 0.03	6.60 ^a ± 0.17	1.08 ^a ± 0.01	6.15 ^a ± 0.16
10% <i>Fagopyrum esculentum</i> + 90% soft wheat flour	23.35 ^b ± 0.68	38.05 ^a ± 0.19	1.63 ^a ± 0.06	6.63 ^a ± 0.11	1.10 ^a ± 0.00	6.07 ^a ± 0.11
20% <i>Fagopyrum esculentum</i> + 80% soft wheat flour	21.55 ^c ± 1.15	32.50 ^a ± 0.22	1.51 ^a ± 0.05	6.52 ^a ± 0.15	0.98 ^a ± 0.01	6.69 ^a ± 0.19
30% <i>Fagopyrum esculentum</i> + 70% soft wheat flour	21.75 ^c ± 0.60	33.09 ^c ± 0.17	1.52 ^a ± 0.10	6.53 ^a ± 0.22	0.99 ^a ± 0.03	6.59 ^a ± 0.15
10% <i>Fagopyrum tataricum</i> + 90% soft wheat flour	18.30 ^d ± 0.36	32.68 ^f ± 0.10	1.79 ^a ± 0.07	6.50 ^a ± 0.13	0.99 ^a ± 0.05	6.60 ^a ± 0.21
20% <i>Fagopyrum tataricum</i> + 80% soft wheat flour	21.40 ^c ± 0.48	36.28 ^e ± 0.25	1.70 ^a ± 0.02	6.54 ^a ± 0.19	1.08 ^a ± 0.07	6.06 ^a ± 0.12
30% <i>Fagopyrum tataricum</i> + 70% soft wheat flour	23.50 ^b ± 0.52	35.28 ^d ± 0.13	1.52 ^a ± 0.04	6.56 ^a ± 0.23	1.05 ^a ± 0.10	6.28 ^a ± 0.17
LSD at 0.05	1.324	0.169	0.506	0.404	0.249	1.204

The results are presented as means for triplicate analyses ± standard deviation (SD)

The data marked with superior letters are significantly different ($p \leq 0.05$)

Table 8 Sensory properties of biscuits with *Fagopyrum esculentum*/*Fagopyrum tataricum*: mean values

Samples	Color (20)	Taste (20)	Odor (20)	Crispiness (20)	Appearance (20)	Overall acceptability (100)
Control (100% soft wheat flour)	18.22 ^a ± 0.32	19.04 ^a ± 1.16	18.52 ^a ± 0.36	17.44 ^b ± 0.50	19.02 ^a ± 0.32	92.24 ^a ± 3.15
10% <i>Fagopyrum esculentum</i> + 90% soft wheat flour	17.12 ^c ± 0.44	18.64 ^a ± 1.22	18.16 ^a ± 0.52	18.02 ^{ab} ± 0.82	19.00 ^a ± 0.28	90.94 ^{ab} ± 2.65
20% <i>Fagopyrum esculentum</i> + 80% soft wheat flour	17.22 ^c ± 0.38	18.74 ^a ± 0.68	17.85 ^a ± 0.69	18.34 ^a ± 0.79	18.82 ^a ± 0.86	91.00 ^{ab} ± 3.54
30% <i>Fagopyrum esculentum</i> + 70% soft wheat flour	15.86 ^d ± 0.52	16.64 ^b ± 0.92	16.66 ^b ± 0.56	18.20 ^a ± 1.03	16.62 ^b ± 0.64	83.98 ^d ± 3.22
10% <i>Fagopyrum tataricum</i> + 90% soft wheat flour	18.28 ^a ± 0.61	18.50 ^a ± 0.86	18.22 ^a ± 0.62	18.30 ^a ± 0.85	16.56 ^b ± 0.38	88.92 ^c ± 2.70
20% <i>Fagopyrum tataricum</i> + 80% soft wheat flour	17.76 ^b ± 0.55	18.86 ^a ± 0.90	18.30 ^a ± 0.78	16.66 ^c ± 0.52	16.96 ^b ± 0.91	89.06 ^{bc} ± 3.05
30% <i>Fagopyrum tataricum</i> + 70% soft wheat flour	17.34 ^{bc} ± 0.45	18.62 ^a ± 1.09	18.58 ^a ± 0.84	18.52 ^a ± 0.92	16.42 ^b ± 0.76	89.90 ^{bc} ± 3.08
LSD at 0.05	0.456	0.697	0.772	0.728	0.833	1.945

The results are presented as means for triplicate analyses ± standard deviation (SD)

The data marked with superior letters are significantly different ($p \leq 0.05$)

often depends on the quality of the components employed [46]. Thus, the specific volume has a significant effect on the quality of the finished product.

Sensory properties. Sensory properties affect the purchase decision. Sensory evaluation of biscuits usually includes such parameters as color, taste, smell, crispiness, and overall acceptability. Table 8 and Fig. 3 demonstrate the sensory properties of the experimental biscuits. The increasing level of *F. esculentum*/*F. tataricum* in the biscuit formulation affected the color of all biscuit samples compared to the control, but there was no significant difference between the color of the biscuit control sample and biscuit with 10% *F. tataricum* (Table 8). Also, the increasing level of *F. esculentum*/*F. tataricum* did not affect significantly on the taste and odor of the biscuit compared to the control sample except 30% *F. escu-*

lentum. As for crispiness, all tested samples had slight differences. There was no significant difference in the appearance of 10 and 20% *F. esculentum* compared to the control sample. Also, there was no significant differences between the 30% *F. esculentum* biscuit and all the samples with *F. tataricum*, while all they significantly decreased compared to the control sample. The same trend between appearance and overall acceptability was noticed. Also, these results were confirmed by the results of the physical properties of biscuits.

Texture profile analysis. Table 9 and Fig. 4 illustrates the texture values for the biscuit samples. Hardness is known to depend on the compressive strength of biscuits. The instrumental hardness test revealed that hardness increased together with the quantity of *F. esculentum*/*F. tataricum*. The immediate increase in hardness

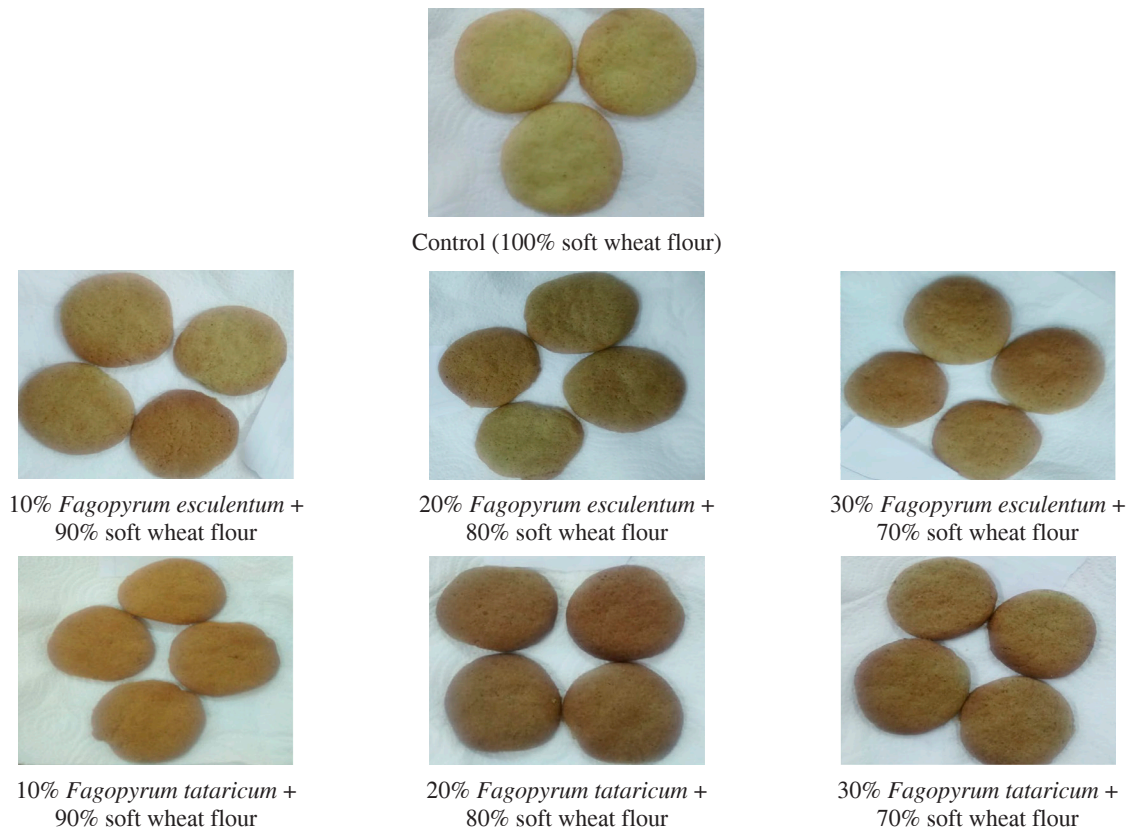


Figure 3 Photos of biscuits with *Fagopyrum esculentum*/*Fagopyrum tataricum*

Table 9 Texture profile analysis of biscuits with *Fagopyrum esculentum*/*Fagopyrum tataricum*

Samples	Hardness, N	Adhesiveness, M·J	Resilience	Springiness, mm	Fracturability
Control (100% soft wheat flour)	12.26	4.00	0.04	1.51	8.98
10% <i>Fagopyrum esculentum</i> + 90% soft wheat flour	13.55	2.00	0.03	2.07	5.70
20% <i>Fagopyrum esculentum</i> + 80% soft wheat flour	10.93	4.00	0.03	2.63	2.01
30% <i>Fagopyrum esculentum</i> + 70% soft wheat flour	12.38	0	0.06	1.39	8.20
10% <i>Fagopyrum tataricum</i> + 90% soft wheat flour	16.83	7.00	0.02	4.24	2.29
20% <i>Fagopyrum tataricum</i> + 80% soft wheat flour	18.13	2.00	0.01	1.61	7.04
30% <i>Fagopyrum tataricum</i> + 70% soft wheat flour	17.49	0	0.04	0.47	1.04

was from 12.26 N for the control biscuits to 17.49 N for the samples with 30% *F. tataricum*. The increase in hardness might have been caused by the increased dietary fiber content with its high water-absorbing capacity. The initial region of negative force produced by the bite quantified the adhesion. In this study, adhesiveness was the negative force area for the first bite. The samples with 20% *F. esculentum* and 10% *F. tataricum* demonstrated the maximal adhesiveness values of 4.0 and 7.0 g/cm, respectively.

Springiness reflects the strength of internal links and the degree to which it may be deformed without

breaking *F. esculentum*/*F. tataricum* enhanced the springiness of the experimental samples compared to control except 30% *F. esculentum* and 30% *F. tataricum*. The sample with 10% *F. tataricum* had the highest springiness (4.24%). These experimental results contradicted those reported in [34, 47].

All the experimental biscuit samples exhibited a slight drop in resilience scores, depending on the *F. esculentum*/*F. tataricum* concentrations. Resilience measures the speed and force with which a sample recovers from deformation. In our study, the sample with 30% *F. esculentum* showed the maximal resilience value of 0.06.

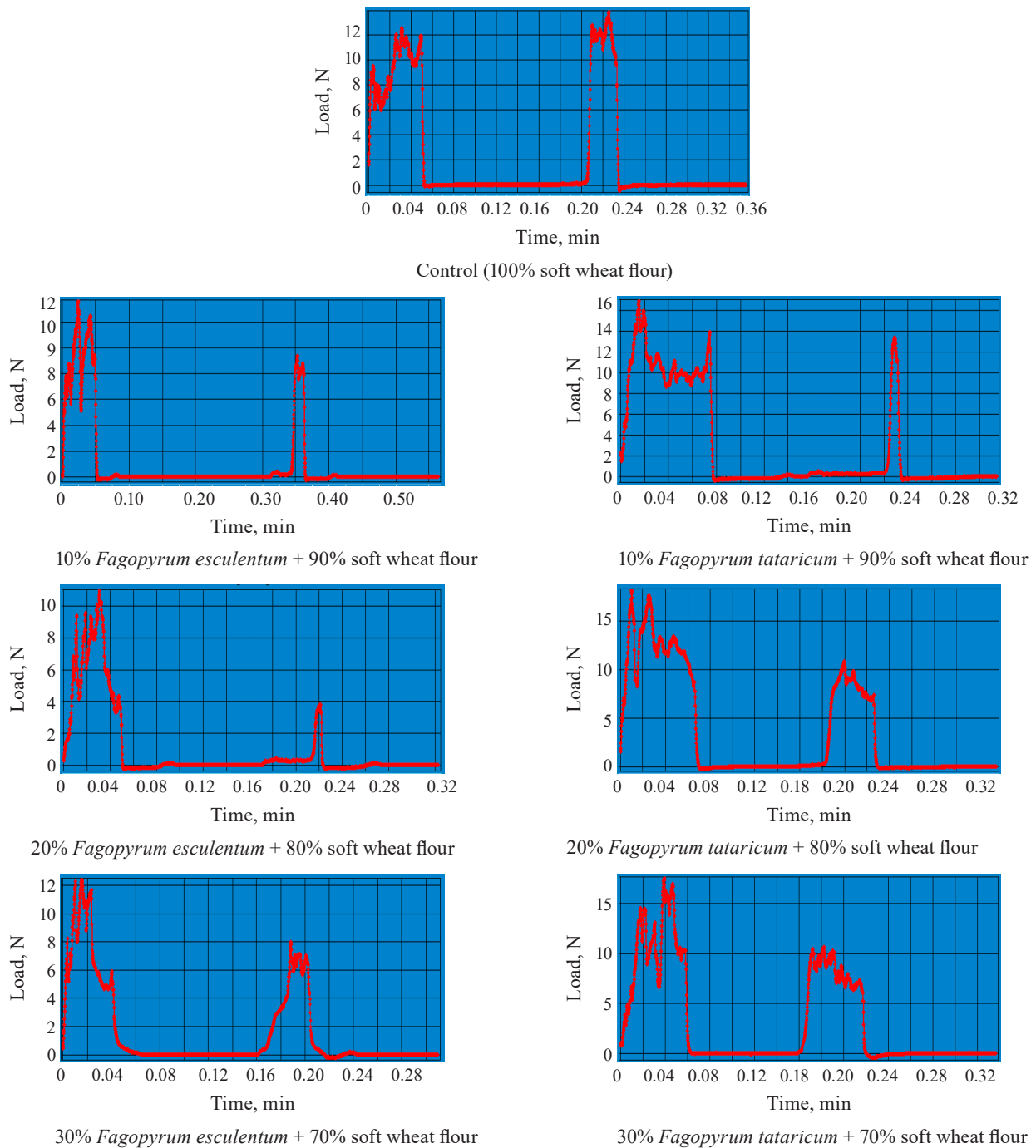


Figure 4 Texture profile of biscuits with *Fagopyrum esculentum*/*Fagopyrum tataricum*

CONCLUSION

Wheat flour biscuits fortified with buckwheat flour had an improved nutritional value. According to the obtained results, the overall acceptability of all the experimental biscuits fell within a suitable range but the biscuits with buckwheat flour up to 20% demonstrated the highest quality. Higher concentrations of *Fagopyrum esculentum* Moench. or *Fagopyrum tataricum* (L.) Gaertn. adversely affected the baking quality, color, and texture of the experimental biscuits. However, the samples with 10% *F. esculentum* or *F. tataricum* demonstrated no significant changes in the sensory profile.

Finally, we can recommend to use 10% buckwheat to improve biscuit quality and alleviate shortages of raw wheat materials.

CONTRIBUTION

The authors were equally involved in the research and are equally responsible for any potential cases of plagiarism.

CONFLICT OF INTEREST

The authors declare that there is no conflict of interests regarding the publication of this article.

REFERENCES

- Okarter N, Liu RH. Health benefits of whole grain phytochemicals. *Critical Reviews in Food Science and Nutrition*. 2010;50(3):193–208. <https://doi.org/10.1080/10408390802248734>
- Gandhi A-P, Kotwaliwale N, Kawalkar J, Srivastav DC, Parihar VS, Nadh PR. Effect of incorporation of defatted soyflour on the quality of sweet biscuits. *Journal of Food Science and Technology*. 2001;38(5):502–503.
- Sudha ML, Vetrmani R, Leelavathi K. Influence of fibre from different cereals on the rheological characteristics of wheat flour dough and on biscuit quality. *Food Chemistry*. 2007;100(4):1365–1370. <https://doi.org/10.1016/j.foodchem.2005.12.013>
- Ibrahim GE, Bahgaat WK, Hussein AMS. Egyptian kishk as a fortificant: Impact on the quality of biscuit. *Foods and Raw Materials*. 2021;9(1):164–173. <https://doi.org/10.21603/2308-4057-2021-1-164-173>
- Lee H, Yuan C, Hammet A, Mahajan A, Chen ES-W, Wu M-R, et al. Diphosphothreonine-specific interaction between an SQ/TQ cluster and an FHA domain in the Rad53-Dun1 kinase cascade. *Molecular Cell*. 2008;30(6):767–778. <https://doi.org/10.1016/j.molcel.2008.05.013>
- Verma KC. Biochemical constituents of buckwheat (*Fagopyrum esculentum* Moench) collected from different geographical regions of Himachal Pradesh. *Molecular Biology Reports*. 2018;45:2681–2687. <https://doi.org/10.1007/s11033-018-4437-8>
- Ahmed A, Khalid N, Ahmad A, Abbasi NA, Latif MSZ, Randhawa MA. Phytochemicals and biofunctional properties of buckwheat: A review. *The Journal of Agricultural Science*. 2014;152(3):349–369. <https://doi.org/10.1017/S0021859613000166>
- Rauf M, Yoon H, Lee S, Hyun DY, Lee M-C, Oh S, et al. Evaluation of *Fagopyrum esculentum* Moench germplasm based on agro-morphological traits and the rutin and quercetin content of seeds under spring cultivation. *Genetic Resources and Crop Evolution*. 2020;67:1385–1403. <https://doi.org/10.1007/s10722-020-00899-3>
- Halbrech B, Romedenne P, Ledent JF. Evolution of flowering, ripening and seed set in buckwheat (*Fagopyrum esculentum* Moench): Quantitative analysis. *European Journal of Agronomy*. 2005;23(3):209–224. <https://doi.org/10.1016/j.eja.2004.11.006>
- Skerritt JH. Molecular comparison of alcohol-soluble wheat and buckwheat proteins. *Cereal Chemistry*. 1986;63(4):365–369.
- Torbica A, Hadnađev M, Dapčević T. Rheological, textural and sensory properties of gluten-free bread formulations based on rice and buckwheat flour. *Food Hydrocolloids*. 2010;24(6–7):626–632. <https://doi.org/10.1016/j.foodhyd.2010.03.004>
- Approved methods of the American association of cereal chemists. AACC; 2000. 1200 p.
- Official methods of analysis. 17th Edition. Gaithersburg: AOAC; 2000.
- Sapers GM, Douglas Jr FW. Measurement of enzymatic browning at cut surfaces and in juice of raw apple and pear fruits. *Journal of Food Science*. 1987;52(5):1258–1285. <https://doi.org/10.1111/j.1365-2621.1987.tb14057.x>
- Hussien AMS, Badr AN, Naeem MA. Innovative nutritious biscuits limit aflatoxin contamination. *Pakistan Journal of Biological Sciences*. 2019;22(3):133–142. <https://doi.org/10.3923/pjbs.2019.133.142>
- McClave JT, Benson PG, Sincich T. *Statistical for business and economics*. Prentice Hall; 1998. 1067 p.
- Sindhu R, Khatkar BS. Composition and functional properties of common buckwheat (*Fagopyrum esculentum* Moench) flour and starch. *International Journal of Innovative Research and Advanced Studies*. 2016;3(7):154–159.
- Ahmad M, Ahmad F, Dar EA, Bhat RA, Mushtaq T, Shah F. Buck wheat (*Fagopyrum esculentum*) – A neglected crop of high altitude cold arid regions of ladakh: Biology and nutritive value. *International Journal of Pure and Applied Bioscience*. 2018;6(1):395–406. <https://doi.org/10.18782/2320-7051.6001>
- Babu S, Yadav GS, Singh R, Avasthe RK, Das A, Mohapatra KP, et al. Production technology and multifarious uses of buckwheat (*Fagopyrum* spp.): A review. *Indian Journal of Agronomy*. 2018;63(4):118–130.
- El-Shenawy M, Hussien AMS, Fouad MT. Production of biscuits from mixture of tiger nut flour, milk permeate and soft wheat flour. *Asian Food Science Journal*. 2020;18(2):11–21. <https://doi.org/10.9734/afsj/2020/v18i230212>
- Hussein AS, Bahgaat WK, Ibraheim GE. Impact of Jameed fortification on physicochemical, antioxidant and volatile compounds of snacks. *Egyptian Journal of Chemistry*. 2022;65(5):1–11.
- Chen H, Rubenthaler GL, Schanus EG. Effect of apple fiber and cellulose on the physical properties of wheat flour. *Journal of Food Science*. 1988;53(1):304–305. <https://doi.org/10.1111/j.1365-2621.1988.tb10242.x>
- Ogunsina BS, Radha C, Indrani D. Quality characteristics of bread and cookies enriched with debittered *Moringa oleifera* seed flour. *International Journal of Food Sciences and Nutrition*. 2011;62(2):185–194. <https://doi.org/10.3109/09637486.2010.526928>

24. Hallén E, İbanoğlu Ş, Ainsworth P. Effect of fermented/germinated cowpea flour addition on the rheological and baking properties of wheat flour. *Journal of Food Engineering*. 2004;63(2):177–184. [https://doi.org/10.1016/S0260-8774\(03\)00298-X](https://doi.org/10.1016/S0260-8774(03)00298-X)
25. Symons LJ, Brennan CS. The effect of barley β -glucan fiber fractions on starch gelatinization and pasting characteristics. *Journal of Food Science*. 2006;69(4):FCT257–FCT261. <https://doi.org/10.1111/j.1365-2621.2004.tb06325.x>
26. Adebowale YA, Adeyemi IA, Oshodi AA. Functional and physicochemical properties of flours of six *Mucuna* species. *African Journal of Biotechnology*. 2005;4(12).
27. Muralikrishna G, Nirmala M. Cereal α -amylases – An overview. *Carbohydrate Polymers*. 2005;60(2):163–173. <https://doi.org/10.1016/j.carbpol.2004.12.002>
28. van Hung P, Maeda T, Morita N. Dough and bread qualities of flours with whole waxy wheat flour substitution. *Food Research International*. 2007;40(2):273–279. <https://doi.org/10.1016/j.foodres.2006.10.007>
29. Renzetti S, Arendt EK. Effect of protease treatment on the baking quality of brown rice bread: From textural and rheological properties to biochemistry and microstructure. *Journal of Cereal Science*. 2009;50(1):22–28. <https://doi.org/10.1016/j.jcs.2009.02.002>
30. de Francischi MLP, Salgado JM, Leitaó RFF. Chemical, nutritional and technological characteristics of buck wheat and non-prolamine buckwheat flours in comparison of wheat flour. *Plant Foods for Human Nutrition*. 1994;46:323–329. <https://doi.org/10.1007/BF01088431>
31. Mustafa AI, Al-Wessali MS, Al-Basha OM, Al-Amir RH. Utilization of cowpea flour and protein isolate in bakery products. *Cereal Foods World*. 1986;31(10):756–759.
32. Rufeng N, Enqi L, Chuangji C, Jiangping Z. A study of the production of healthy biscuit made with tartary buckwheat grown in North China. *Current advances in buckwheat research*. 1995:861–865.
33. Baljeet SY, Ritika BY, Roshan LY. Studies on functional properties and incorporation of buckwheat flour for biscuit making. *International Food Research Journal*. 2010;17:1067–1076.
34. Kaur M, Sandhu KS, Arora A, Sharma A. Gluten free biscuits prepared from buckwheat flour by incorporation of various gums: Physicochemical and sensory properties. *LWT – Food Science and Technology*. 2015;62(1):628–632. <https://doi.org/10.1016/j.lwt.2014.02.039>
35. Kim YS, Ha TY, Lee SH, Lee HY. Effect of rice bran dietary fiber on flour rheology and quality of wet noodles. *Korean Journal of Food Science and Technology*. 1997;29(1):90–95.
36. Hussein AMS, Saber MM, Daoud EM, Alshafei MM, Ziada YM, Gamal A, et al. Formulation and evaluation of biscuits from functional flour mixture to enhance of antioxidants reflecting on nutrition in -patients. *Egyptian Journal of Chemistry*. 2022;65(5):455–466.
37. Ramy A, Salama MF, Shouk AA. Pollards a potential source of dietary fiber for pasta manufacture. *Egyptian Journal of Food Science*. 2002;30(2):313–330.
38. Laguna L, Salvador A, Sanz T, Fiszman SM. Performance of a resistant starch rich ingredient in the baking and eating quality of short-dough biscuits. *LWT – Food Science and Technology*. 2011;44(3):737–746. <https://doi.org/10.1016/j.lwt.2010.05.034>
39. Stojceska V, Ainsworth P, Plunkett A, İbanoğlu Ş. The effect of extrusion cooking using different water feed rates on the quality of ready-to-eat snacks made from food by-products. *Food Chemistry*. 2009;114(1):226–232. <https://doi.org/10.1016/j.foodchem.2008.09.043>
40. Sharma P, Gujral HS. Extrusion of hulled barley affecting β -glucan and properties of extrudates. *Food and Bioprocess Technology*. 2013;6:1374–1389. <https://doi.org/10.1007/s11947-011-0777-2>
41. Sharma P, Gujral HS. Cookie making behavior of wheat-barley flour blends and effects on antioxidant properties. *LWT – Food Science and Technology*. 2014;55(1):301–307. <https://doi.org/10.1016/j.lwt.2013.08.019>
42. Miller RA, Hosney RC. Factors in hard wheat flour responsible for reduced cookie spread. *Cereal Chemistry*. 1997;74(3):330–336. <https://doi.org/10.1094/CCHEM.1997.74.3.330>
43. Arshad MU, Anjum FM, Zahoor T. Nutritional assessment of cookies supplemented with defatted wheat germ. *Food Chemistry*. 2007;102(1):123–128. <https://doi.org/10.1016/j.foodchem.2006.04.040>
44. Ganorkar PM, Jain RK. Effect of flaxseed incorporation on physical, sensorial, textural and chemical attributes of cookies. *International Food Research Journal*. 2014;21(4):1515–1521.
45. Wang N, Hou GG, Kweon M, Lee B. Effects of particle size on the properties of whole-grain soft wheat flour and its cracker baking performance. *Journal of Cereal Science*. 2016;69:187–193. <https://doi.org/10.1016/j.jcs.2016.03.010>
46. Kuchtová V, Minarovičová L, Kohajdová Z, Karovičová J. Effect of wheat and corn germs addition on the physical properties and crackers sensory quality. *Potravinárstvo*. 2016;10(1):543–549. <https://doi.org/10.5219/598>

47. Gujral HS, Mehta S, Samra IS, Goyal P. Effect of wheat bran, coarse wheat flour, and rice flour on the instrumental texture of cookies. *International Journal of Food Properties*. 2003;6(2):329–340. <https://doi.org/10.1081/JFP-120017816>
48. Hunter RS. Scales for the measurements of color difference. In: Hunter RS, editor. *The measurement of appearance*. New York: Wiley; 1975. pp. 133–140.
49. Krishnaswamy GG, Parameshwari S. A concise review on buckwheat materials based ready to serve and ready to eat food products. *Materials Today: Proceedings*. 2022;66:783–788. <https://doi.org/10.1016/j.matpr.2022.04.284>
50. Sofi SA, Ahmed N, Farooq A, Rafiq S, Zargar SM, Kamran F, et al. Nutritional and bioactive characteristics of buckwheat, and its potential for developing gluten-free products: An updated overview. *Food Science and Nutrition*. 2022;11(5):2256–2276. <https://doi.org/10.1002/fsn3.3166>
51. Hassona MM, Hussein AS, Morsy N, Abd El-Aal HA. Chemical, rheological, sensorial and functional properties buckwheat semolina flour composite pasta. *Egyptian Journal of Chemistry*. 2023. <https://doi.org/10.21608/ejchem.2023.172021.7137>
52. Silav-Tuzlu G, Tacer-Caba Z. Influence of chia seed, buckwheat and chestnut flour addition on the overall quality and shelf life of the gluten-free biscuits. *Food Technology and Biotechnology*. 2021;59(4):463–474. <https://doi.org/10.17113/ftb.59.04.21.7204>
53. Farzana T, Hossain FB, Abedin MdJ, Afrin S, Rahman SS. Nutritional and sensory attributes of biscuits enriched with buckwheat. *Journal of Agriculture and Food Research*. 2022;10. <https://doi.org/10.1016/j.jafr.2022.100394>
54. Constantino ABT, Garcia-Rojas EE. Proteins from pseudocereal seeds: Solubility, extraction, and modifications of the physicochemical and techno-functional properties. *Journal of the Science of Food and Agriculture*. 2022;102(7):2630–2639. <https://doi.org/10.1002/jsfa.11750>
55. Sofi SA, Ahmed N, Farooq A, Rafiq S, Zargar SM, Kamran F, et al. Nutritional and bioactive characteristics of buckwheat, and its potential for developing gluten-free products: An updated overview. *Food Science and Nutrition*. 2022;11(5):2256–2276. <https://doi.org/10.1002/fsn3.3166>
56. di Cairano M, Condelli N, Caruso MC, Cela N, Tolve R, Galgano F. Use of underexploited flours for the reduction of glycaemic index of gluten-free biscuits: Physicochemical and sensory characterization. *Food and Bioprocess Technology*. 2021;14:1490–1502. <https://doi.org/10.1007/s11947-021-02650-x>

ORCID IDs

Ahmed M. S. Hussein  <https://orcid.org/0000-0001-6297-3439>

Hala A. Abd El-Aal  <https://orcid.org/0000-0003-2329-6097>

Nahla M. Morsy  <https://orcid.org/0000-0003-0485-2844>

Mohamed M. Hassona  <https://orcid.org/0000-0001-5661-8326>



***Chorizo* sausage with shiitake mushrooms (*Lentinula edodes*) as a fat substitute: quality evaluation**

**Edison Mauricio Rincón Soledad, Mónica Alejandra Arredondo Nontién,
Jose Wilson Castro^{ID}, Dursun Barrios^{ID}, Sandra Milena Vásquez Mejía*^{ID}**

Universidad Nacional de Colombia^{ROR}, Bogota, Colombia

* e-mail: smvasque@unal.edu.co

Received 12.03.2023; Revised 13.05.2023; Accepted 06.06.2023; Published online 11.10.2023

Abstract:

Traditional meat products are made with large amounts of saturated fat and binders such as starch, which increase calories and move away from current consumer trends that seek low-fat products with natural ingredients. Shiitake mushroom has beneficial health properties and it can be used as a fat substitute in processed meat products. We aimed to identify the effects of incorporating shiitake powder into chorizo sausages as a fat substitute.

Shiitake powder was characterized and five formulations of chorizo sausage were developed: control and four experimental samples with 30, 40, 50 and 100% fat substitution (the latter included 50% of shiitake powder and 50% of olive oil).

The experimental sausage showed a greater moisture, lower lipid content, and less cooking loss. The samples with shiitake powder were darker and less red than the control. Texture parameters were not affected by substituting 40% of fat with shiitake powder. The treatment with 40% fat substitution had a greater insoluble fiber content and a lower aerobic mesophile count (CFU/g) than the control. No significant differences were found in the fatty acids profile. The samples with shiitake powder had a moderate level of sensory acceptance which might be associated with the consumers' lack of familiarity with shiitake.

Consumers may accept comminuted sausages in which a maximum of 40% of fat is substituted with shiitake powder. Such products have an adequate nutritional composition, as well as acceptable physicochemical, technological, and microbiological properties.

Keywords: Shiitake, fat substitute, comminuted sausages, processed meat, sensory acceptance

Funding: This work was supported by the Universidad Nacional de Colombia (UNAL)^{ROR} (Project number: HERMES 49072-QUIPU: 302010032172).

Please cite this article in press as: Rincón Soledad EM, Arredondo Nontién MA, Castro JW, Barrios D, Vásquez Mejía SM. *Chorizo* sausage with shiitake mushrooms (*Lentinula edodes*) as a fat substitute: quality evaluation. *Foods and Raw Materials*. 2024;12(1):168–178. <https://doi.org/10.21603/2308-4057-2024-1-598>

INTRODUCTION

Consumption of processed meat products has been questioned in recent years due to their potential contribution to cardiovascular diseases and colon cancer, as well as the impact of the meat industry on the environment [1–3]. With respect to its health effects, saturated fat is a component of meat that has generated the greatest concern.

Consumers have increasingly expressed their preference for natural ingredients and beneficial health effects [4, 5]. This has led the food industry to develop new products and seek ingredients and technologies that satisfy the demands of consumers who are increasingly

better informed. Nevertheless, a gap still exists between the theoretical knowledge of non-meat ingredients and the viability of their incorporation into processed meat products due to synergetic or antagonistic effects among ingredients during processing, as well as their effects on texture or sensory parameters. Therefore, there is a need to study such effects for each ingredient in the product. With this aim, numerous studies have focused on improving the composition of processed meat products so that they contain the nutrients demanded by consumers [6, 7].

Conventional processed meat products such as sausage generally contain added animal fat, which not only

provides sausage with sensory appeal but also contributes to its structure, juiciness, and the desired texture [8]. However, the resulting saturated fatty acids have been associated with long-term negative health effects [9]. Thus, there is a need to substitute animal fat in processed meat products with ingredients that simulate the desired functional and sensory characteristics.

Edible mushrooms are a viable ingredient for replacing meat, fats, salt, nitrites, and phosphates conventionally used in processed meat products. These mushrooms may have beneficial effects on consumers' health due to their bioactive compounds, medicinal effects, and antimicrobial properties [10]. Specifically, shiitake mushrooms (*Lentinula edodes* (Berk.) Pegler) have been demonstrated to have anti-inflammatory, anti-tumor, antiviral, antibacterial, anti-diabetic, and anti-parasite properties, as well as to regulate blood pressure and cholesterol levels [10]. Furthermore, shiitake has been found to have a high content of bioactive compounds, such as phenols, which may act as antioxidants [11].

Shiitake mushrooms have a high level of acceptance when used as an antioxidant and salt substitute in sausages, improving their useful life without deteriorating their color or texture [11]. Additionally, the authors indicate that at levels of 0.8% shiitake reduced lipid oxidation and bacterial growth, as well as improved the sensory quality of the product after one day of refrigerated storage due to its flavor-enhancing components. Meanwhile, shiitake extract added to hamburgers increased consumers' acceptance of color, aroma, texture, flavor, salinity, and general perception, although it provoked changes in some physiochemical characteristics such as pH, yield, and color [12].

Although the use of edible mushrooms in processed meat products has been demonstrated to be successful, fresh mushrooms deteriorate rapidly due to high respiration and metabolic rates [10, 13]. Moreover, they have a high microbiological charge (principally due to bacteria of the genera *Pseudomonas* and *Enterobacter*, as well as molds and yeasts), which degrades mushroom quality soon after harvest, making their use difficult and costly [13, 14]. Therefore, it is important to seek ways of incorporating dehydrated shiitake into processed food products in order to take advantage of their compositional and functional properties.

Given the lack of information on the use of dehydrated shiitake mushroom powder as a fat substitute and the need to make traditional processed meat products healthier, we aimed to determine the influence of shiitake powder incorporated into *chorizo* sausage as a fat substitute on the physiochemical, technological, microbiological, and sensory characteristics of the product, as well as its composition.

STUDY OBJECTS AND METHODS

Shiitake mushrooms were supplied by a local supplier in Funza Cundinamarca, Colombia, and dehydrated in an oven at 40°C for 15 h. Then, the mushrooms

were ground into powder using a food processor, sifted using a #20 sieve (Standard Sieve Series, USA), vacuum packed, and stored at room temperature for two weeks.

Refrigerated pork fat and lean beef were purchased from a local market in Bogotá, Colombia. Other ingredients and additives were obtained from local suppliers specializing in inputs for processed meat products (Tecnas S.A., Colombia). Laboratory chemical reagents for proximate and other analyses were acquired from a local chemical supplier (Elementos Químicos LTDA).

Characterization of shiitake powder. Shiitake powder was characterized using a proximate analysis according to the methodology of the Association of Official Agricultural Chemists [15]. Water retention capacity, oil retention capacity, swelling capacity, pH, color, and solubility of the samples were determined as proposed by Yaruro Cáceres *et al.* [16]. For these parameters, the shiitake powder samples were compared with the samples of commercial oat bran used as a healthy ingredient in processed foods.

Preparation of *chorizo* sausage. Three 8-kg batches of sausage were prepared according to the following procedure. Meat was defrosted and its excess fat was removed. The resulting lean meat was cut and ground using a mill with an 8-mm disk (orifice plate). Pork fat was ground with a 6-mm disc. Liquid smoke was mixed with water to be used in the sausage. Then, the meat was mixed with salt (NaCl and nitral salt), powdered spices, finely chopped onion greens and bell pepper, cold water (1/3 of the total to be used), and artificial coloring with a mixer for approximately 60 s. Following this, soy protein, starch, and another 1/3 of the water were added. Finally, fat or the fat substitute (shiitake powder) was added according to the formula shown in Table 1. The remaining water was added immediately and the mixture was blended with an mixer for approximately 60 s. The temperature of the mixture was maintained below 12°C (beginning with the partially unfrozen meat at < 2°C and adding extra cold water). After that, the mixture was stuffed in 28 mm diameter collagen casings, tied, and scalded until obtaining a constant internal temperature of 72°C. Finally, the sausages were cooled by submerging them in cold water until they reached < 10°C.

Each batch (repetition) was divided into six parts: 500 g for the analysis of pH, texture profile, and color; 500 g for a proximate composition analysis, 500 g for a microbiological analysis; 300 g for a dietary fiber analysis; 300 g for a fatty acids profile analysis, and the remainder for a sensory analysis. Each part was placed in a polyethylene bag, vacuum packed, and refrigerated at 4.0 ± 0.5°C for later analysis. Three independent repetitions of the *chorizo* sausages (control and treatments) were performed during a three-week period, with one week between the repetitions, and three samples were taken for each treatment in each batch of the replicates. The same package (lot) of ingredients was used for each formulation and the mixing process was replicated as described above.

Table 1 Formulation for chorizo sausage containing shiitake mushroom as a fat substitute

Ingredient	Control	Experimental samples with shiitake powder			
		10%	40%	50%	100%*
Lean beef	14	14	14	14	14
Lean pork	50	50	50	50	50
Fat	15	10.50	9	7.50	0
Olive oil	0	0	0	0	7.50
Shiitake powder	0	4.50	6	7.50	7.50
Soy protein	1.50	1.50	1.50	1.50	1.50
Tapioca	2.10	1	1	1	1
Water	8.15	9.50	9.50	9.50	9.50
Spices**	1.53	1.53	1.53	1.53	1.53
Salt	1	1	1	1	1
Nitrite salt curing agent***	0.10	0.10	0.10	0.10	0.10
Liquid smoke	0.25	0.25	0.25	0.25	0.25
Coloring mix****	0.12	0.12	0.12	0.12	0.12
Onion greens and bell pepper	6	6	6	6	6
Total	100	100	100	100	100

* 50% olive oil and 50% shiitake powder

** Powdered garlic, onion, and pepper

*** 97% salt and 3% nitrites

**** Mix of red and orange coloring agents

Characterization of chorizo sausage. All the samples were analyzed for their proximate composition, pH, cooking loss, color, and texture in order to determine which treatment presented the most desirable characteristics for the sausage. Following this, the treatment selected and the control were analyzed for total, soluble, and insoluble dietary fiber, as well as for a fatty acids profile, microbiological and sensory characteristics.

Proximate analysis. The samples' proximate composition was analyzed using the AOAC methods for meat products. Moisture was measured using the AOAC method 950.45; lipids using the AOAC Soxhlet method 991.36 with petroleum ether; crude protein using the AOAC method 990.03 with 6.25 as a conversion factor; and ash using the AOAC method 920.153 [17–20].

Determination of pH. The samples' pH was measured using a laboratory pH meter (Jenway 3520) as proposed by Vasquez Mejia *et al.* [21]. The pH meter was calibrated with buffer solutions with pH of 4.01, 7.00, and 9.21 (Mettlet Toledo In Lab). The equipment automatically corrected to the value expected at the actual temperature. Approximately 5.0 ± 0.5 g of each sample was weighed in a beaker and mixed with 20 mL of water. For each experimental unit, three direct readings of pH of the homogenized solution were taken and the results were averaged.

Cooking loss. The weight of each sample (3 sets of 10 sausages) was recorded before cooking (scalding in water until the interior of the product reached

72°C). After cooking, the sausages were cooled to 10°C and weighed again. Cooking loss, g/100 g was calculated using the following equation:

$$\text{Cooking loss} = \left(\text{Initial sample weight} - \frac{\text{cooked}}{\text{initial}} \text{sample weight} \right) \times 100 \quad (1)$$

Color. Color was analyzed using a ColorQuest XE colorimeter (Hunter Associates Laboratory Inc., Virginia, USA), carrying out an evaluation using the CIE-Lab system (L^* , a^* , b^*), with D65 illumination, aperture size 9.5 mm, and a 10° angle of observation. Each sausage was cut into 2 cm slices, and their color was measured three times from each analytical point as proposed by Vasquez Mejia *et al.* [21]. The lightness value (L^* , with a scale of 0–100) ranged from black (0) to white (100). The first chromaticity coordinate value (a^*) ranged from red (+50) to green (–50), and the second (b^*) from yellow (+50) to blue (–50).

Texture profile analysis. The texture profile of the cooked samples was analyzed through compression tests using a texture analyzer (TA.XT2; Texture, Technologies Corporation, Scarsdale, NY, USA) as described by Vasquez Mejia *et al.* [21]. Texture was measured the day after preparing the samples, which were unrefrigerated and set out to reach room temperature before analysis. For each sample, several pieces from the core were cut out (10 mm in length × 20 mm in diameter) immediately before analysis. For each batch (replicate), 5 pieces were obtained. The pieces were compressed twice until reaching 75% of their original height using a cylindrical acrylic probe measuring 101.6 mm in diameter × 10 mm in height. For this, the probe was set at a test velocity of 1.5 mm/s and a velocity posterior to the test of 1.5 mm/s. The parameters under evaluation included hardness, adhesiveness, cohesiveness, springiness, gumminess, and chewiness.

Analysis of dietary fiber content. Total dietary fiber (including soluble and insoluble dietary fiber) was determined using the AOAC gravimetric enzymatic method 991.43 [22].

Fatty acids profile. Lipids were previously extracted using a 2:1 ratio of chloroform to methanol as a solvent and tricosanoic acid as an internal standard. Fatty acid methyl esters (FAME) were obtained according to the methods of the American Oil Chemistry Society. Saturated and unsaturated fat and *trans*-isomer content were determined by gas chromatography using a chromatograph (model 7890A, Agilent Tech., Santa Clara, CA, USA) equipped with a flame ionization detector and a highly polarized column with a BPX 70 phase (length 60 m, thickness of the layer 0.20 µm, internal diameter 0.25 mm) as proposed by Janiszewski *et al.* [23]. Individual fatty acids were identified by comparing retention times with those for the mixture of the methyl esters of standard fatty acids (Supelco 37 Component FAME

Mix and C18FAME Isomers, Sigma-Aldrich, Darmstadt, Germany) and expressed as a relative proportion of all fatty acids in the sample.

Microbiological analysis. The samples were analyzed according to the methods of the International Commission on Microbiological Specifications for Foods (ICMSF). Immediately after production, the *chorizo* sausages were placed in polyethylene bags, vacuum packed, and refrigerated. On the following day, they were evaluated for aerobic mesophiles, total and fecal coliforms, *Staphylococcus* coagulase, sulphite reducing spores, *Salmonella*, *Listeria monocitogenes*, *Escherichia coli* count, mold count, yeast count, and *Bacillus cereus* count according to the 2008 Colombian Technical Regulation (NTC according to its Spanish initials) 1325 for cooked meat products [24].

Sensory analysis. Sensory analysis was carried out following the methodology of Moghtadaei *et al.* [25]. The samples were randomly selected two days after production, prepared on grill at $110 \pm 3^\circ\text{C}$ for 15 min, randomly numbered with a three-digit code, and placed at 50°C on a tray for the panelists to evaluate in random order. A single sensory session was performed with 70 untrained volunteer panelists (staff and students of the National University of Colombia, 42% women and 58% men, aged 18–52). The panelists analyzed the samples rating their appearance, color, texture, and flavor according to the 7-point hedonic scale, with 1 meaning “dislike very much” and 7 meaning “like very much”. The survey also gathered information regarding their age and frequency of consumption of meat products. After rating the samples, the panelists were asked, “Would you purchase the products consumed in this sensory test?”. Between the samples, they were asked to clean their palate with water and a cracker.

Statistical analysis. Three independent replicates were made using the same ingredients on three different days (the mixing process for each formulation was replicated). All statistical analyses were carried out using the SAS Studio version software (Copyright SAS® On Demand for Academics, 2022). A one-way ANOVA was carried out to compare the samples containing shiitake with the control samples. The Tukey test ($p \leq 0.05$) was applied to compare significant differences.

RESULTS AND DISCUSSION

Characterization of shiitake powder. Table 2 presents the characterization of shiitake powder compared with oat bran used to incorporate fiber and substitute fats in processed meats.

As can be seen, shiitake mushrooms possessed higher percentages of protein and ash and lower percentages of lipids than oat bran, indicating that its nutritional quality was adequate to use in meat products. Studies of shiitake mushrooms carried out by Bisen *et al.* obtained values of 22.8% for protein, 2.1% for lipids, and 6% for ash [26].

The nutritional content of mushrooms, as well as their bioactive compounds, may vary according to the

strain, crop, stage of development, age, storage conditions, and method of extraction [27]. Mushrooms are rich in fiber, carbohydrates, and protein. In particular, they are high in essential amino acids, phenolic compounds (e.g. gallic acid, protocatechuic acid, catechin, caffeic acid, ferulic acid, and myricetin), polyketides, flavonoids, terpenos, steroids, beta carotene, vitamins (including B, C, and D), and minerals (e.g. selenium, zinc, iron, potassium) [27–29]. Fresh shiitakes have an approximate moisture content of $86.3 \pm 2.0\%$, although the level of moisture in dried shiitake varies according to the drying method [30].

Significant differences were found in color between the shiitake powder and oat bran samples, with the former having lower values for L^* (being darker) than the latter. Shiitake powder showed greater values for a^* and b^* . Generally, variations in color among fresh, dried, and rehydrated mushrooms are caused by enzymatic browning or Maillard reactions during their processing [31].

Technological and functional properties, such as water retention capacity, oil retention capacity, solubility, and swelling capacity, were significantly greater in shiitake mushrooms than in oat bran. Therefore, shiitake is expected to have a high level of performance as a functional ingredient, resulting in greater yields of processed meat products. According to Qiu *et al.*, water retention capacity is an important factor in evaluating rehydrated shiitake because it greatly affects sensory properties and it is attributed to the mushroom’s proteins [32]. Having analyzed the secondary structure of the shiitake’s proteins, the authors found a relatively high content of α -helix links (approximately 17.52%), indicating a stable protein structure. They also found a high endothermic peak, which is generally associated with greater thermal stability. According to the authors, despite the condition of the fibrous matter of the cellular wall (β -1-3-glucan and β -1-6-glucan) and the cellular membrane, the fiber contributes little to changes

Table 2 Proximate composition and physicochemical parameters of oat bran and shiitake powder

Parameters	Oat bran	Shiitake powder
Moisture, %	9.29 ± 0.07^a	12.29 ± 0.60^b
Ash, %	4.64 ± 0.01^a	11.56 ± 0.11^b
Lipids, %	4.19 ± 0.14^a	1.79 ± 0.07^b
Protein, %	17.66 ± 0.06^a	25.93 ± 0.53^b
L^*	81.27 ± 0.11^a	75.66 ± 0.41^b
a^*	2.90 ± 0.04^a	3.23 ± 0.33^b
b^*	14.81 ± 0.14^a	16.48 ± 0.80^b
pH	6.31 ± 0.02^a	5.90 ± 0.07^b
Water retention capacity, g/g	3.67 ± 0.41^a	8.87 ± 0.35^b
Oil retention capacity, g/g	2.79 ± 0.04^a	5.34 ± 0.17^b
Solubility, g/g	0.87 ± 0.04^a	4.08 ± 0.12^b
Swelling capacity, g/g	4.57 ± 0.11^a	9.25 ± 0.47^b

Values are given as mean \pm standard error

Different letters in the same row indicate statistically significant differences ($p < 0.05$)

in water retention capacity due to the loss of integrity upon drying and grinding. Nevertheless, the beta-glucan content could positively affect the water retention capacity. It is possible that grinding the shiitake to facilitate its use as a dietary ingredient favored the functional characteristics presented in Table 2, since the finer the powder, the greater its solubility and swelling capacity [33].

Characterization of the chorizo sausage. Proximate analysis. Table 3 presents the proximate composition and physicochemical characteristics of the samples analyzed. As can be seen, moisture and lipids significantly differed ($p \leq 0.05$) among the treatments, with moisture being greater in the experimental samples than in the control. Moisture could be principally attributed to the shiitake's fiber and protein contents that help retain water, as well as varying quantities of water in the formulations, while the lower lipid content in the samples might be down to fat substitution. Ash and protein contents did not show significant differences among the experimental sausage and the control ($p > 0.05$), indicating that despite a high content of shiitake powder (30% or more), which is rich in protein, the proportions employed did not modify these parameters in the final product. Similar results were reported for moisture content ranging from 66.8 to 70.64% in the sausage samples with shiitake [34].

Determination of pH. The results shown in Table 3 indicate that the substitution of fat with shiitake powder did not have any effect on the pH of the final product. Similar results were found by Wang *et al.*, who reported no changes in the pH of sausages in which 25 or 50% of lean meat was substituted with shiitake [34].

Cooking loss. As shown in Table 3, the *chorizo* sausages with shiitake powder used to replace fat had a lower cooking loss than the control ($p \leq 0.05$), apparently due to shiitake's high level of water retention. Given that the capacity of the extenders of meat products to improve water and fat retention determines their level of shrinking upon cooking, it was expected that adding shiitake powder would lead to less contraction in the sausages' diameter during cooking, as was reflected in their yield [35].

Shiitake powder's high water retention capacity (Table 2) allows for greater yields, although a greater quantity of water was used in the samples with shiitake. This is important for the food industry in the search for technological solutions to reduce loss in yield during cooking, since water loss – aside from reducing yield – provokes the accumulation of liquid in the package, causing consequent changes in color and texture, which affects consumer acceptance [36]. Using less fat, as well as adding more water and less starch, as we proposed (Table 1), would allow for healthier processed meat products with fewer calories. Furthermore, additional water compensates for the loss of juiciness in processed meat products with reduced fat. As did the present study, previous investigations using aloe vera as a meat substitute in hamburgers and hydrated wheat bran as a substitute for meat and fats in hamburgers found that cooking loss was minimized upon increasing the use of extenders [5, 37].

Color. The colors of the sausage samples with 30 and 40% fat substitution were statistically ($p \leq 0.05$) less darker (L^*), more yellow (b^*), and less red (a^*) (Table 4). The values of L^* did not show a direct relationship with the concentrations of shiitake powder incorporated. Meanwhile, the values found for a^* may have been influenced by the type of coloring agent used. Additionally, the red color (a^*) resulting from the myoglobin of the meat might have been affected by incorporating shiitake powder, which is dark in color. A study by Martin *et al.* [38] reported the L^* value of 48 and a^* values of 12 to 16 for traditional Spanish cured *chorizo* sausages. Similar values were reported for a^* (24 to 37) in cured dried Spanish sausages in which carmine acid (E-120) was used as a coloring [39].

These results indicate that the color of meat products depends on many factors, including the type of meat used (beef, pork, chicken, rabbit, etc.), other ingredients (wheat flour, smoke, natural and/or artificial colorings, etc.), relative proportions of all ingredients, and technological processes (mixing, scalding, curing/fermenting, high pressure, etc.), all of which vary considerably from study to study. It is expected that non-cured sausages made from ingredients such as those used in our study, including soy protein and starch

Table 3 Proximate analysis and physicochemical characteristics of *chorizo* sausage with shiitake used as a fat substitute

Treatment	Moisture, %	Protein, %	Lipids, %	Ash, %	Total fiber, %	Insoluble fiber, %	Soluble fiber, %	pH	Cooking loss, %
Control	64.36 ± 0.90 ^a	15.54 ± 0.42	13.86 ± 0.50 ^a	1.01 ± 0.04	3.40 ± 0.14 ^a	2.30 ± 0.09 ^a	1.10 ± 0.05	6.23 ± 0.06	5.24 ± 0.33 ^a
30%	68.67 ± 0.29 ^b	15.56 ± 0.27	9.73 ± 0.29 ^b	1.00 ± 0.05	n.a	n.a	n.a	6.24 ± 0.00	4.10 ± 0.07 ^b
40%	66.25 ± 0.79 ^{ab}	15.60 ± 0.62	9.57 ± 0.33 ^b	1.01 ± 0.08	5.68 ± 0.10 ^b	3.82 ± 0.07 ^b	1.86 ± 0.18	6.14 ± 0.06	4.24 ± 0.15 ^b
50%	64.65 ± 0.59 ^c	15.48 ± 0.42	7.23 ± 0.23 ^c	1.01 ± 0.00	n.a	n.a	n.a	6.29 ± 0.03	3.88 ± 0.02 ^b
100%*	66.32 ± 0.24 ^{ab}	15.42 ± 0.29	7.53 ± 0.29 ^c	1.01 ± 0.02	n.a	n.a	n.a	6.46 ± 0.15	3.80 ± 0.02 ^b

n.a – not analyzed

Values are given as mean ± standard error.

Different letters in the same column indicate significant differences ($p \leq 0.05$)

* 50% olive oil and 50% shiitake powder

(tapioca), will have a lighter color, principally due to the use of flours, fat substitution, and artificial coloring.

Texture profile analysis. Adding shiitake powder modified all the parameters of texture, except for adhesiveness (Table 4).

Hardness did not show a significant difference ($p > 0.05$) among the 30 and 40% samples and the control. Similar results for hardness (150.27 ± 19.75) were reported in a sample with 75% substitution of pork meat with shiitake mushroom [34]. Nevertheless, the sausage with 50 and 100% fat substitution were significantly less firm ($p < 0.05$). In general, our results indicated that substituting 50% of meat with shiitake powder decreased hardness, elasticity, and cohesiveness, making the samples less gummy and less chewable. The results for the 40% sample were similar to those for the control with respect to hardness, adhesiveness, springiness, cohesiveness, and gumminess. This indicated that substituting 40% of fat with shiitake powder maintained most of the textural characteristics.

In a previous study by Royse *et al.*, shiitake mushrooms were incorporated into processed meat products without affecting the texture [40]. The greater hardness in the control, as well as in the 30 and 40% sausage samples, may be attributed to the protein structure of shiitake, the structure of meat, and shiitake's fiber that allowed for maintaining the structural network of the product formed by protein and fiber.

The values for springiness and chewiness in our study were lower than those recorded when using adzuki beans to substitute 25% of fat in meatballs, namely 1.19–1.53 and 92.49–145.64 mm, respectively [6].

Gelation of the miosin as a result of hydrophobic interactions and the disulfide-sulfhydryl interactions among proteins has been reported to provide meat systems with greater springiness [41]. Thus, the differences in springiness among the samples in our study may be attributed to the effects of shiitake's dietary fiber. This fiber may interfere with the aggregation of globular heads of miosin, which is the first step in the gelation of proteins during cooking. Furthermore, given that chewiness is a result of gumminess multiplied by springiness, it is expected that a significant increase in springiness caused by adding shiitake powder will directly increase the sample's chewiness.

Based on the proximate analysis, as well as the measurements of pH, cooking loss, color, and texture, we determined that the sample with 40% fat substitution approached the most desirable outcome for these parameters. Thus, we recommend a 40% substitution of animal fat with shiitake powder and only this sample and the control were used in the further analyses of the final product.

Dietary fiber content. Table 2 shows the values for total, soluble, and insoluble dietary fiber of the 40% fat substitution sample and the control. As can be seen, the treatment showed significantly higher values ($p < 0.05$) for insoluble fiber than the control.

Shiitake mushrooms contain dietary fiber which has a high water-retention capacity in addition to increasing

the quantity of insoluble fiber in the final product [42]. This is because fiber reinforces the tridimensional structure of the emulsified protein network, resulting in greater stability, as well as water and oil retention [43].

Fatty acids profile. Table 5 presents the fatty acids profile of the *chorizo* sausage with 40% of fat substituted with shiitake powder as compared to the control. No significant difference was found ($p > 0.05$) for the values of fatty acids between the experimental and control samples. Myristic (C:14), palmitate (C:16), and stearic (C:18) fatty acids were found to make up a large proportion of saturated fatty acids: 41.126% in the control and 36.899% in the experimental sausage. This is consistent with the results of Nieto and Lorenzo as beef and pig fat have a high content of saturated fatty acids [44].

Oleic acid (C18:1n9) was the most abundant mono-unsaturated fatty acid, making up 39.86% of all mono-unsaturated fatty acids in the control and 42.4% in the 40% fat substitution sample. With respect to the poly-unsaturated fatty acids profile, linoleic acid (C18:2 n6) was the most abundant in the control and in the 40% fat substitution sample.

The fact that no significant differences were found in unsaturated fatty acids between the samples under study indicates that the quantity of shiitake powder was not sufficient to increase the amount of unsaturated fatty acids in the final product. Although shiitake contains unsaturated fatty acids, its fat content is low ($< 2\%$) [45]. Therefore, the level of these healthy compounds in the final product can be improved by using higher quantities of shiitake to substitute animal fat (higher than 40%) and/or other sources of unsaturated fatty acids.

While its content of unsaturated fatty acids was not significant, shiitake powder contributed to decreasing caloric intake from animal fats in processed meat products. Additionally, shiitake mushrooms provide antioxidant properties and extend the shelf life of the final product [11].

Microbiological analysis. Table 6 shows the microbiological results of the control sausage as compared to the 40% fat substitution sample. Significant differences ($p \leq 0.05$) were found only in the aerobic mesophile count (CFU/g), with higher values in the control samples, indicating that shiitake may have an antibacterial effect against these microorganisms. According to Pil-Nam *et al.*, at levels of 0.8%, shiitake reduced bacterial growth as well as lipid oxidation [11].

The microbiological parameters indicated that the levels of microorganisms in the control and in the experimental sausage were within those established by Colombia's 2008 Regulation NTC 1325 for cooked meat products [24]. Therefore, the samples were apt for human consumption.

Sensory analysis. Table 7 demonstrates the sensory attributes of the 40% fat substitution sample as compared to the control. Significant differences were found between the general average scores for various characteristics, ranging from 5.4 to 6.3 on a 7-point hedonic scale.

Table 4 Color and texture of *chorizo* sausage with shiitake used as a fat substitute

Treatment	Color		Texture profile analysis						
	<i>L</i> *	<i>a</i> *	<i>b</i> *	Hardness, Newton	Adhesiveness, g·sec	Springiness, mm	Cohesiveness	Gumminess	Chewiness, N/mm
Control	51.17 ± 1.12 ^a	30.40 ± 0.58 ^a	24.53 ± 0.75 ^{ab}	155.66 ± 2.46 ^b	-7.48 ± 2.47	0.87 ± 0.01 ^a	0.27 ± 0.00 ^b	42.79 ± 1.42 ^a	37.15 ± 1.38 ^a
30%	46.76 ± 0.46 ^b	25.79 ± 0.29 ^b	26.15 ± 0.50 ^a	132.63 ± 7.69 ^a	-7.63 ± 2.95	0.68 ± 0.04 ^{b,c}	0.19 ± 0.01 ^b	25.36 ± 6.27 ^{b,c}	16.23 ± 0.88 ^b
40%	46.58 ± 0.45 ^b	25.84 ± 0.52 ^b	28.21 ± 1.67 ^a	145.95 ± 7.53 ^a	-8.17 ± 1.03	0.75 ± 0.03 ^{ab}	0.24 ± 0.00 ^{ab}	35.19 ± 2.48 ^{ab}	26.54 ± 2.55 ^c
50%	49.73 ± 0.48 ^a	14.01 ± 0.14 ^c	18.76 ± 0.29 ^b	75.94 ± 7.27 ^b	-9.95 ± 5.36	0.61 ± 0.01 ^{b,c}	0.21 ± 0.00 ^b	16.81 ± 2.13 ^c	10.26 ± 0.49 ^b
100%*	50.17 ± 0.24 ^a	14.68 ± 0.24 ^c	20.87 ± 0.17 ^{ab}	119.70 ± 11.40 ^{ab}	-4.90 ± 1.09	0.60 ± 0.05 ^c	0.19 ± 0.03 ^b	23.11 ± 3.29 ^{b,c}	13.76 ± 1.09 ^b

Values are given as mean ± standard error

Different letters in the same column indicate significant differences ($p \leq 0.05$)

* 50% olive oil and 50% shiitake powder

Table 5 Fatty acids profile of *chorizo* sausage with 40% of shiitake mushroom as a fat substitute

Saturated fatty acids, %	Monounsaturated fatty acids, %		Polyunsaturated fatty acids, %	
	Control	Experiment	Control	Experiment
C:4	0.07 ± 0.07	0.09 ± 0.09	C14:1	0.13 ± 0.05
C:14	2.15 ± 0.48	1.83 ± 0.27	C15:1	0.02 ± 0.00
C:15	0.12 ± 0.05	0.080 ± 0.002	C16:1	2.58 ± 0.46
C:16	25.62 ± 0.20	23.27 ± 0.81	C17:1	0.332 ± 0.120
C:17	0.55 ± 0.29	0.41 ± 0.08	C18:1n9 <i>trans</i>	0.15 ± 0.00
C:18	12.35 ± 2.37	10.96 ± 0.29	C18:1n9	39.86 ± 0.51
C:20	0.12 ± 0.00	0.13 ± 0.01	C18:1 <i>cis</i>	0.13 ± 0.04
C:22	0.130 ± 0.035	0.130 ± 0.024	C20:1	0.03 ± 0.00
			C22:1	0.07 ± 0.00
Total	41.13	36.89	Total	40.71
			Total	14.06
			Experiment	0.06 ± 0.00
			Experiment	15.47 ± 1.50
			Experiment	0
			Experiment	0.33 ± 0.26
			Experiment	0.40 ± 0.34

Values are given as mean ± standard error

Table 6 Microbiological parameters of *chorizo* sausage with 40% of shiitake mushroom as a fat substitute

Sample	Aerobic mesophiles, CFU/g	Total coliforms, MPN/g	Fecal coliforms, MPN/g	Positive coagulase <i>Staphylococcus</i> , MPN/g	Sulphyte reductor spores, CFU/g	<i>Salmonella</i> (25 g)	<i>Listeria monocytogenes</i> (25 g)	<i>Escherichia coli</i> , CFU/g	Mold count, CFU/g	Yeast count, CFU/g	<i>Bacillus cereus</i> count, CFU/g
Control	1255.0 ± 45.0 ^a	< 3	< 3	< 100	< 100	Absence	Absence	< 10	< 10	17,000 ± 3.0	< 10
Experimental	700 ± 100 ^b	< 3	< 3	< 100	< 100	Absence	Absence	< 10	< 10	28,000 ± 12.0	< 10

Values are given as mean ± standard error

Different letters in the same column indicate significant differences ($p \leq 0.05$)

Table 7 Sensory analysis of *chorizo* sausage with 40% of shiitake powder as a fat substitute

Sample	General product	Appearance	Color	Texture	Flavor
Control	6.01 ± 0.16	6.050 ± 0.075 ^a	5.710 ± 1.169	6.140 ± 1.029 ^a	6.250 ± 1.146 ^a
Experimental	5.61 ± 0.20 ^b	5.650 ± 0.243 ^b	5.660 ± 1.122	5.600 ± 1.332 ^b	5.720 ± 1.452 ^b

Values are given as mean ± standard error

Different letters in the same column indicate significant differences ($p \leq 0.05$)

Incorporation of shiitake powder as a substitute for 40% of animal fat significantly modified all sensory attributes compared to the control. The only exception was color with values of 5.708 ± 1.169 vs. 5.662 ± 1.122 for the control and experimental samples, respectively, corresponding to the rating “like moderately”. Although the experimental *chorizo* sausages were darker and less red – tending toward brown – in the instrumental assessment (Table 4), this had no effect on the panelists’ ratings (Table 7).

On the 7-point hedonic scale, both the samples were rated as “good” to “above average”, corresponding to “like slightly” (point 5), “like moderately” (point 6), and “like very much” (point 7). In all the cases, the consumers rated the control (without fat substitution) higher. Although the 40% fat substitution sample was less accepted than the control, it was not totally rejected with respect to any of the attributes.

In response to the question, “Would you purchase the product?”, 90.77% of the panelists responded that they would purchase the control product, while only 66.15% stated that they would purchase the sausage with shiitake. We recommend that future studies use a panel trained to be able to identify sensory aspects that should be improved in the final product.

To a certain extent, these sensory ratings may be attributed to the consumers’ lack of familiarity with hybrid products (those containing meat and plants as ingredients) and their lack of familiarity with the flavor of shiitake, which has a high content of umami compounds [46]. Although sensory modifications of a conventional product would be better tolerated by those consumers who are familiarized with its health benefits, pleasant sensory characteristics of meat products – e.g., color, texture, and flavor – are essential to their acceptance [47]. In any case, developing foods that contribute to adequate nutrition is still a relevant topic [48, 49]. Therefore, there is a need to further explore which conventional ingredients may be substituted by functional ingredients and to what extent, without affecting the sensory quality of processed meat products.

CONCLUSION

Our study showed that shiitake powder’s technological and functional properties were preferable to those of oat bran, making it viable for incorporation into processed meat products. This functional ingredient provides the product with protein, ash, and fiber, and is low in lipids. While shiitake powder was found to be darker in color than oat bran,

it did not affect the consumer acceptance of *chorizo* sausages with this ingredient.

The *chorizo* sausages in which 40% of fat was substituted with shiitake powder had greater contents of moisture and insoluble fiber, a lower percentage of lipids, less cooking loss, and lower mesophile counts than the control. No differences were found with respect to the protein value or fatty acids profile.

The sausages’ textural parameters were not affected by substituting 40% of fat with shiitake powder. Nevertheless, the samples with 50% fat substitution had a significantly lower hardness than the control.

Finally, the fact that the control was more highly accepted by the panelists than the samples with 40% fat substitution was attributed to their lack of familiarity with hybrid products containing plant ingredients.

CONTRIBUTION

All the authors read and approved the final article. E.M. Rincón Soledad: investigation, formal analysis, writing of the original draft. M.A. Arredondo Nontién: investigation, formal analysis, writing of the original draft. J.W. Castro: investigation. D. Barrios: validation, review and editing. S.M. Vásquez Mejía: conceptualization, methodology, formal analysis, visualization, validation, writing, review and editing.

CONFLICT OF INTEREST

The authors declare that they have no known competing financial interests or personal relationships that may have influenced the results reported in this paper.

ACKNOWLEDGMENTS

The authors would like to thank the sensory analysis panelists for their contribution to the study.

ETHICAL STATEMENT

The study obtained ethical approval from the research ethics committee of the Faculty of Agricultural Sciences – CEIFCA [B.CIERFCA-234-20], Universidad Nacional de Colombia Sede Bogotá. All the panelists gave their informed consent before participating. The study (specifically sensory analysis) was carried out in accordance with the Declaration of Helsinki.

DATA AVAILABILITY

The data supporting this study are available from the corresponding author upon reasonable request.

REFERENCES

1. Kim S-A, Shin S. Red meat and processed meat consumption and the risk of dyslipidemia in Korean adults: A prospective cohort study based on the Health Examinees (HEXA) study. *Nutrition, Metabolism and Cardiovascular Diseases*. 2021;31(6):1714–1727. <https://doi.org/10.1016/j.numecd.2021.02.008>
2. Zhang J, Hayden K, Jackson R, Schutte R. Association of red and processed meat consumption with cardiovascular morbidity and mortality in participants with and without obesity: A prospective cohort study. *Clinical Nutrition*. 2021;40(5):3643–3649. <https://doi.org/10.1016/j.clnu.2020.12.030>
3. González N, Marquès M, Nadal M, Domingo JL. Meat consumption: Which are the current global risks? A review of recent (2010–2020) evidences. *Food Research International*. 2020;137. <https://doi.org/10.1016/j.foodres.2020.109341>
4. Barone AM, Banovic M, Asioli D, Wallace E, Ruiz-Capillas C, Grasso S. The usual suspect: How to co-create healthier meat products. *Food Research International*. 2021;143. <https://doi.org/10.1016/j.foodres.2021.110304>
5. Carvalho LT, Pires MA, Baldin JC, Munekata PES, de Carvalho FAL, Rodrigues I, et al. Partial replacement of meat and fat with hydrated wheat fiber in beef burgers decreases caloric value without reducing the feeling of satiety after consumption. *Meat Science*. 2019;147:53–59. <https://doi.org/10.1016/j.meatsci.2018.08.010>
6. Aslinah LNF, Mat Yusoff M, Ismail-Fitry MR. Simultaneous use of adzuki beans (*Vigna angularis*) flour as meat extender and fat replacer in reduced-fat beef meatballs (*bebola daging*). *Journal of Food Science and Technology*. 2018;55(8):3241–3248. <https://doi.org/10.1007/s13197-018-3256-1>
7. Patinho I, Selani MM, Saldaña E, Bortoluzzi ACT, Rios-Mera JD, da Silva CM, et al. *Agaricus bisporus* mushroom as partial fat replacer improves the sensory quality maintaining the instrumental characteristics of beef burger. *Meat Science*. 2021;172. <https://doi.org/10.1016/j.meatsci.2020.108307>
8. Oh I, Lee JH, Lee HG, Lee S. Feasibility of hydroxypropyl methylcellulose oleogel as an animal fat replacer for meat patties. *Food Research International*. 2019;122:566–572. <https://doi.org/10.1016/j.foodres.2019.01.012>
9. Kouzounis D, Lazaridou A, Katsanidis E. Partial replacement of animal fat by oleogels structured with monoglycerides and phytosterols in frankfurter sausages. *Meat Science*. 2017;130:38–46. <https://doi.org/10.1016/j.meatsci.2017.04.004>
10. Pérez-Montes A, Rangel-Vargas E, Lorenzo JM, Romero L, Santos EM. Edible mushrooms as a novel trend in the development of healthier meat products. *Current Opinion in Food Science*. 2021;37:118–124. <https://doi.org/10.1016/j.cofs.2020.10.004>
11. Pil-Nam S, Park K-M, Kang G-H, Cho S-H, Park B-Y, Van-Ba H. The impact of addition of shiitake on quality characteristics of frankfurter during refrigerated storage. *LWT*. 2015;62(1):62–68. <https://doi.org/10.1016/j.lwt.2015.01.032>
12. Mattar TV, Gonçalves CS, Pereira RC, Faria MA, de Souza VR, Carneiro JdDS. A shiitake mushroom extract as a viable alternative to NaCl for reduction in sodium in beef burgers: A sensory perspective. *British Food Journal*. 2018;120(6):1366–1380. <https://doi.org/10.1108/BFJ-05-2017-0265>
13. Tejedor-Calvo E, Garcia-Barreda S, Sánchez S, Marco P. Effect of bacterial strains isolated from stored shiitake (*Lentinula edodes*) on mushroom biodeterioration and mycelial growth. *Agronomy*. 2020;10(6). <https://doi.org/10.3390/agronomy10060898>
14. Schill S, Stessl B, Meier N, Tichy A, Wagner M, Ludewig M. Microbiological safety and sensory quality of cultivated mushrooms (*Pleurotus eryngii*, *Pleurotus ostreatus* and *Lentinula edodes*) at retail level and post-retail storage. *Foods*. 2021;10(4). <https://doi.org/10.3390/foods10040816>
15. Official Method of Analysis of the AOAC International, 19th ed. Gaithersburg: The Association of Official Analytical Chemists; 2012.
16. Yaruro Cáceres NC, Suarez Mahecha H, de Francisco A, Vásquez Mejia SM, Diaz-Moreno C. Physicochemical, thermal, microstructural and paste properties comparison of four achira (*Canna edulis* sp.) starch ecotypes. *International Journal of Gastronomy and Food Science*. 2021;25. <https://doi.org/10.1016/j.ijgfs.2021.100380>
17. Official Method of Analysis of the AOAC International. Method 950.46. Loss on drying (moisture) in meat, 20th ed. Arlington: The Association of Official Analytical Chemists; 2016.
18. Official Method of Analysis of the AOAC International. Method 991.36. Fat (crude) in meat and meat products, 20th ed. Gaithersburg: The Association of Official Analytical Chemists; 2016.
19. Official Method of Analysis of the AOAC International. Method 990.03. Protein (crude) in animal feed, combustion method, 18th ed. Arlington: The Association of Official Analytical Chemists; 2005.
20. Official Method of Analysis of the AOAC International. Method 920.53. Ash in meat and meat products, 20th ed. Gaithersburg: The Association of Official Analytical Chemists; 2016.

21. Vasquez Mejia SM, Shaheen A, Zhou Z, McNeill D, Bohrer BM. The effect of specialty salts on cooking loss, texture properties, and instrumental color of beef emulsion modeling systems. *Meat Science*. 2019;156:85–92. <https://doi.org/10.1016/j.meatsci.2019.05.015>
22. Official Method of Analysis of the AOAC International, 18th ed. Gaithersburg: The Association of Official Analytical Chemists; 2005.
23. Janiszewski P, Grześkowiak E, Lisiak D, Borys B, Borzuta K, Pospiech E, et al. The influence of thermal processing on the fatty acid profile of pork and lamb meat fed diet with increased levels of unsaturated fatty acids. *Meat Science*. 2016;111:161–167. <https://doi.org/10.1016/j.meatsci.2015.09.006>
24. Norma Técnica Colombiana NTC 1325. Instituto Colombiano de Normas Técnicas y Certificación; 2008.
25. Moghtadaei M, Soltanizadeh N, Goli SAH. Production of sesame oil oleogels based on beeswax and application as partial substitutes of animal fat in beef burger. *Food Research International*. 2018;108:368–377. <https://doi.org/10.1016/j.foodres.2018.03.051>
26. Bisen PS, Baghel RK, Sanodiya BS, Thakur GS, Prasad GBKS. *Lentinus edodes*: A macrofungus with pharmacological activities. *Current Medicinal Chemistry*. 2010;17(22):2419–2430. <https://doi.org/10.2174/092986710791698495>
27. Ramos M, Burgos N, Barnard A, Evans G, Preece J, Graz M, et al. *Agaricus bisporus* and its by-products as a source of valuable extracts and bioactive compounds. *Food Chemistry*. 2019;292:176–187. <https://doi.org/10.1016/j.foodchem.2019.04.035>
28. Buruleanu LC, Radulescu C, Georgescu AA, Danet FA, Olteanu RL, Nicolescu CM, et al. Statistical characterization of the phytochemical characteristics of edible mushroom extracts. *Analytical Letters*. 2018;51(7):1039–1059. <https://doi.org/10.1080/00032719.2017.1366499>
29. Adebayo EA, Martínez-Carrera D, Morales P, Sobal M, Escudero H, Meneses ME, et al. Comparative study of antioxidant and antibacterial properties of the edible mushrooms *Pleurotus levis*, *P. ostreatus*, *P. pulmonarius* and *P. tuber-regium*. *International Journal of Food Science and Technology*. 2018;53(5):1316–1330. <https://doi.org/10.1111/ijfs.13712>
30. Subramaniam S, Wen X-Y, Zhang Z-T, Jing P. Changes in the morphometric, textural, and aromatic characteristics of shiitake mushrooms during combined humid-convective drying. *Drying Technology*. 2021;39(16):2206–2217. <https://doi.org/10.1080/07373937.2020.1760878>
31. Wang X-M, Zhang J, Wu L-H, Zhao Y-L, Li T, Li J-Q, et al. A mini-review of chemical composition and nutritional value of edible wild-grown mushroom from China. *Food Chemistry*. 2014;151:279–285. <https://doi.org/10.1016/j.foodchem.2013.11.062>
32. Qiu Y, Bi J, Jin X, Hu L, Lyu J, Wu X. An understanding of the changes in water holding capacity of rehydrated shiitake mushroom (*Lentinula edodes*) from cell wall, cell membrane and protein. *Food Chemistry*. 2021;351. <https://doi.org/10.1016/j.foodchem.2021.129230>
33. Xu Z, Meenu M, Xu B. Effects of UV-C treatment and ultrafine-grinding on the biotransformation of ergosterol to vitamin D₂, physicochemical properties, and antioxidant properties of shiitake and Jew’s ear. *Food Chemistry*. 2020;309. <https://doi.org/10.1016/j.foodchem.2019.125738>
34. Wang L, Guo H, Liu X, Jiang G, Li C, Li X, et al. Roles of *Lentinula edodes* as the pork lean meat replacer in production of the sausage. *Meat Science*. 2019;156:44–51. <https://doi.org/10.1016/j.meatsci.2019.05.016>
35. Borrajo P, Pateiro M, Munekata PES, Franco D, Domínguez R, Mahgoub M, et al. Pork liver protein hydrolysates as extenders of pork patties shelf-life. *International Journal of Food Science and Technology*. 2021;56(12):6246–6257. <https://doi.org/10.1111/ijfs.15359>
36. Bastos SC, Pimenta MESG, Pimenta CJ, Reis TA, Nunes CA, Pinheiro ACM, et al. Alternative fat substitutes for beef burger: Technological and sensory characteristics. *Journal of Food Science and Technology*. 2014;51(9):2046–2053. <https://doi.org/10.1007/s13197-013-1233-2>
37. Soltanizadeh N, Ghiasi-Esfahani H. Qualitative improvement of low meat beef burger using *Aloe vera*. *Meat Science*. 2015;99:75–80. <https://doi.org/10.1016/j.meatsci.2014.09.002>
38. Martín MJ, García-Parra J, Trejo A, Gómez-Quintana A, Miguel-Pintado C, Riscado A, et al. Comparative effect of high hydrostatic pressure treatment on Spanish and Portuguese traditional chorizos and evolution at different storage temperatures. *Journal of Food Processing and Preservation*. 2020;45(1). <https://doi.org/10.1111/jfpp.15082>
39. Martínez-Zamora L, Peñalver R, Ros G, Nieto G. Substitution of synthetic nitrates and antioxidants by spices, fruits and vegetables in *Clean label* Spanish chorizo. *Food Research International*. 2021;139. <https://doi.org/10.1016/j.foodres.2020.109835>
40. Royse DJ, Baars J, Tan Q. Current overview of mushroom production in the world. In: Zied DC, Pardo-Giménez A, editors. *Edible and medicinal mushrooms: Technology and applications*. John Wiley & Sons Ltd; 2017. <https://doi.org/10.1002/9781119149446.ch2>

41. Savadkoobi S, Shamsi K, Hoogenkamp H, Javadi A, Farahnaky A. Mechanical and gelling properties of comminuted sausages containing chicken MDM. *Journal of Food Engineering*. 2013;117(3):255–262. <https://doi.org/10.1016/j.jfoodeng.2013.03.004>
42. Selani MM, Shirado GAN, Margiotta GB, Saldaña E, Spada FP, Piedade SMS, et al. Effects of pineapple byproduct and canola oil as fat replacers on physicochemical and sensory qualities of low-fat beef burger. *Meat Science*. 2016;112:69–76. <https://doi.org/10.1016/j.meatsci.2015.10.020>
43. Mehta N, Ahlawat SS, Sharma DP, Dabur RS. Novel trends in development of dietary fiber rich meat products – A critical review. *Journal of Food Science and Technology*. 2015;52(2):633–647. <https://doi.org/10.1007/s13197-013-1010-2>
44. Nieto G, Lorenzo JM. Use of olive oil as fat replacer in meat emulsions. *Current Opinion in Food Science*. 2021;40:179–186. <https://doi.org/10.1016/j.cofs.2021.04.007>
45. Pathak MP, Pathak K, Saikia R, Gogoi U, Ahmad MZ, Patowary P, et al. Immunomodulatory effect of mushrooms and their bioactive compounds in cancer: A comprehensive review. *Biomedicine and Pharmacotherapy*. 2022;149. <https://doi.org/10.1016/j.biopha.2022.112901>
46. Harada-Padermo SDS, Dias-Faceto LS, Selani MM, Conti-Silva AC, Vieira TMFdS. Umami ingredient, a newly developed flavor enhancer from shiitake byproducts, in low-sodium products: A study case of application in corn extruded snacks. *LWT*. 2021;138. <https://doi.org/10.1016/j.lwt.2020.110806>
47. Urruzola N, Santana M, Gámbaro A. Aceptabilidad sensorial de una hamburguesa de carne vacuna y vegetales. *Innotec*. 2018;15(1):15–22. <https://doi.org/10.26461/15.03>
48. Sadovoy VV, Shchedrina TV, Trubina IA, Morgunova AV, Franko EP. Cooked sausage enriched with essential nutrients for the gastrointestinal diet. *Foods and Raw Materials*. 2021;9(2):345–353. <https://doi.org/10.21603/2308-4057-2021-2-345-353>
49. Koneva SI, Zakharova AS, Meleshkina LE, Egorova EYu, Mashkova IA. Technological Properties of Dough from a Mix of Rye and Wheat Flour with Processed Sea Buckthorn. *Food Processing: Techniques and Technology*. 2023;53(2):247–258. (In Russ.). <https://doi.org/10.21603/2074-9414-2023-2-2431>


ORCID IDs

Edicson Mauricio Rincón Soledad  <https://orcid.org/0000-0001-8179-9448>

Mónica Alejandra Arredondo Nontién  <https://orcid.org/0000-0002-0899-4703>

Jose Wilson Castro  <https://orcid.org/0009-0003-9311-3468>

Dursun Barrios  <https://orcid.org/0000-0003-3330-3254>

Sandra Milena Vásquez Mejía  <https://orcid.org/0000-0001-7491-5930>



Major food-borne zoonotic bacterial pathogens of livestock origin: A review

Fuad Zenu, Tesfaye Bekele* 

Wolaita Sodo University , Sodo, Ethiopia

* e-mail: tesfayebekele2017@gmail.com

Received 14.02.2023; Revised 09.03.2023; Accepted 04.04.2023; Published online 11.10.2023

Abstract:

Animal food-borne microbes are pathogens that jeopardize food safety and cause illness in humans via natural infection or contamination. Most of those microbes are bacteria that have considerable impacts on public health. Their survival and pathogenicity are due to toxin production, biofilm development, spore formation, disinfection resistance, and other traits. However, detailed information about them is scattered across scientific literature.

We aimed to compile information about major zoonotic bacteria linked with human food of livestock origin and describe their typical features, transmission modes, detection, and preventative approaches. In particular, we addressed the following pathogens that cause food-borne disease worldwide: *Campylobacter*, *Salmonella*, *Listeria*, *Staphylococcus*, *Brucella*, *Clostridium*, *Mycobacterium*, *Colibacillus*, and some others.

Many of those bacteria have substantial reservoirs in food animals, and food products of animal origin are the primary vehicles of their transmission. Human beings become affected by food-borne zoonotic bacteria if they consume raw animal products or foods produced by using unstandardized slaughtering methods or unsanitary preparation and handling procedures. These zoonotic bacteria and their toxins can be detected in food by culturing, serological, and molecular diagnostic methods. They are effectively controlled and prevented by good hygiene, good management practices, cooking, and pasteurization protocols. In addition, there is a need for a centralized surveillance and monitoring system, as well as higher awareness in society of the occurrence, prevention, and control of bacterial pathogens related to food animals.

Keywords: Bacteria, characteristics, control, food-borne disease, livestock, pathogens, prevention and transmissions

Please cite this article in press as: Zenu F, Bekele T. Major food-borne zoonotic bacterial pathogens of livestock origin: A review. *Foods and Raw Materials*. 2024;12(1):179–193. <https://doi.org/10.21603/2308-4057-2024-1-595>

INTRODUCTION

Human beings significantly benefit from livestock products and services. Livestock occupies around 22–26% of ice-free land of the globe, with feed production covering one-third of farmland [1]. Livestock production accounts for almost 40% of the global agricultural GDP in Africa, as well as 33% of protein and 17% of all calories consumed worldwide [2]. The production also provides significant employment opportunities for rural residents [3]. Furthermore, cattle are an important source of food, nutrition, livelihood, and income in underdeveloped countries [4]. It provides industrial raw materials (milk, meat, hides, and skin), as well as high-value protein, to Ethiopian consumers [5].

Foods of livestock origin play an important role in human diet. Nutritionally, they are an important source of protein, carbohydrates, vitamins, minerals, and other

nutrients of good quality. In addition, animal foods are generally more distinctive in flavor or texture and are often more palatable than foods of vegetable origin. However, these livestock-originated foods can be contaminated at any point in the food supply chain: during production, processing, distribution, preparation, and/or final consumption [6]. This results in food-borne disease transmitted to humans through direct or indirect contact with the animal source or related goods. The consumption of infected raw livestock products, such as milk, meat, and eggs, is a major way of transmission [7].

Food-borne diseases, especially those associated with livestock products, are a global public health threat [8]. The occurrence of food-borne diseases in humans increases as they consume more animal products [9]. The increased consumption of animal products (meat, milk, and eggs) is fueled by a rapid human population growth,

urbanization, rising per capita income, globalization, and changing consumer preferences. This leads to a large-scale manufacturing and global transportation of livestock products with exposure to contaminants and food-borne disease transmission [10].

Microorganisms and their toxins, as well as natural toxins, adulterants, and other probable contaminants in animal products (meat, milk, egg, fish, etc.) pose a substantial risk to people [10]. This risk is mostly due to poor farming, slaughtering, processing, and cleaning techniques used. Moreover, a lack of veterinary services and insufficient food safety regulations are common causes of food-borne diseases in developing countries, including Ethiopia [11, 12].

Bacterial pathogens associated with foods originating from animals and resulting in food-borne diseases in humans include *Salmonella*, *Campylobacter*, *Escherichia*, *Listeria*, *Staphylococcus*, *Brucella*, *Clostridia*, *Mycobacteria*, and others [13]. They are the main source of food spoilage and food-borne infections [6]. Food-borne bacteria are a huge threat to public health, and they can cause illness in humans when they consume animal products contaminated with germs or their toxins [12].

Studies conducted in many parts of the world have demonstrated that certain bacterial infections related to animal-derived foods pose a major threat to public health [10]. The majority of their findings, however, are scattered across different articles. Yet, scientific communities and other stakeholders need structured information on this subject.

Therefore, we aimed to:

- review major zoonotic bacterial pathogens associated with foods of livestock origin;
- highlight typical features, detection methods, and transmission modes of these pathogens, as well as prevention and control measures to overcome their effect on humans.

RESULTS AND DISCUSSION

Zoonotic bacteria of livestock-originated food. Bacterial pathogens are the most serious concern among biological risks in terms of food safety for consumers, and they are among the most common global public health problems in recent times [14, 15]. Gram-negative bacteria are responsible for about 69% of all cases of bacterial food poisoning [16].

Even though a variety of pathogens have been identified as causing food-borne diseases, bacteria, such as *Staphylococcus*, *Salmonella*, *Campylobacter*, *Listeria*, *Escherichia*, *Brucella*, *Clostridium*, and *Mycobacterium*, are the most common causes of food-borne disease in humans due to the consumption of animal-originated foods [6, 13].

***Campylobacter*.** *Characteristics.* *Campylobacter* belongs to the *Campylobacter* family which contains the *Arcobacter* and *Bacteroides* genera. Gram-negative, curved or spiral, and microaerophilic bacteria make up the *Campylobacter* genus. This bacterium has 28 species and 8 subspecies. Thermophilic *Campylobacter* spe-

cies, particularly *Campylobacter jejuni* and *Campylobacter coli*, are significant food-borne pathogens of livestock products among these species. The most commonly reported *Campylobacter* species is *C. jejuni*, followed by *C. coli* [12].

Some *Campylobacter* species are thermotolerant and can survive at temperatures ranging from 37 to 42°C, with 42°C and pH 6.5–7.5 being ideal for *C. coli* and *C. jejuni*. They are ubiquitous in nature and have been observed colonizing gastrointestinal tracts of wild and domesticated birds and mammals, as well as all food animals [11].

Source and mode of transmission. *Campylobacter* is found in 100% of poultry (including chickens, turkeys, and waterfowl), cattle, sheep, pigs, and other food animals, as well as wild animals and birds [15]. Human exposure to this pathogen occurs mainly from the consumption of contaminated meat (beef, pork, etc.), unpasteurized milk, and milk products like cheese, as well as from handling and preparation of contaminated foods of livestock origin [11, 17, 18].

As we can see in Fig. 1, *Campylobacter* invades the gastrointestinal tract of animals such as cattle and poultry. Due to the spillage of *Campylobacter*-rich intestinal material, the surface contamination of carcasses is high at the slaughterhouse. Therefore, undercooked meat from these animals poses a threat of pathogen transmission to human after ingestion [19].

The consumption of unpasteurized milk is one of the main routes of *C. jejuni* transmission to people in both developed and developing countries [21]. The partial failure of milk pasteurization in the United Kingdom causes *C. jejuni* to spread from cattle to people [22]. Unpasteurized raw milk has been linked to 80% of *C. jejuni* infection occurrences in California. Contact with cow feces or polluted water, as well as direct contamination due to bovine mastitis, are all potential sources of milk contamination. Pigs are frequently infected with *C. jejuni* and *C. coli*, which should not be underestimated. According to a study conducted in the United States, contaminated meat, pork, and game were responsible for 5% of *Campylobacter* outbreaks between 1997 and 2008 [23].

Detection. Selective culture media, immunological techniques, and molecular approaches have been used to identify *Campylobacter*. Selective agars, such as Preston, Charcoal-cefoperazone-deoxycholate, and Butzler agars, have been developed and tested for their effectiveness in isolating *Campylobacter*. Food samples can be cultured directly onto a selective media. Following isolation, *Campylobacter* bacteria identification is carried out based on their morphological, biochemical, and growth characteristics [22].

Biochemical assays, such as the enzyme-linked immunosorbent assay (ELISA), can be employed as an alternative to growth on agar, as well as to biochemical or phenotypic identification of *Campylobacter*. The polymerase chain reaction (PCR) has recently gained popularity for molecular detection and identification of *Campylobacter* [24].

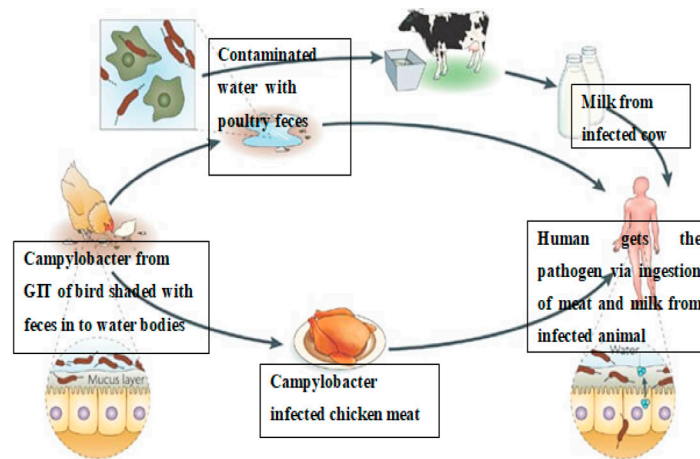


Figure 1 Transmission pathways of *Campylobacter* [20]

Prevention and control. The majority of *Campylobacter* illnesses comes from eating infected foods of animal origin such as meat, milk, and eggs. Therefore, *Campylobacter* infections could be prevented by avoiding the consumption of unpasteurized milk or undercooked meat. To minimize bacterial populations in animals, sanitation and hygiene in livestock barns are essential [25]. *Campylobacter* is found in domestic and wild animals, as well as in the environment. Controlling *Campylobacter* infections in humans should start with measures to minimize infection rates in animal reservoirs utilized for food production, and therefore the risk of their presence in animal-sourced food. Farms should use hygiene barriers to keep out wild animals, perform regular check-ups of animals, and improve their hand-washing facilities [26].

Campylobacter-positive animals are separated and positive poultry flocks are slaughtered to minimize the spread of contamination. Disinfection of feed and water equipment, as well as proper treatment of their dung, has also been suggested to minimize the incidence of *Campylobacter* colonization in cattle [25].

The digestive tract of animals contains a large number of *Campylobacter* species, a possible pollutant of slaughterhouses, environment, and food items. The risk of infection during animal food processing can be minimized by organic acid treatment, UV light, and chemical dip tanks for carcasses. Destroying pathogens or limiting cross-contamination in the kitchen via washing, freezing, or irradiating can help reduce the bacterial transmission to human [27].

Hand washing and separation of ready-to-eat and raw foods are recommended. Cutting boards and utensils that have been used to handle raw meats should be rinsed in hot soapy water before being used to prepare other raw foods. Anyone suffering from an acute diarrheal sickness should avoid food preparation areas until their condition improves. Raw meat, unpasteurized dairy products, and exposure to animals with diarrhea should also be avoided. Before eating, everyone should wash their hands, especially those who work with animals [27, 28].

Non-typhoidal *Salmonella*. *Salmonella* infection in humans results in one of two outcomes: self-limiting gastroenteritis or invasive systemic typhoid fever which is mostly caused by the infecting serovars. *Salmonella* serovars are classified into typhoidal and non-typhoidal *Salmonella*. *Salmonella enteritidis* and *Salmonella typhimurium* are the most frequent non-typhoidal serovars that cause gastroenteritis. *Salmonella typhi* and *Salmonella paratyphi* are typhoidal serovars that cause typhoid fever. About 10–20 million cases of typhoid occur each year, resulting in 100 000–200 000 fatalities in humans worldwide [29, 30].

S. enterica is extremely diverse, with over 2600 distinct serovars. This necessitates understanding the differences between typhoidal and non-typhoidal *Salmonella* as both are of the same species but cause different disease manifestations. Compared to typhoidal strains that are human host-specific, *S. typhimurium* and *S. enteritidis* have broad host ranges. In terms of epidemiology, non-typhoidal *Salmonella* affects people all over the world, whereas typhoidal *Salmonella* is mostly found in underdeveloped nations, such as Southeast Asia and Africa. This could be due to a contaminated living environment and low living standards [31].

Characteristic. *Salmonella* strains are Gram-negative, non-spore-forming, rod-shaped, and motile bacteria that belong to the *Enterobacteriaceae* family [32]. *Salmonella* multiplies best at 35–37°C, pH 6.5–7.5, with little or no oxygen [33]. These heat-sensitive bacteria cannot withstand temperatures > 70°C but they can survive in dried feces, dust, and other dry materials, such as feed and some meals, for a long time [34]. The most common serovars of *Salmonella* that infect livestock and human are shown in Table 1.

Source and mode of transmission. Intestinal tracts of animals (agricultural animals, birds, and reptiles) and people are the principal habitat of *Salmonella* species. Human food-borne illnesses are caused by *Salmonella* transmission from animal products [35]. Human salmonellosis is usually caused by the ingestion of contaminated animal products such as meat, pork, and milk [33].

Table 1 Major serovars of *Salmonella* infecting livestock and human [33]

Animal species	<i>Salmonella</i> serovars
Cattle	<i>Salmonella dublin</i> and <i>Salmonella typhimurium</i>
Sheep	<i>Salmonella typhimurium</i>
Pig	<i>Salmonella choleraesuis</i> , <i>Salmonella typhimurium</i> , and <i>Salmonella typhisuis</i>
Horse	<i>Salmonella typhimurium</i>
Chicken	<i>Salmonella pullorum</i> and <i>Salmonella gallinarum</i>
Human	<i>Salmonella enteritidis</i> , <i>Salmonella typhi</i> , and <i>Salmonella paratyphi</i>

Infected animals used in food production or contaminated carcasses and edible organs are the most common causes of human illness [36]. During slaughtering operations, intestinal content can cross-contaminate carcasses with *S. typhimurium* DT104, a multidrug-resistant definitive type that is primarily transmitted through the consumption of infected beef. Meat usually contains several of the serovars linked to human illnesses. *S. typhimurium*, *S. enteritidis*, and *Salmonella heidelberg* were three of the most common serotypes detected in meat over the last decade [11].

In milk, contamination can arise through a variety of routes. During the febrile stage of the disease, animals may excrete the organisms in milk. Contaminated feces from either a clinically diseased cow or a healthy carrier may contaminate milk during the milking process. Milk can also be contaminated by dairy workers who use unclean water from dirty equipment. *Salmonella*-infected food handlers or sewage-polluted water can contaminate food directly or indirectly. The contaminated milk, in its turn, results in human illness if consumed before proper pasteurization [37].

Since pork is the third most often contaminated meat after fresh chicken and turkey, it is the leading cause of human salmonellosis in the EU. Therefore, monitoring and surveillance efforts have been undertaken across the food chain to assess the danger posed by pork to the general population and to avoid *Salmonella*-borne outbreaks. Pigs can become infected with *Salmonella* from a contaminated environment, feed, or direct contact with diseased animals. At the slaughterhouse, carcasses can be cross-contaminated with excrements of infected or carrier animals causing a public health risk if consumed raw [38].

Detection. *Salmonella* surveillance and monitoring should be based on accurate and efficient detection technologies to ensure food safety. New selective media, modified or adapted conventional processes, immunology-based assays, and nucleic acid-based tests are among commercially available, quick methods for *Salmonella* identification [39]. Selective enrichment media, such as *Salmonella* Shigella agar, Hekaton enteric agar, or deoxycholate agar, as well as broth, are used to culture and isolate bacteria. Food-borne infections are identified with immunology-based approaches such as ELISA, latex agglutination tests, and immunodiffusion tests [40]. *Salmonella* pathogens are detected via PCR, which is a molecular assay [399].

Prevention and control. To control and prevent food spoilage caused by *Salmonella*, biosecurity practices must be used in addition to improved food processing methods, as well as preparation and storage practices [15]. Salmonellosis can be reduced by using attenuated DNA recombinant live *Salmonella* vaccines in combination with a comprehensive control plan in animals and feeds. Humans, especially vulnerable groups, should avoid eating raw or uncooked meat, drinking raw milk or unpasteurized dairy products, as well as cross-contaminating raw and ready-to-eat foods. After coming into contact with animal feces, people should wash their hands properly [35].

Food processing and preparation should involve cooking, reheating, pasteurization of milk, sufficient refrigeration, and the removal of pets and other animals from food-handling areas [14]. After handling uncooked food, cutting boards, knives, and other tools should be washed thoroughly. Uncooked meat should be stored away from ready-to-eat cooked food. Additional secondary contamination control techniques could include cleaning and disinfection, personnel hygiene, and adequate processing [35].

Listeria. Characteristics. Gram-positive, motile, facultatively anaerobic, non-spore producing, and rod-shaped bacteria make up the *Listeria* genus [41, 42]. Of ten species in the genus, *Listeria monocytogenes* is the only one that causes listeriosis in humans. The bacterium can survive at cold temperatures, low pH, and high salt concentrations [11]. In a study by Shamloo *et al.*, *L. monocytogenes* survived a salt concentration of 21% at 4°C and pH = 4 for 19 days [43]. The bacterium is also resistant to disinfectants and can adhere to a variety of surfaces. *L. monocytogenes* can generate biofilm, which can be a cause of contamination in the food processing industry [44].

Source and mode of transmission. Raw foods originating from livestock are the most common sources of *Listeria* species [45]. Foods containing *L. monocytogenes* include ready-to-eat meat products, ground beef, fish and fish products, milk, and pasteurized dairy products such as soft cheese and ice cream [41, 46].

Farmers, butchers, poultry workers, and veterinary surgeons have been reported to contract listeriosis from animal sources as an occupational hazard [46]. At risk for invasive listeriosis are immunocompromised hosts, such as pregnant women, unborn or newly delivered newborns, organ transplant recipients, cancer

and acquired immune deficiency syndrome (AIDS) patients, as well as the elderly [46].

In humans, the most prevalent route of infection is through eating raw animal products such as meat, milk, and pork [47]. The transmission of listeria to humans is also facilitated by cross-contamination of ready-to-eat foods with raw animal products. The highest incidence of *L. monocytogenes* was found in cow meat (26%) followed by goat meat (25%), and sheep meat (17.9%), indicating that red meat is a vehicle for transmission of *L. monocytogenes* to humans [45].

Due to low silage quality and insufficient hygiene, the dairy farm is a favorable environment for the survival and spread of *L. monocytogenes* from cattle into the food chain. *L. monocytogenes* survival in dairy products varies depending on the kind of product. For example, due to reduced pH and moisture content, pathogen development is nearly impossible in hard cheese when compared to soft or semi-soft cheeses. The first listeriosis outbreak in Europe was linked to fresh cheese, and according to an EU baseline study, 0.47% of retail cheese samples tested positive for *L. monocytogenes* [48].

In pork, *L. monocytogenes* is usually discovered in comminuted meats and is found less frequently in freshly-slaughtered pig tissues than in minced pork. Contamination can also arise through the use of tools, hands, boots, gloves, and aprons by manufacturing staff [49].

Detection. Among the procedures used to detect *L. monocytogenes* is enrichment in selective media, subsequent plating on agar plates, and other tests for species identification. Frequently employed is the two-stage enrichment approach with isolation on polymyxin acriflavine lithium-chloride Ceftazidime aesculin manitol (PALCAM) agar and Oxford agar [50]. Molecular approaches are also increasingly being utilized to identify *L. monocytogenes* from food since they are accurate, sensitive, and specific [41].

Prevention and control. Listeriosis can be avoided by thoroughly cleaning all food contact surfaces [51]. To prevent listeriosis and establish consistent management strategies, food-safety control measures must be correctly applied. The most acceptable operational approaches are good hygiene, good manufacturing practice, and sanitation. To limit the risk of infection, vulnerable people (pregnant women, the elderly, and those with compromised immune systems) should avoid unpasteurized dairy products [52]. Food should be protected against *L. monocytogenes* infection by standardized regulatory rules and quality monitoring of meat products. Preventing the spread of bacteria at different stages of the food production chain is one of the most significant techniques to safeguard food from harmful microbes [41].

In the meat industry, non-food contact surfaces, particularly floors and drains, can be a reservoir of *L. monocytogenes* [49]. These areas must be cleaned and sanitized with caution, as they may contaminate

other areas of the food processing facility. Cooking is a good way to protect meat from *L. monocytogenes* infection. The ideal processing procedure would extend the shelf life and safety of the meat product, without compromising its organoleptic or nutritional value, be simple and inexpensive to implement, and avoid causing consumers health risk [51].

Listeria contamination can be greatly reduced in many processed food products by using the Hazard Analysis of Critical Control Points (HACCP) system. To reduce listeriosis, different nations have adopted standards/legislations for the pasteurization of ice cream desserts [41].

***Staphylococcus aureus.* Characteristics.** *S. aureus* is the second most frequent food-borne pathogen in the world after salmonellosis. It is a commensal microorganism that lives on the skin, nose, and mucous membranes of healthy people and animals. However, it is a well-known opportunistic food-borne pathogen that can cause a variety of infectious illnesses of varying severity in humans and animals. This microorganism can survive temperatures ranging from 7 to 48°C, with an optimum of 30 to 37°C, pH 4.2 to 9.3, with an optimum of 7.0 to 7.5, and sodium chloride concentrations up to 15% [53].

These features allow the bacterium to live in a wide range of foods, particularly those that require processing alteration, such as fermented products like cheese [54]. *S. aureus* is a desiccation-tolerant organism that may survive in potentially dry and stressful conditions like the human nose, as well as on the skin and inanimate surfaces like clothing [55].

Source and mode of transmission. Healthy animals carry germs in their nasal passages, throats, and skin, but *S. aureus* is commonly seen in raw milk from mastitic cows. It can be found in a wide range of hosts, including humans and food-producing animals like pigs, cows, goats, chickens, and ducks. Food contamination with *S. aureus* can arise directly from infected food-producing animals or as a result of inadequate hygiene during the manufacturing process, as well as during retail and storage [53].

S. aureus is spread by contaminated animal-source foods [54]. Several food materials are regularly linked to staphylococcal food poisoning, including milk and dairy products, pork, beef, mutton, chicken, and eggs [53]. Raw meat provides a favorable medium for *S. aureus* survival and dissemination in the population, especially the drug-resistant *S. aureus* [56].

Methicillin-resistant *S. aureus* (MRSA) has been discovered at significant levels on US and European farms and in widely sold meats in various investigations, raising concerns among meat workers and consumers. Pig, poultry, and cattle are among those meat-producing animals which are usually implicated with the pathogen. According to a recent study conducted in the United States, 45% of raw pork products and 63% of beef products tested positive for *S. aureus*. A high prevalence of *S. aureus* was found on retail pork products in Iowa,

Minnesota, and New Jersey. These investigations provide clue on the role of commercially-distributed meat as a possible vector for *S. aureus* transmission from farm to the general population [57].

In dairy herds, *S. aureus* is a common cause of bovine mastitis. The prevalence of Methicillin-susceptible *S. aureus* (MSSA) and MRSA was reported to be 84 and 4%, respectively, in a study conducted in Minnesota to determine the herd prevalence of *S. aureus* in bulk tank milk. Udders with clinical or subclinical staphylococcal mastitis can contribute to *S. aureus* contamination of milk by excreting the organisms directly into the milk. In a 1999 *S. aureus* incident in Brazil, for example, cattle mastitis was the primary source of infection, affecting 328 people who consumed unpasteurized milk. Similarly, 293 *S. aureus* isolates were found in 127 bulk tank milk samples from Swiss goats and sheep. Those findings revealed that the consumption of raw or improperly pasteurized milk poses a significant risk to public health [58].

Detection. The ability to produce coagulase is usually the most extensively utilized and widely accepted criterion for identifying pathogenic *Staphylococci*. Mannitol salt agar is a typical medium for the isolation of pathogenic *Staphylococci*. The current standard approach for detecting coagulase-positive *Staphylococci* in food is based on selective enrichment and subsequent isolation of colonies with distinctive morphology, followed by identification using microbiological and biochemical confirmations [54]. Immunological and molecular biology techniques are also useful tools for investigating *S. aureus* contaminations. For the quick detection and identification of MRSA strains, clinical laboratories are increasingly using polymerase chain reaction [53].

Prevention and control. *Staphylococci* are widespread and difficult to eradicate from the environment. To prevent staphylococcal infections and poisoning, methods to stop various mechanisms of transmission are required. Personal hygiene habits among healthcare professionals and food handlers should be improved. Equally effective are the decontamination of equipment, surfaces, and clothing, a judicious use of antibiotics, as well as proper cooking and storage of foods [54].

Staphylococcal infections can be prevented by avoiding contamination and cross-contamination, as well as maintaining critical points. Public education on safe meat handling and other public health interventions could be crucial in preventing the outbreak. Microbiological standards created by the World Health Organization and the US Food and Drug Administration, such as the Hazard Analysis and Critical Control Points (HACCP), Good Manufacturing Practices (GMPs), and good hygiene measures, should be closely followed to avoid *S. aureus* infection. Disinfectants should be used to clean areas where MRSA patients are cared for [57].

S. aureus can survive and produce toxins at temperatures ranging from 6 to 46°C. As a result, the ideal cooking and refrigeration temperatures are above 60°C

and below 5°C, respectively. Other preventive measures include serving food quickly when kept at room temperature, controlling raw food products, disinfecting food processing and preparation equipment, wearing gloves, masks, and hairnets while handling and processing food, as well as frequent hand washing [59].

***Escherichia.* Characteristics.** *Escherichia* is a Gram-negative rod-shaped bacterium that belongs to the *Enterobacteriaceae* family [60]. The majority of *Escherichia coli* are found in the gastrointestinal tracts of animals and humans, whereas some are harmful to humans [61]. *E. coli* is among the most common zoonotic species that poses a public health risk [62]. Several life-threatening food-borne epidemics have been linked to Shiga toxin-producing *E. coli* [63].

E. coli O157:H7 is one of the most well-known serotypes that can infect humans through the ingestion of infected animal foods [60]. It is a well-known Shiga toxin-producing bacterium that is a prominent food-borne and zoonotic pathogen [64].

Source and mode of transmission. Many healthy animals, including humans, have *E. coli* in their gut microbiota. Some strains, however, can cause sickness. Cattle, sheep, and goats are the main reservoirs of *E. coli* O157:H7. In outbreaks, milk and dairy products, as well as improperly cooked meat and other animal food products, have been identified as key sources of infection [65]. The consumption of contaminated animal food and water, fecal contamination of food products, and direct contact with sick animals are the most common routes of *E. coli* O157:H7 transmission to humans [66].

The global prevalence of *E. coli* O157:H7 in beef was found to range from 0.1 to 54.2% in ground beef, 0.1 to 4.4% in sausage, 1.1 to 36.0% in nonspecific retail cuts, and 0.01 to 43.4% in whole carcasses, according to a recent study. The first *E. coli* O157:H7 outbreak was reported in 1982, and it was connected to ground beef, which is still the most common source of food-borne outbreaks today. In the United States, beef was the cause of infection in 78 *E. coli* O157:H7-related outbreaks [67].

Raw milk is a potentially dangerous commodity whose microbiological safety cannot be ensured without pasteurization or a similar treatment. Cheeses prepared from raw milk are extremely prone to bacterial infection. If hygiene and process controls are weak, pathogens may enter cheese during production. Pathogens, such as *E. coli* O157:H7, can be found in raw milk, and mostly they come from milk animals resulting in human disease [68].

Detection. During outbreak investigations, sensitive methods, surveillance, and quality control are recommended to detect *E. coli* O157:H7 [66]. This serotype has been detected in food, environmental, and clinical samples using a variety of methods including culturing in specific media, as well as serological and molecular testing [69].

Biochemical assays and culture isolation of *E. coli* O157:H7 remain the gold standard for identification [70].

Sorbitol-MacConkey (SMAC) agar combined with cefixime and potassium tellurite is one of the most sensitive and discriminating mediums for separating *E. coli* O157:H7 from other *E. coli* serotypes [69]. Colorless colonies will appear if *E. coli* O157:H7 is present, but pink colonies will appear if other *Enterobacteriaceae* are present. Immunoassays and polymerase chain reaction (PCR) technology have made it possible to identify *E. coli* in food and water more quickly. Other techniques include enzyme-linked immunosorbent assays (ELISAs) [71].

Prevention and control. *E. coli*-related food poisoning can be avoided by using the same strategy as is used against other bacteria. Implementing intervention measures across the food continuum, from farm to table, will be necessary for an effective control program to significantly reduce *E. coli* O157:H7 infections. Consumers can also help implement intervention measures in the food handling and preparation process [72].

Pre-harvest *E. coli* O157:H7 control is a method that promotes human health, food, and water safety. The pathogen can also be reduced in animals by implementing proper sanitation procedures throughout food preparation, processing, and transportation management. Preventive measures include food hygiene such as correct meat cooking or intake of pasteurized milk, as well as personnel hygiene. With different degrees of success, post-harvest intervention strategies are used, such as skin and carcass cleaning and the application of antimicrobials [70].

The HACCP approach is used to ensure food safety in the processing industry. This method does not target *E. coli* specifically, but it addresses biological, chemical, and physical risks in general. Food handler training, food premise inspections, and community-based education programs were found to be effective in reducing public exposure to food-borne pathogens in a systematic review of retail and consumer food safety programs. Intervention approaches in cattle, such as probiotics, vaccination, antimicrobials, and bacteriophages, provide another option for increasing herd resistance to infection and subsequent control of *E. coli* O157:H7. Vaccination is a potential method of reducing *E. coli* O157:H7 colonization [70].

Brucella. *Characteristics.* Brucellosis is one of the important zoonotic diseases of livestock worldwide. The most important *Brucella* of veterinary and zoonotic importance that cause abortion and infertility in female and male livestock are *Brucella abortus*, *Brucella melitensis*, and *Brucella suis* [73]. The ability of the pathogen to survive and replicate within different host cells explains its pathogenicity. Its persistence in macrophages and other cell types leads to chronic infections [74].

Source and mode of transmission. In animals, the transmission of *Brucella* can occur either by direct or indirect interaction with diseased cattle or their discharges. The most common route is ingesting feed and drinking water contaminated by the bacteria that

are present in massive amounts in birth products and uterine discharge. Moreover, cattle typically lick their fetuses and newborn calves, which can result in bacterial transmission to humans [75].

Humans typically acquire *Brucella* infection by ingesting raw infected meat, unpasteurized milk, or dairy products. They can also get infected through abrasions that come into contact with fluids or tissues of aborted fetuses of diseased cattle, as well as other work-related practices. Abattoir, farm, and laboratory workers, as well as veterinarians, are known risk groups for *Brucella* infection [76].

Detection. The test samples from which DNA can be extracted most commonly for brucellosis diagnosis include aborted fetuses and food products, such as milk and other foods. The most reliable samples in animals for *Brucella* isolation are spleen as well as lymph nodes (iliac, mammary, and pre-femoral) during the post-mortem inspection [77].

O'Grady *et al.* compared cultural and serological techniques to isolate *B. abortus* from paired supra-mammary, retropharyngeal, and internal iliac lymph nodes of slaughtered animals [78]. Although the micro serum agglutination test and the fluorescence polarization assay were found to be comparatively more sensitive, bacterial culture methods should always be employed for *Brucella* confirmation [79].

Prevention and control. Brucellosis in animals may be controlled by a strict enforcement of measures including testing and slaughtering, vaccination, sanitation, and movement control. The knowledge of brucellosis and its presence in different livestock species is essential for the effective implementation of control measures in food safety. Quarantine and immunization of animals with vaccines are also among important measures of prevention and control [77].

The lack of awareness among farmers and the absence of an effective control strategy have made the situation favorable for *Brucella*. Therefore, animal owners should be made aware of the health impact of brucellosis and the importance of vaccinating their livestock. Public health education should emphasize food and occupational hygiene. Avoiding or discouraging the consumption of raw milk and dairy products, as well as strict protection and safety measures among health workers, will help prevent brucellosis in the human population [80].

Clostridium botulinum. *Characteristics.* *C. botulinum* is a bacterium that produces a dangerous toxin which is reported to be one of the most known lethal substances [81]. *C. botulinum* can colonize the intestinal tract of animals and produce botulism neurotoxin. During unfavorable conditions, *C. botulinum* forms a spore that survives standard cooking and food-processing measures. However, the spore is sensitive to an aerobic environment, acidic pH, and high salt solutions [82]. Spore germination and toxin production are achieved when foods are exposed to anaerobic

conditions, pH > 4.6, low salt and sugar concentrations, and temperatures from 4–12°C [83].

Source and mode of transmission. Botulism is known to affect mammals, birds, and fish, although some species seem to be more susceptible than others. This disease is reported regularly in horses, domesticated ruminants, poultry, wild birds, and aquatic animals. Botulism is not transmitted between animals or people by casual contact. However, it can be acquired by ingesting preformed toxins. Humans contract the toxin by ingesting contaminated livestock products [84].

C. botulinum strains are responsible for numerous botulism outbreaks in humans. Uncooked or minimally heated, chilled livestock products are often involved in the transmission of botulism to humans. *C. botulinum* is a safety risk in home-made or industrial foods that are uncooked or processed with mild heat treatments, as well as stored for long periods even at low temperatures [85]. Meat can be contaminated with fecal *C. botulinum* spores during processing at the slaughter house. Pork meat preparations carry an important risk of botulism in several countries such as France and Poland. In France, type B botulism caused by home-made preparations of pork meat is the most prevalent food-borne botulism [86].

Raw milk contamination by *C. botulinum* results essentially from the cattle environment. Indeed, in farms with a botulism outbreak, the diseased as well as non-symptomatic animals excrete large numbers of *C. botulinum* spores in their feces that are subsequently spread in their local environment, including soil and pasture. Diseased cows are unlikely to excrete botulinum neurotoxin in milk. The toxin is very rarely detected in the serum of cattle with botulism. Thus, the passage of a significant amount of botulinum neurotoxin into milk is very low, with very few outbreaks of human botulism via milk products reported. A report by Dąbrowski and Mędrala shows the presence of botulinum neurotoxin B in the milk of a cow suffering from mastitis [87].

Detection. Food-borne botulism is initially suspected based on the clinical case of the patient. It can be confirmed through a laboratory identification of botulinum neurotoxin and/or those clostridia that produce the toxin in clinical specimens or in suspected food sources consumed by the patient [87].

Several methods are used to detect the toxin. The intra-peritoneal injection of the bacteria to mice remains the most reliable, sensitive, and definitive of all the methods. The presence of *C. botulinum* is detected by injecting the food extract into mice, which are then observed for characteristic symptoms of botulism and ultimate death over a 48-h period. The mouse bioassay is the only standard validated method for the detection of botulinum toxin in foods [88].

Prevention and control. The toxins are typically sensitive and their spores can be destroyed by heating to 85°C for 5 min or by wet sterilization at 120°C for 5 min. Veterinarians who encounter or suspect botulism

should follow their national and/or local guidelines for disease reporting [89].

Feed for animals may be heat-processed and acidified to reduce the risk of botulism. Carcasses should not be allowed to contaminate feed for herbivores, and silage should be monitored for proper acidification. Re-using broiler litter on ruminant farms as feed or bedding increases the risk of botulism. When broiler litter is spread on fields, it should be plowed in immediately. Ruminants with dietary deficiencies should be given feed supplements to reduce the incidence of pica. Vaccines may be available for horses, cattle, sheep, goats, mink, and/or birds in some countries [89].

In humans, the risk of botulism from foods can also be reduced by acidification, moisture reduction, and treatment with salt or other compounds known to inhibit clostridial germination before consumption. Humans should avoid foods from animals with botulism, including meat and milk. Person-to-person transmission of botulinum has never been described, but precautions should be taken to avoid exposure to toxins in body fluids and feces [57].

***Clostridium perfringens*.** **Characteristics.** *C. perfringens* belongs to the *Bacillidial* family and is an important cause of food-borne disease. It produces protein toxins and forms spores resistant to various environmental stresses such as radiation, desiccation, and heat. Vegetative cells grow at temperatures ranging from 6 to 50°C but prefer an optimum temperature between 43 and 47°C, a salt concentration less than 5–8% depending on the strain, and a pH of 5.0–9.0, although 6.0–7.2 is preferred. *C. perfringens* is part of the normal intestinal flora of animals and humans [90].

Source and mode of transmission. *C. perfringens* thrives in high-protein foods of animal origin, such as meat and meat products, meat dishes, and milk. These protein-containing foods, when kept at improper storage temperatures between 12 and 60°C, provide the greatest risk of infection and disease from *C. perfringens*. This is because its spores present after cooking can germinate and potentially grow to high numbers. The risk zone is between 43 and 47°C [91].

Foods can be contaminated during food production, processing, preparation, transportation, and storage. The initial contamination of foods implicated in *C. perfringens* outbreaks might have occurred in the environment, since *C. perfringens* is ubiquitous in soil, in intestinal tracts of animals, and in a variety of ingredients. Raw meat and dairy products can become contaminated if the animal is infected. If consumed raw or after insufficient cooking, these foods may result in bacterial proliferation and toxin production [90].

Detection. Food samples are inoculated into Rapid Perfringens Media (RPM) overnight, then sandwiched into tryptose sulphite cycloserine (TSC) agar, and incubated. Colonies suspected to be *C. perfringens* are then sub-cultured into RPM and incubated again. Typical *C. perfringens* colonies from agar plates are selected and inoculated into a tube of freshly deaerated and

cooled fluid thioglycollate broth. They are incubated in a standard incubator at 35°C for 18–24 h. Then, the cultures are examined by Gram stain and checked for purity. *C. perfringens* is a short, thick, yellowish gray Gram-positive bacillus. DNA is extracted and PCR can also be performed to determine its genotype [92].

Prevention and control. Thermal treatment is one of the most common ways of sterilizing products, as excessive heat destroys the majority of bacterial cells. It has been reported that *C. perfringens* spores are highly heat-resistant, although the resistance patterns vary considerably with the strain and growth conditions, such as the medium and incubation temperature. However, a significant inactivation of *C. perfringens* spores can be achieved by exposing them to high temperatures for a longer period of time. Additionally, cooked food must be chilled rapidly to 41°F (5°C) or less, or kept at hot holding temperatures of 140°F (60°C) or higher to prevent any activation and growth of *C. perfringens* spores [93].

Different types of chemical agents have been proven to be effective in controlling *C. perfringens* such as acetic acid, organic acids, nitrates, and phosphates. In animals, vaccination can be used to control *C. perfringens* B and C [94].

***Mycobacterium bovis*.** **Characteristics.** The *Mycobacterium* genus includes non-spore forming, obligate aerobic, facultative intracellular species. The bacteria's cell walls are rich in lipid, which greatly contributes to their resistance to many disinfectants, common laboratory stains, and antibiotics [95]. *M. bovis* is the main etiological agent of bovine tuberculosis. While the bacteria primarily affect the cattle and other domestic and wild animals, they can also affect human beings [96].

Source and mode of transmission. *M. bovis* is one of the bacteria recognized as a major public health concern. *M. bovis* is the cause of zoonotic tuberculosis in humans, which can be transmitted to people from infected vertebrate animals. It is the most common cause of tuberculosis in humans and cattle [97]. Inhalation and ingestion are two common modes of transmission. Inhalation transmission is mainly by droplet infection. Animals and humans can inhale dust contaminated by sputum, feces, or urine of infected animals. Thus, close housing and overcrowding, along with improper management, increase the risk of the disease in animals. Infected cattle are a possible source of infection as they shed a significant amount of *M. bovis* through droplets into the environment. They may act as a source of intra-herd transmission either directly (animal-to-animal), particularly by aerosol, or indirectly, via infective material (e.g., manure, urine, bedding, contaminated feed, and water) [96].

M. bovis is transmitted from animal to human through ingestion of unpasteurized dairy products and undercooked meat of infected cattle [96]. In an estimate, about 10% of human tuberculosis cases are caused by *M. bovis*, while the majority are caused by *M. tuberculosis*. In the countries where milk is pasteurized and effective bovine tuberculosis control is implemented,

tuberculosis occurrence in humans due to *M. bovis* is very rare. However, in the areas where the disease in bovine is poorly controlled, the disease reports are more frequent [98].

Detection. Different tests can be undertaken to detect *M. bovis* in food samples. The identification of *M. bovis* in raw milk has been described in Tanzania. Microbiological culture remains the gold standard test for detecting *Mycobacterium* species in clinical samples due to its sensitivity and specificity. When tuberculosis lesions are found in a carcass during meat inspection at routine slaughter, a sample of the affected tissue is also sent for mycobacterial culture testing [99].

Enrichment selective media are required to isolate *Mycobacterium* species, especially those containing egg, which is commonly used in veterinary microbiology. One of them is the Lowenstein-Jensen medium made with egg and glycerol favors. After culture, other tests are carried out, such as species identification, antimicrobial susceptibility profile, genotyping, as well as monitoring the human patient's response to treatment [100].

Prevention and control. Tuberculosis needs to be prevented and controlled because it causes a loss of productivity in infected animals and poses a risk of infection to humans. However, it is still a big problem in most developing countries because of financial constraints, scarcity of trained professionals, and lack of political will. Moreover, national governments and donor agencies seem to underestimate the importance of zoonotic tuberculosis in both animal and public health sectors. Therefore, control measures are not applied or applied inadequately [101].

Cattle with tuberculosis must be slaughtered, rather than treated. This is due to the fact that *M. bovis* is resistant to pyrazinamide, which is widely used in the treatment of infections caused by *Mycobacterium tuberculosis* in humans. Meat inspection systems should be strengthened and designed to prevent the consumption of contaminated products by people. All animals entering the food chain should be subjected to ante-mortem and post-mortem inspection. The tuberculin test is valuable in the control of zoonotic tuberculosis because early recognition of preclinical infection in the animals intended for food production eliminates a future source of infection for humans [102].

Standard public health measures used to manage patients with contagious *M. tuberculosis* should be applied to contagious patients with *M. bovis* to stop person-to-person transmission. Hygienic measures should be instituted to prevent the spread of infection. Food containers should be cleaned and thoroughly disinfected, while the consumption of unpasteurized milk, as well as undercooked or raw meat, should be avoided [96].

CONCLUSION

Food-borne zoonotic bacterial infections are the primary causes of human illness worldwide, with a high burden in developing countries. *Campylobacter*,

Salmonella, *Listeria*, *Staphylococcus*, *Escherichia*, *Bruceella*, *Clostridium*, and *Mycobacterium* are the most implicated bacterial pathogens to be found in animal products either from intrinsic infection or environmental contamination with the pathogens or their toxins. Moreover, these bacteria may also infiltrate into the food chain at any stage and affect public health. More importantly, due to the rise of multidrug-resistant strains, most of the bacterial diseases cannot be cured with previous conventional medicaments, exacerbating the problem.

International scientists have regularly isolated the bacteria from food of animal origin, particularly meat, dairy products, and eggs. People may be more susceptible to food-borne zoonotic bacterial infections if they consume raw livestock products, meat supplied from poorly standardized slaughter houses, or use unsanitary food preparation and handling procedures. This calls for a vigorous implementation of effective prevention and control strategies in all food supply

chains to ensure food safety. To this effect, the following recommendations have been put forward:

- coordinated surveillance and monitoring systems for food-borne zoonotic bacterial pathogens should be applied to alleviate their impact on public health;
- the epidemiological information system should be established to cover potential risk factors and incidence of human infections associated with food-borne zoonotic bacterial pathogens; and
- awareness should be raised in the community have the occurrence to prevent and control of food-borne zoonotic bacterial pathogens of livestock origin in humans.

CONTRIBUTION

Fuad Zenu collected the data and wrote the paper. Tesfaye Bekele conceived conceptual frame work and designed the analysis and wrote the paper.

CONFLICT OF INTEREST

The authors declare no conflict of interest.

REFERENCES

1. Phelps LN, Kaplan JO. Land use for animal production in global change studies: Defining and characterizing a framework. *Global Change Biology*. 2017;23(11):4457–4471. <https://doi.org/10.1111/gcb.13732>
2. Balehegn M, Kebreab E, Tolera A, Hunt S, Erickson P, Crane TA, et al. Livestock sustainability research in Africa with a focus on the environment. *Animal Frontiers*. 2021;11(4):47–56. <https://doi.org/10.1093/af/vfab034>
3. Rojas-Downing MM, Nejadhashemi AP, Harrigan T, Woznicki SA. Climate change and livestock: Impacts, adaptation, and mitigation. *Climate Risk Management*. 2017;16:145–163. <https://doi.org/10.1016/j.crm.2017.02.001>
4. Moyo S, Swanepoel F, Stroebel A. *The role of livestock in developing communities: Enhancing multifunctionality*. UJ Press; 2010. 236 p.
5. Eshetie T, Hussien K, Teshome T, Mekonnen A. Meat production, consumption and marketing tradeoffs and potentials in Ethiopia and its effect on GDP growth: A review. *Journal of Nutritional Health and Food Engineering*. 2018;8(3):228–233. <https://doi.org/10.15406/jnhfe.2018.08.00274>
6. Hemalata VB, Virupakshaiah DBM. Isolation and identification of food borne pathogens from spoiled food samples. *International Journal of Current Microbiology and Applied Sciences*. 2016;5(6):1017–1025. <https://doi.org/10.20546/ijemas.2016.506.108>
7. Recht J, Schuenemann VJ, Sánchez-Villagra MR. Host diversity and origin of zoonoses: The ancient and the new. *Animals*. 2020;10(9). <https://doi.org/10.3390/ani10091672>
8. Grujić S, Grujić M. Factors affecting consumer preference for healthy diet and functional foods. *Foods and Raw Materials*. 2023;11(2):259–271. <https://doi.org/10.21603/2308-4057-2023-2-576>
9. Abebe M, Hailelule A, Abrha B, Nigus A, Birhanu M, Adane H, et al. Antibiogram of *Escherichia coli* strains isolated from food of bovine origin in selected Woredas of Tigray, Ethiopia. *Journal of Bacteriology Research*. 2014;6(3):17–22.
10. Haileselassie M, Taddele H, Adhana K, Kalayou S. Food safety knowledge and practices of abattoir and butchery shops and the microbial profile of meat in Mekelle City, Ethiopia. *Asian Pacific Journal of Tropical Biomedicine*. 2013;3(5):407–412. [https://doi.org/10.1016/S2221-1691\(13\)60085-4](https://doi.org/10.1016/S2221-1691(13)60085-4)
11. Dhama K, Rajagunalan S, Chakraborty S, Verma AK, Kumar A, Tiwari R, et al. Food-borne pathogens of animal origin—diagnosis, prevention, control and their zoonotic significance: A review. *Pakistan Journal of Biological Sciences*. 2013;16(20):1076–1085. <https://doi.org/10.3923/pjbs.2013.1076.1085>
12. Heredia N, García S. Animals as sources of food-borne pathogens: A review. *Animal Nutrition*. 2018;4(3):250–255. <https://doi.org/10.1016/j.aninu.2018.04.006>
13. Zhao X, Lin C-W, Wang J, Oh DH. Advances in rapid detection methods for foodborne pathogens. *Journal of Microbiology and Biotechnology*. 2014;24(3):297–312. <https://doi.org/10.4014/jmb.1310.10013>

14. Zelalem A, Sisay M, Vipham JL, Abegaz K, Kebede A, Terefe Y. The prevalence and antimicrobial resistance profiles of bacterial isolates from meat and meat products in Ethiopia: A systematic review and meta-analysis. *International Journal of Food Contamination*. 2019;6. <https://doi.org/10.1186/s40550-019-0071-z>
15. Addis M, Sisay D. A review on major food borne bacterial illnesses. *Journal of Tropical Diseases*. 2015;3.
16. Kebede T, Afera B, Taddele H, Bsrat A. Assessment of bacteriological quality of sold meat in the butcher shops of Adigrat, Tigray, Ethiopia. *Applied Journal of Hygiene*. 2014;3(3):38–44.
17. Dadi L, Asrat D. Prevalence and antimicrobial susceptibility profiles of thermotolerant *Campylobacter* strains in retail raw meat products in Ethiopia. *Ethiopian Journal of Health Development*. 2008;22(2):195–200. <https://doi.org/10.4314/ejhd.v22i2.10072>
18. Wiczorek K, Wołkowicz T, Osek J. Antimicrobial resistance and virulence-associated traits of *Campylobacter jejuni* isolated from poultry food chain and humans with diarrhea. *Frontiers in Microbiology*. 2018;9. <https://doi.org/10.3389/fmicb.2018.01508>
19. Jacobs-Reitsma WF, Newell DG, Wagenaar JA. *Campylobacter jejuni* and *Campylobacter coli*. In: *Manual of diagnostic tests and vaccines for terrestrial animals*. Paris: Office International des Epizooties; 2008. pp. 1185–1191.
20. Young KT, Davis LM, DiRita VJ. *Campylobacter jejuni*: Molecular biology and pathogenesis. *Nature Reviews Microbiology*. 2007;5:665–679. <https://doi.org/10.1038/nrmicro1718>
21. Andrzejewska M, Szczepańska B, Śpica D, Klawe JJ. Prevalence, virulence, and antimicrobial resistance of *Campylobacter* spp. in raw milk, beef, and pork meat in Northern Poland. *Foods*. 2019;8(9). <https://doi.org/10.3390/foods8090420>
22. Fernandes AM, Balasegaram S, Willis C, Wimalaratna HML, Maiden MC, McCarthy ND. Partial failure of milk pasteurization as a risk for the transmission of *Campylobacter* from cattle to humans. *Clinical Infectious Diseases*. 2015;61(6):903–909. <https://doi.org/10.1093/cid/civ431>
23. Taylor EV, Herman KM, Ailes EC, Fitzgerald C, Yoder JS, Mahon BE, et al. Common source outbreaks of *Campylobacter* infection in the USA, 1997–2008. *Epidemiology and Infection*. 2013;141(5):987–996. <https://doi.org/10.1017/S0950268812001744>
24. Jay-Russell MT, Mandrell RE, Yuan J, Bates A, Manalac R, Mohle-Boetani J, et al. Using major outer membrane protein typing as an epidemiological tool to investigate outbreaks caused by milk-borne *Campylobacter jejuni* isolates in California. *Journal of Clinical Microbiology*. 2013;51(1):195–201. <https://doi.org/10.1128/JCM.01845-12>
25. Progress on sanitation and drinking water: 2015 update and MDG assessment. UNICEF and World Health Organization; 2015. 90 p.
26. Humphrey S, Chaloner G, Kemmett K, Davidson N, Williams N, Kipar A, et al. *Campylobacter jejuni* is not merely a commensal in commercial broiler chickens and affects bird welfare. *mBio*. 2014;5(4). <https://doi.org/10.1128/mBio.01364-14>
27. Lake RJ, Horn BJ, Dunn AH, Parris R, Green FT, McNickle DC. Cost-effectiveness of interventions to control *Campylobacter* in the New Zealand poultry meat food supply. *Journal of Food Protection*. 2013;76(7):1161–1167. <https://doi.org/10.4315/0362-028X.JFP-12-481>
28. Chen J, Sun X-T, Zeng Z, Yu Y-Y. *Campylobacter* enteritis in adult patients with acute diarrhea from 2005 to 2009 in Beijing, China. *Chinese Medical Journal*. 2011;124(10):1508–1512. <https://doi.org/10.3760/cma.j.issn.0366-6999.2011.10.013>
29. Mogasale V, Maskery B, Ochiai RL, Lee JS, Mogasale VV, Ramani E, et al. Burden of typhoid fever in low-income and middle-income countries: A systematic, literature-based update with risk-factor adjustment. *The Lancet Global Health*. 2014;2(10):e570–e580. [https://doi.org/10.1016/S2214-109X\(14\)70301-8](https://doi.org/10.1016/S2214-109X(14)70301-8)
30. Evdokimova SA, Karetkin BA, Zhurikov MO, Guseva EV, Khabibulina NV, Shakir IV, et al. Antagonistic activity of synbiotics: Response surface modeling of various factors. *Foods and Raw Materials*. 2022;10(2):365–376. <https://doi.org/10.21603/2308-4057-2022-2-543>
31. Gal-Mor O, Boyle EC, Grassl GA. Same species, different diseases: how and why typhoidal and non-typhoidal *Salmonella enterica* serovars differ. *Frontiers in Microbiology*. 2014;5. <https://doi.org/10.3389/fmicb.2014.00391>
32. Johnson TJ, Wannemuehler YM, Johnson SJ, Logue CM, White DG, Doetkott C, et al. Plasmid replicon typing of commensal and pathogenic *Escherichia coli* isolates. *Applied and Environmental Microbiology*. 2007;73(6):1976–1983. <https://doi.org/10.1128/AEM.02171-06>
33. Kemal J. A review on the public health importance of bovine salmonellosis. *Journal of Veterinary Science and Technology*. 2014;5. <https://doi.org/10.4172/2157-7579.1000175>

34. Radostits OM, Gay CC, Hinchcliff KW, Constable PD. *Veterinary medicine: A textbook of the diseases of cattle, horses, sheep, pigs and goats*. Saunders Ltd.; 2007. 2180 p.
35. Kemal J, Sibhat B, Menkir S, Terefe Y, Muktar Y. Antimicrobial resistance patterns of *Salmonella* in Ethiopia: A review. *African Journal of Microbiology Research*. 2015;9(46):2249–2256. <https://doi.org/10.5897/AJMR2015.7763>
36. Girma G. Prevalence, antibiogram and growth potential of *Salmonella* and *Shigella* in Ethiopia: Implications for public health: A review. *Research Journal of Microbiology*. 2015;10(7):288–307. <https://doi.org/10.3923/jm.2015.288.307>
37. Jones BD. *Salmonella* invasion gene regulation: A story of environmental awareness. *Journal of Microbiology*. 2005;43:110–117.
38. Technical specifications on the harmonised monitoring and reporting of antimicrobial resistance in *Salmonella*, *Campylobacter* and indicator *Escherichia coli* and *Enterococcus* spp. bacteria transmitted through food. *EFSA Journal*. 2012;10(6). <https://doi.org/10.2903/j.efsa.2012.2742>
39. Lee K-M, Runyon M, Herrman TJ, Phillips R, Hsieh J. Review of *Salmonella* detection and identification methods: Aspects of rapid emergency response and food safety. *Food Control*. 2015;47:264–276. <https://doi.org/10.1016/j.foodcont.2014.07.011>
40. Wang J, Li Y, Chen J, Hua D, Li Y, Deng H, et al. Rapid detection of food-borne *Salmonella* contamination using IMBs-qPCR method based on *pagC* gene. *Brazilian Journal of Microbiology*. 2018;49(2):320–328. <https://doi.org/10.1016/j.bjm.2017.09.001>
41. Pal M, Awel H. Public health significance of *Listeria monocytogenes* in milk and milk products: An overview. *Journal of Veterinary Public Health*. 2014;12(1):1–5.
42. Lee SHI, Cappato LP, Guimarães JT, Balthazar CF, Rocha RS, Franco LT, et al. *Listeria monocytogenes* in milk: Occurrence and recent advances in methods for inactivation. *Beverages*. 2019;5(1). <https://doi.org/10.3390/beverages5010014>
43. Shamloo E, Abdimoghdam Z, Nazari K, Hosseini SM, Hosseini H, Alebouyeh M. Long term survival of *Listeria monocytogenes* in stress conditions: High pH and salt concentrations. *Journal of Research in Medical and Dental Science*. 2018;6(6):96–100.
44. Colagiorgi A, Bruini I, Di Ciccio PA, Zanardi E, Ghidini S, Ianieri A. *Listeria monocytogenes* biofilms in the wonderland of food industry. *Pathogens*. 2017;6(3). <https://doi.org/10.3390/pathogens6030041>
45. Al-mashhadany DA, Ba-Salamah HA, Shater A-R, Al Sanabani AS, Abd Al Galil FM. Prevalence of *Listeria monocytogenes* in red meat in Dhamar Governorate/Yemen. *Prevalence*. 2016;2(12):73–78.
46. Şanlıbaba P, Tezel BU. Prevalence and characterization of *Listeria* species from raw milk and dairy products from Çanakkale province. *Turkish Journal of Agriculture – Food Science and Technology*. 2018;6(1):61–64. <https://doi.org/10.24925/turjaf.v6i1.61-64.1641>
47. Girma Y, Abebe B. Isolation, identification and antimicrobial susceptibility of *Listeria* species from raw bovine milk in Debre-Birhan Town, Ethiopia. *Journal of Zoonotic Diseases and Public Health*. 2018;2(1).
48. Analysis of the baseline survey on the prevalence of *Listeria monocytogenes* in certain ready-to-eat foods in the EU, 2010–2011 Part A: *Listeria monocytogenes* prevalence estimates. *EFSA Journal*. 2013;11(6). <https://doi.org/10.2903/j.efsa.2013.3241>
49. Bolocan AS, Oniciuc EA, Alvarez-Ordóñez A, Wagner M, Rychli K, Jordan K, et al. Putative cross-contamination routes of *Listeria monocytogenes* in a meat processing facility in Romania. *Journal of Food Protection*. 2015;78(9):1664–1674. <https://doi.org/10.4315/0362-028X.JFP-14-539>
50. Law JW-F, Ab Mutalib N-S, Chan K-G, Lee L-H. An insight into the isolation, enumeration, and molecular detection of *Listeria monocytogenes* in food. *Frontiers in Microbiology*. 2015;6. <https://doi.org/10.3389/fmicb.2015.01227>
51. Rajkovic A, Smigic N, Devlieghere F. Contemporary strategies in combating microbial contamination in food chain. *International Journal of Food Microbiology*. 2010;141:S29–S42. <https://doi.org/10.1016/j.ijfoodmicro.2009.12.019>
52. Dhama K, Karthik K, Tiwari R, Shabbir MZ, Barbuddhe S, Malik SVS, et al. Listeriosis in animals, its public health significance (food-borne zoonosis) and advances in diagnosis and control: A comprehensive review. *Veterinary Quarterly*. 2015;35(4):211–235. <https://doi.org/10.1080/01652176.2015.1063023>
53. Wang W, Baloch Z, Jiang T, Zhang C, Peng Z, Li F, et al. Enterotoxigenicity and antimicrobial resistance of *Staphylococcus aureus* isolated from retail food in China. *Frontiers in Microbiology*. 2017;8. <https://doi.org/10.3389/fmicb.2017.02256>
54. Argaw S, Addis M. A review on staphylococcal food poisoning. *Food Science and Quality Management*. 2015; 40:59–72.

55. Chaibenjawong P, Foster SJ. Desiccation tolerance in *Staphylococcus aureus*. *Archives of Microbiology*. 2011;193: 125–135. <https://doi.org/10.1007/s00203-010-0653-x>
56. Abebe E, Gugsa G, Ahmed M. Review on major food-borne zoonotic bacterial pathogens. *Journal of Tropical Medicine*. 2020;2020. <https://doi.org/10.1155/2020/4674235>
57. Smith TC, Male MJ, Harper AL, Kroeger JS, Tinkler GP, Moritz ED, et al. Methicillin-resistant *Staphylococcus aureus* (MRSA) strain ST398 is present in midwestern US swine and swine workers. *PLoS ONE*. 2009;4(1). <https://doi.org/10.1371/journal.pone.0004258>
58. do Carmo LS, Dias RS, Linardi VR, de Sena MJ, dos Santos DA, de Faria ME, et al. Food poisoning due to enterotoxigenic strains of *Staphylococcus* present in Minas cheese and raw milk in Brazil. *Food Microbiology*. 2002;19(1):9–14. <https://doi.org/10.1006/fmic.2001.0444>
59. James SJ, Evans J, James C. A review of the performance of domestic refrigerators. *Journal of Food Engineering*. 2008;87(1):2–10. <https://doi.org/10.1016/j.jfoodeng.2007.03.032>
60. Assefa A, Bihon A. A systematic review and meta-analysis of prevalence of *Escherichia coli* in foods of animal origin in Ethiopia. *Heliyon*. 2018;4(8). <https://doi.org/10.1016/j.heliyon.2018.e00716>
61. Bekele T, Zewde G, Tefera G, Feleke A, Zerom K. *Escherichia coli* O157: H7 in raw meat in Addis Ababa, Ethiopia: Prevalence at an abattoir and retailers and antimicrobial susceptibility. *International Journal of Food Contamination*. 2014;1. <https://doi.org/10.1186/s40550-014-0004-9>
62. Geresu MA, Regassa S. *Escherichia coli* O157: H7 from food of animal origin in Arsi: Occurrence at catering establishments and antimicrobial susceptibility profile. *The Scientific World Journal*. 2021;2021. <https://doi.org/10.1155/2021/6631860>
63. Ahmida MR. Molecular identification of certain virulence genes of some food poisoning bacteria contaminating raw milk. *Damanhour Journal of Veterinary Sciences*. 2020;4(2):20–24.
64. Haile AF, Kebede D, Wubshet AK. Prevalence and antibiogram of *Escherichia coli* O157 isolated from bovine in Jimma, Ethiopia: Abattoirbased survey. *Ethiopian Veterinary Journal*. 2017;21(2):109–120. <https://doi.org/10.4314/evj.v21i2.8>
65. Messele YE. Characterization of drug resistance patterns of *E. coli* isolated from milk collected from small scale dairy farms reared in Holeta and Burayu and meat from Addis Ababa abattoirs enterprise and Alema farm slaughter slab. Doctoral dissertation. Addis Ababa University; 2016. 68 p.
66. Abreham S, Teklu A, Cox E, Sisay Tessema T. *Escherichia coli* O157:H7: Distribution, molecular characterization, antimicrobial resistance patterns and source of contamination of sheep and goat carcasses at an export abattoir, Mojdo, Ethiopia. *BMC Microbiology*. 2019;19. <https://orcid.org/0000-0002-4103-5029>
67. Lu Z, Breidt F. *Escherichia coli* O157:H7 bacteriophage Φ 241 isolated from an industrial cucumber fermentation at high acidity and salinity. *Frontiers in Microbiology*. 2015;6. <https://doi.org/10.3389/fmicb.2015.00067>
68. Fusco V, Chieffi D, Fanelli F, Logrieco AF, Cho G-S, Kabisch J, et al. Microbial quality and safety of milk and milk products in the 21st century. *Comprehensive Reviews in Food Science and Food Safety*. 2020;19(4):2013–2049. <https://doi.org/10.1111/1541-4337.12568>
69. Farahmandfar M, Moori-Bakhtiari N, Gooraninezhad S, Zarei M. Comparison of two methods for detection of *E. coli* O157H7 in unpasteurized milk. *Iranian Journal of Microbiology*. 2016;8(5):282–287.
70. Saeedi P, Yazdanparast M, Behzadi E, Salmanian AH, Mousavi SL, Nazarian S, et al. A review on strategies for decreasing *E. coli* O157:H7 risk in animals. *Microbial Pathogenesis*. 2017;103:186–195. <https://doi.org/10.1016/j.micpath.2017.01.001>
71. Mesele F, Abunna F. *Escherichia coli* O157:H7 in foods of animal origin and its food safety implications: Review. *Advances in Biological Research*. 2019;13(4):134–145.
72. Pennington H. *Escherichia coli* O157. *The Lancet*. 2010;376(9750):1428–1435. [https://doi.org/10.1016/S0140-6736\(10\)60963-4](https://doi.org/10.1016/S0140-6736(10)60963-4)
73. Godfroid J, Scholz HC, Barbier T, Nicolas C, Wattiau P, Fretin D, et al. Brucellosis at the animal/ecosystem/human interface at the beginning of the 21st century. *Preventive Veterinary Medicine*. 2011;102(2):118–131. <https://doi.org/10.1016/j.prevetmed.2011.04.007>
74. Ray K, Marteyn B, Sansonetti PJ, Tang CM. Life on the inside: The intracellular lifestyle of cytosolic bacteria. *Nature Reviews Microbiology*. 2009;7:333–340. <https://doi.org/10.1038/nrmicro2112>
75. Tulu D, Deresa B, Begna F, Gojam A. Review of common causes of abortion in dairy cattle in Ethiopia. *Journal of Veterinary Medicine and Animal Health*. 2018;10(1):1–3. <https://doi.org/10.5897/JVMAH2017.0639>
76. Fugier E, Pappas G, Gorvel J-P. Virulence factors in brucellosis: implications for aetiopathogenesis and treatment. *Expert Reviews in Molecular Medicine*. 2007;9(35):1–10. <https://doi.org/10.1017/S1462399407000543>

77. Etter RP, Drew ML. Brucellosis in elk of eastern Idaho. *Journal of Wildlife Diseases*. 2006;42(2):271–278. <https://doi.org/10.7589/0090-3558-42.2.271>
78. O’Grady J, Ruttledge M, Sedano-Balbas S, Smith TJ, Barry T, Maher M. Rapid detection of *Listeria monocytogenes* in food using culture enrichment combined with real-time PCR. *Food Microbiology*. 2009;26(1):4–7. <https://doi.org/10.1016/j.fm.2008.08.009>
79. Ledwaba MB, Ndumnego OC, Matle I, Gelaw AK, van Heerden H. Investigating selective media for optimal isolation of *Brucella* spp. in South Africa. *Onderstepoort Journal of Veterinary Research*. 2020;87(1). <https://doi.org/10.4102/ojvr.v87i1.1792>
80. Acharya KP, Kaphle K, Shrestha K, Garin Bastuji B, Smits HL. RETRACTED: Review of brucellosis in Nepal. *International Journal of Veterinary Science and Medicine*. 2016;4(2):54–62. <https://doi.org/10.1016/j.ijvsm.2016.10.009>
81. Kamaloddini MH, Kheradmand HR. A foodborne botulism occurrence in Mashhad: *Clostridium botulinum* in local cheese. *Journal of Emergency Practice and Trauma*. 2021;7(1):66–68. <https://doi.org/10.34172/jept.2020.01>
82. Sobel J, Tucker N, Sulka A, McLaughlin J, Maslanka S. Foodborne botulism in the United States, 1990–2000. *Emerging Infectious Diseases*. 2004;10(9):1606–1611. <https://doi.org/10.3201/eid1009.030745>
83. Chaidoutis E, Keramydas D, Papalexis P, Migdanis A, Migdanis I, Lazaris AC, et al. Foodborne botulism: A brief review of cases transmitted by cheese products (Review). *Biomedical Reports*. 2022;16(5). <https://doi.org/10.3892/br.2022.1524>
84. Abe Y, Negasawa T, Monma C, Oka A. Infantile botulism caused by *Clostridium butyricum* type E toxin. *Pediatric Neurology*. 2008;38(1):55–57. <https://doi.org/10.1016/j.pediatrneurol.2007.08.013>
85. Rasetti-Escargueil C, Lemichez E, Popoff MR. Public health risk associated with botulism as foodborne zoonoses. *Toxins*. 2020;12(1). <https://doi.org/10.3390/toxins12010017>
86. Mazuet C, da Silva NJ, Legeay C, Sautereau J, Popoff RM. Human botulism in France, 2013–2016. *Bulletin Epidémiologique Hebdomadaire*. 2018;3:46–54. (In French).
87. Dąbrowski W, Mędrała D. Bacterial toxins. In: Dabrowski WM, Sikorski ZE, editors. *Toxins in food*. Boca Raton: CRC Press; 2004. <https://doi.org/10.1201/9780203502358>
88. van Baar BLM, Hulst AG, de Jong AL, Wils ERJ. Characterisation of botulinum toxins type C, D, E, and F by matrix-assisted laser desorption ionisation and electrospray mass spectrometry. *Journal of Chromatography A*. 2004;1035(1):97–114.
89. Madsen JM. Bio warfare and terrorism: toxins and other mid-spectrum agents. *Army medical research inst of chemical defense aberdeen proving ground*; 2005. 8 p.
90. Grass JE, Gould LH, Mahon BE. Epidemiology of foodborne disease outbreaks caused by *Clostridium perfringens*, United States, 1998–2010. *Foodborne Pathogens and Disease*. 2013;10(2):131–136. <https://doi.org/10.1089/fpd.2012.1316>
91. Gui L, Subramony C, Fratkin J, Hughson MD. Fatal enteritis necroticans (pigbel) in a diabetic adult. *Modern Pathology*. 2002;15(1):66–70. <https://doi.org/10.1038/modpathol.3880491>
92. Johansson A, Engström BE, Frey J, Johansson K-E, Båverud V. Survival of *Clostridium perfringens* during simulated transport and stability of some plasmid-borne toxin genes under aerobic conditions. *Acta Veterinaria Scandinavica*. 2005;46. <https://doi.org/10.1186/1751-0147-46-241>
93. Wang G, Paredes-Sabja D, Sarker MR, Green C, Setlow P, Li Y-Q. Effects of wet heat treatment on the germination of individual spores of *Clostridium perfringens*. *Journal of Applied Microbiology*. 2012;113(4):824–836. <https://doi.org/10.1111/j.1365-2672.2012.05387.x>
94. Jay JM, Loessner MJ, Golden DA. *Modern food microbiology*. New York: Springer; 2005. 790 p. <https://doi.org/10.1007/b100840>
95. Birhanu T, Mezgebu E, Ejeta E, Gizachew A, Nekemte E. Review on diagnostic techniques of bovine tuberculosis in Ethiopia. *Report and Opinion*. 2015;7(1):7–14.
96. Verma AK, Tiwari R, Chakraborty S, Neha, Saminathan M, Dhama K, et al. Insights into bovine tuberculosis (bTB), various approaches for its diagnosis, control and its public health concerns: An update. *Asian Journal of Animal and Veterinary Advances*. 2014;9(6):323–344. <https://doi.org/10.3923/ajava.2014.323.344>
97. Lema AG, Dame IE. Bovine tuberculosis remains a major public health concern: A review. *Austin Journal of Veterinary Science and Animal Husbandry*. 2022;9(1).

98. Firdessa R, Tschopp R, Wubete A, Sombo M, Hailu E, Erenso G, et al. High prevalence of bovine tuberculosis in dairy cattle in central Ethiopia: Implications for the dairy industry and public health. *PLoS ONE*. 2012;7(12). <https://doi.org/10.1371/journal.pone.0052851>
99. Cadmus SIB, Yakubu MK, Magaji AA, Jenkins AO, van Soelingen D. *Mycobacterium bovis*, but also *M. africanum* present in raw milk of pastoral cattle in north-central Nigeria. *Tropical Animal Health and Production*. 2010;42:1047–1048. <https://doi.org/10.1007/s11250-010-9533-2>
100. Supply P, Mazars E, Lesjean S, Vincent V, Gicquel B, Lochet C. Variable human minisatellite-like regions in the *Mycobacterium tuberculosis* genome. *Molecular Microbiology*. 2000;36(3):762–771. <https://doi.org/10.1046/j.1365-2958.2000.01905.x>
101. Cousins DV. *Mycobacterium bovis* infection and control in domestic livestock. *Revue Scientifique et Technique*. 2001;20(1):71–85. <https://doi.org/10.20506/rst.20.1.1263>
102. Anaelom NJ, Ikechukwu OJ, Sunday EW, Nnaemeka UC. Zoonotic tuberculosis: A review of epidemiology, clinical presentation, prevention and control. *Journal of Public Health and Epidemiology*. 2010;2(6):118–124.

ORCID IDs

Tesfaye Bekele  <https://orcid.org/0000-0001-6277-9038>



A phytochemical study of the clover growing in Kuzbass

Olga V. Belashova^{1,*}, Oksana V. Kozlova¹, Natalia S. Velichkovich¹,
Anna D. Fokina¹, Vladimir P. Yustratov¹, Andrey N. Petrov²

¹ Kemerovo State University^{ROR}, Kemerovo, Russia

² Russian Biotechnological University^{ROR}, Moscow, Russia

* e-mail: o-belashova@mail.ru

Received 09.04.2023; Revised 30.09.2023; Accepted 03.10.2023; Published online 15.11.2023

Abstract:

In addition to studying bioactive organic compounds in plants, it is increasingly important to determine the biological role of elements in plants growing in environmentally unfavorable areas. One of such regions in Russia is Kuzbass with its intensively developing chemical, metallurgical, and coal mining sectors. In this study, we assessed the plant materials of red clover (*Trifolium pratense* L.), alsike clover (*Trifolium hybridum* L.), and white clover (*Trifolium repens* L.) collected from their natural populations in Kuzbass.

The qualitative and quantitative composition of heavy metals in the clover samples was determined voltammetrically. The contents of molybdenum and phosphorus were measured by the photocolometric method. Total nitrogen and protein were determined by the Kjeldahl method. Nickel, cobalt, and chromium were quantified by spectrophotometry.

We analyzed the plant materials of the clover samples for heavy metals and found that the content of lead was the least in red clover and the highest in alsike clover. Copper varied in a larger range and was minimal in red clover compared to that in alsike and white clover. Zinc was found at higher concentrations of in white and red clover compared to that in alsike clover. The levels of cadmium exceeded the maximum permissible concentrations in all the clover samples. We also revealed that the clover samples contained different amounts of various amino acids, including arginine, valine, lysine, glycine, aspartic acid, and alanine. The plant materials of the clover species growing in Kuzbass can be used to improve the fertility of soil and nitrogen regime. However, the clover species should not be used in bulk feed for farm animals because of high concentrations of cadmium.

Keywords: Clover, *Trifolium pratense* L., *Trifolium hybridum* L., *Trifolium repens* L., soil, microelements, amino acids, heavy metals, plants

Funding: This study was part of the Russian Science Foundation (RSF)^{ROR} project “Fundamentals of obtaining bioactive substances from Siberian medicinal plants and creating phyto-genic feed additives with immunomodulatory effects on their basis” (Agreement No. 23-16-00113 dated May 15, 2023).

Please cite this article in press as: Belashova OV, Kozlova OV, Velichkovich NS, Fokina AD, Yustratov VP, Petrov AN. A phytochemical study of the clover growing in Kuzbass. *Foods and Raw Materials*. 2024;12(1):194–206. <https://doi.org/10.21603/2308-4057-2024-1-599>

INTRODUCTION

Recently, researchers have taken increasing interest in the biological role of metals. In particular, there have been numerous studies of heavy metals, a group of chemical elements with a relative atomic mass of over 40. Standards have been established for the contents of certain metals that are toxic and therefore dangerous for living organisms. The human body contains 81 natural metals out of 92, including 10 vital elements, namely Fe, I, Cu, Zn, Co, Cr, Mo, Ni, Se, and Mn. Permissible concentrations of metals are benefi-

cial for plants, animals, and humans, while their increased concentrations have a negative impact. Numerous studies have shown that metal effects vary depending on their content in the environment and their requirement for microorganisms, plants, animals, and humans. However, rapid industrialization and the resulting global technogenic environmental pollution have led to anomalies of elements (particularly, heavy metals) [1–3].

It is important to determine the contents of heavy metals in environmental objects. Stripping voltammetry is commonly used to measure zinc, cadmium, lead, and

copper. In this study, we aimed to determine concentrations of heavy metals in the clover species growing in various parts of Kuzbass (Russia).

The toxic effects of heavy metals depend on the level of soil pollution, as well as on the properties of a specific metal [4, 5]. In nature, metal ions coexist and form various combinations with each other. Therefore, their toxic effects can both increase (synergistic effects) and decrease (antagonistic effects) [6]. For example, a mixture of zinc and copper is five times more toxic (synergistic effect) than the sum of their toxicity values obtained arithmetically [7]. A combination of zinc and nickel has the same synergistic effect, while zinc and cadmium produce an antagonistic effect, jointly causing unidirectional harm.

Synergism and antagonism can also be observed in multicomponent mixtures of metals. Therefore, the toxicological effect of environmental pollution with heavy metals depends on the mixture of metals, as well as their concentrations and mutual impact on biota. On the other hand, heavy metals and their compounds can have harmful effects on living organisms. In particular, they can accumulate in human tissues and cause a number of diseases [8, 9]. Toxic metals are metals that bring no benefit to biological processes (e.g. lead or copper). However, some elements which usually have a toxic effect on living organisms (e.g. zinc or cadmium) can also have a beneficial effect.

Carbon, hydrogen, oxygen, and nitrogen are organogenic elements. Altogether, they make up 95% of dry plant tissue, with 45, 42, 6.5, and 1.5% of carbon, oxygen, hydrogen, and nitrogen, respectively. The remaining 5% includes macroelements, such as phosphorus, sulfur, potassium, calcium, magnesium, iron, aluminum, silicon, sodium, and others. Metals with concentrations of 0.001% or less are called microelements. They are essential elements that perform important functions in plant life. Their deficiency or excess in plants can cause a number of diseases and even lead to death.

The makeup of elements in plant tissues and organs depends on changes in environmental factors.

Phosphorus is found in the earth's crust at a concentration of 0.08%. It plays an important role in cell energy and is involved in the phosphorylation of cellular proteins using protein kinase enzymes [10]. This mechanism controls many metabolic processes, since phosphate redistributes electrical charges in a protein molecule, changing its structural and functional properties.

Phosphorus deficiency in plants causes the leaves to become small and narrow, as well as changes their color to bluish-green. Moreover, it decreases the absorption of molecular oxygen and changes the activity of respiratory enzymes. On the other hand, excessive phosphorus stops plant growth, delays the ripening of the crop, and inhibits the synthesis of proteins and free nucleotides. Phosphorus interferes with the absorption and transport of iron in plants.

Potassium, an important inorganic osmotic compound, helps regulate water balance in plants. It also

maintains the water status of plants by opening and closing leaf stomata [11]. Potassium is involved in the optimization and transport of photosynthesis, as well as in the activation of photosynthetic enzymes, contributing to the production and transport of carbohydrates [12, 13]. In addition, potassium makes plants more resistant to biotic stress (diseases associated with microorganisms) and abiotic stress (drought, low temperatures, salinity). Thus, plants should be provided with a sufficient amount of potassium, since it takes part in many metabolic processes and regulates the growth of plants.

We found no published data on the accumulation of microelements in red clover (*Trifolium pratense* L.), alsike clover (*Trifolium hybridum* L.), and white clover (*Trifolium repens* L.) depending on the precursor, stage of growth and development, or environmental conditions. Microelements are known to activate metabolic processes. Yet, there is hardly any information on their composition, unlike macroelements [14].

Molybdenum deficiency slows down the synthesis of amides, amino acids, and proteins [15, 16]. Of all plants, clover has the greatest need for molybdenum and often suffers from molybdenum starvation in the fields [11, 17]. Nitrogenase is the key enzyme that catalyzes the fixation of molecular nitrogen in nitrogen-fixing microorganisms (aerobic and anaerobic bacteria, cyanobacteria) and root nodules of legumes. This enzyme catalyzes three coupled reactions: recovery of substrates (N_2 , C_2H_2 , etc.), ATP hydrolysis, and ATP-dependent hydrogen evolution. Nitrogen is bound and recovered on the Mo-Fe protein. Molybdenum protonation is an important step for nitrogen binding, which results in the release of molecular hydrogen. In plants, molybdenum is found mainly in the form of the MoO_4^{2-} anion. This element has the ability to change valency and participate in complex compounds. Legumes contain large amounts of molybdenum and are capable of N_2 -fixation. Experimental studies have shown that molybdenum fertilizers increase the nitrogen content in the leaf part of N-deficient plants with nodule bacteria on the roots. However, nitrates can suppress nitrogenase activity in the plants of the *Fabaceae* family. This may be due to the interception of electrons and ATP molecules by nitrate reductase contained in nodule bacteria. Enzymes compete for molybdenum in nitrogen-fixing cells and nodule bacteria, especially in the budding phase, when their synthesis is most active [18].

Iron is one of the main elements found in the Earth's crust. Its content in plants varies widely from 18 to 3580 mg/kg of dry weight. Iron is a universal cofactor for the processes of growth and development, photosynthesis, hormone synthesis, and respiration [14]. Iron deficiency causes leaves to turn yellow (chlorosis) and rapidly drop.

In Kuzbass, plants of the *Trifolium* genus are the most important perennial plants of the *Fabaceae* family in forage production. These plants are widely distributed in the region's meadows and sparse forests [19]. Their fodder value is determined by their high protein content. In addition to being a low-cost source of plant protein,

these plants can effectively increase soil fertility due to nitrogen absorbed from the atmosphere with the help of nitrogen-fixing bacteria in the nodules of the root system. Clover, one of such plants, is therefore used as a protein and vitamin additive in animal feed. For this, it is harvested in the early phases of the growing season and dried. According to literature, clover has a high content of digestible protein, namely 160–165 g per feed unit. Therefore, about 2 kg of clover grass is equivalent to 1 kg of oat grain. The chemical composition of plant reserve nutrients depends not only on the species characteristics, but also on the growth conditions [20, 21]. Proteins, fats, and carbohydrates, including cellulose, water, and microelements, determine the nutritional value of feed raw material, while bioactive substances provide it with additional properties [17, 22–26]. Noteworthy, enzymes, vitamins, growth substances, alkaloids, phenolic compounds, glycosides, tannins, and other essential bioactive substances play an important role in the processes of growth and development [27–30]. However, there are also toxic substances that can slow down the growth and development of plants and cause many pathological processes in them.

In recent years, Russian scientists have paid great attention to plant raw materials with a high feed value. We know that the plant's biomass directly depends on the content of total nitrogen in the plant [31, 32]. Total nitrogen and protein play a major role in plant growth [33]. No other nutrient can affect food supplies as much as nitrogen, which is why it is called a "growth element" [34, 35]. First of all, it is an essential component of nitrogen-containing organic compounds and is actively involved in the vital metabolic processes during the plant's growth and development. Nitrogen deficiency makes the plant look sickly, changes the color of its leaves, slows down its growth, weakens the intensity of flowering, shortens the period of growth and development, and reduces protein production in the plant. All this decreases the yield and may even cause the plant to die [36].

Nitrogen exchange reactions are determined not only by molybdenum and iron, but also by other metals, including nickel, cobalt, and chromium. These metals affect the ratio of nitrogen forms and the amino acid composition in plant raw materials [9].

Cobalt is found in small quantities in all soils, with larger quantities found in sedimentary rocks. This element accumulates in plants, ranging from 17 to 540 mg/kg ash. Cobalt can be found in different forms, e.g., in ionic form or as part of vitamin B₁₂. Its biological role is to activate glycolytic enzymes (phosphoglucomutase and agrinase), which are involved in the hydrolysis of arginine. Both a deficiency and an excess of this metal can have a negative effect on plant development. Cobalt deficiency reduces the content of chlorophyll and ascorbic acid, while its excess inhibits biosynthesis and lowers the content of protein nitrogen in crops.

The lithosphere and soil are rich in nickel. This microelement promotes the production of vitamin P, increases the activity of redox enzymes, and stabilizes

the structure of ribosomes. Nickel deficiency decreases photosynthetic activity in plants, while its excess can cause necrosis and chlorosis of the green parts of plants.

Chromium is found in various minerals and accumulates in the thin surface layer of soil. This metal is inaccessible to plants. Its content in dry plant mass does not usually exceed 0.02–0.2 mg/kg. Chromium has a dual effect on plant growth and development. On the one hand, this metal is part of many plant enzymes and therefore it affects the biosynthesis of flavonoids and promotes the accumulation of polysaccharides, tannins, carotenoids, cardiac glycosides, and vitamin K. On the other hand, chromium has phytotoxic properties which cause wilting of the aerial parts, damage the root system, and may lead to chlorosis and browning of young leaves. Chromium is also an antagonist of copper, manganese, and boron.

Zinc accumulates in the surface layers of soil and can also be found in some minerals. Its content in plants is 1.2–73.0 mg/kg of dry weight. Like cobalt, zinc ensures the functioning of some enzymes in the glucose oxidation process. Also, zinc plays an important role in the photosynthesis and promotes the production of tryptophan. Its deficiency may disturb phosphorus metabolism, retard the growth of internodes and leaves, as well as cause chlorosis, the development of rosettes, and the accumulation of reducing sugars.

Zinc is a unique metal due to its extensive biogenic properties. It is contained in more than 200 enzymes belonging to all six classes and therefore performs a variety of physiological functions. It is found in all 20 nucleotidyl transferases, as well as in reverse transcriptases. The presence of zinc in these compounds indicates a close relationship with the processes of tumor formation. In addition, zinc stabilizes the structure of DNA, RNA, and ribosomes, as well as plays an important role in gene translation and expression.

Elevated concentrations of zinc have a toxic effect on living organisms. Its excessive accumulation is closely related to anthropogenic activities, which is why high concentrations of zinc are found in industrial areas and agricultural soils over-treated with zinc-containing fertilizers. Many plant species can adapt to zinc excess in soils, but very high levels of this metal can still have a toxic effect. Chlorosis of young leaves is the most common symptom of zinc damage. Moreover, excessive levels of zinc decrease the rate of cell division in plant tissues, as well as impair cell elongation and tissue differentiation. Due to the antagonistic action of zinc towards other metals, its excess in plants reduces the absorption of copper and iron, causing symptoms of their deficiency. Zinc is also an antagonist of cadmium, selenium, and manganese.

Manganese is ubiquitous in rocks and soils. Its content in plants varies from 30 to 500 mg/kg of dry weight. Manganese plays an important biological role in plant growth and development. It is involved in the release of oxygen and carbon dioxide reduced during photosynthesis, regulates the sugar content in leaves,

and participates in the processes of cell growth. Manganese deficiency has a negative effect on the plant, changing its morphology. In particular, it can cause spot chlorosis in the leaves (yellow spots) and tissue necrosis. High manganese contents cause a release of carbon dioxide from plants. Manganese does not interact with calcium or magnesium, but actively interacts with silicon. Manganese is high in plants that synthesize phenolic compounds, tannins, flavonoids, cardiac glycosides, ascorbic acid, carotenes, and vitamin K. Thus, the amount of manganese in clover can be used to estimate its yield and the content of bioactive substances in it. Also, manganese has a beneficial effect on the development and yield of clover seeds.

Copper is an immobile element found in the surface layer of soils. It is part of some proteins and enzymes that accelerate the oxidation of ascorbic acid and diphenols, as well as the hydroxylation of monophenols. Copper also participates in nitrogen-containing metabolism. Its deficiency contributes to stunted growth and flowering, as well as causes chlorosis, loss of turgor, and wilting of plants. Copper excess, on the other hand, affects the metabolism of organic acids and lengthens the period of plant growth and development. The average copper content in plants is 0.6–10.3 mg/kg of air-dry mass. Copper is actively involved in photosynthesis and respiration, as well as nitrogen recovery and fixation in plants. It participates in biochemical processes as part of some oxidase enzymes (e.g., cytochrome oxidase, ceruloplasmin, superoxide dismutase, urate oxidase) that carry out oxidation of substrates with molecular oxygen.

Recently, copper deficiency in soils or its antagonistic interaction with cobalt have been the main causes of concern. Some common signs of copper deficiency in plants include slow formation of reproductive organs and its subsequent cessation, the appearance of puny grains and empty-grained ears, as well as poor adaptation to unfavorable environmental conditions [37]. Wheat, barley, oats, beets, alfalfa, onions, and sunflowers are most sensitive to copper deficiency.

Although lead is found in almost all plants, scientists still lack a full understanding of its role in metabolic processes. According to literature, its low contents inhibit metabolism, while high concentrations have a toxic effect on plants by disrupting photosynthesis and slowing down growth and water absorption by the root system. External negative symptoms include the appearance of dark green leaves, as well as curled old leaves and stunted foliage. Plants exhibit differing resistance to excessive lead concentrations, with cereals being less resistant and legumes being more resistant. Lead has an antagonistic relationship with zinc and a synergic relationship with calcium. The lead content in plants reaches 0.1–10.0 mg/kg of dry weight.

Literature lacks reliable data on the value of cadmium for terrestrial plants. Its toxic effects include slow growth and photosynthesis, inactivated enzymes, disrupted water balance, inhibited reduction of NO₂

to NO, as well as chlorosis [38]. In plant metabolism, cadmium is an antagonist of a number of nutrients (Zn, Cu, Mn, Ni, Se, Ca, Mg, and P). Cadmium is easily transported into plants from the soil and atmosphere. It is the most phytotoxic heavy metal that accumulates in plants (Cd > Cu > Zn > Pb).

Biotechnological methods are widely applied today to determine the nutritional value of plant materials [39, 40]. In studies of plants for animal feeds, great attention must be paid to the content of proteins, since they are functional units of a living cell that are absorbed in the form of amino acids after digestion (MR № 2.3.1.1915-04). Further, these amino acids get involved in plastic metabolism, ensuring the synthesis of their own proteins and other organic compounds [41].

In connection with the above, we carried out a comparative phytochemical study of red clover, alsike clover, and white clover growing in natural populations in Kuzbass. In particular, we performed qualitative and quantitative determination of macro- and microelements, heavy metals, free nitrogen, protein, and amino acids in the experimental plant species.

STUDY OBJECTS AND METHODS

We studied above-ground parts of three types of clover, red clover (*Trifolium pratense* L.), white clover (*Trifolium repens* L.), and alsike clover (*Trifolium hybridum* L.) (Fig. 1). The materials were collected in the natural phytocenoses of Kuzbass (Russia) from the spring of 2023 throughout the flowering period in the summer of 2023. They were selected on the basis of physical factors (adult healthy plants) and visual characteristics (with no toxic effects of anthropogenic pathogens) by using standard methods [42].

The chemical composition of the clover samples was determined by different methods. Phosphorus was measured photocolometrically based on the color intensity of phosphorus-molybdenum blue (from an ash solution). Molybdenum was also determined photocolometrically according to State Standard 18309-72. Copper, zinc, lead, and cadmium were quantified by voltammetry according to Methodological Guidelines 08-47/136 at the chemical and analytical laboratory “GeoBioEcoLab” on a highly sensitive TA-1 voltammetric analyzer that determines nanogram quantities.

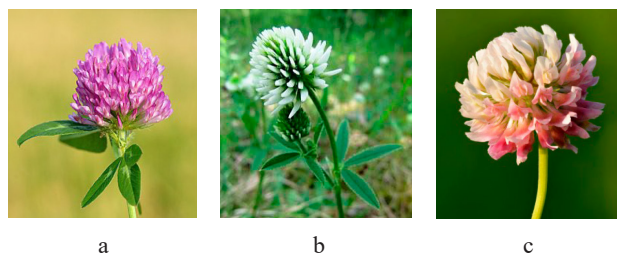


Figure 1 Clover species: (a) red clover (*Trifolium pratense* L.); (b) white clover (*Trifolium repens* L.); and (c) alsike clover (*Trifolium hybridum* L.)

The elemental composition of nickel, cobalt, and chromium was determined by spectrophotometry. This method works by evaporating the substance under analysis, photographing the emission spectrum of the elements excited in the arc discharge zone, and measuring the intensity of the spectral lines of the elements by visually comparing them with those for the reference powders and standard samples. The elements were determined by using atlases of spectral lines and standard spectra.

Cadmium and lead are classified as highly hazardous substances, while copper and zinc are moderately hazardous. Therefore, highly sensitive and accurate methods should be used to measure the contents of these elements. Among such methods is stripping voltammetry that can determine trace amounts. Another advantage of this method is that it can simultaneously determine several components (up to four or five). In addition, a modern polarograph can obtain a linear dependence of the current on concentration in the range of 10^{-8} – 10^{-2} M.

Stripping voltammetry is an electrochemical method that includes the following stages:

1. Electrolytic accumulation of metal ions with a deposit or a metal film forming on the solid electrode coating of the amalgam or on the mercury film electrode. For this, it is important to maintain the rate of the electrode reaction by selecting a constant potential, as well as to constantly stir the solution to ensure a constant flow of the depolarizer from the solution to the electrode surface;

2. A short period of rest of the solution with accumulation potential. The flow moves to the electrode less intensively, causing a rapid drop to the value of the stationary diffusion current; and

3. Electrochemical dissolution of the substance from the electrode surface in the mode of linear potential sweep and strict stabilization of the current flowing between the indicator electrode and the auxiliary electrode.

The current of the dissolution of the concentrated electroactive substance is recorded as a peak. The peak's potential characterizes the nature of the substance, its area indicates the quantity of the substance on the electrode, and its height relates to its concentration.

Stripping voltammetric methods can be anodic (reductive) or cathodic (oxidative).

The height of the peak depends on:

- a) the amount of substance deposited on the electrode (which is a function of its concentration in the solution, accumulation potential, solution composition, temperature, and electrochemical properties of the system);

- b) the conditions of the dissolution process (the area of the active electrode surface, the rate of polarization, and the rate of removal of products from the electrode surface).

Other factors may also influence the peak's height. If the overall electrode process involves a chemical reaction, the peak is determined by the catalytic ability of this reaction, the nature of the reaction products, and the solubility of the resulting compounds.

Stripping voltammetry is a highly sensitive method that can determine nanogram quantities. It is applied to determine low concentrations up to 10^{-2} M, since larger amounts of the isolated sediment saturate the surface, causing a deviation from the direct proportional dependence of the current strength on the concentration. With low concentrations, the error does not exceed 3%.

In stripping voltammetry, just as in polarography, oxygen needs to be extracted from the solution under analysis. This is because at normal temperature and pressure, oxygen is relatively soluble in aqueous solutions and can interfere with the measurement.

Dissolved oxygen is electrolytically reduced, which increases the residual current whose value is poorly reproduced. The presence of dissolved oxygen can lead to other complications in electrochemical measurements. Therefore, in most cases, it is removed by passing through any inert gas that does not require purification. Other methods of oxygen removal (CO_2 in acidic solutions, solid Na_2S in alkaline solutions) have limited use. An inert gas must be passed over the solution throughout the entire analysis. It is important that inert gases should be free of oxygen. UV irradiation is also used in modern methods to remove dissolved oxygen. Thus, stripping voltammetry has high analytical potential and is employed to determine organic and inorganic compounds of various compositions.

In our experiment, Zn, Cd, Pb, and Cu were determined under optimal conditions in aqueous solutions against 0.5 M formic acid under UV irradiation to eliminate the interference of dissolved oxygen. During the analysis, interfering organic substances were destroyed in the electrochemical cell. We selected and tested the conditions for a joint determination of Zn, Cd, Pb, and Cu on a mercury film electrode in a solution of 0.5 M HCOOH with UV irradiation. The optimal conditions included an accumulation potential of 1.4 V and an accumulation time of 30 s for metal ion concentrations in the solution of 0.001–0.05 mg/L. Ion concentrations were determined by adding standard solutions. The air was aspirated through an aerosol filter from perchlorovinyl fiber at a rate of 20 L/min for 25 min.

Amino acids, flavonoids, polyphenols, glycosides, and tannins were determined in the Laboratory for Biotesting of Natural Nutraceuticals at Kemerovo State University. The analysis was performed on a Prominence Shimadzu LC-20 high-performance liquid chromatography system with an SPD-M20A diode array detector and an RF-20 A/20Axs fluorimetric detector.

Total nitrogen and protein were measured by the Kjeldahl method according to General Monograph 1.2.3.0011.15. (OFC.1.5.3.0009.15).

Protein hydrolysates were analyzed by high-performance ion exchange chromatography using a special ninhydrin reagent for the demodulation of eluting amino acids. The samples of plant materials were crushed, weighed, and subjected to complete acid hydrolysis. The resulting hydrolysates were then analyzed.



Figure 2 Air-dried clover samples

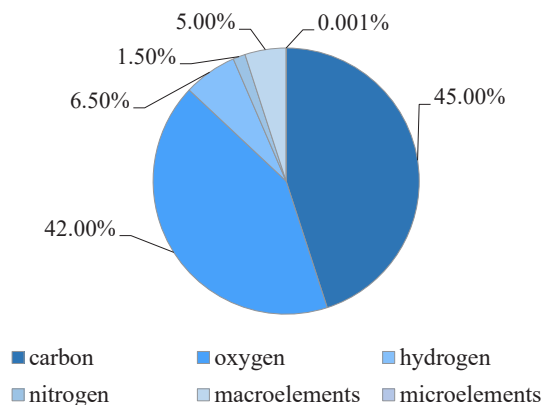


Figure 3 Chemical composition of a combined average clover sample

To prepare the clover materials for the above analyses, they were placed in a thin layer on sheets of parchment paper, covered from dust with another sheet of paper, and left indoors at room temperature for 1–2 days to become air-dry (Fig. 2). Then, the samples were crushed into particles of under 1 cm and distributed on paper in the form of a square. The resulting square was then divided by horizontal and vertical lines into four equal parts, from which samples were taken with a spatula for the laboratory analyses. The weight of the samples depended on the number of analyses, ranging from 50 to 200 g. The samples were then mixed into average samples and placed into labelled glass jars with a ground stopper. In this state, the samples can be stored for a long time, with no change in moisture.

RESULTS AND DISCUSSION

The chemical compositions of the clover species growing in their natural populations in Kuzbass were analyzed for valuable feeding qualities.

As for macroelements, the contents of phosphorus and potassium were almost identical between the clover samples under study (Table 1 and Fig. 4).

As seen from Table 1, the ratios of phosphorus to potassium did not differ significantly.

In particular, the phosphorus content was the highest (6.99 mg/kg) in alsike clover (*Trifolium hybridum* L.) and the lowest (6.48 mg/kg) in red clover (*Trifolium pratense* L.). Potassium was noticeably higher (38.4 mg/kg) in

Table 1 The ratio of phosphorus to potassium in red, white, and alsike clover growing in Kuzbass

Sample	Ratio of phosphorus to potassium, mg/kg
Red clover (<i>Trifolium pratense</i> L.)	5.75
White clover (<i>Trifolium repens</i> L.)	5.80
Alsike clover (<i>Trifolium hybridum</i> L.)	5.23

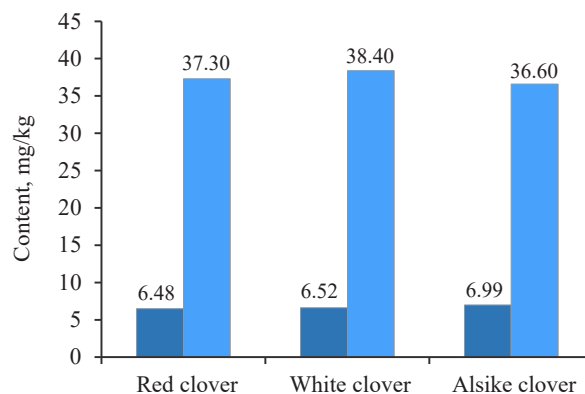


Figure 4 Contents of phosphorus and potassium in red, white, and alsike clover

white clover (*Trifolium repens* L.) and lower (36.6 mg/kg) in alsike clover (*Trifolium hybridum* L.).

The ratio of molybdenum to iron in the clover samples under study is presented in Table 2, while the contents of these elements are shown in Fig. 5.

As can be seen, the content of molybdenum was the highest in red clover (*T. pratense* L.), slightly lower in white clover (*T. repens* L.), and the lowest in alsike clover (*T. hybridum* L.). According to Fig. 5, iron had the highest content (168.51 mg/kg) in white clover and the lowest (135.04 mg/kg) in alsike clover.

One of the advantages of clover over perennial grasses is its higher yield due to nitrogen absorbed by symbiotic nodule bacteria from the atmospheric air. In addition, clover produces its own proteins due to biological nitrogen fixation without any energy costs or expensive nitrogen fertilizers. The ratio of total nitrogen to protein in the experimental clover species ranged from 5.87 to 6.43% (Table 3).

However, we found no direct relationship between the contents of total nitrogen and protein in the clover samples (Fig. 6). For example, white clover (*T. repens* L.) had the highest total nitrogen content of 3.802% and a protein content of 22.73%, while red clover (*T. pratense* L.) had a lower total nitrogen content of 3.715% and a higher protein content of 23.88%. Alsike clover (*T. hybridum* L.) showed the lowest total nitrogen content of 3.683% and the lowest protein content of 21.64%, compared to the other species under study.

Table 2 The ratio of molybdenum to iron in the clover samples under study

Sample	Ratio of molybdenum to iron, mg/kg
Red clover (<i>Trifolium pratense</i> L.)	648.85
White clover (<i>Trifolium repens</i> L.)	755.65
Alsike clover (<i>Trifolium hybridum</i> L.)	894.30

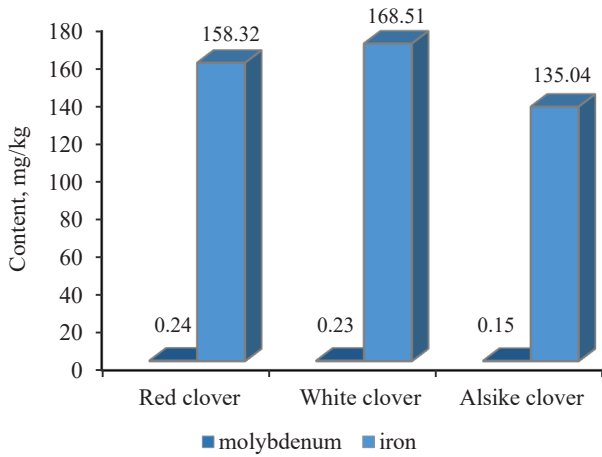


Figure 5 Contents of molybdenum and iron in red, white, and alsike clover

Table 3 The ratio of total nitrogen to protein in red, white, and alsike clover

Sample	Ratio of total nitrogen to protein, %
Red clover (<i>Trifolium pratense</i> L.)	6.43
White clover (<i>Trifolium repens</i> L.)	5.98
Alsike clover (<i>Trifolium hybridum</i> L.)	5.87

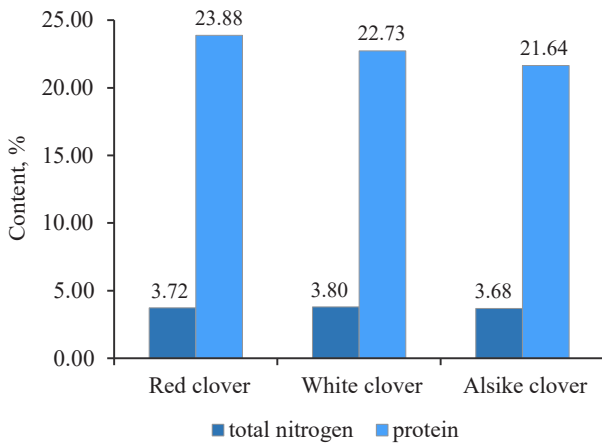


Figure 6 Contents of total nitrogen and protein in the experimental clover species

Noteworthy, the clover genus of the *Fabaceae* family produces up to 80% of protein due to total nitrogen absorbed from the air by nodule bacteria of the root system. This is one of the main advantages of legumes over cereals.

We compared the contents of nickel, cobalt, and chromium as particularly toxic elements with the maximum permissible concentrations established in Sanitary Regulations 2.3.2.10733338-01 for black, green, and brick teas (Figs. 7–9).

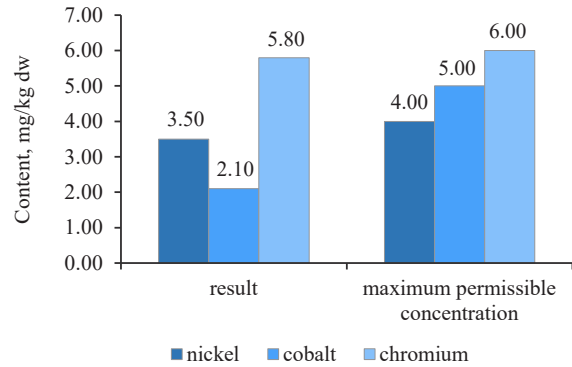


Figure 7 Nickel, cobalt, and chromium contents in red clover and their maximum permissible concentrations

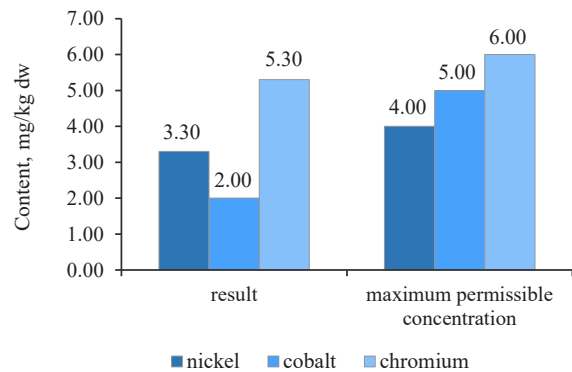


Figure 8 Nickel, cobalt, and chromium contents in white clover and their maximum permissible concentrations

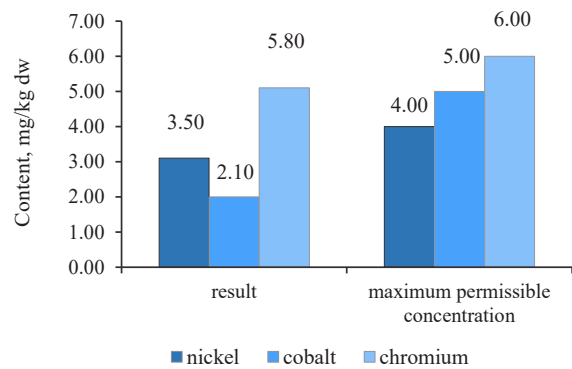


Figure 9 Nickel, cobalt, and chromium contents in alsike clover and their maximum permissible concentrations

As can be seen in Fig. 7, the sample of red clover contained nickel, cobalt, and chromium in permissible concentrations [10, 24, 28].

According to Fig. 8, the sample of white clover contained lower concentrations of these heavy metals than red clover.

As shown in Fig. 9, alsike clover (*T. hybridum* L.) had the lowest concentrations of nickel, cobalt, and chromium, compared to the other samples.

To sum up, all the clover samples complied with Sanitary Regulations 2.3.2.10733338-01. In particular, red clover (*T. pratense* L.) contained the maximum values of chromium, cobalt, and nickel; white clover (*T. repens* L.) showed an average value for nickel, while alsike clover (*T. hybridum* L.) showed the minimum values for all

three metals. Cobalt had almost the same content in all the species, whereas nickel values varied from 3.5 mg/kg in red clover (*T. pratense* L.) to 3.1 mg/kg in alsike clover (*T. hybridum* L.). Thus, the plant materials of the clover species under study do not accumulate chromium, cobalt, and nickel in elevated concentrations. Therefore, these elements have no effect on the plants' growth energy, viability and stability, the synthesis of high-molecular proteins, or the formation of vegetative mass.

The experimental values of heavy metals in the clover species under study are presented in the form of voltammograms in Figs. 10–12.

The voltammograms (Figs. 10–12) indicate the presence of Zn, Cd, Pb, and Cu in almost all the samples of the experimental clover species. The metrological

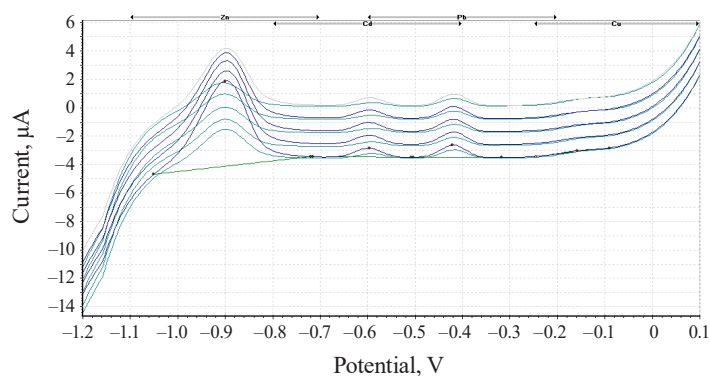


Figure 10 The voltammogram for red clover

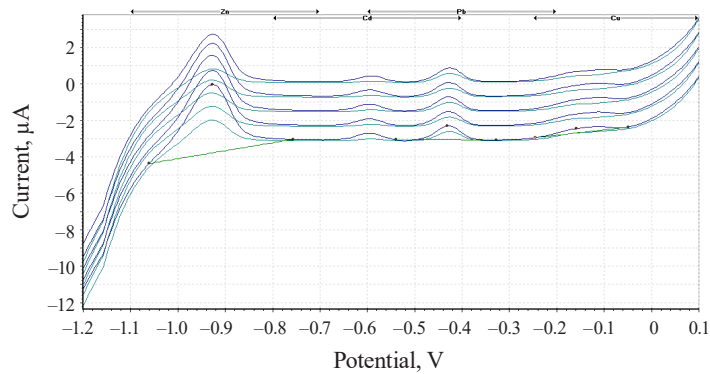


Figure 11 The voltammogram for white clover

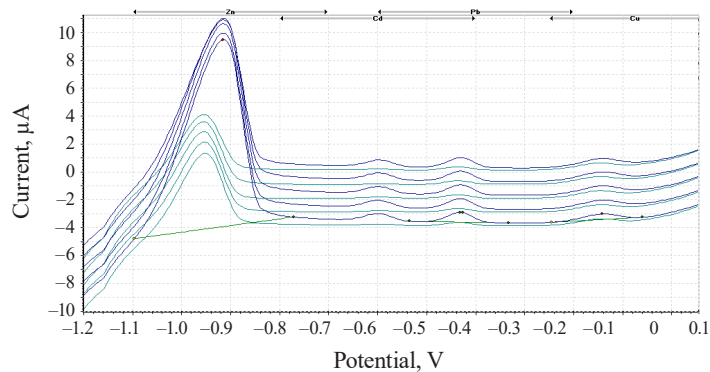


Figure 12 The voltammogram for alsike clover

characteristics for the determination of these heavy metals are presented in Tables 4–6.

We analyzed the contents of Zn, Cd, Pb, and Cu as particularly toxic elements against the maximum permissible concentrations established in Sanitary Regulations 2.3.2.10733338-01 for black, green, and brick teas [34].

According to Table 4, the contents of lead, copper, and zinc in the red clover (*T. pratense* L.) sample were within the permissible levels. However, the cadmium value was over six times the maximum permissible concentration.

As can be seen in Table 5, the sample of white clover (*T. repens* L.) contained lead, copper, and zinc in permissible concentrations, while its content of cadmium was over three times above the maximum level.

As shown in Table 6, the contents of lead, copper, and zinc in the alsike clover (*T. hybridum* L.) sample were within the permissible levels. However, its cadmium value was six times as high as the maximum permissible concentration established in Sanitary Regulations 2.3.2.10733338-01.

To sum up, the contents of lead, zinc and, copper in all the experimental clover samples were within the permissible concentrations by Sanitary Regulations 2.3.2.10733338-01. Cadmium exceeded the standard values in all the three clover species. Zinc was found in almost equal amounts in red clover (*T. pratense* L.) and alsike clover (*T. hybridum* L.), with the maximum value in white clover (*T. repens* L.). The lead content ranged from 3.1×10^{-7} mg/L for white clover (*T. repens* L.) to

5.6×10^{-7} mg/L for alsike clover (*T. hybridum* L.). Copper varied from 3.2×10^{-7} mg/L for alsike clover (*T. hybridum* L.) to 5.1×10^{-7} mg/L for red clover (*T. pratense* L.).

Thus, the plant materials of the studied clover species do not accumulate lead, copper, and zinc in elevated concentrations. Therefore, these metals have no effect on the plants' growth, viability, and stability, as well as the synthesis of high-molecular proteins or the formation of vegetative mass. The elevated cadmium content leads to a lower plant yield and a deteriorated quality of plant products. The accumulation of heavy metals in plant materials has industrial causes. Today, the environment is becoming more and more chemically "aggressive". Cadmium enters the soil in a mobile form and therefore rapidly migrates to plants, producing a negative effect on the environment.

The nutritional value of proteins is determined by the quality and quantity of individual amino acids that proteins are made of. Literature lacks data on the composition of amino acids in the clover species growing in Kuzbass. Therefore, at the final stage of our study, we determined the composition of amino acids in the plant materials of the experimental clover species (Fig. 13 and Table 7).

Red clover is one of the most common plants found in the European part of the former USSR, as well as throughout Western and Eastern Siberia, in a wide variety of environmental conditions, except for marshlands. This is a valuable forage plant with good feeding qualities, which is especially important in places with

Table 4 Metrological characteristics of heavy metals in red clover and their maximum permissible concentrations

Element	Concentration (C_{AV}), mg/L	Standard deviation (S)	ΔC_{AV}	Confidence interval ($\mu = C_{AV} \pm \Delta C_{AV}$), mg/L	Maximum permissible concentration, mg/kg
Cd	6.4×10^{-7}	3.1×10^{-7}	3.8×10^{-7}	$6.4 \pm 3.8 \times 10^{-7}$	1.0
Pb	4.3×10^{-7}	1.1×10^{-7}	1.4×10^{-7}	$4.3 \pm 1.4 \times 10^{-7}$	10.0
Cu	5.1×10^{-7}	2.9×10^{-7}	3.6×10^{-7}	$5.1 \pm 3.6 \times 10^{-7}$	33.0
Zn	4.2×10^{-7}	2.1×10^{-7}	2.6×10^{-7}	$4.2 \pm 2.6 \times 10^{-7}$	23.0

Table 5 Metrological characteristics of heavy metals in white clover and their maximum permissible concentrations

Element	Concentration (C_{AV}), mg/L	Standard deviation (S)	ΔC_{AV}	Confidence interval ($\mu = C_{AV} \pm \Delta C_{AV}$), mg/L	Maximum permissible concentration, mg/kg
Cd	3.4×10^{-7}	1.1×10^{-7}	1.2×10^{-7}	$3.4 \pm 1.2 \times 10^{-7}$	1.0
Pb	3.1×10^{-7}	1.7×10^{-7}	2.1×10^{-7}	$3.8 \pm 2.1 \times 10^{-7}$	10.0
Cu	4.8×10^{-7}	1.9×10^{-7}	2.3×10^{-7}	$4.8 \pm 2.3 \times 10^{-7}$	33.0
Zn	6.3×10^{-7}	2.4×10^{-7}	3.1×10^{-7}	$6.3 \pm 3.1 \times 10^{-7}$	23.0

Table 6 Metrological characteristics of heavy metals in alsike clover and their maximum permissible concentrations

Element	Concentration (C_{AV}), mg/L	Standard deviation (S)	ΔC_{AV}	Confidence interval ($\mu = C_{AV} \pm \Delta C_{AV}$), mg/L	Maximum permissible concentration, mg/kg
Cd	6.2×10^{-7}	2.4×10^{-7}	3.1×10^{-7}	$6.2 \pm 3.1 \times 10^{-7}$	1.0
Pb	5.6×10^{-7}	3.3×10^{-7}	4.1×10^{-7}	$5.6 \pm 4.1 \times 10^{-7}$	10.0
Cu	3.2×10^{-7}	2.9×10^{-7}	3.6×10^{-7}	$5.1 \pm 3.6 \times 10^{-7}$	33.0
Zn	4.1×10^{-7}	1.6×10^{-7}	2.02×10^{-7}	$3.2 \pm 2.2 \times 10^{-7}$	23.0

wet and slightly acidic soils capable of withstanding short-term flooding. Therefore, our next stage was to experimentally determine the content of amino acids in red clover grass.

We found that the experimental samples of the clover species had significant differences in the amino acid composition. According to Table 7, the alsike clover sample had maximum concentrations of all amino acids under study, with the exception of glutamic acid, which was the highest in the white clover sample. Thus, the clover species growing in Kuzbass can provide livestock

with natural feed of high quality due to a wide variety of amino acids in the plants.

Chromatographic analysis was then performed to determine the contents of bioactive substances in the extract of red clover (Fig. 14 and Table 8).

Six substances were found in the red clover extracts, which were chromatographically classified as flavonoids. The following isoflavonoids were identified (in descending order): daidzein, biochanin A, quercetin, genistein, rutin, and apigenin. Their contents varied from 0.4300 mg/g for apigenin to 6.3400 mg/g for

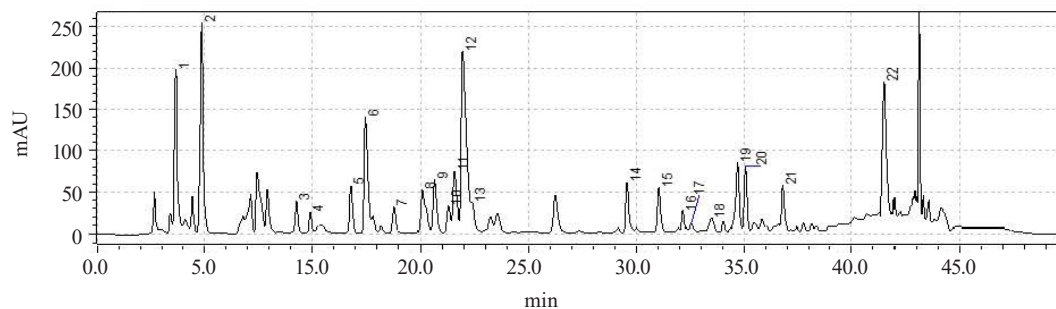


Figure 13 HPLC chromatogram for amino acids in red clover, where: peak 1 – Aspartic acid, peak 2 – Glutamic acid, peak 3 – o-Pro, peak 4 – Serin, peak 5 – Glycine, peak 6 – Histidine, peak 7 – Arginine, peak 8 – Tryptophan, peak 9 – Thr, peaks 10, 11 – Alanin, peaks 12,13 – Proline, peak 14 – Tyrosine, peak 15 – Methionine, peak 16 – Valin, peaks 17,18 – Cys, peak 19 – Isoleucine, peak 20 – Leucine, peak 21 – Phenylalanine, and peak 22 – Lysine

Table 7 Contents of amino acids in clover samples

Amino acid, mg/kg dw	Clover species		
	Red clover (<i>Trifolium pratense</i> L.)	White clover (<i>Trifolium repens</i> L.)	Alsike clover (<i>Trifolium hybridum</i> L.)
Aspartic acid	29.7	35.1	38.6
Tryptophan	7.9	10.3	11.1
Serin	11.8	14.7	15.8
Proline	11.9	11.5	12.2
Glutamic acid	12.1	14.4	13.9
Alanin	12.2	12.7	13.4
Valin	12.5	14.2	14.7
Methionine	2.1	2.1	2.5
Isoleucine	11.2	12.6	12.9
Leucine	20.1	23.1	23.6
Tyrosine	5.2	6.1	7.5
Phenylalanine	12.7	15.3	15.5
Lysine	17.1	19.1	19.7
Histidine	7.4	7.8	8.9
Arginine	24.1	25.2	28.9
Glycine	47.1	51.8	57.7
Total	245.1	276.0	296.9

Table 8 Contents of bioactive substances in the extract of red clover (*Trifolium pratense* L.)

Peak No.	Bioactive substance	Retention time, min	Content, mg/g
1	Quercetin	4.9800	2.8400 ± 0.0048
2	Biochanin A	6.7300	3.1900 ± 0.0053
3	Daidzein	10.0900	6.3400 ± 0.0076
4	Genistein	15.0000	1.2800 ± 0.0031
5	Apigenin	16.9200	0.4300 ± 0.0012
6	Rutin	28.2900	0.6900 ± 0.0015

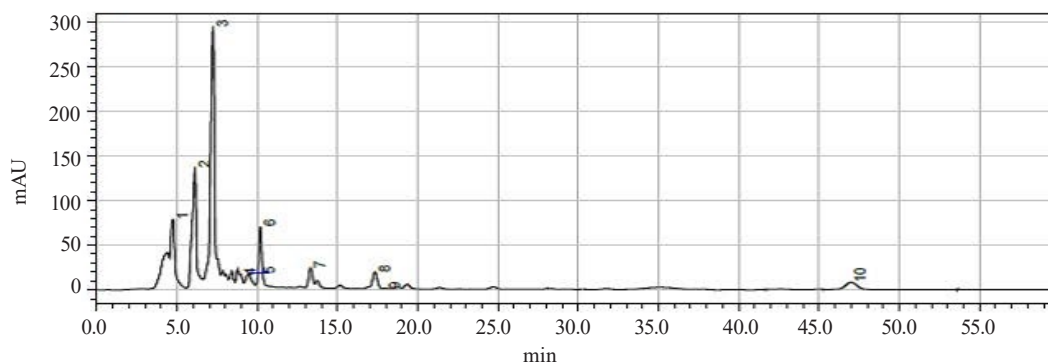


Figure 14 Chromatogram of bioactive substances in the red clover (*Trifolium pratense* L.) extract, where: 1 – quercetin, 2 – biochanin A, 3 – daidzein, 4 – genistein, 5 – apigenin, 6 – luteolin, 7 – formononetin, 8 – naringin, 9 – rutin

daidzein. All of these flavonoids can be successfully used as bioactive substances for therapeutic and preventative purposes.

CONCLUSION

We studied the plant materials of red clover (*Trifolium pratense* L.), white clover (*Trifolium repens* L.), and alsike clover (*Trifolium hybridum* L.) growing in Kuzbass. Our experiments showed no significant differences in their nitrogen content.

The contents of phosphorus and potassium did not differ significantly among the clover species, ranging from 6.48 to 6.99 mg/kg and from 36.6 to 38.4 mg/kg, respectively. The content of cadmium significantly exceeded the maximum permissible concentrations in all the samples, while the contents of zinc and copper were experimentally determined to be minimal. The lead concentration was slightly higher than the standard values in red clover (*T. pratense* L.) and white clover (*T. repens* L.), reaching 10.7 and 11.0 mg/kg, respectively, however, a significant excess of lead (17.5 mg/kg) was detected in alsike clover (*T. hybridum* L.).

The protein content in the clover samples ranged from 21.64 to 23.88%. Such minor differences are due to a high content of total nitrogen synthesized by nodule bacteria in the roots of leguminous plants, on the one hand, and a high content of nitrogen accumulated during the decomposition of root residues during the growing season, on the other hand. All the clover samples had significant amounts of essential amino acids, such as tryptophan, lysine, leucine, isoleucine, methionine, phenylalanine, and valine. This variety of amino acids, and

therefore complete protein, makes the clover a valuable forage plant. The total amount of amino acids was 245.1 mg/kg in red clover (*T. pratense* L.), 276.0 mg/kg in white clover (*T. repens* L.), and as much as 296.9 mg/kg in alsike clover (*T. hybridum* L.).

Thus, the plant materials of red, white, and alsike clover growing in Kuzbass had significant amounts of mineral substances (phosphorus, potassium, molybdenum, and iron), total nitrogen, and protein with essential amino acids. Their contents of particularly toxic elements such as nickel, lead, cobalt, chromium, copper, and zinc did not exceed permissible concentrations. From this we can conclude that these plants can be reliably used to improve the soil's fertility and nitrogen regime. However, the concentration of cadmium in the clover samples was found to be over six times as high as the maximum permissible concentration. This can be explained by the presence of cadmium in fuel and fertilizers, as well as its use in the processing of coal and industrial waste in Kuzbass. Therefore, we would not recommend using the plant materials of the clover species to produce bulk feed for farm animals until the industrial processes in the region become more environmentally friendly and safe.

CONTRIBUTION

All the authors are equally responsible for the research results and the manuscript.

CONFLICT OF INTEREST

The authors declare no conflict of interest.

REFERENCES

1. Aslam M, Aslam A, Sheraz M, Ali B, Ulhassan Z, Najeeb U, et al. Lead toxicity in cereals: Mechanistic insight into toxicity, mode of action, and management. *Frontiers in Plant Science*. 2021;11. <https://doi.org/10.3389/fpls.2020.587785>
2. Chen G, Li J, Han H, Du R, Wang X. Physiological and molecular mechanisms of plant responses to copper stress. *International Journal of Molecular Sciences*. 2022;23(21). <https://doi.org/10.3390/ijms232112950>
3. Asyakina LK, Dyshlyuk LS, Prosekov AYU. Reclamation of post-technological landscapes: International experience. *Food Processing: Techniques and Technology*. 2021;51(4):805–818. (In Russ.). <https://doi.org/10.21603/2074-9414-2021-4-805-818>

4. Budantsev AL. Plant resources of Russia: Wild flowering plants, their composition and biological activity. Vol. 2. The families Actinidiaceae – Malvaceae, Euphorbiaceae – Haloragaceae. St. Petersburg, Moscow: KMK; 2009. 513 p. (In Russ.).
5. Nizamutdinov TI, Suleymanov AR, Morgun EN, Dinkelaker NV, Abakumov EV. Ecotoxicological analysis of fallow soils at the Yamal experimental agricultural station. Food Processing: Techniques and Technology. 2022;52(2): 350–360. <https://doi.org/10.21603/2074-9414-2022-2-2369>
6. Titov AF, Talanova VV, Kaznina NM, Laidinen GF. Plant resistance to heavy metals. Petrozavodsk; 2007. 170 p. (In Russ.).
7. Li X, Wang Z, Bai M, Chen Z, Gu G, Li X, et al. Effects of polystyrene microplastics on copper toxicity to the protozoan *Euglena gracilis*: Emphasis on different evaluation methods, photosynthesis, and metal accumulation. Environmental Science and Pollution Research. 2022;29:23461–23473. <https://doi.org/10.1007/s11356-021-17545-9>
8. Pelikhovich YuV, Begday IV, Kharin KV, Tsesar TA. Heavy metal accumulation in medicinal plants and risk assessment. Science. Innovations. Technologies. 2020;(4):171–183. (In Russ.). <https://doi.org/10.37493/2308-4758.2020.4.13>
9. Goncharuk EA, Zagorskina NV. Heavy metals, their phytotoxicity, and the role of phenolic antioxidants in plant stress responses with focus on cadmium: Review. Molecules. 2023;28(9). <https://doi.org/10.3390/molecules28093921>
10. Capuozzo M, Santorsola M, Bocchetti M, Perri F, Cascella M, Granata V, et al. p53: From fundamental biology to clinical applications in cancer. Biology. 2022;11(9). <https://doi.org/10.3390/biology11091325>
11. D'yakova NA. The content of heavy metals and arsenic in the medicinal plants of the Voronezh region. Russia patent RU 2022620084. 2022. <https://elibrary.ru/AAJXDT>
12. Ho L-H, Rode R, Siegel M, Reinhardt F, Neuhaus HE, Yvin J-C, et al. Potassium application boosts photosynthesis and sorbitol biosynthesis and accelerates cold acclimation of common plantain (*Plantago major* L.). Plants. 2020;9(10). <https://doi.org/10.3390/plants9101259>
13. Li Y, Yin M, Li L, Zheng J, Yuan X, Wen Y. Optimized potassium application rate increases foxtail millet grain yield by improving photosynthetic carbohydrate metabolism. Frontiers in Plant Science. 2022;13. <https://doi.org/10.3389/fpls.2022.1044065>
14. Chen J, Zhang N-N, Pan Q, Lin X-Y, Shangguan Z, Zhang J-H, et al. Hydrogen sulphide alleviates iron deficiency by promoting iron availability and plant hormone levels in *Glycine max* seedlings. BMC Plant Biology. 2020;20. <https://doi.org/10.1186/s12870-020-02601-2>
15. Dyshlyuk LS, Osintseva MA, Kozlova OV, Fotina NV, Prosekov AYu. Antiradical and oxidative stress release properties of *Trifolium pratense* L. extract. Journal of Experimental Biology and Agricultural Sciences. 2022;10(4):852–860. [https://doi.org/10.18006/2022.10\(4\).852.860](https://doi.org/10.18006/2022.10(4).852.860)
16. El'kina GYa. Content of amino acids in plants at different levels of lead in the soil. Agrohimia. 2023;(6):63–72. (In Russ.). <https://elibrary.ru/QOXLOQ>
17. Tabalenkona GN, Silina EV. Influence of habitat conditions on the content and composition of free amino acids of *Plantago media* L. leaves. Proceedings of Voronezh State University. Series: Chemistry. Biology. Pharmacy. 2023;(2):54–61. (In Russ.). <https://elibrary.ru/WSFRVA>
18. Lezhnina MG, Khanina MA, Podolina EA, Rodin AP. The chemical composition of urban gravelate (*Geum urbanum* L.). The Prospects for Innovative Technologies in Medicine and Pharmacy: Proceedings of the 6th All-Russian Scientific and Practical Conference. Volume 2; 2019; Orekhovo-Zuevo. Orekhovo-Zuevo: State University of Humanities and Technology; 2019. p. 161–167. (In Russ.). <https://elibrary.ru/DHIOFC>
19. Prosekov AYu, Ulrikh EV, Kozlova OV, Dyshlyuk LS. Study pectin as vegetable analog pharmaceutical gelatine. Modern Problems of Science and Education. 2014;(5). (In Russ.). <https://elibrary.ru/SZVKBJ>
20. Boyarskykh IG, Siromlya TI. Macro- and trace elements composition of some medicinal plants in the geochemically abnormal environment in the Altai Mountains (Russia). Rastitelnye Resursy. 2022;58(4):376–387. <https://doi.org/10.31857/S0033994622040045>
21. Yermokhin YuI, Bobrenko IA, Bobrenko EG. Microelement composition of agricultural plants in Siberia. Research and Scientific Electronic Journal of Omsk SAU. 2020;21(2).
22. Kruglov DS, Prokusheva DL. The trace-element constituents of the most widespread plants of genus *Artemisia*. Chemistry of Plant Raw Material. 2022;(3):139–149. (In Russ.). <https://doi.org/10.14258/jcprm.20220310800>
23. Hilfiker A, Bovet L. Modulation of the content of amino acids in the plant. Russia patent RU 2799785C2. 2023. <https://elibrary.ru/DXYVMO>
24. Saleh TA. Trends in the sample preparation and analysis of nanomaterials as environmental contaminants. Trends in Environmental Analytical Chemistry. 2020;28. <https://doi.org/10.1016/j.teac.2020.e00101>

25. Babich O, Sukhikh S, Pungin A, Asyakina L, Ivanova S, Prosekov A. Modern trends in the in vitro production and use of callus, suspension cells and root cultures of medicinal plants. *Molecules*. 2020;25(24). <https://doi.org/10.3390/molecules25245805>
26. Babich O, Sukhikh S, Prosekov A, Asyakina L, Ivanova S. Medicinal plants to strengthen immunity during a pandemic. *Pharmaceuticals*. 2020;13(10). <https://doi.org/10.3390/ph13100313>
27. Polozhij AV, Vydrina SN, Kurbatskij VI, Nikiforova OD. *Flora Sibiriae*. Tomus 9. Fabaceae (Leguminosae). Novosibirsk: Nauka; 1994. 280 p. (In Russ.).
28. Popova E. Distribution of heavy metals in plant communities of the West Siberian Arctic and Subarctic. *E3S Web of Conferences*. 2021;284. <https://doi.org/10.1051/e3sconf/202128401009>
29. Sardans J, Peñuelas J. Potassium control of plant functions: Ecological and agricultural implications. *Plants*. 2021;10(2). <https://doi.org/10.3390/plants10020419>
30. Dyshlyuk L, Babich O, Prosekov A, Ivanova S, Pavsky V, Chaplygina T. The effect of postharvest ultraviolet irradiation on the content of antioxidant compounds and the activity of antioxidant enzymes in tomato. *Heliyon*. 2020;6(1). <https://doi.org/10.1016/j.heliyon.2020.e03288>
31. Dolganyuk V, Sukhikh S, Kalashnikova O, Ivanova S, Kashirskikh E, Prosekov A, et al. Food proteins: Potential resources. *Sustainability*. 2023;15(7). <https://doi.org/10.3390/su15075863>
32. D'yakova NA Peculiarities of heavy metal and arsenic trans-medium transition along the chain “soil – medicinal plant material – water extracts”. *Humans and their Health*. 2023;26(1):64–71. (In Russ.). <https://doi.org/10.21626/vestnik/2023-1/08>
33. Rubanka EV, Terletskaia VA, Zinchenko IN. The migration of heavy metals during the extraction of plant materials. *Food Science and Technology*. 2013;24(3):70–72. (In Russ.). <https://elibrary.ru/XIKWEH>
34. Dmitrieva AI, Belashova OV, Ivanova SA, Prosekov AYu, Milenteva IS. Assessment of the content of heavy metals in medicinal plants of Genus trifolium from the growing area on the example of the Siberian federal district. *International Journal of Pharmaceutical Research*. 2020;12(3):1880–1893. <http://dx.doi.org/10.31838/ijpr/2020.12.03.262>
35. Reut AA. The content of biologically active substances to the introduced members of the genus *Hemerocallis* L. *News of FSVK*. 2019;(1):93–96. (In Russ.). <https://doi.org/10.18619/2658-4832-2019-1-93-96>
36. Fashutdinova ER, Sukhikh AS, Le VM, Minina VI, Khelef MEA, Loseva AI. Effects of bioactive substances isolated from Siberian medicinal plants on the lifespan of *Caenorhabditis elegans*. *Foods and Raw Materials*. 2022;10(2):340–352. <https://doi.org/10.21603/2308-4057-2022-2-544>
37. Kamanina IZ, Kaplina SP, Salikhova FS. The content of heavy metals in medicinal plants. *Scientific Review. Biological Science*. 2019;(1):29–34. (In Russ.). <https://elibrary.ru/PQBWFP>
38. Kutlimurotova RKh, Pulatova LT. Study of the amino acid composition of *Asarum europaeum* L plants growing in Uzbekistan. *Universum: Chemistry and Biology*. 2021;86(8):27–30. (In Russ.). <https://doi.org/10.32743/Uni-Chem.2021.86.8.12131>
39. Babich OO, Milentyeva IS, Dyshlyuk LS, Ostapova EV, Altshuler OG. Structure and properties of antimicrobial peptides produced by antagonist microorganisms isolated from Siberian natural objects. *Foods and Raw Materials*. 2022;10(1):27–39. <https://doi.org/10.21603/2308-4057-2022-1-27-39>
40. Dobrosmyslova IA, Sazanova AA, Semenov VG, Tuleubaev Zh, Yesimbekova ZT, Ziyaeva GK. Plant growth and biological productivity after processing with microelements. *The Bulletin the National Academy of Sciences of the Republic of Kazakhstan*. 2021;(1):74–80. (In Russ.). <https://doi.org/10.32014/2021.2518-1467.10>
41. Prosekov AYu, Babich OO, Zaushintseva AV, Belashova OV, Milenteva IS, Asyakina LK, et al. Method for producing curd mass enriched with common skullcap and red clover concentrates. Russia patent RU 2753361C1. 2021. <https://elibrary.ru/DIGWCS>
42. The State Pharmacopoeia of the Russian Federation. Vol. IV. Moscow; 2018. 1926 p. (In Russ.).

ORCID IDs

Olga V. Belashova <https://orcid.org/0000-0002-4706-1850>
Oksana V. Kozlova <https://orcid.org/0000-0002-2960-0216>
Natalia S. Velichkovich <https://orcid.org/0000-0002-9061-1256>
Vladimir P. Yustratov <https://orcid.org/0000-0002-1779-4332>
Andrey N. Petrov <https://orcid.org/0000-0001-9879-482X>

GUIDE FOR AUTHORS FORMATTING REQUIREMENTS FOR ARTICLES

We publish original, previously unpublished English language articles that possess scientific novelty in the field of food industry and related branches of science. The Journal publishes scientific papers, reports, peer reviews, brief scientific communications, letters to the editor, and related news items.

The main requirements for submitted articles are: validity of factual material, clarity and brevity, reproducibility of experimental data. The manuscript should meet the specified formatting standards. Please make sure that the section "Results and discussion" of your article states the novelty of your research.

All manuscripts submitted to the *Foods and Raw Materials* should be written in US English. The manuscript should contain no less than 10 pages in Microsoft Word text editor, abstract, tables, figures, and references included.

Format instructions

- 20 mm margins;
- single line spacing without automatic hyphenation;
- no extra interspaces between words or gaps between paragraphs;
- Times New Roman, size 10.

Structure

(1) **The type of your manuscript** should be clarified in the upper left corner (scientific article, review article, short message, note or letter, etc).

(2) **Title** (< 10 words) should be informative and reflect the main results of the research. The title of the article should be in lowercase letters, with the exception of the first letter and proper names. Please avoid abbreviations.

(3) **First and last names of the authors** are separated by commas. Paternal and middle names should be contracted to the first letter. Spelling should coincide with your ORCID id. Please mark the name of the author responsible for correspondence with an asterisk*.

(4) **Affiliation** is a formal name of the institution, city, postal address with postal code. The names and locations of institutions or companies should be given for all authors. If several institutions are listed, match the institution and the corresponding author with superscript numbers. Please include the e-mail address of the author responsible for correspondence.

(5) **Abstract** (200–250 words) cannot exceed 2000 characters with spaces. The abstract should be original and completely reflect the main results and novelty of the article. The best way to structure your abstract is to let it follow the structure of the article itself: relevance, tasks and objectives, methods, results, and conclusions. Please avoid meaningless introductory phrases and vague, general statements.

(6) **Keywords** provide < 10 keywords identifying the subject and the result of the research. Remember that it is key words that enable your potential readers to find your article on the Internet.

(7) **Introduction** gives a brief review of the publications related to the matter and proves its relevance. Referenced sources should be indexed in international scientific databases. In-text references should be given in square brackets and numbered [beginning with №1] in order of their appearance in the text. If several sources are quoted, they are given in chronological order. Make sure your introduction reflects the objectives of your research.

(8) Study objects and methods:

– Experimental research papers should contain a full description of the subject of the study, consecutive stages of the experiment, equipment, and reagents. Do not forget to specify the original company names of equipment and reagents manufacturers in brackets. If the method you use is not widely known or has been considerably modified, please provide a brief description.

– Theoretical research papers should specify objectives, approximations and assumptions, conclusions and equations. Please do not overload your text with intermediate data and description of well-known methods (such as numerical methods of solving equations) unless you have introduced some novelty into them.

(9) **Results and discussion** should provide a concise description of experimental data. Rather than repeating the data given in tables and graphs, the text should seek to reveal the principles detected. While describing your research results, it is recommended to use the Past Indefinite verb tense. The discussion should not reiterate the results. The discussion should contain an interpretation of the obtained research results (compliance of the results with the research hypothesis, generalisation of the research results, suggestions for practical application and future research).

Each **table** should be made in MS Word (Table – Add Table) or MS Excel and contain no less than three columns. Provide a number and a title for each table.

The Journal publishes color photographs and diagrams.

Mathematical equations should start with a separate line and be typed in the MathType frame as a whole. Mind that it is not allowed to compile formulae from composite elements (e.g. one part of the formula is a table, another part is a text, and some other part is an embedded frame). Please maintain the common settings for fonts, the size of characters and their placement in MathType formulas. Please avoid manual change for individual symbols or formula elements.

(10) **Conclusion** briefly summarises the main results of your research. Naturally, the conclusion should contain the answer to the question posed by the introduction.

(11) **Contribution** should indicate the actual contribution of each author in the research process. *Foods and Raw Materials* observes the CRediT taxonomy of the authors' contributions.

(12) **Conflict of interest** should indicate a real or potential conflict of interest. If there is no conflict of interests, you should write that "the author declares that there is no conflict of interest".

(13) **Acknowledgements** contains expression of gratitude to those who contributed to the research.

(14) **Funding** indicates how the research and the publication of this article were funded. If the study was performed with the support of a grant, specify the number of the grant and its name. State the name of your employer if the study was performed as part of your routine work and did not receive additional funding.

(15) **References** should be formatted according to the standard defined by the editors. The references are given in the order of their appearance in the text. Make sure you have included the DOI, if available.

Please avoid references to publications that are not readily available, e.g. institutional regulations, state standards, technical requirements, unpublished works, proceedings of conferences, extended abstracts of dissertation, and dissertations. Make sure you do not cite unpublished articles. It is not recommended to use more than three references to web resources. Please avoid citing publications that are more than 10 years old.

Self-citation should be well-justified and cannot exceed 10% of the references. Please make sure that at least 50% of the works you cite are less than 5 years old and published in periodicals registered in such data bases as Scopus, Web of Science, etc.

If you mention no references to fresh, 2–3-year-old papers, it might reduce your chances for publication. The references should reflect the actual impact of representatives of the international scientific community on the issue.

The manuscript should be carefully checked and signed by all authors on the first page of the main text. The article will not be published if it fails to meet the requirements. All articles are subject to general editing.

Correspondence and submission of all documents is done by e-mail: fjournal@mail.ru or www.jfrm.ru/en

The editors expect to receive **the following documents**, in Russian or English:

(1) an e-version of your article in MS Word named by the first author's last name (e.g. SmithJ.doc).

(2) a scanned PDF version of your article, the first page signed by all the authors (SmithJ.pdf);

(3) a form with personal information about the author(s). Please do not forget to mark the name of the author responsible for correspondence with an asterisk*. Name the file by the first author's name, e.g., SmithJ_Form.doc;

(4) a scanned PDF version of a cover letter to the editor-in-chief from the responsible organisation with the conclusion about the relevance of the research and recommendations for its publishing. The document should contain the date, reference number, and the signature of the head of the organisation;

(5) a standard copyright agreement.

Please mind that all the files should contain a single document.

For submission instructions, subscription and all other information visit this journals online at jfrm.ru/en/

CONTENTS

Editor's column	ii
Danyo Emmanuel Kormla, Ivantsova Maria N., Selezneva Irina S. Ionizing radiation effects on microorganisms and its applications in the food industry.....	1
Halavach Tatsiana M., Kurchenko Vladimir P., Tarun Ekaterina I., Romanovich Roman V., Mushkevich Natalia V., Kazimirov Alexander D., Lodygin Aleksei D., Evdokimov Ivan A. Chitosan complexes with amino acids and whey peptides: Sensory and antioxidant properties	13
Prasad Jaishankar, Dixit Aishwarya, Sharma Sujata P., Mwakosya Anjelina W., Petkoska Anka T., Upadhyay Ashutosh, Kumar Nishant Nanoemulsion-based active packaging for food products	22
Herrera Nora Gabriela, Villacrés Nelson Adrián, Aymara Lizbeth, Román Viviana, Ramírez Mayra Composite exopolysaccharide-based hydrogels extracted from <i>Nostoc commune</i> V. as scavengers of soluble methylene blue	37
Bugaets Olga N., Bugaets Ivan A., Kaigorodova Elena A., Zelentsov Sergey V., Bugaets Natalia A., Gerasimenko Evgeny O., Butina Elena A. Soybean testa spectral study	47
Eremeeva Natalia B. Nanoparticles of metals and their compounds in films and coatings: A review	60
Perevozchikova Maria A., Domsy Igor A., Sergeyev Alexey A. Hematological parameters of free-ranging moose <i>Alces alces</i> (Linnaeus 1758) (<i>Ruminantia, Cervidae</i>)	80
Evdokimov Ivan Yu., Malkova Angelina V., Irkitova Alena N., Shirmanov Maxim V., Dementev Dmitrii V. Effect of a new probiotic on <i>Artemia</i> cysts determined by a convolutional neural network	91
Romanova Mariia V., Dolbunova Anastasiia N., Epishkina Yulia M., Evdokimova Svetlana A., Kozlovskiy Mikhail R., Kuznetsov Alexander Ye., Khromova Natalya Yu., Beloded Andrey V. A thermophilic L-lactic acid producer of high optical purity: Isolation and identification	101
Gaikwad Vaibhav, Kaur Jaspreet, Rasane Prasad, Kaur Sawinder, Singh Jyoti, Kumar Ankit, Kumar Ashwani, Sharma Nitya, Mehta Chandra Mohan, Pate Avinash Singh Nutritional significance of finger millet and its potential for using in functional products	110
Tikhonov Sergei L., Tikhonova Natalia V., Gette Irina F., Sokolova Ksenia V., Danilova Irina G. Antihyperglycemic activity of colostrum peptides	124
Phuong Do Viet, Nguyen Luu Thao Coffee pulp pretreatment methods: A comparative analysis of hydrolysis efficiency	133
Azizpour Nasim, Razavi Seyed Hadi, Azizpour Mehran, Poul Esmacil Khazaei The effect of post-packaging pasteurization on physicochemical and microbial properties of beef ham	142
Hussein Ahmed M. S., Abd El-Aal Hala A., Morsy Nahla M., Hassona Mohamed M. Chemical, rheological, and sensory properties of wheat biscuits fortified with local buckwheat	156
Rincón Soledad Edicson Mauricio, Arredondo Nontién Mónica Alejandra, Castro Jose Wilson, Barrios Dursun, Vásquez Mejía Sandra Milena Chorizo sausage with shiitake mushrooms (<i>Lentinula edodes</i>) as a fat substitute: quality evaluation	168
Zenu Fuad, Bekele Tesfaye Major food-borne zoonotic bacterial pathogens of livestock origin: A Review	179
Belashova Olga V., Kozlova Oksana V., Velichkovich Natalia S., Fokina Anna D., Yustratov Vladimir P., Petrov Andrey N. A phytochemical study of the clover growing in Kuzbass	194